



NORSK POLARINSTITUTT

RAPPORTSERIE

NR. 97 - OSLO 1997

EDITORS: VLADIMIR VOLKOV, GALINA JU. KOSHELEVA, VASILY
SMOLYANITSKI AND TORGNV VINJE

NATURAL CONDITIONS OF THE KARA AND BARENTS SEAS

PROCEEDINGS OF THE RUSSIAN-NORWEGIAN WORKSHOP -95



ST. PETERSBURG, RUSSIA
FEBRUARY 28 - MARCH 2, 1995

RUSSIAN · NORWEGIAN
WORKSHOP · 95



State Scientific Center
of the Russian Federation
Arctic and Antarctic Research Institute



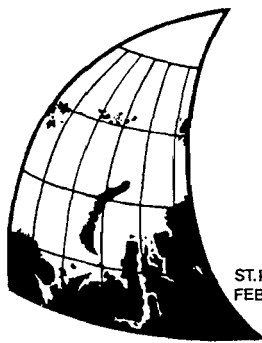


Rapport Nr. 97

NATURAL CONDITIONS OF THE KARA AND BARENTS SEAS

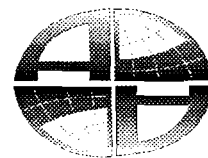
PROCEEDINGS OF THE RUSSIAN-NORWEGIAN WORKSHOP -95

Editors: Vladimir Volkov, Galina Ju. Kosheleva, Vasily Smolyanitsky
and Torgny Vinje



ST. PETERSBURG, RUSSIA
FEBRUARY 28 - MARCH 2, 1995

RUSSIAN-NORWEGIAN
WORKSHOP-95



State Scientific Center
of the Russian Federation
Arctic and Antarctic Research Institute

NORSK POLARINSTITUTT
Oslo 1997

Prepared for publication by:

Arctic and Antarctic Research Institute

Norwegian Polar Institute

Dr.Vladimir Volkov

Dr.Torgny Vinje

Mrs.Galina Ju.Kosheleva

Mr.Vasily Smolyanitsky

Translated into English by:

Miss Irina I.Solov'eva

Mrs N.Yegorova

© Norsk Polarinstitut
Technical Editor: Annemor Brekke
ISBN 82-7666-121-1
Printet November 1997
Gjøvik Trykkeri As

CONTENTS

General information about Workshop 95	10
Preface	12
<i>Plenary reports</i>	13
Volkov, V.A. & T. Vinje: Scientific results of the Russian-Norwegian expedition studies in 1993-1994	15
Engedahl, H., B. Aadlandsvik, & E.A. Martinsen: Production of monthly mean climatological archives of salinity, temperature, current and sea level for the Nordic seas	18
Volkov, V.A. & V.T. Sokolov: Main features of the oceanographic regime of the Kara Sea	19
Ivanov, V.V.: The Kara mouth region, level of knowledge, choice of research priorities	21
Frolov, I. Ye., V. Ye. Borodachev, Ye. U. Mironov: Ice regime of the Barents and the Kara Seas, state and perspectives of studies	23
Polyakov, I., I. Kulakov, S. Kolesov, N. Dmitriyev, A. Naumov: Modelling Kara sea water and ice behaviour	27
Pozdnyshev, S.P., Ye.O. Aksenov, Z.M. Gudkovich, A.A. Panfilov, D.A. Speransky: Modeling of ice cover evolution in the Kara Sea for operational ice forecasting in the summertime	32
Radionov, V.F., V.V. Ivanov, G.I. Baranov & A.P. Makshtas: Western Arctic air circulation and aerosol contamination	38
Ogorodnikov, B.I., V.I. Skitovich, G.A. Luyanene & V.I. Luyans: Radioactive aerosols over Novaya Zemlya and the coast of the Barents sea after 1975	46
Bushuyev, A.V., V.D. Grishchenko, V.G. Smirnov & Yu.A. Shcherbakov: Studies of the Western Arctic Seas using space means	51
Smagin, V.M., S.V. Pivovarov & S.V. Berdnikov: Study of the hydrochemical structure and modeling of the consequences of anthropogenic activities in the Kara Sea	55
Pavlov, V.K., M.Yu Kulakov & V.V. Stanovoy: Modeling of transport and transformation of pollutants in the Barents and Kara Seas	59
Cochrane, S., L. Kjeldstrup, R. Palerud & S. Dahle: Preliminary studies of benthic faunal communities in the estuaries of Ob and Yenisey	64
Khlebovich, V.V. & A.Yu. Komendantov: Biotic communities of the Kara Sea estuarine ecosystems	66
Musatov, E.E.: Late cenozoic sedimentation on the shelf of the Kara and Eastern Barents Seas	67

Livingston, H.D., G.P. Panteleev, F.L. Sayles, Vi. Vi. Ivanov & O.N.Medkova: The history of the radioactive contamination of the Ob river system	68
<i>Physical oceanography</i>	75
Averkiev, A.S., D.V. Gustoev & V.Y. Chantsev: The numerical model of drift of passive impurity in adjacent regions of the Norwegian and Barents Seas	77
Ashik, I.M. & Yu.A. Vanda: Uniform hydrological regions of the Kara Sea and their regime characteristics	81
Ashik, I.M.: Numerical forecasts of surge fluctuations of the Kara Sea level	84
Baskakov, G.A., G.N. Voinov, V.A. Volkov, G.Yu. Kosheleva, V.L. Kuznetsov & V.K. Pavlov: Structure of water circulation in the Kara Sea depending on the type of atmospheric processes	87
Benzeman, V.Yu.: Mezostructure of water density maximal gradients boundary layer relied in Arctic seas by lidar sensing data	92
Bogorodsky, P.V. & A.P. Makshtas: On natural convection in a melt puddle	96
Bulatov, L.V. & S.V. Kochetov: Atlantic water in the Kara Sea	99
Bulatov, L.V.: Role of flaw polynyas in the hydrological and ice regime of the Kara Sea	104
Chviljov, S.V.: Oceanographic database on the Barents Sea as part of creating an oceanographic system on the Arctic ocean	108
Churun, V.N. & L.A. Timokhov: Cold and highly saline water of the Kara Sea	113
Dmitrenko, I.A. & P.N. Golovin: Formation of spatial-temporal temperature non-uniformities in the eastern Kara Sea as affected by the destruction of internal waves	114
Dvorkin, Ye.N., Yu. A. Vanda & P.V. Pavlov: Extreme oscillations of the Kara Sea level	115
Gribanov, V.A., I.A. Dmitrenlo & V.V. Stanovoy: Hydrophysical processes governing mesoscale variability of oceanographic characteristics in the coastal zone of the Kara and Laptev Seas	118
Ivanov, V.V., A.A. Korablev & I.P. Karpova: Manifestation of natural climate oscillations in the Barents-Norwegian seas boundary water masses parameters	121
Høkedal, J.: Observation of spectral downwelling irradiance in the Kara Sea	126
Korobov, V.: Provision of calculated hydrometeorological values for hydrotechnical construction in the south-east of the Barents Sea	130
Kuznetsov, V.L.: Features of the hydrological regime of the Kara Sea in the data of the KAREX-90 expedition	134
Kuz'min, S.B., V.A. Volkov & V.V. Stanovoy: Atlantic water circulation in the region of the continental slope in the north of the Barents Sea	140
Lavrenov, I.V. & J.R.A. Onvlee: Numerical realization of the wave energy propagation in wind wave models	144

Lavrenov, I.V., T.A. Pasechnik, V.I. Dymov & Kudukhov.: Calculation and forecasting model of sea waves and its employment results in the seas of the Arctic Ocean	145
Lebedev, I.A.: Mesoscale mechanisms of heat exchange between different water masses and its probable relation with climate fluctuations in the Barents Sea	150
Lebedev, G.A., G.P. Gavriilo, L.G. Pisarevskaya & A.P. Polyakov: Iceberg active and passive sonar accoustics	151
Makshtas, A.P. & Ivanov, B.V.: Features of sea/air energy exchange processes in the zone of seasonal migration of drifting sea ice	152
Pisarevskaya, L.G. & E. Nygaard: CTD-measurements near a Kara Sea floeberg	160
Pisarevskaya, L.G. & V.A. Volkov: Iceberg induced thermohaline perturbations	163
Semjonov, G.A. & A.M. Bezgreshnov: Numerical simulation of the thermohaline water circulation in the Norwegian-Greenland and the Barents Seas	167
Semjonov, G.A. & S.V. Chviljov: Numerical simulation of interannual variability of the thermohaline water circulation of the Barents Sea in the summer season	171
Vanda, Yu.A. & Ye.N. Dvorkin: Large-scale level oscillations of the Kara Sea	172
Voinov, G.N.: Main features of tidal currents in the Kara Sea	174
Voinov, G.N.: Structure of the tide in Amderma according to the results of a harmonic analysis of sea level observations for a 19-year period from 1962 to 1980	176
Zakharchuk, Ye.A., G.E. Presnyakova: High frequency internal waves in the Kara Sea	179
Zhukov, V.I., V.A. Volkov, V.L. Kuznetsov, S.B. Kuz'min & V.O. Bayandin: Characteristics of currents and hydrological parameters at a standard point in the vicinity of the Dikson Island on the basis of buoy station data NPI-94-K2 from August 24 to September 11, 1994 (the Russian-Norwegian Oceanographic Program, KAREX-94)	183
<i>Hydrology of estuaries and land waters</i>	184
Vinogradova, T.A.: Peculiarities of the water discharge regime in the estuary area of the Ob river	187
Vinogradov, Yu. B.. & T.A. Vinogradova: The problem of estimating the pollutant discharge from the river basins of the arctic zone	191
Volkov, A.V.: A two-layer model of sea/river water interaction in the estuary zone of the sea	196
Grayevsky, A.P.: Water dynamics and structure in the river estuaries of the Kara Sea basin	201
Grayevsky, A.P., V.V. Ivanov, V.S. Latyshev, A.Ye. Antsulevich, N.V. Maksimovich & I.A. Stogov: Results of composite studies of the Pechora mouth area in 1994	205

Doronin, Yu.P., & V.V. Ivanov.: Methods and results of modeling hydrological processes in stratified arctic estuaries	209
Ivanov, V.V.: Inflow and spreading of river water in the Kara Sea	214
Ivanov, V.V. & A.A. Piskun: Water and channel regime in the river deltas	221
Ivanova, A.A.: Features of non-periodic water level fluctuations in the mouth areas of Ob and Yenisey	226
Bessan, G.N., K.A. Klevanny & G.V. Matveyev: Simulation of hydrodynamic and environmental problems in Arctic river deltas with a computer system "cardinal"	229
Kotrekhov, Ye.P.: Study of long-wave processes in the mouth areas of the northern rivers on the basis of hydrodynamic one-dimensional models	235
Medkova, O.N. & D.Yu. Bol'shiyanov: Structure and dynamics of the shores of the Kolguyev Island	237
Medkova, O.N.: Morphology and dynamics of the coastal zone of the Ob gulf	238
Nalimov, Yu.V.: Ice thermal regime of the estuaries of large rivers of the Kara Sea basin	239
Petrov, N.L., A.T. Bozhkov, Yu.V Nalimov & T.I. Nizovtseva: The hydrological database from the stationary observation network in the mouth areas of large rivers in the Kara Sea basin	245
Piskun, A.A.: Characteristics of the free surface curves in the Ob mouth area according to the results of hydraulic calculations	248
Stanovoy, V.V.: Some features of the hydrological regime of the Ob gulf	253
Solovieva, Z.S. & L.V. Antonova: Spatial temporal variability of the ice regime elements in the lower reaches and mouth areas of rivers in the Kara Sea basin	257
Tretyakov, M.V.: Modelling of the halocline dynamics in the river mouth areas taking into account ice dynamics	260
Usankina, G.Ye. & A.P. Balabayev: Features of the freeze-up of the Ob-Taz and Yenisey mouth areas	263
Khrustalev, S.S.: Modelling of water quality dynamics in the northern Ob gulf.	264
Shiklomanov, A.I.: Estimate of the change in the Yenisey river inflow to the Kara Sea as affected by industrial activities in its basin	268
<i>Sea ice</i>	269
Abramov, V.A., S.V. Kliachin & Ye.G. Shvedov: On the question of icebergs in the Arctic seas	271
Aksenov, Ye.O., S.V. Brestkin, A.Ya. Busuyev, V.F. Dubovtsev, S.Yu. Nikolayev & V.S.Porubayev: Russian archived observation data on ice thickness in the Kara Sea	275
Alexandrov, V.Yu. & T.V. Rakhina: Study of the Kara and Laptev sea ice dynamics from satellite images	279

Voevodin, V.A. & V.V. Panov: Very dangerous ice phenomena in the Barents and Kara Seas	282
Gavrilo, V.P., S.M. Kovalev, G.A. Lebedev & O.A. Nedoshivin: First-year Barents and Kara Sea ice: calculated mean multiyear month value of mechanical strength, elastic moduli and potential resistance	283
Gudoshnikov, Yu.P., G.K. Zubakin & A.K. Naumov: Distribution of icebergs in different regions of the Barents and Kara Seas	284
Zubakin, G.K., W.A. Abramov, Yu.P. Gudoshnikov & A.A. Dementiev: Icebergs of the Western Arctic (morphometry, distribution and dynamics)	288
Ivanov, B.V. & Yu.P. Gudoshnikov: Dynamic-stochastic model of drifting iceberg	289
Mironov, Ye.U. & O.I. Babko: Features of the ice conditions in the Barents Sea in the spring-summer of 1993-1994 and tendencies toward their changes in the last decade	290
Polyakov, I., S. Kolesov & A. Naumov: Modelling the variability of the ice cover, temperature and salinity of the Arctic Ocean	293
Smirnov, V.G. & A.V. Grigoryev: The Kara Sea satellite sea surface temperature measurements in September of 1994	298
Smolyanitsky, V.M., V.E. Borodachev, I.E. Frolov S.V. Klyachkin & Ey.G. Shvedov: Usage of the data on sea ice in the GRID format for the Barents and Kara seas areas for the aims of ice informatics	301
Spichkin, V.A. & A.G. Yegorov: Features of changes in summer ice conditions of the KARA Sea in recent years	302
Stepanov, I.V. & V.A. Likhomanov: Stochastic computer simulation of the morphometry of level drifting ice	305
Tripolnikov, V.P.: Methods and techniques for in-situ tests of the ice cover mechanical characteristics	308
Tripolnikov, V.P.: Destruction of ice by explosions	312
Strakhov, M.V., K.P. Tyshko, V.I. Fedotov & N.V. Cherepanov: Spatial temporal variability of ice cover structure of the Kara Sea during its formation and growth	317
Smirnov, V.N., I.B. Sheikin & A.I. Shushlebin: Ice compression and local deformations of an ice floe in the Arctic Ocean	321
Smirnov, V.N., V.A. Nikitin, A.I. Shushlebin & I.V. Sheikin: Results of studies of the effect of wind-induced waves and swell of the ice cover of the Barents Sea	325
<i>Meteorology</i>	329
Alexandrov, E.I., N.N. Bryazgin & A.A. Dementyev: Current changes in climate of the Kara Sea region	331
Bryazgin, N.N. & A.A. Dementyev: Drifting snow transport in the Kara Sea	336
Sadovsky, B.F., A.G. Sharapov & B.I. Ogorodnikov: Concentration of large condensation nuclei at airborne atmospheric sounding over the Barents and Kara Seas	340

Myakoshin, O.I., A.P. Makshtas & A.P. Nagurny: Results of a full-scale experiment on study of solar radiation absorption in the upper layer of the Kara Sea (August-September 1994)	342
<i>Sea ice chemistry and contamination</i>	347
Ivanov, L.M., T.M. Margolina, A.I. Danilov, M.Y. Kulakov & V.K. Pavlov: Radioactive climate of the Kara Sea from the results of the Russian-Norwegian cruise in 1992	349
Lystsov, V.N.: Potential radioecological situation in the regions of the Barents and Kara Seas	350
Namjatov A.A.: Investigation of sediment radioactive contamination at the Kola Bay	351
Nejdanov, G.A. & L.Yu. Kazennov: Results of the express-survey of the Novaya Zemlya bays radioactive pollution	352
Nikitin, A.I., V.B. Chumichev, P. Strand & L. Foyrn: Russian-Norwegian joint investigations of the marine environment radioactive contamination in the areas of radioactive waste dumping in the Kara Sea	353
Korneyeva, G.A., V.P. Shevchenko & G.I. Ivanov: Features of organic matter destruction in water of the Barents and Kara Seas	355
Latyshev, V.S.: Results of hydrochemical studies in the Kara Sea during the expedition Yenisey-93	358
Shevchenko, V.P., G.I. Ivanov, A.A. Vinogradova, A.A. Burovkin & L.Ya. Grudinova: Composition of aerosols over the north-western Kara and Barents Seas in August-October 1994	359
Romanov, V.F. & V.E. Lagun: The diagnostic technologies development for atmospheric pollution transports to the Kara and Barents Seas estimations	363
<i>Biology, sedimentology</i>	371
Alexandrova, O.A. & O.A. Shevchenko: Particulate lipid distribution in the Ob river estuary and the southern Kara Sea	373
Antsulevich, A.E., N.V. Maximovich & I.A. Stogov: Hydrobiological researches in the gulf of Petcora of the Barents Sea and its prospects	376
Barabanova, L.V., L.V. Bondarenko, K.V. Kvitko, V.D. Siminenko, S.A. Kozhin: Phenetical analysis of genetic polymorphism of some invertebrate and plants natural populations in the north-western area of the White Sea for the ecological studies of student biologists	377
Belyaeva, A.N.: Environmental controlling factors reflected in the Kara Sea sedimentary lipids	381
Vedernikov, V.I., G.A. Korneyeva & V.P. Shevchenko: A relationship between the production-destruction processes in sea water of the Kara Sea	385
Gavrilo, M.V.: Marine birds in the Kara Sea ecosystem; coverage and perspective studies	388

Gramberg, I.S., G.I. Ivanov, V.L. Ivanov, Yu.K. Bordukov & V.D. Kryukov: Multidisciplinary investigation of the sea bottom environment of the Western Russian Arctic	389
Denisenko, S.G., N.V. Denisenko, E.A. Frolova, N.A. Anisimova, H. Sandler & S. Dahle: Current state of the bottom fauna and structure of bottom communities in the Pechora Sea	390
Kvitko, K.V., V. Andreyeva, Ja. Kirsanova, N.V. Maximovich, L.N. Tichonova, A. Migunova & Ju. Minichev: Green algae Choricystis (Skuja) Fott - a parasite of the White Sea mussel (<i>Mytilus edulis</i> L.).	395
Kozhin, S.A., L.V. Bondarenko, L.V. Barabanova, K.V. Kvitko, & V.D. Simonenko: Environmental influence to the genetic polymorphism of some invertebrate and brownm algae in the White Sea by the phenetics population method	400
Musatov, E.E. & A. Solheim: Geological correlation and evolution of the eastern Svalbard - Franz Josef Land region: the northern Barents Sea geotraverse	406
Neyelov, A.V. & N.V. Chernova: Fish fauna of the Kara Sea: state of knowledge and key research goals	407
Petrova, V.I.: Polycyclic aromatic hydrocarbons in bottom sediments of the Barents-Kara shelf	412
Pogrebov, V.B., O.A. Kiyko, S.I. Fokin, & V.V. Galtsova: Current ecological state of bottom communities in the Barents and Kara Seas: Results of studies in 1991-1994	415
Sadikov, M.A.: Perspectives of studies of ecological testing grounds 5 in the Arctic	418
Sadikov, M.A.: A chart of ecogeochemical regioning of the western arctic shelf of Russia	421
Chernova, N.V.: State of knowledge of ichthyofauna of the Barents Sea	430
Shevchenko, V.P., A.P. Lisitsin, G.I. Ivanov, O.V. Severina, A.A. Burovkin, Maierova, S.S. Shanin, Ye.A. Romankevich & L.Ya. Grudinova: Quantitative distribution of suspension and suspended organic carbon in the Kara and Barents Seas	431
Shevchenko, V.P., A.P. Lisitsin, G.I. Ivanov, M.Ye. Vinogradov, A.A. Burovkin, V.V. Zernova, S.S. Shanin, Ye. A. Romankevich & A.V. Nescheretov: Ocean sediment fluxes in the Kara and Barents Seas	436

General Information about Workshop-95

Organizers:

AARI- The State Scientific Centre of the Russian Federation Arctic and Antarctic Research Institute (St.Petersburg, Russia)

NP- The Norwegian Polar Institute (Oslo, Norway)

Contributers:

AN - Akvaplan-Niva (Tromse,Norway)

ARROI - All-Russian Research Oceanological Institute (St.Petersburg, Russia)

AIRC - Arctic Innovational Research Centre (St.Petersburg)

BIRAS - Biological Institute of the Russian Academy of Science (St.Petersburg, Russia)

BISPhSU - Biological Institute of St.Petersburg State University (St.Petersburg)

DTAHEM - Dikson Territorial Agency for Hydrometeorology and Environmental Monitoring (Dikson, Russia)

FIMI - Finish University of Marine Research (Finland)

IAP - Institute of Air Physics (Moscow, Russia)

IORAS - Shirshov-Institute for Oceanology of the Russian Academy of Science (Moscow, Russia)

HU - University of Helsinki (Helsinki,Finland)

HPSDI - Hydro-Power Station Design Institute 'Hydroproject', (St.Petersburg, Russia)

KNMI -Royal Meteorological Institute (Netherlands)

KPCI - Karpov- Physical-Chemical Institute (Moscow, Russia)

LARHE SE - Laboratory of the Arctic Regional Hydroecology, State Enterprises (St.Petersburg, Russia)

LIRAS - Limnological Institute of the Russian Academy of Science (St.Petersburg, Russia)

LNPI - Nuclear Physical Institute (St.Petersburg , Russia)

MAGSE - Marine Arctic Geological Survey Expedition (Murmansk, Russia)

MB - Murmansk AARI's Branch (Murmansk, Russia)*MHINUAS* - Marine Hydrophysical Institute of the National Ukraine Academy of Science (Sevastopol, Ukraine)

MEP - Ministry of Environmental Protection (Moscow, Russia)

MI - Microbiological Institute (Moscow, Russia)

MMBI - Murmansk Marine Biological Institute of the Kola Scientific Centre of the Russian Academy of Science (Murmansk, Russia)

MRI - Institute of Marine Research (Bergen,Norway)

MTAHEM - Murmansk Territorial Agency for Hydrometeorology and Environmental Monitoring (Murmansk, Russia)

NDRE - Norwegian Defence Research establishment (Horton,Norway)

NERSC - Nansen Environmental and Remote Sensing Center (Bergen,Norway)

NIERSC - Nansen International Environmental and Remote Sensing Center (St.Petersburg, Russia)

NMG - Northern Marine Geology- Scientific-Productional Association (St.Petersburg, Russia)

NMRI - Norwegian Meteorological Institute (Oslo,Norway)

NORDECO - "NORDECO, INC." Russian-American Joint-Stock Company (Arkhangelsk, Russia)

NRPA -Norwegian Radiation Protection Authority (Norway)

NTAHEM - Northern Territorial Agency for Hydrometeorology and Environmental Monitoring (Arkhangelsk, Russia)

PI - Physical Institute (Vilnius, Lithuania)

PMGSE - Polar Marine Geological Survey Expedition (Murmansk, Russia)

RCMA -Regional Centre "Monitoring of the Arctic" (St.Petersburg)

RIMAM - Research Institute for Mech.App.Math.of the Rostov State University (Rostov-on-Don, Russia)

RSU - Res.Inst.for Mech.App.Math. of the Rostov State Univ., Rostov on-Don

RSHI - Russian State Hydrometeorological Institute (St. Petersburg, Russia)

RSC KI - Russian Scientific Centre- Kurchatov Institute (Moscow, Russia)

SPO - Sea Protection Office 'Morzaschita', (St.Petersburg, Russia)

SHI - State Hydrological Institute (St.Petersburg)

SPbSU - St.Petersburg State University, Microbiological Department (St.Petersburg, Russia)

SPbI SOI - St.Petersburg Department of State Oceanografic Institute (St.Petersburg, Russia)

RINCAN - State Research Institute for Nature Conservation of the Arctic and the North
(St.Petersburg, Russia)

"*System-A*" - "System-A" (St.Petersburg, Russia)

"Typhoon" - "Typhoon" - Scientific-Productional Association (Obninsk, Russia)

UB - University of Bergen (Bergen,Norway)

WOI - Woods Hole Oceanographic Institute (Woodshole,USA)

WU - University of Washington (Seattle,USA)

ZIRAS - Zoological Institute of the Russian Academy of Sciences (St.Petersburg, Russia)

Organizing Committee

Dr.Alexander I. Danilov (AARI, St.Petersburg, Russia)Chairman

Dr.Pal Prestrud (NP, Oslo, Norway)

Dr.Torgny Vinje (NP, Oslo, Norway)

Dr.Vladimir A. Volkov (AARI, St.Petersburg, Russia)

Dr.Sergey M. Priamikov (AARI, St.Petersburg, Russia)

Secretariat

Dr.Vasily L.Kuznetsov (AARI, St.Petersburg, Russia)- Head

Mrs. Natalia B.Yegorova (AARI, St.Petersburg, Russia)

Mrs. Galina Yu.Kosheleva (AARI, St.Petersburg, Russia)

Mr. Sergey B. Kuzmin (AARI, St.Petersburg, Russia)

Dr. Knut Finne (Bergen, Norway)

Dr. Jo Hoekedal (NP, Oslo, Norway)

Mr.Vladislav I.Zhukov (AARI, St.Petersburg, Russia)

Preface

Current publication contains summaries of the reports presented at the workshop and the scientific seminar "Natural Conditions of the Kara and the Barents Seas" held at the State Scientific Center of the Russian Federation - the Arctic and Antarctic Research Institute during the period 28 February - 1 March 1995.

The workshop and the seminar were organized within the framework of the annual Russian-Norwegian Working Meeting between the AARI and the Norwegian Polar Institute (NPI). The aim of the workshop was to assess our level of knowledge about the nature of the region, identify directions of research activities for 1995-1999 and coordinate joint Russian-Norwegian studies. 134 scientists participated in the Scientific Seminar. 16 plenary and 112 poster papers in physical oceanography, meteorology, hydrology of the estuaries and land water, sea chemistry (including contamination transfer and transformation), biology and sedimentology were presented and discussed by representatives from 45 scientific institutions of Russia, Norway and the USA.

As a result of the discussions, the research priorities for Russian-Norwegian cooperation in the Kara and the Barents Seas were outlined for the next 5-year period, which can serve as a basis for the *Agreement on Scientific-Technical Cooperation between Russia and Norway for 1996-1999* with regard to studies in the Arctic region.

It was agreed that studies within the framework of Russian-Norwegian Scientific Cooperation should be related to and coordinated with such large international projects for Arctic studies as *ACSYS*, *AMAP* and *LOICZ*.

Scientists from different institutions emphasized the need to further develop and adopt joint programs for investigating the Barents and the Kara Sea regions under the aegis of the Ministry for Science and Technical Policy of the Russian Federation and the corresponding Ministry in Norway. Participants in the workshop agreed that the State Scientific Center of the RF the Arctic and Antarctic Research Institute and the Norwegian Polar Institute could be coordinators of these programmes.

Current collection of the reports is published according to the recommendations of the workshop.

No corrections or alterations have been made in the contributions received by the Norwegian Polar Institute which has published the report. The contents of the articles are the sole responsibility of the authors.

Plenary reports

February 28 – March 1, 1995

SCIENTIFIC RESULTS OF THE RUSSIAN-NORWEGIAN EXPEDITION STUDIES IN 1993-1994

V.A. Volkov (AARI) and T. Vinje (NP)

Cooperation between the Arctic and Antarctic Research Institute and the Norsk Polar Institute was initiated in 1988 (see Table 1) by signing the known Agreement between the USSR *GKNT* (Ministry for Science and Technical Policy of the Russian Federation now) and the Norwegian Research Council in the area of natural sciences (*NAVF*). Its new stage began in 1993-1994. It is characterized by a significantly expanded study area including the eastern Barents and the Kara Seas with bays and straits, updated scientific programs, improved methodologies, development of a comprehensive approach. Studies of natural communities currently include contamination of water, ice and soil; optical characteristics of sea water; sea/air interaction processes; atmospheric aerosols.

In 1993-1994 the main goal of the scientific program remained study of water-salinity-ice and heat exchange through the main straits, assessment of interannual and interseasonal exchange variability, identification of the mechanisms of water mass transformation and bottom water formation, in particular, of the heat exchange processes between Atlantic water and the layers above and below. In recent years full-scale data necessary for the development of climatic programs were accumulated and the ideas related to transfer and transformation of contaminants in the region were actively evolved. These objectives are consistent with the goals of the international project: "Arctic Climate System Study" (*ACSYS*) within the framework of the World Climate Research Program. They also have a potential with regard to implementing the national programs of Russia and Norway in the framework of the international Arctic Monitoring and Assessment Program (*AMAP*).

In 1993-1994 four Russian-Norwegian expeditions were carried out:

- * two aboard the Norwegian R/V "*Lance*" (1993, 1994) in the Barents Sea
- * two aboard the Russian R/V "*Pavel Bashmakov*" (1993) and "*Ivan Petrov*" (1994) in the Barents and the Kara Seas.

The aim of the joint program onboard the R/V "*Lance*" in 1993 was to study sea/air energy exchange and measure the albedo of puddles. A conclusion about a weak albedo dependence on the puddle depth should be considered an important result. This conclusion was later confirmed by model experiments.

A joint AARI-NP program carried out onboard the R/V "*Lance*" in 1994 was predominantly oceanographic. During the cruise 93 oceanographic stations were occupied and ice samples collected for contamination determination. Due to a favourable ice situation, it was possible to perform observations on the continental slope in the northern Barents Sea and in the Arctic Basin, the region rarely visited by the research vessels. As a result, unique data on warm Atlantic water circulation were obtained. By analyzing these data and the data obtained earlier under the Russian-Norwegian oceanographic program, the pathways of the Atlantic water inflow to the Barents Sea from the north were specified and the water exchange volume estimated.

During the first Russian-Norwegian cruise to the Kara Sea in 1994 aboard the R/V "*Pavel Bashmakov*" the objectives were mainly oceanographic: monitoring of the ice-hydrological regime, study of frontal zones, estimates of the heat-mass exchange between water masses of different origin, study of the influence of icebergs on structure of oceanographic fields, etc. For the first time, a set of hydrooptical measurements (attenuation coefficient and colour index) was conducted.

In 1993 as a result of the specific conditions of atmospheric dynamics, a rare distribution of freshened water on the Kara Sea surface was formed, off the coasts of Novaya Zemlya the area of river water spreading was observed, and in the shallow Ob'-

Yenisey zone even a higher water salinity was recorded. The obtained full-scale data are quite important for verifying the hydrodynamic models and studying the effect of atmospheric processes on changes in the pattern of oceanographic fields within the season.

A detailed hydrooptical survey of the sea made for the first time has allowed a conclusion that water mass transparency in the fall is mainly governed by the distribution of terrigenous material exported by the rivers. The Kara Sea water has a higher attenuation coefficient of directed light as compared with the Barents Sea water. There is no typical feature of water transparency increasing with depth which is usual for most sea areas. Large transparency gradients are observed both in the horizontal and vertical direction. The value of the light attenuation coefficient distribution by depth allows the thermohaline structure components to be revealed.

At present the joint expedition of the AARI-NP (including the *"Akvaplan-Niva"* and the Regional Center *"Monitoring of the Arctic"*) aboard the R/V *"Ivan Petrov"* (Archangelsk) in 1994 is considered to be the largest expedition.

The expedition program included oceanographic, ice, optical, biological and actinometric sections. 23 scientists including 6 Norwegians participated in the expedition. 146 oceanographic stations were occupied and comprehensive information about the ecological state of the Kara Sea environment was collected.

Important scientific results of each of the sections complementing the results of the previous expeditions were obtained. Among the new achievements are: renewal of instrumental multiday observations of currents (as well as of temperature and salinity at a standard AARI point north of Dikson) after a break of several years, as well as a large number of biological samples in the region of the outflow of desalinated water and Kara water. They will allow obtaining estimates of the level of contaminants in biological media and determining the contamination balance components in the marine ecological systems.

The scientific results of the joint Russian-Norwegian studies are described in more detail in numerous more specific presentations at this meeting by the authors of this paper and other scientists, participants of the joint expeditions and from the Russian and Norwegian research institutions.

Table 1.

Main stages of the Russian-Norwegian cooperation (expeditions and meetings)

1986	First meeting
1988	- 15/I Agreement between GKNT and NAVF on technical-scientific cooperation of the Arctic and Northern regions for 1988-92 years - Meeting, Norway (X) - Meeting, Leningrad (XII)
1989	- " <i>G.O.Sars</i> " (III-IV), Norwegian and Barents Seas - " <i>Akademik Shuleikin</i> " (III), Greenland Sea - " <i>H.Mosby</i> " (VI-VII), Greenland Sea - " <i>Akademik Shuleikin</i> " (VII-VIII), Barents Sea - " <i>Lance</i> " (VIII-IX), Barents and Greenland Seas - Meeting, Leningrad (X) - Meeting, Oslo (XII)
1990	- Meeting, Oslo, Bergen (V) - Meeting, Leningrad (VI) - " <i>Professor Multanovsky</i> " (VII-IX), Barents Sea - " <i>Lance</i> " (VII-VIII), Barents and Greenland Seas - " <i>Otto Smidt</i> " (VII-VIII), Barents Sea - Meeting, Leningrad (XII)
1991	- Meeting, Bergen (V) - " <i>Professor Multanovsky</i> " (VII), Greenland and Barents Seas - " <i>Lance</i> " (VIII), Barents and Greenland Seas - Meeting, Leningrad (XI)
1992	- Meeting, Oslo (VI) - " <i>Johan Hjort</i> " (IX), Barents Sea
1993	- " <i>Pavel Bashmakov</i> " (IX-X), Kara and Barents Seas - " <i>Lance</i> " (VIII), Barents Sea - Meeting, S.-Petersburg (XI)
1994	- " <i>Lance</i> " (VII-IX), Greenland Sea and Arctic Basin - " <i>Ivan Petrov</i> " (VIII-X), Kara Sea
1995	- Russian-Norwegian Workshop-95 (II-III) - ...

PRODUCTION OF MONTHLY MEAN CLIMATOLOGICAL ARCHIVES OF SALINITY, TEMPERATURE, CURRENT AND SEA LEVEL FOR THE NORDIC SEAS.

H.Engedahl (NMI), B.A Adlandsvik (IMR) and E.A Martinsen (NMI)

Considered is the use of numerical models to enhance the information contained in oceanographic observations. For this purpose the three-dimensional baroclinic, primitive equation ocean model (*ECOM-3D*) was used to produce climatological dynamically consistent data archives containing monthly mean fields of sea surface elevation, currents, salinity and temperature. The archives cover the North Sea, the Norwegian and Greenland Seas, the Barents Sea, the Kara Sea and parts of the Arctic Ocean with a horizontal grid size of 20km. In the vertical the fields are stored at 31 standard oceanographic levels from 0 to 4500 metres.

First, a Hydrographical Archive was produced based on climatological data from Sidney Levitus and Peter Damm, and refined with observed hydrographic data collected by The Institute of Marine Research (*IMR*). Then, the model was run in diagnostic mode with the fields of salinity and temperature from the Hydrographic Archive held fixed, until a stationary circulation was obtained. The produced dynamically adjusted fields of sea level and current constitute the Diagnostic Archive. To obtain dynamically consistent fields of salinity and temperature together with sea level and current, the model was further run prognostically for seven years, forced by monthly mean wind stress, fresh water runoff, M2 tide, and boundary values taken from the Diagnostic Archive. The so produced archive was denoted the Prognostic Archive.

The Hydrographic and Diagnostic Archives provide a satisfactory description of the monthly mean oceanic circulation in the areas of interest. The Prognostic Archive provides more realistic features and a more detailed structure. In spite of some weaknesses in the model produced circulation, both the Diagnostic and Prognostic Archives should be valuable for regional modelling purposes. The transports through various sections, including the Atlantic inflow through the Shetland-Faeroes channel, are all reasonable, and could be used as boundary conditions for higher resolution ocean models, which were applied for the hindcast simulations. Finally, this work shows the advantages of combining hydrographic observations and numerical models.

MAIN FEATURES OF THE OCEANOGRAPHIC REGIME OF THE KARA SEA

V.A. Volkov and V.T. Sokolov (AARI)

The Kara Sea belongs by type to the ice-covered marginal seas.

The main features of the hydrological regime of the sea are primarily governed by a small amount of solar heat as a result of the high-latitudinal location of the sea, the ice cover presence (the sea area is covered by drifting ice for 9 months during a year), the inflow of cold water from the Arctic Basin, penetration of Atlantic and Barents water and an exceptionally strong freshening effect of the runoff of the great Siberian rivers.

The hydrological regime of the sea is greatly influenced by the highly irregular coastline, relative isolation from the ambient seas and a complicated bottom topography.

Sea water structure is governed by a whole complex of natural processes. The largest amplitudes of fluctuations are observed in the seasonal cycle depending on annual variations of solar radiation and seasonal variations of water phase changes, as well as on changes in water salinity and density characteristics related to the annual cycle of the freshwater balance. The variability of hydrological processes is also affected by freshwater runoff fluctuations, snow and ice melting, ice thickness cover, change in the character and intensity of atmospheric processes, amount of water exchange between the adjacent seas and the Arctic Basin, etc. The maximum variability of hydrophysical characteristics is observed in the upper near-surface layer. With depth, the amplitude of fluctuations of these characteristics gradually decreases and there is a lag in the phase.

Summer processes begin with the end of the ice thickness growth, the onset of surface water heating in the region of discontinuities in solid ice cover, disappearance of young ice as a result of melting, increase in the number of polynyas and fractures, inflow of large volumes of river water that contribute to the development of polynyas acting as a dynamic and thermal factor. Further, the temperature increase and the salinity decrease in the active layer due to snow and ice melting processes are observed. Sea surface becomes ice free due to the temperature and dynamic factors.

Winter processes begin with water reaching the freezing temperature at a given salinity which is accompanied by ice formation. The processes of ice thickness growth result in the increased salinity and the decreased temperature.

The penetration depth of the seasonal variability of water temperature and salinity in the sea depends primarily, on summer heating and winter cooling of sea surface (i.e. on annual air temperature variations), as well as on the initial vertical water density distribution during the warm and cold periods of the year.

Also, the penetration depth depends on the thickness of ice growth in winter, the rate of its melting in the spring-summer, degree of freshening of the surface water layer by the continental outflow, snow and sea ice melting; mixing in the upper sea layer (wave, currents, drifting ice), degree of salination of the upper water layer at ice formation and growth; heat-, salt- and water exchange with adjacent regions.

The distribution of hydrophysical characteristics in the surface sea layer depends to a great extent on prevailing winds and wind-driven currents. In the whole water column it is governed by the water exchange and constant currents related to general water circulation in the Arctic Ocean. The hydrological regime of sea waters can be divided into three regions, depending on the factors governing it.

Thus, the regime of waters in the south-western Kara Sea is governed by surface water of the Kara Sea, Barents water flowing through the southern straits of Novaya Zemlya and bottom water formed as a result of winter cooling and water salination at

ice formation. Barents water being more dense, submerges under surface water and is observed in the western and central sea regions. Barents water in these regions is underlied by bottom water of winter formation.

The regime of the central and eastern sea regions is under a prevailing influence of the continental outflow formed by the Ob'-Yenisey water that flows onto more dense bottom water of winter origin.

The regime of the northern sea region is characterized by the intensive influence of deep Atlantic water flowing to the sea along the deep-water troughs of St. Anna and Voronin. Here the layer of surface Arctic water overlies the layer of winter surface water. The depth of minimum temperatures characterizes the boundaries of winter convection spreading. Surface water is underlied by Atlantic water. Under Atlantic water there is bottom water with a below zero temperature and a slightly greater salinity.

THE KARA MOUTH REGION, LEVEL OF KNOWLEDGE, CHOICE OF RESEARCH PRIORITIES

Ivanov V. V. (AARI)

In accordance with the hydrological- morphometric regioning developed at the AARI, the mouth areas of the Ob', Yenisey, Pyasina and Nizhnyaya Taimyra rivers with the Ob'-Yenisey region of the Kara Sea form the Kara mouth region whose hydrological, hydrochemical and hydrobiological regime strongly depends on the runoff of rivers falling into the sea and on the hydrometeorological conditions of the region.

The entire history of studies in the Kara mouth region is related to the policy of exploration of northern Siberia and development of polar studies in the Russian and the Soviet State.

Systematic instrumental studies of the mouth region, whose the results are still important were initiated in the 1930s. At that time the main Administration of the Northern Sea Route was set up aiming at comprehensive exploration of the territories northward of 62°N. From this time the priority aims and goals of studies of the region were changed many times, although the objectives connected with hydrographic and hydrometeorological support of sea and river shipping were preserved.

During different time periods the priority objectives included:

- study of the mouth region with the aim of choosing the sites for sea and river ports;
- exploration in the lower reaches and mouth areas of rivers with the aim of hydrographic description and development of necessary measures for improving shipping conditions;
- studies of ice conditions for extending the navigation period and then also for all-year-round navigation;
- studies for determining the location of a constantly operating hydrometeorological network for estimating water resources and river water inflow in the sea;
- studies for assessing the effect of the projects under development and of the implemented projects of the hydropower station construction on natural conditions in the basins of the Ob' and Yenisey rivers;
- studies of possible consequences of interzonal redistribution of the river runoff for natural conditions of the Arctic and primarily of the river mouth areas and the Kara Sea;
- a complex of studies of the state of natural conditions of the region and their changes as affected by climate fluctuations and anthropogenic impact.

Thus knowledge on natural conditions of the region was gradually accumulated and methods for stationary and expedition studies, physical and mathematical modelling, calculations and forecasts were developed.

Under present conditions when other Arctic States participate in the studies of the Russian Arctic within the framework of the international programs and projects, the priority goals include estimates of water runoff, thermal, solid, chemical discharge and discharge of nutrients and contaminants at the river boundaries of the mouth areas, their multiyear and seasonal variability; studies of processes of their transport, transformation and sedimentation in the zones from the downstream measuring sections of the rivers to the exit to the sea and further taking into account seasonal and anthropogenic changes in runoff, ice and meteorological conditions.

A particular attention should be given to the regions of accumulating sediments and contaminants in the deltas and bars of rivers, as well as to the zones of river and sea water interaction in the Ob' Gulf, Yenisey Bay and Gulf and the Pyasina Bay.

Naturally, these studies should be of a systematic character and based on stationary and expedition observations, full-scale and laboratory experiments and physical and mathematical modelling.

ICE REGIME OF THE BARENTS AND THE KARA SEAS, STATE AND PERSPECTIVES OF STUDIES

I. Ye. Frolov, V. Ye. Borodachev, Ye. U. Mironov (AARI)

Introduction

One of the fundamental goals of polar oceanography is an analytical description of the ice cover in the northern polar region of the Earth as a complicated multiparameter natural body, which is a link in the climatic system of the globe and which has tremendous influence on human activities.

The ice cover is a significant natural phenomenon of the Barents and Kara Seas, as ice is present over the area much of the year and significantly influences the processes in the boundary layers of the atmosphere and the ocean.

Historical data

Regular sea ice observations in the Barents and Kara Seas were commenced at the beginning of the 20th century. The longest observation series of the ice cover characteristics are available for the study region, as compared with the other Russian Arctic Seas.

As a result, vast data sets were accumulated at the archives of the AARI collected by different methods and from different platforms:

- visual shipborne observations;
- visual airborne observations;
- data from coastal hydrometeorological stations;
- surveys using aircraft SLARs;
- aerial photography;
- satellite observations;
- ice measuring surveys of special expeditions.

Introduction of personal computers on an accelerated pace in recent years has allowed us to commence to set up databases on different sea ice characteristics and develop automated information reference systems. Thus, necessary conditions were created for some evolutionary progress in the area of processing, analysis and presentation of full-scale data.

At the present time the databases on total concentration of sea ice and prevailing age categories were set up. This allowed data exchanges with the World Data Center - (WDC-A) from where the data set on the northern polar region and the Southern Ocean for 1972-1991 in the SIGRID Format was received.

Since a thin layer of the ice cover contains more than 10 components in its composition which change with time and influence the variability of the states of the ice medium, it became necessary to filter quantitative values of each of the components and create charts of their distribution to be further recorded on computer media.

For the last two years the databases on the degree of ice destruction (melting stages), degree of desintegration, icebergs, large fractures in the ice cover, ice thickness, areas of ice massifs and ice cover extent of the Arctic Seas were set up.

Further work with the databases was aimed at obtaining climatic information in the form of charts of the distribution of statistical and probabilistic characteristics.

Studies of ice regime

First studies of the ice regime were performed at the beginning of the 20th century after accumulating first data of sea ice observations. The works of A.Kolchak *"Ice of the Kara and Siberian Seas"* (1909) and E. Lesgaft *"Ice of the Arctic Ocean and a sea route from Europe to Siberia"* (1913) have actually laid the foundation for the concepts and methodology of the Russian school of sea ice studies.

Systematic studies of the ice cover of the Barents and Kara Seas were initiated in the 1920s. The following served as an information basis for theoretical studies:

- Kara sea oceanographic expeditions (1921-1928);
- more than 50 hydrometeorological stations were opened in the 1930s in the Arctic, half of them being in the Barents and Kara Seas;
- regular airborne ice reconnaissance flights from the mid 1930s.

From 1936 regular navigation of transport vessels began along the Northern Sea Route. This fact governed in many respects the direction of future studies, i.e. to reveal typical features in the formation of ice conditions for developing methods of ice forecasts for ensuring safe navigation.

The book of V.Yu.Viese *"A basis of long-range ice forecasting for the Arctic Seas"* (1944) became the first large monography on this problem. The work develops an idea about a natural system of three interacting media: the atmosphere -the ice cover - the ocean. By the example of the areas of the Barents and Kara Seas, the ice cover of the Barents Sea is shown to be a good indicator of climatic changes in the Arctic. Main characteristics of the ice regime of the seas that were used for searching general typical features and prognostic dependencies were considered.

At that time a monograph of N.N. Zubov *"Ice of the Arctic"* was published (1945) where a wide range of ice research problems was considered.

During the 1950s-1960s the main stress was placed on studies of the formation processes of ice conditions at sea, analysis of ice cover evolution under the effect of natural factors and search of quantitative dependencies between them.

The works of the Russian scientists greatly contributed to the solution of this problem. Namely, in the Barents Sea: N.S.Uralov, A.I. Karakash, M.S. Khramtsova, A.A. Lebedev, T.N.Moskal', etc. and in the Kara Sea: Ivanov V.M., Kirillov A.A., Kuznetsov I.M., Spichkin V.A., etc.

Studies of dynamic and thermal processes of ice cover accumulation and destruction - ice formation, growth, drift, deformation, and melting were carried out during this period. These studies are based on numerous observations at coastal polar stations and drifting research stations *"North Pole"*.

Scientific generalizations of studies of this period were made in the monograph of Z.M. Gudkovich, A.A. Kirillov, Ye.G.Kovalev, A.V. Smetannikova, V.A.Spichkin *"A basis for methods of long-range ice forecasting for the Arctic Seas"* (1972) and in some other works.

In the 1970s in connection with the organization of all-year-round navigation in the Kara Sea, a complex of studies of ice cover features in winter - formation and stability of fast ice (V.Ye. Borodachev, A.I. Murzin, etc.), flaw polynyas extent (A.A. Kirillov, V.A. Spichkin, etc), distribution of discontinuities, leads and cracks (Yu.A.Gorbunov, S.M. Losev, etc), were performed.

During the 1970s-1980s a new direction was actively developing - mathematical modelling of the ice cover evolution. This direction contributed to intensive studies of physical processes in ice cover and organization of special full-scale experiments. The expeditions onboard the research icebreaker *"Otto Schmidt"*, as well as radar surveys of the ice cover from aircraft in the Barents and Kara Seas, were of particular interest.

The first numerical models taking into account thermal and dynamic processes include a dynamic-thermodynamic model of Yu.P. Doronin (1970) realized for the Kara Sea. Further, this direction was developed by Z.M. Gudkovich, I.L. Appel', I.Ye. Frolov, I.Yu. Kulakov, S.V. Kolesov, A.N. Zuyev, etc.

At the present time several numerical models are developed at the AARI with a different description of thermal and dynamic processes implemented for the conditions of the Barents and Kara Seas for winter and summer.

In recent years on the basis of databases formed, a complex of studies for generalizing different parameters of ice cover (concentration, age categories, amount of hummocking, degree of destruction, etc.) and of icebergs were carried out. At present, a monograph is being completed which generalizes our current knowledge on the Kara Sea ice regime (V.A.Spichkin, A.G. Yegorov, I.D. Karelin, V.P. Karklin). It will consider in detail the following:

- typical features of the processes of ice formation, ice growth, drift, melting and decay;
- typical features of seasonal and interannual variability of ice conditions;
- typical features of the distribution of the main parameters of the ice cover in different seasons of the year;
- regioning of the sea and typification of ice conditions.

A particular attention in recent years was devoted to applied works in connection with the feasibility studies for exploration of oil-gas condensate fields - Shtockman and Prirazlomnoye fields in the Barents Sea, Bovanenkovskoye on the Yamal peninsula, construction of pipelines in the Baidaratskaya Gulf of the Kara Sea. These works (G.K. Zubakin, V.A. Abramov, Ye.U. Mironov, V.A. Spichkin, etc.) consider local features of ice conditions and formulate principles for monitoring natural conditions and special experimental studies.

Main directions in the ice cover studies for the next few years include:

- completion of databases on all ice cover components;
- creation of an automated information-reference system;
- study of physical processes in the ice cover to improve mathematical models;
- study of the processes forming anomalous ice conditions;
- study of local features of the variability of ice conditions and ice cover parameters for providing support to exploration of oil-gas condensate fields;
- generalization of current knowledge on the ice regime of the Kara and Barents Seas.

References

- 1.Appel', I.L., Gudkovich, Z.M. Numerical modelling and forecasting of the ice cover evolution in the Arctic Seas during melting. St. Petersburg: Gidrometeoizdat, 1992, 144 p.
- 2.Viese, V.Yu. A basis for long-range ice forecasting for the Arctic Seas. Moscow: Glavsevmorput' Publishing House, 1994, 274 p.
- 3.Gudkovich, Z.M., Kirillov, A.A., Kovalev, Ye.G., Smetannikova, A.V., Spichkin, V.A. A basis for the methods of long-range ice forecasting for the Arctic seas. Leningrad: Gidrometeizdat, 1972,348 p.
- 4.Gorbunov, Yu.A., Karelin, I.D., Kuznetsov, I.M., Losev, S.M., Sokolov, A.L. A basis of physical-statistical methods of ice forecasting and calculations for the Arctic Seas up to 30 days in advance. Leningrad: Gidrometeoizdat, 1983,288 p.
- 5.Doronin Yu.P., Kheisin D.Ye. Sea ice. Leningrad: Gidrometeoizdat, 1975, 318 p.

- 6.Zubov, N.N. Ice of the Arctic. Moscow: Glavseморput' Publishing House, 1945, 360p.
- 7.Zubakin, G.K. Large-scale variability of the state of the ice cover in the seas of the North-European Basin. Leningrad: Gidrometeoizdat, 1987,160 p.
- 8.Zubakin, G.K. Natural conditions of the Arctic shelf and their estimate by the example of the Shtockman and Prirazlomnoye fields. Abstracts of the papers of the International conference "Marine fields of oil and gas in Russia", St.Petersburg, 1994, pp.17-19.
- 9.Kolchak, A.V. Ice of the Kara and Siberian Seas. St.Petersburg 1909.
- 10.Lesgaft, E. Ice of the Arctic Ocean and a sea route from Europe to Siberia. St. Petersburg 1913.
- 11.Mironov, Ye.U., Spichkin V.A., Yegorov A.G. Seasonal changes in ice conditions and their interannual variations in the regions of the exploration of the shelf of the Barents and Kara Seas. Abstracts of the papers of the 1st international conference "Exploration of the shelf of the Arctic Seas of Russia". St.Petersburg, 1993, pp.92-93.
- 12.Frolov, I.Ye. A numerical model of autumn-winter ice phenomena for the Arctic Seas. Proc. of the AARI, vol.372, 1981,pp.73-81.

MODELING KARA SEA WATER AND ICE BEHAVIOUR

I. Polyakov, I. Kulakov, S. Kolesov, N. Dmitriyev, A. Naumov (AARI)

For investigating the processes in the Kara Sea a coupled sea ice-ocean model was developed (Polyakov et al., 1994). The model includes a three-dimensional non-stationary baroclinic ocean model with free surface (Polyakov and Dmitriyev, 1993). The model is based on elastic-plastic rheology and is formulated in the Eulerian sense. The model employs ice representation by age gradations: 0-0.1, 0.1-0.3, 0.3-0.7, 0.7-1.2, 1.2-2.0 and more than 2 m. Similar gradations are used in the Russian system for ice data collection. The equations for calculating redistribution of ice concentration and thickness are written for each of age gradations. Thermodynamical part of the ice model is based on the work of Semtner (1976) and Parkinson (1978). This block is also applied for each age gradation separately thus allowing a more accurate simulation of different rates of melting and growth of thick and thin ice (Maykut, 1978) and, respectively, of different heat and salt fluxes on water-ice surface. Open water and nilas included into the first age gradation in the dynamic block of the model are presented here as separate gradations. Parameterization of hummocking is based on controlling the fulfilment of the law of ice mass conservation in the cell and of the condition for total ice concentration not exceeding 1. A special algorithm is used for a difference representation of heat and salt advection, as well as ice mass and concentration (Boris and Book, 1973). It has a high order of the approximation accuracy and preserves the monotonic character of the solution. The momentum exchange between the oceanic and ice blocks of the model is based on the conventional quadratic representation of drag forces.

Calculations of the dynamics and thermodynamics of the Kara Sea were performed for three winter and one summer situations during the period 1993-1994. The boundary conditions were determined by calculating the corresponding situations for the Arctic Ocean on the whole over a coarser grid with a 55.6 km spacing. These solutions were interpolated into the regular grid points of the Kara Sea with a 13.89 km spacing. By means of this procedure boundary conditions for tidal dynamics, baroclinic circulation and wind currents, level oscillations and ice drift for each of the situations considered were obtained.

The initial conditions were determined as a superposition of several constituents. First, mean seasonal temperature and salinity fields (Polyakov and Timokhov, 1994) were used for calculating the baroclinic circulation in the Kara Sea. Secondly, the M2 and S2 tidal waves for the specific phases were simulated. Satellite data were used for the initial ice distribution according to gradations. Similar data were used as a quality criterion of calculations. For this purpose data on level oscillations at coastal stations in the Kara Sea were also used. Calculations were performed on a grid with a spacing of 13.89 km, the vertical resolution in the oceanic block of the model was provided by 17 levels.

Wind stresses were obtained from mean daily charts of atmospheric pressure. Here, the results of calculating the situation during the period 16-23 January, 1993 are presented. The prevailing wind direction during the period was northern, on some days the wind speed exceeded 20 m/s. Fig. 1 shows atmospheric pressure and tangential wind stress as of January 20. Relatively weak pressure gradients were observed in the north-western sea region. The most thick ice was centered in the region between Novaya Zemlya and Severnaya Zemlya Islands. This ice remained practically fast during the calculation period. Young ice 20 cm thick prevailed in the south-western sea.

Southerly winds which contribute to the ice export from the south-western sea caused the export ice drift near the southern shore (Fig. 2) and some shift in the thick ice boundary to the north. Near the southern shores and islands, polynyas and zones of open drifting ice were formed. The distribution of ice more than 1 m thick remained actually unchanged. The position of thick multiyear ice is presented in Fig. 3.

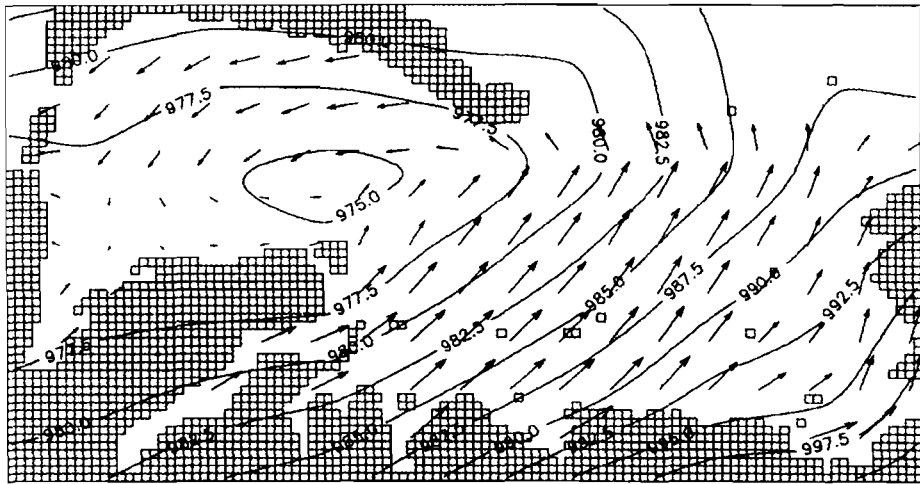


Fig.1. Atmospheric pressure and wind 20.01.1993. — — 10 m/s.

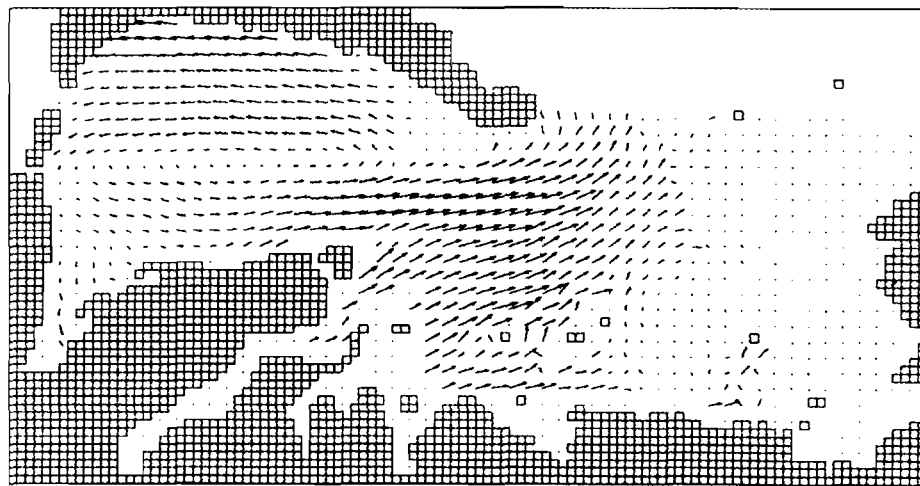


Fig.2. Simulated ice drift 20.01.1993. Scale: — — 50 cm/s.

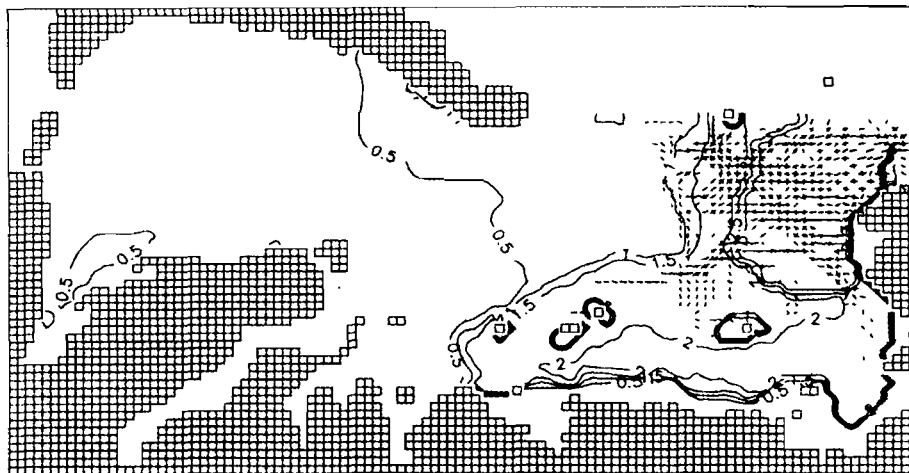


Fig.3. Internal ice stresses and mean thickness 20.01.1993.

The young ice drifting northward (see Fig. 2 with the ice drift vectors) encounters obstacles in the form of the old ice. This forces the young ice to change the drift direction. Likewise large internal stresses occur in the old ice (Fig. 3). These stresses reduce the ice drift rate.

It is important that the ice drift rates near the open sea boundaries were obtained as a result of calculating the situations for the Arctic Ocean on the whole. These boundary conditions provided the realistic calculated ice drift. Otherwise, the shift in multiyear ice should be extremely large. This result underlines the importance of prescribing the correct boundary conditions at vast open boundaries of the Kara Sea.

The direction of surface currents (Fig. 4) and the ice drift is similar, the deviations in current speeds and drift rates do not exceed 1-2 m/s. The tidal constituent in sea level oscillations is evident (Fig. 4). The direction of the near-bottom speeds of currents is mainly opposite to the surface ones. The surface Ekman layer in the vertical structure of currents is well-pronounced.

For estimating the influence of currents on the dynamics of the ocean with ice, additional calculations of the same January situation of 1993 were performed without taking into account the tides. Surface currents and level oscillations are presented in Fig. 5. Neglect of the tides has reduced speeds of currents and rates of the ice drift. Tides significantly influence the formation of sea surface level (compare Fig. 4 and 5). This conclusion is confirmed by comparing the calculated level oscillations and data of coastal stations. The calculated (dashed line) and observed (solid line) variations at the Kharasavey station are shown in Fig. 6. It is apparent that the tidal and nonperiodic components are of the same order.

Let us note that the model has simulated the tidal dynamics of the Kara Sea and the amplitudes and phases of the calculated and observed tidal components are in a good agreement. Some difference between the calculated nonperiodic component of level oscillations and the observed one occurs during the first three days.

The work was fulfilled at the financial support of the Amoco Production Company in the framework of Project 4-Ya-94.

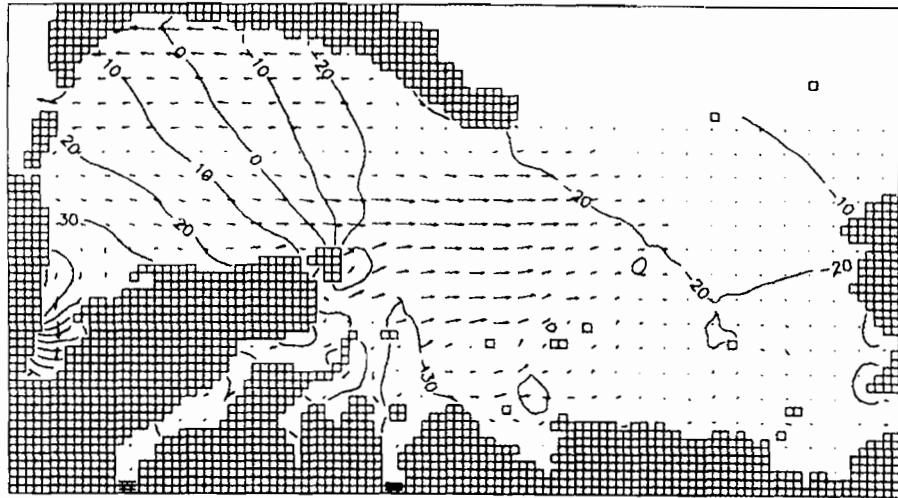


Fig.4. Simulated surface elevation and current 20.01.1993.

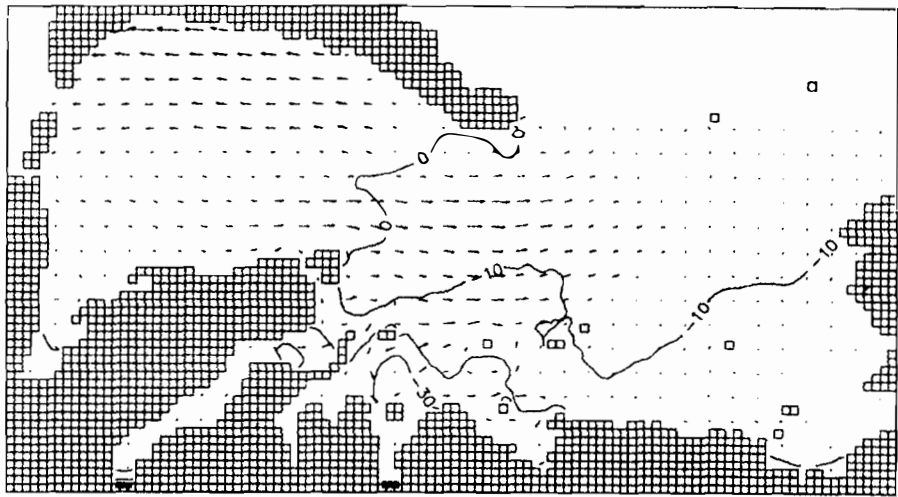


Fig.5. Simulated surface elevation and current (without tides) 20.01.1993.

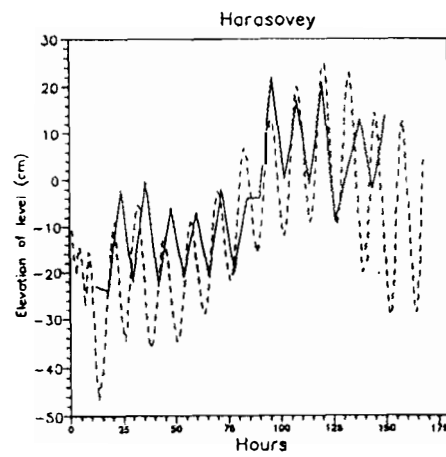


Fig. 6. Calculated (dashed line) and observed (solid line) water level elevation

References

1. Boris, J.P., Book, D.L. Flux-Corrected Transport I: SHASTA - A Fluid Transport Algorithm that Works. *J.Comput.Phys.*, 11, 1973, p.38-69
2. Maykut, G.A.. Energy Exchange Over Young Sea Ice in the Central Arctic. *J.Geophys.Res.* 83, 1978, No C7, 3646-3658.
3. Parkinson, C.L. A numerical simulation of the annual cycle of sea ice in the Arctic and Antarctic. NCAR Cooperative Thesis No. 46. The Ohio State University and National Center for Atmospheric Research, 1978, 191 p.
4. Polyakov, I.V. & Dmitriev, N.Eu. Modelling the vertical structure of the storm surges and tides of a shallow-water basin. *Meteorologiya I Gidrologiya (Meteorology and Hydrology)*, No 12, 1993, p.54-62. - in Russian.
5. Polyakov, I.V. et al. Coupled sea ice - ocean model of the Kara Sea. Tech. Rep.4-YA-94. Arctic and Antarctic Res.Inst., 1994, 194 p.
6. Semtner, A.J. A model for the thermodynamic growth of sea ice in numerical investigation of climate. *J.Phys.Oceanogr.*, No 6, 1976, pp.379-389.

**MODELING OF ICE COVER EVOLUTION IN THE KARA SEA
FOR OPERATIONAL ICE FORECASTING IN THE SUMMERTIME**
S.P. Pozdnyshev, Ye.O. Aksenov, Z.M. Gudkovich., A.A Panfilov, D.A. Speransky
(AARI)

Introduction

A mathematical model of the ice cover evolution as affected by dynamical and thermal factors is considered. Also, the results of using this model for issuing operational ice forecasts for the Kara Sea in the spring-summer season covering the time interval from the onset of snow melting to the beginning of ice formation are presented. The model was developed at the Arctic and Antarctic Research Institute specially for ice forecasting purposes and is to be used for simulating the synoptic and seasonal variability of spatial distribution of the most important sea ice characteristics, such as drift velocity, concentration, ice thickness, position of the drifting ice edge and of pressure zones. The spatial interval of the model is 25 km and calculation of changes in the position of the drifting ice edge is with an accuracy of 5 km. The time interval is 1 day. A seasonal character of the model is governed by the fact that in spring-summer thermal and partly, dynamic processes have significant peculiarities (Appel, I.L., Gudkovich, Z.M. 1992).

Model Description

Changes in the ice conditions are governed by the influence on the ice cover of both the dynamic and thermal processes. Hence the model includes the corresponding calculation blocks.

The dynamic block of the model uses the prognostic fields of surface air pressure averaged over time intervals not less than one day, as initial data. This allows calculating the drift velocity on the basis of stationary momentum balance equations, since a typical time for the drift becoming steady establishment does not exceed 3-4 hours. To determine the ice cover characteristics, connected with the ice mass change, non-stationary equations are used. Ice mass changes over the model time interval (24 hours) insignificantly affect the drift velocity. Hence the numerical solution is by using a method of splitting, when the drift velocity, thermal change in thickness and concentration of the ice cover and their kinematic redistribution are calculated in succession.

The stationary momentum balance equation in the vector form is written as follows:

$$\vec{\tau}_a + \vec{\tau}_w + \vec{F}_c + \vec{F}_b + \vec{F}_p = 0$$

where: $\vec{\tau}_a$ - the tangential stress at the upper ice surface, $\vec{\tau}_w$ - the tangential stress at the lower ice surface, \vec{F}_c - the Coriolis force, \vec{F}_b - the internal interaction force inside the ice, \vec{F}_p - the projection of the gravity force on sea surface.

For calculating the tangential stress at the upper ice cover surface, the gradients of the surface atmospheric pressure field are used.

$$\vec{\tau}_a = K_a (\cos \gamma_a \vec{k} \times \nabla \vec{P}_a + \sin \gamma_a \nabla \vec{P}_a)$$

where: γ_a - the angle of deviation of surface wind from an isobar, $\nabla \bar{P}_a$ the surface pressure gradient, \vec{k} - a single vector perpendicular to the horizontal plane, K_a - the coefficient of proportionality.

The tangential stress at the lower boundary is determined in a similar way:

$$\vec{\tau}_w = K_w (\cos \gamma_w (\vec{W} - \vec{U}_g) + \sin \gamma_w \vec{k} \times (\vec{W} - \vec{U}_g))$$

where: \vec{W} - the drift velocity, \vec{U}_g - the current speed at the lower boundary of the friction layer, γ_w - the angle between the drift vector and the tangential stress, K_w - the coefficient of proportionality.

The Coriolis force and the projection of the gravity force on sea surface are expressed traditionally:

$$\begin{aligned} \vec{F}_c &= -2\rho_i H \vec{\omega}_z \times \vec{W} \\ \vec{F}_p &= -\rho_i H g \nabla \delta \end{aligned}$$

where: H - the ice thickness, $\vec{\omega}_z$ - the angular speed of the Earth's rotation, g - the acceleration of the free fall, ρ_i - the ice density, $\nabla \delta$ - the level surface tilt.

Let us note that the current speed at the lower boundary of the friction layer and the tilt of the level surface are not calculated directly within the model. For forecasting, mean fields of the current speed and level sea surface, obtained by combining field observations and model calculations for the most frequent pressure situations are used.

To calculate the internal interaction force one uses a quasi-viscous description of the ice cover rheology, at which the given force represents the divergence of the internal stress tensor (σ_{ij}):

$$\vec{F}_b = \frac{\partial \sigma_{ij}}{\partial x_j}$$

To prescribe the boundary conditions on the shore is an important part of the problem of determining the ice cover drift. A different approach should be used depending on the fact whether the drift is off-shore or on-shore. In the model, the indicated choice is made by comparing the direction of the coastline and of the drift velocity.

For the on-shore drift, only the velocity component normal to the shore can be assumed to be equal to 0. For determining the component, parallel to the shore, in order to enhance the accuracy of approximating the derivatives at the grid area scale, it is suggested to use the velocity at the external border of a narrow boundary layer of some hundred meters where the velocity gradients are maximum, rather than near the shore, where the condition of the non-drift is fulfilled. In this layer, shear strains and tangential stresses play the largest role, and the viscosity coefficient is assumed to be dependent on the stress normal to the shore.

When the drift is outside the calculation area, at the liquid boundary, the derivative of the velocity is assumed to be equal to the neighboring value of the derivative in the internal calculation area.

In modeling the ice cover characteristics for the period of more than 3 days it is necessary to take into account changes in sea ice thickness and concentration as

affected by thermal processes. Calculation of the heat flux through the underlying surface is based on the heat balance equation:

$$Q_R = Q_\Sigma(1 - \alpha) + Q_T + Q_C + E_A - E_S$$

where Q_R - the resulting heat flux through the surface, Q_Σ - incoming total solar radiation, α - the albedo of the underlying surface, E_S - long-wave radiation of the underlying surface, E_A - long-wave counterradiation of the atmosphere, Q_T - the turbulent heat exchange with the atmosphere, Q_C - the heat flux, connected with evaporation and condensation.

The features of the thermal block are: allowance for the air temperature transformation depending on the underlying surface state and the direction of air transports, as well as the effect of mesoscale inhomogeneity of ice and snow thickness on the melting processes by means of calculating the probability density changes in the ice thickness distribution. The latter allows one to define the time of the melt water appearance on the ice, which induces a sharp change in the ice cover albedo, differences in the melting of level and hummocked ice.

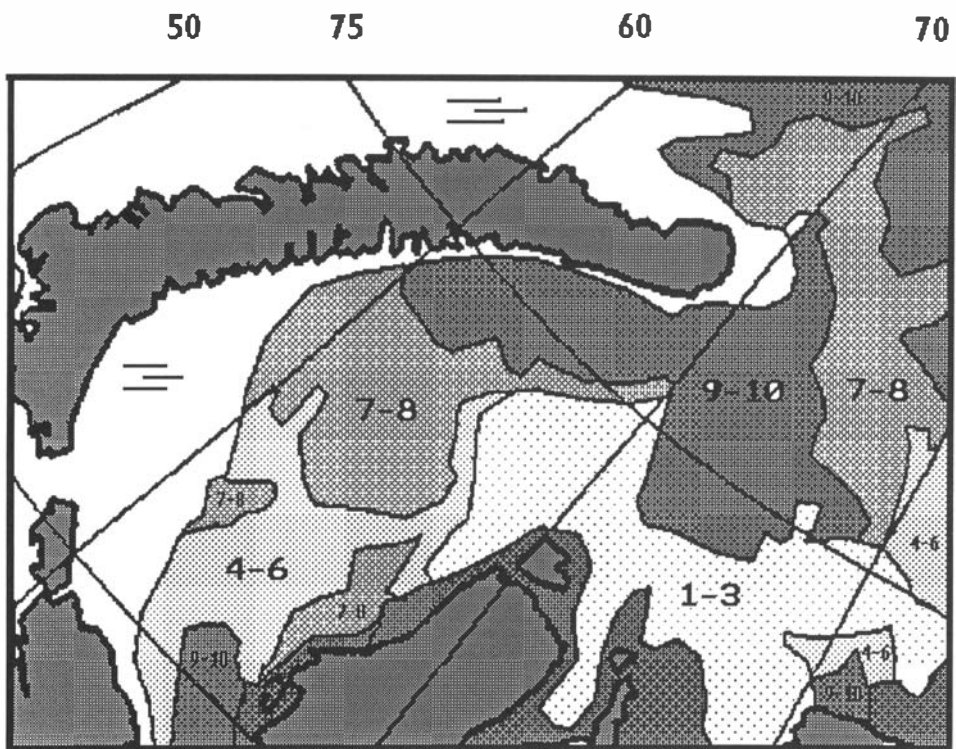
For calculating a kinematic change in concentration and thickness of the ice cover, an original method has been developed which allows suppressing, to a great extent, the effect of the calculation viscosity related to the finite-difference representation of differential equations. In this method ice concentration in the grid cell is governed not only by mean value, but also by the first instant of its spatial distribution.

Results of Model Implementation

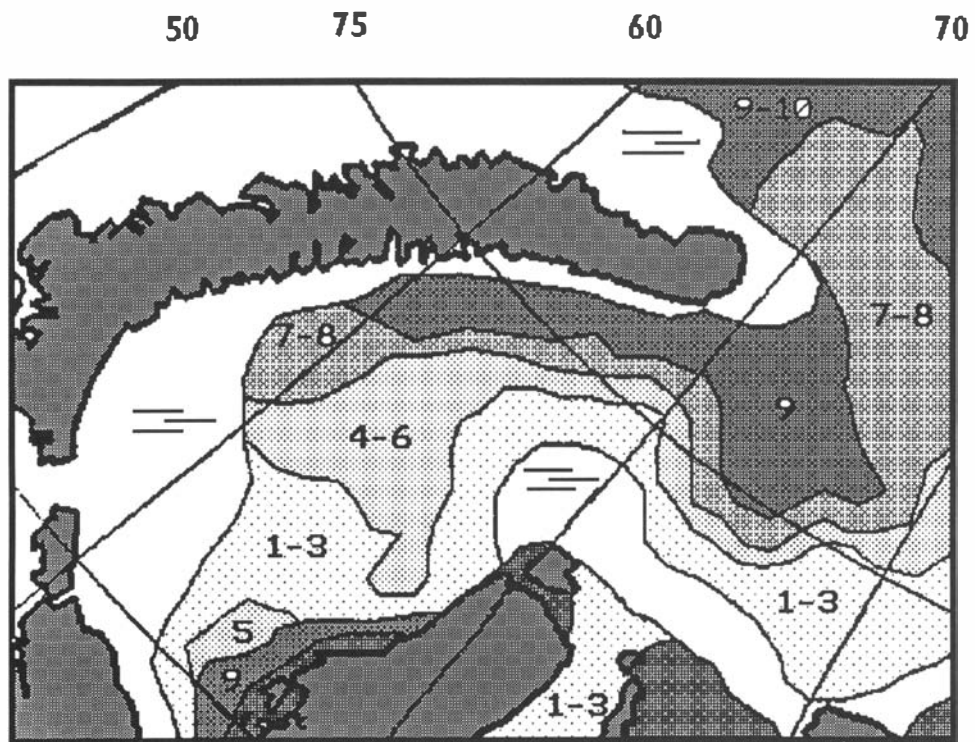
For example, let us consider a forecast of ice concentration redistribution in the south-western Kara Sea. Fig.1 presents the actual distribution for July 12, 1992 which was used as initial one. Fig.2 presents the forecast for July 19, 1992 issued 7 days in advance and Fig.3 presents the actual distribution of concentration for the same date.

Changes in the ice cover concentration for the calculation period are related to the effect of south, south-west winds and intensive melting under the influence of the outflow of warm air masses. The main features of the evolution in concentration as affected by the indicated processes, are seen on the calculated and the actual charts and in our opinion, they coincide.

Instead of the zone of 1-3/10, a strip of open water is formed to the north-east of the Belyi island. The ice patch of 7-8/10 blocking the approaches to the western coast of Yamal has disappeared, but directly along the coast there is still a strip of close ice of 9/10 formed by fast ice fragments and exported from the Baidaratskaya Gulf.



70
 Fig.1. Actual distribution of ice concentration on July 12,1992



70
 Fig.2. Calculated distribution of ice concentration for July 19,1992

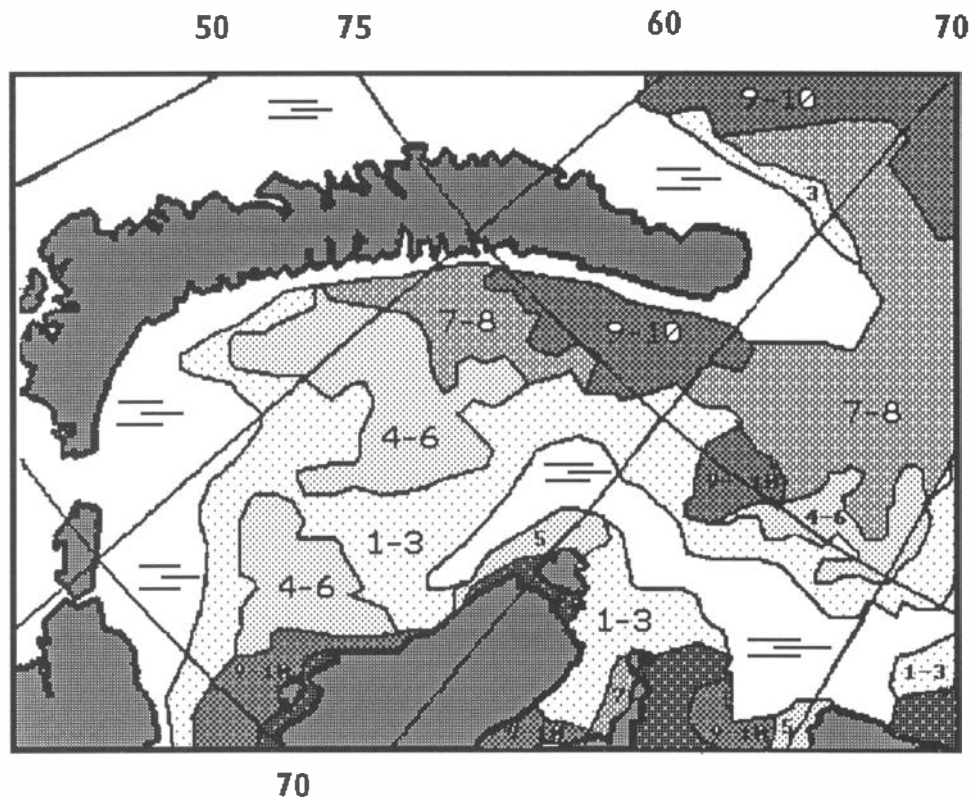


Fig.3. Actual distribution of ice concentration for July 19, 1992.

The zones of 7-8/10 and 9-10/10 off the southern shore of Novaya Zemlya are significantly reduced in size and navigation conditions on the segment Kara Gate strait-Beliy Island have become, on the whole, more favourable.

The differences in the position of the boundaries of the zones are connected both with calculation errors and with the inaccurate prescription of initial information (an increase in the number of zones, small in area, and a large irregularity of their boundaries on the actual chart of July 19, 1992 as compared to the initial chart of July 12, 1992, indicates not only changes in the ice cover, but improved observation conditions as well).

Operational ice forecasts calculated on the basis of this model are regularly issued at the AARI during the navigation period. The background seasonal forecast is issued 1-3 months in advance, the operational forecast is issued 7-8 days in advance, corresponding to the advance period for forecasting surface atmospheric pressure and to the time for updating initial ice information collected over the area of the seas of the Russian Arctic.

The quality of forecasting the ice cover characteristics was verified by a number of model experiments whose results correspond to the actually observed behaviour of the ice cover. Quantitative estimates of the accuracy of calculating the ice drift velocity were performed using data on the coordinates of the drifting radiobuoys "Argos". On average, for calculating the ice drift velocity 5 days ahead, the velocity module error was 20% and the calculation probability of the drift direction at an allowance of 45 degrees was 87%.

Concentration is the main characteristic, used for estimating the verification score of forecasts. The value 0.674σ is used as a root-mean-square deviation of the concentration change for the advance period. At the same time since regular ice data are reported in the form of the charts where zones of standard concentration gradations are delineated: 10-30%, 40-60%, 70-80%, 90-100%, an alternative scheme for the forecast verification is possible. And it is assumed that if actual and prognostic

concentrations in the cell are in one gradation, then the verification score is 100%, if the indicated values are in the adjacent gradations, then it is 50% and in other cases it is 0%.

From the mid 1980s, different working versions of this model were applied for issuing ice forecasts for the Kara Sea area. Mean verification score of the prognostic fields of concentration, calculated by both methods, is 75-80%. For operational application of the model for prognostic purposes, software for automated entry, preparation of initial data, as well as for presenting the calculation results in the form of a traditional chart of the distribution of zones with different ice cover concentration was developed. Three-four hours are required for issuing a forecast 7 days in advance if the model is run within the structure of a usual Russian hydrometeorological center.

References

Appel, I.L., Gudkovich, Z.M. "Numerical modelling and forecasting of ice cover evolution in the Arctic Seas during melting", St. Petersburg, 1992, p.144.

WESTERN ARCTIC AIR CIRCULATION AND AEROSOL CONTAMINATION

V.F.Radionov, V.V.Ivanov, G.I.Baranov, A.P.Makshtas (AARI)

Among the factors influencing climate and the state of the ecosystems the aerosols from anthropogenic sources are of increasing significance. They affect directly or indirectly the optical characteristics and the radiation regime of the atmosphere not only in the vicinity of the pollution source, but also at a significant distance from it. Therefore, estimates of the present state and monitoring of the levels of aerosol air pollution, as well as determination of the contribution of the anthropogenic source appear to be important. Purposeful studies of the aerosol component in the polar regions have been active only for the last 10-15 years. That is why, the obtained fragmentary results cannot yet be fully used for revealing long-term tendencies for changes in aerosol pollution. This possibility is provided by the results of measuring optical atmospheric parameters which also indirectly characterize the aerosol component. In particular, actinometric observations of direct solar radiation that are carried out at some arctic stations from the 1930s allow tracking multiyear changes in atmospheric transparency.

Fig. 1 presents multiyear variations of the T2 parameter (Radionov, 1994, Radionov et al., 1994) characterizing the attenuation of direct solar radiation at the Bukhta Tikhaya station (80°N19, 50°E48) from 1933 to 1939, Dikson Island (73°N30, 80°E14) from 1938 and in Mirny Observatory (66S03, 93E01) in Antarctica from 1956. Mean T2 values for spring (March-May in the Arctic and September-November in Antarctica) and for summer (July-August in the Arctic and December-January in Antarctica) are presented. The T2 parameter may be formally referred to as an optical depth of the atmosphere for broadband radiation in a wide range of wavelengths from 0.4 μm to 4 μm . Major factors influencing T2 variations are changes in atmospheric water vapour and aerosol content (Radionov 1994, Radionov and Marshunova 1992). The dramatic increases in T2, especially well-pronounced in Antarctica, are caused by stratospheric turbidity following the eruption of Mt. Agung (1964), El-Chichon (1982) and Pinatubo and Hudson (1991) volcanos. In both the Arctic and the Antarctic, the increased turbidity after the volcanic eruptions persisted for 1.5-2 years. Two features of the T2 parameter obtained in the Arctic should be stressed:

- There is an upward trend of turbidity in spring in the Arctic. This trend has been shown to be significant at the 99% confidence level. The parameters of the trend $y=a+bx$ are $a=-0.021+0.004$ and $b=(1.1+0.2) \cdot 10^{-3}$. The summer trend is negligible at the 95% confidence level.
- From the second half of the 1950s the values of the T2 parameter in spring exceed those in summer. This effect is nowhere observed except for the Arctic.

An analysis of the obtained data (Radionov and Marshunova 1992) has shown these two features to be connected only with an increase in aerosol turbidity of the atmosphere. The arctic sources proper could not induce the indicated features in multiyear variations of the T2 parameter. This could be only caused by the input of additional aerosol quantities from the sources at temperate latitudes. One of the first explanations for a possible aerosol transport to the Arctic was suggested in (Heidam 1984). The differences in the polar front position in winter and summer account for the observed differences in the turbidity values of the Arctic atmosphere in the winter and summer seasons. But the suggested scheme does not explain a stable increase in T2 and does not describe in detail the transport processes.

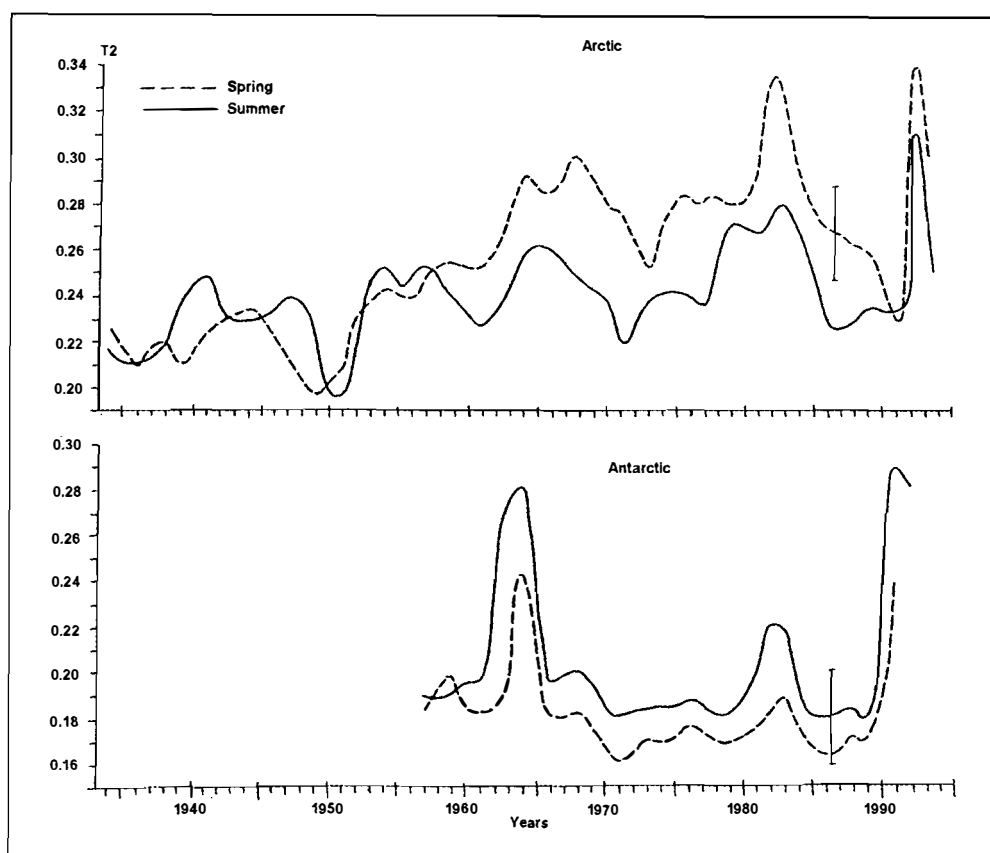


Fig.1. Long-term variations of T2 in the Arctic and the Antarctic.

In principle, two causes for the trend of the T2 increase are possible:

- increase in the number of emissions from the sources;
- intensification of meridional transports of polluted air masses.

Fig. 2 presents data of Barrie (1986) about SO₂ emissions from Europe, acidity of ice from the Agassiz glacier, Ellesmere Island and our record of the turbidity T2 parameter. As is evident, there is a very good agreement between the three presented parameters. Thus, a preliminary conclusion can be drawn that an increase in aerosol turbidity of the atmosphere in the Arctic since the second half of the 1950s was related to an increase in anthropogenic emissions from industrial sources located, in particular, in Russia. What were the circulation conditions during this period? Long thermal-pressure waves are considered one of the most composite characteristics of the general atmospheric circulation. Their classification was developed at the AARI by G.Ya. Vangengeim and A.A. Girs (Dmitriyev 1994). They identified three main atmospheric circulation forms characterizing the prevailing tropospheric transports in the Atlantic-Eurasian sector of the Northern Hemisphere: western W, eastern E and meridional C. The processes of the form W mainly correspond to a zonal atmospheric state, while the processes of the forms E and C - to a meridional state but with a different spatial localization of ridges and troughs (Fig. 4). From the point of view of air mass transport there is a prevailing zonal transport at the form W and the interlatitudinal (meridional) air exchange is enhanced at the forms E and C. As a result, a scheme for air mass transport at different types of the three main circulation forms W, E and C has been formed. It is given in Fig. 4 (Karimova and Chukanin 1988).

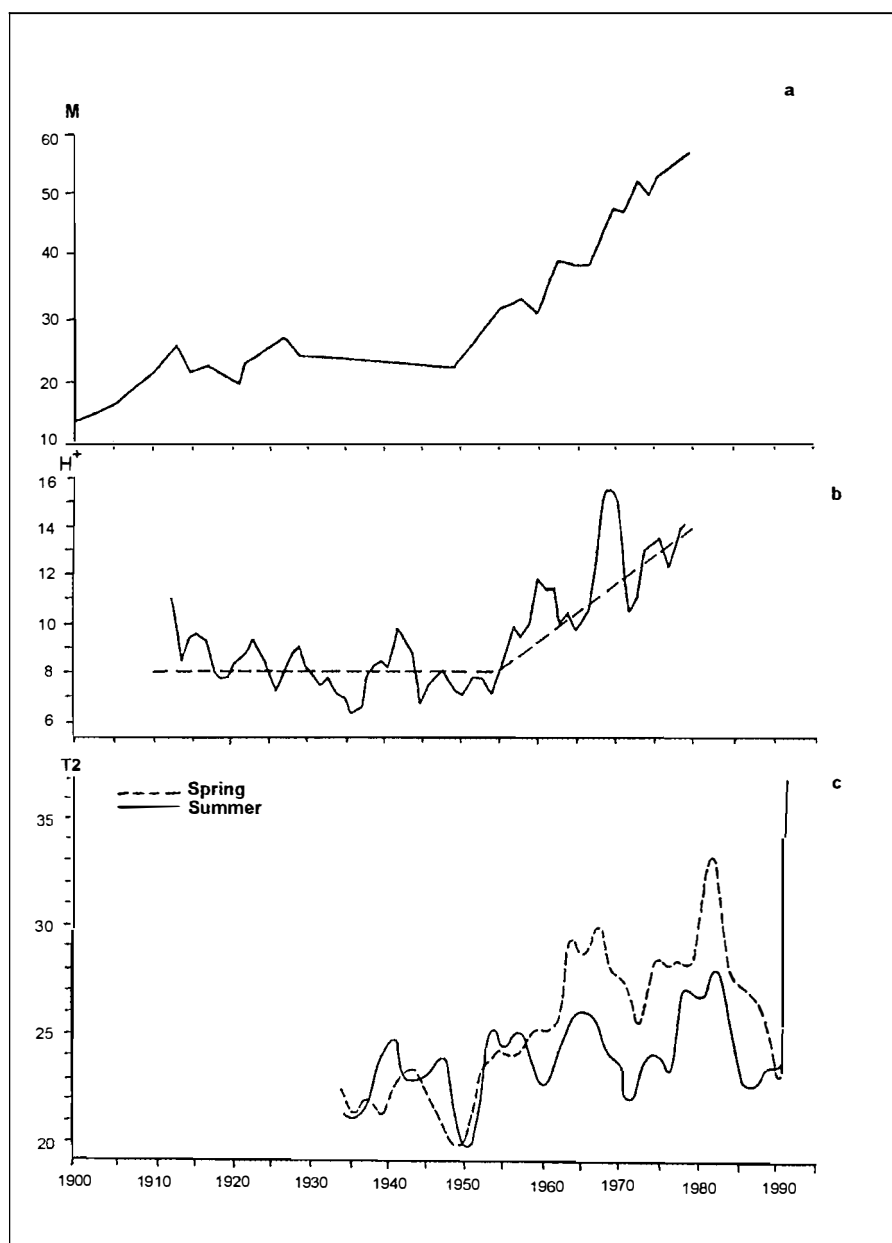


Fig. 2. A comparison of the historical record of SO₂ emission from Europe (a), acidity observations in ice of the Agassiz glacier, Ellesmere Island (b) and turbidity of the atmosphere at Tikhaya Bukhta and Dikson Island (c).

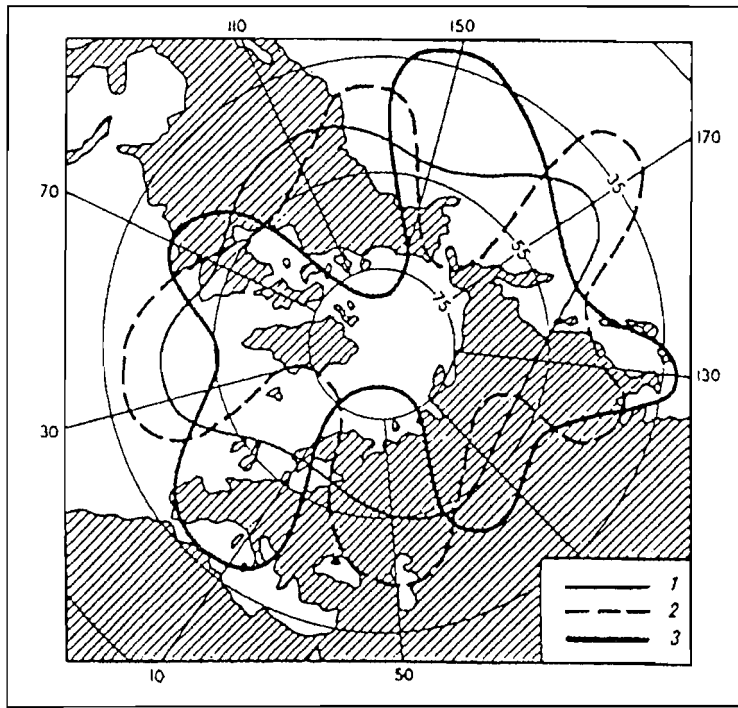


Fig. 3. A scheme of location of altitudinal (500 hPa) ridges and troughs at three kinds of the atmospheric circulation forms: 1 - form W; 2- form C; 3- form E.

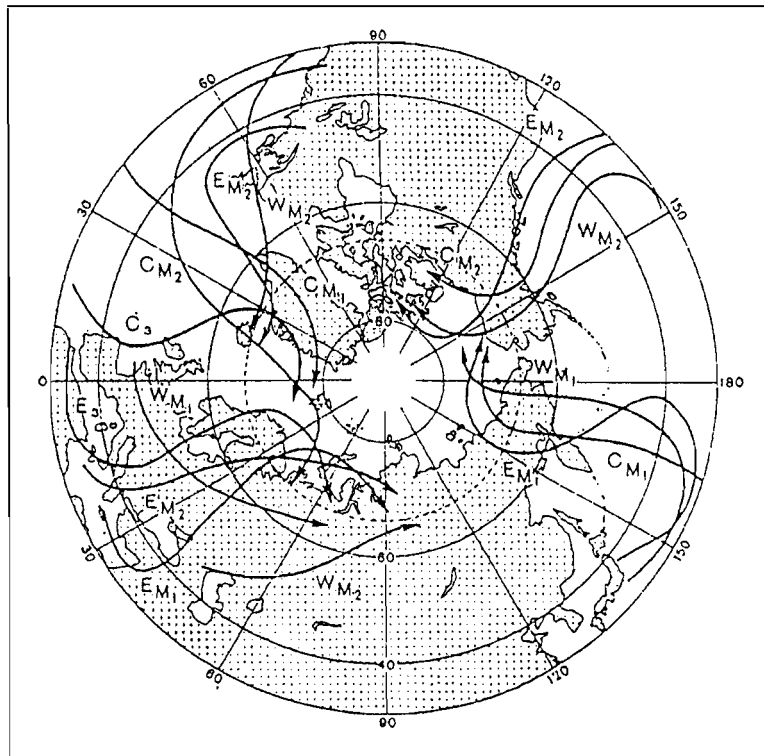


Fig. 4. A scheme of air mass transport

The Department of Long-Range Weather Forecasts of the AARI has prepared a detailed catalogue of multiyear variability of the circulation processes from 1990 up to the present time. In accordance with it the period of 1949-1971 was characterized by a simultaneous or alternating development of the processes of the forms E and C and by the attenuation of the form W processes. Since 1972 the processes of the form E prevailed (Dmitriyev 1994).

Thus, it can be concluded that an increase in emissions of pollutants at temperate latitudes of the European mainland that occurred at the background of prevailing meridional circulation forms has resulted in a stable growth of aerosol pollution of the atmosphere in the western Arctic from the 1950s to the mid-1980s. In the second half of the 1980s there was a tendency for a change in the circulation epochs.

The number of days with zonal transports of the form W, blocking the meridional transport commenced to increase and, respectively, the number of days with meridional forms decreased. But in the same years there was a sharp reduction in industrial production at the territory of the former USSR. As a result, in 1991 for the first time after 1957 the spring values of the T2 parameter became equal to the summer values (see Fig. 1). In this case it is difficult to differentiate explicitly between the influence of the change in the circulation types and the reduction in industrial emissions as a result of "perestroyka" regarding the occurrence of this phenomenon. It is likely that an increase in transparency or a decrease in atmospheric turbidity are related to a decrease in anthropogenic emissions after the industrial recession in the USSR republics.

As a result of these features of aerosol input to the Arctic, one can observe there a unique character of the behavior of aerosol-optical atmospheric parameters. Direct measurements of the aerosol optical thickness of the atmosphere have shown the attenuation of solar radiation due to aerosol particles in the Arctic to be maximum in March-April and comparable by value with the continental conditions (Radionov and Marshunova 1992, Radionov et al. 1994). Such intraannual variations of aerosol extinction with a maximum in spring are observed only in the Arctic.

The results of direct measurements by photoelectric counters of the concentration of aerosol particles more than $0.4 \mu\text{m}$ and $1 \mu\text{m}$ in size are given in Fig. 5. The concentration maxima are observed from January to April. And the concentration of particles in the surface layer is well correlated with the strength of surface inversions (Barteneva et al. 1991). In summer as a result of decreased meridional transports, destruction of the inversion stratification and increased cloudiness and precipitation washing out aerosol particles from the atmosphere, their concentration in the surface layer is 20-30-fold decreased. The aerosol optical thickness of the atmosphere at a wavelength of $0.5 \mu\text{m}$ decreases from 0.25 in April to 0.05 in July. In principle, one could expect the microphysical aerosol parameters in the Arctic to differ from those measured over the mainland. But according to data of measurements in March-April 1994 at the Franz-Josef Land, the character of the size distribution function of the volumes (i.e. mass) of particles turned out to be similar to that in Obninsk in May 1994 (Fig. 6). The measurements were made by means of photoelectric counters A3-5 and Royko in the size range from $0.4 \mu\text{m}$ to $10 \mu\text{m}$ and by an electrostatic counter DAES-2M in the range of $0.005-0.5 \mu\text{m}$.

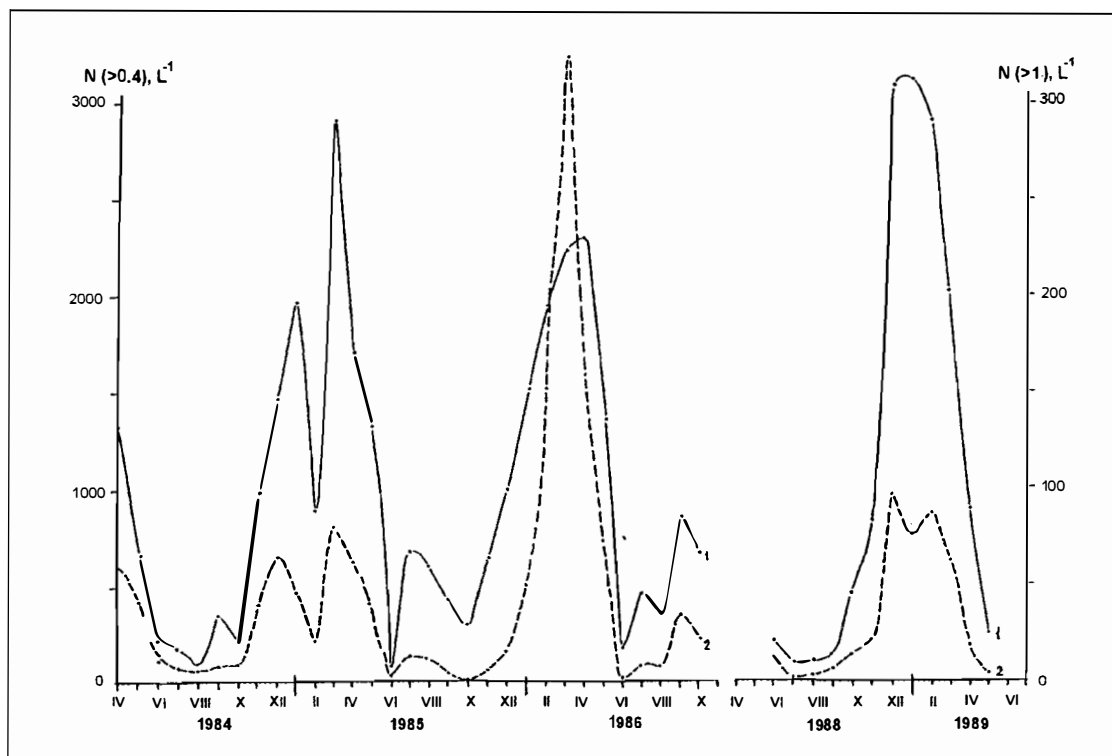


Fig. 5. Interannual variations in the concentration of aerosol particles, 1 - diameter is more than 0.4 μm, 2 - more than 1 μm.

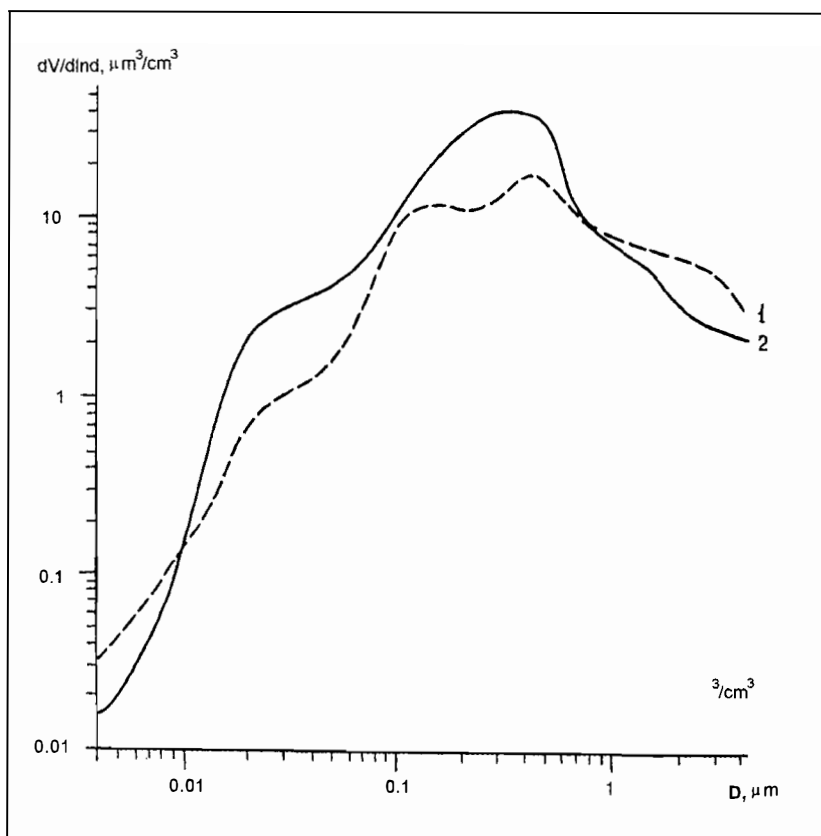


Fig. 6. Size distribution of the volume of aerosol particles: 1 - Tsigler Island, Franz-Josef Land, March-April, 1994; 2 - Obninsk, May 1994.

Moreover, the mass of particles with the sizes from 0.5 to 2 μm turned out unexpectedly to be 1.5-2 times more in the Arctic than over the mainland. The character of the dependency of the variability function on size (a ratio of the standard deviation to mean concentration of particles) in the Arctic is on the whole the same as in most of the points of the Earth, as also in the case of model experiments (Smirnov, 1992). The variability function minimum is in a submicron range of sizes (Fig. 7).

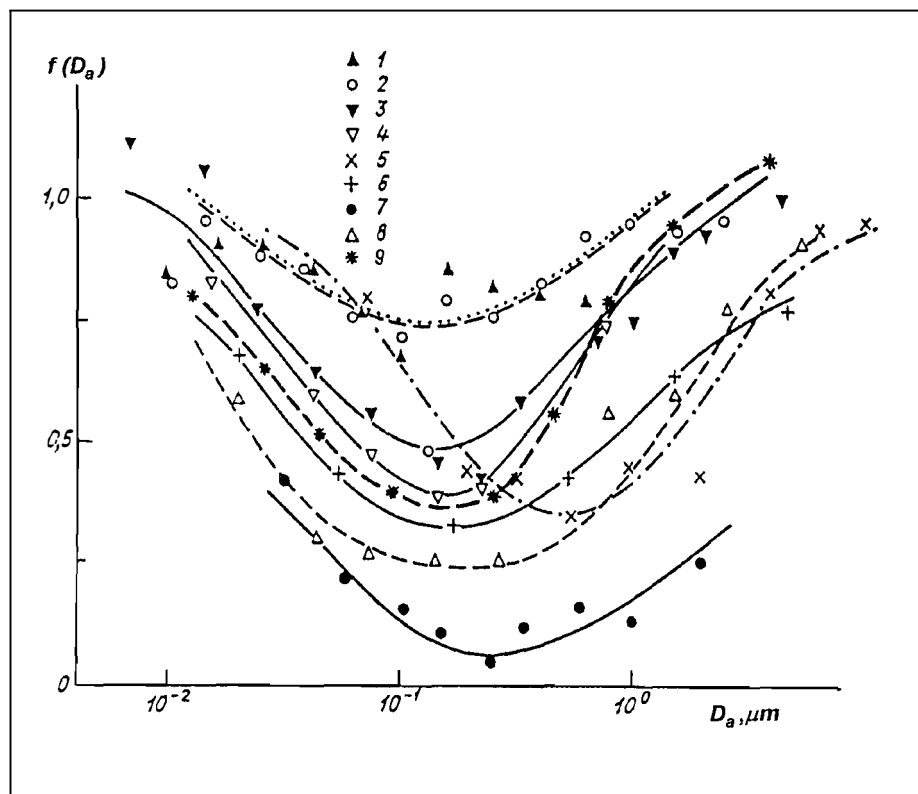


Fig. 7. The variability function of the particle concentration: 1 - the High Plains, the USA; 2 - a district near Moscow; 3 - Obninsk; 4 - haze and fog; 5 - the Atlantic Ocean; 6 - after destruction in "aerosol box" experiment; 7 - typical "aerosol box" experiment; 8 - Wrangel Island, the Arctic; 9 - Tsigler Island, Franz-Josef Land.

This result indicates that the mechanisms for the formation and evolution of the aerosol in the Arctic are close or identical to the continental ones. However the observed effects contradict the existing understanding that microphysical parameters of aerosol particles in the Arctic differ significantly from the continental ones.

New information obtained should be considered a basis for the hypotheses in further studies.

References

1. Barteneva, O.D., Nikitinskaya, N.I., Sakunov, G.G. and Veselova, L.K. Transparency of the atmosphere in visible and near-IR spectra. St. Petersburg: Gidrometeoizdat, 1991, 224 p. (In Russian).
2. Barrie, L.A. Arctic air pollution: an overview of current knowledge. Atmospheric Environment, 1986, vol. 20, No.4, 643-663.

3. Dmitriyev, A.A. Variability of atmospheric processes of the Arctic and its allowance in long-range forecasts, St. Petersburg: Gidrometeoizdat, 1994, 207 p. (In Russian).
4. Heidam, N.Z. 1984. The components of the arctic aerosol. *Atmospheric Environment*, 1994, vol.18, No.2, 329-343.
5. Karimova, G.U., Chukanin, K.I.. A scheme of the transport of pollutants to the Arctic troposphere. In: *Monitoring of climate of the Arctic*. St. Petersburg: Gidrometeoizdat, 1988, 168-181 (In Russian).
6. Radionov, V.F. Variability of aerosol extinction of solar radiation in Antarctica. *Antarctic Science*, 1994, 6(3), 419-424.
7. Radionov, V.F. and Marshunova, M.S. Long-term variations in the turbidity of the Arctic atmosphere in Russia. *Atmosphere-Ocean*, 1992, 30(4), 531-549.
8. Radionov, V.F., Marshunova, M.S., Rusina, E.N., Lubo-Lesnichenko, K.E. and Pimanova, Yu.E. Atmospheric aerosol turbidity in polar regions. *Izv. Acad. Sci., Atmos. Oceanic Phys.*, 1994, vol.30, No.6, 797-801 (In Russian).
9. Smirnov, V.V. Ionization in the troposphere. St. Petersburg: Gidrometeoizdat, 1992, 312 p. (In Russian).

RADIOACTIVE AEROSOLS OVER NOVAYA ZEMLYA AND THE COAST OF THE BARENTS SEA AFTER 1975

B.I. Ogorodnikov, V.I. Skitovich (KPCI), G.A. Luyanene, V.I. Luyans (PI)

Introduction

The composition and concentrations of aerosols are the basic characteristics of mixtures in the free atmosphere. As a result of nuclear tests and the accident at Block IV of the Chernobyl nuclear power station, a large amount of Cs-137 and Sr-90 were injected into the air. The cosmogenic radionuclides Be-7, P-32, P-33 and S-35 are formed in the stratosphere and the troposphere. For some time they are in the state of "free" atoms and then precipitate at aerosol particles. Their future "life" and motion in the atmosphere are to a great extent governed by the properties, chemistry and size of the carriers-particles. The removal of radioactive aerosols from the atmosphere and their distribution at the surface of the Earth depend on mixing of air layers, the content of gaseous, liquid and solid micromixtures, air temperature and humidity, the state of the soil surface and water areas, etc.

The work presents concentrations of Cs-137 in the middle troposphere over Novaya Zemlya and the coast of the Barents Sea in 1975-1990, as well as concentrations, dispersion composition and solubility of carriers-aerosols of radiocesium and cosmogenic radionuclides (Be-7, P-32, 33, S-35) sampled at the heights 2 to 6 km over the Barents Sea in 1989-1990.

Sampling and measurement methods

Sampling was performed from AN-24 aircraft equipped with filter nacelles located on two sides of the frontal part of the fuselage. Each nacelle was equipped with 3 sq.m of the filtering material FPP-15-1.5 or with a package of three filtering layers: *FPA-70-0.15*, *FPA-70-0.3* and *FPP-15-1.5*. During the flight the nacelles were opened at a given height and blown due to dynamic pressure, with a blowing rate of about 16000 m³/h. At linear filtration speeds of 1...2 m/s a three-layer composition of the package allowed determining not only the radionuclide composition and concentrations of aerosols, but also the size distribution of the particles in the diameter range of 0.1..6 μm (Sankov, Yu.A, Budyla, A.K. 1992).

After the end of the flight, the filtering materials were separated into the initial layers and each was compressed into a brick of 50 mm in diameter. During the express-analysis, measurements of the bricks at a semi-conductor detector of the γ-spectrometer allowed determining the levels of radioisotopes of cesium and beryllium. After that the bricks were subjected to radiochemical treatment. The Cs-134,137 isotopes were extracted by potassium-cobalt-ferri-ferrocyanidic sorption. The P-32,33, S-35 and Be-7 radioisotopes were extracted and cleaned-up by means of the method of cation exchange and precipitation using MgNH₄PO₄, Be(OH)₂ and BaSO₄. The residues of P-32,33 and Be-7 were calcinated and weighted. BaSO₄ was washed by ethanol, dried and weighted. Then BaSO₄ was transferred to BaS and oxidized to S. The final clean-up of S-35 was made by sulphur sublimation at a brass disc.

The gamma-spectrometer consisted of a high-resolution semi-conductor Ge(Li) detector and a multichannel amplitude pulse analyzer. The beta-activity of the preparations was measured at low level installations. The quantities of phosphorus radioisotopes were determined by means of the filters-absorbers of beta-radiation of different thickness. In several cases the results were checked by the drop in the activity of the preparations, depending on the time which passed after the end of air sampling. Taking into account the accuracy of chemical operations performed, radiometry,

measurements of filtered air and the determination errors, the quantity of radionuclides were: Be-7-12%, P-32-10%, P-33-22%, S-35-30% and Cs-134, 137<20%.

Results and discussion

In accordance with the Moscow Treaty Banning Nuclear Weapon Tests in three media, the USSR, the USA and Great Britain did not make explosions in the atmosphere in space and under water. France has made its last explosions (as of spring 1995) at the Mururoa atoll (the Pacific Ocean) in 1974. Thus of five nuclear states, only China was active during the study period. The last explosion in the atmosphere at the Chinese testing grounds Lob-Nor took place on October 16, 1980. In total, from data of UN (UN SCDAR, 1985) 450 nuclear explosions of the total strength of 545 Mt were made in the atmosphere. Of them 40% constituted the splitting reactions at which Cs-137 occurred among other fission fragments. In 1976-1980 the total strength of the Chinese explosions due to fission reactions was 2.9 Mt. Thus about 1% of radiocesium was added to the atmosphere during the period of our observations. The underground nuclear explosions have not become a significant source of atmospheric pollution by radioactive substances either.

Figure 1 presents concentrations of Cs-137 in the middle troposphere over Novaya Zemlya. As is seen from the curve of averaged concentrations, there was intense purification of the atmosphere. In September 1976 the content of Cs-137 was about 10 Ku/m³. In 3 years this value has decreased 10-fold. This the "half-life of Cs carriers-aerosols of Cs-137 was 1 year during this period. Then the process slowed down: in August 1983 the concentrations were reduced up to 0.1-0.2 fCi/m³ which corresponded to a "half-life" of 2 years.

The reactor explosion in block IV in Chernobyl in April 1986 has resulted in a considerable pollution of the Northern Hemisphere, including the Arctic region, by a wide range of radionuclides. According to Abagyan A.A. et al., 1986, about 0.5 Mku of Cs-134 and twice as large of Cs-137 were emitted to the atmosphere. Sampling of aerosols during November 29 - December 7, 1989 along the route Moscow-Arkhangelsk-Amderma-Novaya Zemlya and back allowed testing not only Cs-137, but Cs-134 as well. This indicated unambiguously the Chernobyl genesis of the radioactive substance carriers. The concentration of Cs-137 was equal to 7 Ku/m³ which actually corresponded to its level during the initial period of these studies.

In 1990 region two more samples were collected in the Barents Sea: on 12-28 June at the route St.Petersburg - Arkhangelsk - Novaya Zemlya - Arkhangelsk - St.Petersburg - Moscow and on 24-26 October at the route Moscow - Arkhangelsk - Naryan - Mar. The Cs-137 concentrations remained high and were 1.13 and 0.84 fCi/m³, respectively. Thus 4 years after the Chernobyl accident the Cs-137 concentrations exceeded its level in early 1986 by 1-2 orders of magnitude. The contribution of Cs-137 which remained from nuclear tests, to air pollution of the Arctic region became insignificant.

Calculations based on data of Cs-137 distribution in the layers of the package of filtering material, have shown that in 1976-1984 the carriers of this radionuclide had active median aerodynamic diameters (AMAD) in the range of 0.1-0.4 μm. In the sample, collected at the end of 1989, the AMAD of Cs-137 carriers was equal to 0.72 μm and of Cs-134 - 0.76 μm at a standard geometric deviation (σ) of 1.2. It followed that both cesium radioisotopes in aerosols of the Chernobyl genesis were at the same carriers-particles whose size was 2-3 times greater than of Cs-137 carriers in products

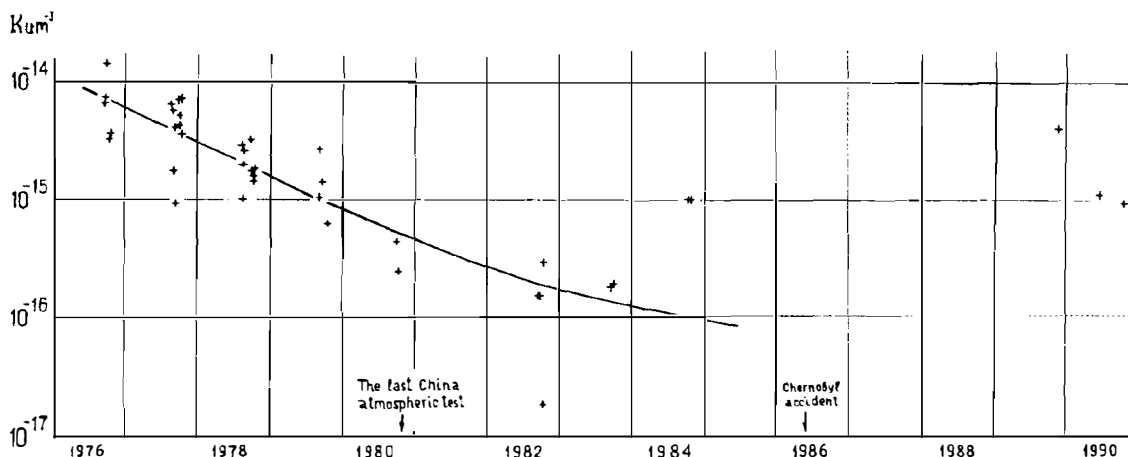


Fig. 1. Concentrations of Cs-137 in the middle troposphere over Novaya Zemlya and the coast of the Barents Sea in 1976-1990.

which remained from the nuclear weapon explosions in the atmosphere by 1976-1984. Measurements of the dispersion composition of aerosols in summer and autumn, 1990 have confirmed the results of the preceding year: the Cs-137 carriers had the AMAD of 0.84 μm (at $\sigma=1.2$) and 0.62 μm (at $\sigma=1.4$), respectively.

Data on the carriers-aerosols of cosmogenic radionuclides Be-7, P-32,33 and S-35 were obtained as a result of the flights in 1989-1990. The concentrations and their ratios are presented in Table 1.

Table 1.
Concentrations and ratios of cosmogenic radioisotopes in aerosols of the middle troposphere in the region of Novaya Zemlya and the coast of the Barents Sea.

Sampling date	Concentration, fCi/m ³				Ratio	
	Be-7	P-32	P-33	S-35	Be-7/P-32	P-33/P-32
29.11.89-07.12.89	132	5.1	3.0	0.8	25.8	0.58
12.06.90-28.06.90	81	4.3	2.7	1.4	18.8	0.62
24-26.10.90	168	4.0	1.9	2.4	41.2	0.47
Mean	127	4.5	2.5	1.5	28.6	0.56

The concentrations of Be-7 and S-35 fluctuated in the range of $\pm 50\%$ relative to mean values. The levels of phosphorus radioisotopes were more stable. For comparison let us note that in April and June 1990 mean concentrations (fCi/m³) of carriers of cosmogenic radionuclides near the earth's surface in the vicinity of Vilnius were: Be-7 - 143; P-32 - 2.2; P-33 - 1.4 and S-35 - 1.2. The AMAD values and σ obtained in the northern region from the results of the distribution of radioisotopes in the layers of filter packages are given in Table 2.

Table 2.

The AMAD values (μm) and σ for carriers-aerosols of cosmogenic radioisotopes.

Sampling date	Be-7		P-32		P-33		S-35	
	AMAD	σ	AMAD	σ	AMAD	σ	AMAD	σ
29.11.89-07.12.89	0.30	1.4	-	-	-	-	0.32	1.2
12.04.90-28.04.90	0.16	3.9	0.12	2.8	0.20	1.9	0.34	2.7
24-26.10.90	0.08	5.0	0.28	1.8	0.08	2.7	0.80	-

As follows from Table 2, the carriers-aerosols of cosmogenic radionuclides had a smaller size than anthropogenic aerosols which contained radiocesium 3-4 years after the accident.

During the flight made in June 1990, aerosols were collected from a larger air volume (about $2 \times 10^5 \text{ m}^3$). This allowed studies of the behavior of carriers-particles of radionuclides of anthropogenic and cosmogenic origin in different liquid media which is important for assessing their behavior after the fallout from the atmosphere to the water surfaces, plants and soils of a different composition. The filtering package was successively treated by deionized water; 0.1 M HCl and then by a hot mixture of concentrated HNO₃ with H₂O₂. The distribution of elements in each of the 4 solutions is presented in Fig. 2.

The solubility of carriers-aerosols of cosmogenic P-32 and P-33 in water was the same and equal to 50%. The solubility of S-35 carriers-aerosols was slightly worse (40%) and of Be-7 carriers - better (60%). The aerosols associated with cesium radioisotopes of Chernobyl genesis were in a sharp contrast to them. Their solubility in water did not exceed 16%. The next treatment of the filter with a sample of hydrochloric acid (0.1M) has shown that the carriers of cosmogenic isotopes are also better dissolved (27-38%) than the radiocesium carriers (12%). After treatment of concentrated hydrochloric acid (6 M) it turned out that not more than 5-10% of cosmogenic radioisotopes and almost 50% of radiocesium are contained in the insoluble residue.

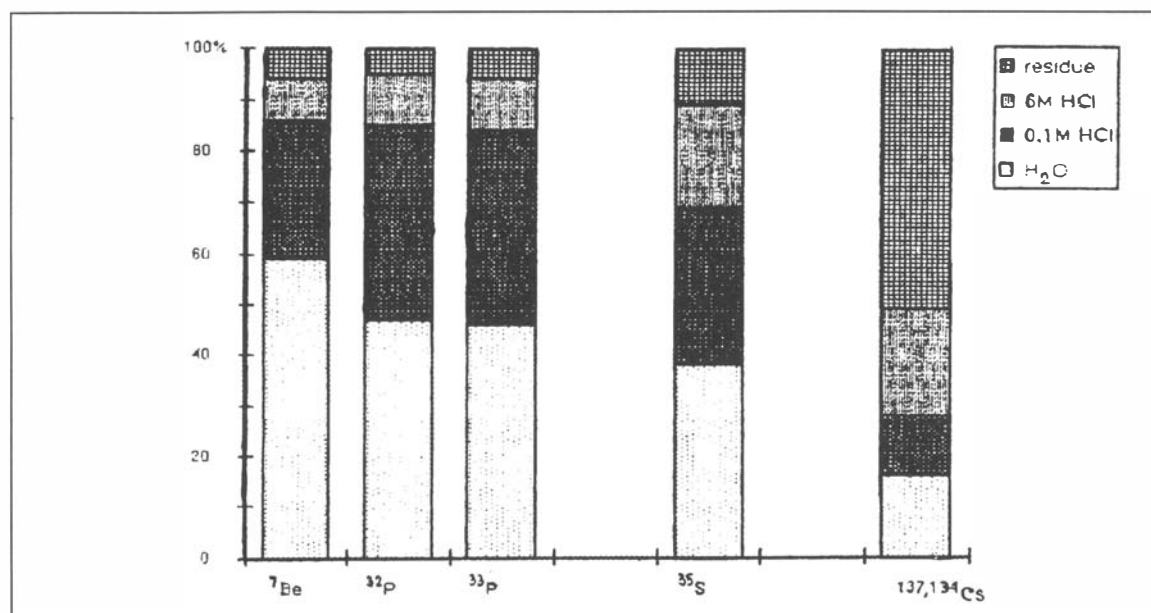


Fig. 2. Solubility of carriers-aerosols of radionuclides in different liquid media.

Conclusion

It was established that in 1976 the Cs-137 concentrations over Novaya Zemlya and the coast of the Barents Sea were about 10 fCi/m³. Prior to 1986 its concentrations steadily decreased with a "half-life" period of 1 year, initially, then of 2 years. The Chernobyl accident has resulted in the increased content of radiocesium by 2 orders of magnitude. Also, the dispersion composition of aerosols has changed. Whereas in 1976-1984 the AMAD of Cs-137 carriers-particles which remained after the nuclear tests in the atmosphere was 0.1-0.4 μm, then in 3-4 years after the accident at block IV in Chernobyl, the radiocesium carriers were 2-3 times larger.

Data on the levels and ratios of the concentrations of radionuclides of cosmogenic origin (Be-7, P-32, 33, S-35) in the middle troposphere at the end of 1989-mid-1990 were obtained. These values over the Barents Sea for Be-7 and S-35 did not significantly differ from the values obtained in Vilnius, but were approximately twice as large as for P-32, 33.

The AMAD of carriers-aerosols of cosmogenic radionuclides was within a range of 0.1-0.4 μm. Studies of solubility of radioactive aerosols sampled in the middle troposphere in summer of 1990 have shown that about 50% of the carriers of cosmogenic radionuclides is transferred to twice deionized distilled water whereas the solubility of radiocesium of Chernobyl genesis does not exceed 16%. After treatment by the diluted and then concentrated hydrochloric acid, only 5-10% of cosmogenic radionuclides remains in the residue and the fraction of the insoluble radiocesium is 50%.

The obtained results are of interest for estimating aerosol precipitation from the atmosphere and its behavior after fallout onto water surfaces, soils and plants.

References

1. Sankov, Yu.A, Budyla, A.K. Environmental Protection, Questions of ecology and control of product quality. - Scientific-technical reference volume. 1992, No.9. pp.35-45.
2. UN SCDAR Exposure as a result of testing of nuclear weapons and nuclear fuel cycle of military significance: UN SCDAR 34th session, Vienna. 10-14 June, 1985.
3. Abagyan A.A. et al. Atomic energy, vol.61, No.5, 1986, pp.301-320.

STUDIES OF THE WESTERN ARCTIC SEAS USING SPACE MEANS

A.V. Bushuyev, V.D. Grishchenko, V.G. Smirnov, Yu. A. Shcherbakov (AARI)

As a result of the rapid advance in methods and technical means which began in the 1950s, remote sensing measurements, including satellite and other platforms, serve as the main tool to-date for environmental studies, hydrometeorological information support of different practical activities and for warning of dangerous and especially dangerous natural phenomena.

The AARI began using satellite information for investigating the Earth's polar regions on a permanent basis in 1967 when a self-contained satellite data receiving facility in the APT mode (APPI) was introduced into operation. The radio visibility zone of all meteorological satellites ("*Meteor*", *NOAA*, "*Okean*") operating in direct data transfer mode provides information retrieval by the APPI of the AARI for all seas of the western Arctic (the Greenland, North, Barents and Kara Seas). At present assembling of the station for satellite data receiving in the HRPT mode is being completed.

In accordance with the directions of the AARI activities, satellite data are mainly used for mapping and investigating the ice cover as the major factor that governs physical and geographical conditions in the Arctic and technology of transport shipping.

During these years as a result of validation and research-methodological studies in the expeditions and at special polygons, information properties of satellite remote sensing means of different ranges and resolution were identified, and hence, ice cover navigation characteristics and their accuracy that are determined on their basis (Table 1). For analyzing this table, one should take into account the difficulty of using the *ERS-1* data operationally which is mainly due to the restricted frame size (100x100 km), the need for wide band communication lines and an irregular mode of work. At present the AARI is oriented to the first three satellites. Estimating data of these satellites, let us note that first-year ice prevails in the seas of the western Arctic. For providing effective support to shipping, its thickness or at least age gradations are required.

On the basis of satellite images in the visible range, vast zones of nilas and young ice can be delineated, the rest, including old ice, belongs to the category of "ice thicker than 30 cm". On the basis of IR images at below zero temperatures (-20°- -30°C), five-six gradations can be identified within a thickness range of 0-120 cm. All other gradations are not discerned either. And finally, using radar images, zones of inclusions or zones of prevailing old ice can be mapped.

Such detailing of the age categories is quite insufficient. Hence, satellite information is supplemented by data obtained from all other data sources.

The possibility for detecting leads which are widely used in arctic shipping is governed by the resolution of the remote sensing means and the contrast of leads relative to the ambient ice in some range or other. The largest contrast is in the visible range being slightly worse in the IR range. On radar images leads among old ice are easily distinguished and in zones of first-year ice only leads covered by grey ice.

The accuracy of determining the location of clear boundaries (fast ice, floes, leads) depends on the accuracy of geolocation. And the accuracy of mapping the boundaries of zones and edges mainly depends on subjective errors of operator drawing them in the interactive mode, and on the adequacy of models for automated delineation of these boundaries.

As a result of constant research during all these years, the systems of interpretation indications, algorithms and software of geographical location, automated and interactive determination of the main ice cover characteristics and preparation of

digital ice charts (Bushuyev, A.V. et al, 1978, Bychenkov, Yu.D., et al, 1983, Guidelines etc., 1985, Handbook etc., 1981) were developed.

The technology for processing satellite videoinformation includes the following stages:

- digitizing of images received in the APT mode;
- geographical positioning of images using orbital data and its correction by ground control points, as a result, the image is transformed into a photographic chart in stereographic projection;
- delineation of the boundaries of zones;
- determination of ice cover characteristics in the delineated zones;
- preparation of an individual ice chart in the letter-digital format KONTUR;
- calculation of ice drift vectors using successive images;
- integration and updating of a current chart of ice situation.

Since all navigation parameters of the ice cover are impossible to determine using only satellite data, satellite ice charts are supplemented by data obtained from all other information sources at the stage of integration and composite ice charts are prepared. There are used data of visual and instrumental ice reconnaissance from aircraft; data from icebreakers and ships; polar stations, as well as from drifting buoys.

A current composite chart contains data of only direct observations. However, there are stored data which can be considered constant and reliably corrected. They include:

- age categories of fast ice,
- amount of hummocking,
- position of stamukhas, hummocking belts, etc.,
- position of the boundaries of zones of inclusions and of prevailing old ice on the basis of drift data,
- first-year ice thickness in the zones whose position and boundaries are tracked from the onset of ice formation.

Thus, there is constant tracking of the ice cover evolution in time and space. For this purpose, a detailed field of the drift vectors is used which is obtained from successive images. This objective is particularly important under conditions of a dramatic decrease in ice reconnaissance flights. Hence, a particular attention is paid to improving the technology for determining drift vectors.

Individual and composite ice charts are prepared in a specially developed letter-digital format KONTUR. This format includes recording of information of each chart in the form of separate sets (layers) - header, main zones, additional zones, linear targets, point targets, ice drift which compose one file. The format provides for entry, storage and transfer of information on all variables characterizing the ice cover state, fully preserving the accuracy in delineating the boundaries of zones and position of linear and point targets. It does not require any converting for further computer-based processing. As compared with facsimile transfer, it is more noise-resistant and reduces the traffic by 2-3 times.

The ice chart in the KONTUR format is transmitted to users via communication lines, converted into a grid format for ice calculations and forecasts and a hard copy can be obtained.

The possibility for obtaining satellite information in the visible and IR ranges is governed by meteorological conditions (the absence of clouds). As is known, the area of such cloud-free zones in the Arctic is equal to 10%, on the average. Hence, the difference in the observation time in different parts of one and the same composite chart can reach 5-10 and even more days. Updating of such diverse observations for the current time instant using actual meteorological fields for the period in the past and

preparation of calculation-analytical composite charts is a separate problem and is outside the scope of the present paper.

As is known, in addition to ice observations, satellite information can be successfully used for investigating processes and phenomena in other natural media. One of such objectives is sea surface temperature (SST) measurements. This problem has been sufficiently well addressed both theoretically and practically for the seas of temperate and equatorial latitudes. However, adaptation of algorithms, technologies and software to the conditions of polar regions has required subsatellite experiments for specifying regional features of the formation of measured radiation SST (seasonal and daily variations, relation to the temperature of lower layers at different conditions of mixing, influence of intermediate medium, etc.). In March-June 1995 such studies were carried out in the Antarctic cruise of the R/V "*Akademik Fedorov*". They are also planned in the Arctic Seas including joint Russian-Norwegian and Russian-German expeditions.

After the satellite data receiving station in the HRPT mode is introduced into operation, regular monitoring of contamination of the Arctic seas by suspended matter is planned with corresponding validation observations.

Methods, software and technologies of ice and other types of observations after testing are incorporated and constantly used at the *Operational Center for Ice and Hydrometeorological Information* of the AARI. Initially it was developed and created as a center of the *Automated Ice and Information System (ALISA)* and its functions were limited to ice observations. However, the interrelation of all hydrometeorological processes required to extend its functions and at present it collects, analyzes and disseminates all hydrometeorological information on the Arctic and the Antarctic.

The output products of the Center include:

- charts of current ice situation (from data of direct observations and calculated-analytical);
- meteorological charts at the main synoptic times (used by research and practical divisions of the AARI);
- medium-range (7-8 days in advance) meteorological and ice forecasts for all Arctic Seas;
- forecasts of sea currents, waves, nonperiodic sea level oscillations;
- navigation recommendations (on request).

The AARI continues to further improve the ALISA system and develop the Center by introducing new technical means for data retrieval and processing, improving automated methods of geolocation and data decoding, improving and developing new models for ice forecasting and calculations, extending databases of operational and regime banks of hydrometeorological data, converting the system to geoinformation technologies. All this aims at increasing the reliability and quality of hydrometeorological information provided to users on an operational basis (Bushuyev, A.V 1991).

In recent years the ALISA system is being adapted for the purpose of providing hydrometeorological information support to international transit shipping along the Northern Sea Route.

Table 1

Accuracy of determining ice cover characteristics, the possibility for satellite observations of ice targets

Characteristics	Range	Satellite type			
		<i>NOAA, Meteor, TV</i>	<i>NOAA, IR</i>	<i>Okean, SLAR</i>	<i>ERS, RSA</i>
Generalized ice cover characteristics					
Concentration	<1	-	-	-	+
total and of observed	1-3	1.0	-	1.0	0.5
age categories (tenths)	4-8	1.5	2.0	2.0	1.0
Age categories (thickness, cm)	9-10	1.0	1.5	1.5	0.2
	5-30	15	5-6	15	10
	30-120	*	gradations	*	*
	120-200	*	*	*	*
Forms, a possibility for observation and accuracy of determining partial concentration (tenths)	Old	*	*	+	+
	<2-20m	-	-	-	-
Rafting (arbitrary units)	20-100m	-	-	-	2.0
	100-2000m	2.0	-	2.0	1.0
	2-10km	1.5	2.0	1.5	0.5
	>10km	1.0	2.5	1.5	0.5
Hummocks (arbitrary units)	0-10	-	-	-	2.0
Snow (arbitrary units)	0-10	-	-	2-3	1-2
Melting stages (arbitrary units)	0-8	-	-	-	-
Compacting (tenths)	0-9	2-3	-	2-3	2-3
	0-3	-	-	-	1-2
Ice targets and boundaries					
Leads with a width more than	km	0.3	0.5	2.0	0.05-0.1
Margins of drift zones					
Boundaries of zones with different drift speeds	km	+	-	-	+
Position of the boundaries of fast ice, position of floes, leads, zones	km	2-3	2-3	3-4	0.5
		5-10	5-10	10-12	1-2
Position of the ice edge: with concentration 1-3/10 more than 4/10		10-15	-	10-20	4-5
		5-10	10-15	10-15	2-3
Drift vectors	km	3-4	3-4	4-5	2-3

Notes: "+" - observed, "-" - not observed, "*" - no differences in the signature of ice of these gradations are observed, however, this ice can be distinguished from all other stages.

References

1. Bushuyev, A.V Development and improvement of the system and methods of ice observations. - Problems of the Arctic and the Antarctic, vol., 1991, 66, pp.170-183.
2. Bushuyev, A.V., Bychenkov, Yu.D. Study of sea ice distribution and dynamics from TV images of "Meteor". Temporal instruction / - L.: Gidrometeoizdat, 1978, 132 p.
3. Bychenkov, Yu.D., Loshilov, V.S., Masanov A.D. Study of the ice cover by means of Side-Looking Airborne Radars (SLAR). A handbook/A.V.Bushuyev,. - L.: Gidrometeoizdat, 1983, 120 p.
4. Guidelines to receiving, processing and using satellite ice information. Determination of the ice cover characteristics from radar images of "Kosmos-1500". Iss. 1. - L.: Reprint of the AARI, 1985. - 75 p.
5. A handbook for airborne ice reconnaissance. L., Gidrometeoizdat, 1981, 240 p

STUDY OF HYDROCHEMICAL STRUCTURE AND MODELING OF THE CONSEQUENCES OF ANTHROPOGENIC ACTIVITIES IN THE KARA SEA

V.M. Smagin, S.V. Pivovarov (AARI) and S.V. Berdnikov (RSU)

The period of hydrochemical studies in the Kara Sea can be divided into several stages. Their results were, as a rule, published at the end of each stage (see references). The most fruitful was the last stage from the early 1970s where regular winter and summer hydrochemical surveys of the sea were carried out and dissolved oxygen, silicon, phosphates, nitrites, nitrates, carbonate system elements, as well as some pollutants were determined. A vast amount of data have been accumulated in the archives of the AARI enabling determination of the hydrochemical structure of the Kara Sea in winter and summer which is necessary for a justified estimate of the state of the marine environment and its possible changes as a result of anthropogenic impacts.

One of the most important factors governing the structure of hydrochemical fields in the Kara Sea is the runoff of the Ob' and Yenisey rivers. There is an extensive zone of mixing of sea and river water in the central part of the sea. The concentration of dissolved silicon is a good indicator of the spreading effect of the river runoff over the sea surface. Fig. 1 shows several variants of the location of the boundary of the river outflow (silica 250 $\mu\text{g/L}$ isoline) in summer which correspond to four types of the extent of the influence of river water at the surface of the Kara Sea. One should note a large variability of the position of the silica 250 $\mu\text{g/L}$ isoline during the summer season.

The zone of the river outflow is characterized by elevated values of specific alkalinity, an anomalous ratio of macrocomponents of the salt composition of sea water and the reduced saturation of the surface layer with oxygen. In addition, the largest vertical gradients of hydrochemical indicators in the halocline are observed in this sea region, especially in summer. Below the halocline, the bottom water layer is characterized by a significant deficit of dissolved oxygen (up to 40%) and the largest supplies of phosphates and nitrates.

An interesting feature of vertical hydrochemical structure in the south-western Kara Sea that is not subjected to the influence of the river runoff in summer, is the existence of the subsurface layer with elevated saturation with oxygen. The formation of the subsurface oxygen maximum is attributed to the conditions forming the summer quasiuniform layer at ice melting, as well as to photosynthetic activity of phytoplankton at a depth of 15-25 m. The subsurface maximum in the south-western sea is observed almost everywhere except for the shallow zones.

The frontal areas of the Kara Sea, as well as deep-sea regions (the troughs: Novozemel'sky, Voronin, St. Anna) are characterized by stratified hydrochemical structure.

Ice conditions greatly influence the formation of hydrochemical fields in summer. In the ice edge vicinity in the surface layer one observes elevated values of dissolved oxygen.

Phosphates and nitrates in the surface layer in summer are almost completely utilized by phytoplankton over the whole area of the Kara Sea. The increase in the concentration of these parameters occurs in the layer of the density gradients. However, near the hydrochemical barriers in the Ob' Gulf and the Yenisey Bay, as well

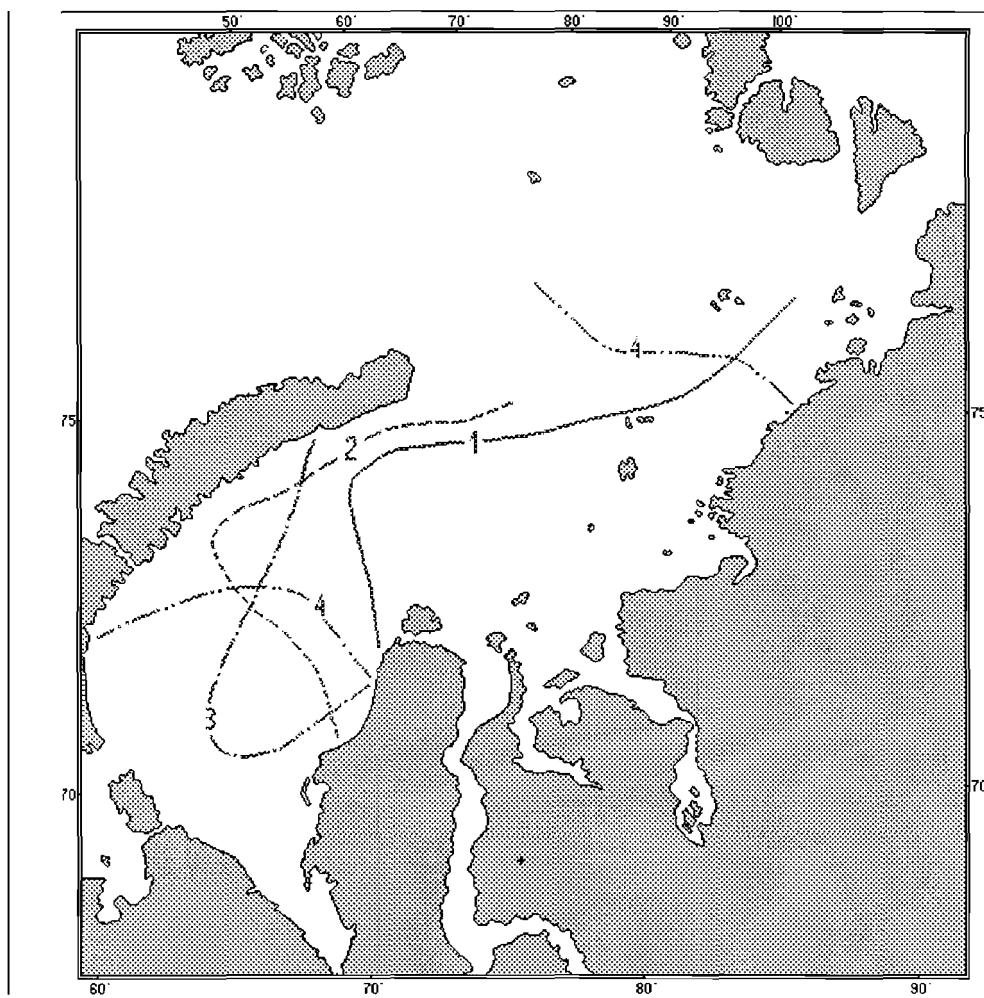


Fig. 1. Position of the 250 $\mu\text{g/Si/L}$ at the surface of the Kara Sea in summertime:
 1 - August 1976, 2 - August 1991, 3 - August 1988, 4 - September 1993.

as in the regions of surface upwellings even in the period of mass blooming of phytoplankton the values of phosphates and nitrates in the surface layer are elevated.

The seasonal change in vertical hydrochemical structure consists in the formation of the upper quasiuniform layer in spring that is supersaturated with oxygen and is devoid of any nutrients. Then, as a result of ice melting and spreading of the river runoff, the summer surface layer is formed. In this layer, changes in oxygen concentration related to water heating and cooling, as well as to changes in the activity of phytoplankton, are noticeable. In autumn and winter the surface and subsurface (spring) layers are combined into one quasiuniform layer which, as a result of convective mixing, is enriched in nutrients. In the regions where convection penetrates down to the bottom, all water column is uniform in hydrochemical indicators.

Unfortunately, a precise description of annual variations of hydrochemical indicators is not yet possible for many regions of the sea due to the absence of data in spring (June-July) and in the period of intensive ice formation. We hope that data gaps will be filled both experimentally during expeditions and by means of a box model which is jointly developed by the AARI and the Rostov University.

The main goals of modelling are as follows: explanation of the features of spatial distribution and seasonal dynamics of hydrochemical and hydrobiological characteristics of the Kara Sea and assessment of possible changes in hydrochemical and hydrobiological regimes as affected by natural and anthropogenic factors.

The following model variables were chosen: water temperature, salinity, level of dissolved oxygen and nutrients (nitrogen, phosphorus, silicon), level of dissolved and suspended organic matter, mineral suspension. Of biological parameters -single-cell algae. Of pollutants - oil hydrocarbons, organochlorines, salts of heavy metals and radionuclides.

On the basis of the statistical analysis of hydrochemical data the Kara Sea was divided into regions. The regions with a typical size of 100 km, uniform in hydrological and hydrochemical parameters were delineated. The exchange of substance and energy between the regions is based on the mass balance. Two layers are delineated by vertical. In each of the layers the following media are considered: water, ice and bottom sediments. A typical time interval is one month.

Changes in any variable of the model are governed by the following processes: advective transfer, mixing and transformation under the effect of a complex of physical, chemical and biological processes. The substance is redistributed between different accumulating media.

The external factors are river runoff, water exchange with the Barents Sea and the Arctic basin. It is assumed that all external factors have seasonal variability, but do not change from year-to-year enabling estimates of some limit state of the marine environment at a definite level of external impact.

The model allows calculations of the distribution of hydrochemical indicators, as well as of some pollutants in space (Fig. 2). Unfortunately, the rates of many processes accounting for transformation of oil products in the Arctic Seas are still unknown. Hence, by using this model only the transfer of the dissolved form of oil hydrocarbons can be estimated by simulating an oil discharge to the sea from additional sources in the locations of its production and transportation.

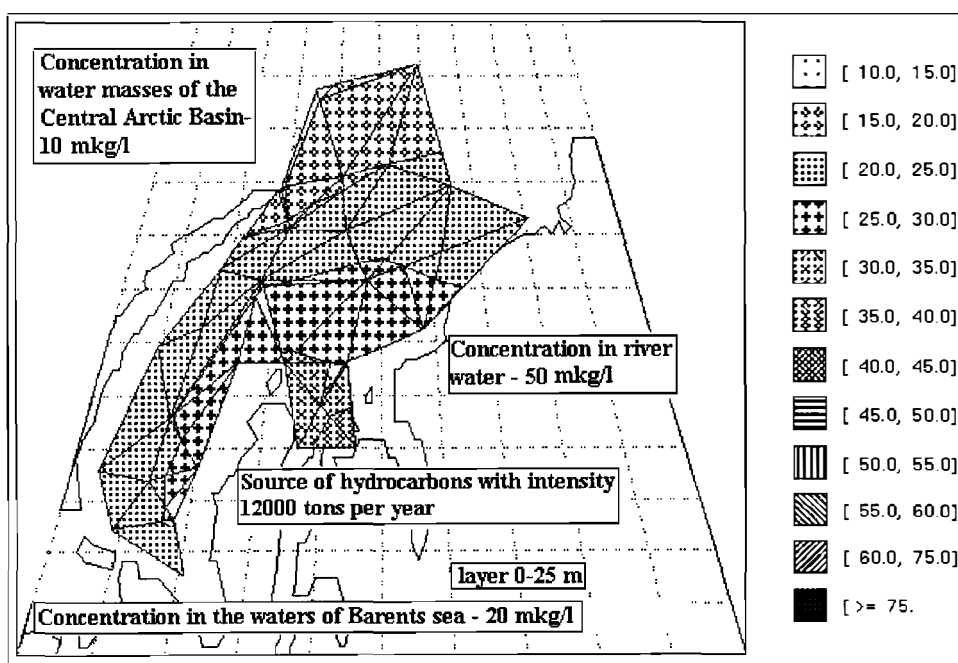


Fig. 2. Distribution of oil hydrocarbons in the Kara Sea in summer ($\mu\text{g/L}$) at a possible pollution source on the Yamal peninsula.

For modelling seasonal dynamics of single-cell algae, the processes of the formation of passive stages were taken into account both due to the physiological features of the dominating algae in the Kara Sea and as a result of the onset of unfavourable conditions for their development. According to the results of simulating

seasonal dynamics of the main groups of diatom algae, the annual primary production of phytoplankton varies from 20 mgC/m² a day for the northern regions to 120mgC/m² a day for the most productive near-mouth areas.

At present, the box model of the Kara Sea allows the main features in the formation of the background hydrochemical regime to be explained and changes in the state of the marine environment as affected by external conditions to be predicted .

References

- 1.Viese, V.Yu. Hydrochemical conditions in the ice edge vicinity in the Arctic Seas. - Problems of the Arctic., 1943, No.2. - pp.13-32.
- 2.Guryanova, A.P., Musina, A.A. Main features in the distribution of oxygen and alkalinity in water of Atlantic origin of the Arctic Seas. - Proc. of the AARI., 1960, Vol.218.- pp.125-158.
- 3.Rusanov, V.P., Vasilyev, A.N. Spreading of river water in the Kara Sea from data of hydrochemical determinations. - Proc. of the AARI., 1976, Vol. 323. - pp.188-196.
- 4.Rusanov, V.P., Yakovlev, N.N., Buynevich, A.G. The hydrochemical regime of the Arctic Ocean. - Proc. of the AARI., 1979, Vol.355. - 144 p.

MODELING OF TRANSPORT AND TRANSFORMATION OF POLLUTANTS IN THE BARENTS AND KARA SEAS

Pavlov V.K., Kulakov M.Yu., Stanovoy V.V (AARI)

The geographical position and climatic features of the Arctic Seas create serious preconditions for disturbing the ecological balance at a possible transfer of contaminants of anthropogenic origin to their territory.

The Arctic Seas present accumulative-transit intermediate natural zones between the regions of the active nature use and contamination and the ecologically clean regions of the central polar basin. In addition, the Barents and Kara Seas had local sources of anthropogenic contamination in the past connected with nuclear tests on the polygon of Novaya Zemlya and dumping of radioactive waste in their areas. The increased activities with regard to exploration of the fields of oil hydrocarbons in these seas, further construction and use of production facilities sharply enhance the possibility for accidental oil and gas-condensate spills.

The *largest* water inflow to the Eurasian subbasin is by jets of the North Atlantic current. This flow washing the coasts of industrially developed countries of Europe and America, is one of the main sources of contaminants transported to the Arctic Ocean.

The *second* source of contamination of the Arctic Ocean is input of contaminants with precipitation. At the present time the radioactivity of precipitation is not large being about 2.1 Bq Cs-137 per 1 sq.m a year.

The *third* source of contamination is the input of contaminants with the continental outflow. In recent years there is also a tendency for a significant decrease in the level of radioactive contamination transported with river runoff.

Dumpings of radioactive wastes over the areas of the Barents and Kara Seas present great danger with respect to radioactive contamination of the Arctic Ocean. Total radioactivity of dumped waste is around 90 PBq.

For estimating the contribution of each of the sources, identify possible areas and trajectories of spreading of contaminants at accidental discharges, the use of mathematical modelling is quite promising.

The model consists of two blocks, namely, a dynamical block and a block of diffusion and advection of non-conservative pollutants taking into account transformation. The dynamical block includes two models:

⇒ A stationary three-dimensional baroclinic model of water circulation and ice drift in the Arctic Ocean (Kulakov, Pavlov 1988). This model is used for calculating trajectories and areas of spreading of contaminants by dissolved long-lived radionuclides, such as Sr-90, Cs-137 from possible sources on seasonal and climatic time scales.

⇒ A non-stationary three-dimensional barotropic model which was used for calculating currents and transfer of possible oil contamination over the Kara and Barents Sea areas.

A natural decay of radionuclides served as a non-conservation parameter in calculations of their transfer and transformation. Calculations of the diffusion and advection of oil spills took into account the decay of oil related to evaporation of the oil patch, photo-oxidation and absorption by drifting ice.

For determining the structure of radionuclide contamination from real and possible antropogenic sources the following numerical experiments were carried out.

- 1. One of the largest injections of artificial radionuclides to the marine environment occurred in the mid 1970s at the plant in Sellafield in northern Scotland. Fig. 1 shows results of

- calculations of the structure of radionuclide contamination of the Arctic Ocean with a period of semi-decay about 30 years in percent age of the concentration in the source in the region of the plant in Sellafield. The source function in the calculations was prescribed in accordance with real levels of radioactive contamination in the North Sea (the value recorded in 1975 was assumed to be 100%). The calculation results have shown that the largest radionuclide contamination of the Barents Sea occurred in 1981 and its value was 3% of the concentration near the source and then a monotonic decrease in the radiation level was observed. This is fully consistent with the results of earlier observations.

A comparison of the calculation results with observation data on the structure of radionuclide contamination in the Barents and Kara Seas in 1982 (Fig. 2) has shown their satisfactory coincidence. This indicates, on the one hand, that the model can be applied for obtaining expert estimates and on the other hand, it allows a conclusion that the discharges at the plant in Sellafield are the main source of radionuclide contamination in the Barents and Kara Seas.

This conclusion does not indicate the safety of the region under consideration, since a potential danger of the radionuclide leak from the dumping sites in the Kara Sea area is quite large. Destruction of the shells of containers may occur both as a result of corrosion and mechanical destruction when interacting with an iceberg or stamukha.

- 2. There were made calculations of the areas of radioactive contamination induced by probable inputs of long-lived radionuclides to marine environment at a possible destruction of the sarcophages of nuclear wastes dumped in the Kara Sea area. Calculations have shown that contaminants are transported by currents from the Kara Sea to the north, then to the Greenland Sea by a jet of the Transarctic current and they may reach the western regions of the North Atlantic. The time for the water with a level of contamination of 1 % of its concentration in the source to reach the coast of Greenland is 3 years, but contamination in the Greenland Sea after a longer period (the quasistationary state is reached in 15 years) does not exceed 3%.

Similar pictures were also obtained for the possible sources in the mouths of large Siberian rivers: Ob', Yenisey and Lena. An analysis of the calculation results has shown the main portion of contamination to fall on the Eurasian subbasin of the Arctic Ocean due to the blocking effect of the Lomonosov ridge.

The increased activities in exploration and production of the oil fields over the Barents and Kara Seas can become an additional contamination source.

For calculating transfer and transformation of oil contamination with known physical-chemical properties - gas-condensate of the Shtockman and oil of Prirazlomnoye fields in the Barents Sea and diesel fuel, numerical experiments were conducted.

Calculations were performed in two stages. At the first stage oil spreading up to the film state on the basis of simplified Fay's equations taking into account advection of the patch and transformation processes was calculated. At the second stage spreading and transformation of the oil film on the basis of resolving the equations of advection and diffusion of a non-conservative mixture were calculated. For calculating advection the Lagrangian approach was used.

Of the processes of oil transformation, the processes of evaporation, photo- and bio-oxidation were taken into account.

Fig. 3 shows an example of calculating spreading and transformation of the discharge of 250 tons of diesel fuel in the Baidaratskaya Gulf. There are shown changes in the form of the fuel patch with time. By area the patch occupies one cell of the calculation grid.

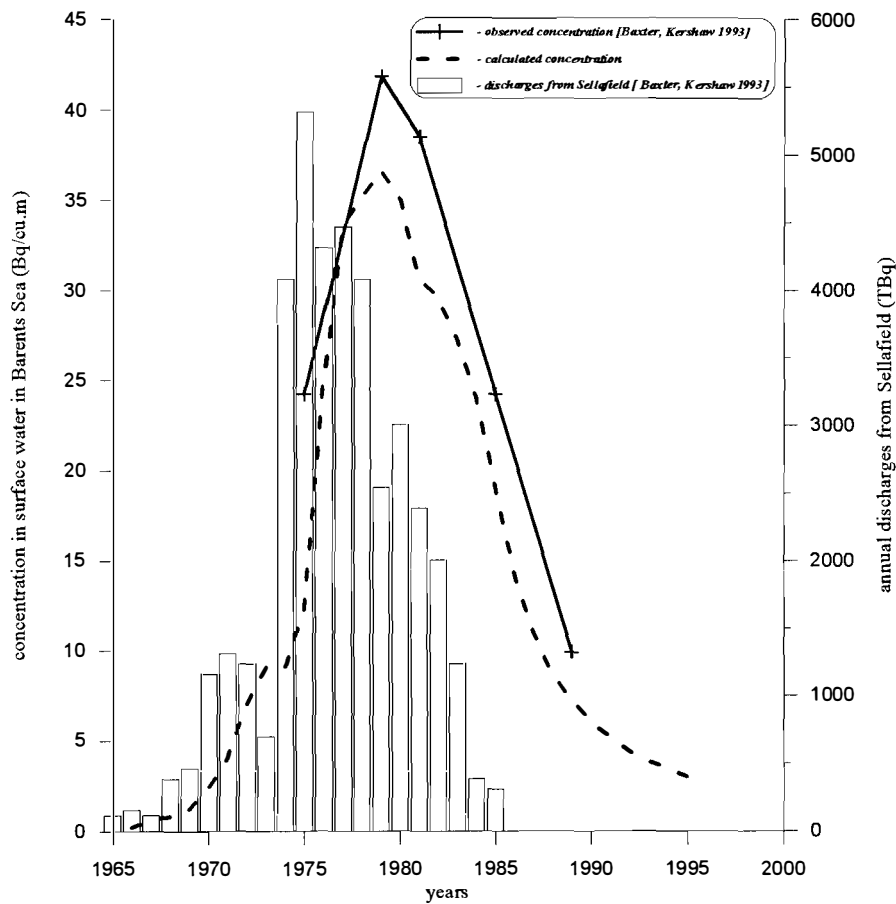


Fig.1. The time-dependent variations of Cs-137 concentration (Bq/cu.m) in surface water in Barents Sea and Sellafield discharge (TBq)

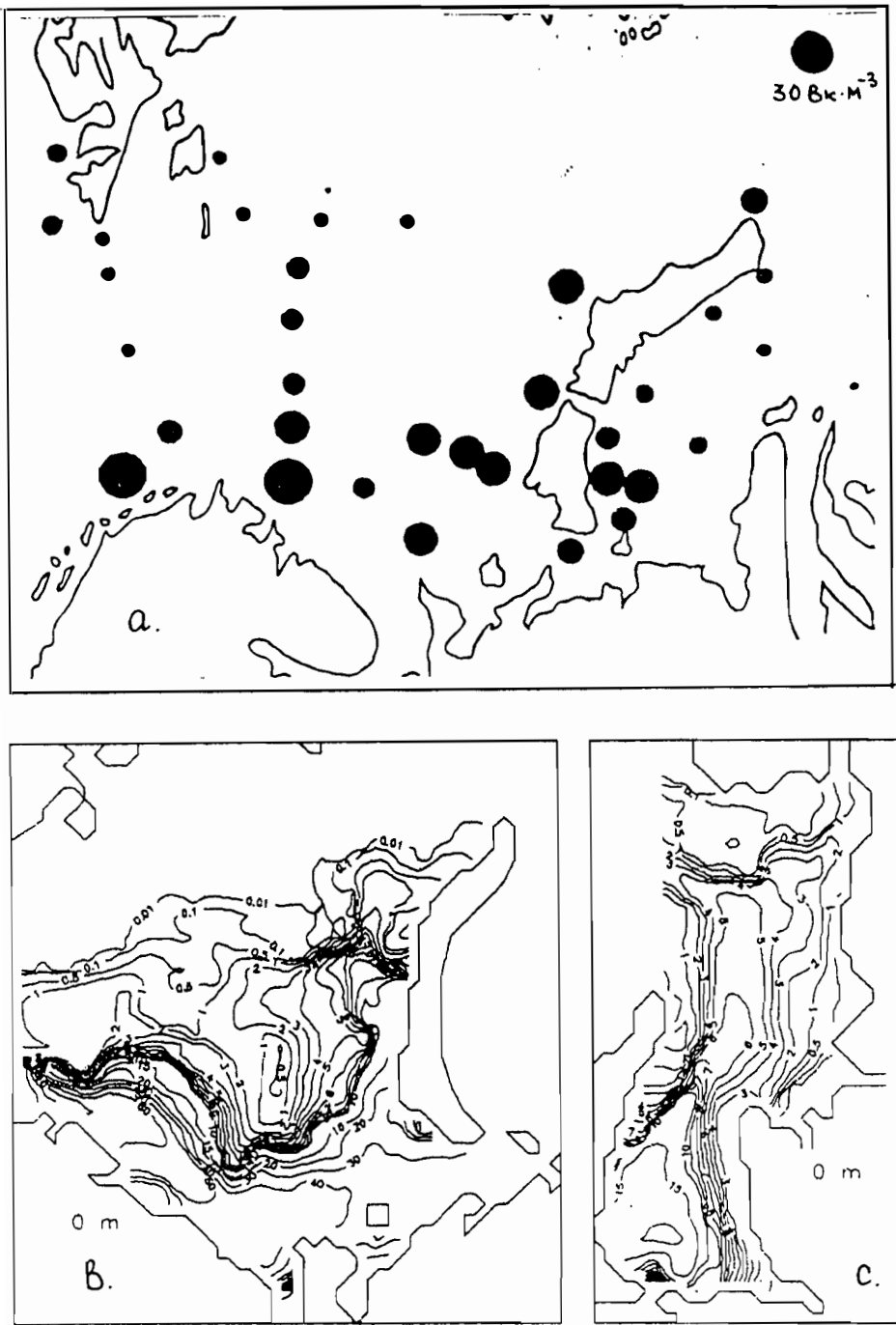


Fig. 2 The distribution of the Cs^{137} concentration (Bq/ cu.m) in the Barents and Kara Seas in 1982 (A) and calculation results of the distribution of the Cs^{137} concentration (%) in the Barents (B) and Kara (C) Seas from the Sellafield plant.

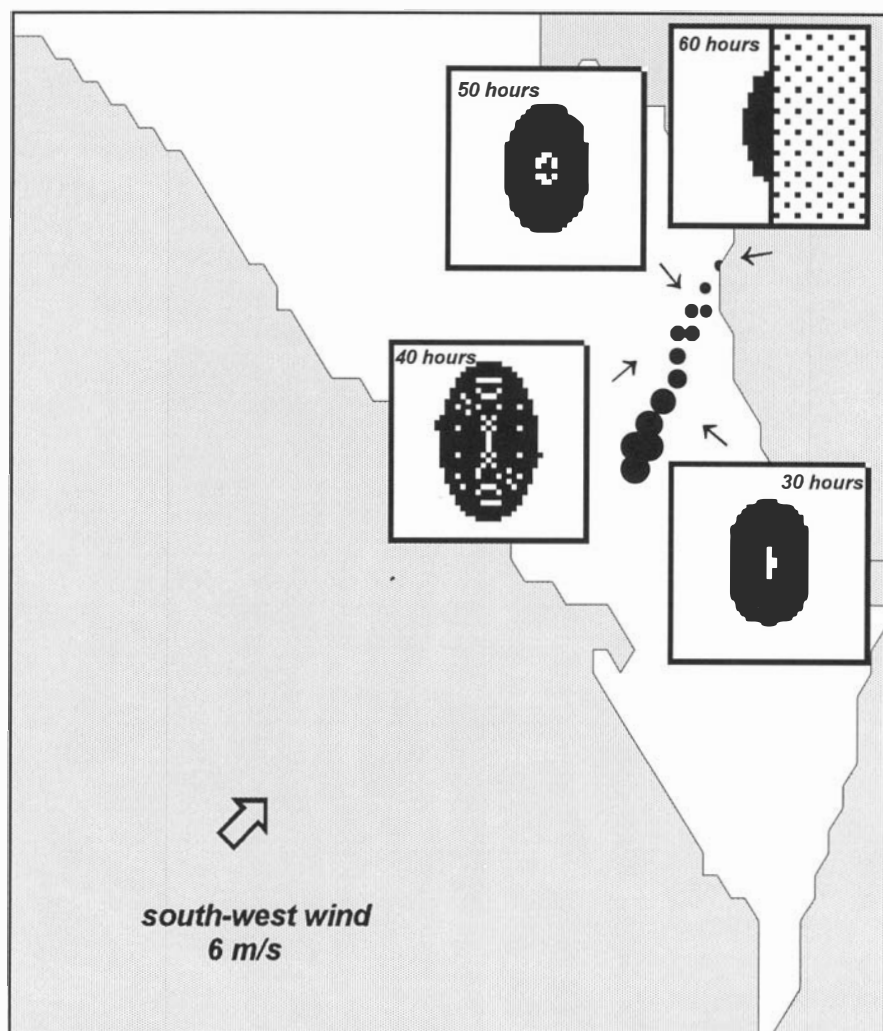


Fig.3. Transport and transformation of the fuel spill (volume 250t.)

The results of calculating the processes of oil transformation allowed determining the "life-time" of the oil spill depending on the wind speed, volume of discharge and ice concentration.

At present the models are being improved, but already now the models presented can be used for forecasting the consequences of accidents in the Arctic Seas

References

Kulakov, M.Yu., Pavlov, V.K. A diagnostic model of water circulation of the Arctic Ocean.- Proc. of the AARI, vol.413, 1988, pp.5-16.

PRELIMINARY STUDIES OF BENTHIC FAUNAL COMMUNITIES IN THE ESTUARIES OF OB AND YENISEY

Sabine Cochrane, Line Kjeldstrup, Rune Palerud & Salve Dahle (APN)

Introduction

Preliminary studies of benthic fauna in the estuaries of Ob and Yenisey were carried out, based on material collected during the "Karex-94" expedition. The biomass of the different animal groups in the communities was recorded (wet weight), as an indication of community composition. Species identification was carried out for the Polychaete worms and Crustacea. Identification of the remaining phyla is scheduled to be completed soon.

The area map* shows the sampling stations included in this first phase of the benthic investigations.

○ - Stations investigated in estuaries of Ob and Yenisey.



Results

Ob stations

The fauna at the mouth of the Ob showed a community mainly composed of Annelid worms, Bivalve molluscs and Crustacea, of which the Mollusca contributed the highest biomass. The polychaete fauna was the most diverse of the five stations sampled, but showed gross dominance of tube-dwelling species *Ampharete baltica*, which is reported from areas of varying degrees of brackish water (Holthe, 1986). Several species of Crustacea are present, the most numerous being the Cumacean *Diastylis* sp.

Further south in the Ob, the faunal composition shows distinct changes from the previous station. The community is 99.9% dominated in biomass by Annelid worms, with only very few representatives of the Crustacea. Of the Annelida, a few individuals of the phylum Oligochaeta, a primarily fresh-water group, are present, while the remainder of the community is exclusively composed of the Polychaete *Marenzelleria* sp., which is known to be tolerant to brackish water. This genus is in need of taxonomic revision, and the origins and taxonomic relationships of the species found in this study are yet unclear. The sparsity of taxa at this station suggests a high degree of environmental stress, with only very few species able to adapt to this highly specialised niche of seasonal salinity variations.

The fauna at the southernmost sampling station in the Ob shows a transition to an exclusively fresh-water community, with the biomass being almost equally divided between

fresh-water Oligochaeta and bivalve Mollusca. This suggests that the bottom water layer is largely composed of purely fresh, rather than brackish water.

Yenisey stations

The outermost station sampled in the Yenisey showed a faunal community dominated in biomass by bivalve Mollusca, with a lesser representation of Polychaeta and Crustacea. Among the Polychaeta, *Marenzelleria* sp. is represented by the highest number of individuals, as was the case at the middle station sampled in the Ob. The Crustacea are dominated in number by members of the Cumacean genus *Diastylis* sp.

The innermost station sampled in the Yenisey contained a faunal community consisting almost exclusively of Annelid worms and Crustacea, which are almost equal in biomass. The Annelida are mainly represented by the polychaete *Marenzelleria* sp., as was the case at the previous station. However, the numbers are considerably lower, perhaps suggesting that the individuals are approaching their limit of tolerance to reduced salinities. The Crustacea are mainly represented by the Amphipod *Pontoporeia affinis*, which is documented to inhabit brackish areas in the Kara Sea (Lindström 1992).

Discussion

These analyses, although of a preliminary nature, highlight several important features of the bottom conditions in the estuarine areas of the Ob and Yenisey. It should be noted that the animals under investigation are extremely small, and generally live submerged within the sediment. Thus, they inhabit a kind of 'micro-niche' where the conditions in the uppermost millimetres of the sediment profile and the bottom centimetre or so of water are the major factors governing the distribution and abundance of this benthic infauna. As a result of this, species which do not tolerate pure fresh-water may be found in areas where oceanographic recordings indicate an even profile of fresh-water. In these cases, it is likely that some saline water is retained in the boundary layer at the sediment-water interface.

It is interesting to note the complete absence of Echinodermata at all five stations sampled, which is likely to indicate the influence of brackish-water, even at the outermost stations. The relative paucity of species represented in the samples, particularly in the case of the Polychaeta, indicates the stressful nature of the benthic environment in these estuarine areas. The transition from a brackish to fresh-water communities is very marked, and can serve to 'map' the extent of influence of the salt-water tongue, which is known to exist in many estuarine areas, at water depths of only a few centimetres above the sediment surface.

In conclusion, the structure of the benthic faunal communities in the estuaries of the Ob and Yenisey are considered largely to be governed by physical factors, the main influence being salinity. Physical factors of the sediment, as well as sedimentation regimes are also likely to play a role in structuring the benthic faunal assemblages.

References

- Holthe, T. 1986. Polychaeta Terebellomorpha. *Marine Invertebrates of Scandinavia* 7: 1-194.
- Lindström, M. 1992. The migration behaviour of the amphipod *Pontoporeia affinis* Lindström. *Walter and Andrée de Nottbeck foundation scientific reports*, No. 7: p 1-18.
- Zettler et al. 1995. Distribution and population dynamics of *Marenzelleria viridis* (Polychaeta, Spionidae) in a coastal water of the southern Baltic. *Arch. Fish. Mar. Res.* 42(2), 209-224.

* area map prepared by Harvey Goodwin (APN)

BIOTIC COMMUNITIES OF THE KARA SEA ESTUARINE ECOSYSTEMS *)

V.V.Khlebovich, A.Yu.Komendantov (ZIRAC)

The Kara Sea estuarine ecosystems are the vastest ecosystems in the Arctic: two rivers, the Ob and Enisey have the annual output equal to more than 1 000 cubic kilometers of fresh water. The biological component of such ecosystems is forming and acting under the effect of a number of abiotic factors. The main factors are the following: the heat, the biogenic and detritic discharges, well-marked halocline and its seasonal tidal, surge displacements. The position of critical salinity zone is masked by the instability of thermohalinic conditions and it is a subject of special biological adaptations.

Biotic communities of estuarine ecosystems are formed by 4 ecological complexes, such as: the euryhaline freshwater, brackish- water, euryhaline marine, and migrating (anadromous) complexes. Each of them has got some own peculiarities in the Arctic, particularly, in the Kara region. As usual, the euryhaline freshwater complex does not withstand the salinity more than 5-8 pro-mille and the euryhaline sea complex does not withstand the salinity which is less than this value. Considering that halocline is exposed to the strong displacement, it can lead to the catastrophic death of euryhaline forms. That fact was noted by the "*Arctic Estuaries-94*" expedition at the stations which had been studied earlier by the "*Enisey-93*" expedition.

The communities of estuarine ecosystems are largely determined by minor amount of species of originally brackish-water complex. The edificators of coenosis are most often the polychaete *Marenzelleria*, bivalve *Portlandia aestivalium* and isopod *Saduria entomon*. The analysis of relations between these species and the salinity allows to consider that they are the indicators of nature processes. *Marenzelleria* is perhaps the physiologically fresh-water species and its presence shows the places where fresh water come to the upper parts of estuaries in winter. *Portlandia aestivalium* indicates the areas of lower part of estuaries exposed briefly to strong freshening. The presence of the sea cockroach *Saduria entomon* characterizes all the estuarine ecosystem. Due to osmoregulation this species can develop dense settlements at low as well as at high salinity but practically this species is inside the estuaries ecosystems because of biotic relation. The estuarine communities of benthic organisms are usually forming round these three species as well as some fish populations.

*) translated by the author

LATE CENOZOIC SEDIMENTATION ON THE SHELF OF THE KARA AND EASTERN BARENTS SEAS *)

E.E. Musatov (ARROI)

Sedimentary processes on the Kara and Eastern Barents Seas Shelf were controlled by distribution of major provenances and depocentres of sedimentation which changed their position several times through Cenozoic. Seismic stratigraphic studies show four main sequences in Cenozoic cover: Paleocene-Eocene marine (only in Southern Kara depression), Oligocene-Miocene lacustrine-alluvial (only in paleovalleys), Pliocene-Pleistocene marine, glacial-marine and glacial and Upper Pleistocene-Holocene glacial-marine and marine. Until Mid-Late Pleistocene vast provenance occurred in the Northernmost part of the region near continental slope of Eurasian oceanic subbasin while depocentres of sedimentation were concentrated in near-shore areas of West Siberia and Pechora lowlands. General direction of terrigenous discharge was from the north to the south. During Pleistocene epoch northern provenance was dissected by deep riftogenous troughs of suboceanic grabens St. Ann and Voronina.

The Late Weichselian time was crucial for evolution of Kara and Eastern Barents Seas environments. Sheet glaciations occurred on the shelf near Franz Josef Land, Novaya Zemlya, Severnaya Zemlya archipelagos as well as on Admiral uplift and Northern Kara plateau. Numerous local (insular) Severnaya Zemlya-type glaciations were controlled by distribution of bottom highs. Low humidity prevented generation of tremendous glaciers similar to Western Barents type. Vast gently undulating plains onshore and offshore Northern Eurasia were at that time a polar desert where major cryolithozone was developed: thick permafrost was created.

The Late Weichselian time developed during maximal shelf erosion: bathymetric, single channel seismic, echo-sounding data and sparker records suggest that paleovalleys existed at modern depths from 50 to 250-300 m. Wide-spread periglacial terrestrial conditions existed in shelfal areas and some islands under continuous deposition of lacustrine-swamp sequences within 24000 to 8000 BP. Glacial-marine Upper Weichselian sediments are established by coring in deep troughs and depressions of Eastern Barents and Kara Seas Shelf at modern depths more than 150-200 m.

Thirteen layers of recent sediments were revealed by coring in St. Ann trough: glacial Late Weichselian tills are overlaid by laminated turbidite-type glacial-marine Latest Weichselian-Early Holocene silty clays and marine Late Holocene clays. Thicknesses of post-glacial deposits vary from few sm on shelfal highs and in outer parts of deep troughs to 5-10 m and even more in modern fjords, near steep slopes of troughs (predominantly silts and clays) and in coastal zones of West Siberia and Timan-Ural regions (predominantly sands).

Total thicknesses of Quaternary sediments vary from 0 m in shelfal areas with exposed bedrock to 100-150 m in deep depressions of pre-Quaternary relief and paleovalleys. For example, Cretaceous rocks are exposed on the bottom of East Novaya Zemlya trough with modern depths more than 400 m. Generally thicknesses of Cenozoic cover and Quaternary veneer are controlled by neotectonic movements of the crust in Eastern Barents and Kara Seas region.

Series of maps and schemes are compiled; map of Quaternary sediments, maps of pre-Quaternary relief and thicknesses of Upper Cenozoic cover and postglacial deposits, geomorphic, neotectonic and palaeogeographic maps, etc.

*) *translated by the author*

THE HISTORY OF THE RADIOACTIVE CONTAMINATION OF THE OB RIVER SYSTEM

*H.D.Livingston, G.P.Pantelev, F.L.Sayles (WOI),
Vl.Vl.Ivanov, O.N.Medkova (AARI)*

- (1) Woods Hole Oceanographic Institution, Woods Hole, MA 02543 U.S.A.
- (2) Arctic and Antarctic Research Institute, St.Petersburg, Russia

As an approach to an assessment of the transport of artificial radionuclides through the Ob river system towards the Arctic Ocean, results are presented from the analyses of a series of sediment cores collected in the Ob delta and estuary in 1994. These cores, collected in areas of sediment accumulation, contain the depositional history at the Ob mouth of substances associated with sediment particles from the whole river system watershed. Several approaches to dating these sediments permitted the development of a chronology for the deposition of plutonium isotopes and Cs-137 - following their first introduction to the environment a half century ago. Some preliminary results for I-129 are also presented from Accelerator Mass Spectrometry (AMS) measurements made by G.M.Raisbeck, F.Yiou (CNRS, Orsay, France) and L.R.Kilius (University of Toronto, Canada).

The sediment cores were collected from a shallow-draft catamaran capable of entering the small lakes (Sor or ox-bow) which are associated with the Ob river system (Fig.1). These lakes are flooded each spring after the ice melts. They are excellent sediment traps which can accumulate the annual pulses of suspended sediment carried by spring/summer floods. Using a Global Positioning System and a depth sounder, we tried to find sites where undisturbed layers of sediment were accumulating. The sediments of a number of these small lakes were sampled with a gravity core, sectioned horizontally and analyzed for radionuclides. Cs-137, Pb-210 and Ra-226 (by its Pb-214 daughter) were measured by Ge gamma spectrometry, Pu isotopes by radiochemistry and alpha spectrometry, and some limited I-129 and I-127 data by Accelerator Mass Spectrometry (Raisbeck et al., above). The downcore distribution of Cs-137 provided the first indication of the record of its depositional history on these cores. The dates of the sediment layers in the cores were determined by the excess Pb-210 method (the amount of Pb-210 not supported by its Ra-226 precursor). Cs-137 profiles in four of the cores are shown in the left panels of Figure 2. Pu-239, 240 data for three of these cores are also shown. At present we have data from eight of the sites sampled in 1994. One of the sites, Ob94-13, is from the Taz estuary and represents a control site which does not receive material transported down the Ob.

The main feature in all of the cores analyzed is a major Cs-137 concentration maximum at various depths downcore. The Pb-210 dating indicates that the time of deposition of the sediments with which these peaks are associated was concurrent with the maximum in deposition of global fallout from nuclear weapons testing in 1961-62. The varying depths of the maximum reflect the differing rates of sedimentation which characterized the cores (0.1-1.6 cm/yr.). The Cs-137 profiles measured, reflect a complex variety of sedimentation regimes - including some where post-depositional erosion is evident. The inventories of Cs-137 (Fig.3), also vary with the nature of sediment accumulation but are always in excess of the estimated integrated fallout delivered to this latitude (based on data from sites in Alaska).

The ratios Pu-239, 240/Cs-137 and Pu-238/Pu-239, 240 can provide evidence of the source of these isotopes. Figure 4 shows the downcore ratio Pu-239, 240/Cs-137 in 5 Ob delta cores and the one from the Taz estuary and compares these values with average values for global fallout and Techa river sediments (referenced in, Panteleyev, G.P., The History of Plutonium and Cs-137 Contamination of the Ob River Delta Sediments, M.Sc.Thesis (submitted), Woods Hole Oceanographic Institute, Woods Hole, MA,

U.S.A.1995) - all at a reference data of 1 August 1994. Figure 5 compares the mean and standard deviation of the downcore ratios Pu-238/Pu-239, 240 with fallout and Techa values (same reference). Finally, the preliminary I-129 results mentioned above, measured in 9 sections from core Ob94-8 are shown in Fig.6. They are plotted against both depth and a Pb-210 derived timescale, and compared against similarly plotted Cs-137 and Pu-239,240 data.

Several conclusions can be drawn from the data collected. The preservation of the record of radionuclide deposition, as described above, can be inferred from the agreement of the Pb-210 dating with the characterization of the mean Cs-137 and Pu peaks in the cores as being derived from the fallout from atmospheric nuclear weapons tests in the 1960's. This was true not only of the Ob delta cores, but also the control core from the Taz estuary. The isotope ratio data are consistent with the fallout source. Mayak contaminated sediments in the Techa river have Pu/Cs-137 and Pu-238/Pu-239,240 ratios close to an order of magnitude lower than those seen in the Ob delta sediments. This strongly indicates that the fallout signal is dominant and that contributions from the Mayak source are either absent or too low to be seen against the fallout record.

The I-129 profile in Figure 5 shows a maximum at a time horizon in the late 1980's. However, the I-129/I-127 profile shows a less pronounced peak at the level of the I-129 maximum and a gradient of decreasing ratios both up and down core - ending up an order of magnitude lower at the deepest point analyzed for I isotopes. This pattern seems consistent with a source or sources of I-129 additional to those discussed above. It is likely that post-depositional migration of solubilized iodine within sediment interstitial water will have affected the observed distribution. In addition to such possible sources as Chernobyl and Mayak, one must also consider venting from underground nuclear tests held at Novaya Zemlya. One such test on August 2, 1987 lead to fission products being detected over Scandinavia (Bjurman, B.et al., J.Environ. Radioactivity, 11, (1990) 1-14). A more detailed Russian report estimates that $3.7 \cdot 10^{13}$ Bq of Iodine radionuclides were released to the atmosphere. The same report lists earlier venting incidents which lead to fission products being detected in the Ob river region, including Salekhard and Khanty-Mansisk (Nuclear explosions in the USSR. Part 1.Northern Test Site. Reference information. Moscow, 1992. 194 pps.).

The main conclusions which can be drawn from this study are: 1. oxbow lakes are excellent sediment traps and do preserve the

historical record of radionuclide deposited there (and, likely, other artificial contaminants),

2. the dominant source of the Pu and Cs-137 in the sediments is global fallout from atmospheric nuclear weapons tests,

3. the contribution of particle reactive radionuclides from "Mayak" is not detectable in comparison to the fallout signal,

4. AMS measurements suggest that these sediments may contain I-129 from a source additional to fallout from atmospheric nuclear weapons tests.

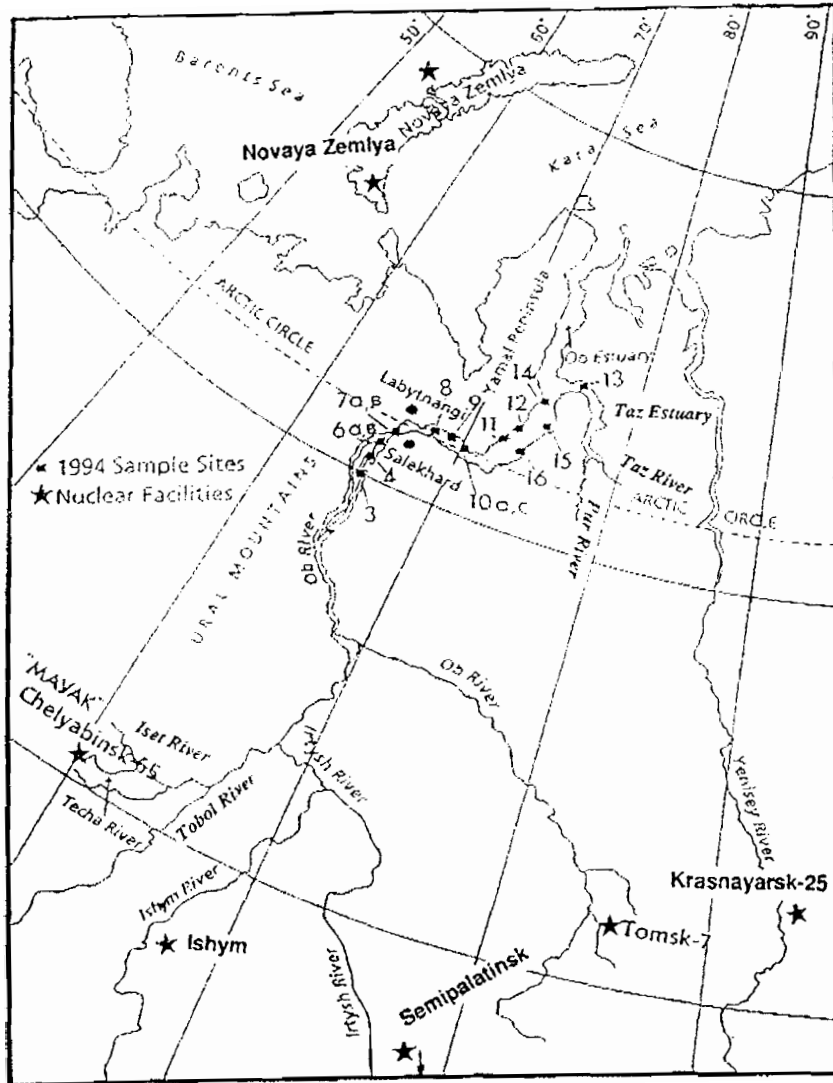


Fig. 1 Map of the Ob River Watershed and sampling locations of the Joint Russian-American Expedition "Ob Estuary-1994".

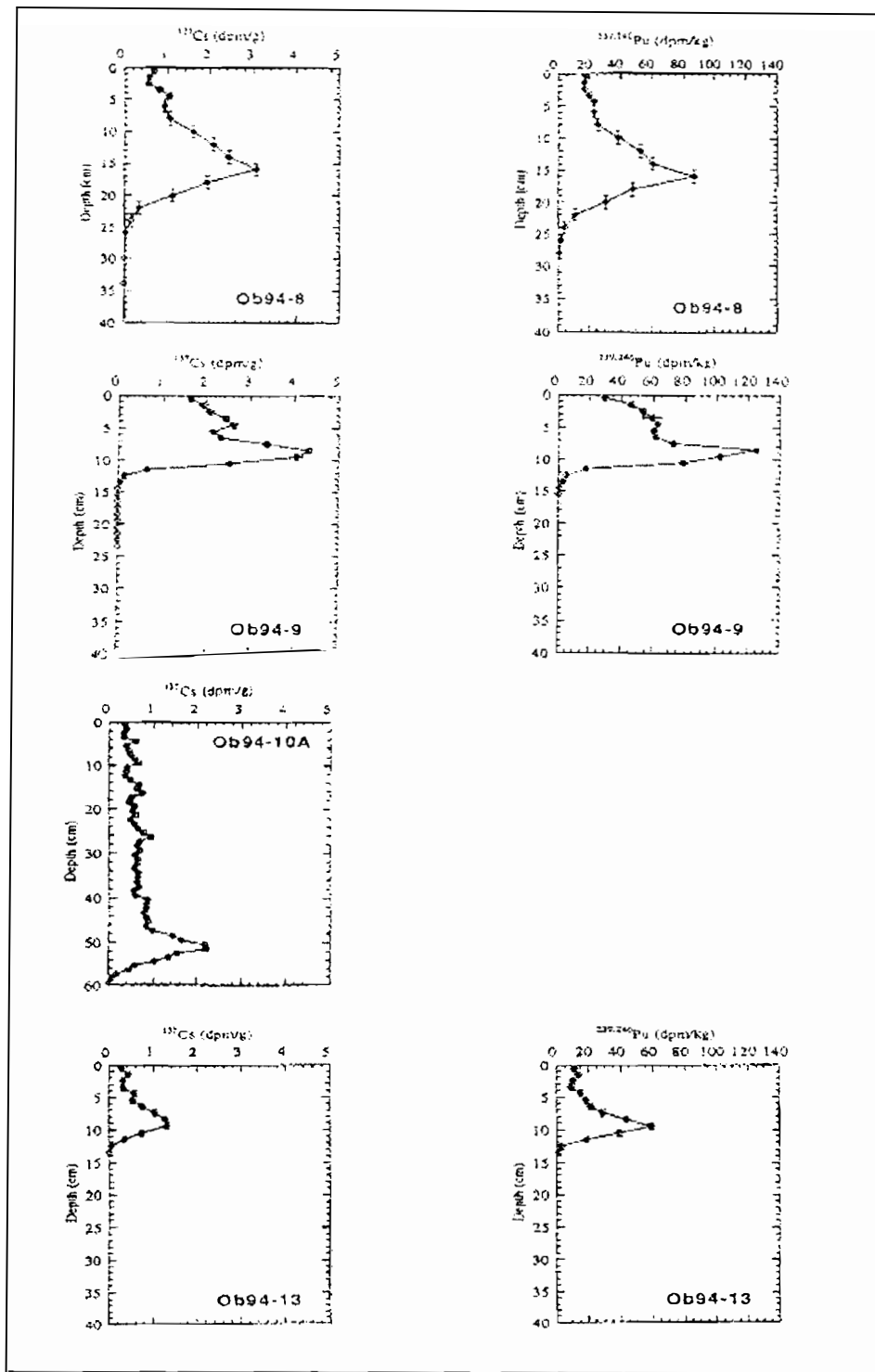


Fig. 2 Pu and Cs-137 profiles in Ob delta (8,9,10a) and Taz estuary (13) cores.

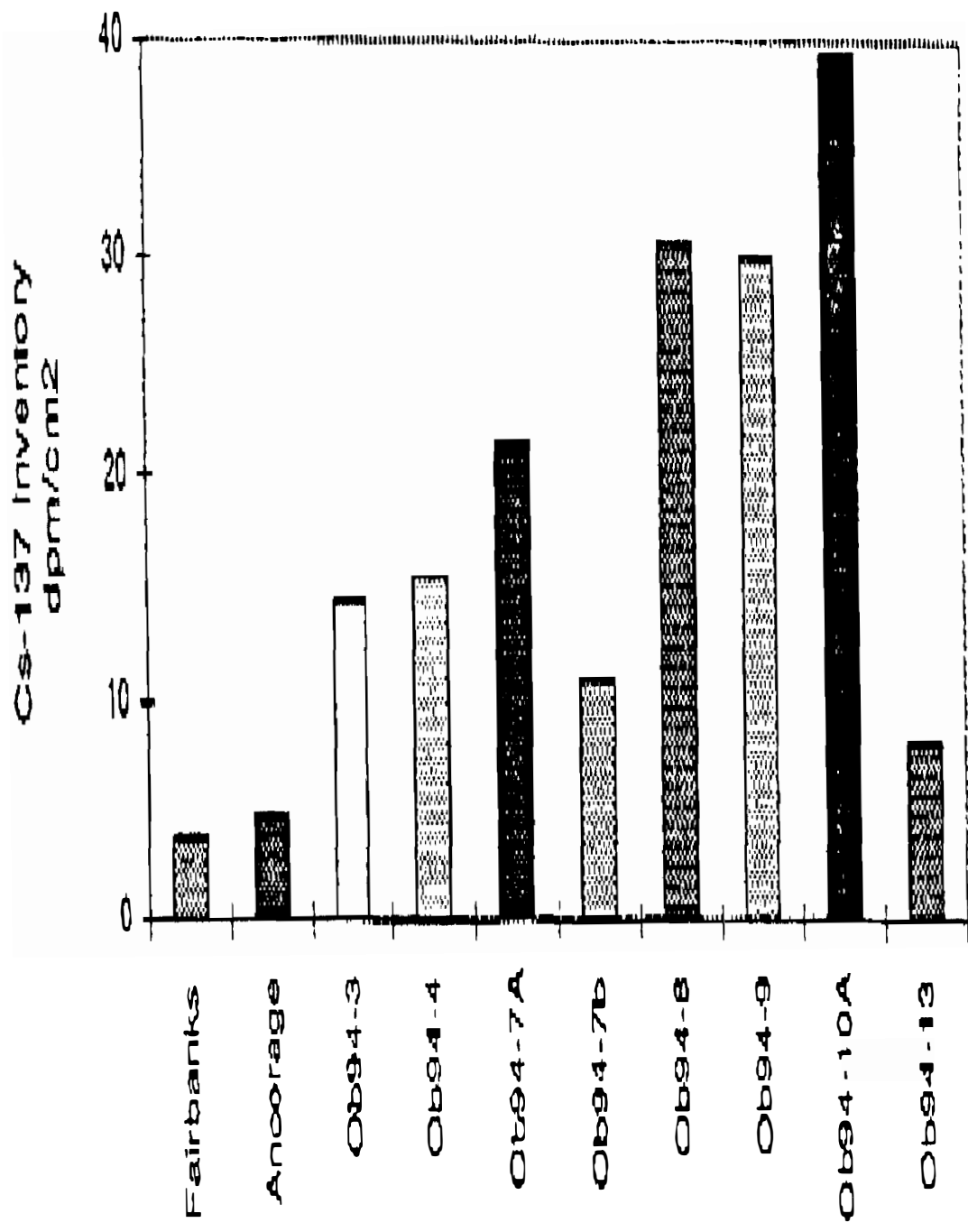


Fig. 3 Cs-137 inventories (dpm/cm²) calculated for Ob delta; Taz estuary sites and estimated for direct Global fallout at Fairbanks and Anchorage, Alaska.

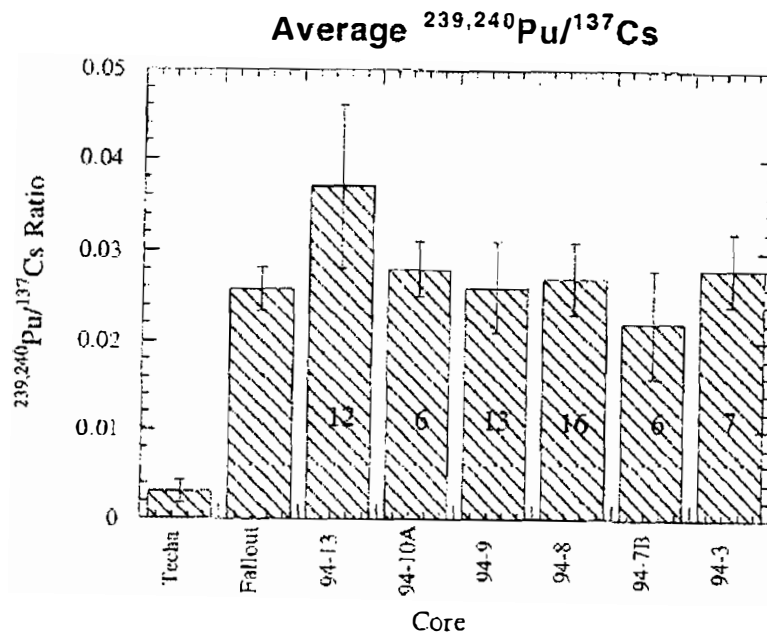
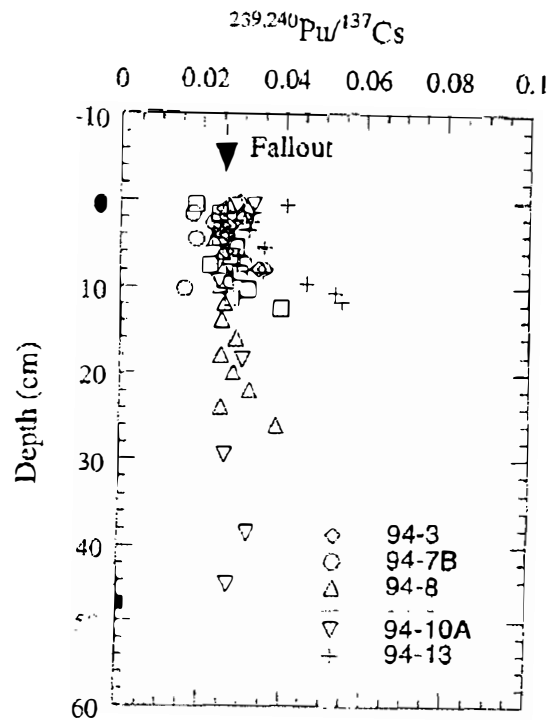


Fig.4 Pu/Cs-137 in Ob delta sediment, bomb fallout and Techa river sediments.

Pu Ratios

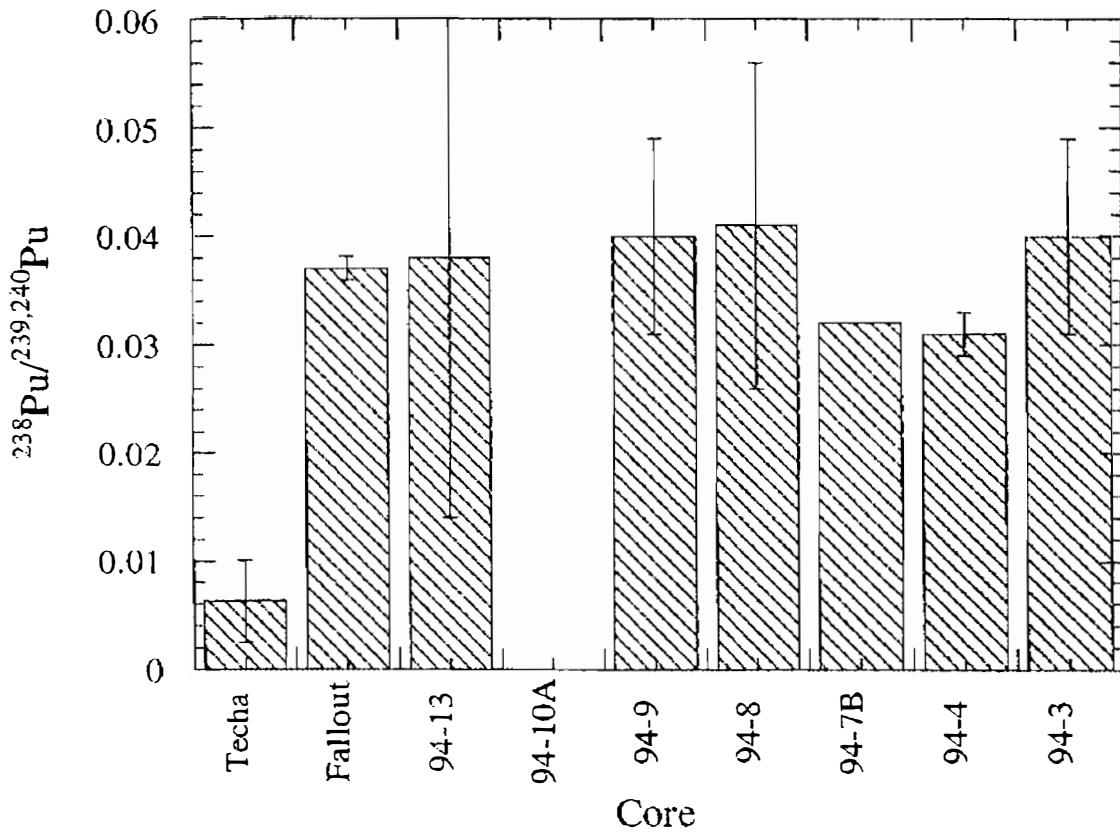


Fig. 5 Pu-238/239,240 in Ob, Techa river sediments and bomb fallout.

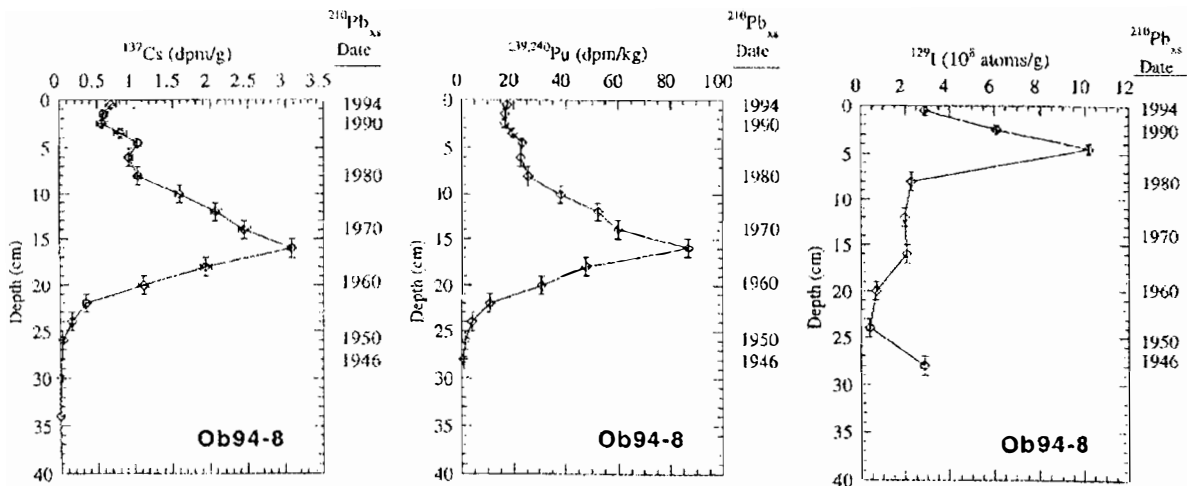


Fig. 6 Pu, Cs-137 and I-129 profiles in Ob delta core 8; dating by Pb-210 method I-129 from Accelerator Mass Spectrometry (AMS) measurements made by G.M. Raisbeck, F. Yiou (CNRS, Orsay, France) and L.R. Kilius (University of Toronto, Canada).

Physical oceanography

THE NUMERICAL MODEL OF DRIFT OF PASSIVE IMPURITY IN ADJACENT REGIONS OF NORWEGIAN AND BARENTS SEAS.

A.S.Averkiev, D.V.Gustoev("Sistema-A"), V.Y.Chantsev(RSHI)

When analyzing the hydrometeorological and fishing information we frequently need to model a particular situation, sometimes in simplified or schematic form. Answering this need is numerical modelling. Although numerical models are not able to provide an unambiguous answer of all issues on fishing forecast, they help in the determination of the mechanisms influencing on fishing and in the classification of situations by certain features.

Thus, the complex of programs, allowing the current speed and passive impurity transport speed to be calculated in the adjacent regions of the Norwegian and Barents Seas, has been worked out. The region under study is within 5° and 33.5° E, and 74.5° N and the coast of the Scandinavian peninsula (Fig.1).

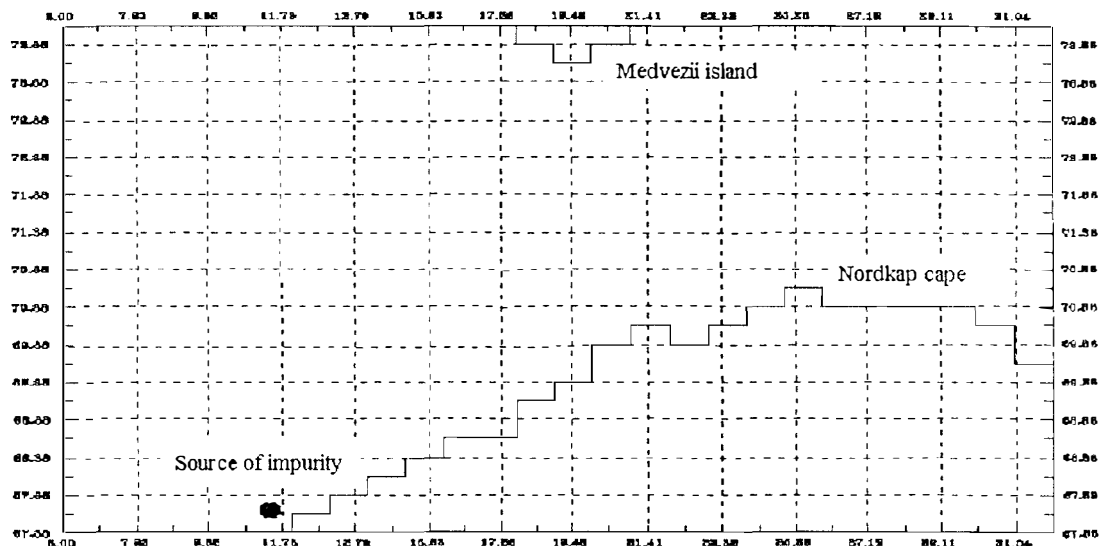


Fig.1 Region under study, calculated grid and location of the impurity source

The circulation calculation is carried out for the upper layer. Geostrophical and drift constituents of current speed are added at points of the $0.25^{\circ} \cdot 1.0^{\circ}$ grid with the 5-day time step in the period March-August.

A geostrophical constituent is found by the dynamic method at standard levels for the reference level of 200m. A drift constituent is done with the help of the tangential wind stress and taken as the mean (constant) value for the upper Ekman layer (the depth to which the wind tangential stress penetrates). The impurity (cod caviar) spreading calculation is performed by the method of random walk.

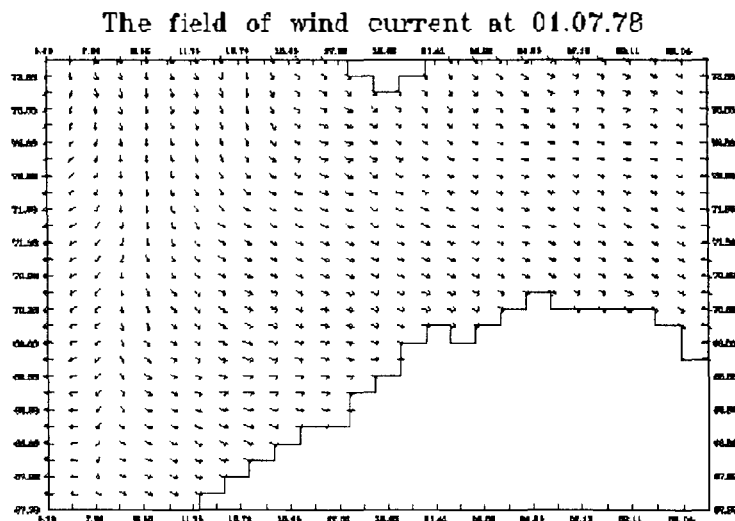
This method allows us to keep track of the marked particles path (the markers path). The resultant vector of the particle drift for one time step consists of the mean drift vector (under the influence of the main flux, i.e. the sum of geostrophical and drift constituents) and the random drift vector. The length of the random drift vector is found from the laboratory and numerical experiments, and it parameterizes the turbulent flow. The direction of vector is prescribed arbitrarily using a random number generator.

1978 and 1983 have been selected for testing calculations since these years are the most representative and well provided with the observational data, and also they differ considerably in thermal and dynamic situations. In calculations of the impurity spreading (movement of markers) the source was not far from the West-Fiord (67.5° N, 11.5° E) (refer to Fig.1). It is suggested that the main cod reproduction takes place here. The source was

operating for a month (6 five-day time steps), i.e. from the 5th of March till the 5th of April. It is apparent that beyond the Fiord the cod caviar moves towards the north and north-east with the main flows.

A number of numerical experiments were performed to investigate the influence of thermal and dynamic conditions of this region on the hydrobionts spreading, being in the passive stages of development. In order to learn the relative contribution of the geostrophical and drift (Fig.2a,b) constituents to the resultant transport the calculations considering these constituents separately from each other were carried out.

a)



b)

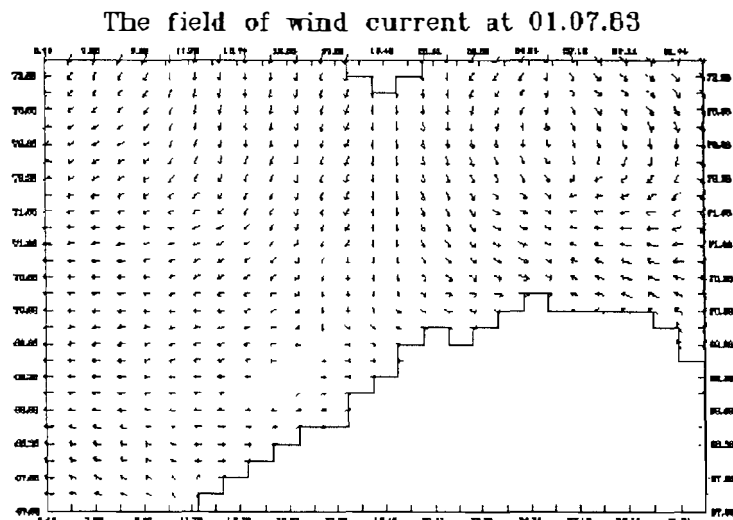
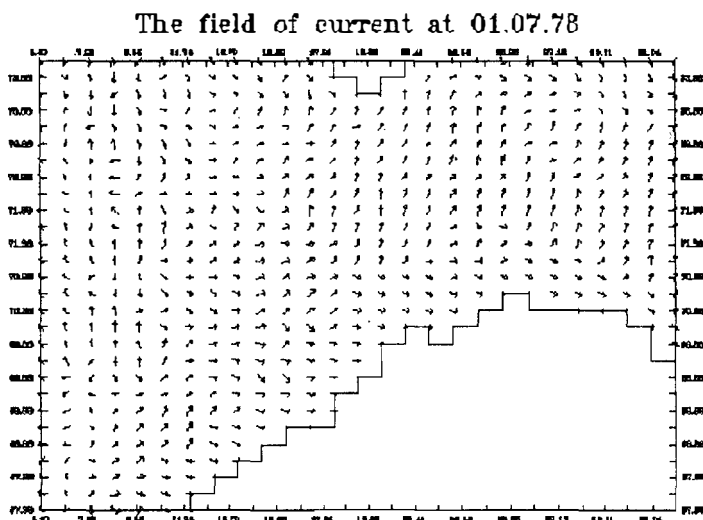


Fig.2 Drift current constituents in the region under study in 1978(a) and 1983(b).

Contributions of the constituents to the resultant speed vector are approximately the same for the whole region. But as predicted, the geostrophic constituent is the major transporter to the north and north-east, and the drift constituent either increases or reduces the transport depending on the prevailing baric situation. The contribution of the random constituent is determined when the markers transport is being calculated. It parameterizes the turbulent motions and does not exceed 10-12 percent of the resultant speed length (Fig.3a,b).

a)



b)

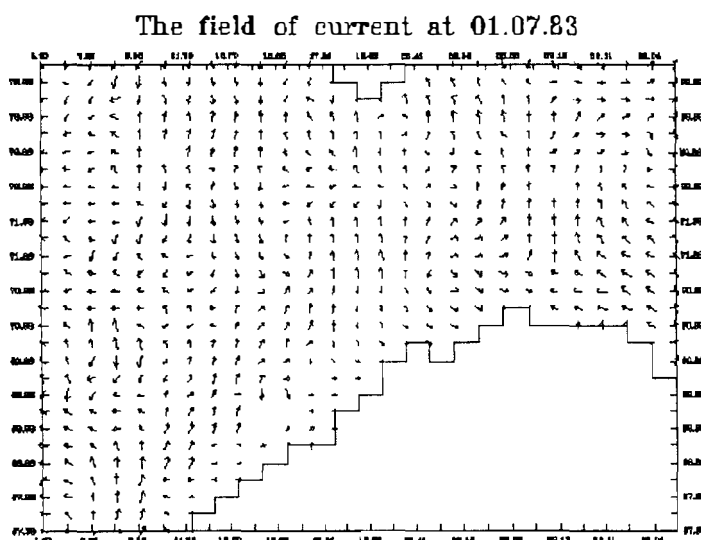


Fig.3 Resultant speed vector for the region under study in 1978 (a) and 1983 (b)

Modelling of the passive impurity transport clearly illustrates that the hydrobionts distribution over the water area differs rather significantly depending on thermal and dynamic conditions (for example, cold and warm years). In this case, in 1978 all the impurity remained within the Norwegian Sea water area, in 1983 about 95 percent of it was moved to the Barents Sea (Fig.4a,b).

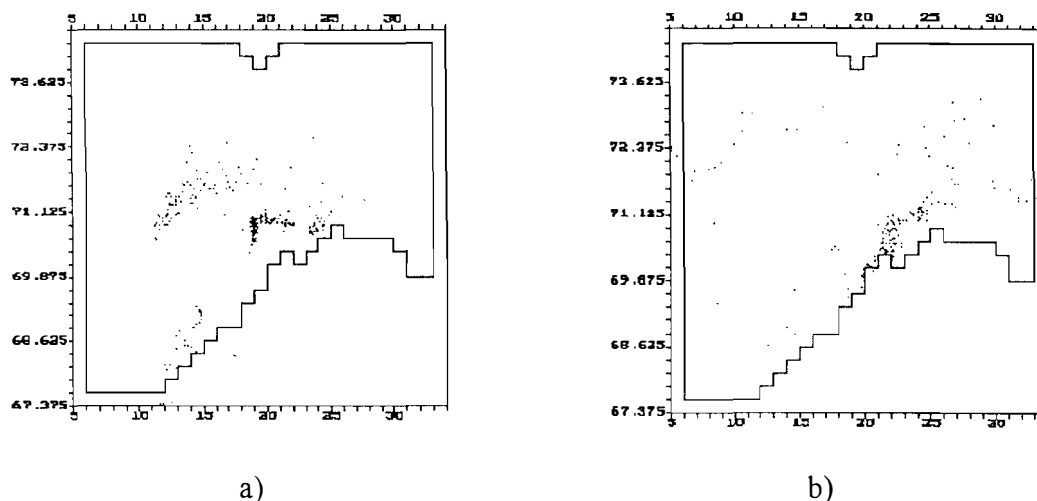


Fig.4 Final impurity distribution over the Norwegian and Barents Seas water area in 1978 (a) and 1983 (b)

Thus, the testing calculations show that the model is correct and can be used for further calculations. For more close analysis the archives on hydrological and fishing data available now at relevant institutions should be involved.

UNIFORM HYDROLOGICAL REGIONS OF THE KARA SEA AND THEIR REGIME CHARACTERISTICS

I.M. Ashik, Yu. A. Vanda (AARI)

Studies of the hydrological regime of sea areas, development and improvement of marine hydrological forecasting methods, optimization of the network of sea stations and other problems of scientific and applied character require a preliminary delineation of regions that differ in physical-geographical features, hydrological conditions and variability both on seasonal and synoptical scales.

For regioning of the Kara Sea a uniform character of surge level oscillations was chosen as the main characteristic. Level fluctuations are considered to be an integral characteristic of the dynamic state of the hydrosphere. The regioning has been made using techniques of objective classification in accordance with an algorithm described by Gruza and Ran'kov (1970). As a matrix of distances characterizing similarity of objects, the matrix of maximums of mutual correlation functions of surge level oscillations is employed. There were used data of sea level observations at four fixed synoptic hours at 16 polar stations located on the coast and islands of the Kara Sea.

An analysis of the results of calculations has shown a significant difference in the character of surge level oscillations for the south-western and north-eastern sea regions. In turn, three regions can be identified in the north-eastern sea: Northern, Central and Coastal regions with the North-Taimyr subregion in the latter (Fig.1).

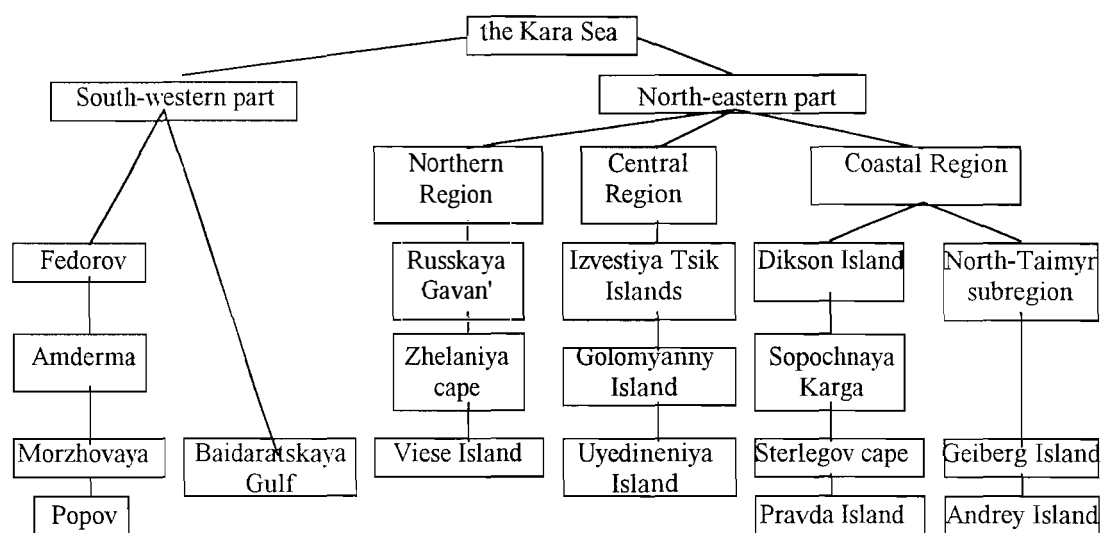


Fig. 1. A scheme of regioning of the Kara Sea on the basis of objective classification of surge level oscillations.

As is known, the character of surge oscillations of the sea level is governed by a combination of the dynamic and conservative factors. The dimensions of the Kara Sea are comparable to those of pressure systems inducing surge level oscillations which allows speaking about a relative uniformity of the dynamic factor for its entire area. Thus, the differences in surge level oscillations for different regions of the Kara Sea should primarily be governed by morphometric features of these regions: configuration and orientation of the coastline, bottom relief. When delineating the boundaries between uniform regions, it was attempted to take into account to a maximum extent the features of morphometry.

The boundary between the south-western and north-eastern regions of the Kara Sea passes from Belyi Island to the north-eastern tip of Novaya Zemlya (Fig. 2). The south-western Kara Sea is characterized by a strong non-uniformity of bottom relief at the background of comparatively large depths: in the western zone of this region there is the Novozemel'sky Deep with maximum depths exceeding 400 m, over most of the area depths from 50 to 100 m prevail and only in the south-easternmost zone of this region—the Baidaratskaya Gulf, mean depth is about 20 m. Unfortunately, the Baidaratskaya Gulf is not covered by observations of sea level oscillations which does not allow us to unambiguously identify it as a separate region. However, in view of its position, evidently, the Baidaratskaya Gulf can be delineated as a subregion of the south-western Kara Sea.

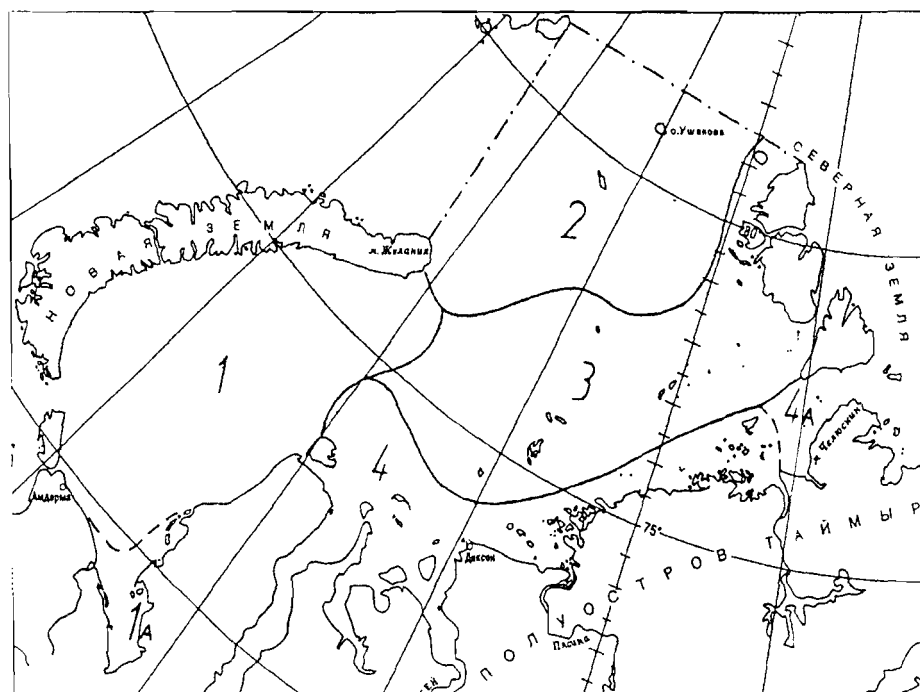


Fig. 2. Uniform hydrological regions of the Kara Sea. 1 - south-western part; 1a - Baidaratskaya Gulf; 2 - the Northern Region; 3 - the Central Region; 4 - the Coastal Region; 4a - the North-Taimyr subregion

In the north-eastern Kara Sea the boundary between the Northern and Central regions passes in the vicinity of the 100m isobath from the north-eastern tip of Novaya Zemlya Island to Shmidt Island, and the boundary between the Central and Coastal regions - in the vicinity of a 25 m isobath along the continental coast (Fig. 2). The morphometry of all three regions is rather complicated. In the central zone of the Northern region there is the Central Kara Elevation with Ushakov and Vise Islands, east of it is the Voronin trough with maximum depths exceeding 300 m, and westward is the St. Anna trough with maximum depths exceeding 600 m. The depths of the Central region vary from 20-30 to 100-150 m and of the Coastal region do not exceed 20-25 m except for the North-Taimyr subregion whose mean depth is about 100 m.

The coastline limiting the north-eastern Kara Sea is oriented from north to south along the eastern coast and from the north-east to the south-west along the southern coast. The coastline of the south-western sea forms a semi-closed contour opened from the north-eastern side.

Thus, it is evident that the delineated areas, regions and subregions have a significantly different morphometry which governs the difference in the character of surge oscillations of the sea level.

By using a numerical model described by Ashik (1994), there were calculated and plotted dependence graphs of surge fluctuations on the speed and direction of regional wind for the delineated uniform regions. Calculations indicate that an effective surge direction for the stations located in the south-western Kara Sea (Amderma st.) and in the Northern region (st. at the Viese Island) of its north-eastern zone is north-west-south-east. However, at one and the same wind force the value of level oscillations in the south-western sea exceeds the value of these oscillations in the Northern region by 1.5-2 times. For the Central region (st. Izvestiya Tsik Islands) and the Coastal region (st. of Dikson Island) an effective surge direction is west-east, however, the value of level oscillations in the Coastal region at one and the same wind force exceeds by about 5 times such oscillations in the Central Region. At the same time the values of level oscillations in the Northern and Central regions are close to each other at one and the same wind force.

The regioning of the Kara Sea made is on the whole in good agreement with the results obtained earlier by analyzing seasonal level oscillations (Dvorkin et al, 1979), as well as spectra of free oscillations (Proshutinsky, 1993). A consistency of the results of the Kara Sea regioning when using different methods, proves an objective existence of uniform regions and their correct localization.

References

1. Ashik I.M., Numerical methods of sea level oscillations and ice concentration in the Laptev and East-Siberian Seas. - In: "Scientific results of the expedition "LAPEX-93", St. Petersburg, Gidrometeoizdat, 1994, pp.199-209.
2. Gruza G.V., Ran'kov E.Ya., On the principles for automatic classification of meteorological objects. - Meteorology and Hydrology, 1970, No.8, pp.12-22.
3. Dvorkin Ye.N., Zakharov Yu. V., Mustafin N.V., Seasonal and multiyear variability of the Kara Sea level. - 1979, Proc. of the AARI, vol.361, pp.63-71.
4. Proshutinsky A.Yu., Level oscillations in the Arctic Ocean.- St. Petersburg, Gidrometeoizdat, 1993, 216 p.

NUMERICAL FORECASTS OF SURGE FLUCTUATIONS OF THE KARA SEA LEVEL

I.M. Ashik (AARI)

Surge level oscillations in the Kara Sea can reach significant values and considerably influence economic activities of different onstitutions. Primarily, this concerns shipping and cargo operations at the roadstead in shallow regions: at crossovers of river mouth regions, in bar areas, in straits and at unloading points, but it is also of importance for drilling activities on the shelf.

Since 1991, prognostic calculations of non-periodic level oscillations over the areas of the Russian Arctic Seas are carried out all-year-round on an operational basis at the Center of Ice and Hydrometeorological Information of the AARI (CIHI). The calculation methods are based on using a coupled two-dimensional ice-hydrodynamic model describing the dynamics of interacting water masses and ice cover.

$$\begin{aligned} \frac{\partial \bar{U}}{\partial t} + 2\bar{\omega}_z \bar{U} &= -g(H + \xi)\nabla\xi + \frac{(H + \xi)}{\rho_w} \nabla P_a + \frac{1}{\rho_w} \left((1 - C)\bar{\tau}^s + C\bar{\tau}^i - \bar{\tau}^b \right), \\ \frac{\partial \xi}{\partial t} &= -\text{div}(\bar{U}), \\ \frac{d\bar{u}_i}{dt} + 2\bar{\omega}_z \bar{u}_i &= -g\nabla\xi + \frac{1}{\rho_i h C} \left(\bar{\tau}^i - \bar{\tau}^w \right) + \bar{F}, \\ \frac{\partial C}{\partial t} &= -\text{div}(C\bar{u}_i), \end{aligned}$$

where t is time; $\bar{U} = \int_0^{(H+\xi)} \bar{u} dz$ is a vector of a full flow; $\bar{\omega}_z$ is the Coriolis parameter; g is acceleration of the gravity force; ξ is the deviation of the level from a non-disturbed state; H is a non-disturbed sea depth; P_a is atmospheric pressure; ρ_w is water density; $\bar{\tau}^s$, $\bar{\tau}^i$, $\bar{\tau}^w$, $\bar{\tau}^b$ is the tangential friction at air-water, air-ice, ice-water and water-bottom boundaries, respectively; \bar{u} and \bar{u}_i are a mean-by-vertical vector of the current speed and the ice drift vector; ρ_i is ice density; h is the ice thickness; C is the concentration function; \bar{F} is the forces of internal interaction in the ice cover.

The tangential stress at the ice-water and water-bottom boundaries is calculated by means of quadratic dependencies

$$\bar{\tau}^w = R_w \rho_w (\bar{u}_i - \bar{u}) |\bar{u}_i - \bar{u}|, \quad \bar{\tau}^b = K \rho_w \bar{U} |\bar{U}|,$$

where $K = \frac{K_w}{(H + \xi)^2}$; $K_w = 2.6 \cdot 10^{-3}$ is the friction coefficient at the water-bottom

boundary, $R_w = 5.5 \cdot 10^{-3}$ is the friction coefficient at the ice-water boundary.

The tangential stress at the ice surface is assumed to equal the tangential stress at the water surface and is calculated from the dependence

$$\bar{\tau}^s = \bar{\tau}^i = 12.0 \left(1 - \exp(-0.002W^2) \right)$$

where W is wind speed in m/s.

For including internal interaction forces into the model, the approximation is used in the form:

$$\bar{F} = \eta \nabla^2 \bar{u}_i + \lambda \frac{\partial}{\partial x_j} \text{div}(\bar{u}_i) - \frac{\partial P_i}{\partial x_j};$$

$$P_i = -K_p \text{div}(\bar{u}_i), \text{ for } \text{div}(\bar{u}_i) < 0;$$

$$P_i = 0, \text{ for } \text{div}(\bar{u}_i) \geq 0,$$

where $\lambda = \eta = 10^{10} \text{ cm}^2/\text{sec}$ are coefficients of the volumetric and shear viscosity, respectively; $K_p \cong 10\eta$ is the compression coefficient.

At the solid boundaries of the domain the condition of non-flowing is assumed, at liquid boundaries for water the condition of radiation is set and for ice - a free flow. As initial conditions for water and ice, the state of rest is assumed, the concentration function is prescribed in accordance with the real ice distribution. The ice thickness is considered to be constant both in time and space and is assumed to be equal to 2 m.

The calculation domain covers the coastal seas of the Russian Arctic from the Kara to the Chukchi Sea with grid spacing of 55.56 km (Fig. 1).

A sequence of surface air pressure fields reported from the European Center for Medium-Range Weather Forecasting and information on the distribution of fast ice and concentration of drifting ice over the calculation domain serve as initial information.

Wind speed and direction near the water surface are calculated from the dependencies in the form:

$$W = k_1 W_g, \quad A = A_g - \alpha$$

where $k_1 = \frac{h}{h+1}$, $h = 0.25 * 1.212 W_g$, $\alpha = 41.26 \exp(-0.07 W_g) - 11.27 \exp(-0.48 W_g)$,

W_g, A_g are speed and direction of the geostrophic wind.

An assessment of the results of prognostic calculations showed the methods to be highly effective both for ocean dynamics elements and the ice drift regardless of the season of the year (Fig. 2). The verification score of forecasting level oscillations in the Kara Sea for the first 24 h is 90-95% on average, decreasing by about 10% with an increase in the advance period for each successive 24 h for the first four days of forecasting. In case of forecasting 5-6 days in advance, the verification score is stable at the 50-60% level. Mean absolute error for 12 stations of the Kara Sea from July to October 1994 was 5 cm for the first day of the forecast, 13 cm for the second day, 16 cm for the third day and mean absolute error was about 20 cm for the forecast for 4-6 days. Thus, the quality of forecasting sea level oscillations is to a great extent governed by the quality of forecasting surface atmospheric pressure fields used in calculations.

A relative simplicity of the calculation scheme and a high technology of the methods allow adapting the model to any area with minimum expenses.

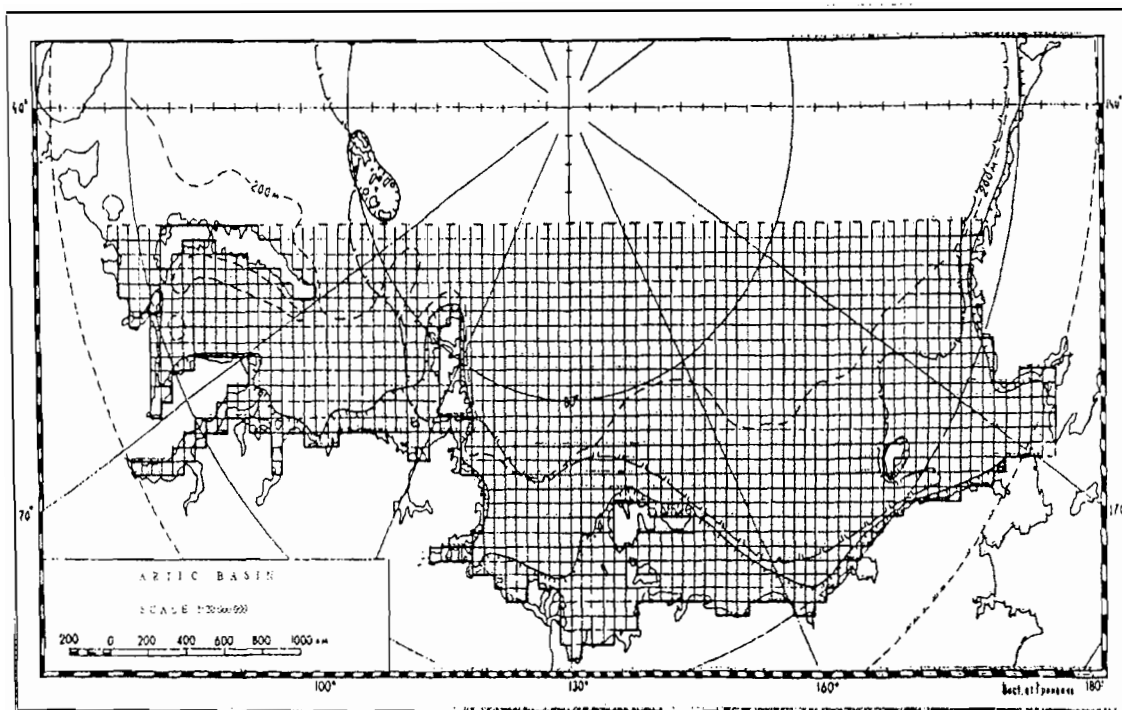
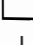
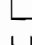
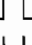
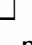


Fig. 1. Calculation domain : — — — - a 200-m isobath;   - mean multiyear position of the drifting ice edge at a minimum extent;   - mean multiyear boundary of fast ice at a maximum extent.

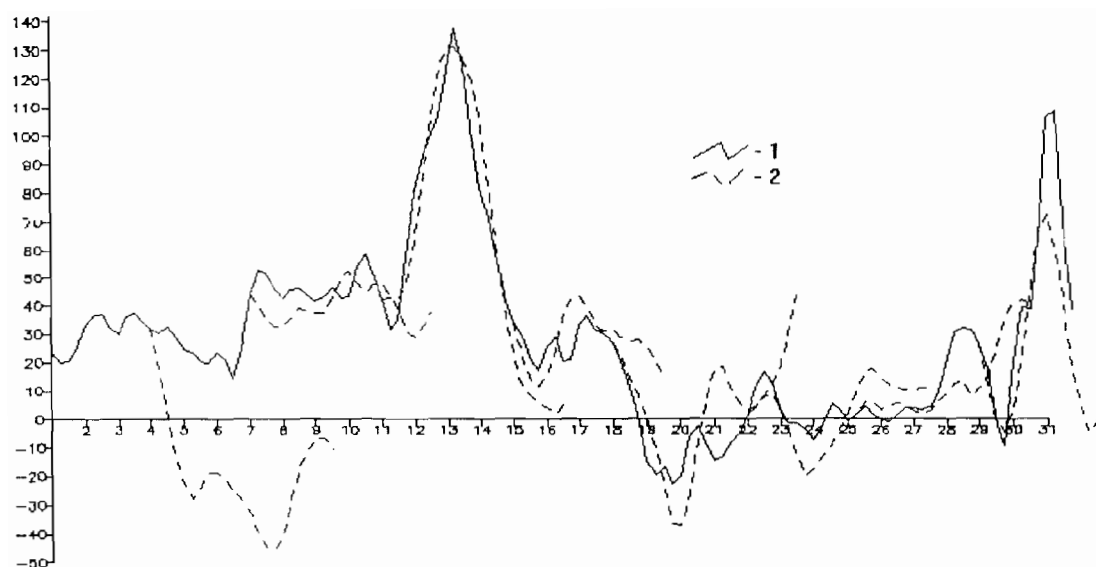


Fig. 2. Sea level oscillations at the Shaitansky bar (Sopochneya Karga station) in the Yenisey Bay in August 1994 (1 - actual level, 2 - prognostic level).

STRUCTURE OF WATER CIRCULATION IN THE KARA SEA DEPENDING ON THE TYPE OF ATMOSPHERIC PROCESSES

G.A. Baskakov, G.N. Voinov, V.A. Volkov, G. Yu. Kosheleva, V.L. Kuznetsov, V.K. Pavlov
(AARI)

Temporal and spatial structure of currents in the Kara Sea in summer (August-first half of October) is rather complicated. It depends, primarily, on the intensity and variability of atmospheric conditions (a comparative proximity of the Icelandic Low), as well as on a large inflow of freshwater and a strongly irregular bottom relief.

In the Kara Sea both tidal and non-periodic currents are well-pronounced. The ratio of dispersions of their mean speeds is from 10 to 62% in different sea regions.

Tidal currents over much of the sea, mainly in its deep-sea zone, are semi-diurnal (Fig. 1). A vast zone with irregular semi-diurnal currents is located in the coastal strip along the Taimyr peninsula as well as off the Yamal peninsula and in Kara Gate and Yugorsky Shar straits. Most considerable speeds of tidal currents are observed in Kara Gate, Yugorsky Shar and Malygin straits where they are 64, 136 and 83 cm/s, respectively.

In the open area of the Kara Sea tidal currents are stronger than non-periodic, whereas in the coastal area it is vice versa - non-periodic currents are stronger than tidal (Fig. 2).

The speeds of non-periodic currents in the open part of the Kara Sea do not usually exceed 10 cm/s; in the coastal sea strip the speeds are larger.

Non-periodic currents-density currents (i.e. constant in the first approximation) and wind-driven currents were calculated by means of a three-dimensional stationary hydrodynamic model developed by Pavlov and Kulakov (1987).

Density currents were calculated according to observation data of water temperature and salinity on the basis of 12 hydrological surveys in the Kara Sea from 1971 to 1989. The results of calculations of currents by years were averaged and fields of density currents at levels: surface, 10, 25, 50, 100, 200, 300 m and at the near bottom level were obtained. In particular, as is seen from Fig. 3, at a level of 10 m a constant water transport to the north-east prevails. Only in the south-western sea region where speeds of currents are very small, a less ordered water circulation was observed.

The typification of the pressure fields over the Kara Sea in summer (August-first half of October) developed by Dmitriyev and Zeltser (1988), was used as a meteorological basis for calculating wind-driven currents. Of the total number of 18 types of fields identified by the authors, four have the largest occurrence frequency: ZnW and ZnN (with a total occurrence frequency of 28.7% according to the number of cases) that are characterized by the dominance of SE and SW winds over the sea, as well as ZnE and ZnS (total occurrence frequency of 27.1%) at which NE and N winds prevail (Figs.4-7). Figs. 8-11 show fields of wind-driven currents at sea surface in summer at these types of pressure fields calculated by means of the model. As is seen from the considered charts, the northward water outflow prevails at the surface at types ZnW and ZnN and an opposite process - the southward water outflow prevails at types ZnE and ZnS. The speeds of wind-driven currents differ in larger variability in space at each type of the pressure fields.

Model calculations were compared with full-scale data - wind-driven currents calculated on the basis of long-term (26 days) measurements of currents by current meters BPV-2 west of Belyi island at a level of 10 m in August-September 1979 (see the table 1).

Table 1.

Wind-driven currents calculated on the basis of full-scale data

Type of pressure field	ZnW	ZnN	ZnE	ZnS
Number of days	14	1	3	8
Current direction, mean	342	339	225	187
Current speed modulus, (in conventional units)	0.4	0.4	0.5	0.6
Stability criterion "K"	0.70	-	0.65	0.65

In the table the stability criterion "K" is a ratio of the vector speed to the speed modulus. Current directions calculated by full-scale data given in the table are, first of all, in good agreement with model calculations (Fig. 4-8), secondly, both of them reflect to a full extent changes in directions to reverse ones at changes in the types of pressure fields (ZnW or ZnN to ZnE or ZnS and vice versa).

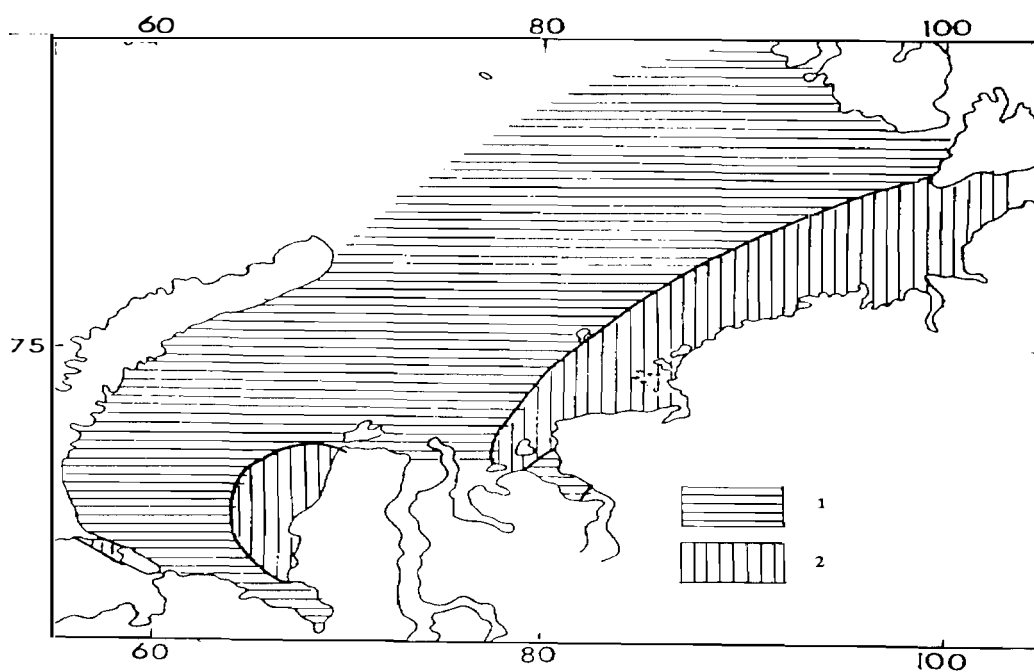


Fig. 1. A character of tidal currents (after Voinov);
1 - semi-diurnal, 2- irregular semi-diurnal

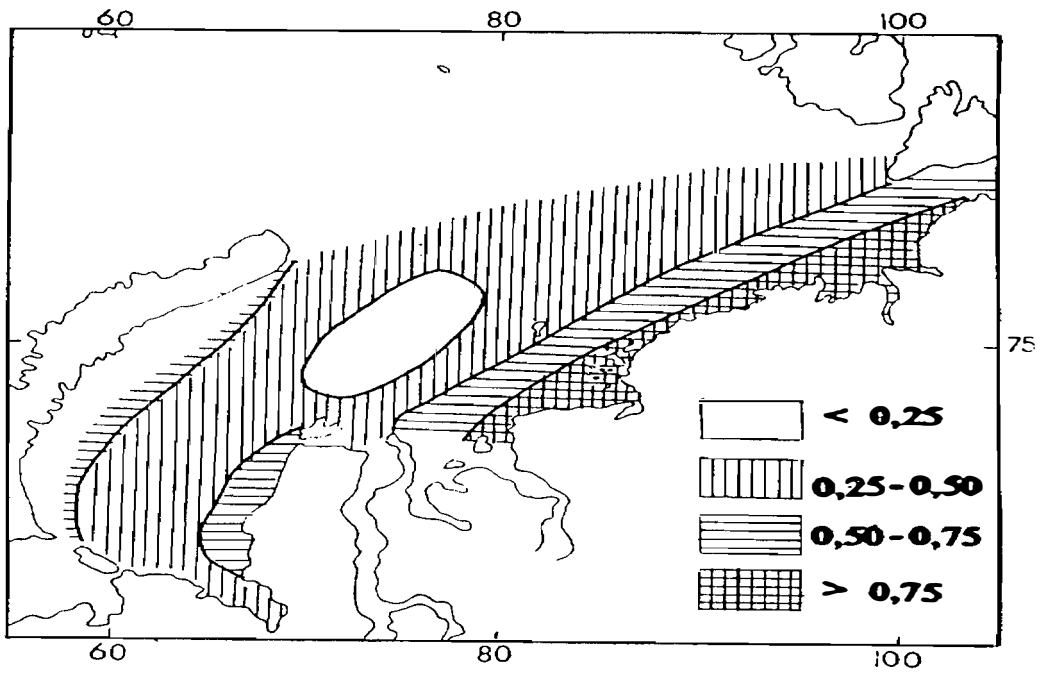


Fig. 2. A ratio of the mean speed of a non-periodic current to that of the total current at a level of 10 m.

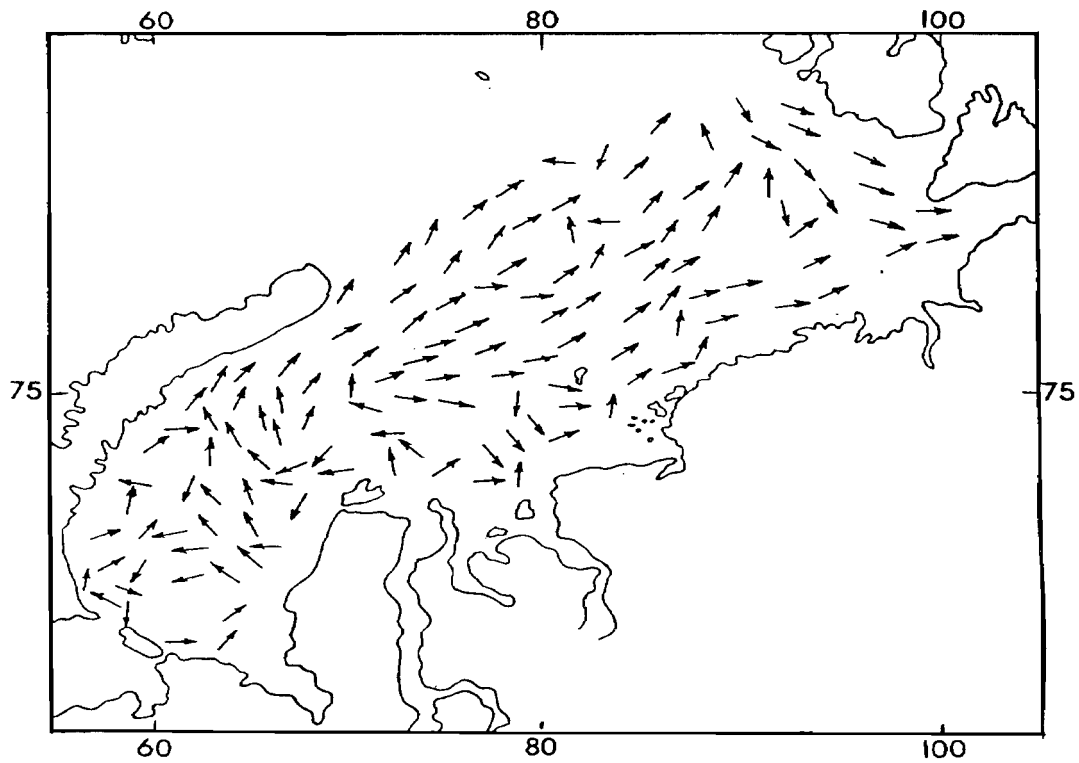


Fig. 3. Calculated density (constant) currents at a level of 10 m in summer. Speeds of currents are given in cm/s.

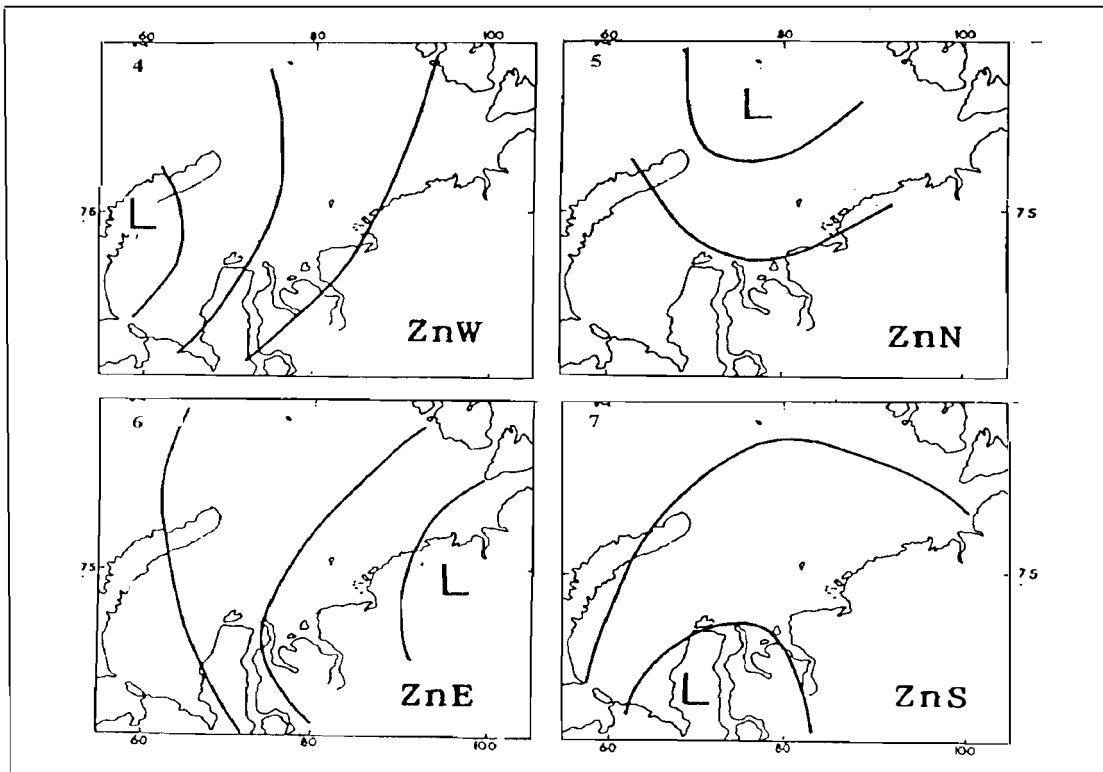


Fig. 4-7. Types of pressure fields, summer (after Dmitriyev and Seltzer).
L - a center of the cyclone.

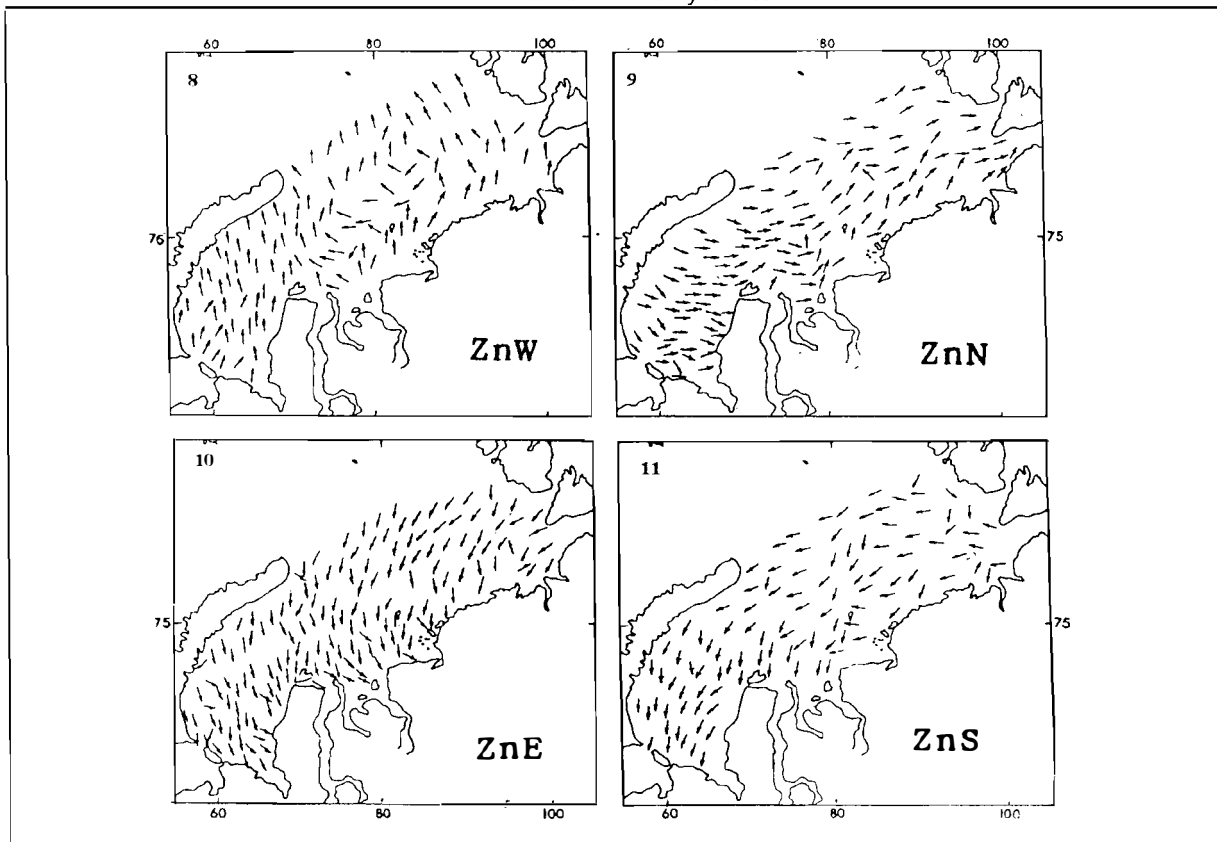


Fig. 8-11. Calculated wind-driven currents at sea-surface in summer
at ZnW, ZnN, ZnS types of pressure fields. Speeds of currents are given in cm/s.

References

1. Kulakov M.Yu., Pavlov V.K., A diagnostic model of water circulation in the Arctic Ocean. 1987, Proc. of the AARI, vol.413, pp.5-16.
2. Dmitriyev A.A., Sel'tzer P.A., Report on the research study "Development of the method for detailed forecasting up to 3 days by days (temperature, precipitation, wind, pressure and their extreme values) for the Arctic in the warm period of the year", 1988. Gidrometeorological archive of the AARI, 100 p.

MEZOSTRUCTURE OF WATER DENSITY MAXIMAL GRADIENTS BOUNDARY LAYER RELIED IN ARCTIC SEAS BY LIDAR SENSING DATA

V. Yu. Benzeman (AARI)

In 1988-1989 the expedition of the AARI carried out experiments of sensing in the surface water layer of the Arctic Seas using a lidar complex Makrel-2 onboard the aircraft-laboratory IL-18 DORR.

A laser generates impulse emission with a wavelength in the green part of the spectrum. The penetration depth of the ray is up to 35 m from the surface.

The last expedition with lidar sensing experiments in all Arctic seas of the Russian Federation took place in August-September 1989 and included 115 air observation hours.

The location depth of optical inhomogeneities in sea water was recorded automatically using the reflected echo-signals of polarization and depolarization windows every 15 m of the flight. The recording of such inhomogeneities is related to the reflection of a monochromatic laser ray from suspended matter (phytoplankton) whose geometrical dimensions are comparable to the emission wavelength (532 nm).

The flight routes of the aircraft-laboratory (Fig. 1) at upper water layer sensing were over standard transects of oceanographic stations. They were occupied at the same time (August-September) by the oceanographic expeditions of the institute in the Barents and Kara Seas onboard the research icebreaker "Otto Schmidt" and the R/V "Akademik Shuleikin", in the Laptev and East-Siberian Seas by the R/V "Mezen" and in the Chukchi Sea by the R/V "Professor Khromov" and the hydrographic ship "Dmitry Laptev". Of a large number of oceanographic stations occupied, about 140 stations coincided in the location with the flight tracks. They were used for comparison with data of lidar sensing.

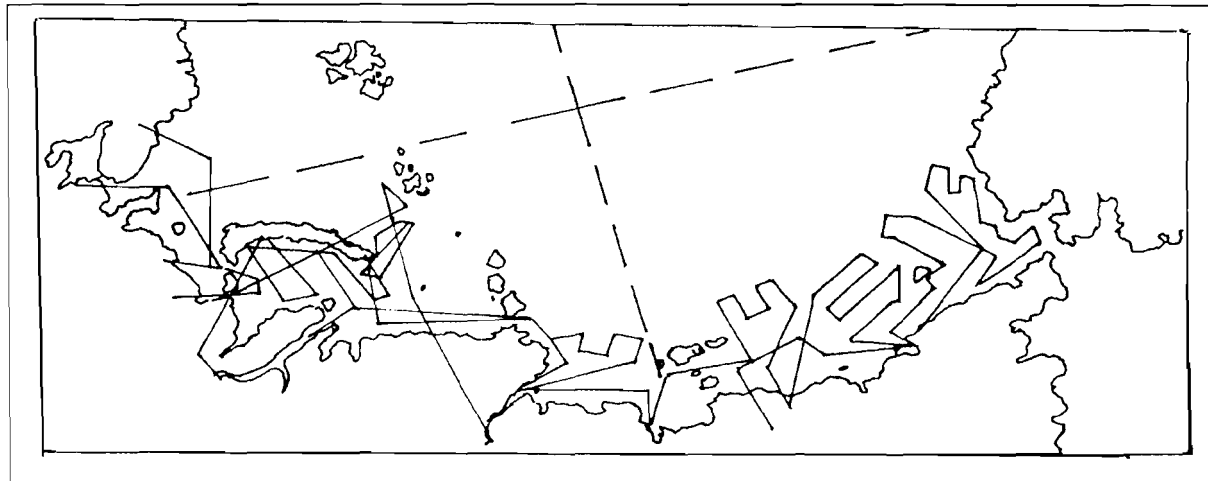


Fig. 1. A diagram of the flight routes.

Laser echo signals were computer-processed by means of the nonparametric methods of the theory of decision making. Then these data were separately plotted for a polarized and depolarized windows on the charts in accordance with the flight routes. The charts contained depths of lower boundary of the maximum density gradients obtained from lidar data. The same depths of the lower boundary of the maximum density gradients obtained independently from data of the vertical distribution of water density at oceanographic stations carried out by the indicated research ships were plotted on them.

On the basis of the charts, assuming these data to be reference data, charts of deviations - errors Δ were constructed, in spite of large deviations in time (10-20 days) of some oceanographic measurements from lidar sensing.

These charts are presented in Fig. 2 (a, b, c). Only those flights and their parts where oceanographic stations were occupied are plotted on the charts. Completely shaded sections of the route are places where depths of the lower boundary of the pycnocline measured by means of aircraft lidar sensing coincided actually completely $\Delta=0-5$ m with an accuracy up to errors of recording the levels, with similar characteristics obtained by means of oceanographic stations. The obliquely hatched parts of the route designate places where $\Delta= 5-10$ m. The non-hatched parts of the routes are zones where deviations were very large $\Delta > 10$ m.

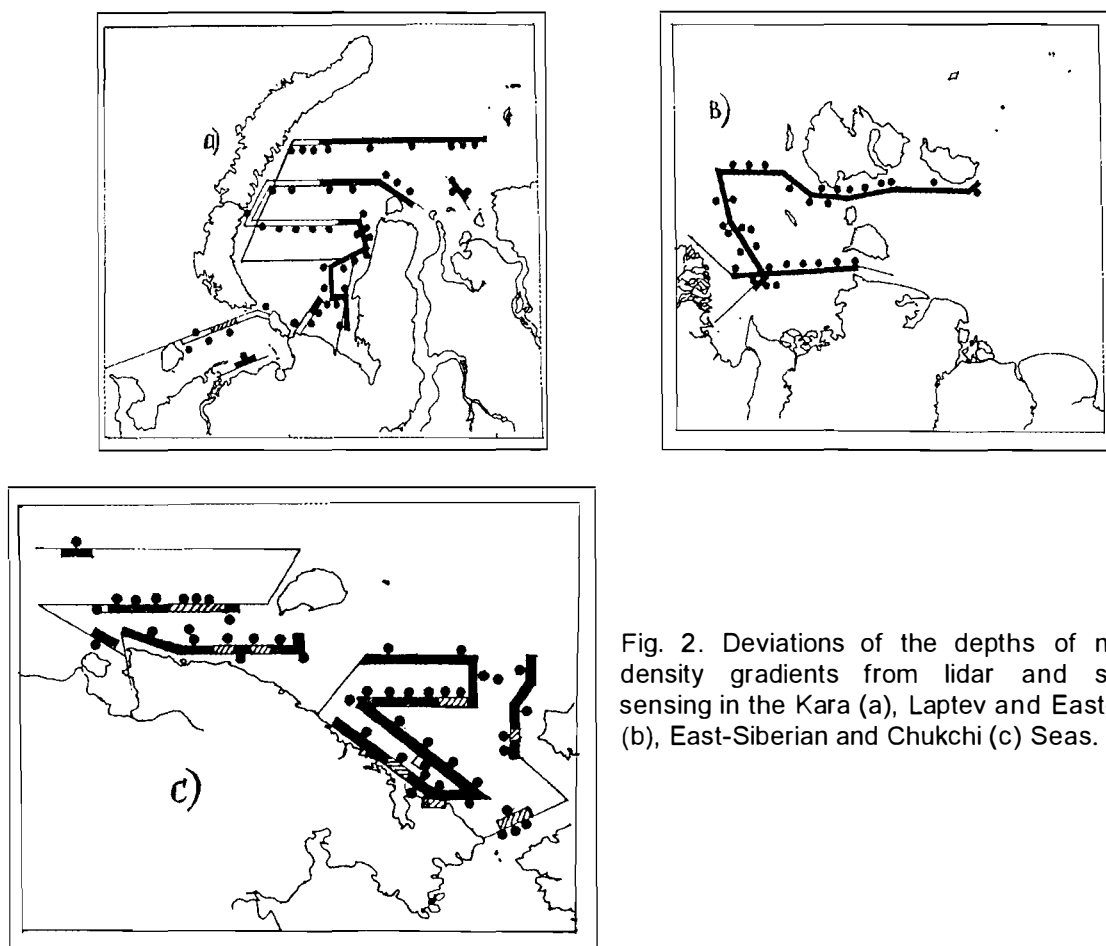


Fig. 2. Deviations of the depths of maximum density gradients from lidar and shipborne sensing in the Kara (a), Laptev and East-Siberian (b), East-Siberian and Chukchi (c) Seas.

Black circles on the same charts indicate locations of oceanographic stations occupied by ships used for comparison. The charts of deviations Δ clearly show the geography of inaccurate lidar recording in some regions of the lower boundary of the layer of the maximum density gradients.

The region of the western Kara Sea where deviations of lidar and oceanographic data are very large, is sufficiently sharply pronounced. Further east the coincidence is complete and in the regions of the East-Siberian and the Chukchi Seas there are deviations of $\Delta=5-10$ m in some places, as to the rest the coincidence here is also complete.

It should be mentioned that this region is characterized by a large difference in time between lidar sensing and many oceanographic stations.

Let us consider the statistics of deviations of Δ of lidar and oceanographic data.

Deviation value Δ (in m)	Kara Sea			East			Over all seas		
	0-5	6-10	>10	0-5	6-10	>10	0-5	6-10	>10
Number of stations	34	10	15	49	23	2	83	33	17
Percent, %	58	17	25	66	31	3	62	25	13

As is seen, 13% of oceanographic stations have large deviations Δ . The remaining 87% of oceanographic stations (116 stations) confirm, on the whole, lidar measurements in the region of these stations. There is a distinct division of deviations Δ over the regions which is related to the features of water masses in different regions. By their optical properties, to be exact, by the presence of underwater optical inhomogeneities in sea water, they govern the physics of the laser emission transmission in the medium and errors in the measurements of the maximum density gradients. It should be noted that statistics for comparing with lidar data do not include oceanographic stations made onboard the research icebreaker "Otto Schmidt" in the north-western Kara Sea, since as a result of lidar calibration in this region and the oceanographic stations themselves it is seen that their comparison is impossible in this region.

Let us try to explain to what the indicated deviations Δ are related. As is seen from the preceding section, for two calibrations (off Yamal - the R/V "Akademik Shuleikin" and in the Chukchi Sea - the hydrographic vessel "Dmitry Laptev") of three there was a complete coincidence at large maximum values of the vertical water gradient $(\partial\sigma_t/\partial z)_{\max} > 0.2$.

For the third calibration performed jointly with the icebreaker "Otto Schmidt" north of the Zhelaniya cape, the discrepancy in the pycnocline between lidar and oceanographic data is very large $\Delta=20$ m. The values of the maximum gradient is very small $(\partial\sigma_t/\partial z)_{\max} \approx 0.02$. That is, there is an obvious tendency: at small water density gradients the deviation in the pycnocline is large and at larger gradients the coincidence is actually complete.

To make it clear, the values of the maximum water density gradients were calculated for seventy of oceanographic stations used for comparison with lidar data, largely from the western Arctic.

Fig. 3 presents a graph of the distribution of these gradients by stations depending on the values of deviations in the depth of the lower boundary of the water pycnocline according to lidar measurements and oceanographic stations. The concentration of small deviations ($\Delta < 5$ m) within $(\partial\sigma_t/\partial z)_{\max} = 0.15 - 0.55$ in conventional sigma units per one meter is evident. Large deviations ($\Delta > 14$ m) at small gradient values < 0.15 units/m are sharp and apart. Approximately, the dependence of the error of lidar Δ determination of the maximum density gradient depth on the water density gradient value can be expressed as:

$$\Delta = f(1/(\partial\sigma_t/\partial z)) \text{ or } \Delta = k (1/(\partial\sigma_t/\partial z))$$

where $k = a \cdot \exp(-(\lambda_2 + \lambda_1))$ and λ_2 and λ_1 are decrements of the function damping within which the points in Fig. 3 are located.

Further, it is possible to specify the parameters of Δ dependence on $(\partial\sigma_t/\partial z)$ on condition of a large number of calibrations, as well as new oceanographic surveys in the seas at a simultaneous remote sensing of the upper water layer in the Arctic seas.

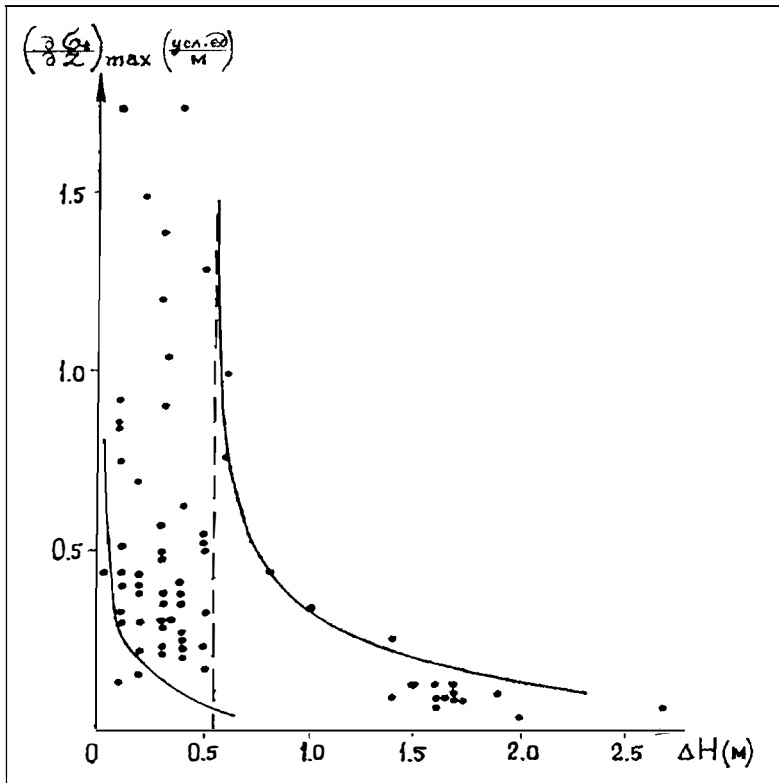


Fig. 3. Dependence of the deviation values Δ on the maximum density gradients $(\partial\sigma_1/\partial z)_{\max}$

On the whole, the geography of the distribution of minimum errors of Δ describes well the spreading of river (desalinated) water in the Arctic Seas.

To conclude, it should be mentioned that recording of the lower boundary profile of the maximum water density gradients measured by the lidar is actually continuous with an interval of 0.5-1 s. This allows investigation of the mesostructure, and even the microstructure of this conventional surface over large areas at a very large rate on different scales of its spatial distribution in the Arctic Seas from micro- to synoptic ones.

ON NATURAL CONVECTION IN A MELT PUDDLE

P.V. Bogorodsky and A.P. Makshatas (AARI)

1. Puddles can be considered an important component of the Arctic climatic system (Moritz et al., 1993). In summer when they cover up to half of the total area of drifting ice, solar radiation absorbed by them per unit area is several times greater than the absorption by the snow-ice cover (Nazintsev 1964). The shortwave part of the incoming solar radiation ($0.35\text{-}0.7\mu$) is absorbed either directly by the puddle bottom providing an increase in the salinity of the bottom water layer due to melting of sea ice, or in the ice cover thickness and the subice sea layer resulting in intensive melting of the bottom ice surface (Wadhams and Martin 1990). The remaining portion of solar radiation (with a wave-length more than 0.7μ) is directly absorbed by water of the puddle. Both indicated processes along with the energy exchange processes at the upper surface lead to the formation of the thermohaline structure of the puddle (Fig.1, Eicken et al. 1994), which can be conventionally represented as a two-layer one. Calculations show the heat fluxes governed by the absorption of solar radiation directly in the puddle and the lower lying ice cover to be approximately equal. Hence, it is important to estimate the mechanism for convective heat transfer to the ice (Appel' and Gudkovich 1979).

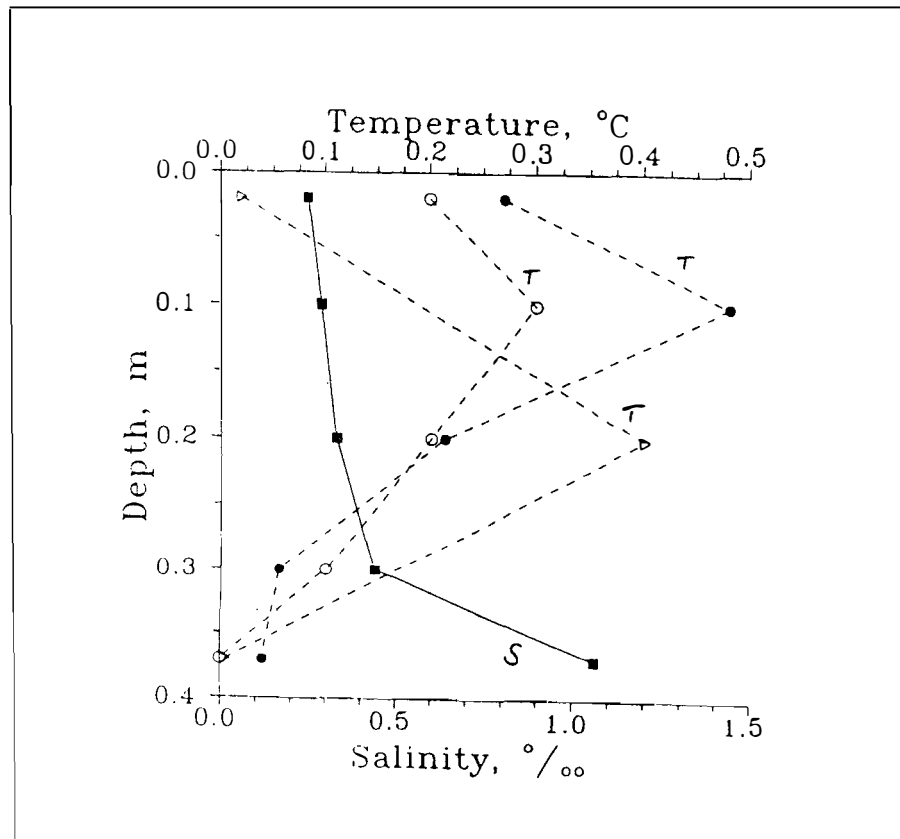


Fig.1. Temperature (T) and salinity (S) profiles in the puddle.

2. Let us consider a system of two horizontal layers of fluid cooled from below. A warmer and fresher upper layer and cold and saline lower layer (both with temperatures between the freezing and maximum density points) are restricted to external free (from above) and solid (from below) surfaces.

The lower external boundary is assumed to be isothermal and isoconcentrated, the upper - heat and salt isolated. The axis z is directed upward, the beginning of coordinates is at the lower boundary. The full thickness of the system H ; h is the ratio of the thickness of the lower layer to H . The coefficients of viscosity, heat conductivity, temperature conductivity, diffusion and heat and salt expansion of the both fluid layers - $\eta_m, \nu_m, \lambda_m, \chi_m, D_m, \alpha_m, \beta_m$ ($m=1$ for the lower layer and $m=2$ for the upper layer). The equilibrium gradients of temperature A_m and salinity B_m in each layer are constant and connected with the continuity condition at the interface of the layers: $\lambda_1 A_1 = \lambda_2 A_2, D_1 B_1 = D_2 B_2$. For such a system the linearized equations of the thermoconcentrated convection in the non-dimensional form for the neutral amplitudes of velocity w_m , temperature θ_m and salinity σ_m with a wave number k are written in the form ($\delta = d^2/dz^2 - k^2$)

$$\begin{aligned} \delta^2 w_m + k^2 a_m Ra \theta_m + k^2 b_m Rs \sigma_m &= 0 \\ \delta \theta_m + c_m f_m w_m &= 0 \\ \delta \sigma_m + d_m^2 w_m &= 0 \\ a_1 = b_1 = c_1 = d_1 = f_1 &= 1 \\ a_2 = \nu/\alpha, b_2 = \nu/\beta, c_2 = \lambda, f_2 = \chi, d_2 = D \\ \alpha = \alpha_1/\alpha_2, \beta = \beta_1/\beta_2, \chi = \chi_1/\chi_2, \eta = \eta_1/\eta_2, \mathbf{D} = \mathbf{D}_1/D_2, \lambda = \lambda_1/\lambda_2, \nu = \nu_1/\nu_2 \\ Ra = g\alpha_1 A_1 H^4 / \nu_1 \chi_1, Rs = g\beta_1 B_1 H^4 / \nu_1 D_1 \end{aligned} \quad (1)$$

The criterion of stability of the system is conventional Ra and concentration Rs of the Rayleigh number expressed through the full thickness H and parameters of the lower layer. The boundary conditions (primes indicate differentiation) at three interfaces - lower ($z=0$), upper ($z=1$) and intermediate ($z=h$) are:

$$\begin{aligned} z=0: w_1 = w_1' = \theta_1 = \sigma_1 &= 0 \\ z=1: w_2 = w_2'' = \theta_2 = \sigma_2 &= 0 \\ z=h: w_1 = w_2 = 0, w_1' = w_2', \eta w_1'' = w_2'', \theta_1 = \theta_2, \sigma_1 = \sigma_2, \lambda \theta_1 = \theta_2, D \sigma_1 = \sigma_2 \end{aligned} \quad (2)$$

3. The main contribution to instability of the two-layer convective systems is made by longwave disturbances ($k \rightarrow 0$, Gershuni and Zhukhovitsky 1986), which can be represented in the form of the series by even powers of k :

$$(w_m, \theta_m, \sigma_m) = (w_m, \theta_m, \sigma_m)^{(0)} + k^2 (w_m, \theta_m, \sigma_m)^{(1)} + o(k^2) \quad (3)$$

For the considered system $a_2 \cong b_2 \cong c_2 \cong f_2 \cong 1; d_2 < 1$ (Horne 1969). After some manipulations the system of equations (1) for the first-order terms is reduced to the form:

$$\begin{aligned} w_m^{(1)IV} &= -R \\ (\theta_m^{(1)})'' + w_m^{(1)} &= \\ (\sigma_m^{(1)})'' + d_m^2 w_m^{(1)} &= \end{aligned} \quad (1')$$

where $R = Ra + Rs$. The boundary conditions coincide with (2). Integration of (1') and substitution of the amplitudes to (1) results in the expression for the critical number R :

$$R = \frac{1440[D + 2h(1-D)(1-h)]}{\mathbf{D}(4p_1 h^6 - 15p_2 h^5 + 15p_3 h^4 - 9p_4 h + p_5)} \quad (4)$$

$$p_1 = D^2 - 6D + 5, p_2 = D^2 - 5D + 4, p_3 = D^2 - 4D + 3, p_4 = D^2 - D, p_5 = 5D^2$$

Limiting cases $h \rightarrow 0$ and $h \rightarrow 1$ correspond to transition to a one-layer system with the properties of the upper and lower fluids and critical numbers $R = 288D^{-2}$, $R = 288$ respectively.

The latter result is also obtained at $D=1$, i.e. at the absence of the difference in properties between both fluids.

Fig. 2 shows the form of function (4). It should be noted that according to the statement of problem only those parts of curves which correspond to D less than unit have real sense. The remaining lie outside of the interval of physically possible values of parameter D .

The arguments for the existence of the described mechanism of instability under full-scale conditions are unknown to the authors. Nevertheless using described mechanism one can explain the deep stabilization of a melt puddle (appr. 40 cm). It may be proposed that decreasing of ratio D conditioned by growth of the lower layer salinity sharply increases the instability threshold (keeping in mind long wavelength instability) that result in termination of mixing.

This study was performed with financial support of the Russian Foundation for Basis Research (Project No.95-05-15315a).

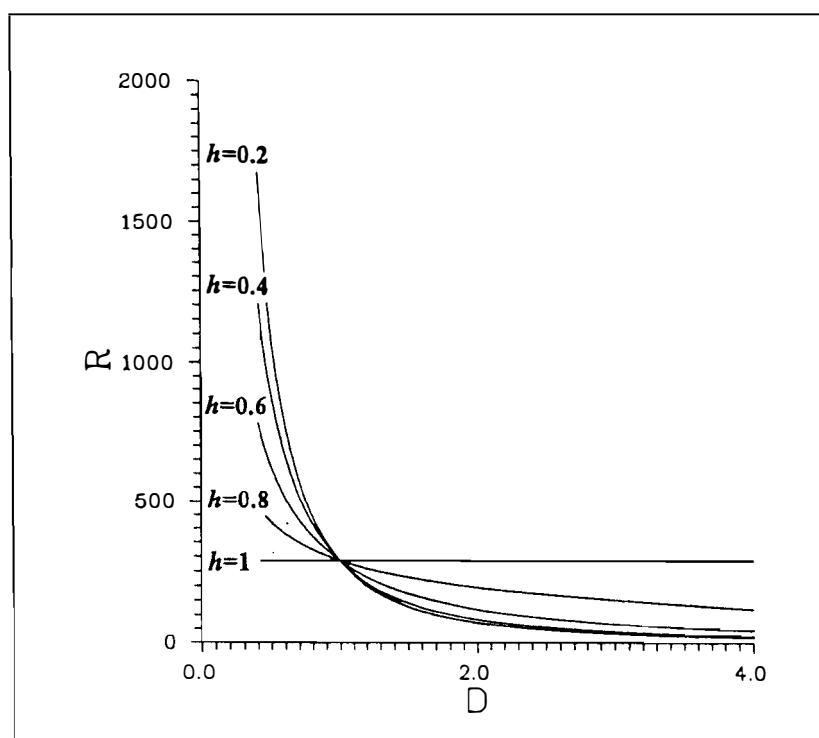


Fig. 2. The form of the function $R(D)$.

ATLANTIC WATER IN THE KARA SEA

L. V. Bulatov, S. V. Kochetov (AARI)

Atlantic water inflows to the Arctic Basin through Fram strait and spreads over its areas in a deep layer about 600 m thick. It penetrates the Kara Sea through three deep-water troughs: the St. Anna, Voronin and the trough along Novaya Zemlya and the Franz-Josef Land (Fig. 1).

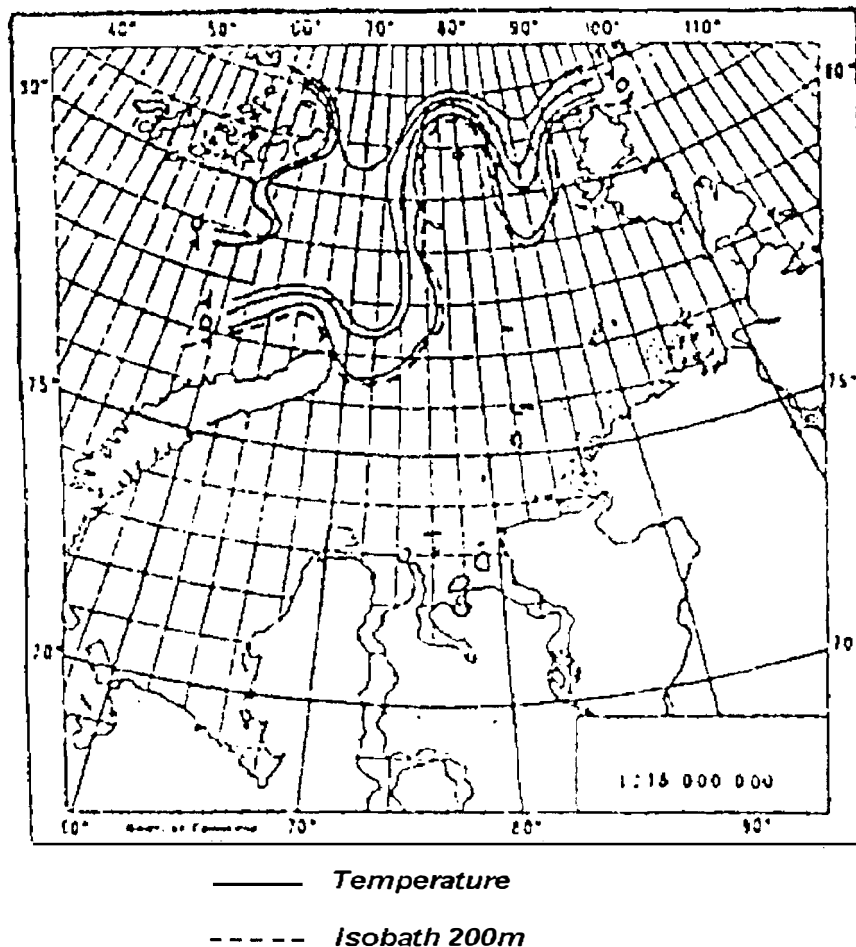


Fig. 1. Maximum temperature of Atlantic water

Quite a lot of attention has been given to studies of Atlantic water (see references). At the present time new data were collected by airborne expeditions "Sever" that allow one to specify horizontal and vertical structure of Atlantic water, its transformation on the continental slope.

Atlantic water is characterized on the basis of analyzing materials of hydrological observations performed at five transects crossing the indicated troughs: Zhelaniya cape - Salm island, Salm Island - Viese Island, Graham-Bell Island - Ushakov Island, Ushakov Island - Shmidt Island, Vise Island - Dlinnyy Island.

Deep water which has positive temperature, i.e. its boundaries are the upper and lower zero isotherms, is assumed to be Atlantic water.

An analysis has shown that in the region of the trough between Novaya Zemlya and Franz-Josef Land with depths up to 400 m the width of the Atlantic water flow is about 100 miles and the thickness of its layer is 200-250 m. The maximum temperature of this water is observed at a depth of about 150 m where it reaches $+1.00^{\circ}$ - $+1.50^{\circ}$. The salinity of Atlantic water varies within 34.80-34.90 per mil.

In the north-western Kara Sea there is the St. Anna trough - a deep-sea tongue of the Arctic Basin with depths up to 600 m. The length of this trough is 250 miles. Its width in the north of the sea is 90 miles. The core of the flow of Atlantic water is observed along $68-70^{\circ}\text{E}$ meridians. The width of the flow of Atlantic water at its entering the St. Anna trough is about 60 miles and the thickness of the layer is 450 m. In the western region of the trough Atlantic water spreads up to the shore and in the eastern one its boundary passes at about 30 miles from the shore. The maximum temperature is observed at a depth of about 200 m being about 2° in winter and $+1.5^{\circ}$ in summer (Fig. 4).

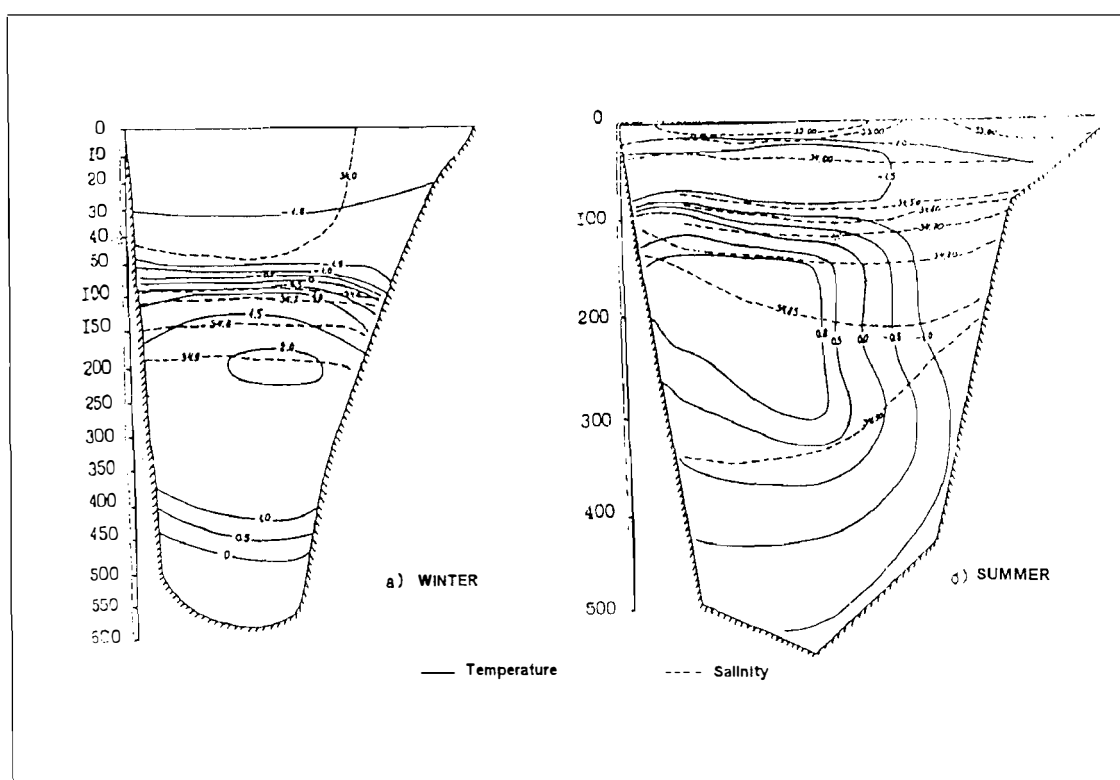


Fig. 4. Water temperature and salinity distribution at the transect Graham-Bell Island - Ushakov Island

In winter the flow of Atlantic water is more intensive than in summer, as in winter air transports with a southern component prevail over the Kara Sea. Surface water with ice is exported northward and the inflow of Atlantic water along the deep-sea troughs increases as a compensation. Observations point out that in winter the layer of Atlantic water is 50-100 m more thick and the maximum temperature is $0.5-1.0^{\circ}$ higher than in summer.

At the transect Salm Island - Viese Island located 60 miles southward, the width of the flow of Atlantic water is 100 miles, the thickness of the layer is 400 m and the maximum temperature is about 1.5° . Atlantic water flows to this region both from the north from the Arctic Basin and from the west from the Barents Sea.

One can follow the changing characteristics of Atlantic water when it moves from north to south along the St. Anna trough in the data of transects along 70°E

meridian. The transect begins in the vicinity of the North Pole (at 88°N) and ends off Belyi Island in the Kara Sea (Fig. 3).

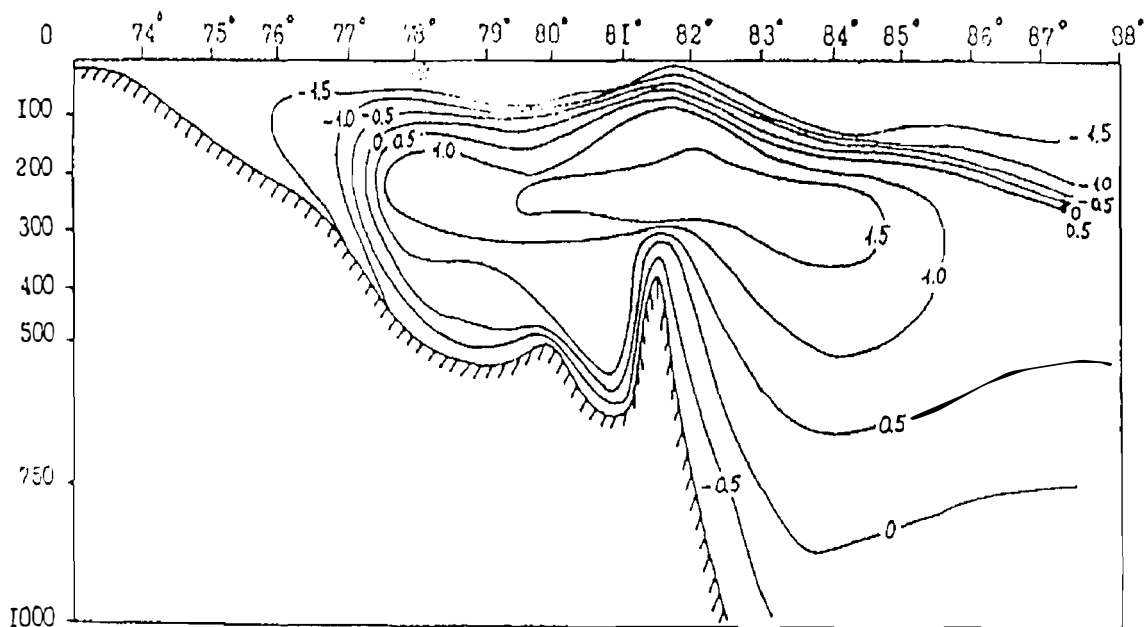


Fig. 3. Distribution of water temperature at the transect along 70°E from the North Pole to Belyi Island

At the beginning of this transect the thickness of the layer of Atlantic water is 500 m and the maximum temperature is about 0.7° (at a level of 400 m). The upper and lower boundaries of Atlantic water are located, respectively, at levels of 250 and 750 m. In moving southward the thickness of the layer of this water and the temperature increase. In the vicinity of 84°N the thickness of the layer of Atlantic water in exceeds of 700 m and temperature reaches 1.7°. The core of Atlantic water is located near 82°N where temperature reaches 2°. A sharp change in all characteristics of Atlantic water occurs in the vicinity of the continental slope. There is a well-defined dependence of Atlantic water spreading on the submarine relief. The continental slope serves as a barrier of some kind to spreading of Atlantic water and it is evident that heat of this water has the largest influence on those sea regions where the continental slope is dissected by deep-water troughs. When entering the St. Anna trough, Atlantic water spreads in a layer of almost 500 m thick: from a level of 100 m to the bottom (600 m). Its maximum temperature is 1.7-2.0°C. Advancing southward the temperature in the flow core changes insignificantly. A sharp temperature decrease is observed in the vicinity of the continental slope. Here, for 5-10 miles the temperature decreases from +1.5° to -1.0°C. The layer of Atlantic water becomes thinner rising closer to the surface. This creates the conditions for convection spreading during the autumn-winter period down to the depth where Atlantic water is located, its entrainment into convection and heat transfer to the surface. Atlantic water spreads along the St. Anna trough up to the Zhelaniya cape. Observation data indicate that Atlantic water significantly affects ice thicknesses in the Kara Sea. Repeated measurements of the ice thickness made in different years during hydrological surveys, indicate that ice thickness above the St. Anna trough is almost 1 m less than in the other sea regions. Vertical temperature and salinity profiles show the convection in the regions with small ice thicknesses reaching the layer of Atlantic water. During the autumn-winter period Atlantic water releases about 7 kcal/cm² of heat.

In the north-eastern Kara Sea there is the Voronin trough with depths more than 400 m. The length of the trough is about 120 miles and the width is about 60 miles. Atlantic water is observed here only in the northern region of the trough. In summertime the maximum temperature is about 0° and in wintertime it is almost 1° higher (Fig. 5). In winter, water with positive temperature penetrates up to parallel $79^{\circ}30'$ (Fig. 2).

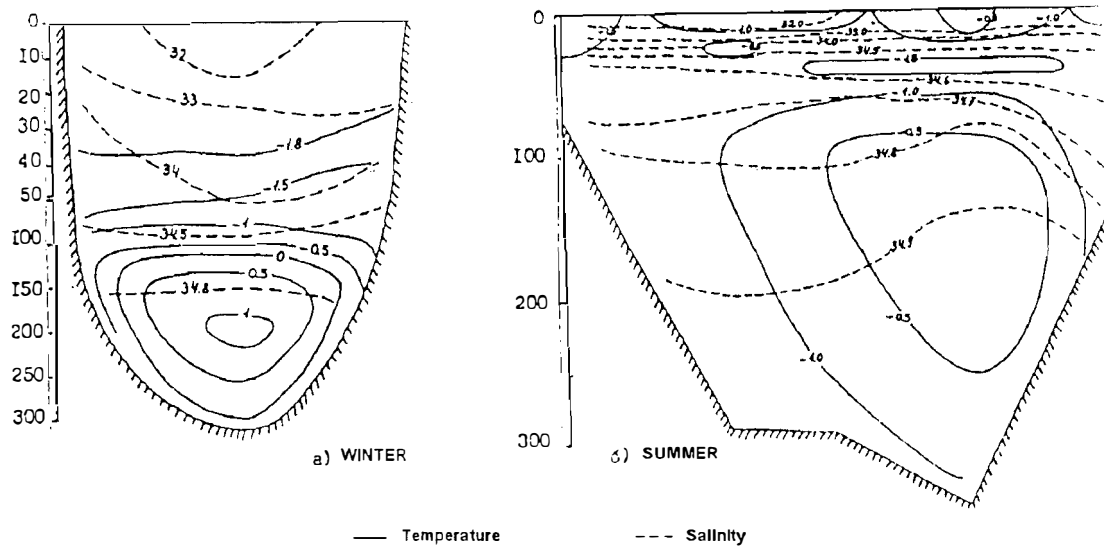


Fig. 5. Water temperature and salinity distribution at the transect Ushakov Island-Shmidt Island

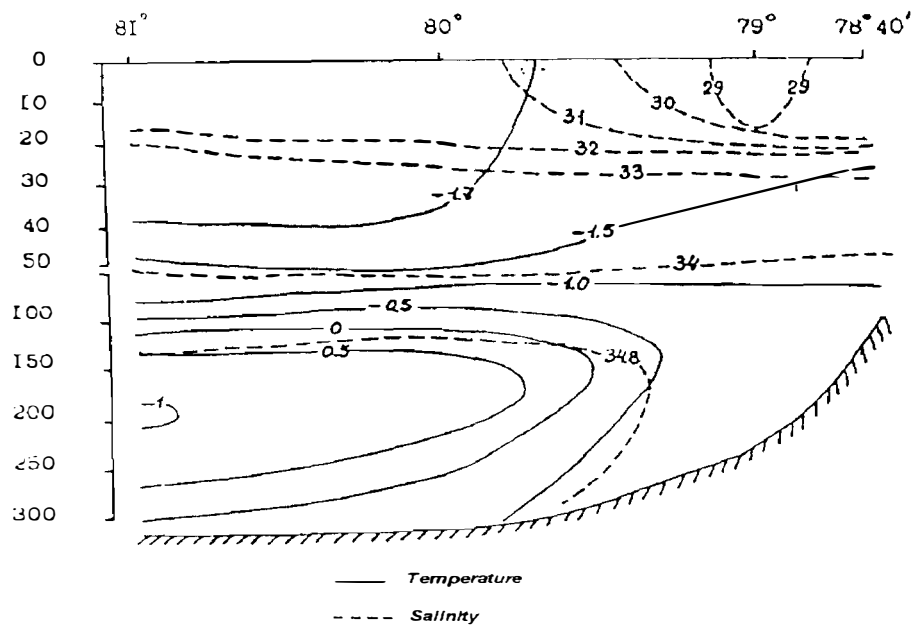


Fig. 2. Water temperature and salinity distribution at the transect along 85°E

At a contact of Atlantic water with Arctic water a frontal zone is formed whose width is 5-10 miles on average and the horizontal temperature gradients can reach 0.4 degrees per mile. Contact zones follow along deep-sea troughs since during the autumn-winter

period, as a result of convective mixing which in shallow regions rapidly reaches bottom, water becomes more dense, sinking along the slopes of the troughs thus replacing less dense water.

All these facts allow a conclusion that the role of Atlantic water in the heat regime of the Kara Sea is high. In the autumn and winter periods they directly affect the surface layers, slow ice formation and reduce ice thickness. In summer, heat of Atlantic water does not get to the surface, being lost due to heating of intermediate cold water. During the autumn-winter period Atlantic water releases upward to the bottom ice surface from 6 to 8 kcal/cm² of heat.

References

Panov V.V., 1961: The role of Atlantic water in the hydrological and ice regime of the Arctic Seas (by the example of the Kara Sea). Problems of the Arctic and the Antarctic, No. 8, pp.75-77.

Timofeyev V.T., 1962: Influence of deep Atlantic water on the formation and melting of ice in the Kara and Laptev Seas. Oceanology, vol.2, iss.2, pp.219-225.

Shpaikher A.O., 1965: Influence of Atlantic water on the formation of the hydrometeorological regime of the Arctic Seas. Proc. of the Central Institute of Forecasting, iss. 142.

Timofeyev V.T., 1960: Water masses of the Arctic Basin. L.: Gidrometeoizdat, 190 p.

ROLE OF FLAW POLYNYAS IN THE HYDROLOGICAL AND ICE REGIME OF THE KARA SEA

L. V. Bulatov (AARI)

In winter the Kara Sea is completely ice-covered. In the coastal regions fast ice is established. Behind fast ice at off-shore winds polynyas are formed, their occurrence frequency being 70-100% for the period of February to June. In some years the width of polynyas reaches 200 km and the length measures hundreds of kilometers.

Flaw polynyas produce a considerable influence on the formation of the hydrological and ice regime of the Kara Sea: in winter intensive ice formation, salination and convection, strong heat release to the atmosphere are connected with them; in spring these are strong heat accumulators and centers of clearing from ice, since at this time a maximum solar radiation influx is observed (15-16 kcal/cm² a month).

The formation of polynyas usually indicates a favourable development of the processes of ice disappearance in the sea and its heating. Polynyas surrounded by ice, remain the only zones of the sea that accumulate heat. The intensity of accumulation can be quite large - through June alone the heat content of the sea may increase to 10 kcal/cm².

The heat content of the surface layer of the Kara Sea was calculated successively from one 10-day period to another beginning from the moment of heat balance passing through zero to positive values. The calculation methods are presented by Bulatov and Zakharov (1967). Calculations are performed separately for the south-western and north-eastern Kara Sea. They have shown heat accumulation by the sea surface layer in the ice-free zones to begin from the second 10-day period of May (Fig. 1). The only zones of open water at this time are flaw polynyas.

The most intensive heat accumulation occurs during a comparatively short time interval following immediately the process of sea becoming ice-free. With the increased temperature in the surface layer and an increase in heat losses related to it due to turbulent exchange, radiation and evaporation, the intensity of heat accumulation decreases. The amount of absorbed heat depends to a greater extent on the dates of occurrence of open water (Bulatov and Zakharov, 1976). In the regions that become ice-free early, the heat content of the surface layer reaches its maximum in August. Then, cooling of the surface layer begins, being at first slow, then becoming increasingly more intensive due to the heat release to the atmosphere. A probable maximum of the heat content is 18.0 kcal/cm² in the south-western Kara Sea and 14.8 kcal/cm² in the north-eastern region. Water temperature at the surface at the moment of the maximum heat content reaches 10° in the south-western sea and 7° in the north-eastern sea.

These temperatures should be considered as ultimate under current meteorological conditions in the Arctic. Ultimate temperatures mean the end of heat accumulation by the surface sea layer.

Marginal regions are characterized by different conditions where heat absorbed by open water is completely lost due to ice melting.

Sea surface temperature remains close to 0°, hence, intensive heat accumulation is constantly maintained both due to solar radiation absorption and to turbulent exchange (Fig. 2). Calculations show that in the regions of the ice edge about 45 kcal/cm² can be absorbed and lost due to ice melting for five summer months. This heat is enough to melt ice about 6 m thick.

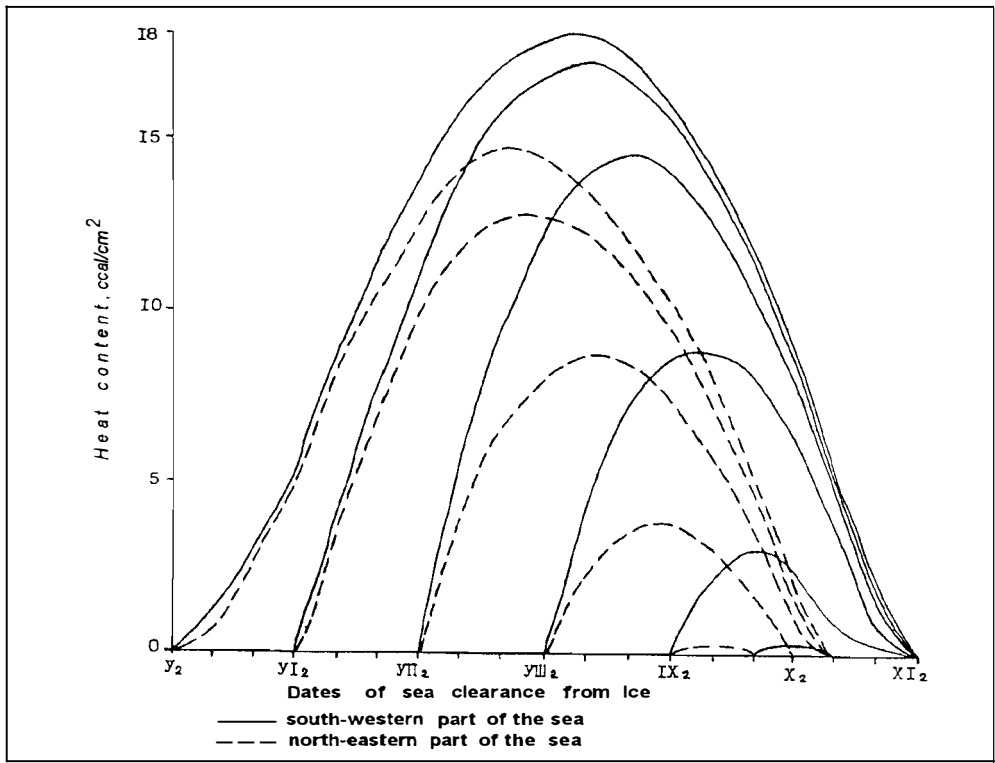


Fig. 1. Heat accumulation and loss by the surface layer of the Kara Sea, Time of the sea becoming ice-free for south-western sea, north-eastern sea, heat content, kcal/cm²

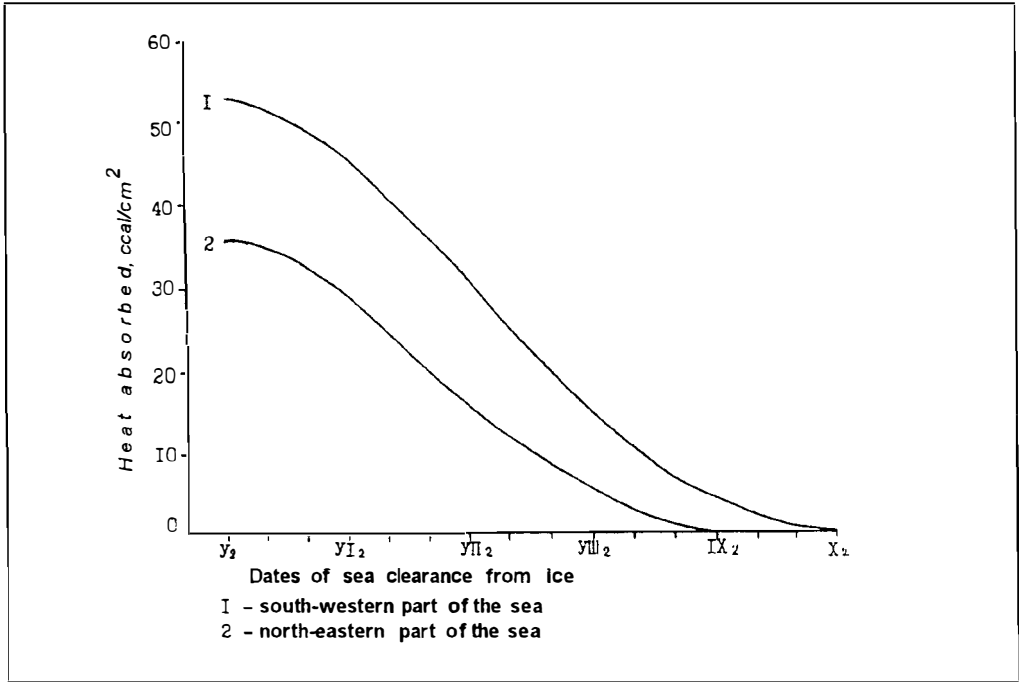


Fig. 2. Possible heat accumulation in the ice edge region of the Kara Sea. Time of the sea becoming ice-free south-western sea north-eastern sea absorbed heat, kcal/cm²

Large accumulating capacity of polynyas is confirmed by actual observation data. Fig. 3 presents heat content of the polynya which had formed behind fast ice in the middle of May and then developed to large dimensions at the time of the hydrological survey on July 13-25.

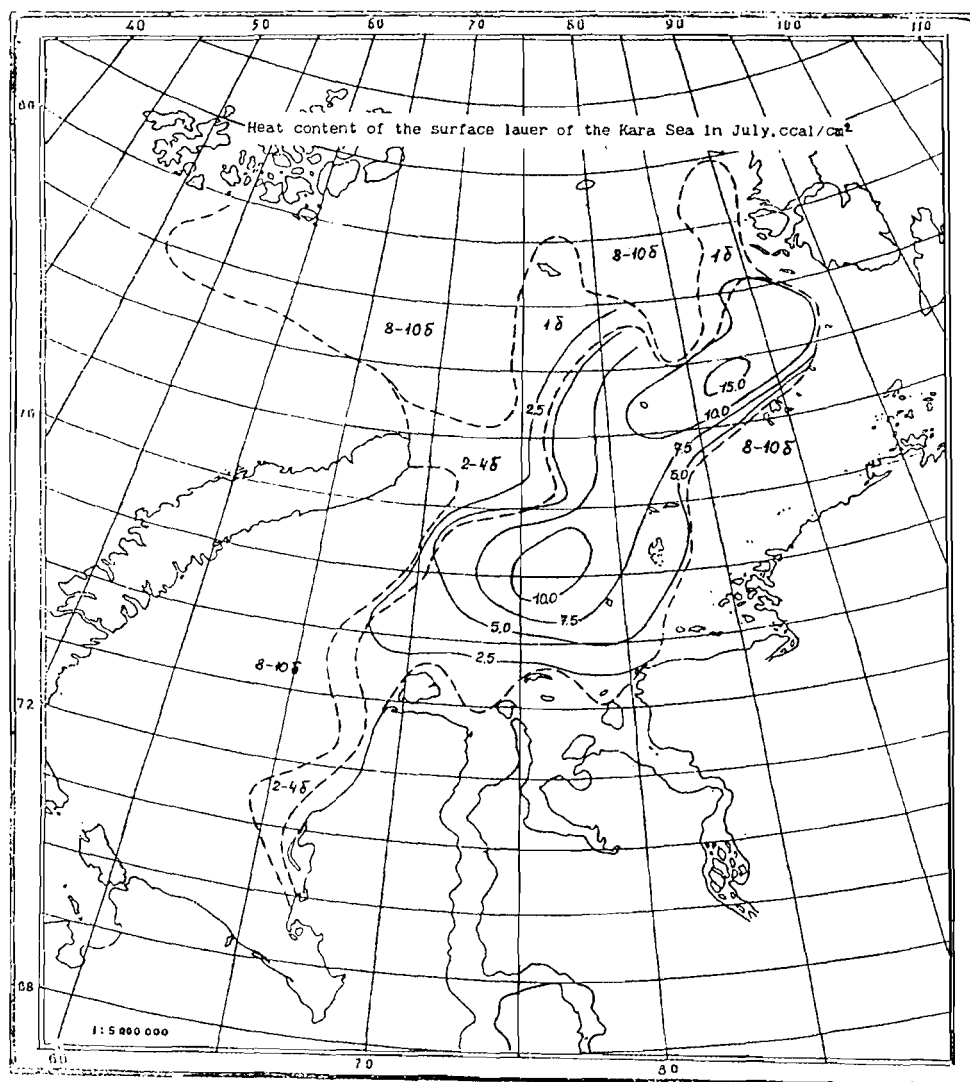


Fig. 3. Heat content of the surface layer of the Kara Sea in July, kcal/cm²

In the central zone of the polynya heat content reaches 10-15 kcal/cm². High heat content values in the polynya do not fully reflect atmospheric heat accumulation, since part of this heat is lost due to ice melting. Heat losses due to melting can be easily determined from freshening of the surface layer in the regions not subjected to the influence of the continental outflow (Bulatov and Zakharov, 1966). In this case only the northern half of the polynya meets this condition. Calculations have shown that at the time of the survey heat losses due to melting were about 15 kcal/cm² on average. Since in addition to this, 10 kcal/cm² were lost due to heating of the surface layer, the total amount of heat absorbed by the polynya from the moment the sign of the heat exchange changed to a positive one, was about 25 kcal/cm². This equals 74% of the incident solar radiation.

Thus, an enormous role of polynyas as heat accumulators and centers of ice destruction in the sea has been confirmed.

References

Bulatov L.V., Zakharov V.F., 1967: Some features of heat accumulation and loss in the south-western Kara Sea. Proc. of the AARI., vol.257, pp.119-124.

Bulatov L.V., Zakharov V.F., 1966: On estimating the amount of ice melted in open sea. Problems of the Arctic and the Antarctic, iss.22, pp.127-128.

Bulatov L.V., Zakharov V.F., 1976: Formation of the thermal regime of surface water in the Arctic Seas. Proc. of the AARI, vol.319, pp.63-72.

OCEANOGRAPHIC DATABASE ON THE BARENTS SEA AS PART OF CREATING OCEANOGRAPHIC SYSTEM ON THE ARCTIC OCEAN.

S. V. Chviljov (AARI)

Database

The basic idea of the database structure is an ordinary conception typical of modern databases: the greatest body of information being kept in a minimum of files. Each file contains the unique group of the data. No duplication of the groups can be done fundamentally: data of one field is kept in a single file. The only exception is the fields used for file linking. This approach excludes (or reduces to a minimum) the duplicate records and simplifies records processing and updating. Fragmentation of the data by periods and observational regions is not allowed as it is usually done in so called "special-purpose" databases. The two-year experience in handling data suggests that this line of attack is justified.

By August, 1995 the database had already included the information from more than 190 000 oceanographic stations or, in other words, from more than 1 900 000 observational levels of the Arctic Ocean (Fig.1).

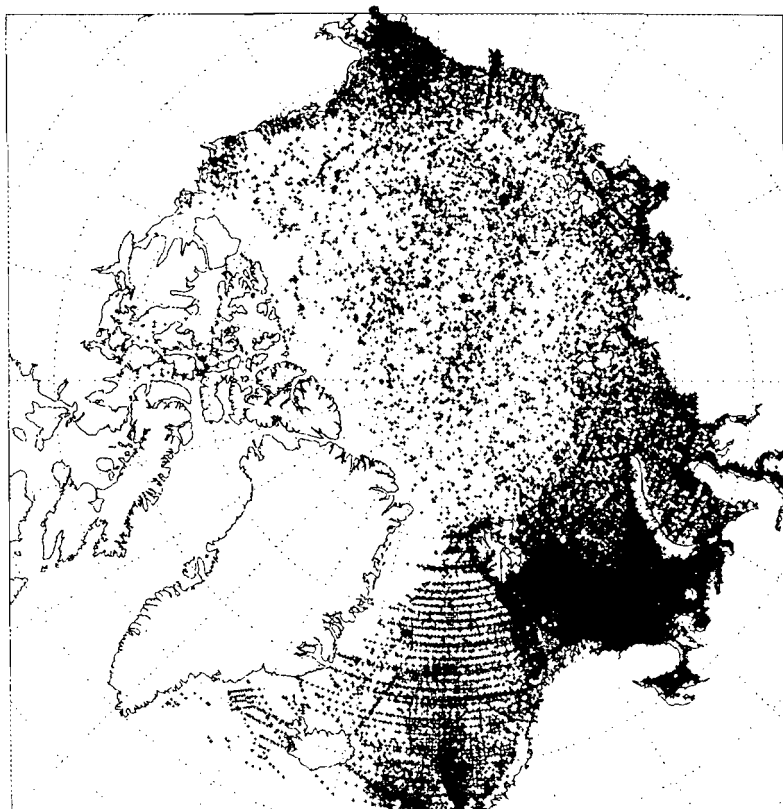


Fig. 1. Position of oceanographic stations in temperature and salinity fields of the Arctic Ocean

129 005 oceanographic stations (65 %) refer to the Barents Sea. The parameter composition of the Barents Sea data is as follows: temperature (100%), salinity (85%), oxygen (20%), pH (2%), PO₄ (14%), SiO₂ (9%), NO₂ (5%), NO₃ (5%). 92% of the oceanographic stations were identified by the name of a vessel. Research vessels of the Former Soviet Union and Russia, owned by the Federal Service for Hydrometeorology

and Monitoring of the Environment and the Committee on Fishery of the Russian Federation, are mainly presented. Most observations were carried out by means of Nansen bottle. The observational period for the Barents Sea covers the time from 1900 till 1993: 0.7% falls within the range between 1900 and 1929, 4.4% - in the 30s, 2.6% - in the 40s, 15.8% - in the 50s, 23.5% - in the 60s, 27.0% - in the 70s, 21.4% - in the 80s and 4.5% - between 1990 and 1993 (Fig. 2).

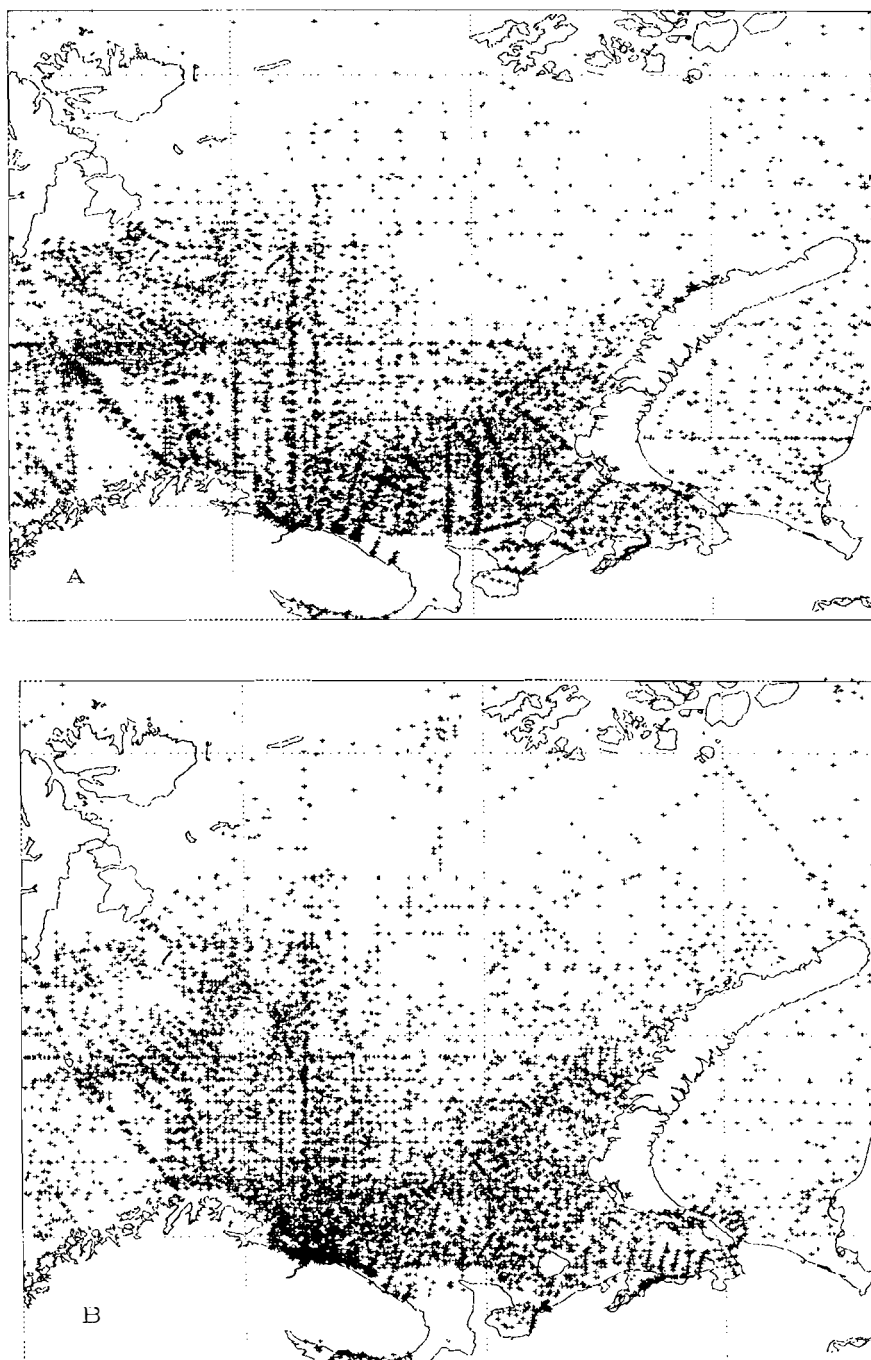


Fig. 2. Position of oceanographic stations in temperature and salinity fields of the Barents Sea: in the 1960s (a), 1970s (b).

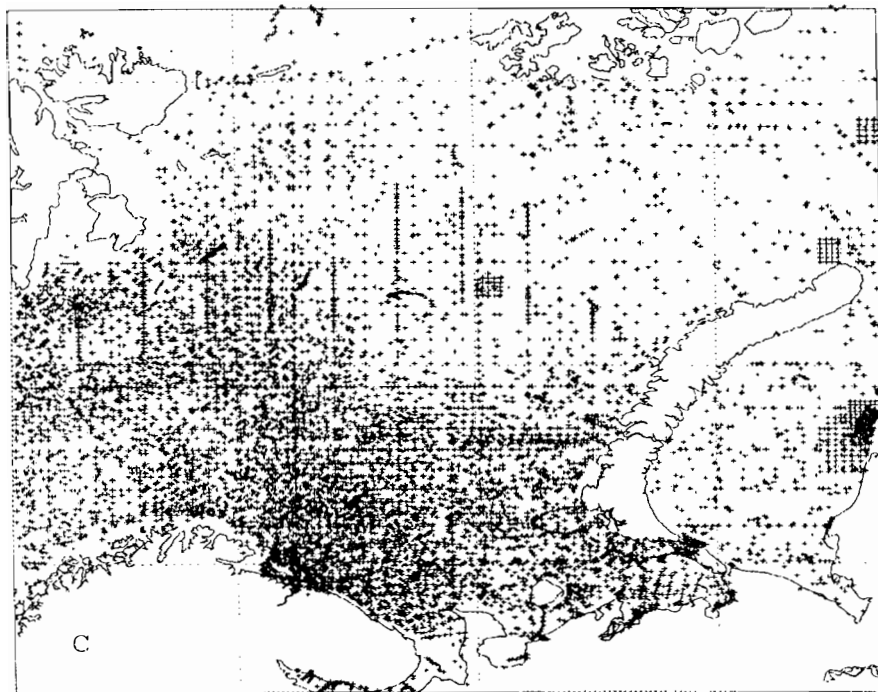
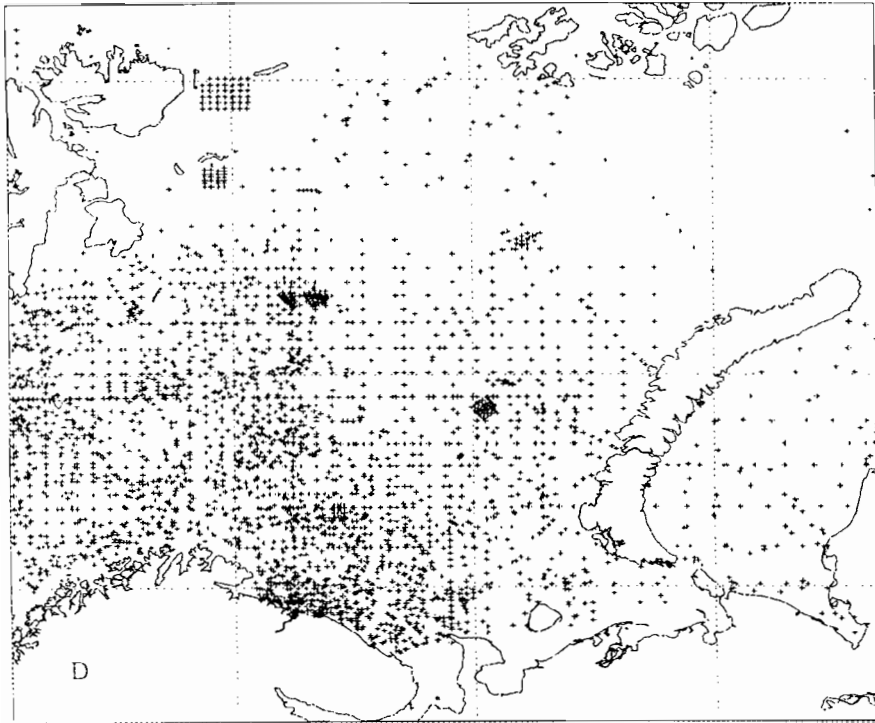


Fig. 2. Position of oceanographic stations in temperature and salinity fields of the Barents Sea: in the 1980s (c) and 1990-1993 years (d) .

Oceanographic system

The control system of the oceanographic database for IBM-compatible personal computers was worked out with the help of the FoxPro 2.5 for DOS in 1993-1995. This system is intended for those oceanographers who work with great data sets on IBM-compatible personal computers. Because of the convenient menu that also supports a "mouse" the system has become simple for any user to operate.

Basic items of the system are as follows:

- Data input: screen ("manual") input, import from ASCII-files, quality control for data input. Deletion of duplicate records (oceanographic stations and/or observational levels)
- Data quality control in the main database
- Output and visual representation (mapping) of the data. "Visual representation" is the interface between the database and the Surfer package
- Working with the database inventories: development, view mode, comparison of the inventories

When the body of available information and the speed of data processing of this system are compared with those of the similar ones for DOS, the system seems to be the best among them, which can be proved by the following:

- Based on the fact that a station includes about 20 observational levels, the number of the oceanographic stations simultaneously accessible to be processed can be equal to 50 million (CD-ROM disks, NODC, USA, include now 4.6 million of oceanographic stations in temperature field and 1.3 million in salinity field for the whole World Ocean during the whole observational period).
- For an "ordinary" PC 486 DX/66 MHz with a usual hard disk, in the case of the most complicated inquiry, it takes us about 3 minutes to do the data output from the database counting 198 183 deep-zone oceanographic stations (or 1 965 257 observational levels) and approximately 10 seconds for the inquiry like "within the coordinate range ... for the period ... to output the parameter ... at a depth ... ". Access to an oceanographic station by given co-ordinates, date and time is practically instantaneous.

The non-network version of the system was used on 19 personal computers till October, 1995. The main troubles noticed by end-users have been already eliminated by now.

The purpose of further development of the system is to connect the system with the Local Area Network and develop the Windows-version using the FoxPro 3.0 (Visual) for Windows-95.

In late 1995-early 1996 the database was steadily supplemented by the addition of oceanographic observations from both the Russian and Western expeditions in the Arctic Ocean. The database structure and capabilities of the FoxPro enable us to do it.

Outlook of productivity

According to our estimations, the total historical observational data set for the Arctic Ocean seems to contain 500 000 oceanographic stations.

While searching the given value in an indexed file the maximum of references is determined as $\log_2 N$, where N is the quantity of records in this file.

Consequently, when the database is increased from 190 000 to 500 000 oceanographic stations (i.e. by 163%) there will be a rise in the time of the data output by not more than 8%.

Thus, using even rather "modest" personal computers system makes possible the supporting and quick processing of the databases which are comparable with the total historical oceanographic data set for the Arctic Ocean in the body of information.

References

1. S.V.Chvilyov. Control system of the oceanographic database for IBM-compatible personal computers to be developed using the FoxPro package. , 1995. Preparation of the sea ice and hydrometeorological database. St.Petersburg, Hydrometeoizdat, pp. 84-92. In Russian
2. V.T. Sokolov, V.Yu.Karpiy, N.V.Lebedev, S.V.Chvilyov, Oceanographic database for the Arctic ocean. Preparation of the sea ice and hydrometeorological database, 1995 . St.Petersburg, Hydrometeoizdat, pp. 6-12. In Russian

COLD AND HIGHLY SALINE WATER OF THE KARA SEA

V.N. Churun, L.A. Timokhov (AARI).

A phenomenon of the formation of cold and very saline water in winter whose density may exceed that of deep and bottom water is a unique feature of the Kara Sea.

In order to identify the regions of its formation, data of oceanographic observations carried out by the "Sever" expedition in 1977-1989 and 1993 in the Kara Sea were used. The main attention was given to oceanographic stations where extreme salinity values exceeded 34 ‰ from the surface to the bottom at a quasiuniform water temperature distribution.

In the Kara Sea there are clearly identified two regions of water localization with extreme thermohaline characteristics. The first region is confined to the Baidaratskaya Gulf. Here in winter water with a temperature $-1.98 \dots -1.56$ C and salinity 34.04 - 35.29 ‰ is formed. An arbitrary density of such water is 27.40-28.41 units. The physical-geographical location of the Baidaratskaya Gulf, its shallow character, absence of the river runoff and cyclonic character of water motion contributes to the process of water column salination at ice formation. The most probable mechanism of the formation of a stable-stratified state of the water column is a continuous process of salinity convection at an absence of significant vertical temperature gradients. It is possible that tidal currents play a significant role in vertical salinity advection (N.Ye. Dmitriyev, 1993).

The second region of the formation of water with extreme thermohaline characteristics is located at the shallow plateau between the Viese and Ushakov islands. The temperature of this water is $-1.98 \dots -1.59$ C with salinity reaching 34.16-35.21 ‰. An arbitrary water density in this region is a little higher than in the south-western Kara Sea being 27.49-28.35 units. The main cause for the formation of water with such characteristics in winter is a sufficiently large inflow of saline (up to 34 ‰) surface water from the north.

Water with close extreme characteristics of temperature ($-1.99 \dots -1.89$ C) and salinity (34.17 - 35.17 ‰) is also observed in winter in the south-eastern Pechora Sea. Here along with the hydrographic features of the region and a significant reduction in the river runoff in winter the decisive factor in the formation of cold and very saline water is an inflow of the Barents Sea water.

Occasionally such extreme temperature and salinity values in winter were observed in the vicinity of the Zhelaniya cape, along the eastern coast of Novaya Zemlya, off the Franz-Josef Land, as well as north of Severnaya Zemlya. But most frequently and over a more extensive area such phenomena are observed at the plateau of the Central Kara Upland. The proximity to the plateau of the St. Anna and Voronin troughs suggests that this region of the Kara Sea with the above mentioned regions plays a large role in the formation of deep and bottom water of the Arctic Basin.

**FORMATION OF SPATIAL-TEMPORAL TEMPERATURE NON-
UNIFORMITIES IN THE EASTERN KARA SEA AS AFFECTED BY THE
DESTRUCTION OF INTERNAL WAVES**

I.A.Dmitrenko, P.N.Golovin (AARI)

In summer of 1994 oceanographic observations were carried out in the eastern Kara Sea from board the R/V "Professor Multanovsky" at two long-term stations with duration of 14 and 17 hours. Time interval of soundings was 30 minutes at spatial resolution not less than 5 cm. Sampling and sounding by fluorimeter were performed simultaneously.

As a result of the studies, high gradient interlayers of cold water are recorded at depths of 13-14 m in the water layer between the seasonal and main thermocline. The thickness of interlayers varied from 3 to 5 m, vertical temperature gradients were reaching 0.7 C/m. A distinguishing feature of observed intrusions is their isopycnic character, natural density stratification remained undisturbed at their advection by mean flow.

Similar isopycnic intrusions of warm and cold water were found in the course of the expedition studies of 1993-1994 in the Laptev Sea under the Russian-German Program "the Laptev Sea System". Its spreading is confined to the locations of outflow hydrofronts and occurrence is related to a sharp thermocline of the outflow hydrofronts appearing due to convergent processes in the near frontal zone. In this case any horizontal momentum, for example, induced by a system of inertia currents, can serve as an initial precondition of their generation.

A composite analysis has shown that occurrence of such intrusions in the eastern Kara Sea is related to destruction of the ridges of internal waves formed in the lower main thermocline. This is also confirmed by the fact that intrusions are characterized by enhanced values of the chlorophyl "a" fluorescence whose local maxima are observed everywhere in the region of the main thermocline location. Same pattern is observed with regard to the level of oxygen dissolved in water.

An isopycnic character in this case is governed by the process of isopycnic advection of intrusions from the nearby sea regions where corresponding salinities are recorded in the region of the main thermocline location.

EXTREME OSCILLATIONS OF THE KARA SEA LEVEL

Ye.N.Dvorkin , Yu.A. Vanda,P. V.Pavlov(AARI)

The shelf zone of the Kara Sea is rich in mineral resources. In recent years the activity for search, exploration and industrial production of sea oil-gas-bearing fields in this region have increased. Planning and provision of safety of shipping, designing and construction of marine oil-gas producing complexes, as well as hydrometeorological support of their exploitation require comprehensive evidence on different elements of the hydrometeorological regime, in particular, information on sea level oscillations. This is a factor which can actively influence human activities in the coastal Arctic zone. Let us note that multiyear observations of sea level oscillations at island and coastal stations are especially valuable, as among other indicators of dynamic processes in the hydrosphere of the shelf zone of the Kara Sea information on sea level is most fully and objectively presented.

Main initial data used for investigating features of extreme level oscillations of the Kara Sea were multiyear series (more than 35 years) of level observations at 4 synoptic times at 23 coastal and island stations (Fig. 1). Considering that marine activities in the Kara Sea can be carried out all-year-round, extreme level values were analyzed for all months of the annual cycle.

Level oscillations in the Kara Sea are of extremely complicated character and are governed by a combination of the dynamic and conservative factors. The dimensions and position of the Kara Sea allow considering the action of the dynamic factor to be sufficiently uniform over its area. Thus, differences in the character of level oscillations, features in the formation of extreme oscillations in some regions of the Kara Sea are primarily governed by the morphometry of these regions: bottom topography, coastline position, etc. River runoff also plays a considerable role in the regime of extreme level oscillations in the Kara Sea.

By morphometric indications the Kara Sea can be divided into several regions, its northern part being one of them. In the center of the northern Kara Sea there is the Central Kara Elevation restricted from the west by the St. Anna trough with depths exceeding 600 m and from the east by the Voronin trough with depths about 200-300 m. Thus, the depth in this sea region is quite large and the amplitude of extreme level oscillations at the stations located in this region (Zhelaniya cape, Viese Island, Uyedineniya Island, Golomyanny Island, Krasnoflotsky Islands, Geiberg Island, Solnechnaya inlet, Cheluskin cape) is rather small not exceeding 200 cm. Absolute maximums and minimums at most stations of this region do not exceed 100 cm.

With the decrease in depths of the regions, the amplitude of extreme level oscillations begins to increase comprising 200-250 cm for the stations Bolvansky Nos, Se-Yakha, Izvestiya Tsik Islands, Russky Island and 250-300 cm for the stations Yugorsky Shar, Amderma, Ust'-Kara, Tadibeyakha, Dikson Island, Sterlegov cape, Pravda Island, Kharasavey Cape. Whereas the absolute maximum value for the stations of the first group varies from +100 cm to +130 cm and of the minimum from -80 cm to -100 cm, these values comprise from +130 cm to +170 cm and from -110 to -130 cm for the second group, respectively.

A sharp increase in the amplitude of extreme level oscillations at the stations Antipayuta (434 cm) and Sopochnaya Karga (436 cm) as compared to other stations, is governed by the position of these stations in the mouths of such rivers as Taz and Yenisey, rather than by the morphometry of the regions of their location. The absolute maximum at these stations is almost twice as large as the absolute minimum and is observed in June at the time of the spring flood. The secondary maximum at these stations observed in September-October is +144 cm and +196 cm at a minimum of -147 cm and -174 cm, respectively. Thus, the amplitude of level

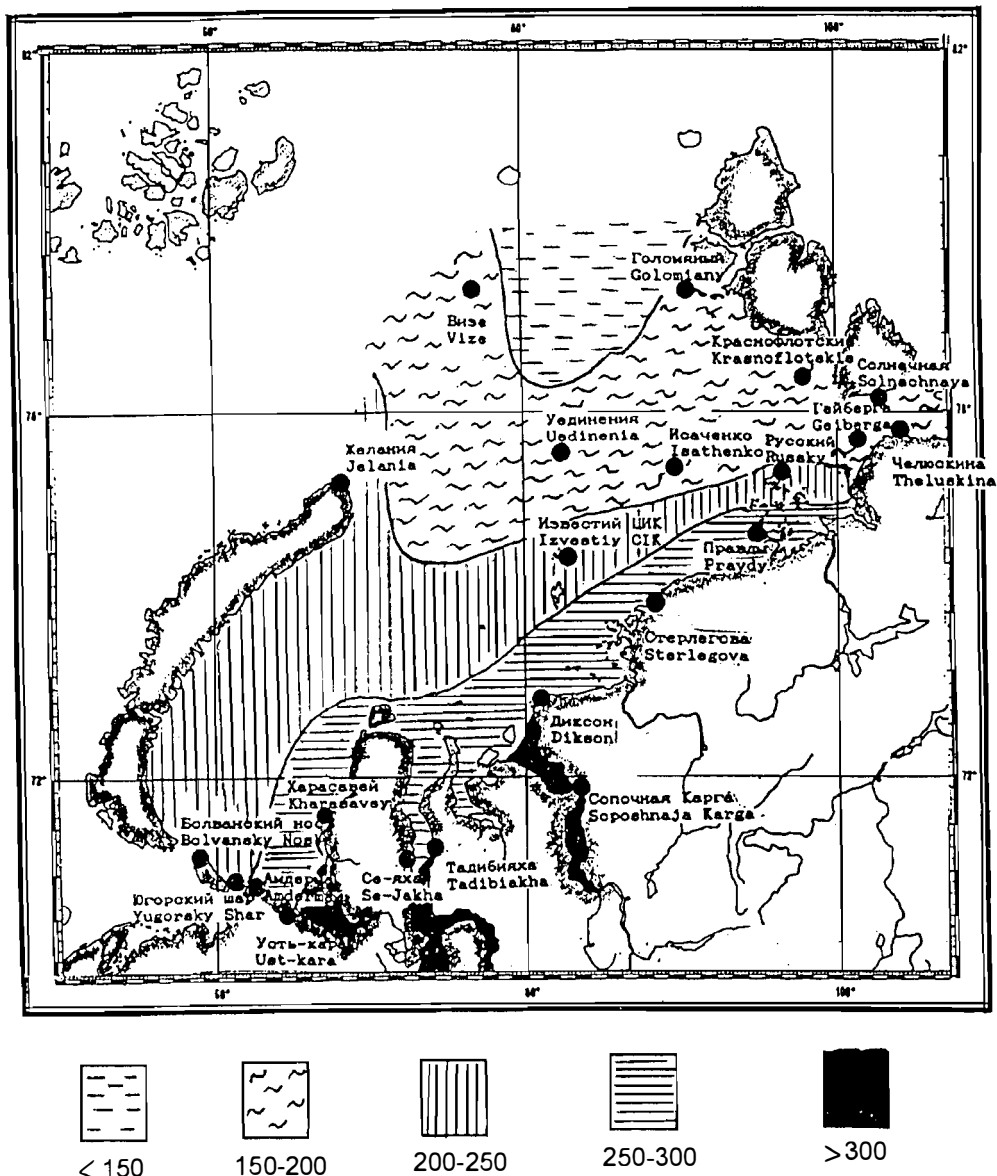


Fig. 1. Location of sea level observation sites and areas of amplitudes of extreme level oscillations in the Kara Sea (cm)

oscillations governed by the influence of sea factors alone at these stations is 291 cm for Antipayuta and 370 cm for Sopochnaya Karga.

A well-pronounced maximum at the time of the spring flood is observed at all stations located in the mouths of the rivers (Ust'-Karga, Se-Yakha, Tadibeyakha, Antipayuta, Sopochnaya Karga), as well as at some others: Bolvansky Nos cape, Kharasavey cape, Dikson Island, Sterlegov cape, but the value of the absolute maximum at these stations does not already exceed the absolute maximum governed by the influence of sea factors.

A characteristic feature of the regime of extreme level oscillations in the Kara Sea is the excess of the values of absolute maximums over the values of the absolute minimums. The only exception are four stations: Krasnoflotskiy Islands, Golomyany Island, Izvestiya Tsik Islands and Solnechnaya inlet where the value of the absolute minimum exceeds that of the absolute maximum by 5-15 cm. At some stations (Yugorskiy Shar, Kharasavey cape, Zhelaniya cape, Isvestiya Tsik Islands, Isachenko Island, Geiberg Island, Viese Island, Solnechnaya inlet, Krasnoflotskiy Islands,

Golomyany Island) the difference in the values of the absolute maximum and the absolute minimum is comparatively small being not more than 15 cm). At the stations Bolvansky Nos, Amderma, Ust'-Kara, Se-Yakha, Dikson Island, Sterlegov cape, Uyedineniya Island, Cheluskin cape the excess of the absolute maximum value over that of the absolute minimum is 25-35 cm. The most significant difference between the values of the absolute maximum and minimum governed by sea factors is observed for the stations Pravda Island and Russky Island where it is equal to 50-55 cm.

It is obvious that the existence of this feature in the regime of extreme level oscillations indicates a uniform character of effective surge directions for most stations of the Kara Sea and the excess of northerly wind speeds over southerly wind speeds which is confirmed by the analysis of the wind regime of separate regions of the Kara Sea.

Absolute level maximums of the Kara Sea are subjected to a well-pronounced seasonal variability. At most stations of the Kara Sea where the effect of river runoff is comparatively small, there is a sharp increase in the absolute maximums in September and persistence of their increased background up to March after which beginning from April the values of the absolute maximums sharply decrease and remain comparatively small up to August. Such a character of the seasonal variability of absolute maximums is in accordance with the Icelandic Low becoming more active in the autumn-winter period and hence, the increased cyclonic activity over the Kara Sea area. At some stations, as mentioned above, a secondary maximum is observed which is related to the spring flood. Absolute level minimums in the Kara Sea have a similar character of the seasonal variability.

Thus, the most significant level oscillations in the Kara Sea are observed along the Yugorsky and Yamal coasts, in the Ob' and Taz Gulfs, in the Yenisey Bay and east of it along the coast of the Taimyr peninsula up to the Nordenskjold archipelago, i.e. in the coastal shallow zone limited approximately to a 20-25 m isobath. Unfortunately, due to the absence of observations, extreme level oscillations in the Baidaratskaya Gulf and along the Novozemel'sky coast cannot be characterized, however, an analysis of the morphometry of these regions suggests a possibility for significant sea level rises and drops in the Baidaratskaya Gulf and comparatively small level oscillations in the region adjacent to the coast of Novaya Zemlya.

A general character of the spatial location of the regions of absolute amplitudes of extreme level oscillations in the Kara Sea is illustrated in Fig. 1.

The study performed can be considered as a basis for preparing a specialized regime-reference handbook on extreme level oscillations in the Kara Sea.

HYDROPHYSICAL PROCESSES GOVERNING MESOSCALE VARIABILITY OF OCEANOGRAPHIC CHARACTERISTICS IN THE COASTAL ZONE OF THE KARA AND LAPTEV SEAS

V.A. Gribanov, I.A. Dmitrenko, V.V. Stanovoy (AARI)

The results of the analysis of observation data obtained at multiday oceanographic stations in the coastal zone of the Kara and Laptev Seas are presented. Spectral structure features of mesoscale hydrophysical processes and the effect of river runoff were established.

The specific features of hydrophysical processes in the Arctic Seas in summer are governed by significant freshwater runoff of the Siberian rivers whose maximum falls on the Kara and Laptev Seas. The coastal sea regions are most affected by river runoff.

In the estuaries the pycnocline is formed when the desalinated water flows onto a more saline and, as a rule, colder sea water. The depth of the pycnocline is small in the coastal zone gradually increasing toward the head of the estuary. In this region with small depths the hydrophysical processes in the pycnocline are influenced both by the proximity of sea surface and the bottom. Hence, the internal waves in the estuaries are, as a rule non-linear, have the finite amplitude and there is a large probability for the occurrence of hydrodynamic instability. The maximum of the spectral density function is observed at the pycnocline depths at inertial and tidal frequencies. The increase in spectral density at frequencies of shallow tides of 3, 6 and 8 hours is typical.

For the regions of open sea with a well-pronounced quasistationary upper mixed layer and the pycnocline, the maximum of the spectral density function of temperature and salinity variations is observed in high gradient layers - the pycnocline and the thermocline coinciding in depth.

The most complicated processes are observed in the coastal zones which are characterized by small depths, the presence of frontal zones and the absence of a stationary upper quasiuniform layer. The pycnocline is located in the surface layers which leads to specific dynamic processes in these zones - generation, interaction and decay of the internal waves, entrainment and mixing processes, developed mesoscale turbulence.

As a result of analyzing the observation material at multiday oceanographic stations, it was found that in the shallow coastal zone even in the absence of the outflow currents there is observed a well-pronounced baroclinicity and the spectral structure of processes is characterized by the presence of subsurface maxima at inertial and tidal frequencies (Fig. 1 a). An analysis of the data collected in the coastal zone of the East-Siberian Sea allows similar conclusions of the prevailing effect of the internal tidal waves on the formation of the vertical distribution of oceanographic characteristics.

In shallow water regions in the zone of the river runoff effect spectral maxima are shifted to the surface (Fig. 1b). And a monotone decrease in the spectral density values with depth suggests a barotropic character of the motions. Since the outflow lense thickness does not, as a rule, exceed 5-7 m, the barotropic motions in this case can be attributed to the processes of entrainment and convergence at outflow hydrofronts, as well as to the processes of internal waves exiting to surface levels, their decay and the formation of the "internal" surf effect.

Thus, a spectral analysis of the observation data at multiday stations in different zones of the Kara and Laptev Seas suggests that the most intensive mesoscale processes are manifested near the inertial and tidal frequencies being confined to high-gradient water layers. However, in the coastal zones the largest mesoscale variability is observed in the surface layer in the region of hydrofronts (Fig. 2).

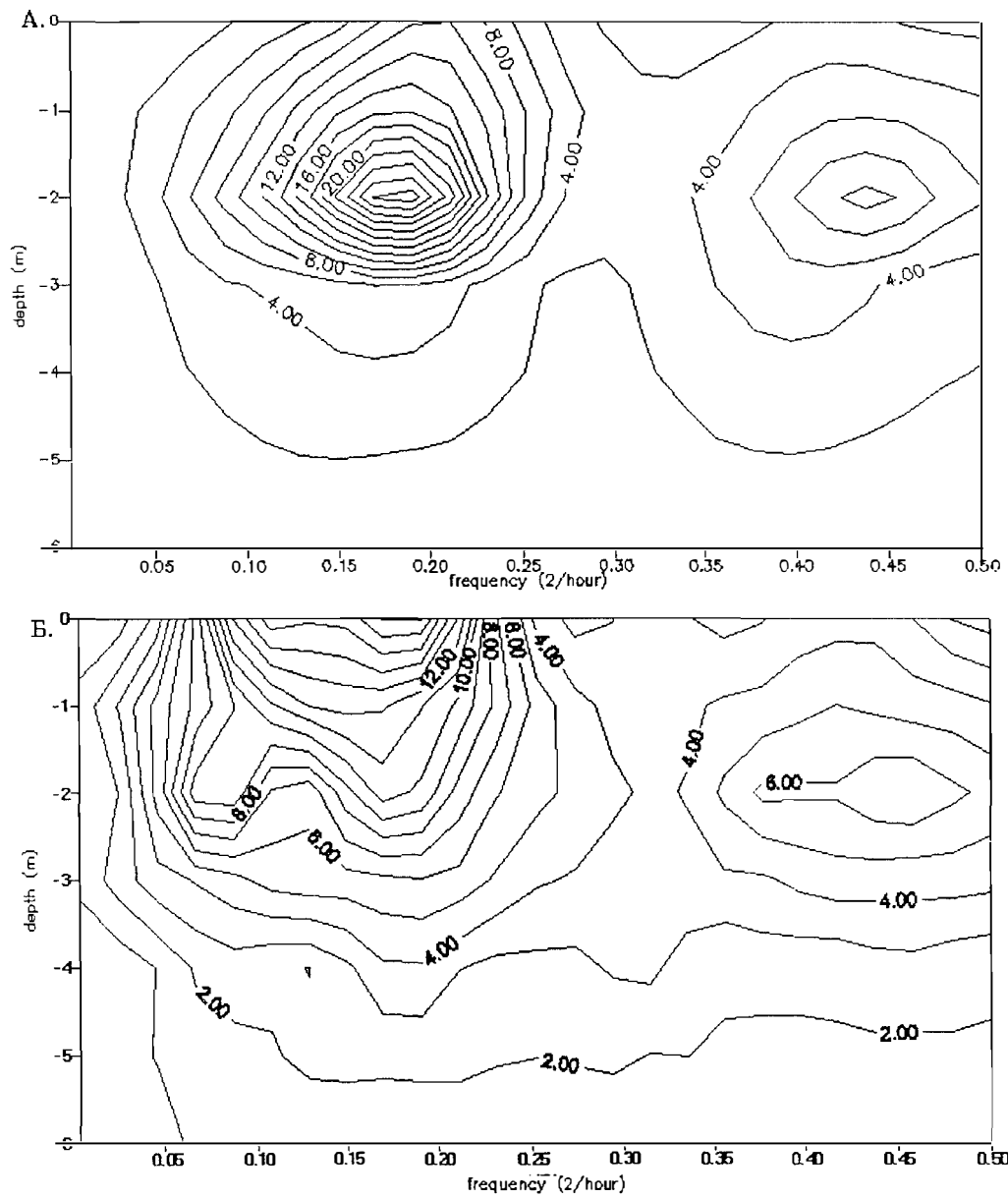


Fig.1. Spectral density of the water salinity fluctuations on the multiday stations in the coastal zone of the Laptev Sea

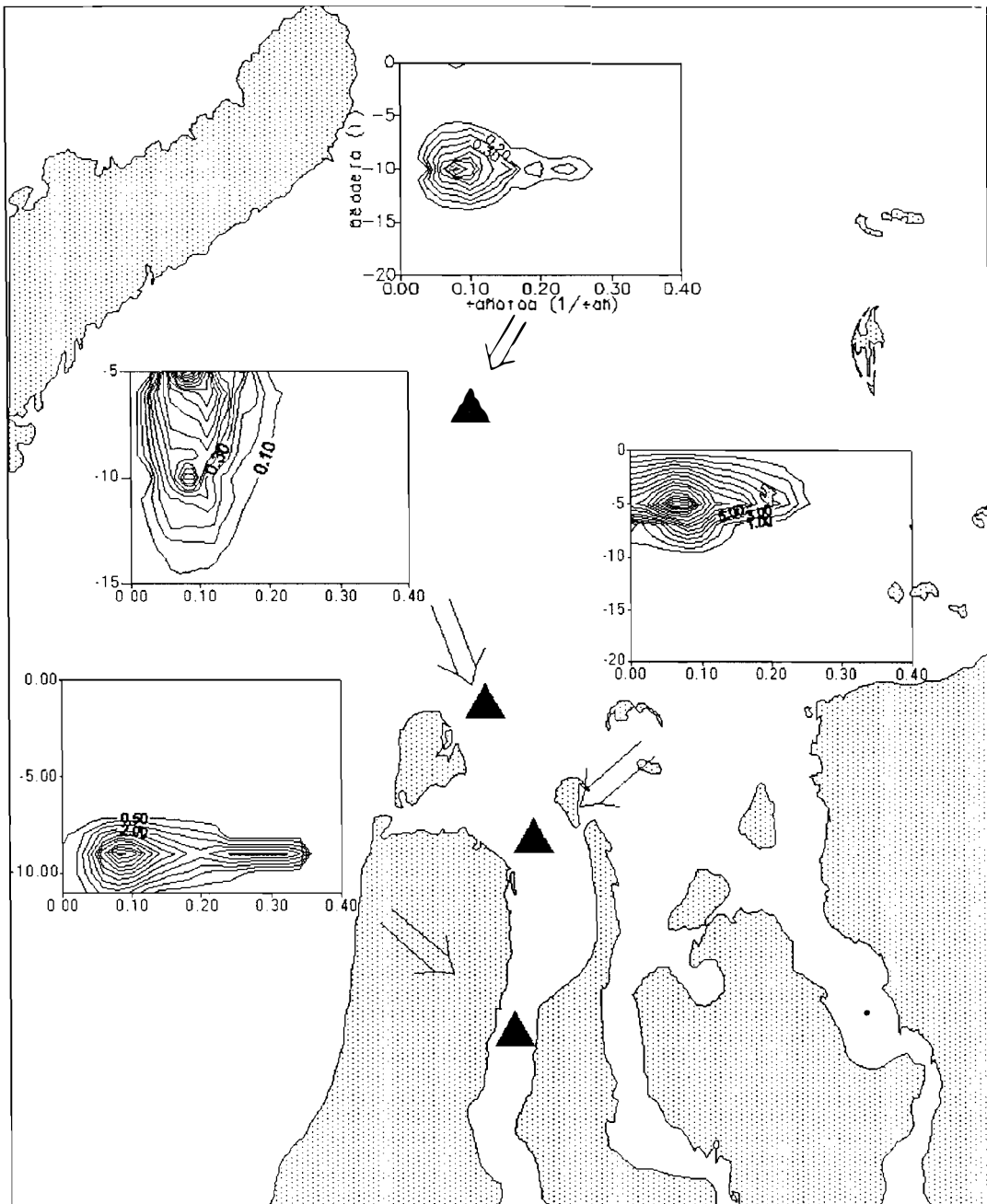


Fig. 2. Spatial variability of the spectral density of the water temperature

MANIFESTATION OF NATURAL CLIMATE OSCILLATIONS IN THE BARENTS-NORWEGIAN SEAS BOUNDARY WATER MASSES PARAMETERS

V.V.Ivanov, A.A.Korablev (AARI), I.P.Karpova ("Systema-A")

Global warming observed in the Northern Hemisphere since the mid 1960s, caused the increased fresh water outflow from the Arctic Basin to the North Atlantic. Presumably, this had resulted in a noticeable decrease in convective activity in the Greenland and the Norwegian Seas that was recorded ten years later (Aagaard, Carmack, 1989). The most probable explanation of the observed time shift between these events is as follows. Large-scale salinity anomalies of the Arctic origin which govern conditions for the development of convection in polar regions, extending in the subpolar gyre system, penetrate the convective zones of the Greenland and the Norwegian Seas only with water of the North Atlantic current, rather than directly from the north from the Arctic Basin. If this is the case, a haline "signal" of the same sign should be present along the whole of the motion trajectory of Atlantic water within the North-European Basin including the West Spitsbergen and the Nordcapp currents.

Using this hypothesis as a basis, temporal variability of water mass parameters at the boundary between the Norwegian and the Barents Seas was estimated and its possible connection with the current climatic tendencies was analyzed.

Method and algorithm of studies

Structurization of the available set of oceanographic observations is of principal importance for investigating the climatic trends. As a result, the spatially connected areas of a sufficiently uniform character are delineated. These areas can be interpreted as water masses and their variability can be analyzed separately. This approach allows revealing the true variability pattern which in the case of a randomly chosen spatial averaging area can be considerably distorted. The present study uses an algorithm of multiple classification based on the cluster analysis methods for water mass identification (Prim, 1957). The calculation algorithm includes the following stages:

- formation of oceanographic data sets in regular grid points for different time moments;
- calculation of mean values and mean quadratic deviations in grid points;
- transformation of the parameters into a dimensionless form;
- calculation of the shortest connection network;
- division into classes (water masses) and determination of their parameters.

After identification of water masses, their mean boundaries are assumed to be constant in time and for each of the time moments (oceanographic surveys) mean parameters are calculated by means of averaging within the class boundaries.

The results of 55 oceanographic surveys at the transect Nordcapp - Spitsbergen regularly made by PINRO ships from 1981 to 1990 and containing data on temperature, salinity, dissolved oxygen, phosphates and silicon, served as initial data.

Main results

According to the results of classification, two classes (51 and 53) were identified. They can be considered modified by Atlantic water intruding into the Barents Sea (Fig. 1 and Table 1). However, in spite of a considerable similarity in the values of separate parameters (salinity, silicon), the cross-correlation analysis between separate parameters inside the classes has revealed the Atlantic origin of the water mass forming class 51 (high positive TS correlation and high negative correlation Tsi (Reid, 1979) and presumably, the local origin of the water mass forming class 53 due to mixing of

Atlantic water with water of the Barents Sea (high negative TS correlation and a weak correlation dependence between the temperature and silicon).

Table 1.

Water mass statistics for different classification steps.
Section NordCape - Bear isl. Data averaged for whole Year (55 section 1981-1990)

PAR- PAR	I	II	III	IV	I				II				V	
					7	8	14	16	21	27	28	29	51	53
knot:	288	199	182	153	15	15	14	16	10	12	13	35	73	64
PAR MEAN VALUE														
t	3.64 2	3.550	3.543	3.503	3.573	3.301	2.663	3.216	0.358	2.853	5.851	5.446	2.609	4.336
s	34.9 16	34.984	34.998	35.01 1	34.921	35.00 5	34.337	34.437	34.528	34.743	34.585	34.893	35.01 3	35.01 7
o2	7.13 9	7.072	7.057	7.039	7.025	6.971	7.466	7.433	8.135	7.581	6.998	7.446	7.153	6.912
po4	0.76 5	0.828	0.839	0.854	0.658	0.794	0.400	0.375	0.582	0.622	0.601	0.616	0.879	0.841
si	5.01 4	5.481	5.560	5.698	4.561	5.505	2.821	2.755	3.131	3.794	4.056	4.093	5.733	5.767
PAR_SSD MEAN VALUE														
t	1.27 4	1.006	0.950	0.866	0.836	0.491	1.094	1.298	1.447	2.455	1.813	1.652	0.852	0.827
s	0.13 9	0.084	0.071	0.055	0.069	0.034	0.260	0.255	0.330	0.382	0.259	0.188	0.043	0.055
o2	0.27 7	0.223	0.209	0.188	0.218	0.150	0.261	0.246	0.393	0.491	0.323	0.360	0.177	0.188
po4	0.15 9	0.133	0.131	0.129	0.067	0.073	0.123	0.170	0.229	0.212	0.199	0.224	0.125	0.132
si	1.53 9	1.445	1.432	1.434	0.777	0.815	0.790	0.533	1.854	2.034	1.498	1.657	1.356	1.521
PARAMETER MIN-MAX														
t	0.16 4 6.04 3	1.455 5.470	1.450 5.320	1.450 5.272	3.199 4.254	2.721 4.074	2.544 3.185	3.027 3.389	0.164 0.582	2.396 3.165	5.449 6.043	4.633 5.998	1.450 3.951	3.170 5.133
s	34.4 57 35.0 45	34.712 35.045	34.798 35.045	34.87 4 35.04 5	34.745 34.997	34.98 3 35.02 5	34.257 34.569	34.368 34.500	34.512 34.557	34.711 34.769	34.457 34.669	34.718 34.975	34.97 9 35.04 5	34.93 9 35.04 4
o2	6.79 0 8.13 9	6.790 7.529	6.790 7.415	6.790 7.264	6.899 7.152	6.891 7.021	7.339 7.527	7.404 7.469	8.095 8.169	7.532 7.659	6.911 7.019	6.991 7.286	7.041 7.257	6.790 7.063
po4	0.55 4 0.96 9	0.680 0.969	0.699 0.969	0.747 0.969	0.561 0.702	0.749 0.844	0.373 0.460	0.346 0.417	0.554 0.629	0.600 0.645	0.567 0.666	0.676 0.661	0.804 0.969	0.783 0.909
si	2.94 6 7.00 5	4.285 7.005	4.386 7.005	4.649 7.005	3.845 5.069	5.025 5.975	2.670 3.127	2.534 2.997	2.946 3.454	3.439 4.114	3.755 4.533	3.625 4.540	4.905 7.005	4.930 6.423

Temporal variability of oceanographic parameters (Fig.2) confirms the initial hypothesis of large-scale salinity anomalies penetrating the Barents Sea with water of the Nordcapp current. The decrease in salinity of the water mass of Atlantic origin (class 51) beginning from 1985 is consistent with a similar tendency in the central Norwegian Sea (Ivanov, Korablev, 1994). However, this freshening is extremely little connected with temperature variations in this water mass characterized by a cycle of 8-10 years. Similar cyclicity is traced in the variability of the dissolved oxygen and main parameters of class 53. A probable explanation of the observed temporal variations is as follows: since class 53 contains water of local origin, the variability of its parameters reflects the effect of hydrometeorological processes forming the given water mass in the Barents Sea and the northern Norwegian Sea. The same processes should, obviously,

affect Atlantic water flowing from the south which is manifested in the least conservative parameters of class 51 - temperature and dissolved oxygen. This study was performed with the support of the Russian Fund for Basic Studies (Grant No.95-05-14935-a).

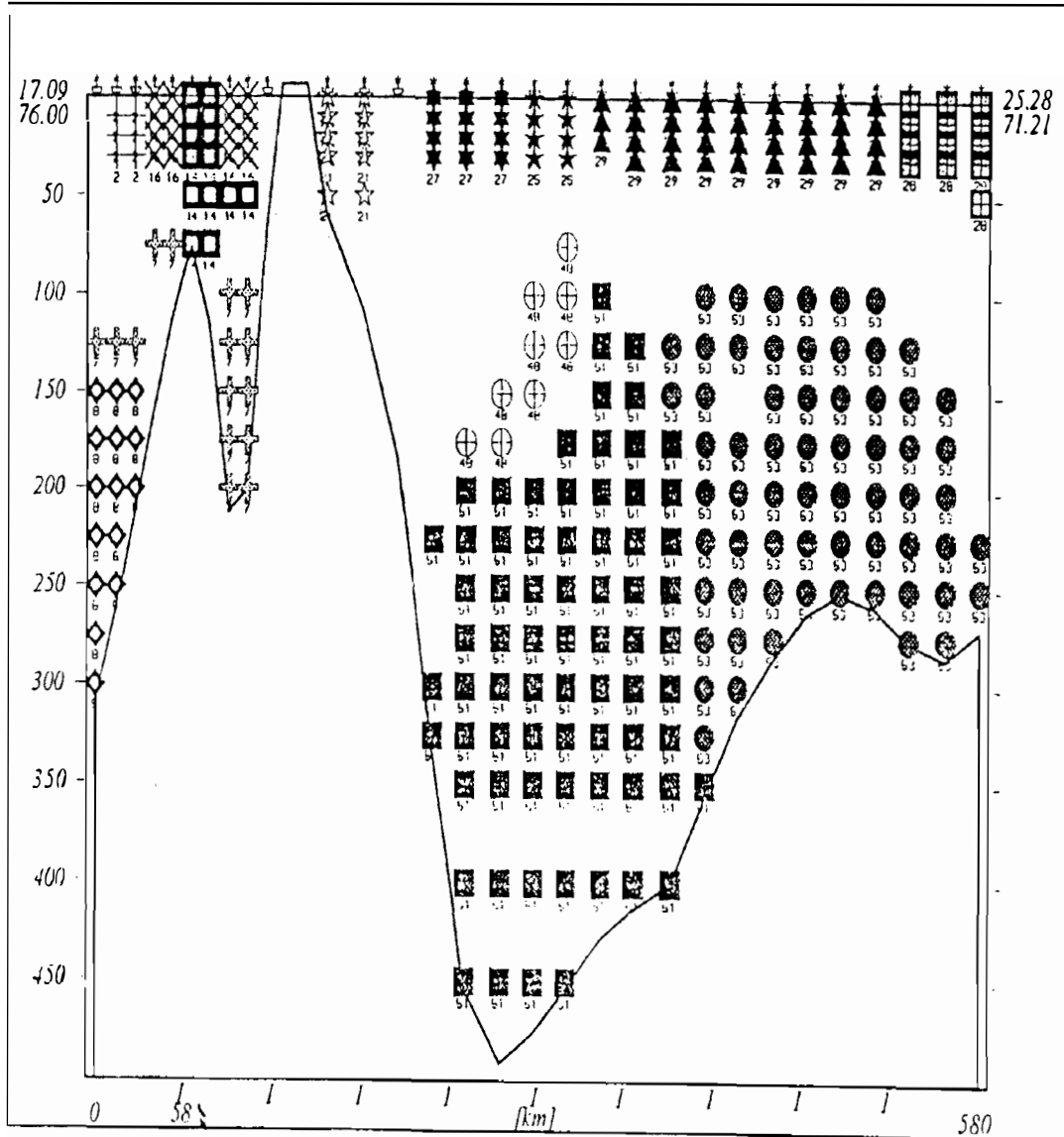


Fig. 1 Section NordCap - Bear isl. CLASSIFICATION RESULT WHOLE YEAR (55 sections 1981-1990) Parameters: 10 (t, s o2, po4, si, ssd_t,ssd_s,ssd_o2,ssd_po4,ssd_si) Recalculation step:5 Classes: 54

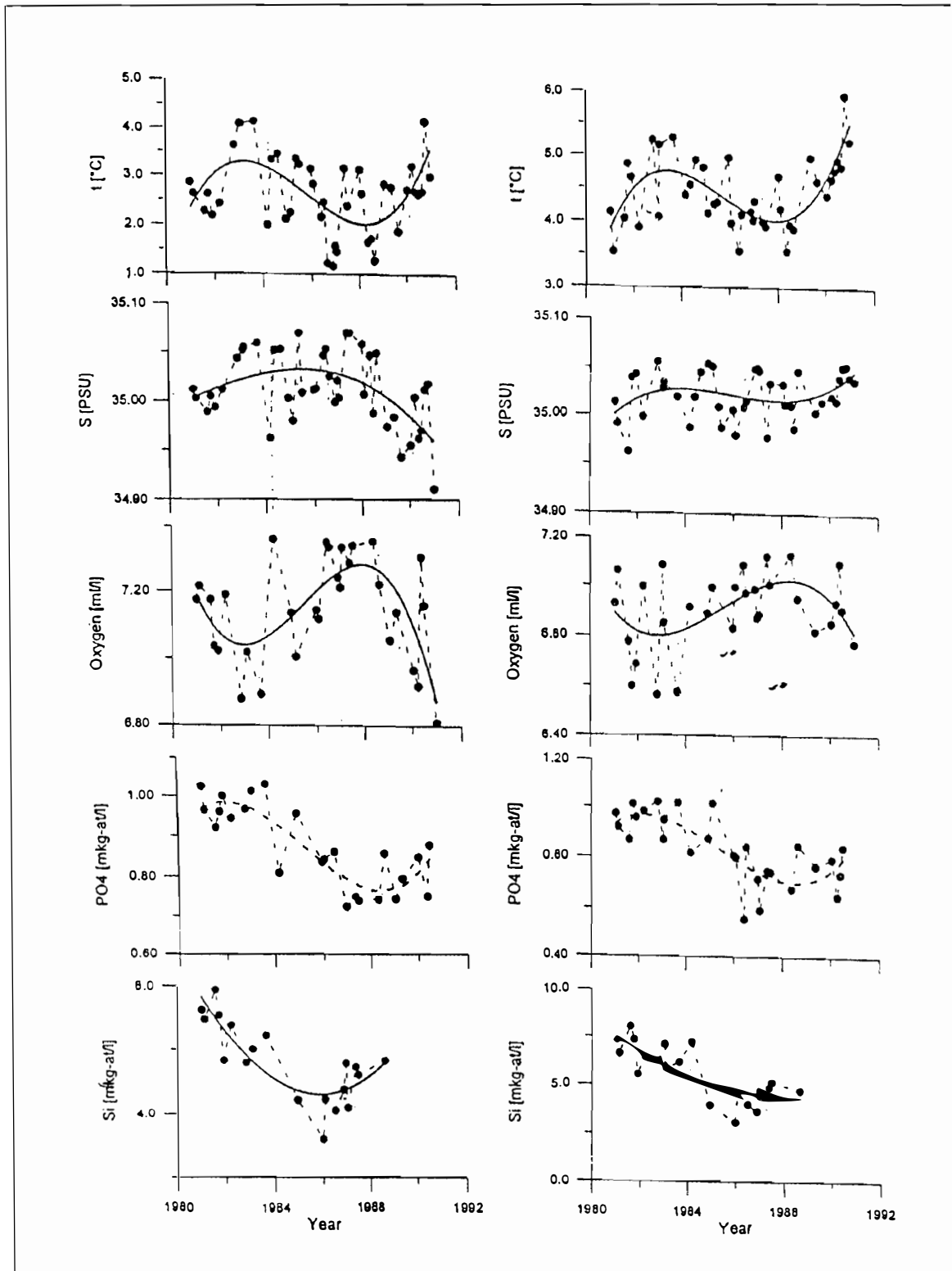


Fig.2 Temporal variability of the oceanographic characteristics spatially averaged within classes 51 and 53 Section NordCape - Bear isi.

References

Aagaard K., Carmack E., The role of sea ice and fresh water in the Arctic circulation. 1989, Journ.of geoph.res. V.94.,NC10.-P.14,485-14,498.

Ivanov V.V., Korablev A.A., Is the intensity of the deep convection in the Nordic Seas an indicator of the long-term climate variability? (Abstract), WCRP, ACSYS Book of Abstracts (Nov. 7-10, Goeteborg Sweden) O-16. 1994

Prim R.C., Shortest connection networks and some generalizations// 1957, Bell Syst. Techn.J., 36,N6, P.1389-1401□

Reid J.R., On the contribution of the Mediterranean Sea outflow to the Norwegian-Greenland Sea. 1979, Deep-Sea Res., 26A, P.1199-1223.

Observations of spectral downwelling irradiance in the Kara Sea

Jo Høkedal*
Norwegian Polar Institute, Oslo

Introduction

The motivation of this work is to distinguish fresh/brackish water of different origin in the Kara Sea. Traditionally watermasses are distinguished by use of CTD observations. Since we can not make use of different salinities for the rivers, only the temprature is left, which is not enough.

Instead we will make use of the fact that the rivers contains different amounts of suspended and particulate matters, and thereby attenuate light in different ways. By finding the attenuation as function of wavelength for the rivers we get characteristical attenuation spectrums.

It is commonly known that the attenuation of light is a complicated function of wavelength (λ), but a simple exponential function of depth (z), ($E_\lambda(z) = E_\lambda(0) \exp(-K_\lambda z)$) where $E_\lambda(0)$ is the irradiance at the surface at wavelength λ .

Figure 1

From irradiance observations at different wavelengths at two or more depths (as an example the left figure shows the irradiance just above the surface and at 1, 2 and 5 m depth). From this we easily find the attenuation as a function of wavelength for the stations (dashed lines for three stations in Baydaraskaya Bay at the right figure). To get the charateristical attenuations spectrum the average value of the stations is calculated for each observed wavelength (solid curve).

Figure 2

This figure shows the attenuation spectrums for each of the water types.

Figure 3

As we see the type "Sea" is almost identical to Jerlov's oceanic type III [2]. The deviation increases with decreasing wavelength. This and the rather low salinities (25 – 31 psu) strongly suggests that yellow substance has been brought into the region with fresh water. Thus I use:

- The attenuation of irradiance is mainly a absorption phenomen.

* Now at the University of Oslo. E-mail: johoh@geofysikk.uio.no

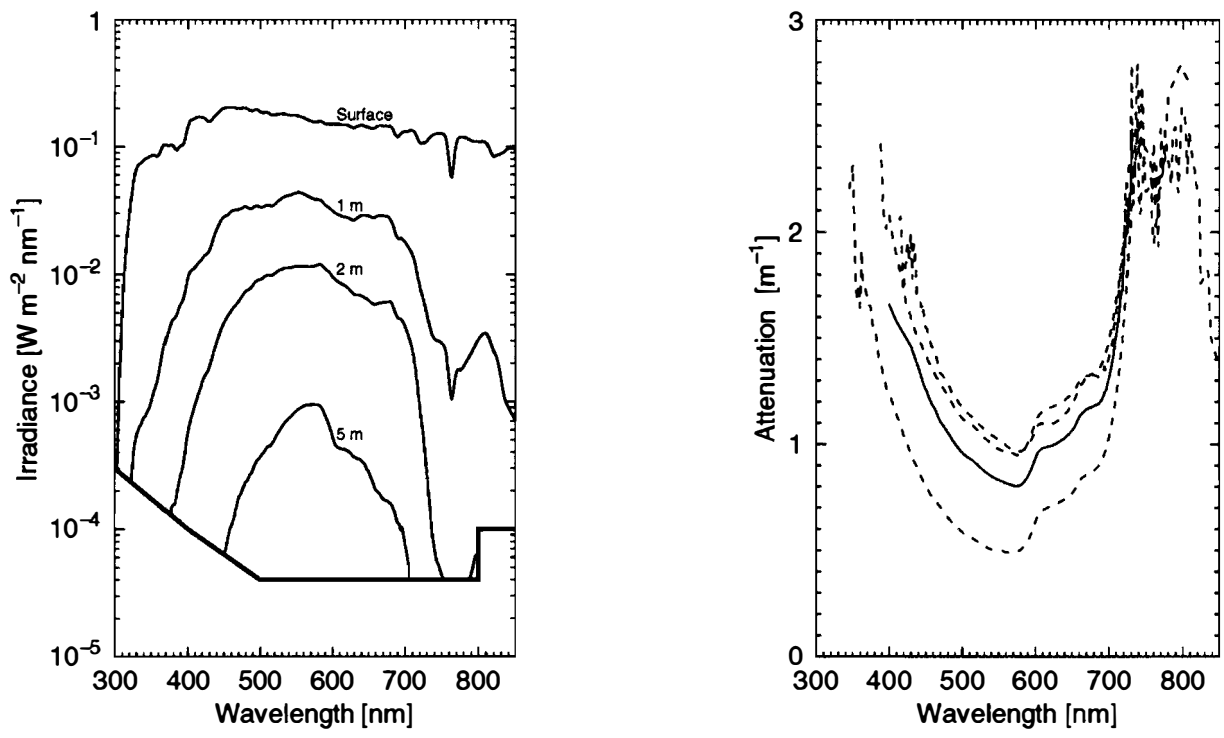


Figure 1: *Left*: Irradiance as function of wavelength at some depths at station C (N 69° 49.85' E 61° 14.40').
Right: Spectral attenuation at 3 stations in Baydaraskaya Bay and the average value of them.

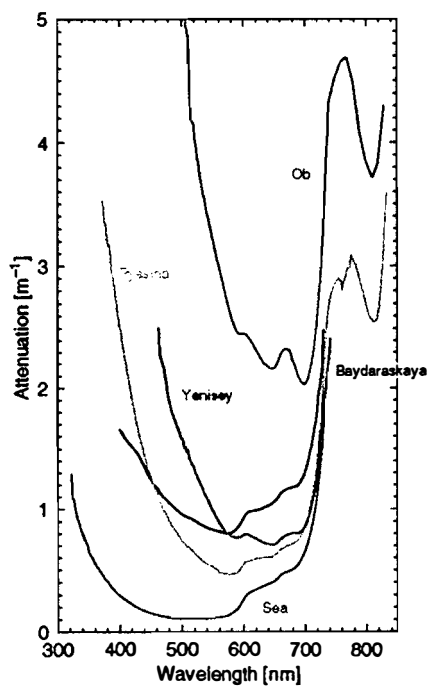


Figure 2: Characteristical attenuation spectras for some rivers/regions.

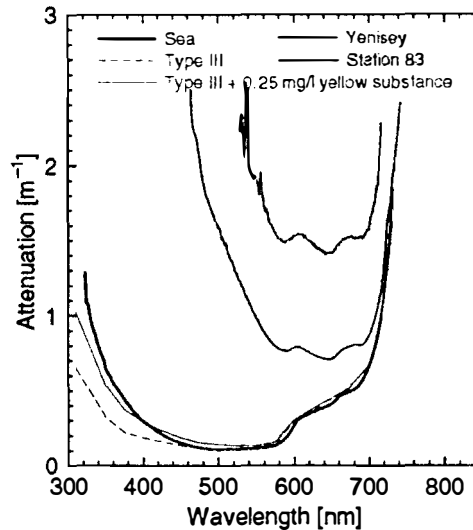


Figure 3: The similarity between the characteristic Yenisey attenuation spectrum and the observed one at station 83 (N 72° 5.97' E 82° 0.14'). Difference between water type “Sea” and Jerlov’s oceanic water type III due to yellow substance.

- Yellow substance absorb according to an exponential function of wavelength

$$a_y(\lambda) = a_y(\lambda_0) \exp[-0.014m \cdot (\lambda - \lambda_0)]$$

where $a_y(\lambda_0)$ is the absorption due to yellow substance at any fixed wavelength. (Højerslev [1]).

- The attenuation due to yellow substance at 450 nm with a content of one mg/l yellow substance is: $a_y(\lambda_0 = 450nm) = 0.212m^{-1}$. (Nyquist [3]).

Jerlov’s oceanic water types are waters free of yellow substance, thus it is just to add the attenuation of yellow substance. As we see out of the figure 0.25 mg/l gives a fairly good agreement with the observed type “Sea”.

Also the characteristic Yenisey attenuation spectrum and the attenuation from station 83 are shown. (It should be noted that this station has *not* been used when the characteristic spectrum has been determined.) As we clearly can see the observed spectrum is similar to the characteristic one, it is only shifted $0.7m^{-1}$ toward a higher attenuation. Suspicious readers will at figure 2 see that the observed attenuation at this station does not correspond to any other attenuation spectrums.

Figure 4

As we saw in the previous figure we can determine which water type an observation is from by comparing curves.

An other way is calculating the ratio between attenuation values for two and two selected wavelengths at each station. These pair of numbers may then be plotted in a diagram.

Wavelengths selected are either those of maximum transmission of the Schott filter B12, V9 and R1, or among the wavelengths that will be observed by SeaWIFS. Combinations of wavelengths are then chosen not only to get the points spread, but also to get them collected in separate groups.

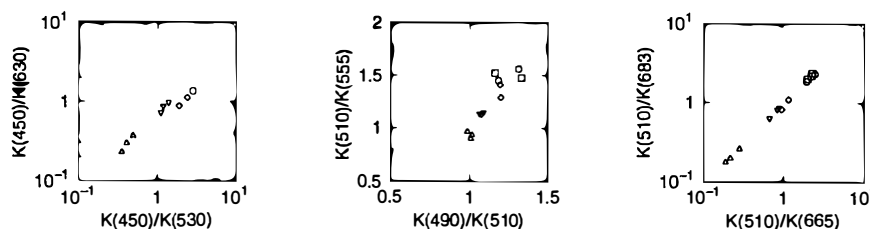


Figure 4: Ratios between the observed attenuation coefficients for some wavelengths in different regions. (∇ =Baydaraskaya, \square =Ob, \diamond =Pyasina, \triangle =Sea and \circ =Yenisey)

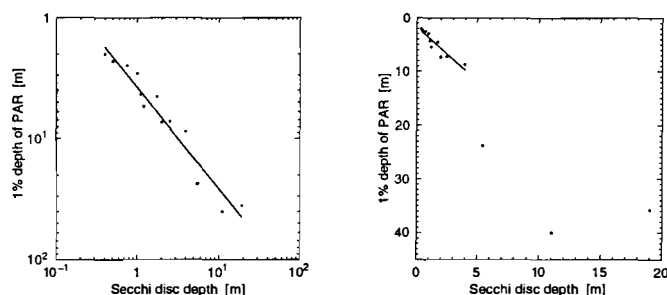


Figure 5: 1% depth of photosynthetically active radiation (PAR) as function of Secchi disc depth.

Figure 5

The penetration of light defines the photic zone, the lower limit of which is generally marked by the depth where surface photosynthetically active radiation (PAR) is reduced to 1%.

Two relations with this depth and the Secchi disc depth are found. At the left figure the exponential relation is

$$Z_{1\%} = 3.78S^{0.837}$$

where $Z_{1\%}$ is the 1% depth of PAR, and S is the Secchi disc depth.

At right a linear relation is found

$$Z_{1\%} = 1.58 + 2.04S$$

where only stations with Secchi disc depth less than 5 m are used.

References

- [1] Højerslev, N. K., *Natural Occurrences and Optical Effects of Gelbstoff*. Inst. Rep., Geophys. Inst. Dept. of Phys. Oceanography, Univ. of Copenhagen, 1988.
- [2] Jerlov, N. G., *Marine optics*. Elsevier Oceanography Series, 14, 1976.
- [3] Nyquist, G., *Investigation of some optical properties of sea water with special reference to lignin sulfonates and humic substances*. Thesis Dep. Annal. Mar. Chem., Gothenburg 1979.

PROVISION OF CALCULATED HYDROMETEOROLOGICAL VALUES FOR HYDROTECHNICAL CONSTRUCTION IN THE SOUTH-EAST OF THE BARENTS SEA

V. Korobov ("Nordeco")

Introduction

The design and construction of hydrotechnical structures, drilling platforms and corresponding communication lines in the off-shore zone require extreme environmental characteristics. As a rule, systematic multiyear observation data for the specific points of the area are absent. Therefore, the required characteristics of the main values are derived by means of calculations using the archived synoptic data and verified models of wind, waves, currents and so on. In view of the labor-consuming calculation methods, these characteristics are usually calculated for 20-25 most strong storms. At the next stage the convolution integral of the distribution of storms and of hydrometeorological parameters with the subsequent calculation of values that are probable once in a prescribed period is estimated.

In this case for the distribution of storm characteristics the Poisson's distribution is prescribed, as a rule, since this law describes rare events. The Poisson's formula is also attractive by the fact that it allows obtaining elegant analytical solutions of the convolution integral in a number of cases.

Such an approach is widespread for calculating maximum waves, currents and levels. The algorithms used are based on Langbein (1949) and Petrauskas & Aagaard (1971) where corresponding formulas and ratios are inferred.

All calculations have a common block which contains statistical characteristics of storms. We have made studies of the empirical functions of storm distribution in the south-eastern Barents Sea. As initial data, the wind observation series over a network of coastal and island hydrometeorological stations (HMS) of Rosgidromet for the period 1960-1992 were used.

In view of ambiguous determinations of storm criteria in handbooks and literature, we have considered two threshold wind speeds $V > 10$ m/s and $V > 15$ m/s. An event was assumed to be a storm when wind speed not lower than the threshold one was observed at least at two HMS for not less than 6 hours. The wind gusts between the observation times were not taken into account.

The estimates of the density of distributions of the number of storms were found by means of the χ -square criterion. The storm was considered an event without taking into account its duration. The distributions widespread in hydrometeorology were considered: normal, log-normal, Weibull's, exponential, gamma, Poisson's and some others.

Taking into account a monsoon character of the wind regime (Wind and waves in the ocean and the seas, 1974) and the large interannual variability of the storm activity (Kabatchenko & Korablev, 1988), the calculations were performed for samplings of monthly, seasonal and annual series. By a season is meant the time interval during which there is a change in hydrometeorological conditions, rather than its calendar period. According to data of multiyear observations (Hydrometeorology and hydrochemistry of the USSR seas, 1974), the following boundaries of the seasons were assumed: spring - May-June, summer- July-August, autumn - September-October, winter - November-April.

Main results

Calculations were performed separately for two wind speed gradations $V > 10$ m/s and $V > 15$ m/s. This separation is rather statistical than physical: at a threshold wind speed of 10 m/s the confidence of obtained estimates increases.

Let us consider monthly and annual samplings (Table 1). In this table, as well as in other tables gaps mark the values below 0.10.

Table 1

Distribution of the number of storms ($V > 10$ m/s)

N	Distribution law	I	II	III	IV	V	VI	VII	VII I	IX	X	XI	XII	year
1	Erlang's	0.39	0.43	-	0.23	0.35	0.46	0.81	0.57	0.57	0.24	0.77	0.34	0.91
2	Gamma	0.38	0.24	-	0.26	0.35	0.46	0.32	.069	0.53	0.28	0.70	0.31	0.88
3	log-normal	0.23	-	0.77	0.16	-	0.15	0.41	0.38	0.92	0.15	0.83	0.12	0.93
4	Weibull's	0.71	0.56	-	0.24	0.28	0.46	0.37	0.76	0.46	0.32	0.69	0.62	0.55
5	Normal	-	-	-	-	-	-	-	-	-	0.30	-	0.38	0.54
6	Poisson's	-	-	-	-	-	-	-	-	-	-	-	0.25	-

Among monthly samplings the empirical functions most frequently - in half of cases, are best of all approximated by the Weibull's distribution, but the degree of their coincidence with this law is relatively small and does not exceed 0.76. Likewise, for annual samplings quite a good agreement (0.88-0.93) was obtained for the Erlang's, gamma and log-normal distributions. There is a noticeable decrease in the χ -square values in April and October when there is a change in the atmospheric circulation pattern over the north of the European part of Russia. The χ -square for seasonal samplings is a little higher, as compared with monthly values (Table 2). For each season the empirical functions are approximated by their own distribution law.

Table 2

Distribution of the number of storms by seasons ($V > 10$ m/s)

N	Distribution law	Spring	Summer	Autumn	Winter
1	Erlang's	0.33	0.71	0.78	0.37
2	Gamma	0.72	0.62	0.72	0.38
3	log-normal	0.18	0.68	0.72	0.81
4	Weibull's	0.54	0.65	0.74	0.21
5	Normal	-	-	0.37	0.19
6	Poisson's	-	-	-	-
7	Exponential	0.53	0.88	-	-

The χ -square criterion values for the threshold wind speed of 15 m/s are considerable lower (Table 3, 4). This fact can be attributed to a significant decrease in the number of storms (events), especially from May to September with the increase in the threshold storm wind speed. The empirical distributions of monthly samplings are most often approximated by the exponential law; the χ -square values reach that of 0.83. For annual samplings the largest χ -square value (0.38) was obtained for a log-normal distribution.

Seasonal distributions (Table 4) in two cases are better approximated by the gamma-distribution, in autumn and winter the χ -square values being much larger than in spring and summer. The latter is attributed to a large number of storms in the

autumn-winter period as compared with the spring-summer season enabling the formation of statistically more reliable samplings.

Table 3.

Distribution of the number of storms ($V > 15$ m/s)

N	Distribution law	I	II	III	IV	V	VI	VII	VII I	IX	X	XI	XII	ear
1	Erlang's	0.51	0.40	0.13	0.18	-	-	-	-	-	0.26	0.14	0.54	0.14
2	Gamma	0.59	0.63	0.43	0.41	-	-	-	-	0.16	0.62	0.67	0.27	0.24
3	log-normal	0.31	0.32	-	-	-	-	-	-	-	0.47	0.53	-	0.38
4	Weibull's	0.58	0.54	0.41	0.34	-	-	-	-	-	0.59	0.63	0.36	0.29
5	Exponential	-	-	0.83	0.41	0.17	0.13	-	0.52	-	0.45	0.33	0.83	0.27

Table 4

Distribution of the number of storms by seasons ($V > 15$ m/s)

N	Distribution law	Spring	Summer	Autumn	Winter
1	Erlang's	-	-	0.31	0.48
2	Gamma	0.11	0.30	0.77	0.47
3	log-normal	0.12	0.26	0.70	0.80
4	Weibull's	0.12	0.27	0.73	0.83
5	Poisson's	-	-	-	-
6	Exponential	-	0.18	0.50	0.69

Conclusion

The studies mentioned above allow a number of conclusions, some of them being of a preliminary character.

1. The existence of the Poisson's distribution for the distribution of storms was confirmed neither for monthly, nor for seasonal, nor for annual samplings.

2. A significant variance in the theoretical laws for approximating empirical dependencies was found.

3. A dependence of the distribution law type on the threshold of the truncated storm sampling for monthly series was established. At wind speeds more than 10 m/s the Weibull's distribution prevails and at speeds more than 15 m/s the exponential distribution.

4. The majority of seasonal storm samplings are approximated by different laws for each of the seasons; for annual series it is preferable to use a log-normal distribution.

5. It appears that for developing regional probabilistic models for calculating extreme hydrometeorological parameters in convolution integrals, one should refuse from the approximation of storms by means of the Poisson's distribution, at least, until the procedures proving that storm distributions can be described by the Poisson's distribution, are found. Instead it is preferable to use other distributions selecting their type from Tables 1-4 depending on the time scales of the problems to be resolved.

6. Further studies should aim to:

- exclude the trends and cyclicity in the interannual activity from initial samplings with a subsequent approximation by theoretical laws;

- search for a composition or sewing together of two distribution laws or more that describe the process. As a special case, one law can be considered, but with different distribution parameters.

References

Langbein W.B., Annual floods and partial duration flood series. - 1949, Trans.Amer.Geophys. Union, v.30, No. 6, pp.879-881.

Petrauskas C., Aagaard P., Extrapolation of historical storm data for estimating design wave height. -1971, J.Soc.Petroleum Eng., v.11, No.1, pp.23-37.

Wind and waves in the oceans and the seas. Reference data.- 1974,L.,Transport,359 p.

Kabatchenko I.M., Korobov V.B., Interannual variability of storm activity in the seas of the USSR. -1988, M., Dep. in VNIIGMI-WDC 11.-2.88, No.737-gm 88, 7 p.

Hydrometeorology and hydrochemistry of the seas of the USSR Volume 1. The Barents Sea. -1991, L., Gidrometeoizdat, 281 p.

FEATURES OF THE HYDROLOGICAL REGIME OF THE KARA SEA IN THE DATA OF THE "KAREX-90" EXPEDITION

V.L. Kuznetsov (AARI)

By analyzing data of oceanographic survey "KAREX-90" that was carried out from August 22 to September 3, 1990, it is possible to trace features of the regime characteristics of the Kara Sea during the navigation period of 1990.

Two natural synoptic periods (NSP) can be identified in the synoptic situation over the Kara Sea at that time, from August 23 to 27 and from August 27 to September 2. The first NSP was formed by the cyclone passage over the northern region of the sea from south-west to north-east. The second NSP was governed by the high pressure ridge over much of the area. The center of the anticyclone was west of the Zhelaniya Cape.

The character of isotherms on the surface of the area (Fig. 1) displays a direct water temperature dependence on the duration of radiation heating with a shift of the drifting ice edge to the north-east. Only in shallow areas along the Yamal coast and in the river run-off zone where turbulent processes are most active, this dependence is broken.

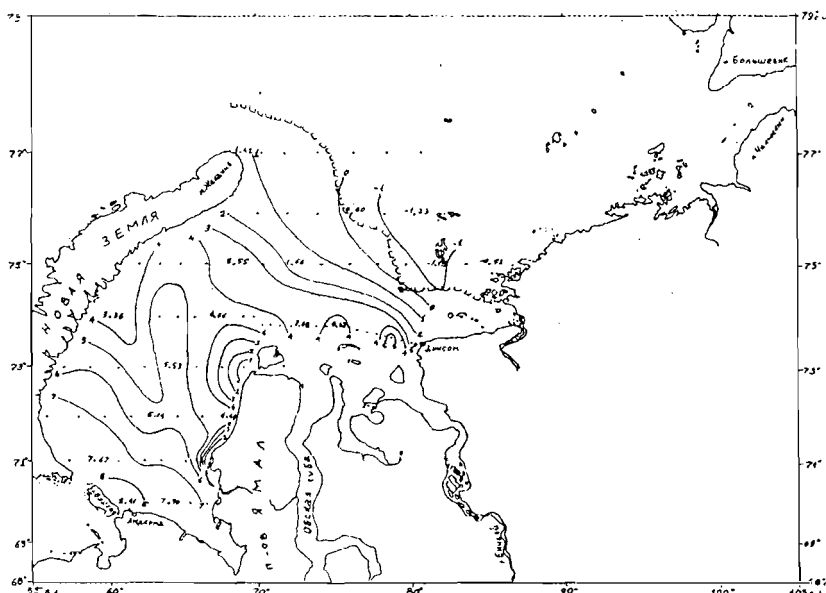


Fig. 1. Distribution of sea surface temperature in the Kara Sea. August 22 - March 9, 1990.

As compared with mean multiyear values, given in /2,3/, sea surface temperature in the region of the Kara Gate Strait is 2 C above the normal value. Further along the route up to 65 E it is within the normal range and from Belyi Island to the Sterligov Cape it is 1-2 C below the normal value in spite of anomalously small ice cover extent in the south-western sea.

Salinity distribution in the surface layer (Fig. 2) stresses the influence of advection of river and Barents water and ice melting processes. Variations in isohalines at sea surface indicate the western type of the spreading of river water /1/. A sharp increase in salinity and a decrease in temperature along the western Yamal coast, from the Kharasavey cape to Skuratov cape, is probably caused by the water level drop,

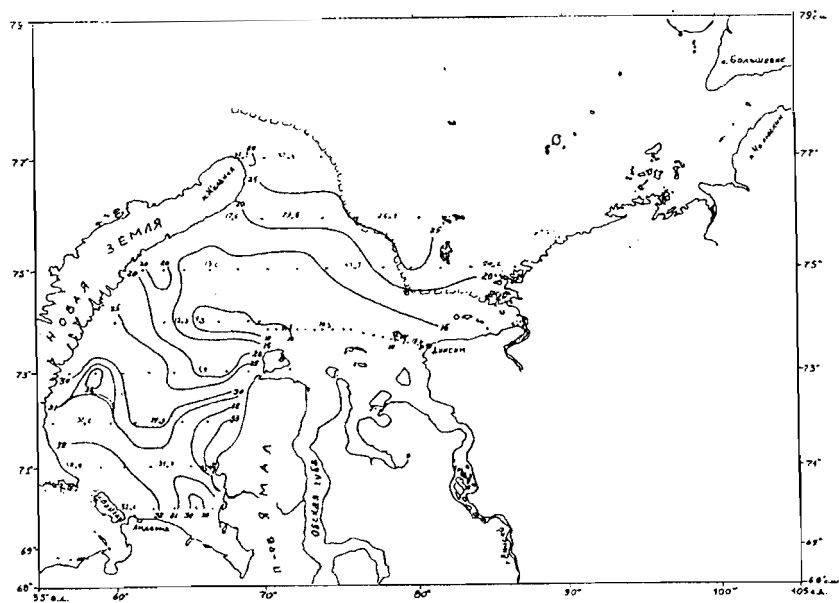


Fig. 2. Distribution of surface water salinity in the kara Sea. August 22 - March 9, 1990.

upwelling and wind mixing on the shoals. Calculations of the heat content of water in the Kara Sea showed that water of the active surface layer in the south-western region has the largest heat content from 50 to 65% (Figs. 3, 4).

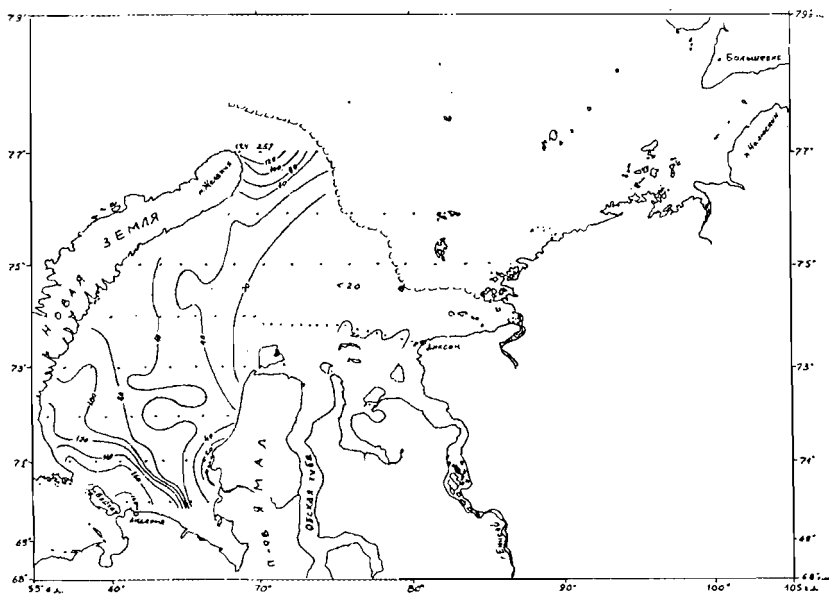


Fig. 3. Integral (from surface to the bottom) heat content of water in the Kara Sea. August 22 - March 9, 1990. KJ/cm2

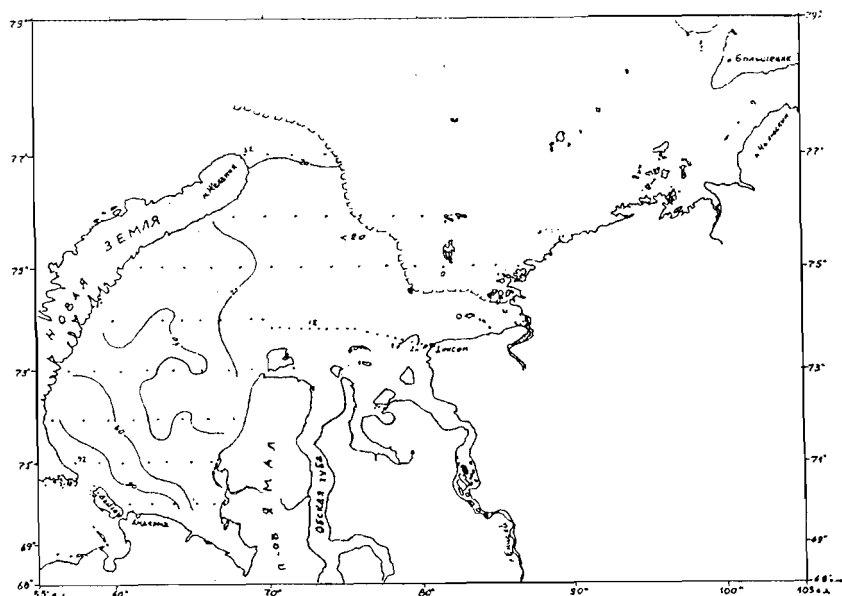


Fig. 4. Heat content of the water layer in the Kara Sea from the surface to a depth of 25 m. August 22 - March 9, 1990. KJ/cm².

Water heat content of the layer of intermediate Kara water is small and Barents water is vice versa, rich in heat. Its presence distinctly increases the integral heat content of the entire water column and variations in isolines indicate spreading of this water within the region. And of course, Atlantic water off the Zhelaniya cape makes a significant contribution.

A comparison of data of the charts of heat distribution with those obtained in 1985, 1986 suggests that the year 1990 is an exceptional one, and probably, anomalous with regard to surface layer heating by solar radiation and also with a considerably larger inflow of warm Barents water. Calculations of the meridional water transport at the transect Belyi island-Dikson island by a dynamical method has shown that southward transport east of Vil'kitsky island exceeds the northward transport by a factor of three: 0.25 and 0.08 cu.km/h and components of geostrophic speeds in the southern direction are up to 20 cm/s.

For calculating thermohaline speeds of the Kara Sea a method of mathematical modelling was also applied by means of the diagnostic model suggested by Pavlov /5/.

Thermohaline circulation (Fig. 5) differs from classical circulation given in /8/ in that the East-Novozemel'sky and Yamal currents have a reverse sign and in the Yenisey near mouth estuary the vectors are directed to the Yenisey Bay. The countercurrent to the bay was governed by the hydrological front located at a level of 10 m where river runoff waters were transformed to brackish intermediate cold waters.

Since the model of Pavlov and Kulakov /5/ allows calculating thermohaline circulation combining it with wind-driven circulation, patterns of currents for two synoptic situations corresponding to NSP of the beginning and the end of survey, were obtained.

Circulation presented in Fig. 6, is formed by the density field and the wind field corresponding to synoptic conditions presented at the chart (wind of the western quarter prevailed over the area). In the central sea a cyclonic gyre was formed, part of

the flow coinciding in direction with thermohaline one (in the region of the meander near the ice edge), has higher current speeds.

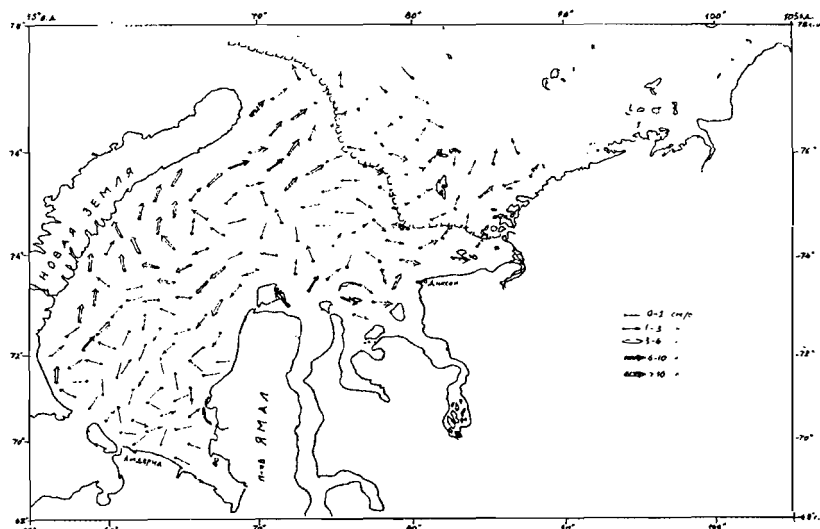


Fig. 5. Thermohaline circulation at the surface of the Kara Sea. Results of calculations are based on observation data from August 22 to March 9, 1990.

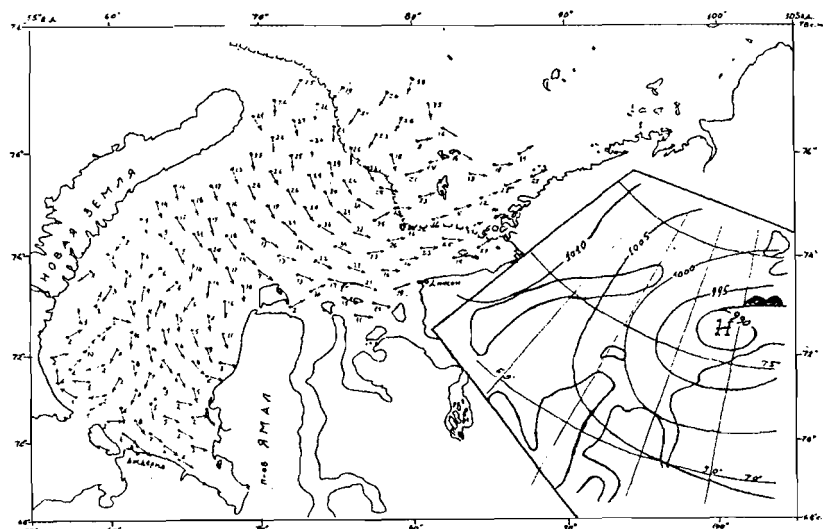


Fig. 6. Combined circulation of wind and thermohaline current at the surface of the Kara Sea. Results of calculation are based on observation data from August 22 to March 9, 1990 and the atmospheric pressure field for August 25, 1990. The synoptic situation of August 25, 1990 is shown on the chart (right-hand side).

The following pattern of wind-driven currents taking into account thermohaline circulation was obtained for the second half of the oceanographic survey (Fig. 7). The wind field typical of the second NSP was prescribed and namely: uniform wind induced by the high pressure ridge, 70 deg direction, 10m/s speed. A field of actually unidirectional and equal vectors of currents was obtained.

The deviations in the direction occur in shallow areas and at a counteraction of density currents. In the zones where the directions coincide (the river water hydrofront zone), the speed increases and where they are opposite (in the estuary, along the Taimyr coast, near the ice edge) the speeds decrease and vectors deviate from the direction of the general transport.

Both patterns of non-periodic currents obtained do not confirm the classic circulation pattern. It is known that a common pattern of water circulation at the surface of the Kara Sea is compiled by using data of separate instrumental observations

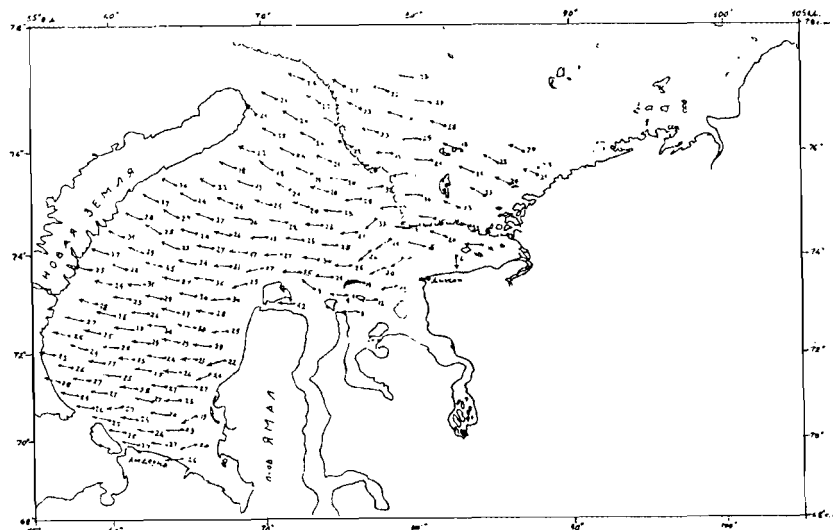


Fig. 7. Combined circulation of wind and thermohaline currents at the surface of the Kara Sea. Results of calculation are based on observation data from August 22 to March 9, 1990 at the wind of 70 ...; 10 m/s.

of currents, instrumental and visual observations of the drift of ships, ice, floating objects and taking into account data of the bottle mail and calculating currents by means of the dynamical method. For confirming this circulation pattern it would be necessary to conduct a long series of instrumental observations of currents in the main flows identified: Novozemel'sky, Yamal, West Taimyr, Litke, St. Anna. By means of mathematical modelling one may obtain a pattern close to a common one when prescribing a definite wind field as it was done by Proshutinsky on a barotropic model on condition of the south wind prevailing /7/.

An analysis of the results of the "KAREX-90" expedition allows the following conclusions:

- in connection with early dates of ice disappearance there was an anomalously long heating of the surface layer in the southwestern sea, the upper quasiuniform layer was 10 m which is above the norm;
- the ice cover extent of the north-western region of the sea was anomalous, water with a temperature close to the freezing point was observed at the surface. The onset of the autumn-winter processes was earlier than the norm;
- the salinity in the river runoff zone was 2-3 per mil above the norm;
- river runoff was spreading over the sea area according to the western type;
- along the western coast of Yamal from the Kharasavey cape to Skuratov cape the upwelling phenomenon with the formation of the hydrological front in the seaward zone was tracked;
- stratification of water masses was close to mean multiyear one;

- the inflow of Barents water increased, there was an inflow of transformed Atlantic water with a core at a level of 180 m along the St. Anna trough to the region of the Zhelaniya cape;

- water heat content in the south-western sea in 1990 clearly exceeded corresponding values for 1985, 1986.

According to model calculations there prevailed in the field of thermohaline currents:

- the North-eastern transport along the Novaya Zemlya shore;

- the flow along the frontal divide between surface river and Arctic water;

- West-Taimyr current;

- mean speeds in the flows were from 3 to 5 cm/s, the maximum being 11 cm/s.

- atmospheric processes during observations formed the wind field over the area which induced wind-driven currents with speeds five times exceeding those of density currents.

References

1. Antonov V.S. Spreading of river water in the Arctic Seas. Proc. of the AARI, vol. 208, L., Sea transport, 1957, p.15.

2. Baskakov G.A., Moretsky V.N. et al. A brief hydrometeorological description of the Arctic Seas. L., Archives of the AARI, 1965, 59p.

3. Moretsky V.N., Shpaikher A.O. et al. Hydrometeorological regime of the southern Kara Sea (a description for pilots). Archives of the AARI, 1961.

4. Kuznetsov V.L. Features of thermohaline structure of the Kara Sea water. A Work Report during the 11th cruise of the R/V "Professor Multanovsky", vol. 1, part 2, L., Archives of the AARI, 1986.

5. Kulakov M.Yu., Pavlov V.K. A diagnostic model of water circulation of the Arctic Ocean. Proc. of the AARI, vol. 413, 1988, pp. 17-23.

6. Nikiforov Ye.G., Shpaikher A.O. Typical features in the formation of large-scale fluctuations of the hydrological regime of the Arctic Ocean. L., GMI, 1980, 272 p.

7. Proshutinsky A.Yu. Modelling of water circulation and level oscillations in the Kara Sea. A Work Report during the 11th cruise of the R/V "Prof. Multanovsky", vol. 1, Part 2, L., Archives of the AARI, 1986.

8. The Soviet Arctic (seas and islands of the Arctic Ocean). M., Nauka, 1970.

ATLANTIC WATER CIRCULATION IN THE REGION OF THE CONTINENTAL SLOPE IN THE NORTH OF THE BARENTS SEA

S. B. Kuz'min, V. A. Volkov, V. V. Stanovoy (AARI)

An inflow of Atlantic water to the Barents Sea is considered to be one of the governing factors in the formation of the hydrological regime and climatic changes in this area and adjacent regions. That is why, it is most important to specify the circulation features of this water when it inflows to the Barents Sea, as well as give a quantitative assessment of this inflow. The Atlantic water circulation in the region of the continental slope in the north of the Barents Sea has been most sparsely studied in this respect. This is related to an occasional character of data collection here due to heavy ice conditions typical of this region even in summertime.

This presentation analyses hydrological data obtained in the years of favorable ice conditions. Of the last 10 years three years were selected when the most complete data on this region were collected. 1984 - the R/V "Otto Schmidt" the 17th cruise (July-September); 1990 - the R/V "Otto Schmidt" the 37th cruise (July-August); the R/V "Professor Multanovsky" the 27th cruise (July-September); the R/V "Lance" (August 1994).

On the basis of the analysis it has been found that the main inflow of Atlantic water in the north of the Barents Sea occurs between the Victoriaoya and Franz-Josef Land (FJL) through the Franz-Victoria trough in two flows (with occurrence of two typical cores at depths of 100-300 m): large western and smaller eastern directed south and south-east, respectively.

The speeds of thermohaline flows calculated from data of 1984 (for the levels: 100, 150, 200, 250, 300 m) are about 5-10 cm/s here, reaching a maximum of 15 cm/s in the region of the inflow of the eastern branch of Atlantic water (Fig. 1, 2). It should be mentioned that similar speeds correspond to an enhanced inflow of Atlantic water which, probably, took place in 1984. The 1990 data show a weak non-uniform field of thermohaline flows indicating the attenuated inflow. And the presence of Atlantic water in the southern part of the Franz-Victoria trough and south-east of the FJL confirms the circulation pattern. A similar non-uniformity in the inflow of Atlantic water is reported by I.A. Lebedev (the Murmansk Branch of the AARI). An approximate estimate of Atlantic water transport through this trough is about 1 Sv according to data of the "Lance" expedition in 1994.

An inflow of Atlantic water through the strait between Spitsbergen (Svalbard) and Belyi island (Kvitoya) is very weak (1984) being actually absent (1990, 1994). Further evidence is provided by the results of processing a series of annual data from the buoy station deployed in this strait by Norwegian specialists in 1980 (the R/V "Ymer") and recovered in 1981 (the R/V "Lance"). These results showed the filtered currents (i.e. after using a low-frequency filter) to be weak (the speeds of about 2 cm/s) with a mean annual flow here, probably, not exceeding 0.2 Sv in the north-eastern direction (Aagard K, Foldvik A., Gammelsrod T. and Vinje T. 1983). An insignificant and also irregular from year-to-year inflow of Atlantic water through the Hinlopen strait supplements the circulation pattern.

In conclusion it should be noted that data obtained in 1994 (the R/V "Lance") are very important for understanding a complete circulation pattern of Atlantic water in the north of the Barents Sea and can be used for further detailed analysis.

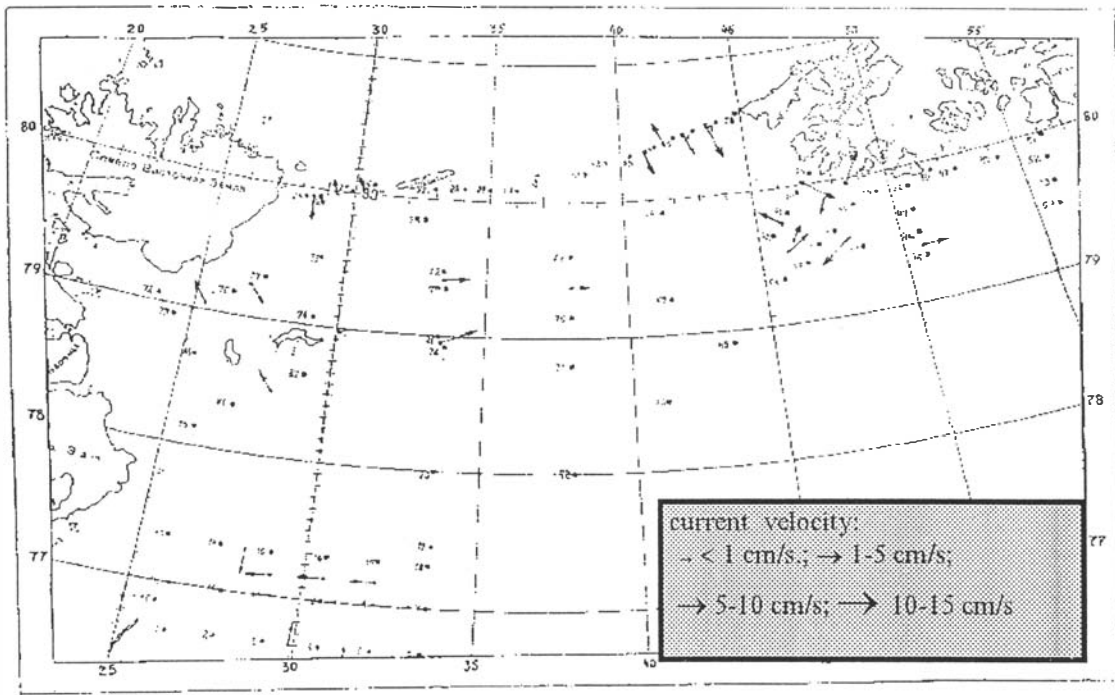


Fig. 1. Thermohaline flows at a level of 150 m. Results of calculations from oceanographical stations, the 17th cruise of the R/V "Otto Schmidt" (July-September 1984)

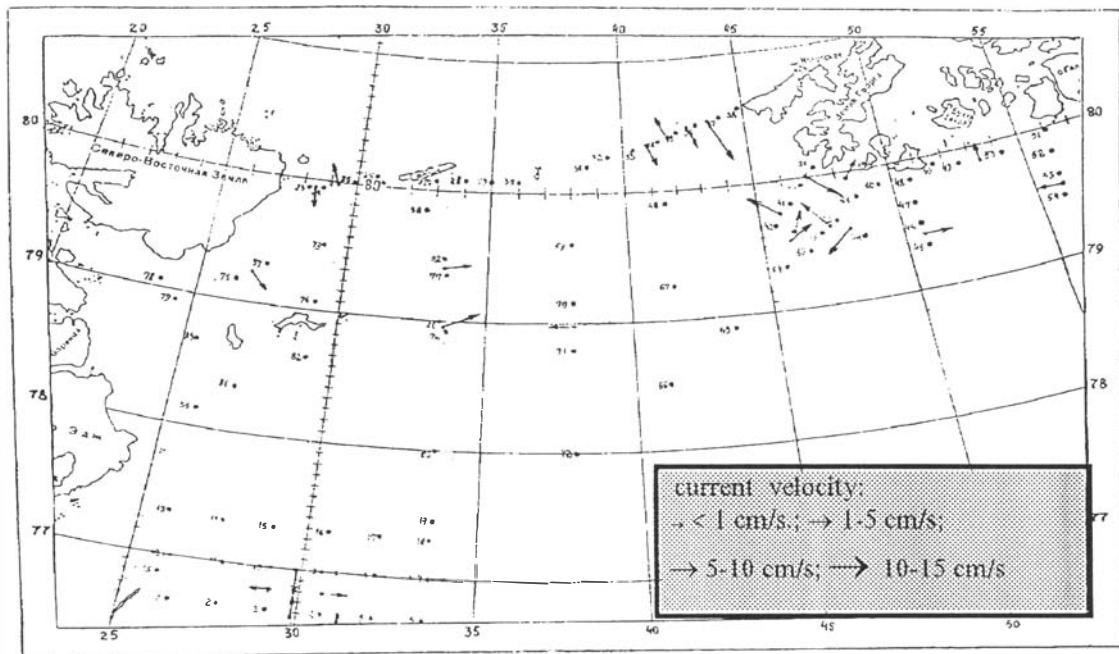


Fig. 2. Thermohaline flows at a level of 200 m. Results of calculations from oceanographical stations, the 17th cruise of the R/V "Otto Schmidt" (July-September 1984)

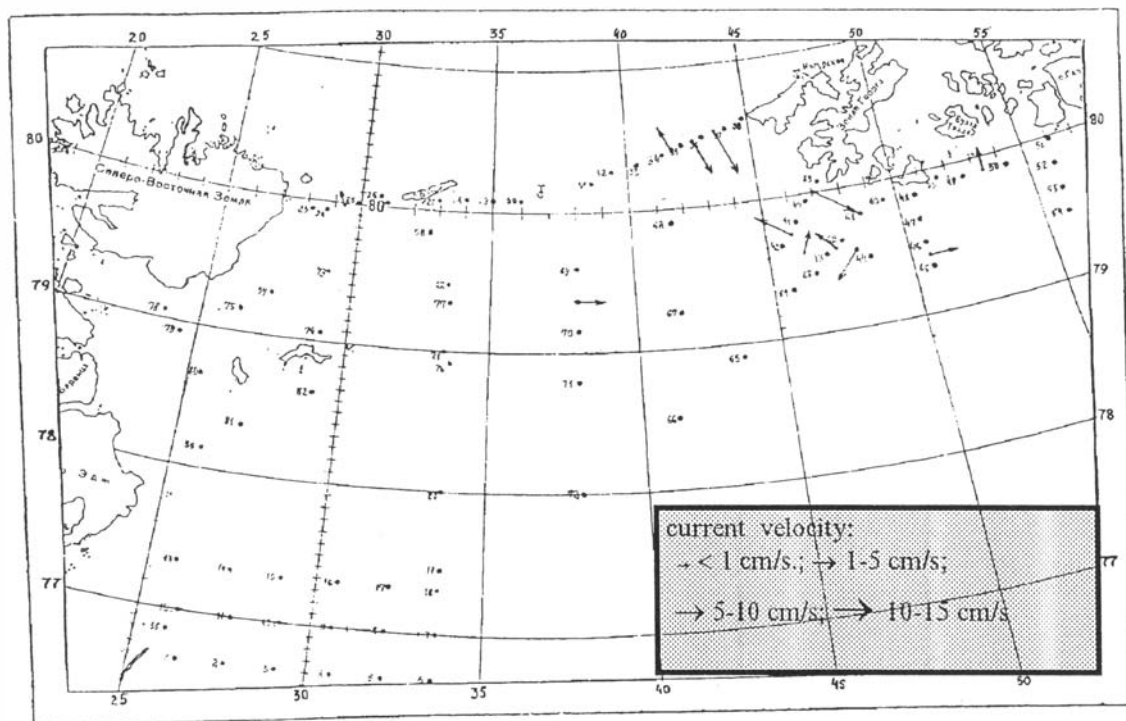


Fig. 3. Thermohaline flows at a level of 250 m. Results of calculations from oceanographical stations, the 17th cruise of the R/V "Otto Schmidt" (July-September 1984)

References

1. Denisov V.V., Zuyev A.N., Lebedev I.A., Large-scale oceanographic surveys and their methodological significance for comprehensive studies of the Barents Sea (by the example of the "BAREX-84" expedition). 1991, The Problems of the Arctic and the Antarctic. - No. 65, pp.121-132. In Russian.
2. Novitsky V.P., Constant currents in the north of the Barents Sea. 1961, Proc. of GOIN, issue 64, pp.1-32. In Russian.
3. Ozhigin V.K., On the frontal zones of the Barents Sea. 1989, Questions of productive oceanology of the Northern Basin. - Murmansk, pp.89-103.
4. Savinov V.M., Some comments to the method for calculating boundaries of Atlantic water in the Barents Sea. 1990, Ecological reproduction and protection of biological resources of the seas of the Northern Europe: Abstracts of the papers of the 3d All-Union Conference, Murmansk, June 25-29, pp. 50-51. In Russian.
5. Tantsyura A.V., Dominating surface currents of the Barents Sea. 1958, The research-Technical Bulletin, PINRO.
6. Tantsyura A.V., On seasonal changes in currents of the Barents Sea. 1973, Proc. of PINRO, iss.34.
7. Tantsyura A.V., On the currents of the Barents Sea. 1959, Proc. of PINRO, iss.11.
8. Timofeyev V.T., Water masses of the Arctic Basin. 1960, L., Gidrometeoizdat.

9. Timofeyev V.T., Panov V.V., Indirect methods of identification and analysis of water masses. 1962,L., Gidrometeoizdat.
10. A.F. Treshnikov, G.I. Baranov., Structure of water circulation in the Arctic Basin. 1972,L., Gidrometeoizdat.
11. Aagard K., Foldvik A., Gammelsrod T and Vinje T. One-year records of current and bottom pressure in the strait between Nordaustlandet and Kvitoya, Svalbard, 1980-1981. 1983,Polar Research 1 n.s., pp.107-113.
12. Midttun L., Formation of dense bottom water in the Barents Sea.1985, Deep-Sea Research, 32(10): pp.1233-1241.

NUMERICAL REALIZATION OF THE WAVE ENERGY PROPAGATION IN WIND WAVE MODELS

I.V.Lavrenov(AARI),J.R.A.Omlee(KNMI)

Successful solution of the hindcast or forecast wind wave problem depends on the quality of physical model and on the accuracy of wind velocity. Nevertheless errors of the energy balance numerical realisation can be no less than the errors coming from the wind value and from the unsatisfactory implementation of the wind wave physics in the model.

Present state-of-the art wave models are formulated in the terms of a wave energy spectrum discretized into a large number of spectral bands. The finite width of these bands introduces non-trivial complications for the computation of the wave propagation. Ideally, the energy of a wave disturbance of small initial extent will spread out smoothly over the sea or ocean in the course of time. In most of the presently operational models, however, the spectral resolution is so coarse that the so-called "garden-sprinkler" effect: most of the energy of the propagating wave becomes concentrated along the basic directions of the model which are closest to the direction of wave propagation in the area of initial source, while in the other directions the wave energy is underestimated. One consequence of this phenomenon is that the arrival of swell originating from distant storms is often poorly predicted.

The original correction term was been derived to remove garden-sprinkler effect of the energy balance equation solution for the case of wave propagation at the ocean. By using the simple approximation of correction term and the semiLagrangian numerical method the original interpolation-ray numerical (INTERPOL) has been offered to solve energy balance equation on the spherical surface.

The accuracy of two different propagation schemes, namely the first-order difference scheme (FOUS) implemented in the most advanst wind wave model WAM (WAMDI group,1988) and the INTERPOL has been assessed for the case of pure swell propagation at the ocean. It was found that for the FOUS propagation scheme with 12 directions the local errors in wave height due to numerical realisation of the energy propagation could become of the order of 30-50% within 24 hours.

The INTERPOL method results proved to be much closer with the analytical solution than the FOUS. Moreover, due to the absolute stability of the method this higher accuracy could be achieved by using much larger propagation time step, and therefore at substantially lower computational expense.

The main future of the INTERPOL method is that it may be applicable to solve the energy balance equation with a fine space grid by using larger time step than its allowed by the traditional finite-difference schemes. The INTERPOL method is superior not only to the first-order upwind scheme. It could be regarded as a general alternative for the numerical realization of energy balance equation in the wind wave models.

CALCULATION AND FORECASTING MODEL OF SEA WAVES AND ITS EMPLOYMENT RESULTS IN THE SEAS OF ARCTIC OCEAN

I.V.Lavrenov, T.A.Pasechnik, V.I.Dymov, Kudukhov(AARI)

At present mathematical models are used for calculating waves. Usually, models are based on the so-called "ideal conditions for wave formation" which are used for calibration, testing and verification of the calculated results /1,2,3/. As a rule, in such cases data of full-scale observations normalized to wind speed at a 10 m level are used. It is assumed that the wind speed itself remains unchanged along the fetch and the universal character of the normalized values of the wave elements remains valid for all wind speeds. Examples can be found in such known guiding documents as SNIP /4/, Handbook of the Register /5/, etc. This approach does not take into account the reverse influence of waves on wind and it is not justified to use data of full-scale studies obtained at mean wind speeds (7-15 m/s) for the cases of strong storm wind speeds (20 m/s and more).

Some authors /6,7/ show the inconsistency of the approach described above and suggest to use normalization to friction velocity which allows taking into account a non-linear character of interaction between waves and wind. Normalization of full-scale data to friction velocity makes them more universal which provides a possibility for using them in calculations of waves at large wind speeds and thus, for more accurate prediction of especially dangerous waves.

This work describes a new spectral-parametric model of the wind-induced wave SPD2 where integral values of the wave elements (wave energy, frequency of the maximum of the wave spectrum, etc.) are normalized to friction velocity. The results of this version of the model are compared with an earlier SPM model elaborated at the St. Petersburg branch of GOIN where the wave forming factors are normalized to wind speed at a 10 m level. As a result of testing these models, it turned out that for storm wind speeds the values of the wave heights calculated using an updated model version, can significantly exceed the wave heights obtained without taking into account normalization to friction velocity. The article presents the results of comparing model calculations and prediction of the wave elements with full-scale instrumental measurements from a drilling platform in the North, Norwegian and Greenland Seas.

It is shown that the suggested model allows obtaining more accurate heights of the storm waves in the seas and the oceans.

1. Equation of the wave energy balance in the spectral form

The wave energy balance equation in the spectral form on the spherical surface is written as /6/:

$$\frac{\partial S}{\partial t} + \frac{1}{\cos \varphi} \frac{\partial}{\partial \varphi} (\dot{\varphi} \cos \varphi S) + \frac{\partial(\dot{\theta}S)}{\partial \theta} + \frac{\alpha(\dot{\beta}S)}{\partial \beta} = G \quad (1)$$

where: φ - latitude, θ - longitude, t - time, S - spectrum, β - angle of the wave vector direction, G - source function describing physical mechanisms forming the wind wave spectrum.

The equation characteristics (1) are the following ratios describing spreading of wave packets along the geodesic curve.

$$\dot{\varphi} = \frac{C_g}{R} \sin \beta; \quad \dot{\theta} = \frac{C_g}{R} \frac{\cos \beta}{\cos \varphi}, \quad \dot{\beta} = -\frac{C_g}{R} \operatorname{tg} \varphi \cos \beta; \quad (2)$$

where C_g - group speed, R - the Earth's radius.

2. System of equations of the parameters of the wind wave spectrum

As a result of the effect of integral operators /2/ on the equation of the wave energy balance (1), the following system of equations relative to the spectrum parameters can be arrived at wave energy m_0 and the general direction of wave propagation $\bar{\beta}$:

$$\begin{aligned} \frac{\partial m_0}{\partial t} + CW_* \frac{\sin \bar{\beta}}{R} \frac{\partial m_0}{\partial \varphi} + CW_* \frac{\cos \bar{\beta}}{R} \frac{\partial m_0}{\partial \theta} &= G_1 g / W_* m_0 \\ \frac{\partial \bar{\beta}}{\partial t} + D \frac{\sin \bar{\beta}}{R} \frac{\partial \bar{\beta}}{\partial \varphi} + D \frac{\cos \bar{\beta}}{R} \frac{\partial \bar{\beta}}{\partial \theta} &= 5 \times 10^{-5} \left(\frac{\omega_m}{W_* g} \right)^{1.51} \times \omega_m \sin(\bar{\beta} - \beta_U) \end{aligned} \quad (4)$$

(where φ - latitude, θ - longitude, R - the Earth's radius, $D = 0.45g / \omega_m$, ω_m - frequency of the spectrum maximum, W_* - friction velocity, β_U - wind direction.

The spectrum wave energy is connected with the dimensionless frequency of the maximum by the following empirical ratio /6,7/

$$\omega_m^* = 0.37(m_0^*)^{-0.34} \quad (5)$$

where $*$ - the sign of normalization to friction velocity.

The coefficients C and G_1 are derived from the following ratios:

$$\begin{aligned} C &= \alpha^{1/\gamma} \gamma x_*^{\gamma-1/\gamma} \\ \alpha &= 0.0075 C_d^{\gamma/2-1}, \quad \gamma = 1.355 \\ G_1 &= \frac{2\gamma \alpha^{1/\gamma} \alpha_1 x_*^{-0.5/\gamma}}{\text{sh}(2\alpha_1 x_*^{0.5})}, \quad \alpha_1 = 0.000156 \quad (6) \\ x_* &= \left(\frac{1}{\alpha} \text{arctg}(m_0^* / 3450)^{0.5} \right)^2 \end{aligned}$$

The resistance coefficient C_d is determined through friction velocity

$$\left(\frac{W_*}{W} \right)^2 = C_d \quad (7)$$

The SPD2 model assumes the following relation between the resistance coefficient and the wave development stage suggested by Davidan /7/:

$$\ln C_d + 0.267 / \sqrt{C_d} = 3.67 - 0.667 \ln \tilde{\omega}_m - 1.333 \ln W_{10} \quad (8)$$

where W_{10} - wind speed at a level of 10 m, $\tilde{\omega}_m$ - maximum frequency normalized to W_{10}

3. Swell calculation

In the spectral-parametric wave model the swell is calculated by solving the equation of the wave energy balance (1) with a zero source term. Let us rewrite this equation in the form of a full derivative /6/:

$$\frac{\partial S}{\partial t} + \frac{\partial S}{\partial \varphi} \dot{\varphi} + \frac{\partial S}{\partial \theta} \dot{\theta} + \frac{\partial S}{\partial \beta} \dot{\beta} = 0 \quad (9)$$

It is assumed in the model that wind waves and swell can interact which results in the energy exchange between waves and swell /2/.

As a result of the numerical solution of the equation system (3)-(8), the wave elements at a prescribed wind field are calculated: height of the waves, their period and direction of propagation.

4. Results of calculations

The first stage of calculations included estimates of the wave elements for the most simple conditions of the wave formation: calculation of waves along the fetch at a constant gradient wind speed at a 10 m level. Calculations were performed using two versions of the spectral-parametric model: on the basis of the model described above taking into account normalization to friction velocity (SPD2) and the previous version of the model (SPM) developed earlier at the St. Petersburg branch of GOIN /2,3/ with normalization to wind speed at a 10 m level (without taking into account friction velocity). The results of calculating mean wave heights along the fetch for different wind speeds are presented in Table 1.

Table 1.

Changes in mean wave heights along the fetch for different wind speeds W. The first line - fetch in km; second - mean wave height (in m), calculated using the SPM program (without friction velocity); third - mean wave height calculated using the SPD2 program (without taking into account friction velocity).

W=10 m/s																
X	50	100	150	200	250	300	350	400	450	500						
h	0.6	0.9	1.0	1.2	1.3	1.4	1.5	1.6	1.6	1.6						
h _d	0.6	0.8	1.0	1.1	1.2	1.3	1.3	1.4	1.4	1.4						
W=20 m/s																
X	100	200	300	400	500	600	700	800	900	1000	1100	1200	1300	1400	1500	
h	1.9	2.6	3.2	3.6	4.0	4.3	4.6	4.9	5.1	5.4	5.6	5.8	6.0	6.2	6.3	
h _d	2.3	3.2	3.8	4.3	4.7	5.1	5.4	5.7	5.9	6.1	6.3	6.5	6.6	6.7	6.8	
W=30 m/s																
X	200	400	600	800	1000	1200	1400	1600	1800	2000	2400	2800	3200	3600	4000	4400
h	4.1	5.7	6.8	7.7	8.5	9.2	9.8	10.4	11.0	11.5	12.4	13.3	14.0	14.2	14.2	
h _d	6.0	8.1	9.7	11.0	12.0	13.0	13.8	14.5	15.2	15.8	16.8	17.7	18.5	19.1	19.5	19.8

As follows, for small wind speeds the wave heights h calculated from the SPM model turn out to be larger than the wave height h_d calculated from the SPD2 model, whereas for large wind speeds (more than 15 m/s) a reverse situation is observed - the wave heights obtained from the SPD2 model become much larger than those of the SPM model and this difference increases with the further increase in wind speed.

After test calculations we have performed prognostic calculations of the elements of the wind waves over the area covering the Arctic Seas including the Barents, Norwegian, Greenland and North Seas. As initial information, prognostic surface pressure fields up to 6 days in advance from the European Center for Medium Range Weather Forecasting were used (in the GRID system). Information was presented for calculations with a 24 h time interval in grid points of 5x5 degrees of the geographical coordinate system. Calculations were performed twice a week during three months and a half from the end of July to the beginning of November 1994. An example of such calculation is given in Fig. 1.

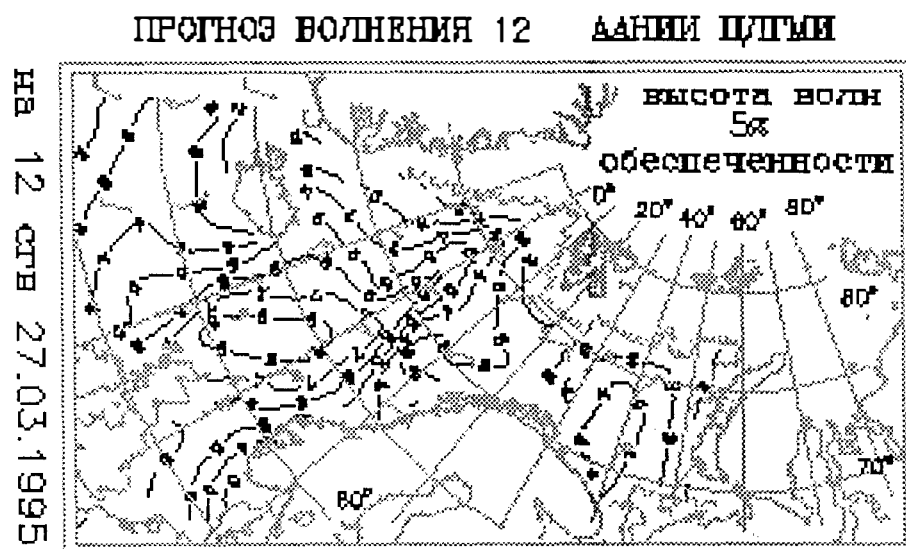


Fig.1 Example of the prognostic calculations of the elements of the wind waves for 27 March 1995 performed by the AARI.

Results of calculations on a model were compared with data of instrumental observations of waves from off-shore structures located in the Norwegian, the Greenland and the North Seas. The number of simultaneous observations of the waves for each synoptic time was about 25 (to be more exact, their number could change from 20 to 30). As a result of linear interpolation using 4 points, the accuracy of the diagnostic and prognostic calculations was determined.

The results of the calculations made show that the RMS error in calculations of the wave heights using the last version of the spectral-parametric model SPD2 is 10-20% less than when using the SPM model.

5. Conclusion

The article presents the improved version of the spectral-parametric model of the wind waves which uses normalization to wind friction velocity. On the basis of this model tests, as well as diagnostic and prognostic calculations of waves in the seas of the Arctic Ocean, were performed.

The tests of the model have shown it to be able to calculate storm waves with a higher accuracy than its previous analogues.

References

1. Ocean wave modeling (SWAMP grWp). Plenum press, New York, 1985.
2. Theoretical grounds and calculation methods for wind waves (ed. by Davidan I.N.) L., Gidrometeoizdat, 1988, 264 p.

3. Davidan I.N., Lavrenov I.V., Pasechnik T.A. et al. A mathematical model and a method of operational calculations of wind waves in the seas of the USSR, *Meteorologiya i Gidrologiya*, 1988, No.11, pp.81-90.
4. Construction norms and rules (SNiP), Loads and impacts on off-shore structures. M., Stroyizdat, 1983, 264 p.
5. Reference data on wind regime and waves in the oceans. M.-L. Transport, 1956, 234 p.
6. Lavrenov I.V., Mathematical modeling of wind waves in the World Ocean under conditions of its spatial non-uniformity. 1992, Author's summary of the Ph.D. thesis, the AARI, 28 p.
7. Problems of study and mathematical modeling of wind waves. St. Petersburg, Gidrometeoizdat, 1995.

MESOSCALE MECHANISMS OF HEAT EXCHANGE BETWEEN DIFFERENT WATER MASSES AND ITS PROBABLE RELATION WITH CLIMATE FLUCTUATIONS IN THE BARENTS SEA

I.A. Lebedev (MB)

The summarized information about specific mechanisms of warm atlantic waters interaction with cold deep and intermediate layers is discussed. The data were collected by the research vessels "Lance" (Norway), "Otto Schmidt" and "Professor Molchanow" (Russia) in the northern part of the Barents Sea in 1989-1990.

The examining of fine structure and modeling have shown that intrusion layering is conditioned mainly by double diffusive processes in the region (Kuzmina, Lebedev, Rodionov, 1994).

The materials of detailed oceanographic surveys allowed to distinguish a few local regions of cold intermediate layer destruction near some coastal and frontal zones. There was an intensification of the heat flux from atlantic waters towards the sea-surface observed in the local regions due to the favorable combinations of the different factors. The influence of isopycnal movements, intrusions with corresponding development of double-diffusive convection, destruction of internal waves in a coastal zone is discussed. The numerical solution of heat condition equation was used for the estimations of efficient vertical heat fluxes and ice melting rate. The locations of more intensive heat exchange zones coincided with the regions of systematic formation of polynyas in winter and spring time. Probable, the considered features can cause the abnormal early clearing of the Barents Sea northern part from ice in summer, that observed in some years.

The observations of "Otto Schmidt" allowed to reveal the cases of warm thermocline eddies formation in the zone of Nordcap current waters submerging on the latitude about 77 N (Kostyanov, Lebedev, Novikov, Rodionov, 1992). The experiments of "Professor Molchanow" showed that cold intermediate layer could be also divided to separate cells as a result of local vertical movements. There is more intensive heat exchange near the borders of the cells (Lebedev, 1993).

Evidently, all this features can influence upon short-term climatic fluctuations of thermohaline fields. On the other side the mesoscale processes depend on variability of atlantic waters inflow or on intensity of cold deep water formation (in connection with inclemency of winters). The detailed study of these phenomena can be used for climate investigations as a whole. The program of the study must be based on combination of special observations in the concrete regions and examining of the large-scale thermohaline anomalies variability for multiyear period. For the last purpose, the all accessible archives of data and mathematical methods of objective analysis of oceanographic fields (Golubev, Zuev, Lebedev, 1992) can be used.

ICEBERG ACTIVE AND PASSIVE SONAR ACOUSTICS

G.A.Lebedev, V.P.Gavrilo, L.G.Pisarevskaya, A.P.Polyakov(AARI)

Field data from AARI expeditions to the Barents and Kara seas are analysed. It is shown that sound velocity perturbations in the vicinity of a drifting iceberg can lead to the lack of echo-signal at the ship's sonar as well as the significant underestimation of iceberg draft at the distances about 4-6 km. Field studies of the noise levels produced by a melting iceberg in the frequency band from 20 Hz to 20 kHz at the distance from 15 km up to 10 m and calculated corresponding acoustic power of 0.06 to 0.024 W show that an iceberg can be detected by its noise at the distances of tens of kilometers in the frequency band tens and hundreds of Hz.

FEATURES OF SEA/AIR ENERGY EXCHANGE PROCESSES IN THE ZONE OF SEASONAL MIGRATION OF DRIFTING SEA ICE.

Makshtas A.P., Ivanov B.V.(AARI)

Studies of physical processes in the zone of seasonal migration of drifting sea ice were performed on the basis of hydrometeorological observations on a mesoscale oceanographic 60x80 mile polygon in the north-western Barents Sea. During observations air temperature (T_a) and humidity, wind direction and speed (u), underlying surface temperature (T_w) and incoming longwave radiation were continuously measured; the amount of total cloud cover (n) and ice cover concentration (N) were estimated visually. Then, using hourly averaged values of the governing meteorological parameters and an algorithm suggested by Makshtas (1991), vertical turbulent fluxes of sensible (H) and latent (LE) heat, longwave (R_g) and short-wave radiation balance and the sea-to-atmosphere heat flux through the snow-ice cover or water surface (Q) as a residual heat balance term were calculated.

For analyzing spatial-temporal variability the meteorological parameters and heat fluxes were averaged over the area of 20x10 miles on the polygon segment oriented from south to north (32°-33°30'E, 75°40'-77°20'N). The choice of the site was governed by the latitudinal location of the ice edge at the polygon in July and December.

As is seen from Fig. 1, in summer the spatial variability of actually all characteristics was governed by large-scale advective processes in the atmosphere typical of this period of the year. First, this is cyclonic circulation which contributes to the inflow of air masses from temperate latitudes to the Arctic Basin. One can note only a regular decrease in water temperature from south to north governed by the preceding winter cooling of the mixed layer. Mean temperature gradient in the range of 75°40' - 77°20'N decreased from July to August from $2.4 \cdot 10^{-5}$ °C/m to $1.4 \cdot 10^{-5}$ °C/m.

In the fall actually all characteristics that govern sea/air energy exchange attain an explicitly latitudinal character along with the decrease in the mean sea surface temperature gradient up to $2.2 \cdot 10^{-5}$ °C/m in October and $3.5 \cdot 10^{-5}$ °C/m in December. It becomes especially distinct with the occurrence of young ice in the northern part of the study region (Fig. 1,2). As is apparent, turbulent heat fluxes over the ice cover do not exceed 10 W/m^2 and actually do not change in the value, whereas over open water already at a distance of 20 miles from the edge they reach $30\text{-}40 \text{ W/m}^2$. Timachev and Makshtas (1994) attribute the indicated effect to the processes of transformation of the boundary atmospheric layer at the transfer of the air mass from the ice cover to open water governed by a simultaneous increase in the temperature of the underlying surface and its aerodynamic characteristics.

It was impossible to investigate the spatial variability of short-wave radiation and the sea-to-atmosphere heat fluxes during the experiments because of their clearly pronounced variability within the day. Due to this circumstance, Fig. 2 presents main heat balance characteristics of the zone of seasonal migration of drifting sea ice that were averaged over the time of the polygon observations (the duration of each of the surveys was 7-10 days). A comparison of data in Fig. 2 with the main energy exchange characteristics calculated on a zero-dimensional quasistationary sea ice cover model (Fig.3) which uses as external parameters mean multiyear, mean monthly data on the meteorological characteristics of the study region of the Barents Sea (Atlas of the Oceans, 1990) from (Makshtas, Ivanov, 1990), shows their qualitative consistency. This allows a sufficiently convincing suggestion that the use of relatively simple thermodynamical models of sea ice for climatic studies of sea/air interaction processes in the regions where seasonal migration of the ice cover is mainly governed by *in situ* processes. is adequate, at least for the summer-fall period.

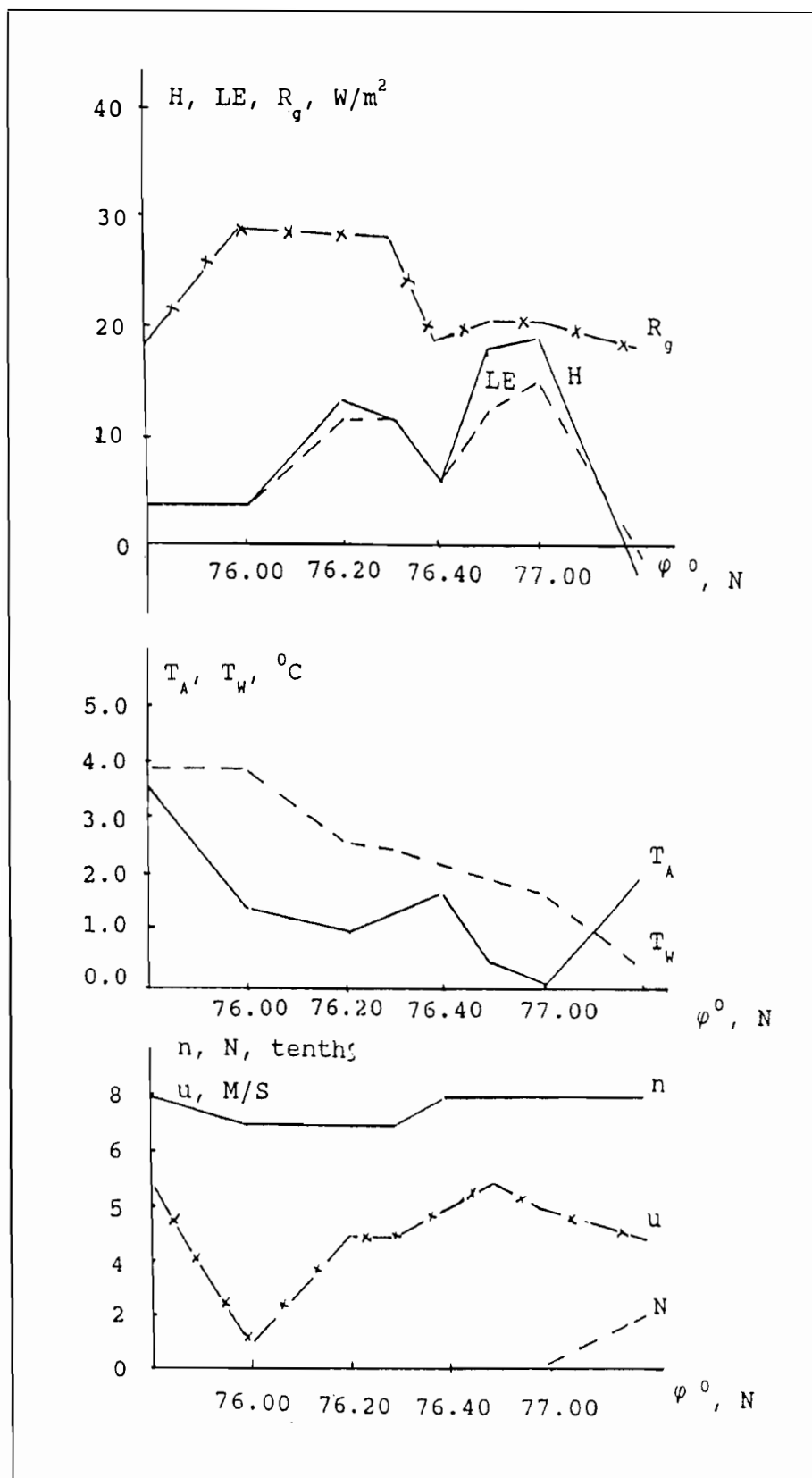


Fig. 1. Distribution of main characteristics of the subsurface atmospheric layer in the zone of seasonal migration of drifting sea ice; a-July H, LE - vertical turbulent fluxes of sensible and latent heat, R_g - longwave radiation balance; T_a - air temperature at a height of 13 m; T_w - temperature of the underlying surface; n - amount of total cloud cover, N - ice cover concentration; u - wind speed.

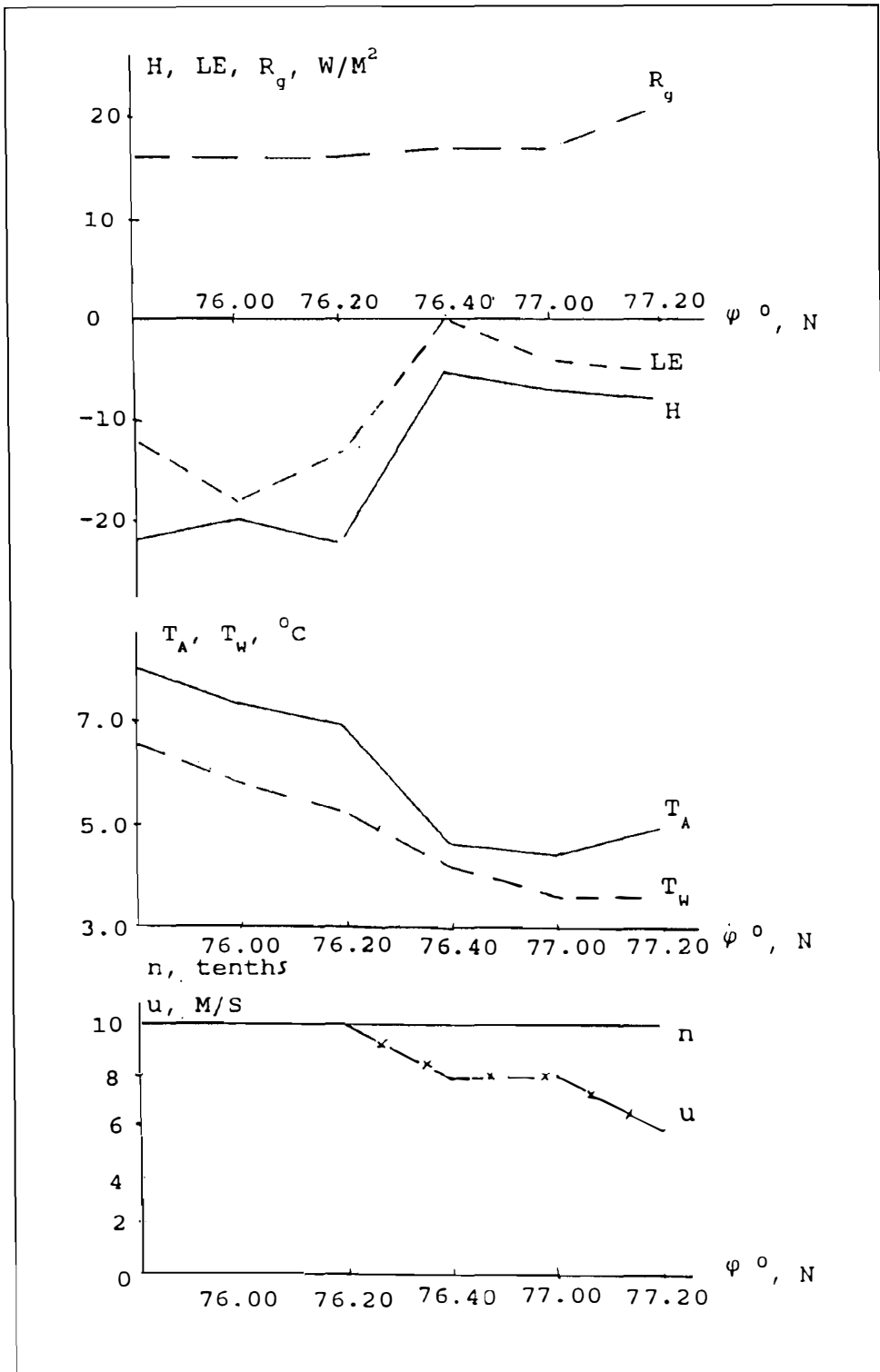


Fig. 1. Distribution of main characteristics of the subsurface atmospheric layer in the zone of seasonal migration of drifting sea ice; b-August. H, LE - vertical turbulent fluxes of sensible and latent heat, R_g - longwave radiation balance; T_a - air temperature at a height of 13 m; T_w - temperature of the underlying surface; n - amount of total cloud cover, N - ice cover concentration; u - wind speed.

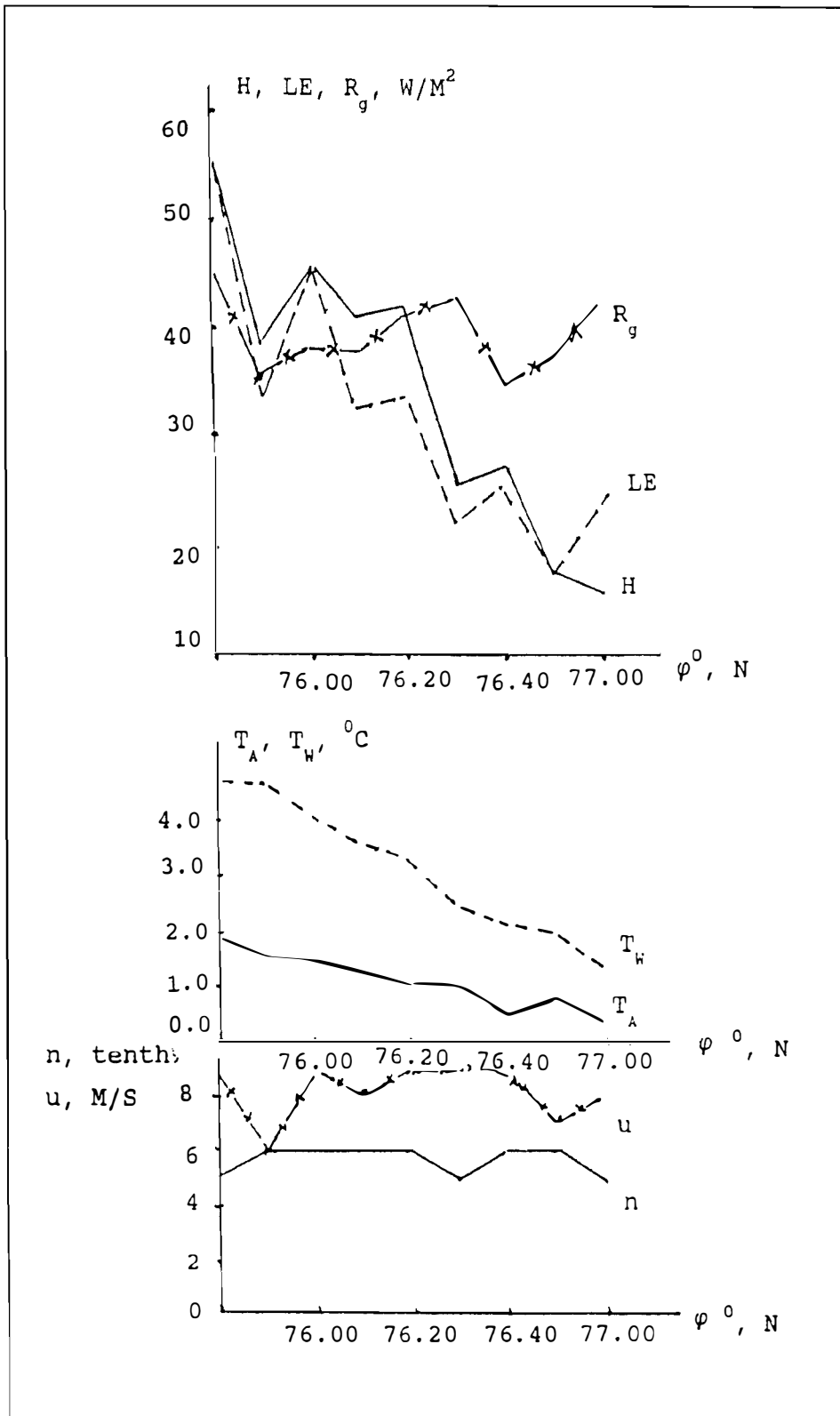


Fig. 1. Distribution of main characteristics of the subsurface atmospheric layer in the zone of seasonal migration of drifting sea ice; c-October, H, LE - vertical turbulent fluxes of sensible and latent heat, R_g - longwave radiation balance; T_a - air temperature at a height of 13 m; T_w - temperature of the underlying surface; n - amount of total cloud cover, N - ice cover concentration; u - wind speed.

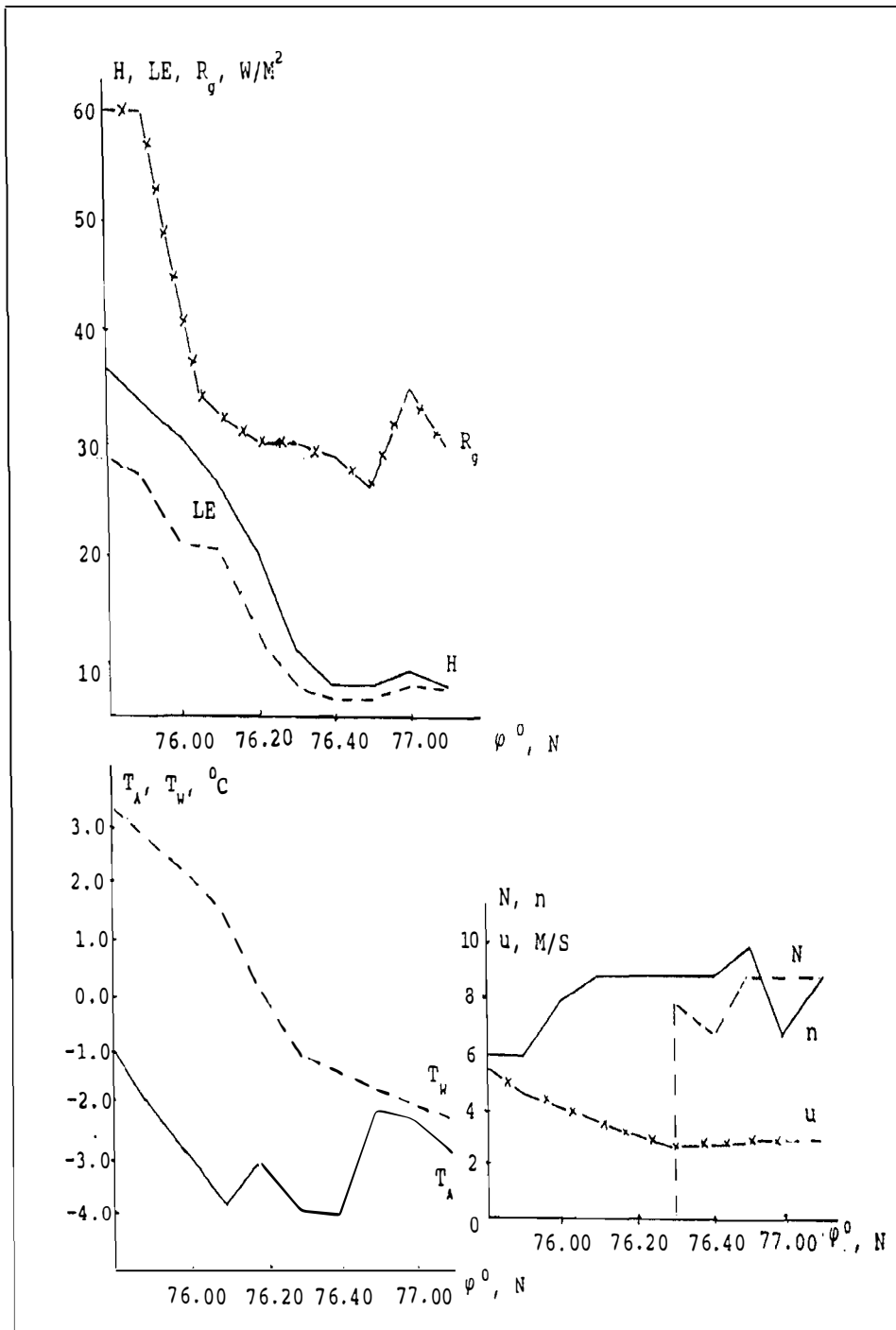


Fig. 1. Distribution of main characteristics of the subsurface atmospheric layer in the zone of seasonal migration of drifting sea ice; d-December. H, LE - vertical turbulent fluxes of sensible and latent heat, R_g - longwave radiation balance; T_a - air temperature at a height of 13 m; T_w - temperature of the underlying surface; n - amount of total cloud cover, N - ice cover concentration; u - wind speed.

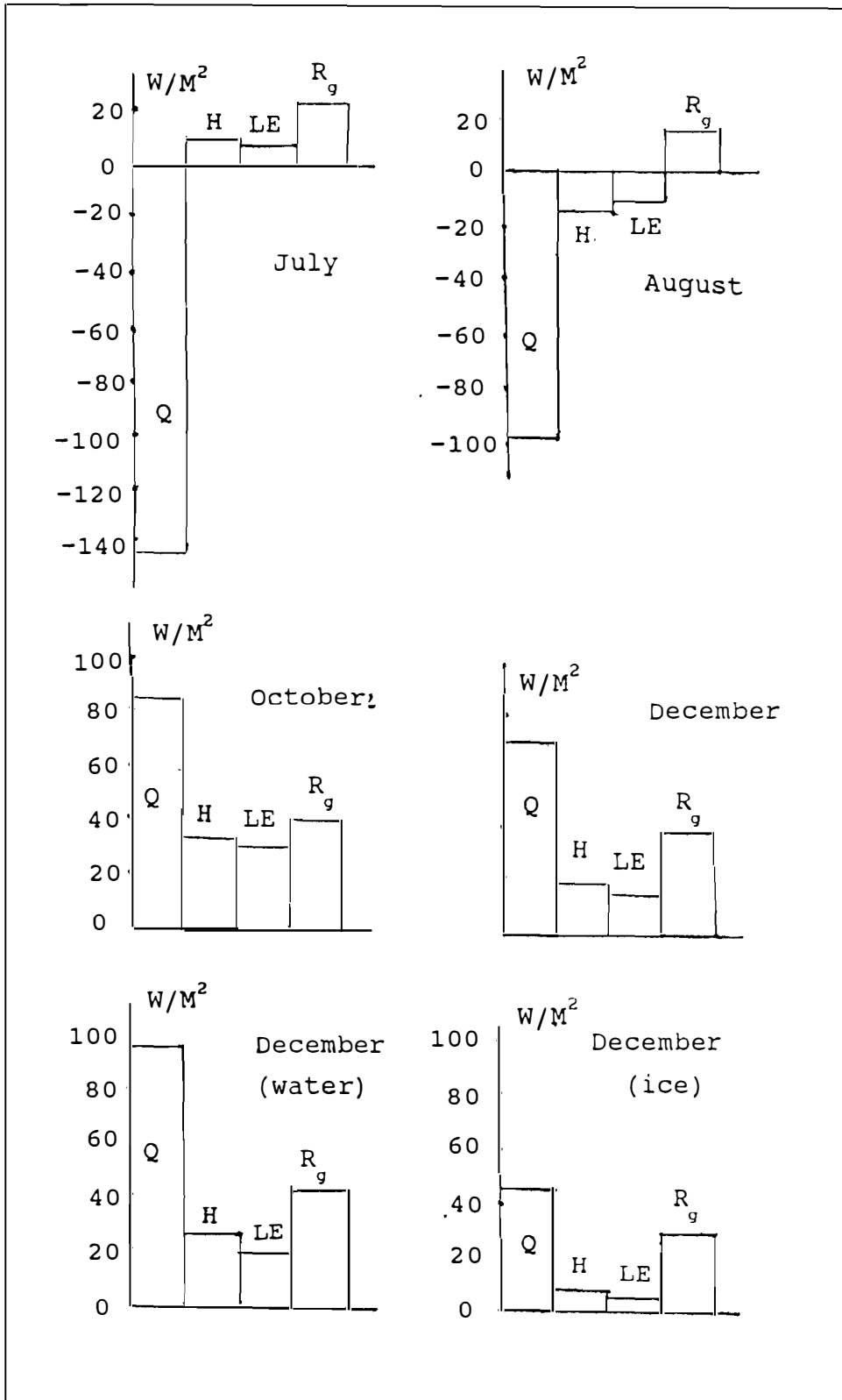


Fig. 2. Histograms of mean surface heat balance values in the Barents Sea in the zone of seasonal migration of drifting sea ice.

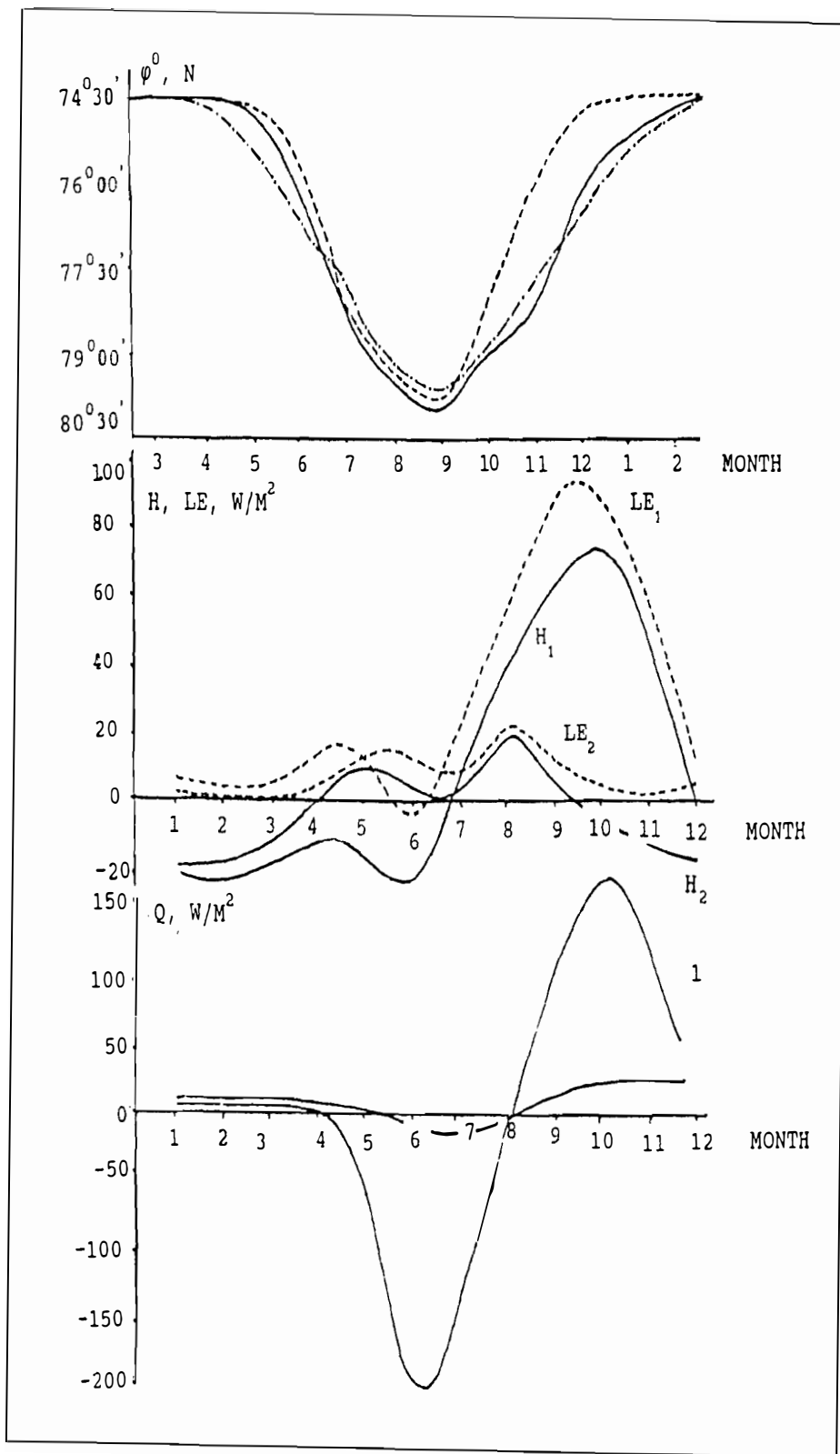


Fig. 3. Model estimates of seasonal migration of the sea ice cover - open water boundary in the western Barents Sea at a prescribed depth of the mixed layer of 100 m (1), 30 m (2) in the data of the Atlas of the Oceans (3) and main surface heat balance constituents at latitudes $74^{\circ}30'N$ (index 1) and $82^{\circ}00'N$ (index 2).

This study was performed with the financial support of the Russian Fund for Fundamental Studies (Project No 95-05-15315a).

References

Makshtas A.P. Sea/air interaction processes in the Arctic Basin. In: Sea/air interaction in the Northern polar Area, 1991, Gidrometeoizdat, pp.47-94.

Makshtas A.P., Ivanov B.V. Spatial-temporal variability of ice cover characteristics in the zone of its seasonal variability. 1990, Proc. of the AARI, vol.420, pp.71-80.

Atlas of the Oceans. The Arctic Ocean. 1980, Publ. by the USSR Ministry for Defence - Navy.

Timachev V.F., Makshtas A.P., 1994. Parameterization of energy exchange processes in the marginal zone of drifting ice. In: Typical features of large-scale processes in the Norwegian energy active zone and adjoining regions. St. Petersburg, Gidrometeoizdat, pp.164-178.

CTD-MEASUREMENTS NEAR A KARA SEA FLOEBERG.

Pisarevskaya L.G. (AARI) and E. Nygaard (NPI)

Since theoretical estimates of Nesyba (1977) of iceberg induced upwelling several laboratory and field investigations were done for its verification. Yet the hazardness of performing CTD-measurements in the close proximity of the iceberg walls in the rough seas and the difficultness of extracting iceberg induced perturbations out of natural spacial/temporal variability of the thermohaline stratification prevented scientists from getting a clear picture of iceberg-ocean interaction.

It was 1994 year expedition to the Kara sea that gave a possibility of detecting upwelling by using a natural tracer in the form of a 7-m thick warm layer entrapped by salt-stratification into an almost uniformly cold background. This warm layer could be traced along the whole 30-km transect (CTD stations 26,27,28,29,30,31). Due to the absence of available icebergs for study we approached instead a floeberg in the extremely calm weather condition. The floeberg consisted of heavily-ridged sea ice amidst scattered ice floes (78deg 17min N, 86deg 17min E). It had a length about 12 m, a height above sea-level of 4-5 m, and an estimated keel draft of 15-20 m. The measurements of temperature and conductivity versus depth (CTD) with a OTS-1500 probe revealed general warming of the cold surface layer near the floeberg (Fig.1, left). Superimposed on this warming trend there was an interleaving, step-like structure with the vertical dimension of 2-3 m, which seemed to correspond well to estimates based on laboratory experiments of Huppert and Turner (1978). Less evident yet quite noticeable in the data is appearance of the warmer and less saline water close to a floeberg at the depth of the supposed draft (about 10-12 m), meaning that the ambient water goes also downward thus forming a low-density zone below pycnocline.

Both features are traceable through the field and laboratory data of the other investigators. In 1987/88 year AARI expedition to the Southern ocean 31 CTD-stations were done in the vicinity of 5 free-drifting icebergs. Upwelling out of the cold water layer (remnants of winter water) into the seasonal warm surface layer can be well traced through the temperature and salinity data on Fig.1, right (from unpublished expedition data). Intrusions of thus upwelled water spreading asides into the ambient water form inversions in the profiles and resemble much of a floeberg case pattern. Weak stratification makes the whole water column to take part in the upward motion. More evident upwelling event can be seen through the data obtained in the Weddell sea (Bagryantsev et al, 1994; Abaza et al, 1995), though the authors treated the feature as internal wave manifestation according to the idea proposed by Pisarevskaya and Popov (1989).

Though it was later shown that a solid body (iceberg) moving across the pycnocline generates internal waves (Shishkina et al, 1995), it is interesting to consider another mechanism that can explain the revealed perturbations. The air bubble release while ice melting was shown to increase the intensity of convection (Josberger, 1980). Knowledge of ice melt rate depending on temperature and velocity of ambient fluid (Weeks and Mellor, 1974, Bannov-Baikov et al 1989) and available estimates of Ashton (1974), basing on Kobus equations (1968) on ambient water entrainment into the bubble plume give us significant values (Volkov and Pisarevskaya, 1995). Thus for a middle-sized Antarctic iceberg of 1000 x 1000 m, a draft of 300 m and a relative speed of 5 cm per second in a warm layer of 2 degrees Celsius we get 1700 m³ per second of entrained water to be delivered to the ice surface with the overall temperature exceeding freezing point. In the case of a Kara sea floeberg the amount will be modest (about 0.15 cubic meters per second), yet noticeable at the distance of performed measurements.

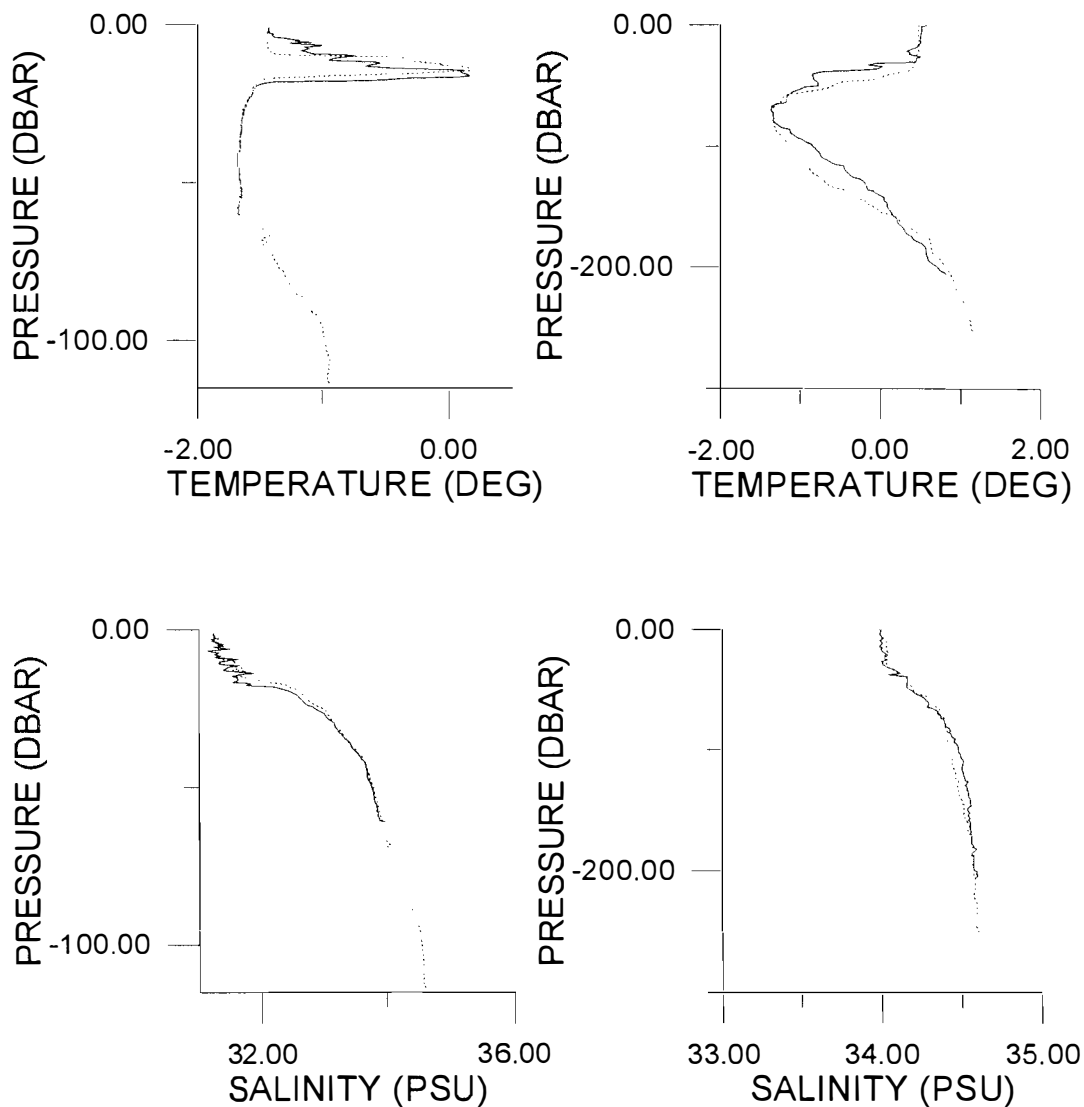


Fig.1. Temperature (upper) and salinity (lower) vertical distributions near the Kara sea floeberg (left), and an Antarctic iceberg (right) with the dimensions of 140 x 200 meters and elevation above the sea level of 15 meters. Solid line corresponds to the closest distance and dashed line - to the farthest, that is for the floeberg case - 10 and 100 meters, for the iceberg case - 730 and 3700 meters respectively.

Thus we come to the conclusion that air bubble release during glacier ice melting can upwell warm salty water from below pycnocline to the sea surface as well as heat to the ice cover, making icebergs a unique re-distributor of ocean heat and salt fluxes. Large Antarctic icebergs with their bottoms reaching warm deep water are able to provide the large zones of upwelled water, reported to be seen in the iceberg infested waters (Egorova et al, 1987) and may in some specific conditions form extensive areas of ice-free water like Weddell Polynya.

References

1. Neshyba S , "Upwelling by Icebergs",1977,Nature. No 267 (5611), pp.507-508.
2. Huppert H.E. and Turner J.S., "On Melting Icebergs",1978,Nature 271(5640), pp.46-48.

3. Bagryantsev N.V., Klepikov A.V., Chuguy V.I., Shil'nikov V.I., " Oceanographic Measurements Near the Drifting Iceberg in the Southern Ocean" 1994, Inf. Bullut. SAE, No 118, pp.32-44.
4. Abaza V.P., Korostelev V.G., Popov I.K., "Disturbances of the Thermohaline Structure of the Ocean Surface Layer in the Icebergs' Wake",1995,Doklady RAN, vol.342, vyp. 5, pp.1564-1567.
5. Pisarevskaya L.G. and Popov I.K., " Iceberg Wake Spatial Structure", Trudy AANII, No 417, pp.140-144. 6. Shishkina O.D., Vasilyeva V.V., Pisarevskaya L.G., 1995 "Internal Waves Generated by a Drifting Iceberg: Theory and Experiments", Izvestiya RAN, Fizika Atmosfery i Okeana, vol.6, (in press).
7. Josberger E.G., " The Effect of Bubbles Released From a Melting Ice Wall on the Melt-Driven Convection in Salt Water.", 1980 ,Journal of Physical Oceanography, Vol 10(3), pp.474-477.
8. Weeks W.F. and Campbell W.J., "Icebergs as a Fresh Water Source: an Appraisal",1973, Journal of Glaciology, 12, p.207-233.
9. Bannov-Baikov Yu.L., Golovin Yu.L., Totubalin Yu.Yu., Cherepanov N.V., " Fresh Ice Melt Rate Dependance on the Temperature and Speed of the Ambient Flow", 1989, Trudy AANII, vol.417, pp.106-113.
10. Ashton G.D., " Air Bubbler Systems to Suppress Ice"1974,CRREL Special Report 210, 42 p.
11. Kobus H.E., " Analysis of the Flow Induced by Air-Bubbler Systems",1968,Chapter 65 of Part 3. Coastal Structures, vol.11, Proceedings Eleventh Conference on Coastal Engineering, London. England, New York: ASCE, pp.1016-1031.
12. Volkov V.A. and Pisarevskaya L.G., "Iceberg induced convection patterns" in extended abstracts of the eighth meeting of the Working group ",1995,Laboratory Modelling of Dynamic Processes in the Ocean", St.Petersburg, June 6-8,1995, pp.158-159.
13. Egorova V.A., Kazansky M.M., Kononova S.A., " Thermohaline water structure near the ice shelves and ice bergs", 1987,Zapiski po Gidrografii, No 217, pp.35-39.

ICEBERG INDUCED THERMOHALINE PERTURBATIONS.

Pisarevskaya L.G. and Volkov V.A. (AARI)

To estimate iceberg induced thermohaline perturbations several hydrological surveys were performed in the Barents sea in 1989-1992 according to the Soviet - Norwegian Oceanographic Program. Overall analysis of the temperature and salinity data in the presence of drifting icebergs of the 1990 year cruise of the r/v PROFESSOR MULTANOVSKY made it possible for us to outline the typical effects for an iceberg that is drifting in summer in the Barents sea

(Volkov and Pisarevskaya, 1991):

1) lense of warmer and less saline water in the surface layer and corresponding deepening of pycnocline by several meters,

2) lense of colder and less saline water piercing warm atlantic layer at the depth of the supposed iceberg draft and lower,

3) upwelling of the bottom water. The striking similarity of this picture with the description

of the chimneys in the Northern Atlantic (Scott and Killworth, 1991) makes it tempting to consider icebergs to be the origin of the described features.

Laboratory experiments of Petterson (1904,1907) gave the true idea of the process that takes place in the World ocean. Huppert and Turner (1978) gave the values for thickness of intrusion layers depending on the ambient water stratification. Nevertheless it was only 1994 year expedition to the Kara sea onboard the r/v IVAN PETROV that draw our attention to evident dense water upwelling along an ice wall, its spreading asides in the form of intrusions and subsequent pycnocline lowering (Pisarevskaya and Nydaard, 1996).

We rule out the following process: denser water being upwelled in the vicinity of an ice wall (air bubble release enhances ambient water entrainment into the rising plume), spreads asides in layers. Their thickness is defined by ambient water density stratification. Usually in the data treating process this interleaving (fine structure) especially in the region of high gradients, is averaged, but raw data from the Kara sea expedition in 1994 depict it very well.

So the colder and less saline water lense at the depth of the iceberg draft and lower (Fig.1) is produced not by iceberg meltwater input, but by continuous sinking of the whole abovementioned system. High compressibility of the cold ocean water with pressure leads to water level denivelation and surface water convergence over the sinking zone (this is the way of warmer and less saline water lense formation).

The results can be applied to marginal ice zones, river freshwater intrusions on shelf, shelf- deep ocean interaction, that is - to all frontal zones.

Iceberg frontal zone positioning (Fig.2), also marked by Wadhams and Crane (1991) in the Southern ocean gives a chance of tracing warm water fronts through iceberg spatial distribution.

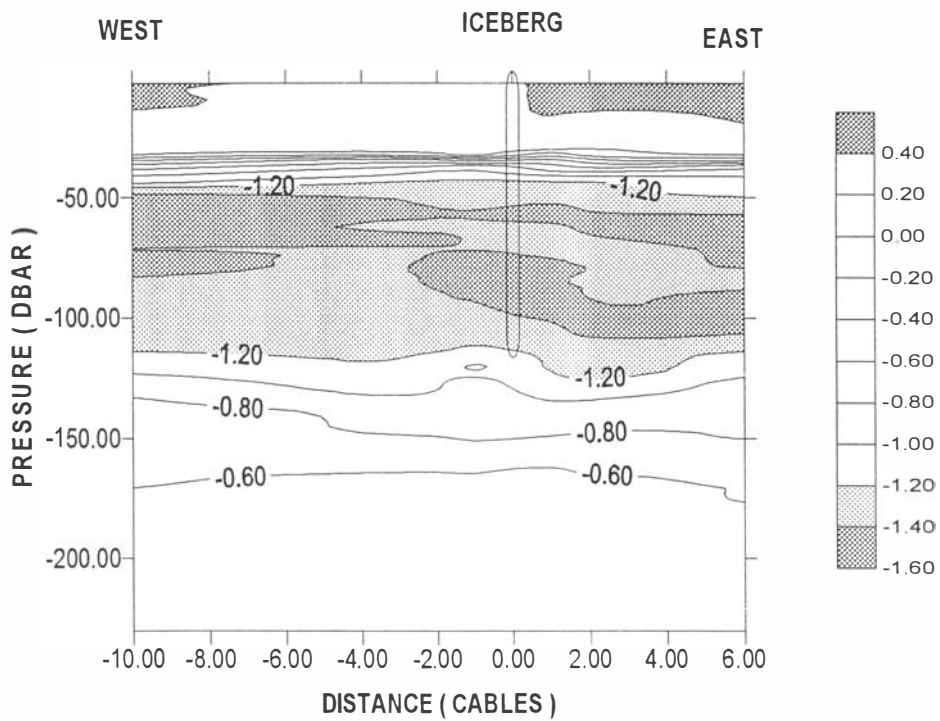
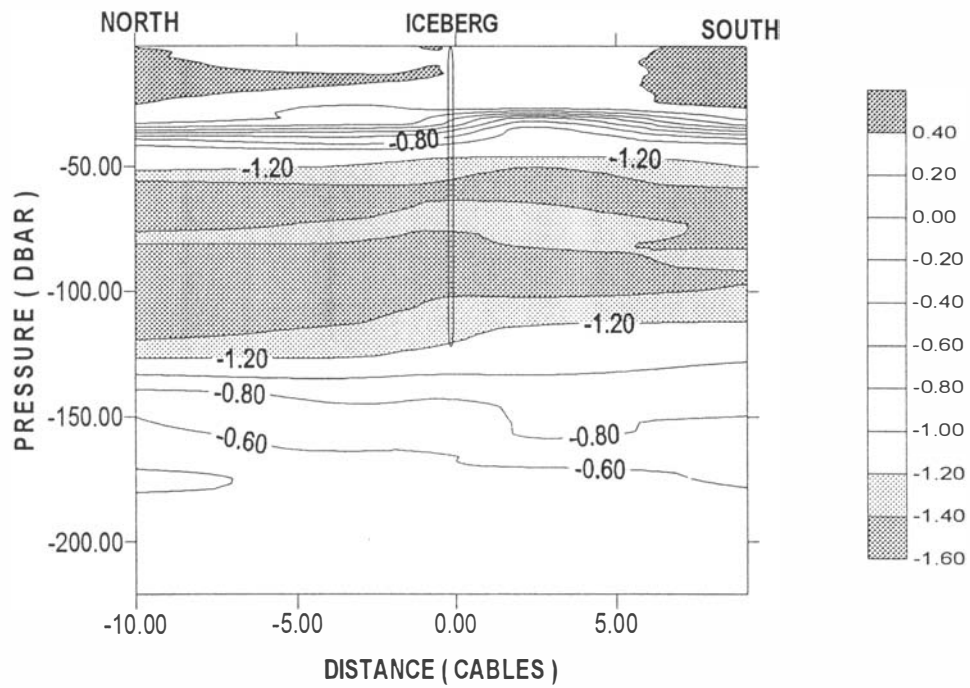


Fig.1. Temperature distribution along North-South (upper) and West-East transect according to the data from the r/v "Johan Hjort" 1992 cruise to the Barents sea. Iceberg draft was measured to be about 118-125 meters, iceberg lateral dimensions werew about 220 x 40 meters. It drifted to the South-West.

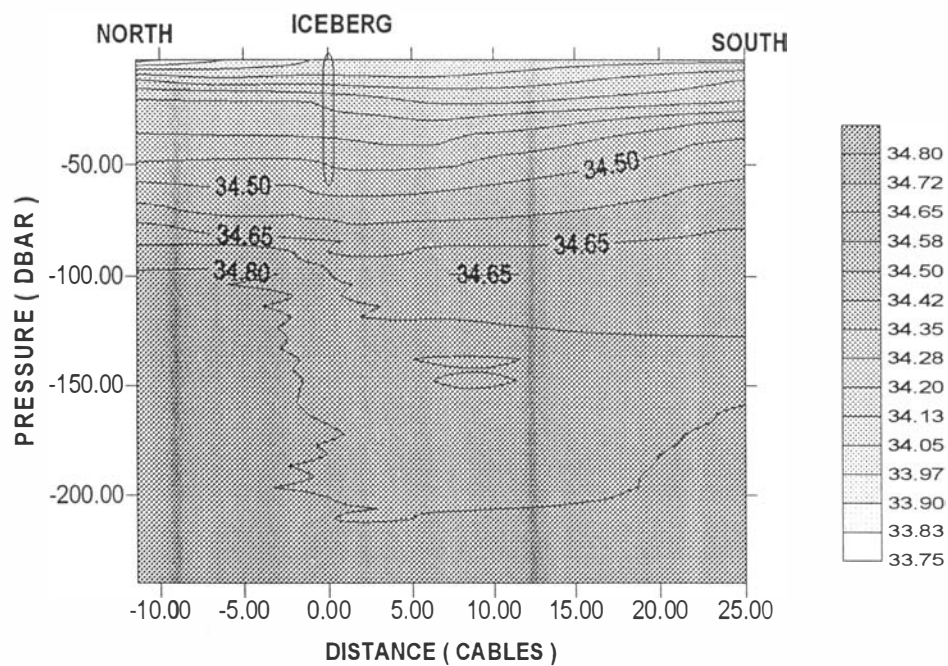
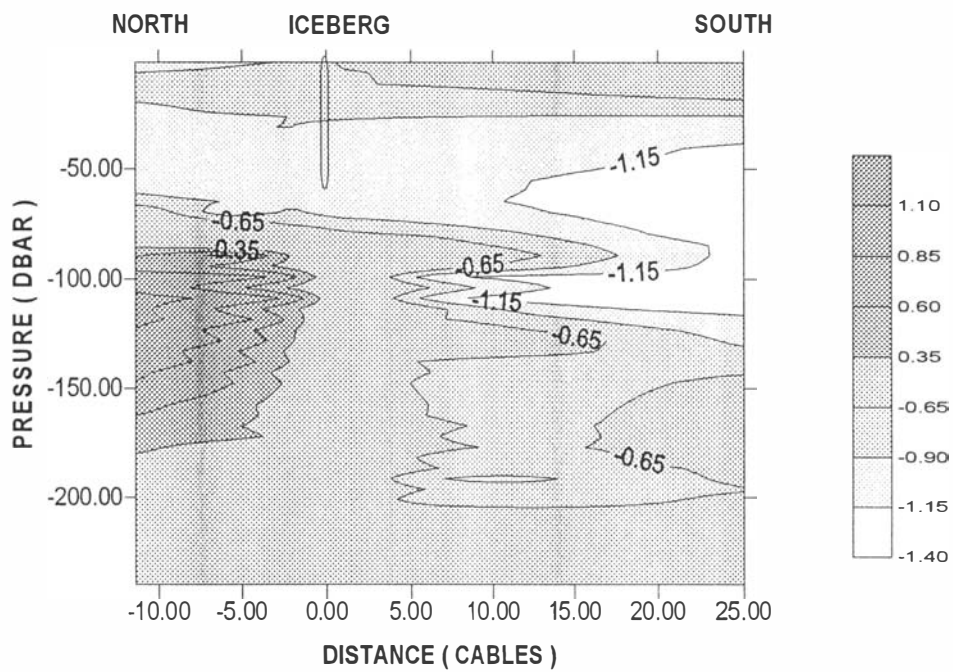


FIG.2. Temperature (upper) and salinity (lower) distribution along North-South transect according to the data from the r/v "Akademik Shuleikin" 1989 year cruise to the Barents sea. Iceberg draft was estimated to be about 70 meters, its lateral dimensions were about 180 x 120 meters.

References

1. Volkov V.A. and Pisarevskaya L.G., " Cooling and Mixing of Ocean Waters by Drifting Icebergs" Proceedings of the II-nd International Symposium on Integrated Global Ocean Monitoring, IGOM-II, 15-20 April, 1991.
2. Scott J.C., and Killworth P.D., "Upper Ocean Structures in the South-Western Iceland Sea - a Preliminary Report.", 1991, In P.C. Chu and J.C. Gascard (ed) Deep Convection and Deep Water Formation, 1991, Elsevier Publishers B.V., pp.107-121.
3. Petterson O., "On the Influence of Ice-melting Upon Oceanic Circulation", 1904, Geographical Journal, 24, pp.285-333.
4. Petterson O., "On the influence of ice-melting Upon Oceanic Circulation", 1907 , Geographical Journal, 30, pp. 273-333.
5. Huppert H.E. and Turner J.S., "On iceberg melting" , 1978, Nature, vol.271, No 5640, pp.46-48.
6. Pisarevskaya L.G. and Nygaard, " CTD-measurements near a Kara-sea floeberg". 1996. This issue.
7. Wadhams P. and Crane D.R., " SPRI participation in the Winter Weddell Gyre Study 1989" 1991, Polar Record, v. 27, No 160, pp.29-38.

NUMERICAL SIMULATION OF THE THERMOHALINE WATER CIRCULATION IN THE NORWEGIAN, GREENLAND AND THE BARENTS SEAS

G.A. Semjonov, A.M. Bezgreshnov(AARI)

Water circulation of the Norwegian, Greenland and Barents Seas is known to primarily form under the influence of water-heat exchange through the straits connecting these seas with the Arctic Basin and the Atlantic Ocean. For correctly prescribing water transport through the straits correlated with heat and salt fluxes, the region of the Norwegian, Greenland and Barents Seas was approximated as part of a common circulation system: the Arctic Basin - the Norwegian, Greenland and Barents Seas - the Atlantic Ocean. For this purpose, a three-dimensional baroclinic model of large-scale water circulation of the Arctic and Atlantic Oceans was constructed based on full equations of ocean hydrothermodynamics using Bussinesque and hydrostatics approximations written in the spherical coordinate system with the pole situated in the region of Greenland. This allowed obtaining the curves of the speeds of currents in the straits correlated with the temperature and salinity fields (with good spatial resolution (about 30 km).

Within the framework of the constructed model diagnostic (20 days) and adaptation calculations (10 days) for climatic summer and winter were performed. A diagram of currents in the system of the Arctic Ocean-Straits-North Atlantic was obtained with resolution at all points of the study area suitable for analysis. This diagram (see Fig. 1) shows all main surface large-scale currents and eddies, such as: Gulfstream, North-Atlantic (NAC), Transarctic, East-Greenland (EGC), West-Spitsbergen (WSC) and Norwegian currents; an anticyclonic eddy in the Arctic Basin and the Norwegian Sea; a cyclonic eddy in the Greenland Sea. As a result of calculations, the following transports were obtained for main currents and eddies: Gulfstream - 40.2 Sv, North-Atlantic current - 8.6 (in winter) and 5.2 (in summer), Transarctic current - 10.8 and 6.1, an anticyclonic eddy in the Arctic Basin - 8.4 and 7.2, a cyclonic eddy in the Greenland Sea - 6.2 and 6.1, an anticyclonic eddy in the Norwegian sea - 8.0 and 7.0. The main feature of circulation in the lower ocean layers is the presence of a countercurrent under the Gulfstream (below 1500 m), under the Transarctic current and under the anticyclonic gyre in the Arctic Basin (below 300 m) and under the cyclonic gyre in the Greenland Sea (below 1500 m). Under the East-Greenland current below the depth of polar water (0-200 m) there is a system of cyclonic and anticyclonic eddies spreading down to the bottom.

The constructed model adequately simulates the main circulation characteristics of the Norwegian, Greenland and Barents Seas both using the archived data of Levitus (1982) and of the AARI. The water budgets for the Norwegian, Greenland and Barents Seas are presented in Table 1. Data for "Budget 1" and "Budget 2" are taken from Earth Sci. Rev., 30 (Hopkins, 1991). The presented results were obtained without taking into account the wind effect. The difference in the estimates of transports in the straits for winter and summer calculated by means of the model is attributed to the difference in the initial salinity and temperature fields.

To conclude, it can be mentioned that the model allows investigating water mass circulation in the Norwegian, Greenland and Barents Seas without a-priori prescribing mass, heat and salt fluxes in the straits connecting the study basin with the Atlantic and the Arctic Ocean since they are calculated according to the model.

Table 1

Transports in the straits of the Norwegian, Greenland and Barents Seas (in Sverdrups)

Strait	Transport estimates		Model transports			
	budget 1	budget 2	AARI data		Levitus data	
	mean annual		winter	summer	winter	summer
Fram to (EGC) from (WSC)	7.1 -5.6	7.73 -7.20	2.5 -3.7	4.0 -10.0	6.0 -12.3	4.1 -14.4
Denmark To (Irminger) From (EGC)	0.6 -5.7	0.60 -5.28	-- -4.1	-- -2.8	-- -2.9	-- -2.1
Fareo-Iceland To From	1.3 -1.0	3.0 -0.7	2.0 --	0.8 --	0.9 --	0.2 --
Fareo-Shetland To (NAC) From	2.0 -1.4	5.35 -1.4	2.1 --	2.0 --	2.0 --	1.9 --
Spitsbergen-Franz-Josef Land To From	-- --	0.9 --	1.4 --	6.1 --	6.4 --	10.4 --
Franz-Josef Land- Novaya Zemlya To From	-- -1.9	-- -1.9	-- -0.2	-- -0.1	-- -0.1	-- -0.1
Total	-3.60	3.10	0.00	0.00	0.00	0.00

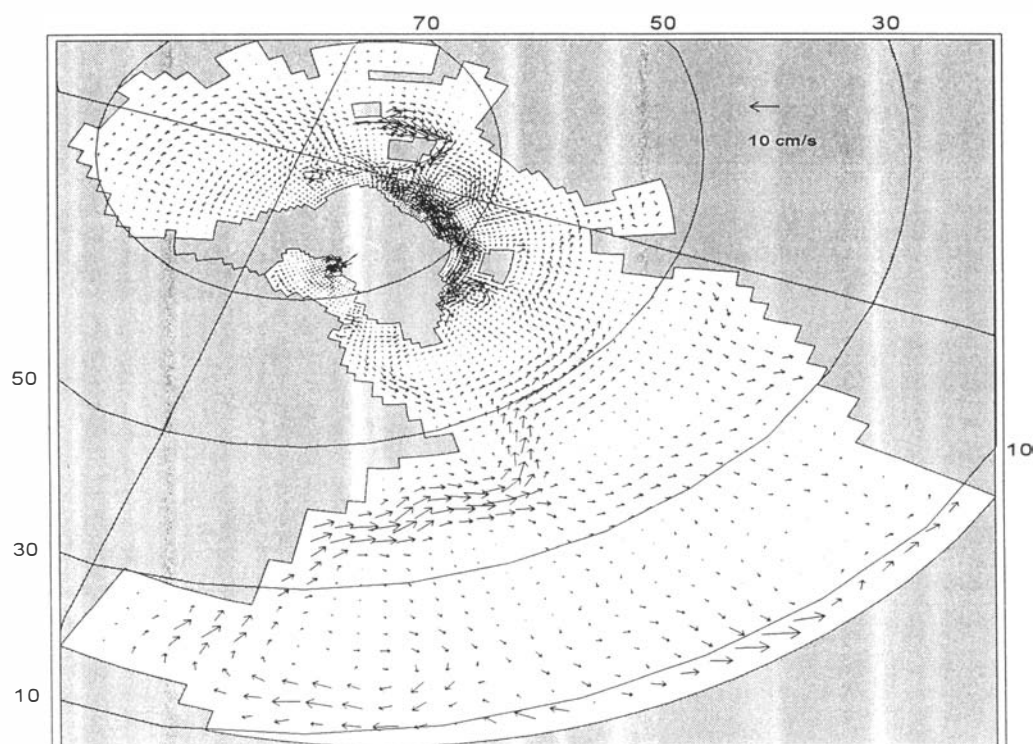


Fig. 1. Field of currents at a depth of 10 m for climatic summer.

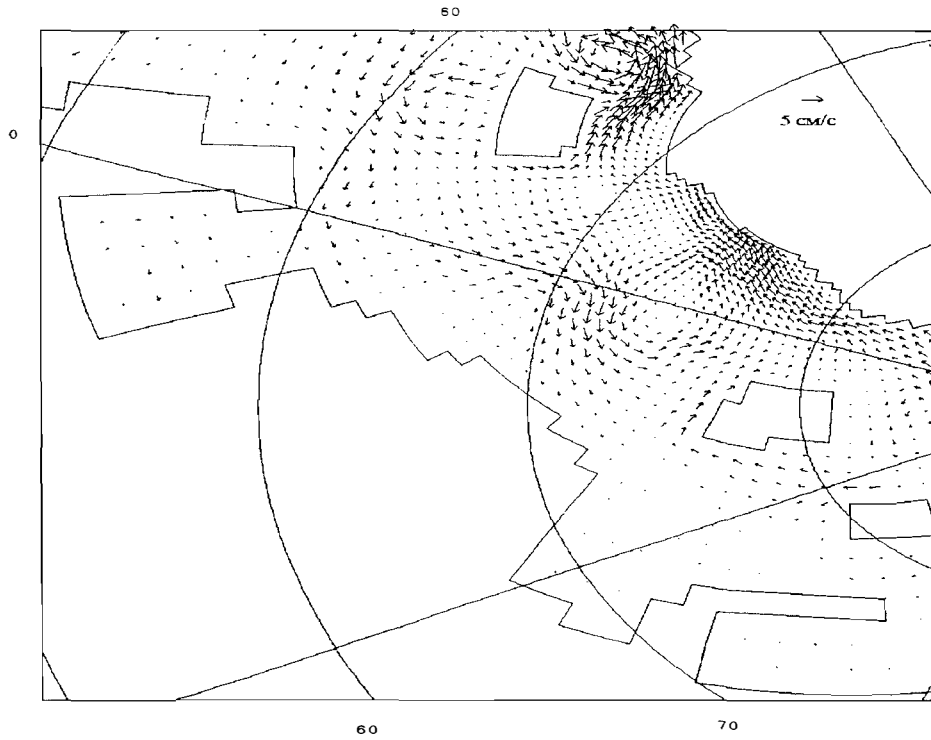


Fig. 2. Field of currents at a depth of 10 m for climatic winter in the archived data of the AARI.

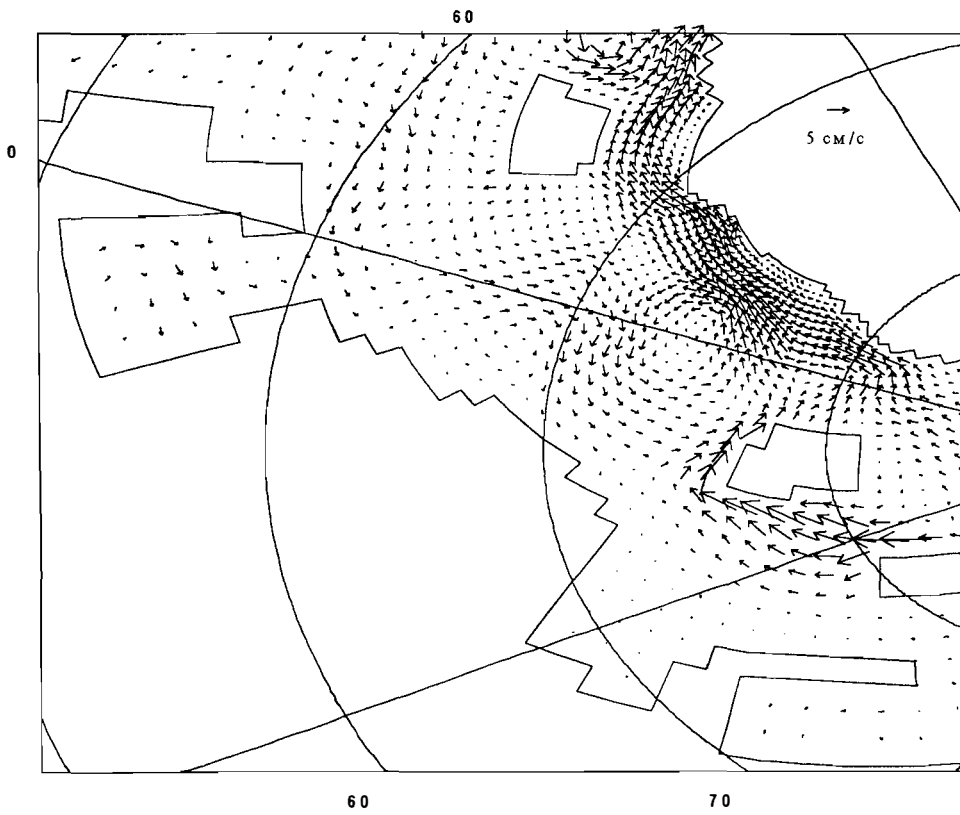


Fig. 3. Field of currents at a depth of 10 m for climatic summer in the archived data of the AARI.

References

Levitus, S., Climatological atlas of world ocean. -1982,OAA, Professional Paper 13, p.174.

Hopkins, T.S. The GIN Sea - a synthesis of its physical oceanography and literature review 1972-1985. -1991,Earth-Sci.Rev., 30., 175-318.

NUMERICAL SIMULATION OF INTERANNUAL VARIABILITY OF THE THERMOHALINE WATER CIRCULATION OF THE BARENTS SEA FOR SUMMER SEASON

G.A. Semjonov , S.V. Chviljov (AARI)

Non-stationary, three-dimensional, baroclinical model of circulation, based on full equations of ocean hydrothermodynamics, has been constructed for investigation of interannual variability of currents of the Barents Sea during summer season. For realization of the model method of splitting problem in to physical processes has been used. It simplified original system appreciably and application of effective numerical methods for its solution became possible.

Results of three of numerical diagnostic adaptive experimentson calculation of water circulation are submitted. In first experiment average fields of temperature (T) and salinity (S) for August-September 1980-1992 have been used. In second and third ones fields of T and S observed in August-September 1984 and 1987 have been used.

The used hydrodynamic model represented structure of fields of currents adequately: the received results are consistent with knowledge about permanent currents of the Barents sea. To the south-west of Zemlya Frantsa Josifa for the first time anticyclonic eddy, caused by hill with great difference of depths, has been located.

Observed values of T identify summer of 1984 as moderate warm and 1987 as cold. But general pattern of currents in 1984 and 1987 was very similar. It is caused by large influence of bottom topography into forming of structure of currents of the Barents sea.

There is direct bond between anomalies of currents and anomalies of water T: both for sea and for separate areas. In comparison with average values in warm 1984 eastern component of currents prevailed, in cold 1987 western one prevailed. As heat conditions of sea depend on flow of warm atlantic waters from the west, the amplification (moderation) of eastern transfer of waters caused to relative increase (decrease) of T in 1984 (1987).

The interannual variability is particularly pronounced in jets of currents and large scale eddies. High-rate (in comparison with 1987) flow of atlantic waters in 1984 raised the rates of all currents.

LARGE-SCALE LEVEL OSCILLATIONS OF THE KARA SEA

Yu. A. Vanda, Ye. N. Dvorkin (AARI)

Knowledge of the typical features of large-scale level oscillations and positions of mean sea level is required to address many current scientific and practical problems. Data on sea level for a sufficiently long period are used as a height datum for leveling the Earth's surface. A comparison of mean levels for different periods allows finding eustatic level oscillations of the World Ocean. A change in mean levels with time at some sea points is used for determining secular motions of the Earth's crust.

By using the Kara Sea as an example, an analysis of large-scale level oscillations has been made and tendencies for changes in mean level in a multiyear plan (about 50 years) have been determined on the basis of 22 coastal and island stations in this sea.

All observation points in the Kara Sea are characterized by well-pronounced seasonal variations in sea level. The minimum level is observed in April and the maximum in June, October and December. Seasonal level oscillations are mainly caused by changes in atmospheric pressure, wind, sea water density and also in runoff of rivers. Depending on the character of seasonal level changes and their spatial differences, zonation of the Kara Sea can be performed. The boundaries of the delineated regions are shown in Fig. 1 by solid lines. Four regions are delineated.

In order to enhance the reliability of calculations of long-term oscillations a method of smoothing mean annual level values by 5-year periods was used. This allows one to track a general character of multiyear level changes, reduce errors of calculations of mean rates of these changes, as well as exclude to some extent the influence of hydrometeorological factors on interannual changes in sea level. Calculations have enabled revealing a non-uniform character of mean rates of multiyear level changes in different regions of the Kara Sea and plotting a chart of zones of multiyear level rise and drop that are, probably, related to the areas of sinking and rising of shores, respectively. As is seen from Fig. 1, zones of multiyear level rise and drop (dashed lines) within the Kara Sea alternate, with zones of the level drop covering the north-western sea including the coasts of the Novaya Zemlya, Viese, Golomyanny islands and regions of the Ob' Gulf, Taz Gulf and the Yenisey Bay, and zones of the level rise the rest of the sea. The largest rates of multiyear changes in sea level are observed at the following points: positive - Solnechnaya inlet (+4.7 mm/year) and Tadibeykaha (-3.8 mm/year).

In addition to the indicated features in the general tendencies for changes in the Kara Sea level, one may mention a quasiperiodic character of the variability of mean annual levels. For the sites located along the mainland shore and in the central sea, the period of these changes is close to 20-22 years and in the points Zhelaniya cape (north of Novaya Zemlya Island), Vieze Island, Golomyany Island the periodicity of 10-12 years is observed. It is interesting that the periodicity of atmospheric pressure changes at all Kara Sea points is close to 10-12 years.

Studies of multiyear changes in the Kara Sea level should be continued using data on geomorphology, geology, geodesy and other disciplines which will allow revealing the nature of these changes and explaining their features in different regions of the sea.

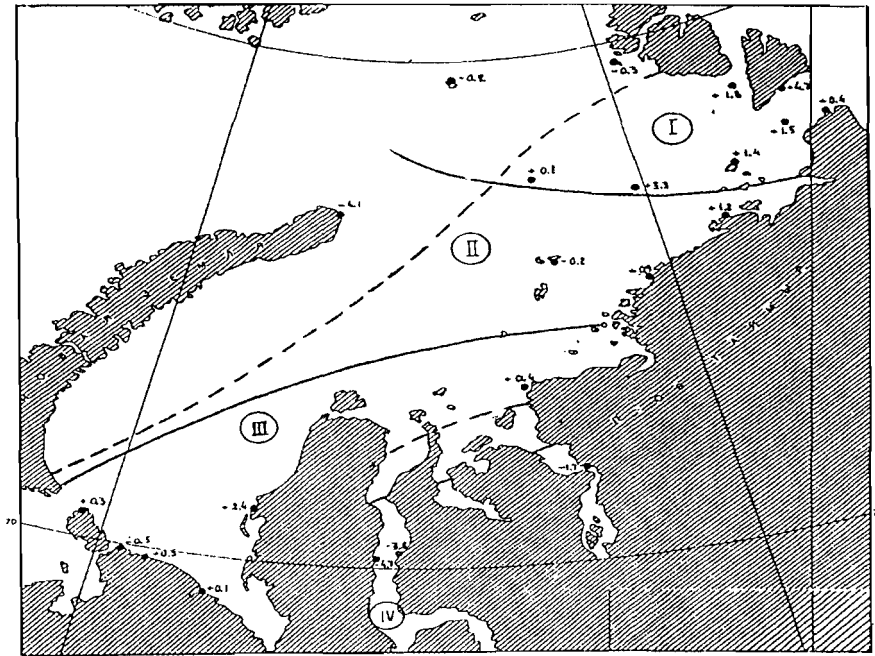


Fig. 1. Rates of multiyear level changes (mm/year), regions of their positive and negative values, regions of uniform seasonal changes in the Kara Sea level.

MAIN FEATURES OF TIDAL CURRENTS IN THE KARA SEA.

G.N.Voinov(AARI)

An analysis of the regime of tidal currents on the basis of the results of a harmonic analysis of current observation data at 245 self-contained buoy stations from 1956 to 1980 in summer is presented.

In the work on studies of the Arctic seas tidal current regime carried out on the basis of the data from the field tide measurements (G.N.Voinov, 1983) the modern methods on analysis of tides, such as Dudson's method (1954) and the method of least squares (MLS) were applied.

The distribution maps of the largest possible speed and character of the tidal current are presented. The distribution of the greatest possible velocity is shown in Fig. 1a. From the picture it follows that the maximum velocity in the open sea is observed to the north of the Ob Bay and it can reach 60 cm/s. From this region to the other ones of the open sea the velocity decreases, it does not exceed 20 cm/s in the deep zone as well as on the water area adjacent to the Taimyr Peninsula. The increase in velocity up to 30-35 cm/s is recorded near the islands located in the deep zone of the sea.

The velocity also increases up to 45-70 cm/s in the Baidaratskaya, Ob and Yenisey Bays. The highest velocity of the current is observed in the Kara Gate, Yugorsky Shar and Malygin Straits, being respectively equal to 64, 136 and 82 cm/s.

The character of tidal current is presented in 1b. The values of the character of the tidal current were calculated according to A.I.Duvanina's criterion.

Referring to Fig.1b, the currents are of semi-diurnal character on the largest part of the sea, especially in the deep zone. The extensive area with irregular, semi-diurnal currents is located in the Taimyr Peninsular coastal zone. The areas of similar character of currents are recorded near the Yamal Peninsular and in the Kara Gate and Yugorsky Shar Straits.

It is well to bear in mind that the character of tidal currents may differ essentially from the character of the tide. The zones with a irregular, semi-diurnal character are observed only in the Kara Gate, Yugorsky Shar Straits, along the Yamal Peninsular, in the region to the west of the Severnaya Zemlia Islands, near the islands of the central part of the sea, and in the southern Vilkitsky Strait. On the rest of the water area the tide is of semi-diurnal character.

The lunar semi-diurnal tide M_2 dominates in the Kara Sea and gives the good first approximation of tidal motion in the sea.

In the Kara Sea the tide M_2 is characterized by the presence of two main amphidromic systems. The main amphidromy is located in the SW Kara Sea and governs the structure of the tide and tidal current in this part and in the central Kara Sea. The second amphidromy is near the Komsomoletz Island, Severnaya Zemlia. There is a rotation of cotidal lines in an anticlockwise direction in both amphidromic systems and the systems correlate with Taylor amphidromies.

The coordinates of the centres of two amphidromic systems mentioned above are given in Table . Evidently, now extra experiments are needed to locate exactly the centres of these amphidromies. In consequence of the strong tidal wave reflection from the coast, the nodal zones appear in the Baidaratskaya Bay, near the Bely and Shokalsky Islands. The Baidaratsky Bay nodal zone is the most pronounced among them, and it transforms into the non-pronounced amphidromic system.

The presence of the other amphidromic systems in model calculations, for instance, near the Dickson Island or near the Mikhailov Peninsular, is in contradiction with the observational data.

The results of a harmonic analysis of current observations from ice in winter have shown fast ice to have a considerable influence on tidal current components. However, the expression of variability of the tidal current constituents is not simple due to fast ice effect.

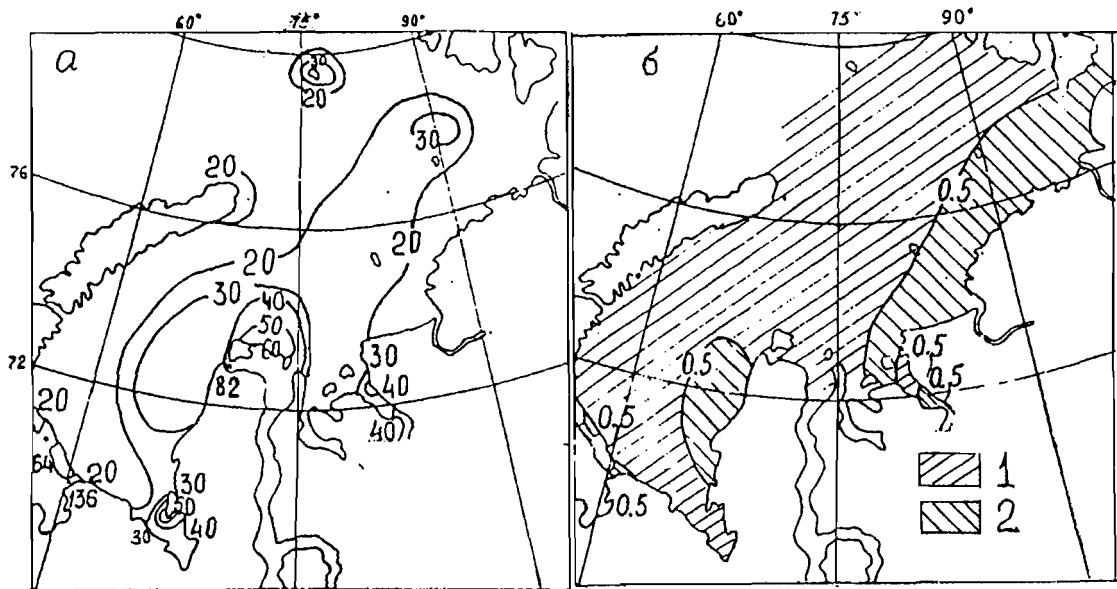


Fig. 1. The greatest possible velocity of tidal current in the layer 0-25m in summertime, cm/s (a) and the character of tidal current (b):
 1- semi-diurnal current;
 2- irregular semi-diurnal current

Table 1

Coordinates of the centres of the amphidromic systems M_2 in the Kara Sea

number	Latitude, western	±	Longitude eastern	±
1	73° 45'	0.5°	65° 00'	1°
2	80° 15'	0.25°	89° 00'	0.5°

The effect of fast ice on the tidal current increases with a decrease in sea depth and an increase in the distance the wave under fast ice passes. And the dumping of the wave M_2 current speed reaches, as compared with summer, in some areas 60% and the phase change constitutes up to 67°.

STRUCTURE OF THE TIDE IN AMDERMA ACCORDING TO THE RESULTS OF A HARMONIC ANALYSIS OF SEA LEVEL OBSERVATIONS FOR A 19-YEAR PERIOD FROM 1962 TO 1980

G.N.Voinov(AARI)

A harmonic analysis of the tide in Amderma, the Kara Sea, for the period of sea level observations from 1962 to 1980, equal to the period of the revolution of lunar nodes - 18.61 was performed (163153 hours).

The analysis program is divided into two stages. At the first stage, the convolution of a series is carried out using Fourier transform with a resolution by frequency of 0.0022 deg/h. Then identification of the harmonics exceeding the background noise using astronomical constituents from the potential expansion of Cartwright-Taylor (1971) and Cartwright-Edden (1973) (452 harmonics) and shallow water constituents (121) is performed. At the final stage the harmonic analysis proper is employed on the basis of the least-square method for the selected constituents.

Hence, the analysis program combines the advantages of the Fourier transform, most fully shown by Franko and Harari (1988) and of the least-squares as implemented by Foreman and Neyfeld (1991).

As a result of such an approach by analyzing on the basis of the least-squares, the matrix of linear equations is significantly reduced.

According to the results of the analysis, it is found that the ratio of energy of oscillations in the long-period, diurnal, semidiurnal and the rest of the tide species (including 1/6- day species) is, respectively, 29.0, 5.6, 65.3 and 0.02 % of the total variance of the tide.

In the long-period species the main contribution is made by the annual constituent S_a , whose amplitude reaches 13.2 cm. This harmonic is modulated by two satellites with an amplitude of about 2 cm. But to clear up their stability in time and include into the prediction, the analysis of observations for a longer period than 19 years is required. Let us note that the lunar monthly tide M_m and the lunar semi-monthly M_f have amplitudes smaller than those in the theory of the potential, being equal to 0.492 and 0.626 of their equilibrium values, respectively.

Depending on the background noise in a corresponding tide species, satellites were determined in the clusters of constituents from the 2d- and 3d-order potential terms. In the clusters of the main diurnal and semidiurnal constituents from 3 to 9 satellites were resolved.

In the diurnal and semidiurnal species the main satellites of the 2d-order potential term are close in the amplitude and phase lags to the theoretical ratios that are predicted on the basis of the potential theory. However, in the clusters of constituents $2Q_1$, σ_1 , Q_1 , ρ_1 , 0_1 , M_1 , P_1 , K_1 , J_1 , $2N_2$, N_2 , M_2 , L_2 the satellites of the 3d-order potential term and some satellites of the 2d-order potential term differ in amplitudes and phase lags theoretical ratios. The constituents M_1 and J_1 have satellites of the 3d-order potential term which exceed the main lines in their clusters in the amplitude. A similar result for the harmonic M_1 was also observed by Amin (1981).

For the constituents μ_2 and J_1 there is observed an anomalous decrease in the amplitude near the main line. At present it is difficult to find the cause for this phenomenon, since it can be a result of the proximity of the amphidrome or a result of interference with a shallow water constituent.

Following the principles developed by Cartwright (1968), the constituents L_2 and $2MN_2, \lambda_2$ and $2Mv_2$ were separated using the response functions. The radiation (or shallow water) contributions to the harmonics T_2 and R_2 are 27 and 91%, respectively.

The results of the tide analysis with a superresolution allow a more effective calculation of nodal modulation as compared to standard calculations. At this method the nodal angles (U)

and coefficients (F) are determined from the ratios of the amplitudes and phase lags of constituents obtained from observations. A more justified method for introducing nodal correction reduces the interannual scatter and scatter within a year in the values of harmonic constants earlier inferred from short-range observations. By interannual scatter is meant the scatter in the values of the harmonic constants, determined from annual tide analyses for 19 years, and by scatter within a year - determined from monthly tide analyses.

For the main constituents Q_1 , O_1 , K_1 , N_2 , M_2 , L_2 , S_2 , K_2 the errors of mean vector values of harmonic constants, determined from the annual tide analyses, decrease in the amplitude from 0.4% (M_2) to 8.6% (L_2) and in the phase lags from 0.2 deg (K_2 and S_2) to 4.1 deg (L_2). As to the constituents M_1 and J_1 , the calculation of the standard nodal correction does not give positive results for them, but introducing modulations using a cluster from observation radically improves the values of the harmonic constants.

More complicated appears to be the annual variability of the harmonic constants of the tide according to data of the analyses for a month.

As is currently understood (Voinov G.N. et al., 1987) the annual variability, at least for the main semi-diurnal harmonics M_2 and S_2 , is pronounced in the form of the seasonal variability resulting from changes in ice conditions in the Arctic seas. However, it can be experimentally shown that the seasonal(annual) or semi-annual variability always occurs for any of the harmonics derived if the satellite harmonic is not taken into account or the ratios for separating the harmonics differ from the theoretical ones. This conclusion is not new and was demonstrated by Godin (1970) by the example of the constituent K_1 .

When analyzing the tide for a month for the constituent M_2 , the satellite harmonics, i.e. the harmonics that are not resolved for such a period, are OP_2 , $MTS_2(H_1)$, $MST_2(H_2)$ and MKS_2 . The standard analyses of the tide for a month the influence of these harmonics on M_2 is not taken into account.

When deriving the constituent S_2 , the theoretical ratios for the harmonics K_2 , T_2 and R_2 are usually used. In Amderma the real ratios for the harmonics T_2 and R_2 differ from the theoretical ones.

After correcting the harmonic constants of the M_2 and S_2 tide from the influence of the indicated satellite harmonics, the annual periodicity in the amplitudes and the phase lags disappears. Thus, one should, probably, correct the problem of the variability of the harmonic constants of the tide which occurs in the tide at the Amderma due to the shortcomings of short-term analyses of the tide, rather than to the influence of ice conditions.

The results of the analysis of the tide permit a purely harmonic prediction of the tide without introducing the nodal correction, as is shown by Zetler et al. (1985). To clear up the effectiveness of such prediction, the variance of the residual series (observations minus prediction) at a standard (quasiharmonic) and accurate harmonic predictions was found.

For standard prediction there were used 40 constituents (including the harmonics H_1 and H_2) obtained as the means from annual analyses for 19 years. At accurate prediction (142 harmonics) the residual dispersion was 11.21 cm^2 less for 19 years on the total, as compared to standard calculation.

Let us note that in some years (3 cases) the residual variance was not observed to decrease at accurate prediction. An analysis of the residual series has shown that in these cases the residual dispersion in the diurnal and semi-diurnal species of the tide was also always less at accurate prediction as compared to standard one. The deterioration in the accurate prediction in these years was due to a long-period species of the tide and was induced by the anomalous behavior of the constituent Sta .

On the whole, accurate harmonic prediction has obvious advantages as compared to the standard (quasiharmonic) method for tide calculation. This is confirmed by the decrease in the tidal "cusps" in the spectra of residual series.

References

- Cartwright D.E., Taylor R.J., New computations of the tide-generating potential. 1971, *Geophys. J.R. Astr. Soc.*, vol.23, No.1, pp. 45-74.
- Cartwright D.E., Edden A.E., Corrected tables of tidal harmonics. 1973, *Geophys. J.R. Astr. Soc.*, vol.33, No.3, pp.253-264.
- Franko A.S., Harari J., Tidal analysis of long series. 1988, *Inter. Hydrogr. Rev.*, vol. LXV, No.1, pp.141-158.
- Foreman M.G.G., Neufeld E.T., Harmonic tidal analyses of long time series. 1991, *Inter. Hydrogr. Rev.*, vol. LXVIII, No.1, pp.85-108.
- Amin M., On analysis and prediction of tides on the west coast of Great Britain. 1982, *Geophys. J.R. Astr. Soc.*, vol.68, No.1, pp.57-58.
- Voinov G.N., Dvorkin Ye.N., Mandel' S.Z., The influence of the ice cover on tidal phenomena. 1987, Abstracts of papers. In the volume "The 3d Congress of Soviet Oceanographers. Section - Ocean Physics and Chemistry. Polar and Regional Oceanography." L., *Gidrometeoizdat*, , pp.159-160.
- Godin G., The resolution of tidal constituents. 1970, *Inter. Hydrogr. Rev.*, vol.XLII, No.2, pp.133-144.
- Zetler B.D., Long E.E., Ku L.F., Tide predictions using satellite constituents. 1985, *Inter. Hydrogr. Rev.*, vol. LXII, No.2, pp.135-142.

HIGH-FREQUENCY INTERNAL WAVES IN THE KARA SEA

Ye. A. Zakharchuk (AARI), G.E. Presnyakova (SPbSU)

During the Russian-Swedish Expedition "Ecology of Tundra-94" aboard the research expedition vessel "Akademik Fedorov" in August-September 1994 the ocean soundings in the coastal regions of the Laptev, Kara and Barents Seas in the seasonal pycnocline layer have shown short-period (minutes) temperature and salinity variations. Above and below the pycnocline such variations were not found. Variations were most intensive in the south of the Kara Sea where in the seasonal pycnocline layer at fixed level there were observed very intensive temperature and salinity variations with a maximum range reaching more than 5°C in temperature and about 2 ‰ in salinity (Fig. 1). Observations at the station for 29 hours have also shown vertical shifts of the upper pycnocline boundary at a depth ranging from 9 to 13 m and a change in thickness from 4 m at the beginning of observations to 0.4 m at the end of observations at the 18 m sea depth in this location.

For investigating the temporal variability of the observed temperature variations in the north a small experiment was performed on August 22, 1994. Onboard the moored ship temperature observations were carried out at a fixed level of 11.2 m (the upper thermocline layer) for almost an hour with an interval of 4 seconds. The thermocline thickness was 1 m. As a result, a series of 540 values was obtained. The analysis of this series has shown the temperature to change from 2.70 to 8.17 degrees during the experiment (Fig.2). Fluctuations with a cyclicity of 10-12 minutes were most intensive. Temperature fluctuations in the cycles of 2.2 and 3.0 minutes were less pronounced. As is apparent from Fig.1, 10-12 minute temperature fluctuations have a clear non-linear wave structure. These waves can be identified as high frequency internal non-linear gravitation waves and 2-3 minute variations in temperature are probably connected with turbulence or shorter-period internal waves.

Assuming that frequency of internal waves is close to that of buoyancy, the Brunt-Vaisala frequency was calculated for the pycnocline layer of mean density profile. The period corresponding to this frequency and equal to 10.4 minutes turned out to be close to the period of the observed internal waves. On the basis of the dispersion ratio (1) taken from Konyayev and Sabinin (1992), we can estimate the phase speed of waves C for long waves in a two-layered fluid:

$$C = \sqrt{g'Hh / (H+h)} \quad (1)$$

where $g' = g\Delta\rho / \rho$ is the reduced acceleration of a free fall, $\Delta\rho = \rho_2 - \rho_1$ is the difference in densities of water layers, H and h are thicknesses of the upper and lower uniform layers.

The phase wave speed estimated by means of (1) turned out to be 124 cm/s. The wave lengths of 744-893 m correspond to such phase speed at periods of 10-12 minutes.

One can calculate the amplitude of internal waves A by means of the formula which follows from the heat transfer equation

$$A = \frac{\sigma_t}{\Delta T / \Delta Z} \quad (2)$$

where σ_t - is the mean quadratic deviation of temperature for the time of the experiment, $\Delta T / \Delta Z$ is change in water temperature in the thermocline layer. The amplitude thus estimated was equal to 1.2 m.

The obtained lengths of internal waves are in a good agreement with the SAR results of the Russian "Almaz-1" satellite (Viter et al., 1993) in the east of the Barents Sea. The image from this satellite clearly shows a packet of internal waves 4-6 km long consisting of 14-20 separate waves at the exit from the Kara Gate. The wave length in

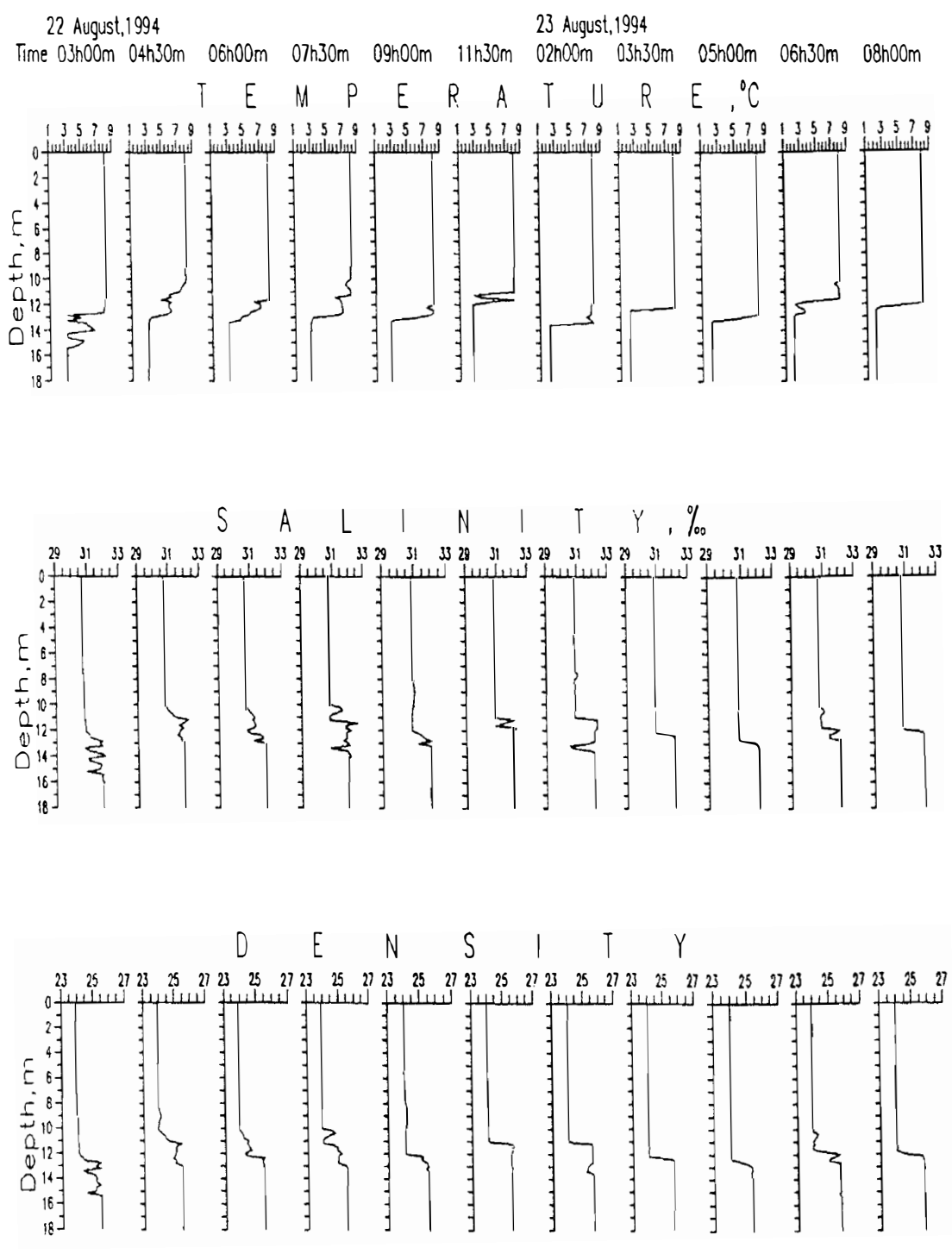


Fig. 1. Vertical temperature, salinity and density profiles in the southern Kara Sea.

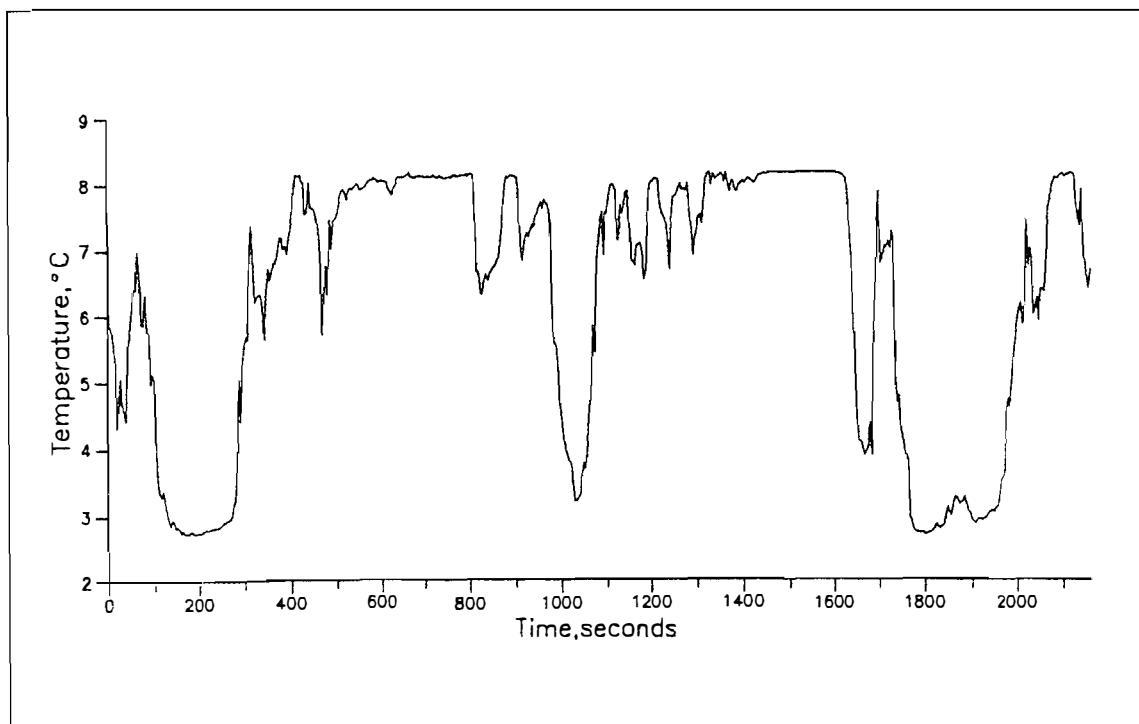


Fig. 2. Change in water temperature at a level of 11.2 m in the southern Kara Sea.

the packet is 200-400 m on the western segment of the wave front and 400-800 m - on the eastern one.

It is interesting to note that in a month a sea sounding was made almost at the same point onboard the ship "Ivan Petrov" during the Russian-Norwegian expedition "KAREX" in the south of the Kara Sea. Analysis of vertical temperature and salinity profiles has shown that due to cooling and wind increase there was complete mixing of water layers and no short-period temperature and salinity fluctuations were observed.

In conclusion we may note that high-frequency internal waves can strongly complicate observations of the forms of fine thermohaline structure. Thus, in the regions like the southern Kara Sea when soundings are made at vertical temperature and salinity profiles in the thermo- and halocline layers there will be observed small-scale temperature and salinity fluctuations due to the influence of internal waves.

But they will not be connected with lenses or intrusion layers. The life-time of intrusions according to Fedorov (1991) varies from hours to days. These are comparatively stable formations. In our case timescales of the largest variability of temperature were equal to 10-12 minutes. Hence, the forms of fine thermohaline structure in such regions can only be found by averaging a large number of vertical temperature and salinity profiles. According to the obtained results, the interval between soundings should not exceed 5 minutes.

Since small-scale variations in temperature and salinity in the pycnocline layer were observed almost at all stops of the vessel, it may be suggested that high-frequency gravitation internal waves are quite widespread, at least in the coastal waters of the shelf seas of the Arctic Ocean. That is why, under expedition conditions when investigating fine thermohaline structure, first, a control sounding should be made for finding high-frequency internal waves and estimating their period if they are present, and only after that the interval between soundings at a given point should be determined.

The results obtained show that studies of the forms of fine thermohaline structure should be carried out together with studies of internal waves.

References

V.V. Viter, G.A. Yefremov, A.Yu. Ivanov, K.Ts.Litovchenko, S.S. Semenov, A.V. Smirnov, Yu. G. Trokhimovsky, P.A. Shirokov, V.S. Etkin, Spacecraft "Almaz-1" - "OKEAN-I" program: preliminary results of high-resolution radar observations of processes in the ocean. 1993, Internal waves. Study of the Earth from space, No. 6, pp.63-74.

K.V.Konyayev, K.D.Sabinin, Waves inside the ocean. 1992, St.Petersburg, Gidrometeoizdat, 271 p.

K.N. Fedorov, Selected proc. on physical oceanography. 1991, Leningrad. Gidrometeoizdat. 310 p.

**CHARACTERISTICS OF CURRENTS AND HYDROLOGICAL
PARAMETERS AT A STANDARD POINT IN THE VICINITY OF THE
DIKSON ISLAND ON THE BASIS OF BUOY STATION DATA NPI-94-
K2 FROM AUGUST 24 TO SEPTEMBER 11, 1994 (THE RUSSIAN-
NORWEGIAN OCEANOGRAPHIC PROGRAM, KAREX-94)**

V.I.Zhukov, V.A.Volkov, V.L.Kuznetsov, S.B.Kuz'min(AARI), V.O.Bayandin(SPb SOI).

The buoy station NPI-94-K2 (station coordinates: 74 00N; 80 00 E) was deployed in the Kara Sea in August-October of 1994 during the expedition aboard the R/V "Ivan Petrov"

The place of deployment was related to the objective of tracking the region of the Yenisey river fresh water outflow and assessment of frontal zones both at the surface and in the near-bottom layer. This location was also interesting for the study of the regime of the coastal Siberian current and estimates of transport for different types of water masses.

It should be noted that the indicated point is standard for instrumental observations of the Kara Sea currents that are carried out by the AARI and has a long series of hydrometeorological information.

Meters for determining temperature and salinity parameters, current speed and direction with a 10 minute interval between measurements were used at the station.

In the course of processing the collected data an analysis of temporal variations of water temperature and salinity, current speed and direction by two levels (10.5 and 30 m) was performed. Also, spectral densities of total currents; invariant characteristics (using methods of V.A. Rozhkov); characteristics of tidal currents in this zone were analyzed.

Two water masses can be identified in the deployment region: transformed brakish water of the river runoff that forms an upper quasiuniform layer and Kara water proper located below the pycnocline and formed by winter convection. A tidal component plays a significant role in the currents (>50%). Tidal currents are mainly formed by the wave incoming from the north.

During the indicated period in this region there was a well-pronounced eastern transport of the continental water runoff in the surface layer and advection of Kara water in the direction of the mainland in the near-bottom layer. An analysis of the correspondence of the regime of currents with the actual synoptic situation during the station operation was performed (by the classification of Dmitriyev A.A. and P.A.Seltser).

Part “Hydrology of estuaries and waters of land”

February 28, 1995

PECULIARITIES OF THE WATER RUNOFF REGIME IN THE MOUTH AREA OF THE OB' RIVER

VINOGRADOVA (SPBSTU)

One of the main factors forming the hydrological regime of the Ob' mouth area is the river runoff. Its absolute value, multiyear and seasonal variability govern in many respects such characteristics as the heat sink, the discharge of sediments and pollutants, as well as the location of the hydrofront and of the zone of reverse currents.

The spatial-temporal variability of the runoff characteristics in the Ob' mouth area has been poorly covered by observation data due to the great length of the water body (more than 1000 km), a lengthy spring flood process and the complexity of identifying only the runoff characteristics among the regime forming factors.

The dynamics of the runoff characteristics over the mouth area was obtained by modeling based on a one-dimensional hydrodynamical model. At the river boundary of the mouth area a runoff hydrograph was prescribed, at the sea boundary - seasonal or surge sea level oscillations. In addition, the density non-uniformity of the flow in the northern zone of the area, the duration of the freeze-up period, ice breakup dates over the gulf area and a lateral inflow were taken into account.

As a result of calculations, the spatial-temporal variability of the following characteristics was obtained: the runoff component of the level, water discharges, mean current speeds over the section in the mouth area of Ob' for the observed and model situations.

The following typical features of the process during the flood wave passage were obtained:

- in the mouth zone of the river, at a 6-time increase in the flood wave height, mean speeds over the section and water discharges change by 3 times, in the estuary these ratios are more significant - at a 1.0-1.5-time increase in the wave height, mean speed increases by 7 times;

- at the passage of the flood wave along the mouth area, a significant decrease in the water level from 6 m to 0.3 m and an almost complete flattening out of the runoff hydrograph are observed. The latter is typical of the affluents with small tilts of the water surface;

- ice conditions have an additional influence on the flattening out of the runoff hydrograph and the value of the maximum water discharge, increasing, on average, the value of the maximum water discharge by 10%;

- seasonal variations in sea level reduce the value of the maximum water discharge approximately by 12%;

- the rate of the propagation of the wave ridge in the river mouth area has significant values increasing in the estuary by 3-4 times more as compared to the river zone;

- ice conditions and the background sea level influence the time lag of the maximum or the given runoff levels and water discharges. Hence, the dependencies of water discharges and runoff components have an ambiguous form;

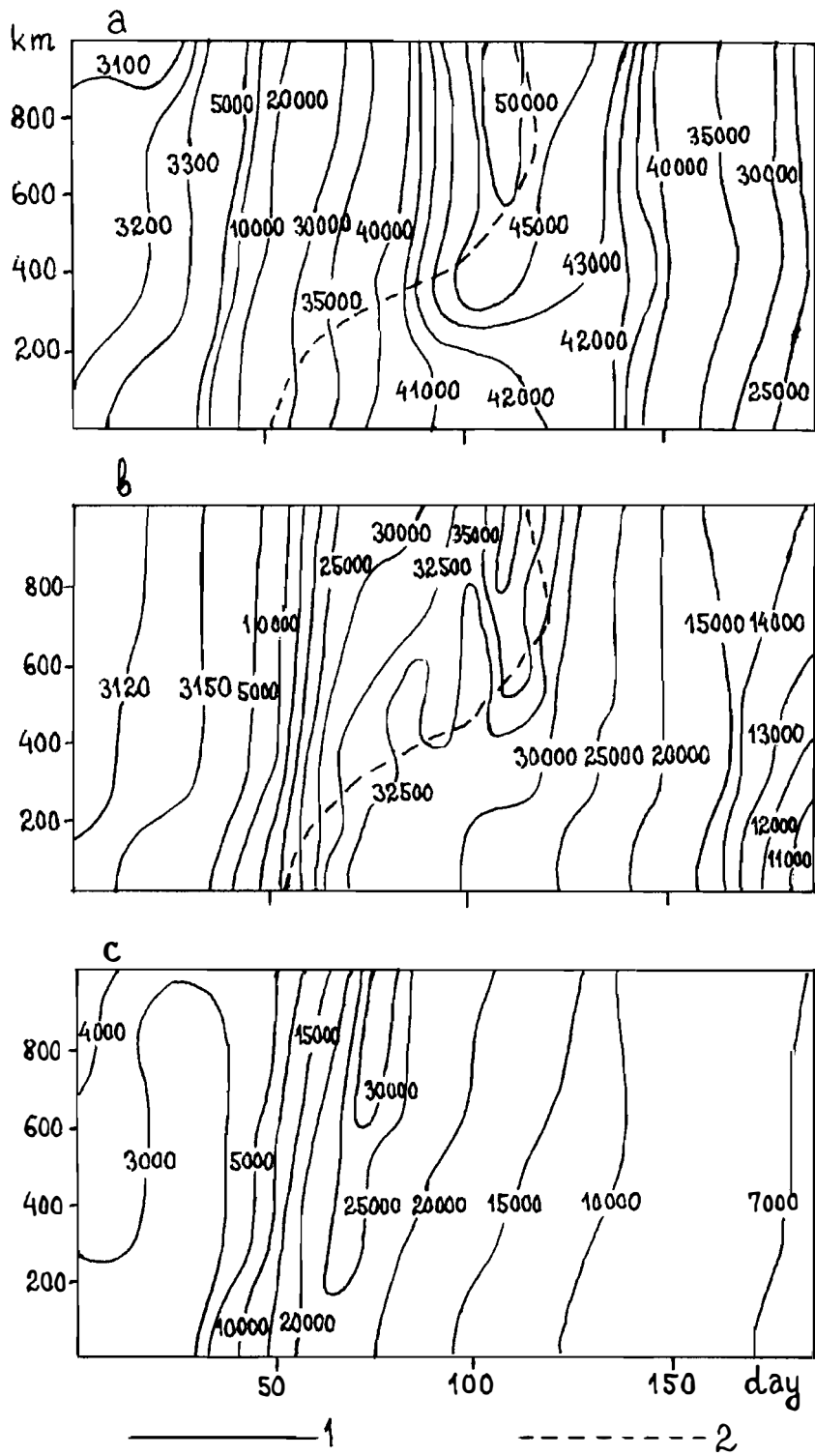


Fig. 1. Calculated isolines of water discharges (m^3/s) in the coordinates of the system: time - distance a) high water year; b) average water content; c) low water year; (1) isolines of water discharges (2) a curve of the ice breakup (disappearance) dates in the area.

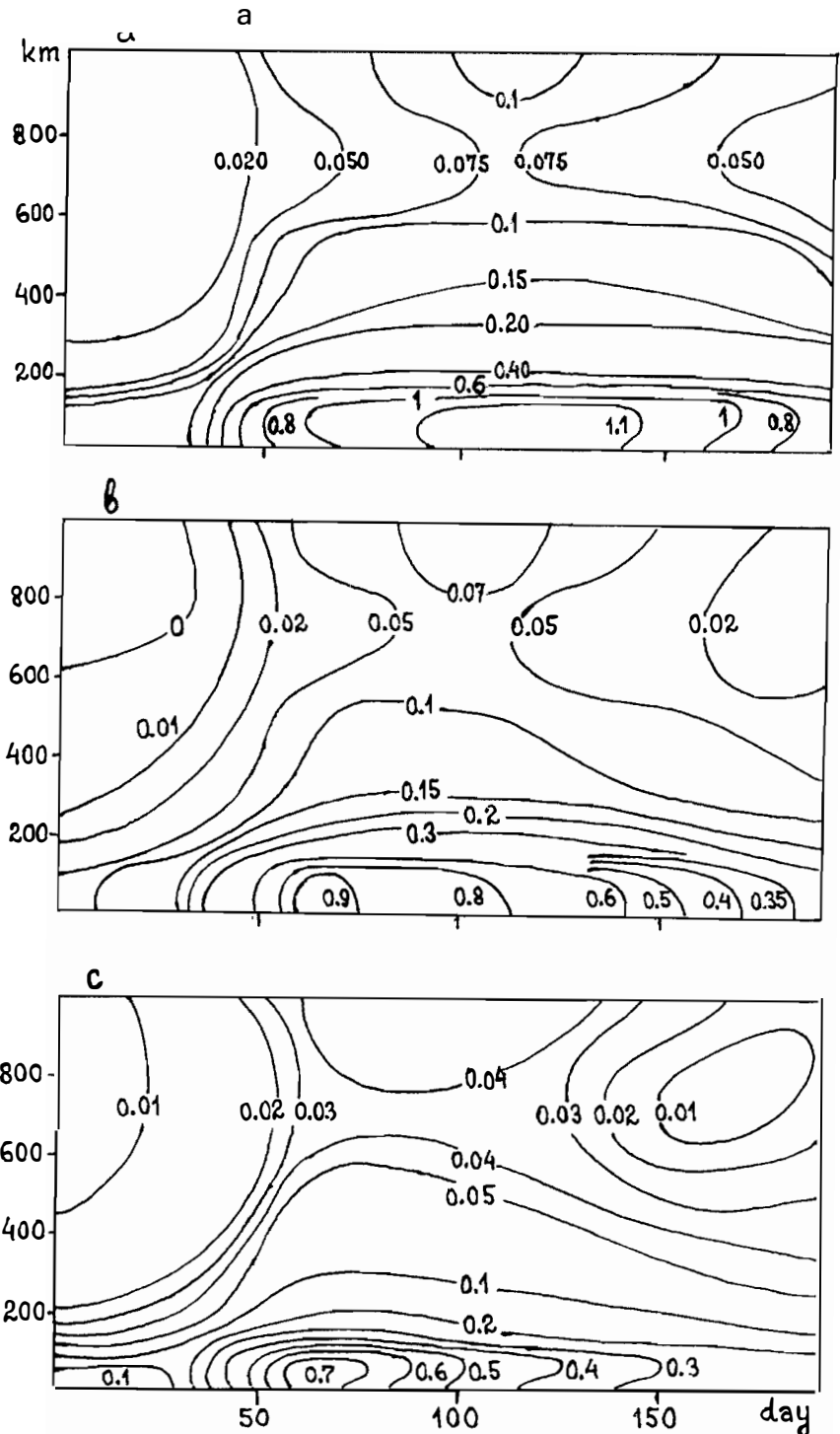


Fig. 2. Calculated isolines of runoff current speeds (m/s) in coordinates of the system: time - distance.
 a) high water year; b) average water content; c) low water year.

- ice conditions influence transformation of the runoff hydrograph, contributing to the increase in the maximum water discharges, formation of additional peaks at the hydrograph, as well as to the "delayed flood recession;

- seasonal sea level variations influence changes in the runoff hydrograph and redistribution of water discharges; the increase in discharges related to the indicated factor in the southern zone of the estuary is 3-5% and in the northern zone - 10-15%.

Estimates of the runoff speeds of currents and rates of water discharges are presented in the regime diagrams in Figs. 1 and 2. They show how these characteristics change (from April 1 to September 30) in high-, average- and low water model years over the entire territory of the Ob' mouth area (from Salekhard to the exit to the sea). In Salekhard, the runoff hydrographs were synthesized from water discharges of a 2%, 50% and 98% probability which corresponded to high-, average- and low water years. In determining the runoff characteristics, one should take into account that the rate of the wave ridge propagating in this body is large and the time lag is small, respectively. Seasonal sea level oscillations (especially at the points close to the sea boundary) increase the time lag of the maximum, and early breakup dates can reduce it. All these factors do not permit obtaining an unambiguous dependence of the time lag on the water discharge /1/.

The main feature of the regime of the runoff change in the Ob' mouth area is a large dynamics of water discharges at insignificant changes in the runoff component of the levels and speeds of the current. During the low water period in the estuary, water discharges under the influence of non-periodic oscillations can reach zero or negative values (at the level rise) and then dramatically increase at the level drop /2/.

References

1. Vinogradova T.A. Typical features of the flood wave propagation in the Ob'-Taz mouth area. Author's summary of the thesis, L., 1987, 19 p.
2. Vinogradova T.A. Analysis of the interaction between the flood waves and level oscillations in the estuaries, bays and gulfs of the Siberian rivers. Proc. of the 5th All-Union Hydrological Congress, L., 1990, vol.9, pp.150-157.

THE PROBLEM OF ESTIMATING THE POLLUTANT DISCHARGE FROM THE RIVER BASINS OF THE ARCTIC ZONES

Vinogradov Yu.B. (SHI), Vinogradova T.A. (SPbSU).

A pollutant spreads within the river basin either uniformly, or tending to some fixed points. After it is transferred to the basin, it spreads very fast through different media, water and soil being the most important of them.

Then the pollutant or its derivatives are present at any moment of time within the river basin in the following associations: in the biocenosis, in the soil substance, in soil and ground water, in water of lakes and swamps and in the channel running water. The "storage" time of the pollutant, corresponding to the extent of its dynamics, varies rather widely - from hours to many years and decades.

The described picture of the initial stage of the pollutant fate is corrected by a number of factors: by the relief and landscape in the pollution area, seasons, weather conditions, the presence or absence of the snow cover, humidity and temperature of soil.

The basins under consideration are characterized by the presence of permafrost rocks which serve as a cryogenic bed and prevent penetration of the pollutant into the ground water. Thus their influence upon the general ecological situation is very important. Nevertheless, the pollutant can penetrate the ground water in the zones of taliks which exist at some sites near the drainage divides and also under the lakes and river channels.

The dynamics of the pollutant within the river basin and its escape beyond it are governed by the water dynamics and river runoff through the downstream measuring sections of the basin. Hence it is necessary to consider the movement of water and of the pollutant jointly throughout the diverse land part of the hydrological cycle.

For calculating water and pollution discharge, a sufficiently complicated physically justified composite modeling system "DISCHARGE-EROSION-POLLUTION" is used. Fig. 1 presents a block-diagram of its components. This system includes ten soil layers, up to 15 levels of the regulating capacities of the underground discharge and up to 15 levels of the waterways according to the classification of Horton-Straler. This, probably covers all possible sizes of the river basins up to the Amazonka river. The ideology and modeling features are given in /1, 2, 3/.

The content of this universal system and its algorithm strongly differ from few other known models with the distributed entry and parameters. The main differences primarily refer to such important questions as surface and underground runoff formation, dynamics of soil waters and phase transitions in soil, prechannel and channel runoff transformation.

The model is oriented to the most simple routine meteorological information (temperature and air humidity deficit, precipitation layer and liquid precipitation duration) but the techniques are used which increase its effectiveness.

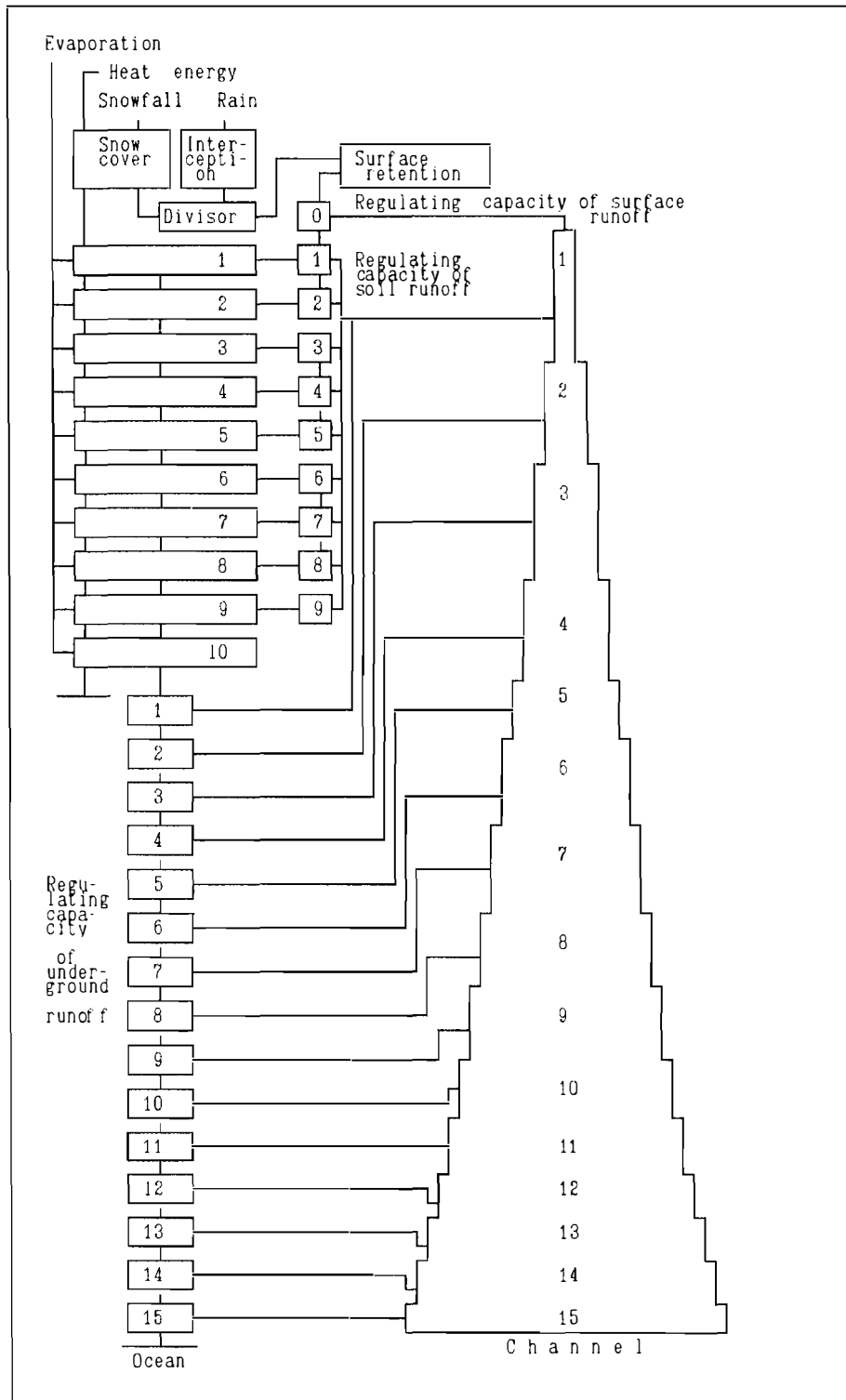


Fig. 1. Elements of the modeling system.

By depth, soil is divided into ten calculation layers, usually (but not necessarily) uniform and equal to 0.1 m.

The output of the model is a continuous runoff hydrograph at the downstream measuring section during the required number of years. Simultaneously, such variables of the state of the model system are calculated as soil temperature and humidity, temperature, water supply and density of the snow cover at any calculation point.

The calculation time interval can be any, but it is convenient to assume it to be equal to one day or less.

For the Arctic winter, the blocks of the model which calculate phase transitions of soil water, are most important. The model performance under conditions of permafrost and seasonal melting of soils for tundra landscapes has been positively evaluated.

The suggested modeling system can, in principle, be used for the river basins of any size (from fractions to million sq.km) and in any geographical zone.

The modeling system has been successfully run for estimating and predicting the dynamics of pollution in the regions of the fall of two stages of rockets at their experimental launches. "Naryan-Mar" (Malozemelskaya tundra) and "Koida" (the interfluvium of Kuloy and small rivers falling to the White Sea) were considered as two of such regions. The calculation results for the Naryan-Mar region are given in Tables 1-3. In this case the rocket fuel - 1,2 dimethylhydrazin is assumed to be a pollutant. During modeling the pollution patchiness was taken into account.

At the present time the model system "DISCHARGE-EROSION-POLLUTION" is being improved.

Table 1.

A decrease in the pollution layer in the soil core 1 m deep "Naryan-Mar"

No. of the year	0	1	5	10	15	20	25	30	35	40	45	50
Pollution layer 10 ⁻⁴ m	2. 28	2. 26	2. 12	1. 96	1. 82	1. 67	1. 53	1. 41	1. 29	1. 17	1. 06	0. 96

Table 2.

Dynamics of the pollution layer in the soil core (Naryan-Mar)
The pollution layer of 10 m^5

No. of the year	No. of the calculation soil layer									
	1	2	3	4	5	6	7	8	9	10
0	15.0 0	7.80	0	0	0	0	0	0	0	0
1	9.34	10.0 0	2.16	0.77	0.21	0.11	*	*	*	0
5	3.38	9.50	5.26	2.12	0.62	0.26	0.04	*	*	0
10	0.76	6.00	5.94	4.12	1.67	0.94	0.19	*	*	0
20	0.04	1.71	3.33	4.66	3.04	2.92	0.94	0.02	*	0
30	*	0.43	1.30	3.02	2.89	4.24	2.12	0.09	*	0
40	*	0.11	0.45	1.55	1.99	4.22	3.12	0.25	*	0
50	*	0.03	0.14	0.72	1.15	3.40	3.59	0.57	*	0

Note: designation * indicates the difference from 0

Table 3.

Indicators of the pollutant discharge

No. of the year	the thickness of the calculation layer is 10^{-6} m	Relative Concentration 10^{-8} m	Concentration 10^{-5} kg/cu.m
5	4.58	34.4	27.5
10	2.63	19.7	15.2
15	1.39	10.4	8.32
20	0.72	5.40	4.32
25	0.36	2.71	2.17
30	0.18	1.35	1.08
35	0.09	0.68	0.54
40	0.05	0.34	0.27
45	0.02	0.17	0.14
50	0.01	0.08	0.07

References

1. Vinogradov Yu.B. Mathematical modeling of the runoff formation processes. Experience of a critical analysis. L., Gidrometeoizdat, 1988, 312 p.
2. Vinogradov Yu.B. The ecological orientation of hydrology in the system of environmental science. In: Papers on problems of modern hydrology", Gidrometeoizdat, in press.
3. Yu. Vinogradov, T.Vinogradova. Hydrological cycle modeling for arctic river basins. Arctic climate system study. A book of abstracts. Gothenburg. 1994. H-10.

A TWO-LAYER MODEL OF SEA/RIVER WATER INTERACTION IN THE ESTUARY ZONE OF THE SEA

A. V. Volkov (RSHI/AARI)

The problem of studying the processes in the area of sea/river water interaction has become very important lately in connection with various activities on the sea shelf. The thickness of the upper layer which consists of fresh river or mixed river and sea water is one of the most important parameters of the hydrological conditions in the estuary zone of the sea.

Due to a great density difference between the upper freshened and lower (consisting of sea water) layers, the exchange of heat, salt and momentum is strongly restricted. As a result, in the autumn season the rate of cooling and hence the date of new ice formation on the shelf of the Arctic Seas depends only on the temperature and thickness of the upper freshened layer and the ocean-to-atmosphere heat flux.

For calculating dynamic and thermohaline characteristics of the processes of sea/river water interaction, a two-layer model with entrainment was applied. The equation system of the model is as follows:

$$\frac{\partial \xi}{\partial t} + \frac{g}{f} J(\xi, H) + \frac{g}{f\rho_0} J(\rho_1 h_1 + \rho_2 h_2, H) + \frac{1}{f\rho_0} \text{rot}_z \tau^0 - \frac{g}{2\alpha' f\rho_0} [\rho_1 \nabla^2 \xi + h_1 \nabla^2 \rho_1 + h_2 \nabla^2 \rho_2 - (\rho_2 - \rho_1) \nabla^2 h_1] = 0 \quad (1)$$

$$\frac{\partial h_1}{\partial t} - \frac{g}{f} J(\xi, H) - \frac{g}{f\rho_0} J(\rho_1 h_1 + \rho_2 h_2, H) + \frac{2gh_1}{f\rho_0} J(\rho_1, h_1) + \frac{g}{2\alpha' f\rho_0} [\rho_1 \nabla^2 \xi + h_1 \nabla^2 \rho_1 + h_2 \nabla^2 \rho_2 - (\rho_2 - \rho_1) \nabla^2 h_1] = WE \quad (2)$$

$$\frac{\partial \rho_i}{\partial t} + \frac{g}{f} J(\xi, \rho_i) + \frac{1}{f\rho_0 h_i} \text{rot}_z [\rho_i (\tau^{i-1} - \tau^i)] - \frac{1}{f\rho_0 h_i} \text{rot}_z (\tau^{i-1} - \tau^i) - K_{L\rho} \nabla^2 \rho_i = \frac{\rho_i}{f\rho_0 h_i} \quad (3)$$

$$-fV_i = -g \left\{ h_i \frac{\partial \xi}{\partial x} + \frac{h_i^2}{2\rho_0} \frac{\partial \rho_i}{\partial x} + (i-1) \frac{h_i}{\rho_0} \frac{\partial \rho_{i-1}}{\partial x} - \left(\rho_i - \rho_{i-1} \right) \frac{\partial h_{i-1}}{\partial x} \frac{\tau_x^{i-1} - \tau_x^i}{\rho_0} \right\} + \dots \quad (4)$$

$$fU_i = -g \left\{ h_i \frac{\partial \xi}{\partial y} + \frac{h_i^2}{2\rho_0} \frac{\partial \rho_i}{\partial y} + (i-1) \frac{h_i}{\rho_0} \frac{\partial \rho_{i-1}}{\partial y} - \left(\rho_i - \rho_{i-1} \right) \frac{\partial h_{i-1}}{\partial y} \frac{\tau_y^{i-1} - \tau_y^i}{\rho_0} \right\} + \dots \quad (5)$$

where:

$$\text{WE (6)} = \frac{2}{3} \frac{c}{\Delta b h_1} \frac{V_1^3}{h_1}$$

Here ρ_i , h_i , U_i and V_i - density, thickness of the layer and horizontal velocity components $i=1$ for the upper layer, $i=2$ for the lower layer, ζ - free surface level, f - Coriolis parameter, X- and Y-axes are directed to the east and north, respectively, τ - friction forcing, \tilde{Q} - density flux, $H = h_1 + h_2$.

The expression (6) for computing the entrainment rate corresponds to the model of the upper quasi-homogenous layer in the open ocean /Kraus, 1979/.

As boundary conditions for the free surface level, the expressions obtained by Sarkisyan (1977) were used. At the solid boundary for the normal velocity component the assumption of non-flowing was used and for the tangential component - the assumption of free sliding; at the liquid boundary the assumption of free flowing was applied. The boundary conditions for the density and thickness of the upper layer at the solid boundary had the form of the normal gradients equal to zero and at the liquid boundary - conditions of free emission.

Calculations were performed for a hypothetical rectangular grid 100x100 km which approximates the estuary zone of large arctic rivers. The depths and density values were roughly the same as on the shelf of the Arctic Seas. The initial thickness of the upper freshened layer was equal to 9 m. The spatial resolution was 10 km, the temporal resolution - 100 s, the water discharge through the mouth - 30000 m³.

As a result of modelling for the period up to 30 days, the core characteristics of dynamic and thermohaline processes in the estuary zone were obtained. It was found that river water flowing from the mouth, shifts to the east due to Coriolis forcing. Thus eastward currents prevail in the upper (Fig. 1a) and westward currents in the lower (Fig. 1b) layers. Also, as a result of modeling, the presence of the sea water inflow in the lower layer of the river estuary was established. The transformation (salination) rate of river water, resulting from interaction with a sea water layer (Fig. 2 and 3) was determined, as well as the character of the distribution of the free surface level over the modeling area. The influence of the atmospheric processes was not taken into account (heat, density and momentum fluxes at the upper boundary of the freshened layer were equal to zero).

A comparison of the model results with data of the hydrological surveys conducted in this region onboard the research vessels, has shown this model to simulate the main features of the dynamic and thermohaline processes in the estuary zone and to allow estimates of the thickness of the upper freshened layer with a sufficient accuracy (up to 1-2 m).

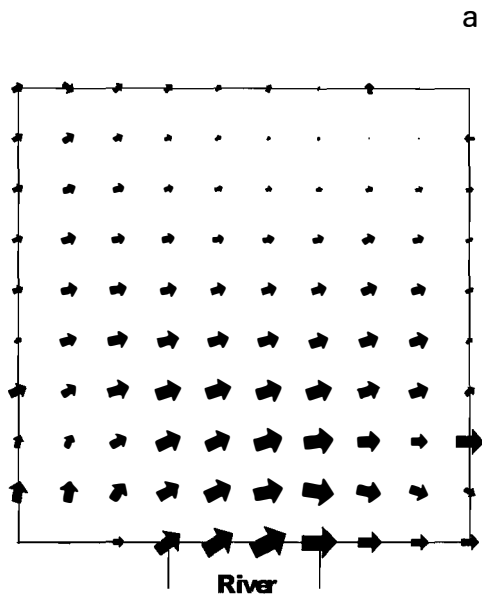


Fig. 1. Currents (1cm = 25 cm/s): a) in the upper layer

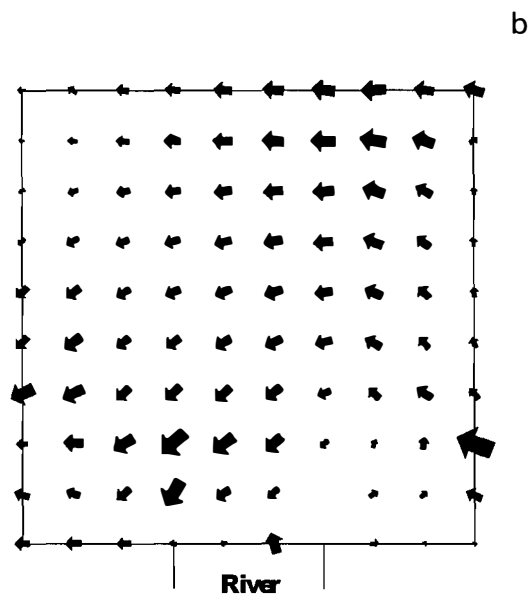


Fig. 1. Currents (1cm = 25 cm/s): b) in the lower layer

a

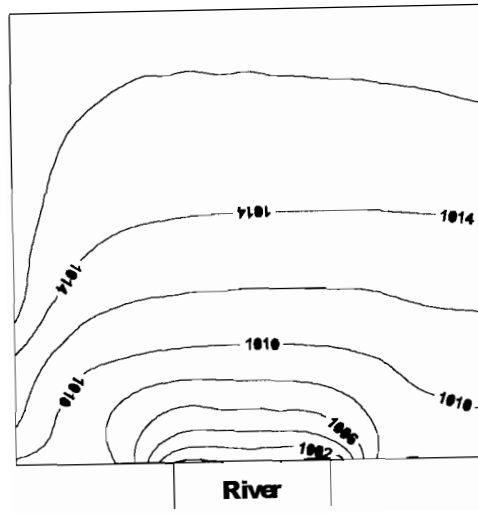


Fig. 2. Density at different levels in 20 days (kg/m..); a) in the upper layer b) in the lower layer.

b

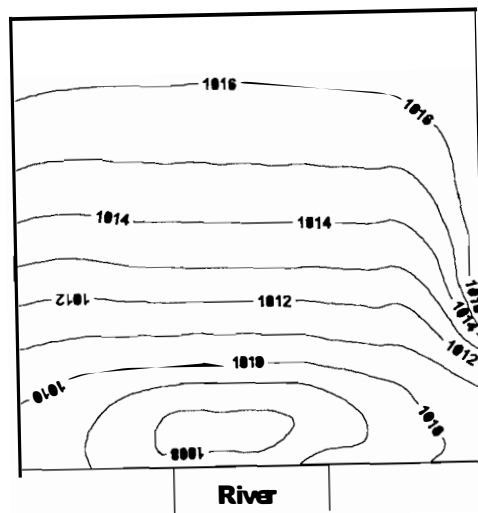


Fig. 2. Density at different levels in 20 days (kg/m..); b) in the lower layer.

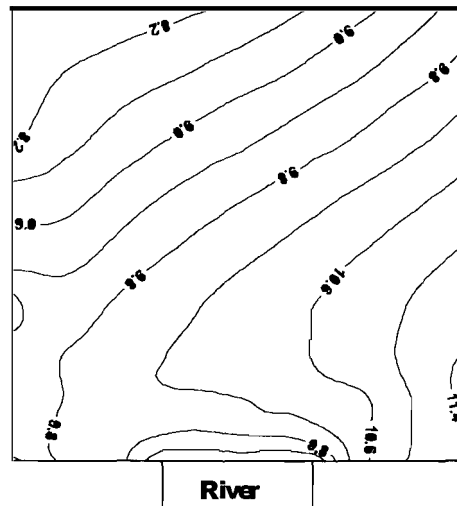


Fig. 3. Thickness of the oper layer in 20 days.

References

1. Kraus E.B. (ed), Modeling and prediction of the upper ocean layers, L.: Gidrometeoizdat, 1979. - 367 p.
2. Sarkisyan A.S., Numerical analysis and prediction of sea currents, L.: Gidrometeoizdat, 1977. - 187 p.

WATER DYNAMICS AND STRUCTURE IN THE RIVER ESTUARIES OF THE KARA SEA BASIN

A.P. Grayevsky (State Enterprise "LARGE")

As a result of specialized hydrological studies carried out by the AARI during the period 1972-1986 in the river estuaries of the Kara Sea Basin (Yenisey in 1972-1975, 1979-1984, Ob' in 1976-1980, Pyasina in 1984-86), the formation features of water dynamics and structure, characteristic of the mouths of the Arctic rivers of the estuary type, which have mouth areas with deltas and semi-closed gulfs and bays (estuaries) with a free water exchange, were revealed.

An analysis of water dynamics variability was carried out on the basis of data of long-term observations of the components of currents at bench mark stations of hydrological polygons in different seasons of the year, including the period of break-up and ice disappearance (Yenisey 1981-1982). It allowed an assessment of the effect of the processes of different temporal scales (seasonal, synoptic, tidal) on the regime of currents depending on the season and river water content and determination of spatial scales of the effect of these processes /1,2/. Fig. 1 shows by the example of the Yenisey estuary typical temporal scales of the variability in speeds and the contribution of energy significant zones to the total dispersion of the process along the mouth area which explicitly reflect the decrease in the effect of tidal and surge waves on the variations in the current speeds with a distance from the sea boundary of the estuary (Fig. 2).

Studies of the formation of thermohaline water structure at different phases of the hydrological regime allowed obtaining a number of typical features characteristic of this type of estuaries.

By using the cluster analysis method, the features of the distribution of water masses forming the water ecosystem of the mixing zone were found on the basis of the Yenisey estuary /3/.

It was found, in particular, that except for the spring flood there are three zones with water masses differing in hydrophysical and hydrochemical indicators (Fig. 3) in the estuaries with open water exchange, including a zone of river water, a zone of sea water and a zone of mixed water, subdivided into subtypes depending on the prevalence of some properties or other (II-IV in Fig. 3).

On the basis of the cluster analysis it was confirmed that the thermohaline characteristics in which water salinity is most important are the governing ones for identification of sea water in the Arctic estuaries and chemical characteristics govern only the sub-type of water masses in the mixing zone.

An analysis of the variability of the water thermohaline structure allowed one to determine typical temporal scales of the processes, producing the greatest influence on the formation of the estuary water structure depending on the season of the year and river runoff variations. It has also shown that except for the spring flood when the effect of river water is decisive over much of the estuary, the largest influence is

produced by the non-periodic factors expressed in the form of surges. At significant surges there is a radical modification in the water structure pattern with the change in the distance of the boundaries of sea water penetration to the river and outflow of river water to the sea. Simultaneously, there is a change in the conditions of mixing of river and sea water with properties becoming equal with depth and the increase in the gradients of properties by the length of the estuary (Fig. 4). The reconstruction of the main typical properties in the distribution of water masses is, as a rule, observed during the next 2-3 days after the end of the phenomenon.

The effect of tidal phenomena in the river estuaries of the Kara Sea Basin is much smaller. It is expressed in the development of internal waves induced by them in the

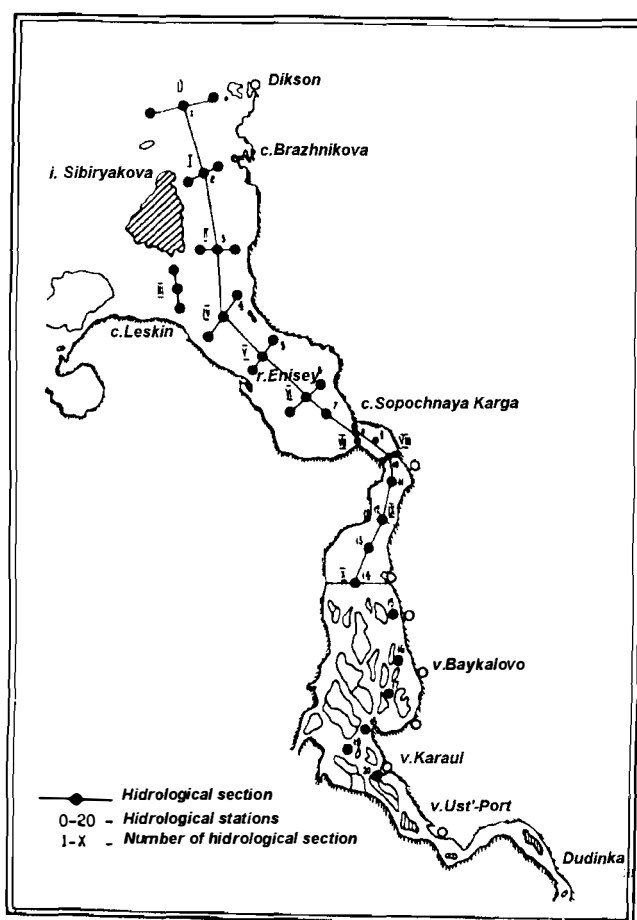


Fig. 1. A diagram of the hydrological polygon in the Yenisey estuary.

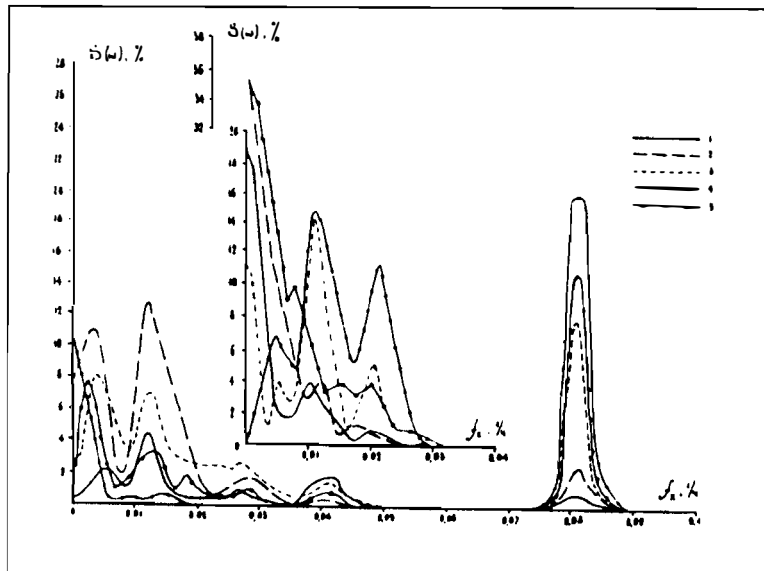


Fig. 2. Spectral densities of current speeds: a - total, 6 - remaining (from observations of 1974). 1 - a section in the near-delta region (Lipatnikovo) 2 - a section at the delta head (Ust'Port) 3 - a section near the sea margin of the delta (Baykalovo) 4 - a section at the head of the Yenisey Bay (Sopochnaya Karga) 5 - a section near the sea boundary of the mouth area (Brazhnikovo).

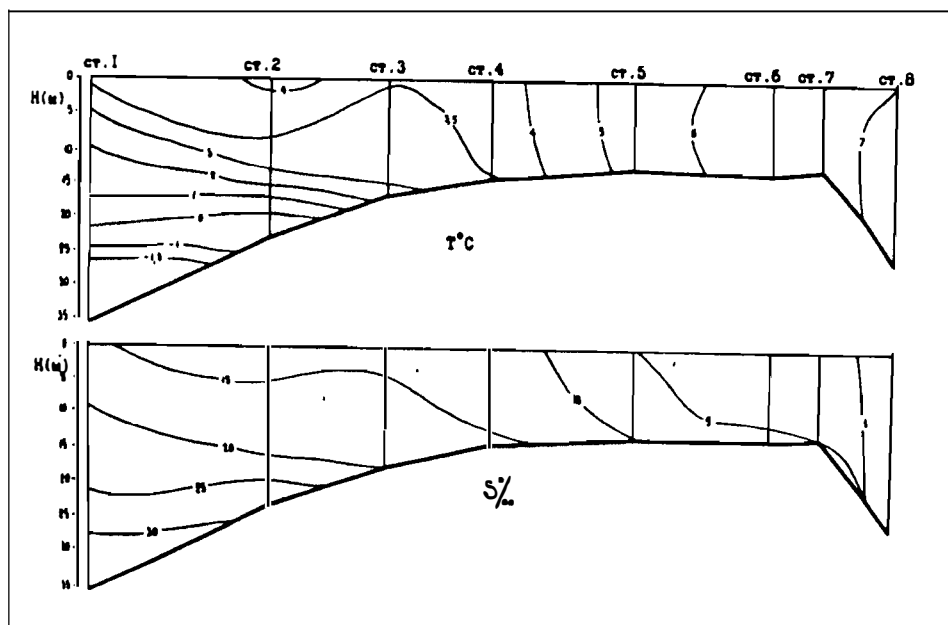


Fig. 3. T-S distribution at intensive wind mixing from data of the survey of September 10-14, 1982.

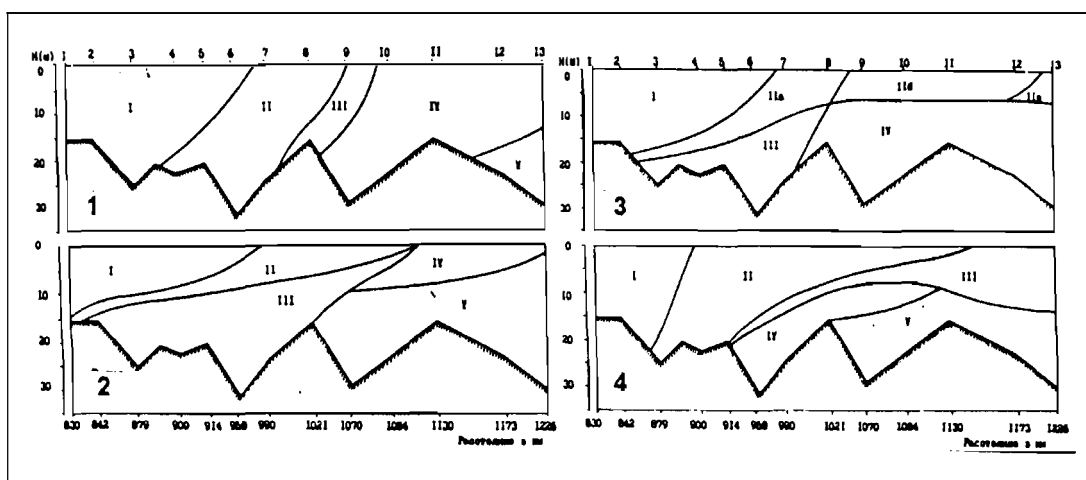


Fig. 4. Distribution of water masses of the Yenisey estuary on the basis of the clusteranalysis of hydrological surveys performed during the period: 1 - September 10-14, 1982 2 - from March 22 to April 4, 1983 3 - from July 29 to August 13, 1982. 4 - September 21-28, 1983.

zone of river and sea water division governing periodical variations in water temperature and salinity supporting the processes of mixing and transfer of water masses due to large vertical and horizontal shifts of water particles.

To conclude, it should be mentioned that the observed features of the formation of water dynamics and structure permitted one to specify for this type of estuaries the limit boundaries of sea water penetrating the river and of reverse currents of different origin, features of river water spreading in the sea and the regioning of the mouth areas of the Arctic rivers on the basis of these indications.

References

1. Grayevsky A.P., Kotrekhov Ye.P. Temporal variability of a rapid flow in the Yenisey mouth area. - Proc. of the AARI. - 1983. - vol. 378. - pp.39-50.
2. Grayevsky A.P. Water dynamics of the Yenisey mouth area under conditions of the regulated runoff. - Water resources. -1987. - No.6. - pp.159-163.
3. Ivanov V.V., Kirpichenok T.Ye., Grayevsky A.P. Methods for a composite estimate of the water state in the river mouths on the basis of a cluster analysis of multifactor information. - water resources. - 1987. - No.4. pp.100-104.

RESULT OF COMPOSITE STUDIES OF THE PECHORA MOUTH AREA IN 1994

A.P. Grayevsky (State Enterprise "Large", V.V. Ivanov, V.S. Latyshev (SRC AARI), A.Ye. Antsulevich, N.V. Maksimovich, I.A. Stogov (SPbSU).

Composite expedition studies of the AARI under the program "Estuary-Pechora 94" financially supported by the Ministry for Science of the RF, allowed collecting vast full-scale data covering the present-day state of the hydrological, hydrochemical, hydrobiological regime and contamination of the estuary of the Pechora river. The region of the expedition studies, the location of the hydrological polygon and main observations are given in Fig. 1. Estimates of the variability in the estuary water dynamics have shown that during winter and summer-fall low water period the largest influence on the regime of currents in the gulf is produced by periodical (tidal) factors. Their contribution into the total dispersion of the variability in the speeds of currents reaches 65-90%. The data of calculations performed on the basis of long-term observations of currents from self-contained stations situated uniformly along the length of the gulf (Voinov (G.V.) are presented in Table 1. They sufficiently well confirm the dominating influence of the tides on the regime of currents in the estuary.

Table 1

Table 1. A ratio of the energy of tidal and nonperiodic variations of currents at stations (for level 5m) in the Pechora gulf

1	Total dispersion	Tide
dispersion		
st.	cm^2 / s^2	cm^2 / s^2
% of the total		
2	1110 / 2209	1076 / 1891
96.9 / 85.6		
3	817 / 1139	662 / 964
80.9 / 84.6		
4	2138 / 424	1647 / 236
77.0 / 55.8		

*numerator - meridional current constituent
denominator - longitudinal current constituent*

Non-periodic (surge) phenomena cause a short-term modification in the pattern of the field of speeds and formation of uniaxial currents which govern transports of considerable water masses. The contribution of the runoff constituent sharply decreases on the segment from the sea edge of the delta to the outer boundary of the river bar and its effect on the current regime in the Gulf is less by an order of magnitude than that of other factors. A sharp decrease in the runoff speeds at the exit to the Pechora Gulf reduces the transport capability and governs sedimentation of suspended sediments. This is clearly manifested by water becoming more light and by increased transparency.

A characteristic feature of the thermohaline structure of the mixing zone water in the Pechora Gulf is a comparative thermal water uniformity at significant vertical and horizontal salinity gradients. Under the conditions of intensive storm events in 1994, the properties were observed to become equal with depth with a dramatic sharpening of horizontal gradients that govern the frontal development of the mixing processes (Fig. 2a and b).

One of the peculiarities of the hydrochemical regime was the presence of large changes in the water state parameters (SiO_3 , PO_4 , NO_2 , pH, Alk, O_2). They were confined to local areas in the estuary and consistent with the transition zones of different water masses delineated by thermohaline characteristics (river water zone, mixed water zone and sea water zone). (Fig. 2). Local sources of a sharp change in the levels of some hydrochemical elements, found within the mixed water zone and at its boundary, allow an additional regioning of the mixed water zone into sub-types. The variability of the water state parameters is governed to a great extent by the change in the conditions of life activity of phytoplankton which depend on water temperature and salinity and are related to an input of a large amount of dead organic matter into water. The processes of organic substance destruction and chemical processes thus governed, form the distribution pattern of hydrochemical elements in the estuary and adjacent regions and agree quite well with the zones in the Pechora estuary delineated by hydrophysical and hydrobiological indications.

Studies of the species type, abundance and distribution of plankton and bottom organisms have demonstrated a spatial division of the estuary into three different and quite stable zones - fresh, brakish and sea waters, being characterized by inherent biota. A zone with brakish intermediate water has depleted fauna, also including a number of typically mesohaline elements not inhabiting the other adjacent zones (Fig. 3).

The boundaries between the faunistic zones can be delineated quite accurately. Their position does not in general depend on currents, tides, hydrometeorological situations and seasons that were studied. In other words, there are three different but related water bodies confined in one.

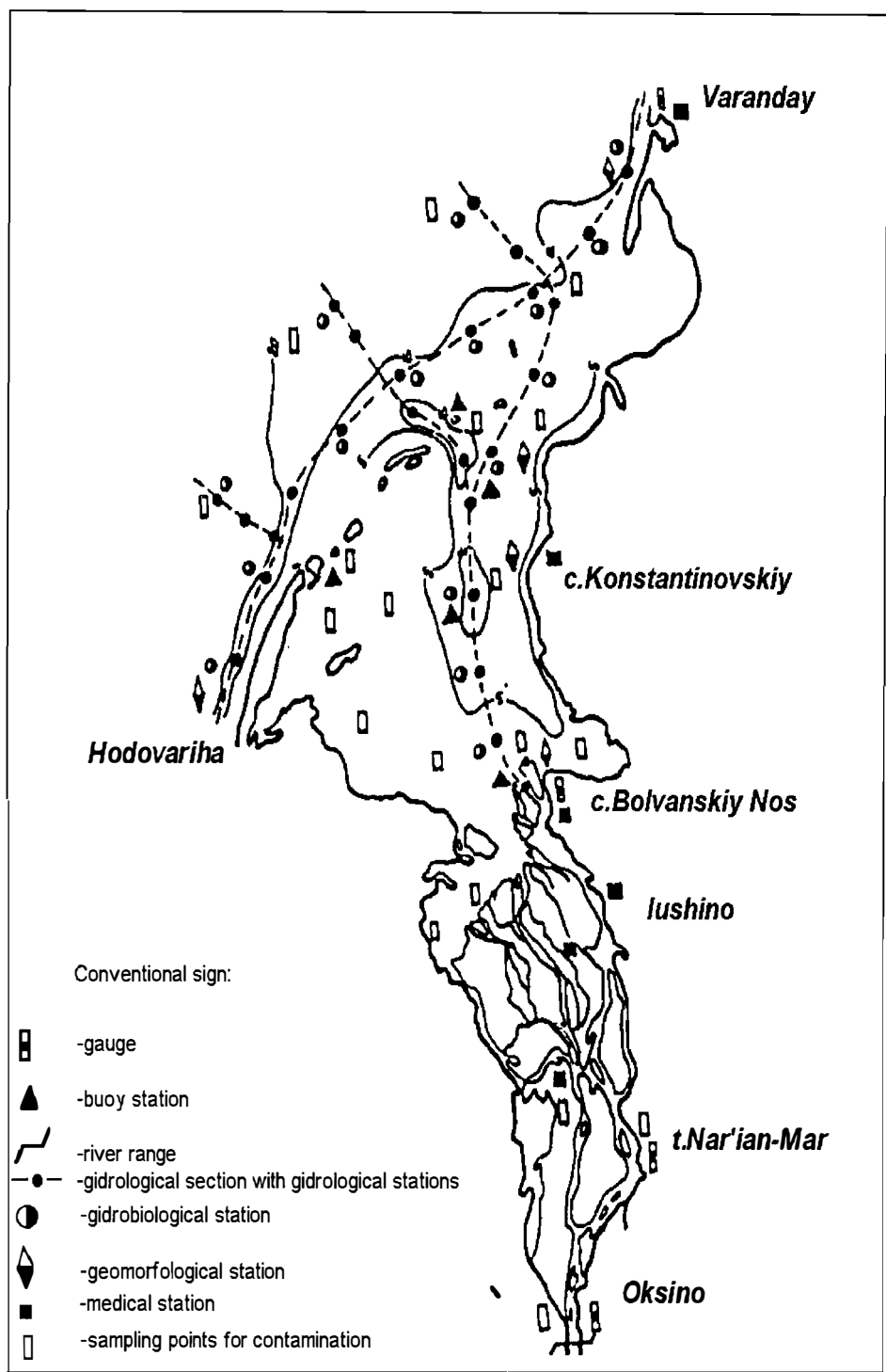


Fig.1 The region of research and types of observation of multi-purpose expedition "Estuary-Pechora 94"

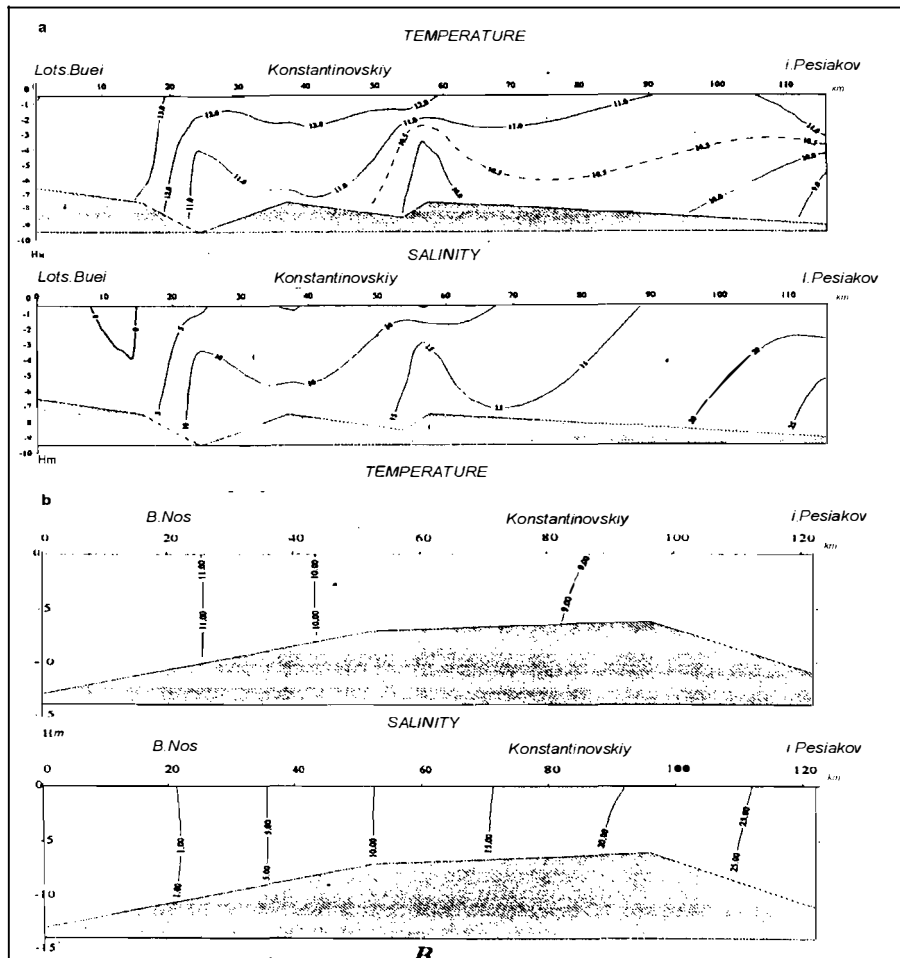


Fig. 2. Water temperature and salinity distribution on a longitudinal transect of the Pechora Gulf from the materials of the survey: a - July 22-25, 1994 (quiet weather), b - August 25-26, 1994 (after a storm).

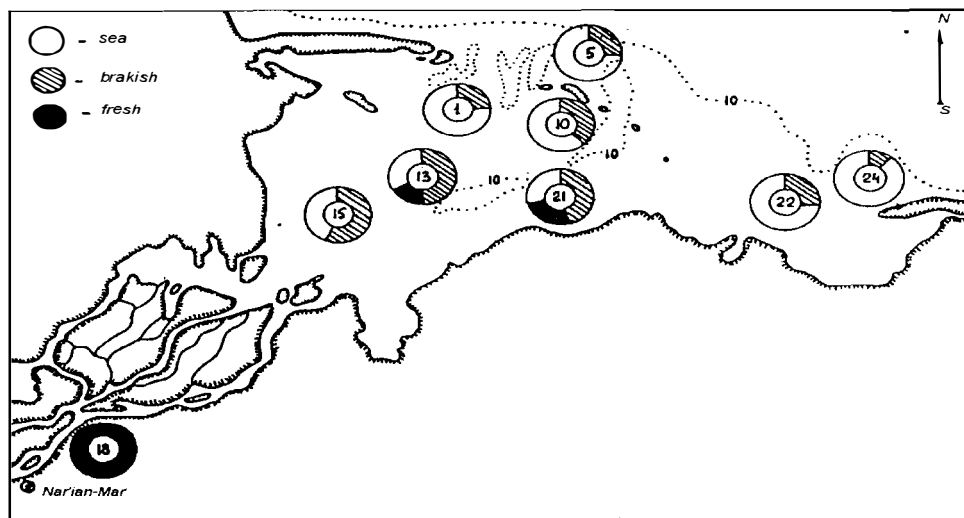


Fig. 3. A ratio of sea, brackish and fresh water forms of zooplankton at the stations of the Pechora Gulf in August 1994.

METHODS AND RESULTS OF MODELING HYDROLOGICAL PROCESSES IN STRATIFIED ARCTIC ESTUARIES

Doronin Yu. P. (RSHI) Ivanov V.V. (SRC the AARI)

One of the priority objectives related to the rational use and protection of the Arctic estuaries is to study hydrological processes in the zone of river/sea water interaction /7/. This governs the need for developing mathematical models which allow the description of the seasonal variability in the hydrological characteristics of the estuary for several years. As a result of joint studies of the AARI and RSHMI, along with earlier used balance, box and one-dimensional hydrodynamic models, three types of models were developed and tested in practice: profile by vertical, two-layered plane and a three-dimensional models.

The two-dimensional profile models which describe the hydrological processes in the Arctic estuaries with different detailing, are widespread /1-3, 5, 9/. The most complete variant of the two-dimensional profile model includes a non-stationary linear motion equation, as well as the equations of hydrostatics, continuity, state, heat and salt diffusion, turbulence energy balance, ice growth and melting /1, 3/. This model simulates annual variations of water temperature, salinity, longitudinal and vertical current speed components and ice thickness averaged over the width of the estuary. In addition to bathymetric data, the model required prescribing the annual distribution of the river runoff, water temperature at the sea and river boundaries, salinity at the sea boundary and meteorological characteristics. By means of this model, annual variations of hydrological and ice characteristics were calculated for the Ob' Gulf (Fig. 1 and 2), the Yenisey Gulf and the mouths of Kolyma and Yana river mouths. The results of modeling have shown the model to simulate the main features of the spatial distribution and temporal variability of the calculated characteristics. This model can be most successful for calculating the annual variability of the distance of penetration of sea water to the estuary. When calculating the characteristics for which the longitudinal distribution is not as decisive as for temperature, there are difficulties in interpreting the calculated results which govern the characteristics averaged over the estuary width and their comparison with observation data.

For investigating the spatial variability of the halocline characteristics not only along the estuary, but also along its width and in the near mouth sea area, a plane two-layered model was constructed /4, 5, 9/. The model considers the upper desalinated layer and the lower layer of near bottom sea water. The model describes the spreading distance of the near-bottom layer along the estuary, the spatial thickness and salinity distribution in the upper and lower layers, as well as their seasonal variability connected with the distribution of the river runoff within a year. The initial system of model equations includes the non-stationary linear motion equations averaged by the layer thickness taking into account the Coriolis forces,

friction at the upper and lower boundaries of the layers, baroclinic and barotropic components of the pressure gradient. Also, the equations of hydrostatics, continuity, salt transfer and the equation of state are used. The model was tested by the example of the Ob' Gulf including the near mouth sea zone to the calculation area. As shown by test results, the model simulated most successfully the main features of the calculated characteristics during the period of the maximum values of the river runoff at which there is a sharp and a sufficiently narrow boundary in the salinity between the layers. In winter with the decreased river runoff this boundary is dispersed and the differences in the salinity of the layers diminish which makes difficult application of the model.

For eliminating these difficulties, a three-dimensional model was developed. It allows us to calculate evolution of the three-dimensional fields of salinity, temperature, currents, concentration and the ice drift rate for the arctic estuary within a year [5, 6, 10]. The initial system of model equations includes the stationary linear motion equations taking into account the Coriolis force and the vertical friction coefficient, the hydrostatics, state, heat and salt transfer equations, as well as the equations for calculating the enumerated ice characteristics. This model was used for calculating annual variations of hydrological and ice characteristics for the Ob'-Yenisey mouth region, including the Ob' Gulf, the Yenisey bay and the Ob'-Yenisey sea region (Fig. 3), as well as for the south-eastern Laptev Sea, including the Yana bay and the Buor-Khai inlet. In addition to the capabilities of the two first types of the models it was possible by using a three-dimensional model to more fully simulate the ice state taking into account the influence of the river heat sink on the formation of ice melt sources and drift changes due to occurrence of open water areas.

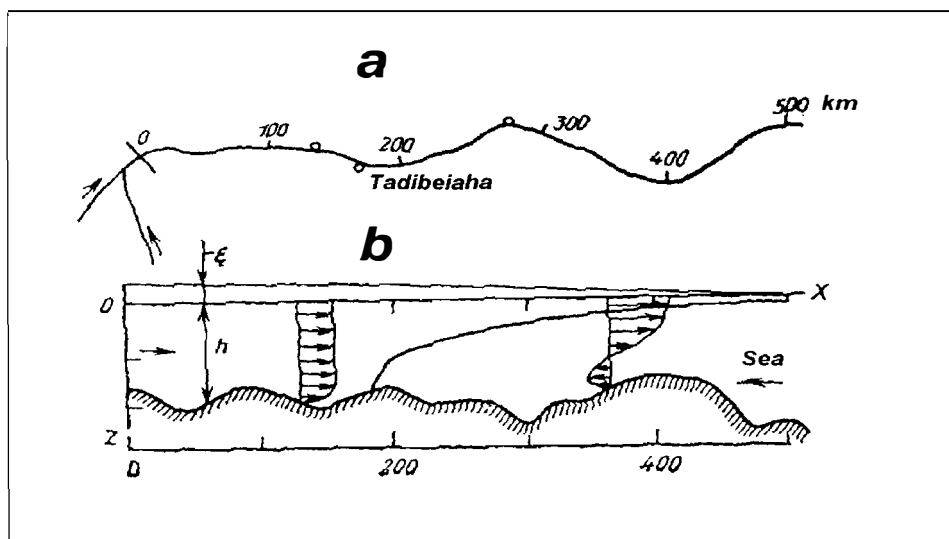


Fig. 1. A scheme of the Northern Ob' Gulf (a) and the longitudinal profile of the calculation area (b).

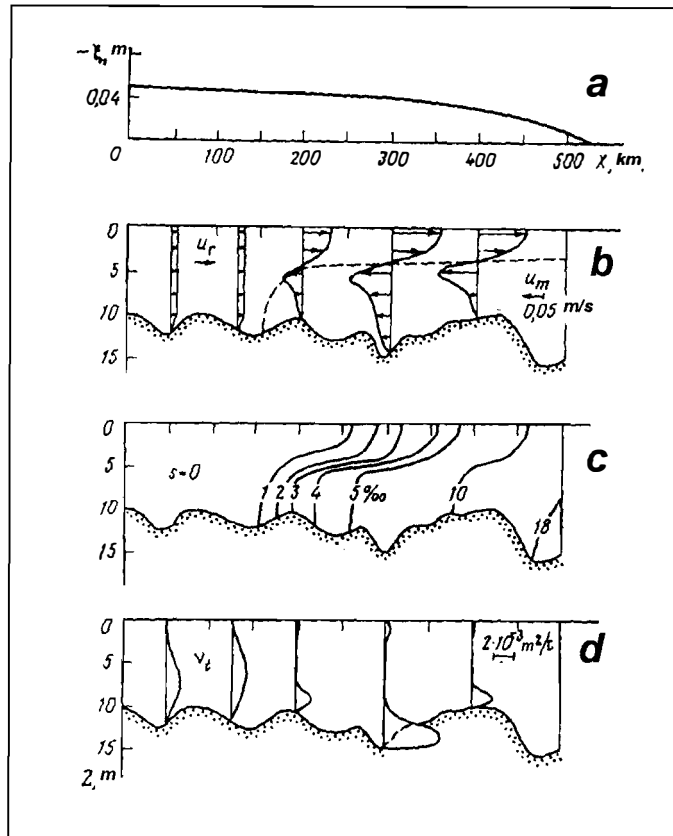


Fig. 2. Calculated vertical profiles in the northern Ob' Gulf for the conditions of April 1972. a) - the free surface of the flow ξ ; b) - the horizontal current speed component u m/s; c) - the salinity s (‰) ; d) - the turbulent viscosity coefficient ν_t m^2/s .

The fields of water temperature and salinity are modelled in more detail. Due to the natural dependence of modeling results on open boundary conditions, it is advisable to use a three-dimensional model as a specific model for a more extensive area where the influence of a free boundary is less pronounced.

The complication of the models from the first to the third type is accompanied by the requirement to increase initial and current information. That is why the choice of the model type strongly depends not only on the problem set, but also on the volume and reliability of available hydrometeorological data.

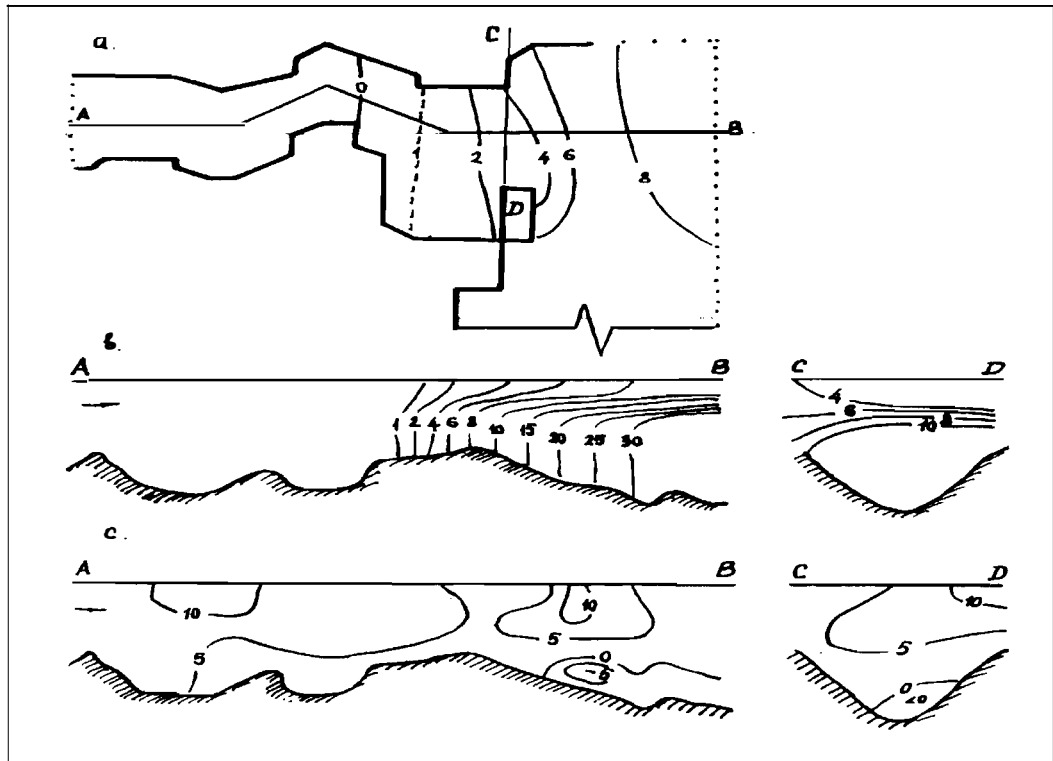


Fig. 3. The distribution of the calculated hydrological characteristics in the northern Ob' Gulf for September 1, 1972 a) - water salinity (‰) at the surface, b) - water salinity(‰) at the sections AB and CD, c) - the longitudinal current speed component (cm/s) at the AB and CD sections (the positive direction - towards the sea) . .

References

1. Doronin Yu.P. Modeling of vertical structure of the mouth area of the river with a sea halocline, 1992, No.8, pp.76-83.
2. Doronin Yu.P. Processes of sea/river water interaction in the near-mouth sea areas (physical grounds and numerical modeling) - Proc. of the 5th All-Union Hydrological Congress, vol.9, River mouths. L., Gidrometeoizdat, 1990, pp.122-129.
3. Doronin Yu.P., Ivanov V.V., Svyatsky A.Z. Mathematical modeling of river/sea water interaction processes in the mouth of rivers in the Arctic zone. - Proc. of the 5th All-Union Hydrological Congress, vol.9 (River mouths). L., Gidrometeoizdat, 1990.
4. Doronin Yu.P., Lukyanov S.V. Mathematical modeling of sea/river water interaction in the near-mouth sea area by means of a two-layer model. - Meteorology and Hydrology, 1944, No.10, pp.70-77.
5. Doronin Yu.P., Lukyanov S.V., Tsarev V.A. Mathematical models of the hydrology of the estuary and the near-mouth sea areas. - Proc. of the RSHMI, 1994, pp.15-31.
6. Doronin Yu.P., Tsarev V.A. Mathematical modeling of the Arctic shelf hydrology for estimating anthropogenic impacts. - Proc. of the 1 International conference "Exploration of the shelf of Russia", RAO 93, pp.330-337.

7. Ivanov V.V. Main results and the immediate objectives of studies of the lower reaches and mouth areas of the Arctic rivers./ Problems of the Arctic and the Antarctic, 1978, No.54, pp.52-53.
8. Ivanov V.V., Svyatsky A.Z. Numerical modeling of sea water intrusion to the river mouths at a seasonal time scale. - Water Resources, 1987, No.5, pp.116-122.
9. Lukyanov S.V. A two-layer model of water circulation in the near-mouth sea area. - Modeling and experimental studies of the hydrology of the shelf seas: Proc. of LHMI, No.10, 1988, pp.148-158.
10. Doronin Yu.P., Ivanov V.V., Tsarev V.A. Ice cover simulation for the Arctic estuary./IAHR. Proceeding of the 10th International Symposium on Ice, Espoo, Finland, August 20-23, 1990, vol.4, pp.210-218.

INFLOW AND SPREADING OF RIVER WATER IN THE KARA SEA

V. V. Ivanov (RF SRC the AARI)

Freshwater of the continental runoff in spite of its insignificant value in the total volume of the Kara Sea water and significantly different physical-chemical properties, indirectly influences the motion pattern of the water masses by mixing with saline water. Even a comparatively small freshwater amount results in the formation of lighter desalinated water in the surface layer preventing deep sinking of the whole water mass of the supercooled surface layer /1,7/.

The main mass of river water flows to the Kara Sea from the basins of large rivers Ob', Yenisey, as well as Pyasina and N.Taimyra and forms, as a rule, one area of freshened surface water which reaches the largest value at the end of August or in September, depending on the water capacity of the year. The form of the area of spreading is governed by the hydrometeorological conditions in the sea.

Along with river waters, dissolved and suspended pollutants flow to the sea and spread there. Hence for estimating the levels and the extent of pollution spreading in the sea, not only the concentration of pollutants, but the volume of the river water inflow to the sea, as well as areas of their spreading should be known.

The mean annual inflow to the Kara Sea is 1350 cu.km which is equivalent to a layer of 152 cm relative to the total sea area being the largest among other seas. This is primarily related to the vast area of the watershed sea basin equal, to 6039.1 thousands of sq.km, and to the ratio of this area to that of the sea (885.2 thousands of sq.km). For the Kara Sea this ratio is 6.82, whereas for the Arctic Seas on the whole it is 2.8, for the Arctic Ocean Basin - 1.53 and for the World Ocean - 0.33 /6/.

First estimates of the total inflow of river water to the Kara Sea were made in 1957 /2/. They were obtained from processing the measured water discharges at downstream measuring gauges of large rivers for the period 1936-1950 and by using a chart of mean annual runoff for the non-studied watershed zones. After 1957, similar estimates were made repeatedly and they differed in the period of processing the measured discharges and in the use of different charts of mean annual runoff. The last most complete estimate was given in the work with a processing period up to 1970 /5,6/.

Materials on the runoff of large rivers of the Kara Sea Basin accumulated for the last years, as well as the methods developed for indirect estimates of the river runoff from the non-studied territories allow more reliable and detailed evidence on the volumes of incoming freshwater to the sea to be obtained. This is important both for the ecological and the climatic studies of the Kara Sea Basin.

The total mean annual river water inflow to the Kara Sea was calculated on the basis of runoff data at the downstream hydrometric

gauges of the 7 largest rivers Ob', Nadym, Pur, Taz, Yenisey, Pyasina and N.Taimyra (Fig. 1) /4/. For the regions located below the downstream measuring gauges, as well as for interfluves of large rivers and islands where hydrometric observational data are actually absent, the river water inflow was estimated using a map of the mean annual Arctic outflow /3/. The resulting data for separate rivers and the Kara Sea are presented in Table 1. As follows from the table, the inflow of river water to the Kara Sea from the basins of Ob' and Yenisey constitutes 85.8% and taking into account the water inflow from Pyasina and N.Taimyra - 94.2% of the total inflow to the sea.

Tabl.1

Table 1 Mean annual river water inflow to the Kara Sea

River	Watershed area of the river		Mean annual inflow to the sea			Multi year-variability Cv	Down stream gauge			Location of the halo	
	sq.km	% of the watershed of the sea	sq.km	mm (sea layer)	% of the inflow of the sea		Location	Distance to the exit to the sea, km	Area observations %	winter	summer
Ob'(with Nadym, Pur and Taz)	2945000	48.2	540	610	40.0	0.14	Salekhard	1097	91.2	north. Ob' Gulf (Trekhubornyy Cape)	north. Ob' Gulf (Pavlov Cape)
Yenisey	2590000	42.4	618	698	45.8	0.07	Igarka	1226	94.2	delta	Yenisey bay
Pyasina	182000	3.0	77.6	88	5.8	0.16	Ust'-Tareya	271	72.4	delta	Pyasina bay
Taimyra	124000	2.0	35.2	40	2.6	-	Zeleny Yary	106	80.6	river	Taimyra gulf
Small rivers of the interfluves and islands	198000	4.4	79.2	124	5.8	-	-	-	-	-	-
On the whole for the Kara Sea Basin	6110000	100	1350	1525	100	0.08	-	-	-	-	-

The area of the Kara Sea is 885.2 thousand sq.km

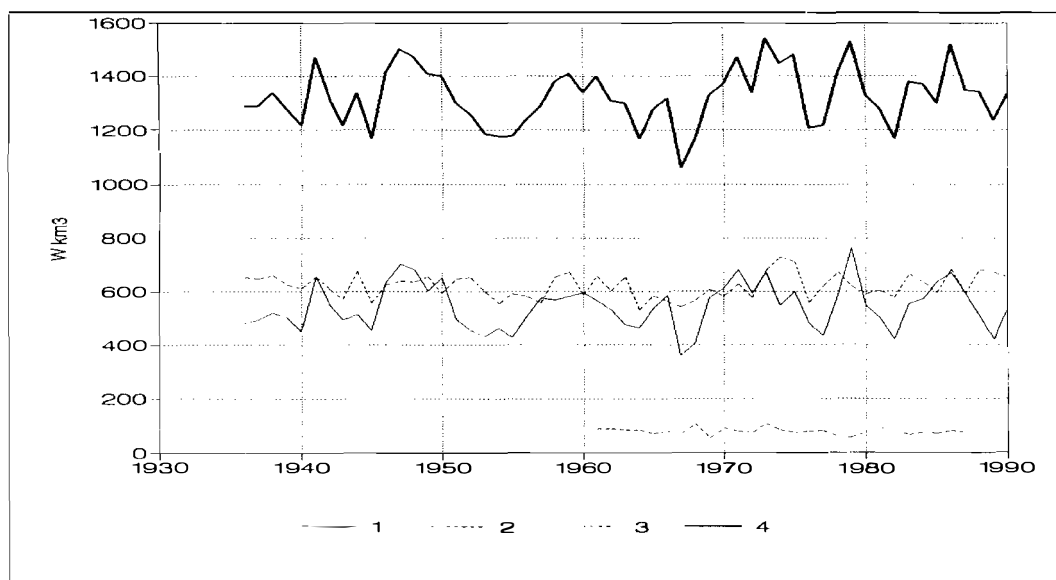


Fig. 1. Multiyear variations of the river water inflow in the Kara Sea 1 - Ob'; 2 - Pur; 3 - Yenisey; 4 - Pyasina; 5 - total.

Mean multiyear variability of the total river water inflow to the Kara Sea is given in Fig. 2. As is apparent, there is absent any significant relationship in multiyear variations of the total river water inflow from the Ob' and Yenisey to the Kara Sea, since the watersheds are situated in different climatic regions. The variation coefficients for separate rivers vary from 0.07 (Yenisey) to 0.18 (Nadym) at a general variation coefficient for the Kara Sea being 0.08. An exceptionally small variation coefficient for Yenisey is also explained by the fact that the watersheds of Yenisey and its largest tributaries Angara, Podkamennaya and Nizhnyaya Tunguska are in different climatic regions.

To delineate the areas of desalinated water spreading in the Kara Sea, both thermohaline and hydrochemical characteristics were used. Generalization of data of hydrochemical observations performed from 1930 to 1948 allowed Smirnov /11/ to outline the boundaries of the maximum water freshening in the surface layers of the Kara Sea.

During the same period Antonov /1/, by using thermochemical characteristics, not only defined the areas of spreading of continental waters in the Kara Sea, but also established the main types of their spreading. The author indicated that by salinity and alkalinity only the maximum spreading of freshened water in the sea in the summertime can be determined, irrespective of the sources of freshening.

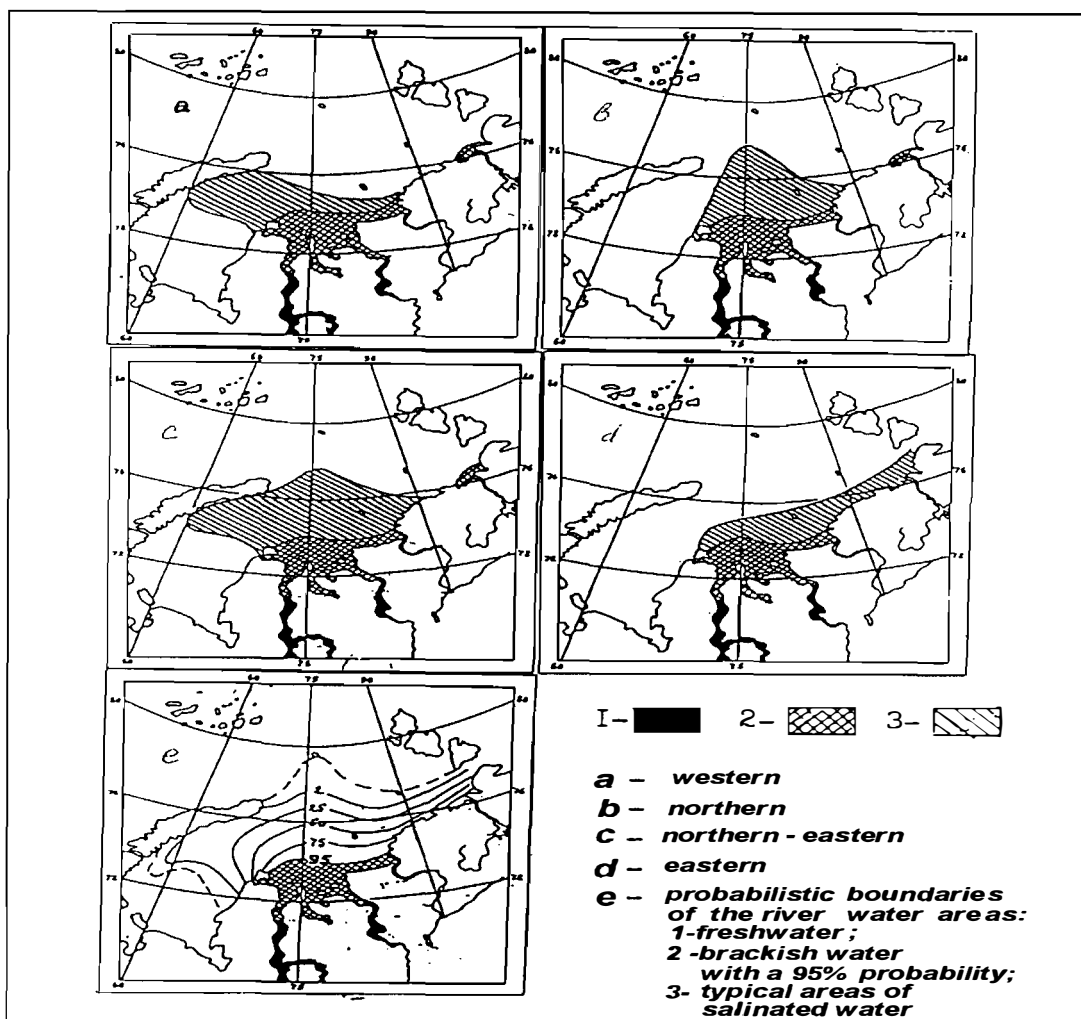


Fig. 2. Types of areas of river water spreading in the Kara Sea (a, b, c,d) and the probable distribution of their boundaries over a multiyear period in the summertime (e)

It should be remembered that in addition to river waters, the inflow of freshwater to the sea occurs due to ice melting and atmospheric precipitation (to be more exact, the precipitation excess over evaporation). However, while these sources are observed over the entire sea area, the freshening due to the river runoff is clearly evident in the region of the fall of large rivers.

As shown by further studies, the dissolved silicon appears to be a more conservative characteristic for identifying areas of river waters in the Arctic Seas. Waters of the large Siberian rivers serve as its main source (3000-5000 $\mu\text{g/l}$), whereas the level of silicon in sea water is an order of magnitude smaller and is less than 250 $\mu\text{g/l}$ [12].

In view of the accuracy of the analytical methods of silicon determination in sea water, the isoline with a silicon level of 500 $\mu\text{g/l}$ can be assumed to be the boundary of river water area. In this case the zone between isolines of 250 and 500 $\mu\text{g/l}$ should be considered the area of complete river water transformation to sea water. The boundaries of the areas of freshened waters identified by means of the alkaline-salinity

coefficient and equal to 700 and isooxygen of a 100% saturation, are between the isolines of silicon levels of 250 and 500 ug/l. The comparison of the areas of freshened waters in the Kara Sea for the period from 1965 to 1977 based on thermohaline and hydrochemical characteristics has shown the general pattern to be preserved. This allows data for the past years to be used for identification of the areas and their typification /10/.

The results of the generalization of data on silicon solubility in surface water of the Kara Sea for the summer period 1965-1990 have mainly confirmed the presence of three different types of river water spreading: western (1974), northern (1965) and eastern (1973) (Fig. 2a-2c). Simultaneously the presence of intermediary types related to the changed meteorological situation over the sea in the second half of the navigation period (September-October) was identified. The most well-pronounced intermediary type is characterized by the presence of two ridges - to the north and west (Fig.2d). In the first half of the summer season the area of river water was spreading northward and in the second - westward. Another case which disturbs the typical positions of the area of freshened water spreading in the second half of the navigation period is a partial or complete separation of the area of freshened water due to the latitudinal transports and a dramatic decrease in the river runoff in the pre-winter period.

An analysis of the annual charts of the areas of river water spreading in the Kara Sea for a multiyear period indicates the relationship between the type of river water spreading in the sea and the character of the air mass transport over the sea. However, no reliable relations between the volume of the total river water inflow in the sea, type and extent of spreading of river water were found.

Fig. 2e presents a chart of the probabilistic boundaries of the river water areas in the Kara Sea in summer from 1965 to 1990 over the whole observation period. The chart shows the boundaries of the river water areas with a prescribed probability.

It follows that annually a considerable region of the Kara Sea area is subjected to a direct influence of river waters whose spreading in the sea in different years varies within a wide range. However, as a rule, the boundary of spreading of river water in the sea passes seaward of the adopted boundaries of the estuaries of Ob', Yenisey, Pyasina and N. Taimyra determined from hydrological-morphological indications. This allows a conclusion to be drawn that the Ob'-Yenisey region of the Kara Sea between the adopted boundaries of the estuaries of these rivers and the isolines of river water spreading with a 95% probability is simultaneously the mouth region of the Kara Sea and the estuary ecosystem which are strongly influenced by the inflow of river water and pollutants from the rivers.

It should be noted that currently available data on the distribution of the inflow of river water and pollutants to the Kara Sea within a year are based on the observation data at the downstream measuring gauges of large rivers located at a distance of several hundreds (Pyasina) up to 1

thousand kilometers and more (Ob', Yenisey) from the exit to the sea. The lag time of river waters and pollutants from the downstream gauges to the exit to the sea at different rivers and in different seasons varies significantly and changes from several 10-day periods to several months. Simultaneously, transformation and deposition of pollutants in these regions occur. Especially, these changes are pronounced in the Ob'-Taz mouth area. Hence it is incorrect to identify estimates of the inflow of water, sediments and pollutants at the sea boundary of the estuaries with estimates at the downstream river gauges.

Changes in the characteristics of sediments and pollutants along the length of the mouth area are non-uniform, significantly varying at a sharp change in the morphometric, hydrodynamic and thermohaline characteristics. Such regions include: internal deltas and river bars where main deposition of river sediments occurs and the hydrofront zone in the estuaries where different physical-chemical processes take place. The pattern of changes in the pollution characteristics is sharply complicated if the estuaries are formed by more than two large rivers or if there are large pollution sources at the local watershed of the estuary (for example, the Ob'-Taz Gulf).

The complexity of the processes of transfer, transformation and deposition of sediments and pollutants in the large mouth areas of rivers requires monitoring of fresh water inflow, sediments and pollutants not only at the downstream river gauges, but also along the longitudinal sections of the estuaries and further up to the boundary of the river water areas in the sea. It is necessary to organize observations of the water state by depth at the sea boundary of the estuaries with identification of the zones of direct and reverse flows. Taking into account that location of hydrofronts in the estuaries of large rivers shifts over several hundred kilometers during a year, monitoring of water dynamics and changes in the pollution characteristics in this zone, especially in the presence of ice phenomena by means of observations is expensive and not always possible /8, 9/. Hence for obtaining evidence on the character of transport and transfer of water masses along the length of the estuary and in the river water areas in the Kara Sea, full-scale data are desirable to combine with numerical modeling.

References

1. Antonov V.S. Distribution of river water in the Arctic Seas. - Proc. of the AARI, 1957, vol.208, No.2, pp.25-52.
2. Antonov V.S., Morozova V.Ya. The total continental runoff to the Arctic Seas. Proc. of the AARI, 1957, vol.208, pp.13-24.
3. Atlas of the Arctic. L., Izd. GUGK, 1985, 204 p. (sheet 97-98).
4. Annual data on the regime and water quality in the seas and marine river mouths, vol.4, p.2, the Kara Sea Basin 1978-1991.
5. Ivanov V.V. Mean annual surface outflow in the Arctic. - Proc. of the AARI, 1976, vol.323, pp.101-114.

6. Ivanov V.V. Freshwater balance of the Arctic Ocean, Proc. of the AARI, vol.323, L., 1976, pp.138-144.
7. Ivanov V.V., Nikiforov Ye.G. Methods for estimating possible changes in the hydrological regime of the Kara Sea as affected by interbasin river runoff removal. Proc. of the AARI, 1976, vol. 314, pp.176-182.
8. Ivanov V.V., Svyatsky A.Z. Numerical modelling of water intrusion to the river mouths at a seasonal time scale. Water resources, No.5, 1987, pp.116-121.
9. Ivanov V.V., Kirpichenok T.Ye., Grayevsky A.P. Methods for a comprehensive assessment of the water state in river mouths based on cluster analysis of multivariate information. Water resources, No.4, 1987, pp.100-104.
10. Ivanov V.V., Rusanov V.P., Gordin O.I., Osipova I.V. Interannual variability and spreading of river water to the Kara Sea. - Proc of the AARI, 1984, vol.368, pp.74-81.
11. Smirnov A.A. Penetration of river water to the Kara and Laptev Seas. - Proc. of the AARI, 1955, vol.72, No.2, pp.93-104.
12. Shpaikher A.O., Rusanov V.P. Silicon distribution as an indicator of water masses in the seas of the Siberian shelf. - "Problems of the Arctic and the Antarctic", 1972, No.40, pp.64-70.

WATER AND CHANNEL REGIME IN THE RIVER DELTAS

Vi.Vi.Ivanov, A.A. Piskun (SRC AARI)

Deltas of the rivers in the Kara Sea Basin (Fig. 1) are considered to be the important links in the system of natural mouth complexes. The possibilities for their rational use are closely connected with the hydrological regime whose important components are liquid runoff and solid discharge mutually governing the character of channel processes in the deltas under conditions of a complicated river/sea interaction.

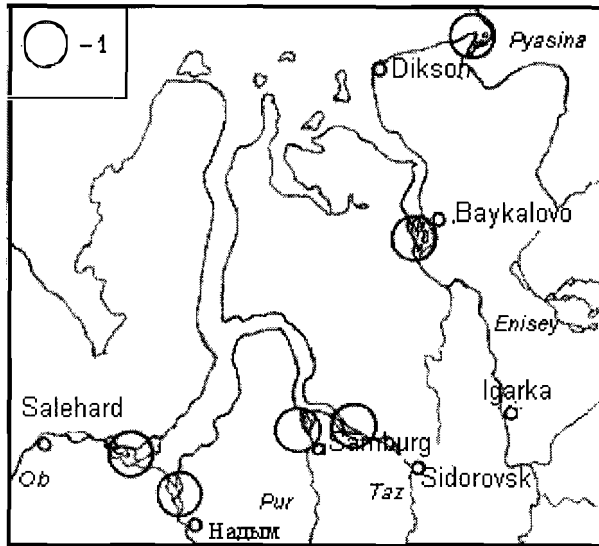


Fig. 1. A scheme of the location of deltas of the main rivers in the Kara Sea Basin. 1. river deltas.

An analysis of the level of knowledge of the water and channel regime in the river deltas of the Kara Sea Basin has shown that their studies were carried out by expeditions of the AARI and other institutions (Table 1), as well as by means of aerodynamic models (Table 2) and calculation methods /7-9, 14, 20, 24/. Most completely covered by full-scale observations (mainly during the period of the open channel) appear to be delta arms of Ob' /1, 3, 5, 13, 17, 21-24/ and Yenisey /4, 6, 11, 12/, however, data are not sufficient to plot reliable water discharge curves. Observations in the Nadym delta /17/ are mainly centered in the crossover zones since studies were made for providing favourable shipping conditions. In the Pur and Taz deltas /16,19/ the expedition measurements of water and sediment discharges cover most arms. However, a maximum number of measurements at one section does not exceed 8 on Pur and 4 on Taz and thus, these measurements should be considered as survey data. Aerodynamic modeling was performed for the Ob', Yenisey, Pyasina deltas and for separate zones of the Nadym, Pur and Taz deltas /2, 10, 15/. Numerical modeling of water dynamics was carried out for the Ob' delta 20/. Hydraulic calculations of the distribution of discharges and levels were performed for the Ob' Yenisey, Pur and Taz deltas /8, 9, 11/ and for the Ob' delta such calculations were conducted taking into account the channel regime /14/.

Table 1

Current state of the level of knowledge of water and channel regime in the deltas of rivers in the Kara Sea Basin based on the expedition data River delta Characteristics Ob', Nadym ,Pur , Taz , Yenisey ,Pyasina

Characteristic	River delta					
	Yenisey	Ob	Nadym	Pur	Taz	Pyasina
Total number of hydrometric sections	20	101	23	54	20	8
The largest number of water discharge measurements at one hydrometric section	17	12	8	4	17	46
Total number of measured discharges of sediments	95	+	47	>80	+	-
Number of samples for granulometric composition of sediments:						
-suspended	9	-	-	-	-	-
- bottom	57	+	>50	>60	+	+
The number of buoy stations	7	-	-	-	4	4
Number of temporary level stations	4	5	4	6	2	7
Connection with the gauge datum of stations with the state height network	no	yes	no	no	no	no
Years of studies	1935-39 1977-83	1971- 76	1969, 1970, 1982	197 0, 198 3	1973- 74, 1976,19 80 1982	1984-86

Note: "-" measurements were not made;

"+" measurements were made but their number was not determined.

Table 2

Main characteristics of aerodynamic models of the deltas of rivers in the Kara Sea Basin

Object	Year	Scale of the model		Range of discharges, m ³ /s	Number of the water regimes studied
		plane	vertical		
à) River deltas					
Ob	1963	1:200 00	1:500	11000	5
Pur	1971	1:350 0	1:150	1080- 3680	5
Taz	1972	1:350 0	1:125	1200- 5800	5
Yenisey	1966	1:150 00	1:500	17000- 55000	10
Pyasina	1988	1:800 0	1:200	2080- 8560	5
b) Mouth crossovers					
- in the near-delta zone:					
Yenisey	1962	1:500 0	1:500	16100- 59600	9
Nadym	1975	1:500 0	1:200	400-1450	3
- in the delta:					
Yenisey	1973	1:600 0	1:500	11550- 60000	5
Nadym	1977	1:250 0	1:250	400-1450	5

An assessment of the level of knowledge and generalization of the results of the preceding studies of the water and channel regime of the river deltas of the Kara Sea Basin performed in this study, will be used for planning and conducting further studies of natural environmental elements in the region.

References

1. Antonov V.S., Maslayeva N.G. The Ob' river lower reaches and mouth (a hydrological and navigation overview), L., Gidrometeoizdat, 1965. -82 p.

2. Antonov V.S., Gilyarov N.P., Ivanov V.V. Experimental studies of the water regime of the Ob' river delta. // Problems of the Arctic and the Antarctic. - 1965, No.20, pp.23-30.
3. Gilyarov N.P., Ivanov V.V. Results of laboratory studies of the water regime of the mouth zones of large rivers. Proc.of the Fourth Hydrological Congress, vol. V, L., Gidrometeoizdat, 1975, pp.381-387.
4. Grayevsky A.P., Kotrekhov Ye.P., Matveyev A.A., Yefimtsev A.V. Results of studies of currents in the mouth zone of Yenisey in the summer-autumn season.//Proc. of the AARI, 1980, vol.358, pp.55-74.
5. Zhizhanov A.V. Results of the expedition hydrological studies of the Ob' mouth area in 1977-1979.//Proc. of the AARI, 1980, vol.394, pp.51-62.
6. Zayets G.M., Miloshevich V.A., Mikhinov A.Ye., Sidorchuk A.Yu. Distribution of water runoff and suspended sediments in the Yenisey river delta. // In: Methods of estimating the influence of the removal of runoff on the hydrometeorological regime of the northern regions. VINITI Dep., No.4489-82, M., 1982.- pp.125-137.
7. Ivanov V.V. On the temporal variability of runoff and levels in the deltas of rivers in the Arctic. - //Proc. of the AARI, 1970, vol.290, pp.6-17.
8. Ivanov V.V. A method for hydraulic calculations of the water regime elements in river deltas. //Proc. of the AARI, 1968, vol.283, pp.30-63.
9. Ivanov V.V., Vinogradova T.V., Ivanova A.A., Makeyev V.M., Piskun A.A., Yankina V.A. Possible changes in hydrological conditions in the mouth areas of rivers under the influence of water use activities. //Proc. of the Vth All-Union Hydrological Congress, vol.4, L., Gidrometeoizdat, 1990, pp.370-377.
10. Ivanov V.V., Gilyarov N.P. Experimental studies of the runoff redistribution in the Yenisey delta. //Proc. of the AARI, 1972, vol.297, pp.103-115.
11. Ivanov V.V., Grayevsky A.P., Piskun A.A. An assessment of the distribution and possible redistribution of runoff in the branches of the Yenisey delta.//Problems of the Arctic and the Antarctic, 1984, No. 58, pp.15-25.
12. Ivanov V.V., Kotrekhov Ye.P. An assessment of the river runoff influence on the regime of levels of the mouth zone of Yenisey.//Proc. of the AARI, 1976, vol.314, pp.120-151.
13. Ivanov V.V., Makeyev V.M. The role of long-term ocean level oscillations and vertical motions of the earth's crust in the development of the mouth areas of rivers in the Arctic zone.// Water resources, 1987, No.4, pp.123-128.
14. Ivanov V.V., Mikhalev M.A., Marchenko A.S., Piskun A.A., Chernin K.Ye. The hydraulic method for calculating water and channel regime in multibranch river channels. //Proc. of the AARI, 1984, vol.378, pp.5-22.
15. Ivanov V.V., Piskun A.A., Gilyarov N.P. Experimental studies of runoff redistribution in the deltas of Pur and Taz rivers for river shipping. //Proc. of the AARI, 1980, vol.358, pp.75-92.
16. Korotayev V.N., Chalov R.S. Modern processes of delta formation in the mouth area of Pur and Taz rivers. //Proc. of the AARI, 1976, vol.314, pp.162-175.
17. Levashov A.A. Features of channel processes at rivers of the zone with deep freezing of ground. Authors's thesis of the candidate of Geographical Science, L., 1976.

18. Makeyev V.M., Bol'shiyanov D.Yu., medkova O.N., Savin V.B., Fedorov B.G. Features of the morphology of the valley of the mouth zone of Ob' and the formation history of the modern delta. In: Geographical and glaciological studies in polar countries. L., Gidrometeoizdat, 1987, pp.125-136.
19. Makkaveyev N.I., Korotayev V.N., Chalov R.S. Results of studies of channel processes in the mouths of rivers Pur, Taz, Yana and Indigirka.// Problems of the Arctic and the Antarctic, 1980, No.55. - pp.54-60.
20. Piskun A.A. Numerical modeling of water dynamics in the Ob' delta at surges.// Water resources, 1987, No.5, pp.129-135.
21. Razumikhina K.V. Methodological aspects of estimating the discharge of sediments in the river delta (by the example of Ob').// Vestnik Len.universiteta, 1983, No.24, Geology. Geography, iss.4, pp.61-72.
22. Razumikhina K.V. Current regime of the discharge of sediments in the mouth area of the Ob' river.// Vestnik Len.universiteta, 1984, No.24, pp.65-73.
23. Savin V.B. Features of channel deformations under conditions of permafrost (by the example of the Ob' river).// Abstracts of the Fifth All-Union Hydrological Congress. Subsection: River mouths. Leningrad, October 20-24, 1986. pp.30-31.
24. Smirnova Z.S. Hydrological and morphometric characteristics of the main branches of the Ob' river delta.//Proc. of the AARI, 1970, vol.290, pp.145-157.

FEATURES OF NON-PERIODIC WATER LEVEL OSCILLATIONS IN THE MOUTH AREAS OF OB' AND YENISEY

Ivanova A.A. (AARI)

Water level oscillations of a synoptic temporal scale were studied at the sections of the four shallow water zones in the mouth areas of Ob' and Yenisey. One bar zone was situated in the south of the Ob' Gulf, three bars and crossovers in the Yenisey mouth area (a bar in the south of the bay, two crossovers - the first in the delta near the Baikalovo settlement and the second in the near-delta zone of the river near the Lipatnikovo settlement). Similar observations were earlier conducted in separate zones /1-5/. With accumulation of initial information it became necessary to improve the existing methods for short-range level forecasting for all zones of the mouth areas of Ob' and Yenisey which limit shipping. Hence a combined statistical analysis of the characteristics influencing the process of water level changes for the mouth areas of the rivers with the largest bays was performed.

Water level observations at the Yamsale bar of the Ob' Gulf were conducted during the summer-autumn navigation periods and in the Yenisey mouth area all-year-round. The observation series in all study zones are of different duration. Observation data of water levels at bars and crossovers during the synchronous periods were analyzed along with water levels at the sea and river boundaries of the river mouth areas and wind characteristics over the bays. For the navigation periods during the years with large, small and average water content of Ob' and Yenisey, the regression equations were calculated. In winter they were calculated for each month for a number of years, since the ice thickness increases gradually from month-to-month and appreciably influences the water level oscillations.

By using the stepwise regression methods, it was estimated how the water levels of bars and crossovers were affected by the tangential wind stress projections to the general direction of the flows at the representative sections of bays, as well as water levels at the sea and river boundaries of the mouth areas taking into account the lag time /6/. Unlike the previous studies, the predictors were taken in the form used in a one-dimensional hydrodynamic model /7, 8/. By means of this model it is possible to solve the problems of the motion of long waves in such large, remote and non-uniformly studied regions as the mouth areas of Ob' and Yenisey without dividing them into fragments /9-12/. The extent of the influence of the predictors on water level variations differs both in respect of each of these two bodies and separate zones in them, the water content of the navigation periods, the absence and the presence of the ice cover and ice thicknesses in the dynamics of their increase by months. The stepwise regression analysis allows quantitative estimates of the influence of the river and sea levels and wind characteristics on the water level oscillations in the summer and winter navigation periods.

An analysis of the weight coefficients of the equations allows the following suggestions:

1. In all study zones the local winds over the areas of estuaries of the Ob' and Yenisey have a significant influence. The regression coefficients reach the values of 0.30-0.60.

2. In the estuary and in the delta of the Yenisey river the influence of sea level oscillations is most large (the regression coefficients vary from 0.35 to 0.85 at the bars). At the second crossover this influence decreases (0.30-0.60). In winter the sea influence at the bar increases from month-to-month with the growth in ice thickness over the area of the bay through February and the corresponding equation coefficients increase from 0.46 to 0.80, beginning to decrease in March-April (up to 0.68). From October to February the effect of the local winds also gradually abates with the regression coefficients decreasing by the module from 0.21 to 0.01.

3. The influence of level oscillations at the river boundary of the Yenisey mouth area is considerable in the region of the second crossover. At the bar of Ob' the inflow of river water to the Gulf influences the value of the free terms of the regression equations.

The multiple regression coefficients are sufficiently large (up to 0.95). The obtained equations are used for short-term forecasts of water levels for providing all-year-round navigation at the segments of the Northern Sea Routes. The largest errors are obtained in forecasting the extreme water levels. Hence an analysis of the conditions for the surge level rises which occur at the influence of the winds of the northern direction on the surface of the region, was performed.

The process of occurrence of extreme surge level rises for each zone is specific. At the bar of Ob' the turn of the local wind to the east at the end of a 3-4 day period of the persistent northerly on-shore wind induces an additional level increase. At the bar of Yenisey a similar influence results from the change in the wind direction to the western one after a 2-day effect of the northerly or the north-westerly on-shore wind on the region of the bay. This is governed by the general direction and the local turns of the coastline of the bays in the regions of the bars and occurs at the passage of the corresponding pressure formations over their areas.

At the crossover in the Yenisey delta, an additional level rise results from the wind increase on some segment or other of the wind channel with persistent northerly and north-westerly on-shore winds for not less than two days. Further influence of the winds of the northern direction does not play any role.

At the second crossover the largest surge level rises are those which are subjected to the least transformation when shifting from the delta. They have a more smooth diagram of the level change with time and more long duration of high levels. Waves with a sharp top coming from the delta, rapidly transform from catastrophic to usual surge level rises.

Due to the specific features of their formation and transformation the extreme level rises on all the study segments are observed at different time and the development of the methods for forecasting these dangerous phenomena should be a special study. The genesis of the formation and transformation of the minimum surge water level oscillations, as well as a quantitative estimate of the influence of the inflow to the Ob' Gulf on the non-periodic water level oscillations at the Yamsale bar has been insufficiently studied.

References

1. Maslayeva N.G. To calculations of surge level oscillations in the lower reaches of Yenisey. - Proc./AARI, 1968, vol.283, pp.71-78.
2. Smirnova L.N. Forecasting of surges in the Ob' mouth area. - Proc./AARI, 1974, vol.308, pp.27-34.
3. Uranov Ye.N. A method for forecasting surge level oscillations at the Turushinsk crossover in the Yenisey delta. -
4. Uranov Ye.N. Analysis and forecasting of the sea background level variations in the Yenisey estuary. - Proc./AARI, 1975, vol.314, pp.152-161.
5. Proshutinsky A.Yu., Uranov Ye.N. A composite method for forecasting surge level oscillations in the Yenisey estuary in winter 2-3 days in advance. - Proc./AARI, 1985, vol.389, pp.78-86.
6. Ivanova A.A. Water level oscillations in the Yenisey mouth area during the summer-autumn navigation period. - Proc. of the AARI, 1991, vol. 424, pp.122-127.
7. Voyevodin A.F., Nikiforovskaya V.S., Ovcharova A.S. Numerical methods for resolving the problem of unsteady water motion in the river mouth zones. - Proc. of the AARI, 1983, vol. 378, pp.23-34.
8. Stolyar S.Ye. Taking into account wind effect in calculations of unsteady water motion in the river mouth zones. - Proc. of the AARI, 1983, vol.378, pp.35-38.
9. Ivanov V.V., Kotrekhov Ye.P. Experience of hydrodynamic calculation of nonperiodic level oscillations. - Problems of the Arctic and the Antarctic, 1971, iss.38, pp.45-55.
10. Kotrekhov Ye.P. On calculation of the storm-driven long wave travel along the river mouth zone. - Proc. of GGI, 1972, iss. 204, pp.130-140.
11. Kotrekhov Ye.P. Full-scale studies and numerical calculations of surge phenomena in the mouth area of the Yenisey. Water resources, 1984, No.2, pp.49-61.
12. Vinogradova T.A. Study of the hydraulic regime of extreme water level rises in the Ob'-Taz and Yenisey mouth areas. - In: Papers of young scientists and specialists. Questions of land hydrology. - L.: Gidrometeoizdat, 1980, pp.131-138.

SIMULATION OF HYDRODYNAMIC AND ENVIRONMENTAL PROBLEMS IN ARCTIC RIVER DELTAS WITH A COMPUTER SYSTEM 'CARDINAL'

*Bessan G.N.(HPSDI 'Hydroproject')Klevanny K.A. and Matveyev G.V.
(SPO 'Morzaschita')*

1. Introduction.

The modelling system CARDINAL (Coastal Area Dynamics Investigation Algorithm) is a computer program for solving various hydrodynamic and water pollution problems in two and three dimensional approaches. It allows currents, surface levels and concentrations of pollutants in any complicated water domain to be calculated . CARDINAL was designed as a simple tool for engineers, researchers, managers, and staff of environmental protection agencies. It may also be useful in theoretical investigations and for educational purposes. The program makes it possible to determine the influence of various hydrotechnical structures on hydrodynamics and water pollution and to suggest optimal solutions. The method of the solution is based on curvilinear boundary-fitted coordinates and mapping of a given domain onto a canonical one. It uses implicit high-order numerical schemes. A detailed description of the program is given in [1,2].

2. Application of the model.

The modeling system CARDINAL is used in many organizations for the realization of dozens of projects. Among them are projects connected with river deltas and estuaries. They include calculations of water dynamics and dispersion of pollutants in the Neva Bay and the Eastern Gulf of Finland for the choice of optimal locations outfalls of treatment plants, study of the impact of the St.Petersburg Flood Protection Barrier on the Bay pollution , the forecast of spreading of warm water discharged from a design thermal-power station. It may also be used for the river deltas of the Barents and Kara Seas. One of the examples concerns computations of storm surge propagation in the Kolyma River delta.

The mathematical model study of an interaction of the Kolyma River flow and long waves generated in the Arctic Ocean was undertaken in connection with designs of Kolyma and Ust-Srednekan hydro-power stations located 1894 and 1677 km from the river mouth, respectively. Despite these long distances, surface levels in the river mouth depend on the regimes of water discharges from the stations. Surface levels, in turn, influence the navigation conditions as depths in the navigation channels in the river mouth are 4 - 6 m and fall to 2 - 3 m during long wave oscillations generated by storm surges and tides in the Arctic Ocean. Thus it is desirable to have a tool for forecasting surface levels in the river delta depending on water levels in the ocean and water discharges from the power stations.

The area of computations was 128 km long and comprises the Kolima delta from Ambarchik to Nizhnekolimsk (Fig.1). The curvilinear grid consists of 4125

grid points (125 along the river and 33 across it). Surface levels were assigned at the sea boundary and discharges were assigned at the river one.

At the first step a steady river flow was modelled. An expedition of Hydroproject Institute fulfilled hourly measurements of surface levels at the points Zeleny Mys and Kray Lesa from 20 June 1991 to 28 August 1991 [3]. Data of surface levels in Ambarchik were available from measurements of the Hydrometeorological Service.

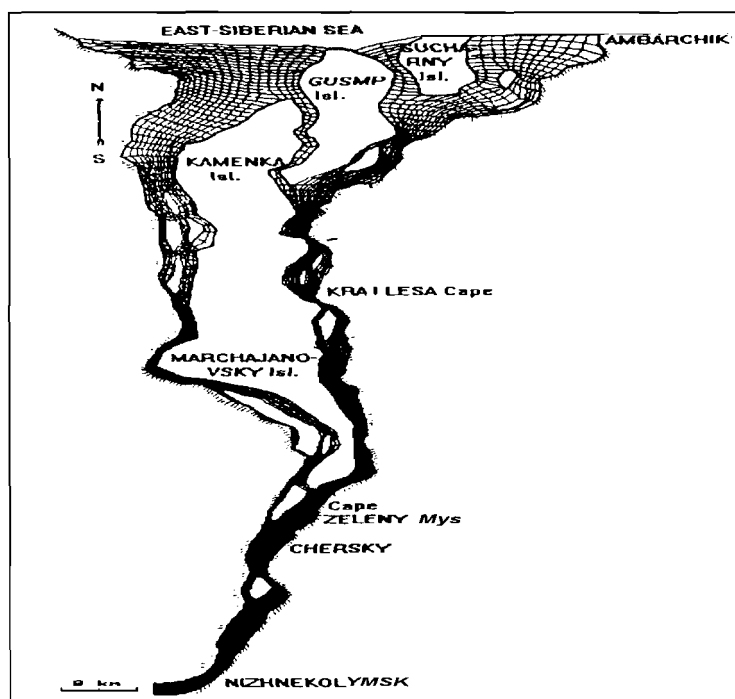


Fig.1 Curvilinear grid for the Kolima River delta.

According to these measurements, average water level difference between Ambarchik and Zeleny Mys was 7 cm and between Ambarchik and Kray Lesa this difference was 4 cm. The river discharge was about 2900 m³/s. These surface level gradient values were obtained in the model with Manning's roughness parameter equal to 0.012.

At the second step the real unsteady situation from 21 to 25 July 1991 was simulated. During 21 July and until 6:00 on 22 July the water level in Ambarchik decreased by on 35 cm. Then a long wave coming from the Arctic Ocean increased the water level in Ambarchik by 98 cm at 17:00 on 23 July. After that the water level in Ambarchik decreased. According to the Hydroproject measurements, the wave height increased during its propagation and in Zeleny Mys it was equal to 113 cm.

The computational time step was 60 s, the horizontal eddy viscosity coefficient was 20 m²/s. It should be noted that at the river boundary in Nizhnekolymsk the assigned discharges were extrapolated from data for Kolymsk located 75 km south of Nizhnekolymsk by multiplying by coefficient 1.29 which was obtained taking into account water intake in this part of the river. This

introduced an error because during propagation of long waves up the river, the discharges in Nizhnekolymsk should differ significantly from then in Kolymsk.

Time histories of water levels in Nizhnekolymsk (computed), Zeleny Mys, Kray Lesa (computed and measured) and in Ambarchik (measured) are presented in Fig.5. During the first two days the measured and computed values are rather different as the initial conditions taken from the steady solution differ from unknown natural conditions for the moment of the computation start, but after that the computed and measured results are a reasonably consistent, especially for the Kray Lesa point. According to computations, the wave height increased during its propagation up the river to Zeleny Mys and also to Nizhnekolymsk. So the computational domain should be prolonged for further investigation of long wave propagation.

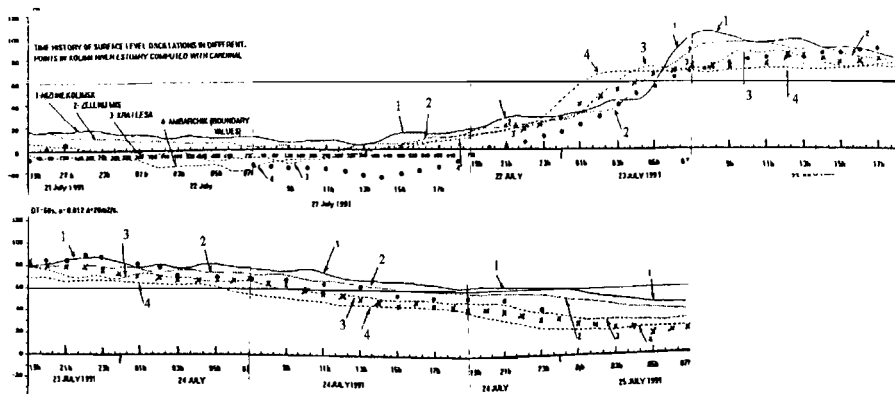


Fig.5 Computed and observed time histories of surface level oscillations in different points in the Kolyma River delta on 21 - 25 July 1995. o - observed levels in Zeleny Mys; x - observed levels in Kray Lesa. Computed: 1 - Nizhnekolymsk, 2 - Zeleny Mys, 3 - Kray Lesa. 4 - Ambarchik (assigned from observation as a boundary condition).

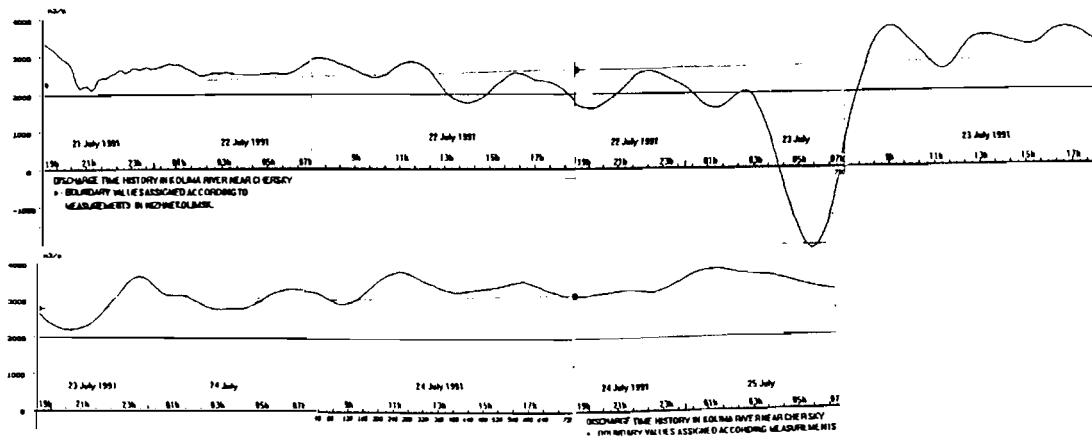


Fig.6 Computed time history of discharge in the Kolyma River near Chersky. Positive values correspond to the flows to the sea and negative ones - to the south ward flows up the river.

In the river mouth the discharge into the river reached, according to the model, 15000 m³/s at 2:00 on 23 July. Results in Fig.6 prove that the wave reached the area near Chersky at 5:00 on 23 July and the flow directed up the river has discharge here up to 2000 m³/s. A place of meeting of the inflow and outflow currents of the moment of 7:00 on 23 July was located near Zeleny Mys and the spatial distribution of depth averaged velocities in this moment here is presented in Fig.2. Four stages of the long wave penetration are shown in Fig.3 as surface level profiles along the east river shore. A considerable cross sectional non- uniformity of surface level distribution in the river branches was obtained. Fig.4 represents bird's eye views of the surface levels for six different time moments.

The results proved that the model can be applied for implementation of water management systems which allow in particular, control of navigation conditions in the Arctic river deltas and estuaries in the presence of hydro-power stations in regions subjected to storm surges and tides.

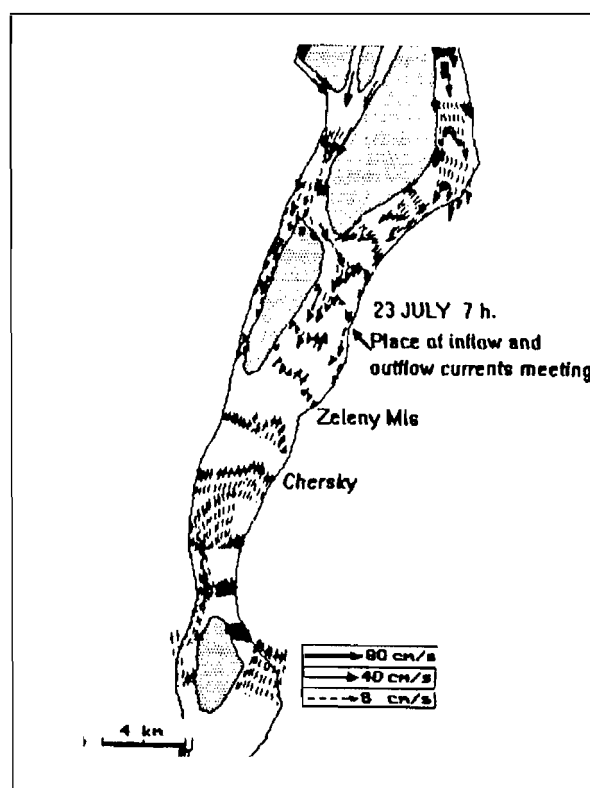


Fig.2 Velocity field in a part of the Kolyma delta near Zeleny Mys in the moment of meeting of the inflow and outflow currents (23 July, 7:00).

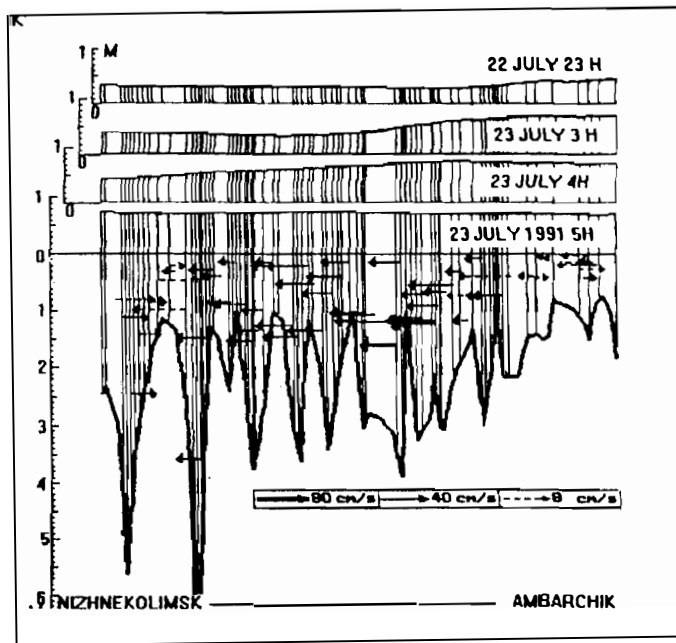


Fig.3 Surface level profiles from Nizhnekolymsk to Ambarchik along the east river shore in different moments of the long wave propagation up the river. For the last moment depth profile and depth averaged velocities are given.

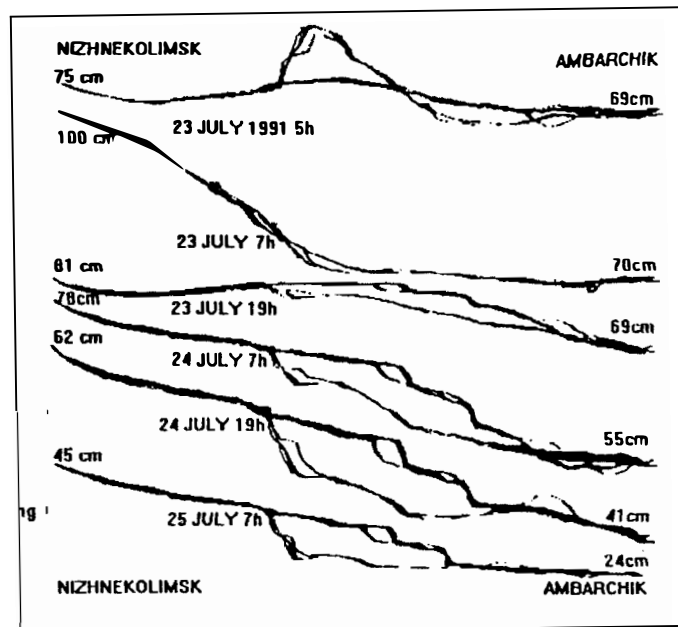


Fig.4 Bird's eye views on the surface levels in the Kolima delta for six different time moments. Point of viewing: to the east from the river, zero vertical angle (i.e. view from the land).

References

1. Klevanny K.A., Matveyev G.V. and Voltzinger N.E. 'An integrated modeling system for coastal area dynamics', *Int. J. for Numerical Methods in Fluids*, v.18, p.181--206, (1994).
2. Klevanny K.A. and Matveyev G.V. 'Application of the integrated modelling system CARDINAL for estimation of environmental impacts of coastal engineering in the Gulf of Finland', In: *Proc. 4th Int. Conf. on Coastal and Port Engineering in Developing Countries, Rio de Janeiro, Brazil*, v.3, p.2120 -2134, (1995).
3. Hydrological Field Works in the Kolima River Delta in 1991. Technical Report of the Hydroproject Design Institute, N GD 367/26, St.Petersburg, 27p. (1991).

STUDY OF LONG-WAVE PROCESSES IN THE MOUTH AREAS OF THE NORTHERN RIVERS ON THE BASIS OF HYDRODYNAMIC ONE-DIMENSIONAL MODELS

Ye.P.Kotrekhov(LIRAS)

Among the dynamic processes in marine river mouths long-wave motions induced by natural and artificial changes in the river runoff and also by tides, surges, etc., play a dominating role. The study of such processes on the basis of limited full-scale data is related to considerable difficulties. At some allowances following from the features of long-wave motions, they can be described by means of the theory of "shallow water" using one-dimensional models. Some experience in this field has been gained with regard to the studies and calculations of water regime characteristics of the mouth areas of such rivers as Yenisey, Pechora, Severnaya Dvina, Tuloma along with the Kola Bay of the Barents Sea.

Taking into account that almost all river mouth areas under consideration include multibranch deltas special methods have been applied to solve one-dimensional equations of shallow water. And numerical methods created in different years at the Institute of Hydrodynamics of the Siberian Branch of the Russian Academy of Sciences (RAS) were widely used. A modification of one of these methods developed specially for the Pechora river delta, allowed describing unstable water motions in the complex system of channels at the presence of inner (delta) reservoirs and taking into account difficult water exchange between them and water flows.

Model verification was performed by using full-scale data on levels, water discharges and current speeds. An estimate of the accuracy of model calculations using an available set of initial data and various calculation algorithms was made. As a result of multiyear studies, the methods for an optimal schematic presentation of the mouth areas of rivers of different type, prescription of initial hydraulic-morphometric characteristics, initial and boundary conditions, etc. have been tested. This allowed formulating respective recommendations for the use of available numerical methods and calculations of unstable water motion in marine river mouths.

During the studies main typical features of the propagation and transformation of long waves of different nature moving both downstream and upstream the river channel have been found. In particular, the effect of river runoff on the spreading extent and attenuation process of the waves of surges and tides has been assessed in a wide range. On the basis of full-scale data on currents and numerical calculations the range of the changes in the flow speeds and a character of their relation with water level fluctuations at surges and tides have been revealed.

Also, the questions of the interfection of long waves under conditions of multibranch deltas have been considered. As a result of the studies made for the mouth of the Severnaya Dvina river, a technique for the analysis and calculation of water level constituents has been suggested for the case of the interaction of the tide and storm surge under conditions of a complicated river delta. By the examples of calculating storm surges for different water bodies and numerical

experiments the required details of taking into account wind have been found and corresponding recommendations for its prescription in numerical model obtained. By the example of the Kola Bay of the Barents Sea and the mouth area of the Tuloma river the influence of the bottom relief and the hydrotechnical structure (hydropower station dam) on the tidal wave propagation in the presence of the effect of its reflection from the obstacle has been investigated. For the same water body using numerical experiments the transformation features of the flood waves in the Kola Bay, formed in the basins of the Kola and Tuloma rivers, as well as of the wave flash at the Nizhne-Tulomskaya hydropower station were revealed.

STRUCTURE AND DYNAMICS OF THE SHORES OF THE KOLGUYEV ISLAND

O.N. Medkova, D.Yu. Bol'shiyanov(AARI)

The Kolguyev Island with 3150 sq. km area is situated in the south-eastern Barents Sea. The island is composed from the surface by Quaternary aleurite-sand-clay and aleurite-clay deposits with a large amount of fragmental debris. The thickness of deposits in the central part of the island is 75-125 m increasing southward up to 145-150 m.

Round contours of the island in the plan and a radial pattern of the hydronetwork are governed by recent tectonic motions.

A total length of the shores of the island is 278 km, 52% of them being relatively stable, 40% are subjected to active abrasion and over 8% there is accumulation of terrigene material.

High western and northern shores are almost everywhere subjected to thermoabrasion. Mean annual rate of the cliff edge retreat is 1.5 m and maximum one reaches 4 m. The material incoming to the coastal zone feeds two strong sediment flows along the shore that round the island from the north-west and east. In the south-eastern part of the island it is deposited forming two large spits - Flat Western and Eastern Koshka 80 and 72 km respectively with an extensive shallow water zone between them.

The Western Koshka spit is relatively stable. In distal part of the Eastern Koshka there is a shore aggra

ation reaching 4-5 m, in proximal one during the period 1948-1968 the thermoabrasion`rate was up to 1.5-2.0 m a year. It is here that with the oil exploration and production on the island in the 80s the construction of industrial and living facilities and roads began. Non-consideration of the tendencies in the dynamics of the coastal zone resulted in a number of negative consequences. Thus, the production of sand-gravel pebble and flotsam (logs) in the quantity of 1.1 mln cu. m/year from the beach near the proximal part of the Eastern Koshka spit resulted in active irreversible eroding of the coast northward and retreat of the this part of the spit. The eroding rate increased to 2-3 m/year. Some of the ecologically dangerous constructions, in particular the oil pipeline passing across the shore zone for oil loading to tankers are under a threat of being destructed.

MORPHOLOGY AND DYNAMICS OF THE COASTAL ZONE OF THE OB' GULF

Medkova O.N. (AARI)

On the basis of analyzing the direction and intensity of modern shore processes, distribution of the shore types, character of sedimentation and effect of different exogenic factors two areas are delineated: western and eastern and three latitudinal zones.

The differences in the Yamal and Taz-Gydan' shores are attributed to a joint effect of a number of endogenic and exogenic factors: inheritance from the preceding subaerial stage of the development of the Ob' river valley, morphostructure of the territory, differentiated character of recent tectonic motions and Coriolis force.

Latitudinal differences are mainly governed by the features of hydrological regime, direction and value of the alongshore sediment transport (AST) oriented on the whole to the Gulf head. A transverse sediment drifting is insignificant.

In the northern zone (up to the Tambey settlement latitude talassogenic factors prevail: strong wave and tides governing a predominant development of the abrasion shores. At a general AST direction southward in the lower part of the underwater coastal slope (UCS) mainly along the eastern coast there are observed accumulative forms increasing in the northward direction.

The dynamics of the shores in the middle most extensive and narrow zone of the Gulf (up to Kamennaya spit) is governed by its internal (estuary) regime also subjected to the river runoff effect mainly from the Taz Gulf. The effect of waves and tides is weaker here. There is a stronger tendency toward accumulating sediments at UCS (especially on the left bank where large accumulative forms are formed). In many places the AST is broken by the zones of divergence, convergence or zones without a clearly expressed direction. In the first zones a tendency towards the shore erosion is observed, in the second (especially) and in the third zones - towards its aggradation.

The river runoff of the Ob' has already a significant influence on the dynamics of the coastal zone in the southern shallow part, particularly isolated from the sea. The effect of the tides is small, the role of surges is large and in the near delta zone a considerable role is also played by the outflow current and flood level rises. In some zones the AST is characterized by different directions and a small value (especially near the western shore). All this governs the development of mainly accumulative processes.

ICE THERMAL REGIME OF THE ESTUARIES OF LARGE RIVERS IN THE KARA SEA BASIN

Nalimov Yu. V. (AARI)

A number of studies are devoted to the mouth areas of the rivers in the Kara Sea Basin /1-11/. This article presents a generalized evaluation of the ice-thermal regime of the estuaries of large rivers in the Kara Sea Basin.

The studies of the ice-thermal regime of the Ob'-Taz Gulf, the Yenisey and Pysina Bays were based on data from a network of polar stations and winter expeditions of the Amderma and Dikson Territorial Administrations of the Hydrometeorological Service, as well as on data of airborne ice reconnaissance, airborne ice, actinometric and thermal surveys carried out by the AARI. As a result of the observations, the dates, regions of the onset and the character of ice formation, freeze-up and break-up for each of the estuaries were determined /10, 12/.

In the estuaries, ice formation begins actually simultaneously in the northern and southern regions of the gulfs and bays at the end of September-beginning of October (Fig. 1a, b). Then in the southern regions of the estuaries ice dams are formed between the shores where ice expands northward and southward.

Ice formation in the northern region of the Pyasina river delta begins from the shallow zones and gradually spreads northward to the sea regions and southward to the river region (Fig. 1c).

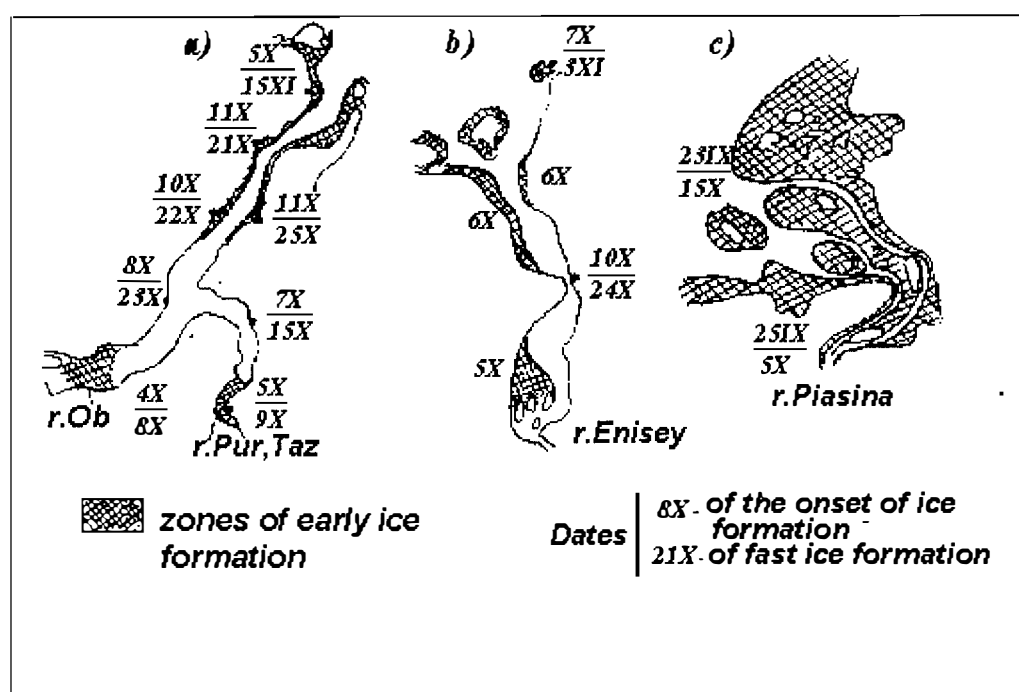


Fig. 1. Dates of ice and land fast ice formation.

On average, the range of the ice drift period in the autumn in the estuaries is 24-27 days with the exception of the Ob' Gulf in the area from the polar station Tadibeyakha to the traverse of the Tambey station where the range

reaches 41 days. In the estuaries the mean period of the ice drift is not more than 10-15 days.

The ice growth in the estuaries depends on a number of factors /12/ which govern both the ice structure and texture. Much of the Ob' Gulf is covered by freshwater ice and the Yenisey and Pyasina Bays by brackish ice.

As a result of actinometric observations, a dependence of the albedo of new ice on its thickness with growth was obtained /6/. Fig. 2 presents this dependence.

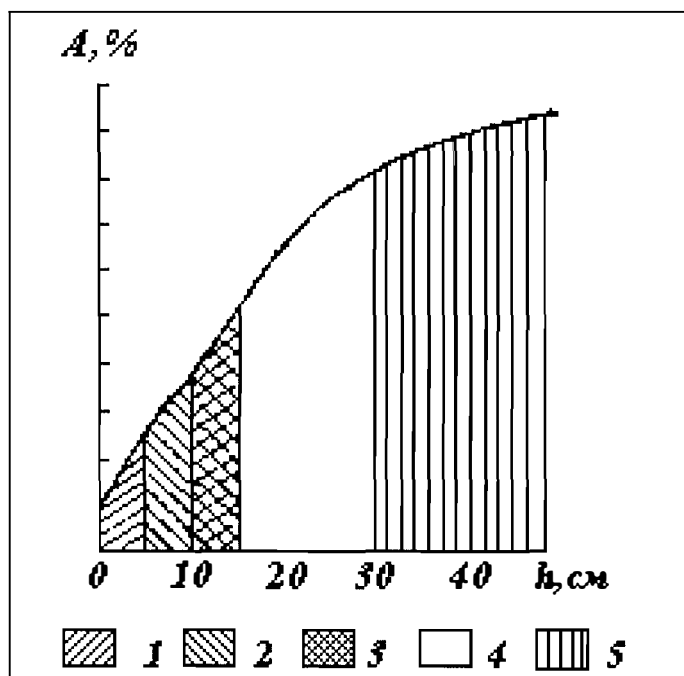


Fig. 2. Dependence of new ice albedo on its thickness. 1 - dark nilas; 2 - light nilas; 3 - grey ice; 4 - grey-white ice; 5 - white ice.

In October, ice in the estuaries of the Kara Sea Basin reaches, on average, the thickness of grey-white ice (up to 30 cm) and in March-April of medium first-year ice (70-120 cm) and thick first-year ice (more than 180 cm). Ice thickness in the estuaries is greater than in the lower reaches of rivers and in the coastal sea regions. In the northern Ob' Gulf the maximum ice thickness reaches 250 cm and in the Yenisey Bay - 270 cm. In the Pyasina Bay ice can also reach such values.

In the southern regions of the estuaries, ice is, as a rule, level, the amount of hummocked ice being 0-20%, whereas in the northern regions it is 40-60% with patches of hummocked ice of 100%. The snow depth on the ice in the southern regions of the estuaries is usually 60-80 cm, and in the northern regions 20-50 cm.

Spring decay of ice in the Ob'-Taz Gulf and the Pyasina Bay occurs under the effect of a complex of hydrometeorological factors and in the Yenisey Bay predominantly under the influence of river water heat /12, 13/. The albedo value of the snow-ice cover in the estuaries of the Ob'-Yenisey rivers depending on the extent of ice decay and contamination, are presented in Fig. 3 /14/.

Fig. 4a, b, c presents the character and dates of the ice decay. A characteristic feature of break-up in the estuaries of the Ob'-Taz Gulfs and the Yenisey Bay is the retreat of the ice edge to the north as affected by river water heat. In the Ob' and the Taz Bays ice melting is preceded by its break-up, drift and changes in the edge configuration, whereas over much of the Yenisey Bay, land fast ice melts along the midstream (Fig. 4a,b), /13/.

The character of the ice break-up in the Pysina river estuary in the delta region adjacent to the sea, sharply differs from a typical break-up process in the estuaries. The break-up mechanism is as follows: flood water exiting to the near-sea zone of the Pyasina river, floods the ice frozen to the ground. Ice over deepwater channels is torn away from the general mass and surfaces. Narrow ice strips are formed over the channels, repeating their configuration. Then these strips break-up and ice which composes them, drifts to the edge of the unbroken fast ice. In the Pyasina river mouth area break-up of these strips and ice clearance usually occur in the third 10-day period of July (Fig. 4c).

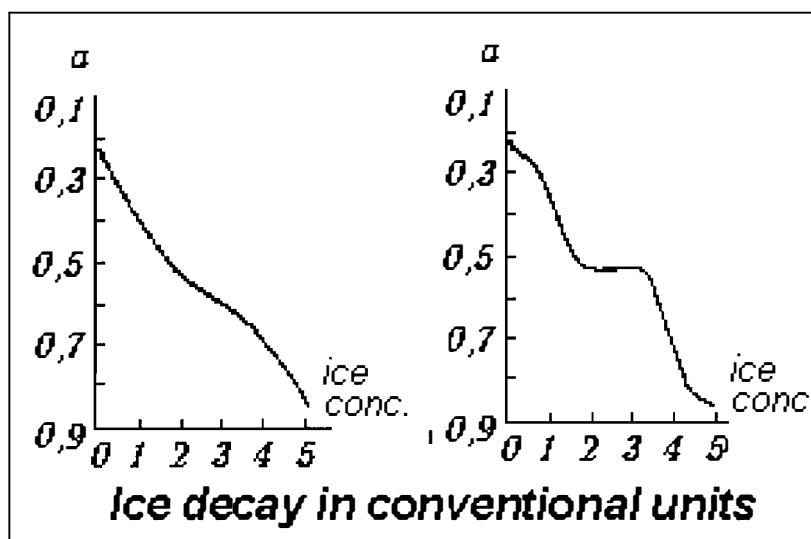


Fig. 3. Albedo values of the snow-ice cover at pollution of the ice area of 10-40%.

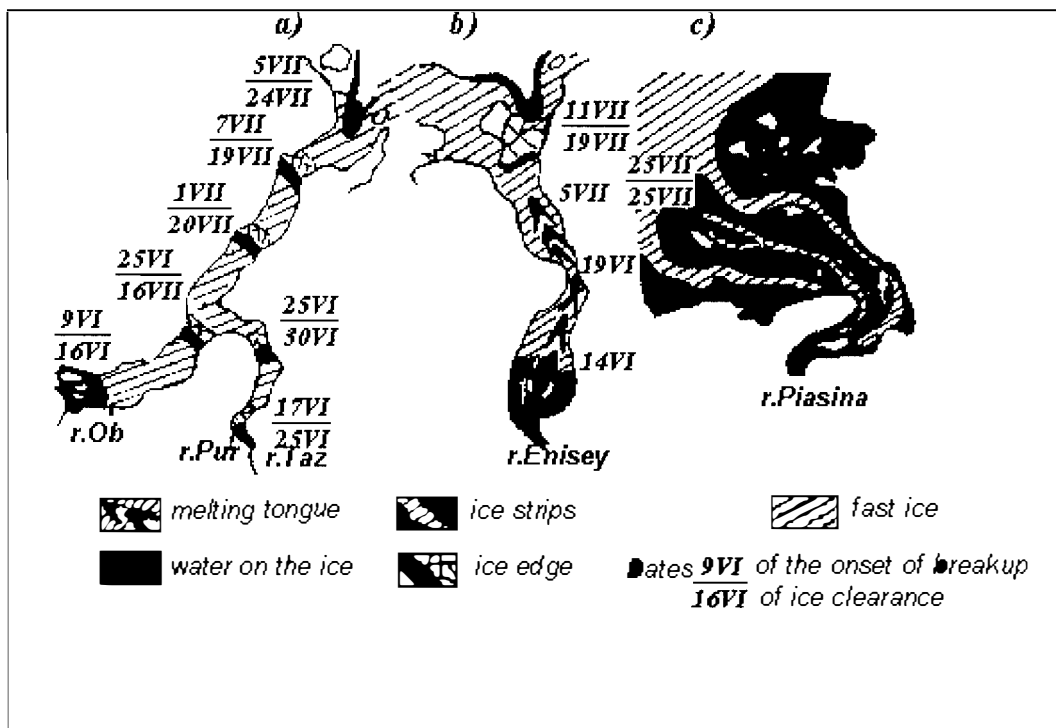


Fig. 4. The character and dates of break-up in the estuary zones of the rivers.

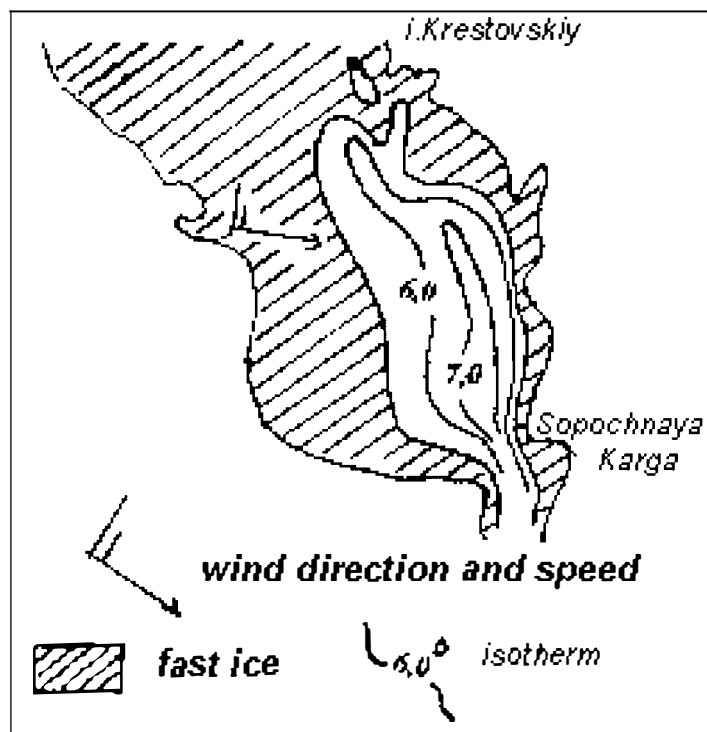


Fig. 5. Deviation of the warm river runoff in the Yenisey Bay as affected by wind

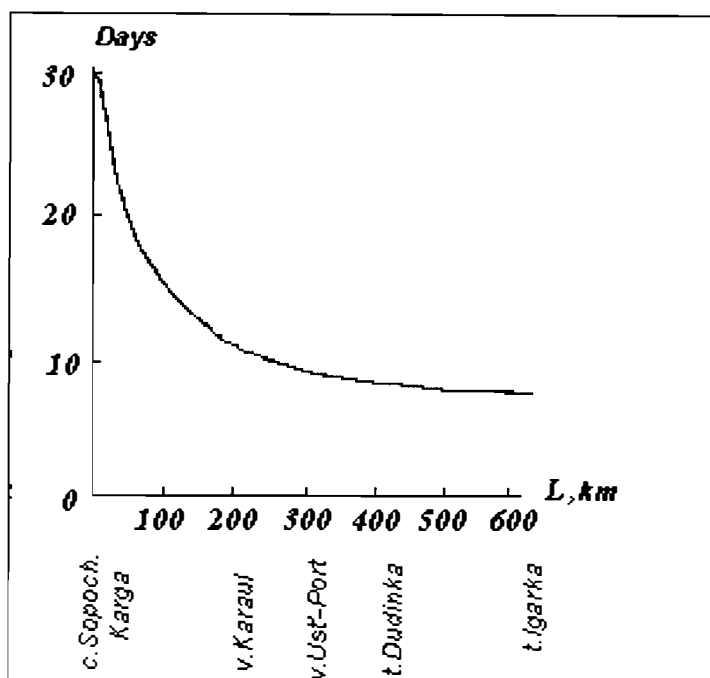


Fig. 6. The period (a day) of water temperatures becoming equal along the channel section in the Yenisey mouth after being ice cleared.

In spring, warm water flows to the estuaries from rivers contributing to ice melting (Fig. 5,6), /15/. At the sea margin of the delta the water temperature reaches 14-17 ..C, while in the northern regions of the estuaries it is close to sea water temperature. In the freshwater regions of the estuaries the process of ice formation begins when water reaches a temperature of 0.2 C in the autumn /16/.

References

1. Antonov V.S., Maslayeva N.G. 1965: Low reaches and the mouth of the Ob' river (a hydrological-navigation description), L. Gidrometeoizdat, 82 p.
2. Antonov V.S. 1962: Yenisey (a hydrological-navigation description). Proc. of the Arctic and Antarctic Research Institute, "Marine Transport" Publishers., L., 99 p.
3. Antonov V.S., Ivanov V.V., Nalimov Yu.V. Typical features of the ice regime of navigable rivers in the Arctic zones. - "Problems of the Arctic and the Antarctic", 1964, Mo.15, pp.11-17.
4. Antonov V.S., Ivanov V.V., Nalimov Yu.V. Distribution of spring dams at the rivers of the Arctic zone of Siberia. - Proc. of the AARI, 1972, vol.297, pp.116-122.
5. Burdykina A.P. Features of break-up in the mouth area and lower reaches of Yenisey. - Proc. of the AARI, 1970, vol.29, pp.34-55.
6. Grayevsky A.P., Nalimov Yu.V., Timerev A.A. Reflectivity of young ice in the estuaries of the Arctic rivers. - Proc. of the AARI, 1980, pp.35-39.

7. Zotin M.I. Features of break-up in the lower reaches and the mouth of rivers falling to the northern seas by the example of Yenisey. - Proc. of GOIN, 1962, No.66, pp.24-34.
8. Ivanov V.V. Break-up of the ice cover in the lower reaches and the mouth of the Yenisey river - Problems of the Arctic and the Antarctic", 1963, No.2, pp.141-146.
9. Ivanov V.V., Komov N.I. Features of break-up of the ice cover in the near-mouth area of Yenisey at extremely low levels. - Problems of the Arctic and the Antarctic", 1970, No.35, pp.19-25.
10. Ivanov V.V., Nalimov Yu.V. Results of airborne expeditions in the lower reaches and mouth areas of the rivers in the Arctic zone. Problems of the Arctic and the Antarctic", 1981, No.51, pp.79-91.
11. Nalimov Yu.V. Influence of dam formation on the break-up regime of the ice cover in the near-mouth area of Yenisey. - Proc. of the AARI, 1972, vol.297, pp.127-137.
12. Nalimov Yu.V. Heat balance methods for calculating the elements of the ice regime in the estuaries of the Siberian rivers. - Proc. of the All-Union Hydrological Congress, 1990, River mouths, vol. 9, pp.182-189.
13. Nalimov Yu.V. Assessment of the role of factors of the ice cover melting in the mouths of the Arctic rivers (by the example of the Yenisey river mouth). - Proc. of the AARI, 1972, vol.297, pp.60-68.
14. Nalimov Yu.V., Timerev A.A. Values of the snow-ice cover albedo in the lower reaches and mouths of the Arctic rivers. - Meteorology and Hydrology, 1974, No.5, pp.64-68.
15. Nalimov Yu.V. Study of the thermal regime of the Yenisey mouth river for calculation and prediction of break-up. - Proc. of the AARI, 1976, vol. 314, pp.104-111.
16. Nalimov Yu.V. Application of the radiation thermometer in the mouth areas of the Siberian rivers. - Problems of the Arctic and the Antarctic, 1971, No.38, pp.129-132.

THE HYDROLOGICAL DATABASE FROM THE STATIONARY OBSERVATION NETWORK IN THE MOUTH AREAS OF LARGE RIVERS IN THE KARA SEA BASIN

Petrov N.L., Bozhkov A.T., Nalimov Yu.V., Nizovtseva T.I. (AARI)

An automated information system with a specialized hydrological database of observations over a stationary network in the mouth areas of rivers of the Kara Sea was developed for providing reliable storage of accumulated observation data, a quick access and their subsequent processing in accordance with the requirements of the State Water Cadastre.

Initial information on the mouth bays and gulfs of the Kara Sea Basin was selected from data of polar stations stored at the archives of the AARI and on the mouth areas of rivers from the published Hydrological Yearbooks.

The database includes hydrological observations for 30-40 years obtained at 38 stations and gauge sites in the river mouth areas of the Kara Sea Basin. Of them, 24 are situated in the river mouth zones and 14 in the mouth bays and gulfs. The database includes the following hydrological parameters: water levels and discharges, water temperature, salinity and density, waves, ice phases and snow depth on the ice.

Some problems were encountered in the process of analyzing initial information for including into the database. On the one hand, data of observations at standard synoptic times from 1976 to 1979 are absent at the AARI. On the other hand, during the decades covered by the database, the methods of observations, initial processing and recording of data in the logs and tables were repeatedly changed and improved. Some observation points situated on the coast of the bays and gulfs operate under the sea program /2/ and the stations situated in the lower reaches and deltas of rivers belong to the river stations /3/ which makes difficult automated processing of observation data. This shortcoming in the observation system will be eliminated after a new Guiding Document on observations over a network of stations in the river mouth areas is introduced within the framework of the hydrometeorological network /4/.

Observation information which is included to the database is subjected to automated initial processing and analysis: based on hourly values, values at synoptic times, mean daily, 10-day period values and mean monthly values are determined /2-4// It is possible to obtain maximum and mean values of the elements for any prescribed observation period.

The suggested database was developed for IBM-compatible PC which is managed by the MS DOS operating system and is realized in Turbo Pascal 7.0. Data are entered to the database in DBMS (Database Management System) formats Paradox 3.5. The communication between the information system and the database is maintained by means of Paradox Engine 3.0 functions.

The structure of the database is based on the relational model type. The database consists of the following files related to the key fields: the list of water bodies, the list of observation points with reference data, the measured values of the parameters (data at synoptic times in the mouth bays and gulfs and mean daily values in the river mouth areas) (Fig. 1).

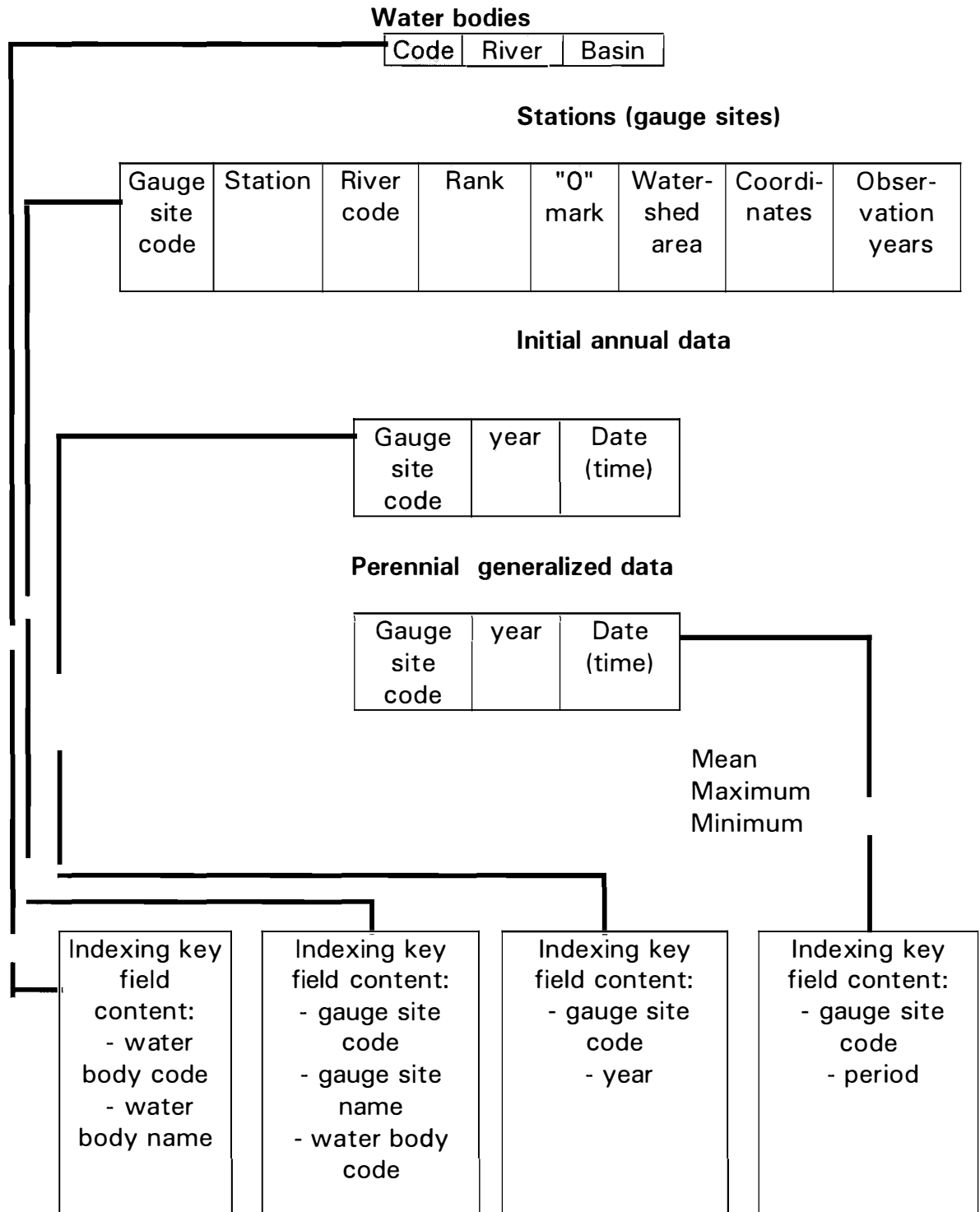


Fig. 1. Structure and relationship between the tables of the hydrological database in the river mouth areas.

The created information system is accessible for the users of any level of computer skill and presents an integrated medium including a multilevel system of the User's menu, a system of context-dependent promptings, full-screen editor for input, correction and display of information which performs the initial syntactic and semantic control of input data.

The User has a possibility for regulating data processing: calculations of mean and sampling of extreme values over the prescribed observation period.

Data contained in the database can be output for printing in the tabular form or converted to the formats of statistical programs (GIDSTAT and STATGRAPHICS) to be used in applied problems.

The developed information system can be used for storage of any hydrological data which are observed within the framework of standard programs of the stationary network.

References

1. Composition of data of the State Water Cadastre., Moscow, 1981, 21 p.
2. A Manual for hydrometeorological stations and gauge sites. Issue 9, Part I. Gidrometeoizdat, Leningrad, 1984, 312 p.
3. Manuals for hydrometeorological stations and gauge sites. Issue 2, Part II. Gidrometeoizdat, Leningrad, 1975, 263 p.
4. A Guiding Document. Methodological instructions: Hydrological observations and work over the hydrometeorological network in the mouth areas of rivers. Gidrometeoizdat, Moscow, 1993, 188 p.

CHARACTERISTICS OF THE FREE SURFACE CURVES IN THE OB' MOUTH AREA ACCORDING TO THE RESULTS OF HYDRAULIC CALCULATIONS

A.A. Piskun (AARI)

As is known, evidence on the height of the free surface level in the mouth areas of rivers is necessary for calculations of the chart datum and design levels, estimates of the water balance components and mass transfer, determination of the areas and volumes of flooding of the flood-plains and deltas, parameterization of mathematical models and for other purposes.

For river zones which are outside the influence of backwater from the sea, this evidence is usually obtained using the relation plots between the respective water levels combined into one system of the heights along the river length. For the mouth river areas whose water regime is governed not only by the river runoff, but also by sea level, the height of the free surface of the level can be obtained by hydraulic methods [7,8]. The use of these methods for the mouth bodies was substantiated by Grishanin [3] and earlier implemented by Ivanov [4-6]. A similar approach was also used in this work with regard to the Ob' mouth area (Fig. 1).

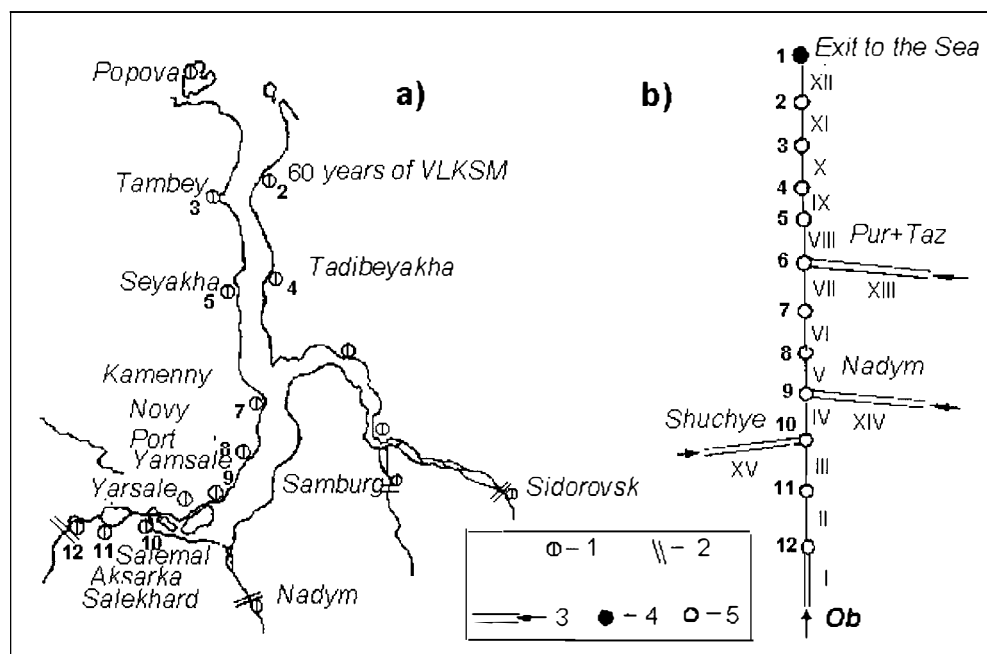


Fig. 1. The Ob' mouth area (a) and its calculation scheme b) 1 - level gauge sites; 2 - hydrometric sections; 3 - zones with the prescribed water discharges; 4 - a point with a prescribed level mark; 5 - calculation points.

The Ob' mouth area which extends over more than 1000 km, has a complicated character of the water regime, depending both on the runoff of the Ob' (about 84% of the water volume discharged to the Gulf), Nadym (about 3%), Pur and Taz rivers (about 13%) and the background sea level, surge and tidal phenomena. Fig. 2 provides some impression about the variability of mean annual, mean monthly levels and of the levels at standard synoptic times along the length of the Ob' mouth area.

The hydraulic calculation scheme (Fig. 1) included 15 segments and 12 points confined to the level gauge sites. In addition, the scheme included the confluence point of the Ob' and Taz bays (near the Trekhbugorny cape). For obtaining the main

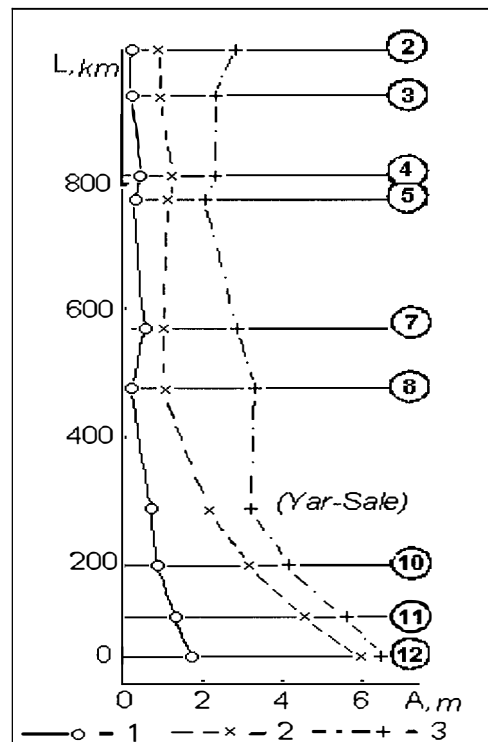


Fig. 2. The amplitude (A) of the oscillations of mean annual (1), mean monthly (2) levels and levels measured at synoptic times (3) /1, 2/ at the gauge sites along the length (L) of the Ob' mouth area. The numbers of the points correspond to the points of the calculation scheme.

calculation parameters - resistance modules of the zones, mean monthly levels of permanent gauges and water discharges at the downstream measuring sections were used /1, 2/ (Fig. 3).

A preliminary analysis of the height position of the corresponding levels obtained from the relation plots of the levels along the length of the mouth area, has shown that at the minimum river runoff and even under mean hydrological conditions (at the water discharge in the Ob' river of 12500 m³/s), we obtain the reverse level surface slopes on the segment of the gulf between the Kamenny and the 60 years of VLKSM gauge sites. This indicates the need for correcting the gauge datum planes in the

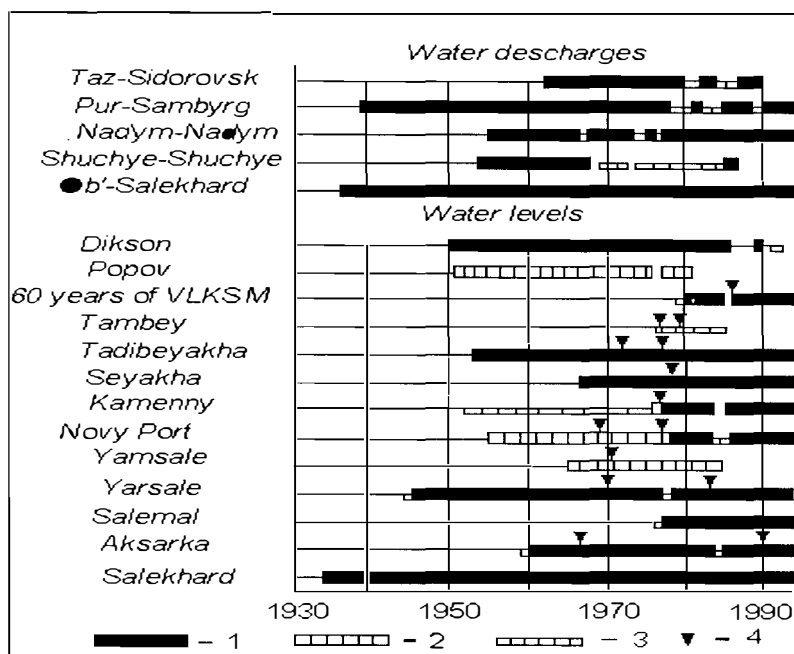


Fig. 3. Duration of observations of water discharges and levels at the sections and gauge sites used for calculation, 1 - all-year-round observations; 2 - seasonal; 3 - discontinuous observations; 4 - a year of the gauge datum plane change.

mouth area. In connection with the absence of reliable data on the levels at the sea boundary of the calculation area, the levels of the Tambey, Popov and Dikson points were used.

The results of hydraulic calculations for the conditions of the absence of backwater have shown good agreement between the calculated and full-scale data at the corresponding levels at the gauge sites along the length of the mouth area.

Fig. 4 presents the calculated longitudinal profiles of the free surface in the Ob' mouth area at the established water motion regime which illustrate the influence of backwater. They show that at the increase in mean monthly sea level from the least to the largest value at the maximum mean monthly Ob' discharge equal to 43400 m³/s, the influence of level oscillations ends within the Ob' delta. At the minimum mean monthly discharge (6640 m³/s) this influence spreads upstream Salekhard.

For all points of the calculation scheme, the plots (Fig. 5) and analytical expressions for determining water height marks at the calculation points were obtained. For the zones of the dependencies of mean level (or level drop) on the total discharge of river water (or water discharge at the calculation section) there were also calculated sea level marks. Fig. 6 presents one of the dependencies which can be used under prescribed boundary conditions for determining free surface marks at any point of the mouth area, also beyond the observation points.

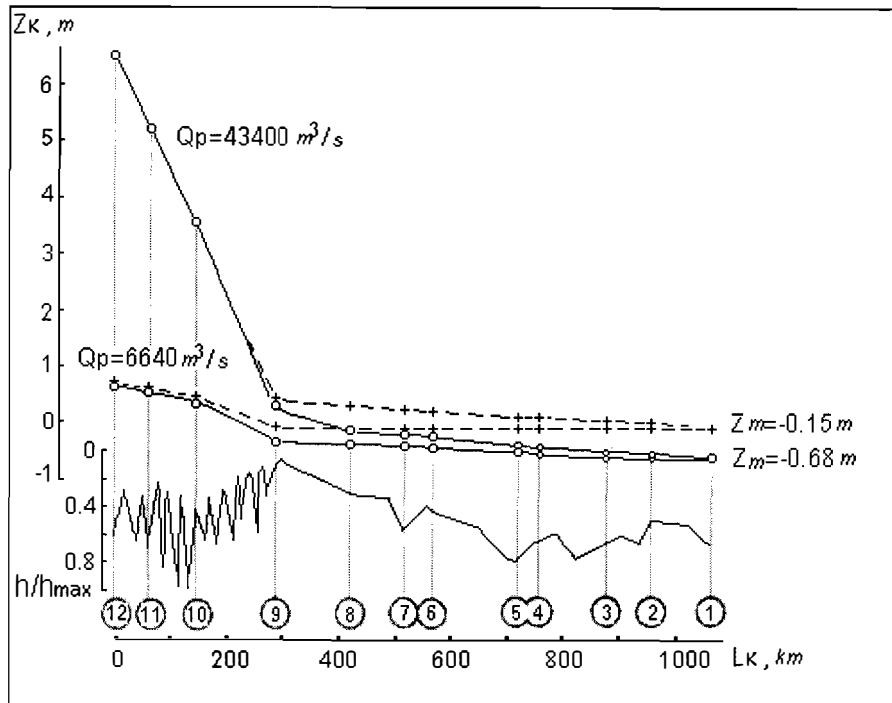


Fig. 4. The calculated longitudinal free surface profiles in the Ob' mouth area for the largest and the least mean monthly values of boundary conditions. Z_m - sea level marks; L - the distance from Salekhard; h/h_{max} - a ratio of mean depth at the sections to the largest depth in the mouth area.

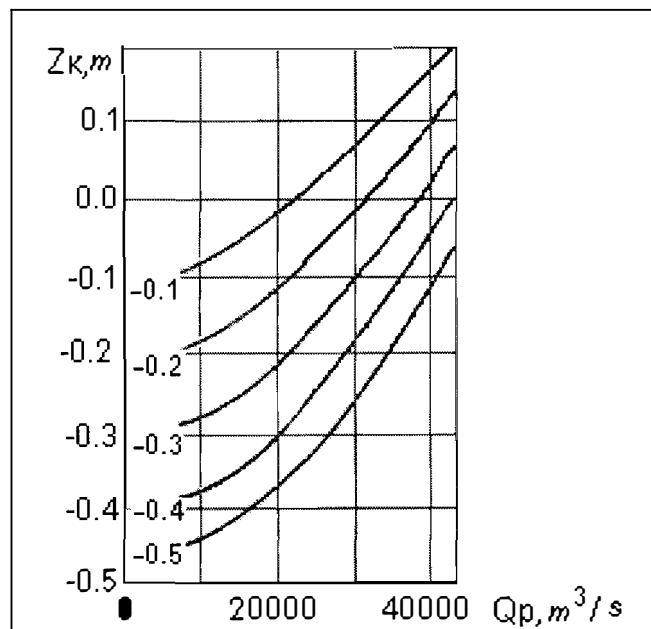


Fig. 5. Dependencies of the level heights near the Trekhbugorny Cape (Z_k) on the river runoff (Q_p) and sea level (Z_m - figures near the curves).

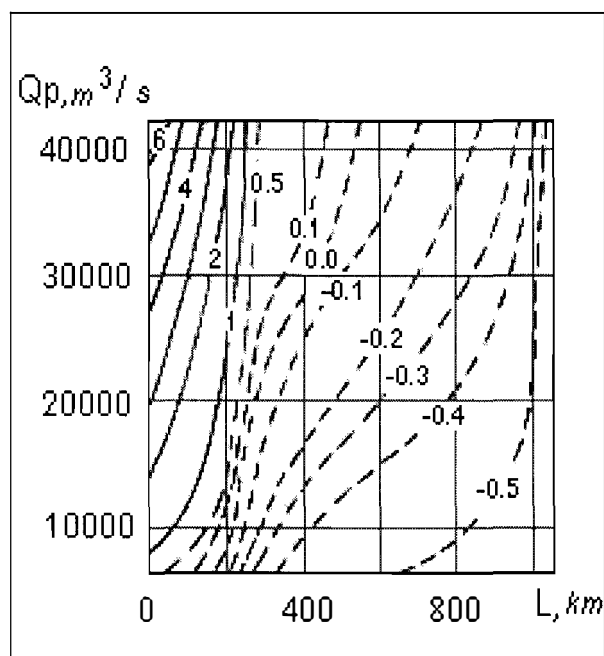


Fig. 6. Isolines for determining level heights (in meters) along the length of the Ob' mouth area under mean hydrological conditions of the sea.

The studies performed have shown that for more reliable estimates of the characteristics of free surface of levels in the Ob' mouth area it is necessary, primarily, to update the height basis of the level gauge sites and arrange at a least an annual cycle of level observations at the sea delta edge (Yamsale) and at the sea boundary of the Ob' Gulf (Popov).

References

1. Hydrological Yearbooks. Vol. 6, No. 0-3.
2. The State water Cadastre. EDM, vol. 4, P.II.
3. Grishanin K.V. The hydraulic calculation of the water regime elements in the deltas of the rivers in the Arctic zone. - Proc./AARI, 1967, vol.278, pp.5-21.
4. Ivanov V.V. On calculation of the chart datum in the mouth of rivers of tidal seas. Proc./AARI, 1961, vol.256, pp.104-106.
5. Ivanov V.V., Mednikova E.S. The hydraulic calculation of relations between levels and discharges in river deltas by means of an Electronic Digital Computing Machine. Proc./AARI, 1970, vol.291, pp.44-57.
6. Ivanov V.V. A method for calculating the runoff component of level oscillations in the river mouths. Proc./AARI, 1968, vol.283, pp.12-29.
7. Rakhmanov A.K. On the question of constructing free surface curves for natural water courses. - Hydrotechnical construction, 1934, No.10, pp.1-4.
8. A guidebook for calculation of the elements of the hydrological regime in the coastal zone of the seas and in the mouths of rivers at engineering explorations. M.: Gidrometeoizdat, 1973, 535 p.

SOME FEATURES OF THE HYDROLOGICAL REGIME OF THE OB' GULF

V.V. Stanovoy (The AARI)

The paper presents the results of studies which continue earlier studies /1-4/.

The Ob' Gulf is an extensive shallow zone of interacting river and sea waters. The vertical salinity gradients of water can reach 10 per mil/m and the horizontal ones up to 1-2 per mil /km. There is a significant interannual, seasonal and intraseasonal variability in the position of the hydrofront.

The interaction zone is influenced by dynamic factors, the most significant of them being the flood wave, wind-driven currents and tides.

The speeds of constant runoff currents during the period of navigation calculated by means of a hydrodynamical model, gradually decrease in the surface layer from 7-12 cm/s in the southern region of the gulf up to 1-3 cm/s in the northern region. With depth the speeds decrease and near the bottom they are about half as large as at the surface. Nonperiodic runoff wind currents in the Ob' Gulf were calculated using a three-dimensional hydrodynamical model over a 20x8 km grid of the gulf for prevailing winds. Winds of the main directions with a speed of 5-10 m/s have the largest occurrence frequency during the navigation period (Fig. 1). According to Snopova, (1976) the occurrence frequency of these five pressure situations during the navigation period is about 78%.

At south winds when the directions of the wind and runoff currents in general coincide, the field of currents is sufficiently uniform. At the north, east and west winds the field of currents presents rather a complicated pattern and numerous eddy formations are traced in the Ob' Gulf area. The speeds of a nonperiodic current on the surface change within a wide range reaching 20-25 cm/s in some places. With depth the speeds decrease. The maximum inflow of sea water to the gulf in the surface layer is observed at the north winds and in the near-bottom layer at the south winds.

The maximum tides are observed in the northern Ob' Gulf where the tide value on the western shore reaches 1.8 m and on the eastern shore (Shokal'sky island) there is a non-pronounced amphidrome with the tide value of 0.37 m. When travelling southward along the gulf the tidal wave gradually dissipates up to the values of 0.1-0.2 m in the southern gulf. The maximum speeds of tidal currents reach 0.8 m/s near the western shore in the northern Ob' Gulf.

One of the most important dynamical factors in the northern Ob' Gulf is the existence of the internal gravitation waves. They are closely interrelated to the dynamics and thermohaline structure and are observed at all daily and multiday oceanographic stations both in summer and in winter under the ice, their length being several tens of kilometers and their

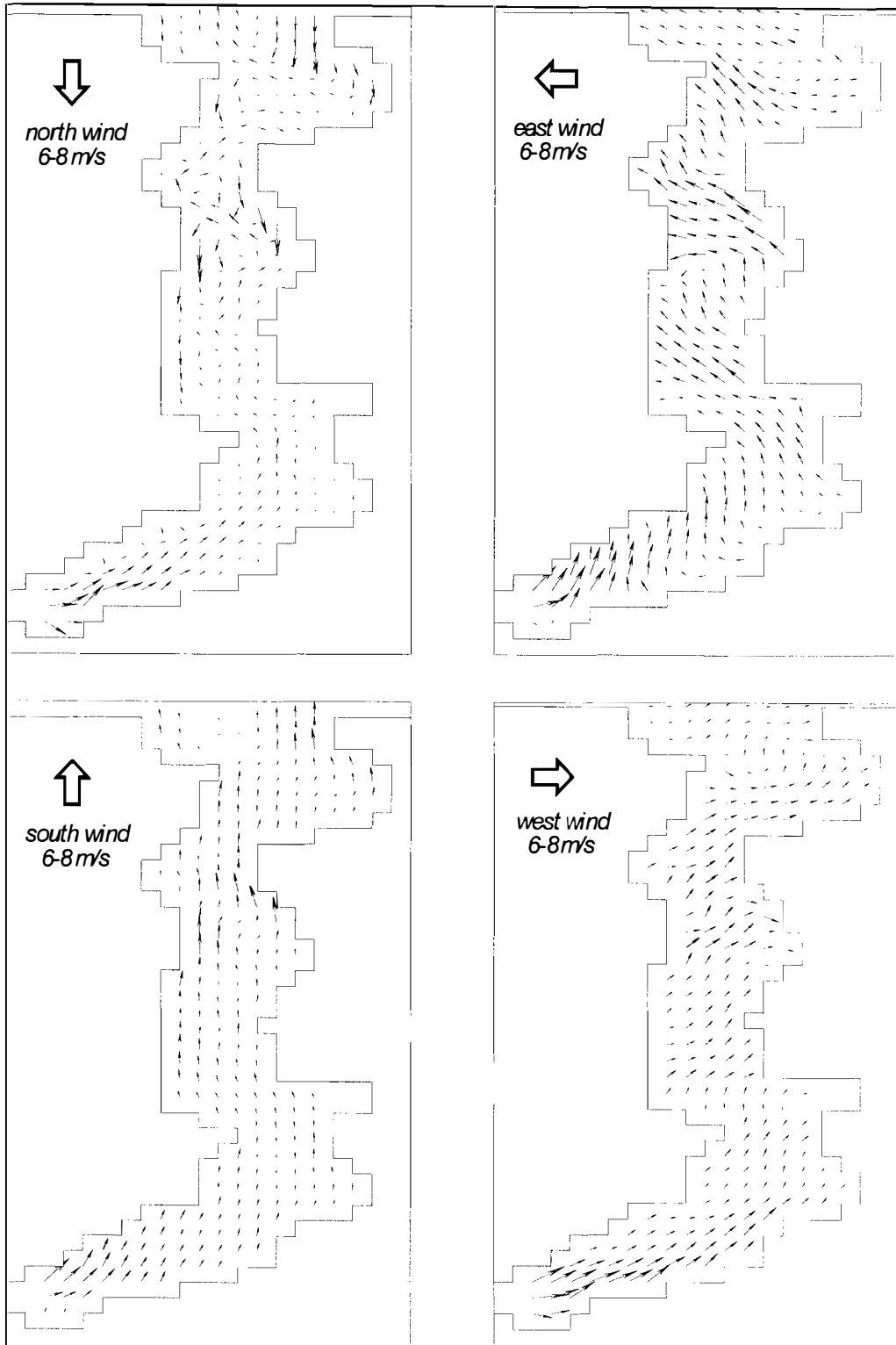


Fig.1 The calculated fields of the surface current in the Ob' Gulf

values reaching half of the depth in shallow regions. Such waves are, as a rule, unstable and their decay causes unstable stratification. The decay of the internal waves at dynamical or gravitation instability can result in the formation of turbulence and erosion of the pycnocline.

The internal waves of tidal frequencies are well traced, i.e. the baroclinic tides play a significant role in the dynamics of the northern Gulf (Fig.2).

Small depths contribute to the generation of non-linear cnoidal internal waves which have a property of mass transfer, i.e. at propagation of a packet of internal waves, the residual current is induced. The passage of the non-linear internal waves of the finite amplitude can significantly change the vertical structure and contribute to the formation of fine thermohaline structure. The internal waves can change water salinity in the pycnocline by 10-15 per mil for several hours.

The ice cover influences the internal waves when the pycnocline is located sufficiently close to the bottom ice surface. A combination of the ice cover and small depths contributes to the formation of the non-linear internal waves. There are also cases of the occurrence of solitons (Fig. 3). According to rough estimates, the amplitudes of solitons can reach 5-6 m (at a depth of 18-20 m), the period of about 45 hours and the speed of travel of about 0.7 m/s. When a soliton passes, the water salinity value can change by more than 15 per mil.

Thus, small depths, strong river runoff, a peculiar configuration of the coastline, the presence of fast ice cover and intensive water dynamics cause the processes, inherent to a well-pronounced frontal zone in the Ob' Gulf, in particular, its northern region, to occur in a more pronounced and dynamical form.

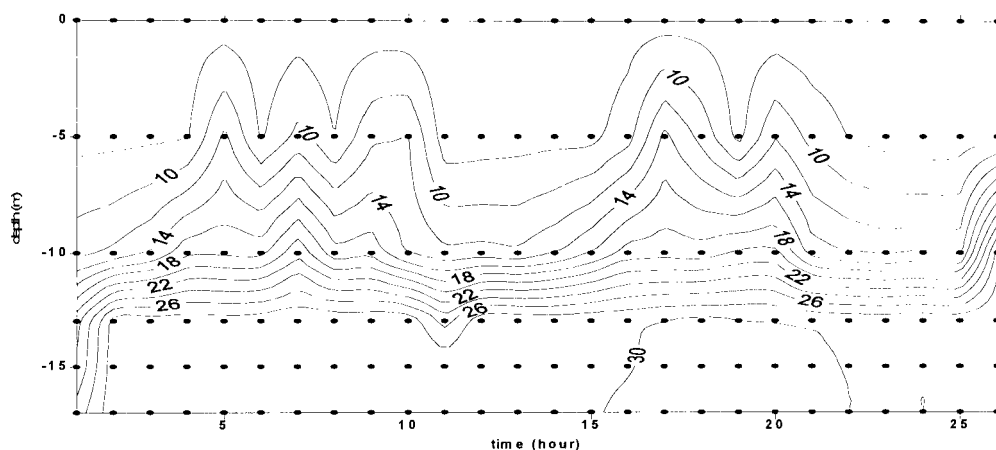


Fig.2 Vertical distribution of the water salinity. Multihour station in the northern part of the Ob' Gulf-August

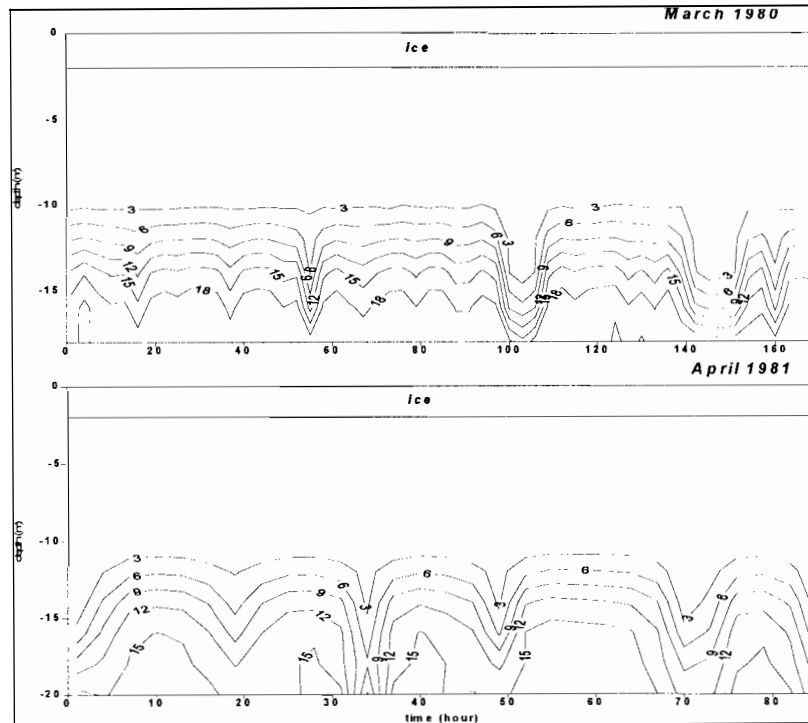


Fig.3 Vertical distribution of the water salinity. Multiday station in the northern part of the Ob' Gulf

References

1. Pavlov V.K., Stanovoy V.V. Calculation of climatic characteristics of runoff-wind currents of the Ob' Gulf. - Proc. of the AARI, vol.380, 1983, pp.49-54.
2. Stanovoy V.V. The influence of tidal phenomena on the variability of thermohaline structure in the northern Ob' Gulf. - Proc. of the AARI, vol.394, 1984, pp.19-22.
3. Stanovoy V.V. Features of studies of thermohaline structure in baroclinic estuaries. - In: Abstracts of the II All-Union Conference "Dynamics and thermal conditions of rivers, water reservoirs and estuaries", vol. 2, M., VNIIGMiM, 1984, pp.193-194.
4. Stanovoy V.V. The hydrodynamical model for calculating tidal phenomena in baroclinic estuaries. In: Abstracts of the All-Union Meeting "Study of natural conditions of low reaches and mouths of rivers in the Arctic zone for hydrometeorological support of people's economy", L., AARI, 1985, pp.27-29.

SPATIAL-TEMPORAL VARIABILITY OF THE ICE REGIME ELEMENTS IN THE LOWER REACHES AND MOUTH AREAS OF RIVERS IN THE KARA SEA BASIN

Z.S. Solovieva, L.V. Antonova (the AARI)

For analyzing spatial-temporal variability of the ice regime in the lower reaches and mouth areas of the rivers of the Kara Sea Basin the following characteristics were assumed: the dates of the onset of stable ice formation, ice disappearance, the period with stationary ice (freeze-up) and ice thicknesses at the end of the winter season based on data of the stationary network. Earlier data which used common criteria both regarding the length of the rivers and their mouth areas were investigated /3/.

The process of stable ice formation in the basin under consideration begins in late September on the Pyasina river and spreads south-west for two weeks including all medium rivers of the Basin - Nadym, Pur and Taz. Only the lower reaches of large rivers Ob' and Yenisey with their large heat content freeze one-two weeks later September 15-20).

The break-up process of the rivers in the study basin and their clearance from ice occurs under the effect of both thermal and mechanical factors.

First, (third 10-day period of May) the break-up takes place in the lower reaches of Ob' (downstream from Salekhard), Yenisey (downstream from Igarka) and Nadym river, then in the tributaries of these rivers and medium rivers Pur and Taz (first half of June). The break-up in the Pyasina river occurs in the second half of June and the estuaries of the Ob' and Yenisey at the end of June-July, i.e. the whole Kara Sea Basin is covered by the break-up wave for two months.

The duration of the period with stationary ice on the rivers of the region increases from 7 months in the lower reaches of Ob' and Yenisey up to 8 months in the mouth of Nadym, Pur and Taz and in the south of the estuaries of Ob' and Yenisey and up to 8.5 months on the Pyasina river and in the north of gulfs and bays (Fig. 1).

An analysis of long-term tendencies in the variations of the dates of the onset of ice phases on large rivers Ob' and Yenisey for a 55-year period shows that in the 1940s there was a tendency toward later freeze-up and earlier break-up and hence, a tendency toward a decreased period with ice. In the 1950-1960s and up to the early 1970s there was a clear tendency for earlier freeze-up and later break-up and as a result, an increase in the period with ice /5/.

During the next years there was again a change in the sign in the variations toward later formation of stationary ice and earlier break-up resulting in a slight decrease in the period with stationary ice, however, it did not reach the level of the late 1940s (Fig.2).

The character of ice thickness variations at the end of the winter season is in good agreement with variations in the break-up dates.

Thus, an analysis has confirmed earlier conclusions of V.S.Antonov /1/, V.F.Zakharov /2/, N.D. Vinogradov et al. /4/ of the tendency for relative cooling or warming in different periods of the Arctic detected in the other elements of the hydrometeorological regime.

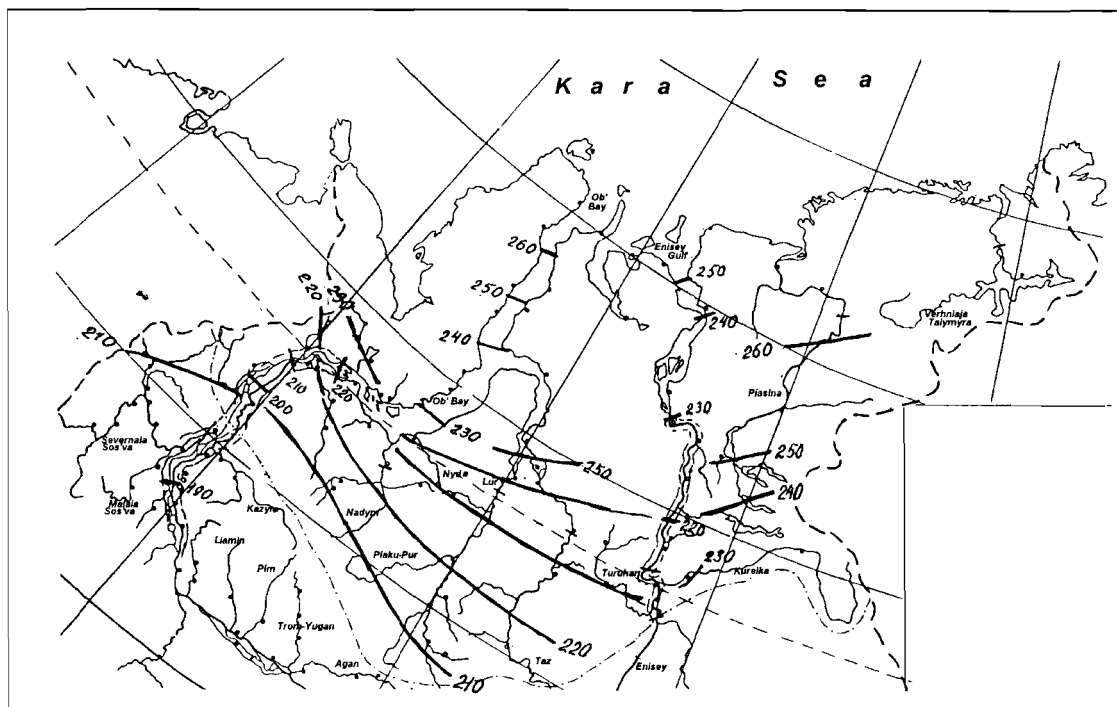


Fig. 1. Duration of the freeze-up period.

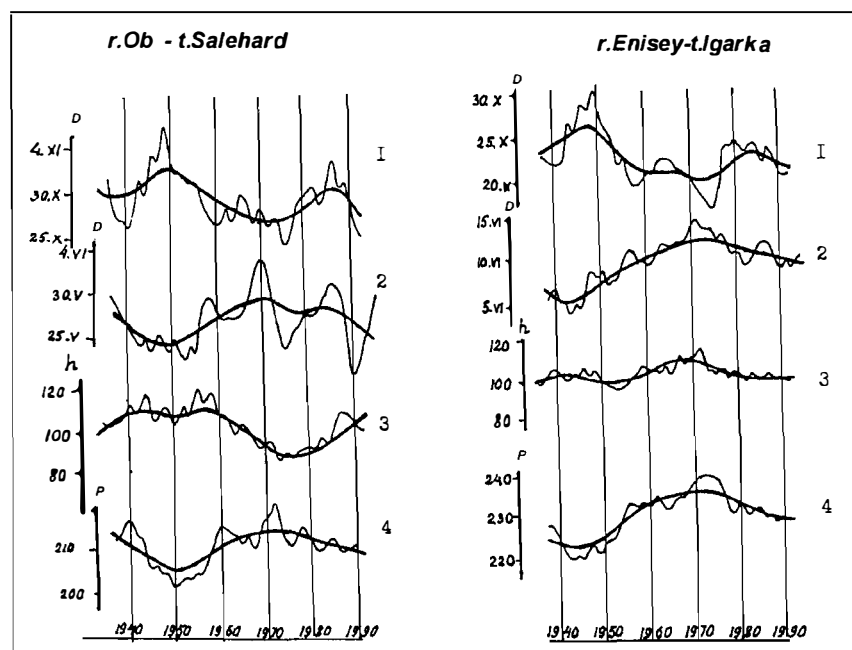


Fig. 2. Multiyear variations in the ice regime elements in the mouth regions of Ob' and Yenisey: - freeze-up, 2 - the onset of spring ice motion, 3 - ice thickness as of April 30, 4 - duration of the period with ice.

References

1. Antonov V.S. The ice indicator of the current tendency for climate cooling in the lower reaches of Yenisey. - Problems of the Arctic and the Antarctic, 1975, No.. 46, pp.84-90.
2. Zakharov V.F. Cooling of the Arctic and the ice cover of the Arctic Seas. - L.: Gidrometeoizdat, 1988, 408 p.
3. Ivanov V.V., Solovieva Z.S., Usankina G.Ye. Revealing of anomalies in the freeze-up and break-up dates of the lower reaches and mouth areas of the rivers of Siberia. - Proc. of the AARI, 1980, vol.358, pp.5-24.
4. Ivanov V.V., Solovieva Z.S., Antonova L.V. Tendencies for ice regime changes in the lower reaches and mouth areas of the Arctic rivers . - In: The climatic regime of the Arctic at the border of the 20th and the 21st century. Ed. by Dr. B.A.Krutskikh. - L.: Gidrometeoizdat, 1991, 200 p.
5. Solovieva Z.S. Typical features of temporal variability of the break-up dates of the lower reaches and the mouths of the rivers of Siberia. - Proc. of the AARI, 1983, vol.378, pp.113-132.

MODELING OF THE HALOCLINE DYNAMICS IN THE RIVER MOUTH AREAS TAKING INTO ACCOUNT ICE DYNAMICS

M. V. Tretyakov (AARI)

In addition to a two-dimensional profile mathematical model of the halocline dynamics in the river mouths under the conditions of a variable discharge by the length of the delta arm /3/, constructed in 1993 at the RSHNI, a model with a supplementary block of the ice cover genesis was developed. The obtained mathematical model calculates main hydrological characteristics (current speed, water temperature and salinity, date of ice occurrence, ice growth and melting).

The model is based on the non-stationary motion, continuity, heat and salt transfer equations /1, 4/. The continuity equation under the conditions of a variable discharge by the length of the arm has the form:

$$b(x) \frac{\partial \xi}{\partial t} \frac{\partial}{\partial x} \left(b(x) \int_0^{H(x)} U dz \right) = Q_i \delta(x - x_i)$$

where $Q_i \delta(x - x_i)$ - water outflow from the main channel, $\delta(x - x_i)$ - delta

function, $b(x)$ - flow width, ξ - deviation of the level from non-disturbed free surface, $H(x)$ - flow depth, t - time, U - horizontal velocity.

For calculating the turbulence coefficient, the equation of the turbulence energy balance in the framework of a semi-empirical theory of the boundary layer turbulence, as well as a ratio for the turbulence scale are used /1, 2/. The ice part includes three equations: the equation for calculating the water freezing temperature, the equation for calculating the ice thickness change during the period of growth and the equation for the period of melting /1/. The ice growth formula works when the surface water temperature becomes below the freezing temperature. At a positive value of the heat flux, the thickness of the melted ice is calculated.

As boundary conditions, water temperature and salinity profiles, as well as water discharge by the length of the arm taking into account lateral inflow (outflow), air temperature and humidity, wind speed and the radiation balance are prescribed at the river and sea limits of the calculation area /6/. At the open surface of the estuary, the wind stress and heat flux are determined from meteorological information. In the presence of ice the water temperature at the ice bottom surface is assumed to be equal to the freezing temperature and the friction stress to be proportional to the current speed.

For taking into account the relief irregularities, the method of bottom rectification was used. The curvilinear area is transformed to atherectilinear one by introducing a dimensionless variable /1/.

The model is computer-based in Turbo Pascal with a graphic display of the dynamics of the salinity fields and the ice thickness in the calculation process. By means of this model it is possible to simulate the

major features of annual variations of the thermohaline, dynamic and ice thermal characteristics in the Arctic estuaries.

The model was adapted and tested relative to the Kolyma delta. Fig. 1 presents the calculated distance of saline water penetration (L) (along the near-bottom isohaline of 1 per mil). Fig. 2 shows the longitudinal distribution of salinity at the time of the largest distance of sea water penetration to the river. The model reliably reflects the ice processes of this body (Fig. 3). The difference in the simulated and mean multiyear dates of ice clearance and of the dates of the onset of ice formation does not exceed 10 days /5/. The calculated ice thickness and the character of ice growth and melting correspond to full-scale observations.

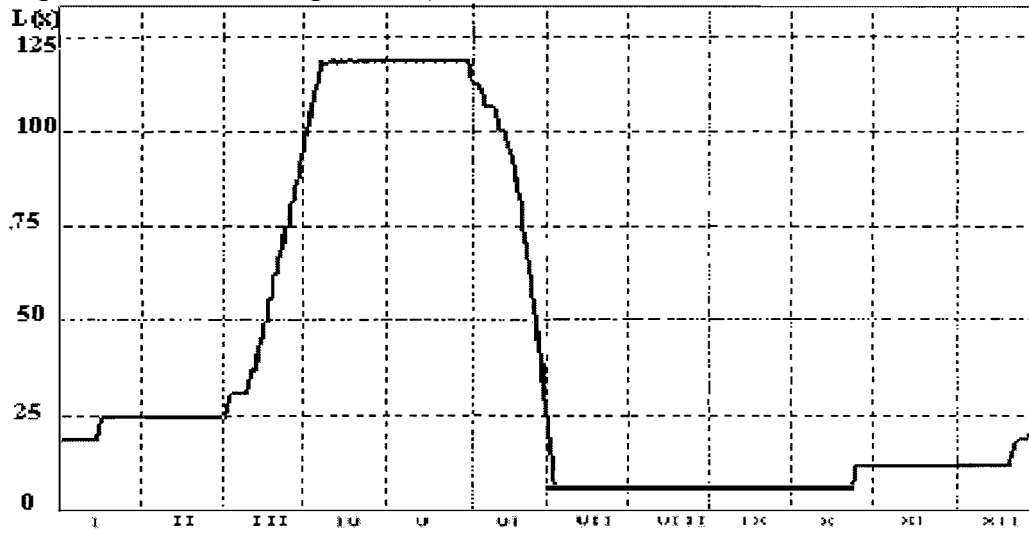


Fig. 1. The distance of sea water penetration to the Kamennaya branch of the Kolyma river.

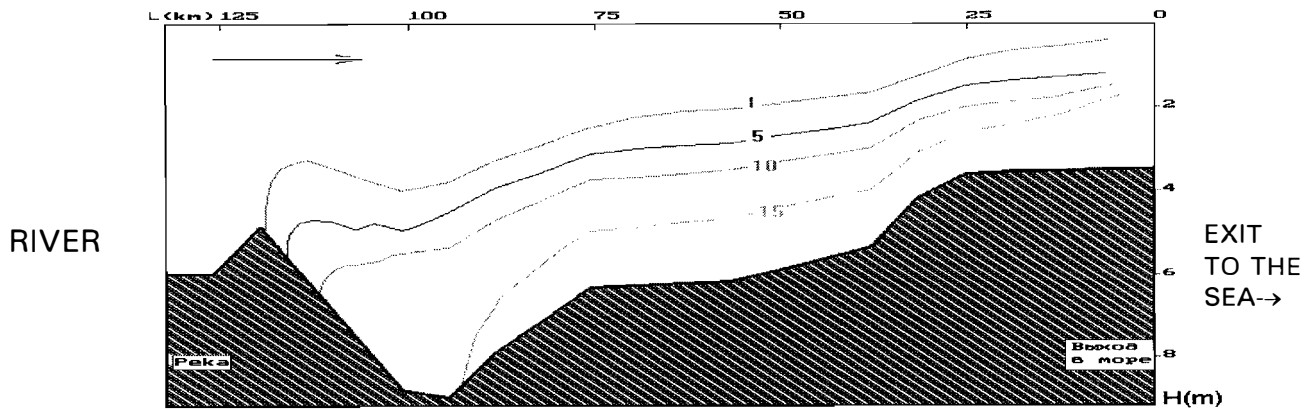


Fig. 2. Spreading of sea water in the Kamennaya branch of Kolyma, calculated for the end of June (isolines-isohalines, per mil).

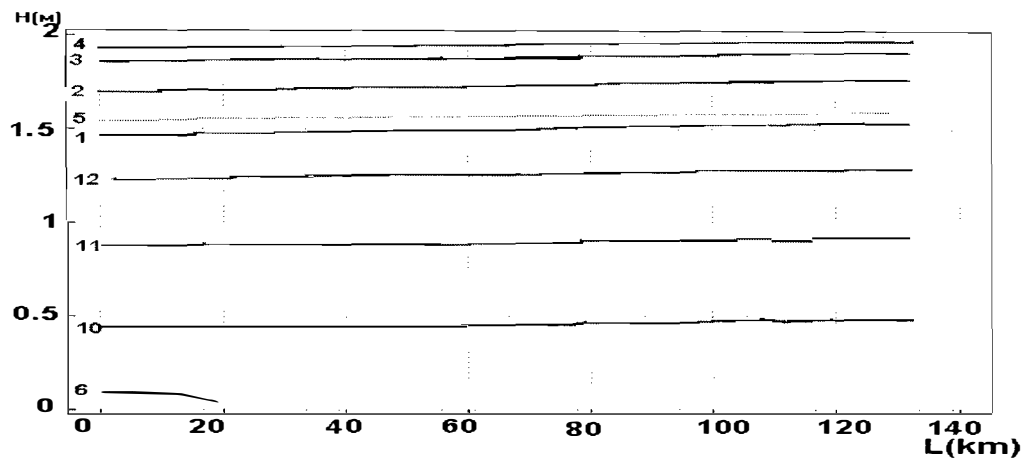


Fig. 3. The calculated ice thickness at the end of the month during the period of its growth (10-12, 1-4) and melting (5, 6).

It is planned to use the model for salinated deltas of Yenisey, Pyasina and other deltas with the halocline, as well as for the large estuaries with a lateral inflow.

References

1. Doronin Yu.P. Modeling of vertical structure of the river mouth area with a sea halocline. - *Meteorologiya i Gidrologiya*, 1992, No.8, pp.76-83.
2. Doronin Yu.P., Svyatsky A.Z., Ivanov V.V. Mathematical modeling of the processes of river/sea water interaction in the mouths of the rivers in the Arctic zone. - *Proc. of the 5th All-Union Hydrological Congress, vol. 9 (River mouths)*., L., Gidrometeoizdat, 1990, pp.163-170.
3. Doronin Yu.P., Lukyanov S.V., Tsarev V.A., Ivanov V.V. Methods and results of modeling of the hydrological processes in the stratified arctic estuaries (in the present volume).
4. Ivanov V.V., Svyatsky A.Z. Numerical modeling of sea water intrusion to the river mouths at the seasonal temporal scale. - *Water resources*, 1987, No.5, pp.116-122.
5. Ivanov V.V., Solovieva Z.S., Usankina G.Ye. Revealing of anomalous dates of freeze-up and break-up of the lower reaches and mouth areas of Siberia. - *Proc./AARI*, 1974, vol. 358, pp.5-24.
6. A scientific-applied handbook on the USSR climate, series 3, multiyear data, parts 1-6, No.24, 1990, 624 p.

FEATURES OF THE FREEZE-UP OF THE OB'-TAZ AND YENISEY MOUTH AREAS

G.Ye.Usankina ,A.P.Balabayev (AARI)

This study was an initial stage in solving applied problems of a wider scope connected with long-range forecasting of the dates of ice formation.

The freeze-up dates in the mouth areas of the Kara Sea Basin have a significant (up to a month and more) amplitude of variations. Determination of the typical features in interannual variations of the dates of the onset of the ice phase is of great importance for developing methods of forecasting both for choosing the methods of the studies and for selecting the most predictable initial characteristics.

The study presents the results of spatial-temporal statistical analysis on the basis of information on the freeze-up dates from the stationary observation network and airborne ice reconnaissance flights. 19 time series in the points located in the Ob'-Taz and Yenisey mouth areas have been considered.

In order to substantiate the use of the methods of multi-dimensional statistical analysis when solving the forecastings problems, verification of hypotheses of a random and stationary character of the series, as well as of their belonging to the normal distribution law was performed.

The calculation results have shown that almost for all considered time series the hypothesis of a random character, i.e. of the absence of relations within the series was not contradicted. The suggestion of the stationary character (uniformity) was not confirmed only for two time samplings at the Yenisey river (Igarka and Dudinka towns). It is likely to be related to economic activities and, particularly for the Dudinka town, to all-year-round navigation in the lower reaches of Yenisey. The hypothesis about the considered series belonging to a normal distribution law was not contradicted. Using theoretical curves of the distribution law, optimal for each series, extreme possible freeze-up dates are determined.

An analysis of self-correlating functions of the remainder of the smoothed series of the freeze-up dates has indicated an existence of a 1-2 year cyclicity in their interannual fluctuations.

A spatial analysis of the freeze-up dates performed using current information and methods has confirmed the correctness of the zonation of the study region by the freeze-up dates made by the author in the late 1970s.

MODELING OF WATER QUALITY DYNAMICS IN THE NORTHERN OB' GULF

S.S. Khrustalev (RF SRC the AARI)

The work aims at modeling the dynamics of water quality in the stratified zone of the Ob' Gulf in the wintertime based on the following characteristics: oxygen level, BOD₅ and inorganic nitrogen forms (ammonium, nitrate, nitrite) averaged over the river width.

For applying the mathematical model, the northern Ob' Gulf was selected which is part of the Ob'-Taz mouth area beyond which sea water does not spread. The distinguishing feature of the regime in the northern Ob' gulf is the existence of a stable vertical density stratification in all seasons of the year. According to observation data, it is not destroyed either during the flood period or by constant tides. The main factor maintaining a stable density stratification in the zone of river/sea water interaction in the Ob' Gulf is penetration of saline water near the bottom. The location of the boundary of sea water in the northern Ob'-Taz mouth area during a year does not remain stable. Depending on the value of the river runoff, the presence of the ice cover and hydrometeorological conditions it changes over a wide range. The largest penetration of sea water to the gulf is observed in March-April when there are the least freshwater inflow, the largest salinity at the sea boundary and the low background level in the Kara Sea. The least intrusion is observed in July-August when the largest river water inflow, the least salinity at the sea boundary and the high background sea level are observed. The distribution of the river water inflow within a year has the greatest influence on intrusion of sea water in the Ob' Gulf. The discharge of fresh water in the vicinity of the Trekhbugorny cape is, on average, 16800 cu./s, varying within 4000 - 55000 cu.m/s. The amplitude of seasonal variations of the background level is 0.3-0.4 m. Seasonal variations in salinity in the surface layer at the sea boundary in the mouth area reach 20-25% /6/.

It should also be noted that the Ob' Gulf is a unique water body which is of large economic, social and nature protection importance. It is a zone of the enhanced ecological risk as a result of human oil and gas exploration activities. But the ecological state of this body is insufficiently studied and the behaviour of pollutants and water quality elements, especially in the zone of sea water intrusion is actually non-investigated. Thus modeling of water quality dynamics in this water body is of important scientific and applied significance.

To resolve this problem, a profile two-dimensional mathematical model is used, based on the equation of transfer and transformation of water dissolved substances /7/. To take into account the destruction of mixtures, parameterization of the processes of transformation of DO-BOD and inorganic forms of nitrogen is applied /1, 2, 4/.

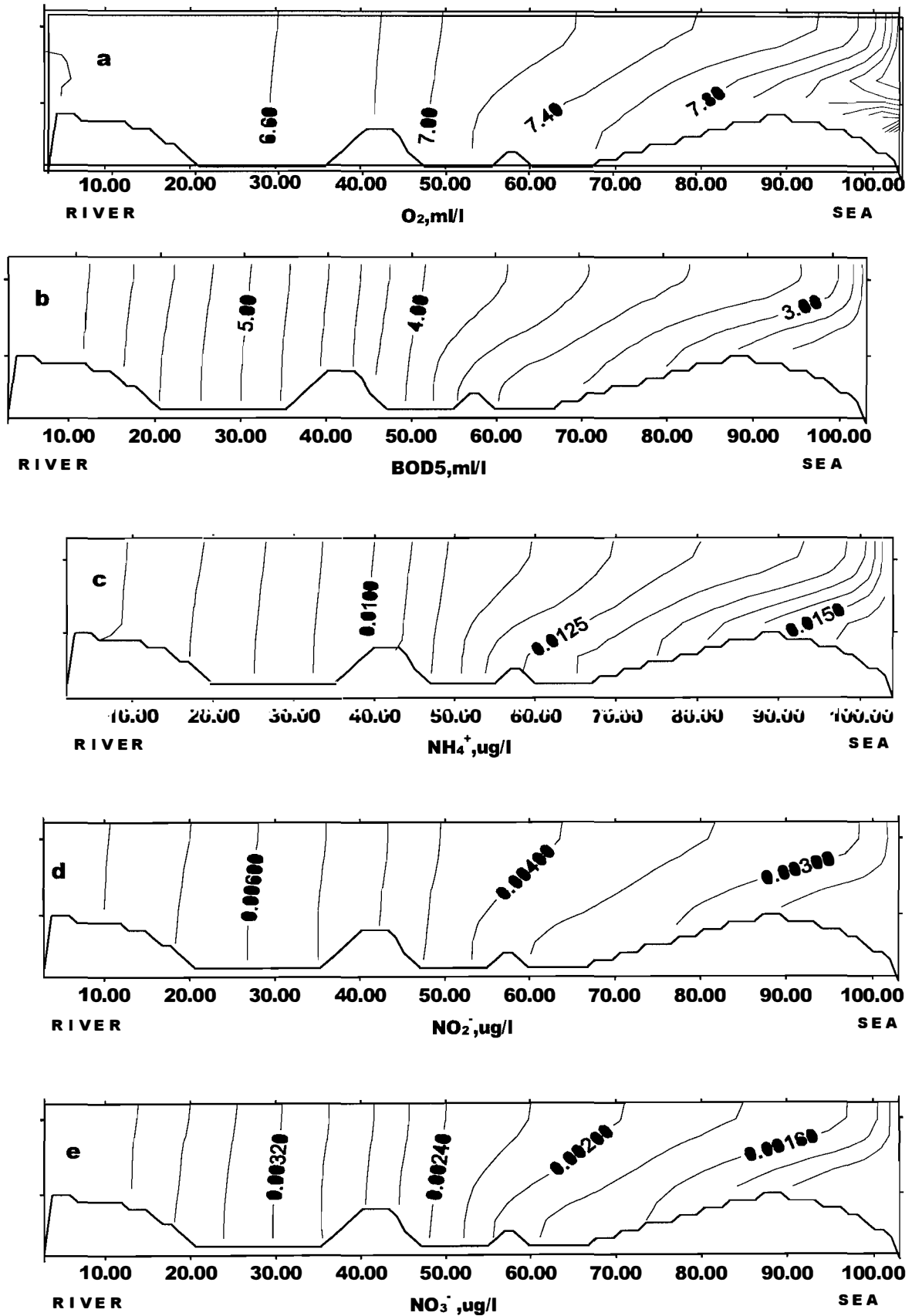


Fig. 1 Vertical profiles of water quality elements in the northern Ob' Gulf. a - oxygen, ml/l; b - BOD5, ml/l; c - ammonium, ug/l; d nitrite, ug/l; e - nitrate, ug/l;

At the initial moment the content of the water quality elements at each point of the calculation grid is equal to zero. As boundary conditions, the profiles of the calculated characteristics at the boundaries of the calculation areas and the substance fluxes at the water surface and near the bottom are calculated. The model is computer-based in Turbo Basic language with a graphic depiction of the fields of water quality characteristics under study /5/. Data on the current speed and turbulence coefficient profile are calculated using a profile two-dimensional mathematical model of the halocline dynamics in the river mouths /3/.

The calculation zone presented a scheme of the northern Ob' Gulf 500 km long from the Trekhbugorny Cape to the Poyelov Cape. The Trekhbugorny Cape was assumed to be the river boundary of the calculation area. The width of the Gulf in the delineated calculation area varies from 35 to 85 km at mean by section depths from 12 to 20 m. The horizontal spacing is 5 km, the number of points - 101, the vertical spacing - 1 m, the number of points - 21, which is consistent with /6/.

As a result of numerical experiments for average conditions in February, a spatial distribution of oxygen, BOD5 and three inorganic nitrogen forms is obtained (Fig. 1).

The distribution of oxygen in the southern part of the calculation zone is practically linear by vertical with a small decrease in the content when moving from the surface to the bottom. In the zone of sea/river water interaction there is a dramatic lamination by vertical which is probably, related to the saline water wedge blocking oxygen penetration to the near-bottom layer where the content is 2-2.5 ml/l less than in the surface layer (Fig. 1a).

The BOD5 decreases when moving toward the sea, but while in the southern part the changes by vertical are insignificant, in the halocline zone the BOD considerably changes with depth which is related to the low oxygen content in the lower layer and to a greater BOD of river water as compared to sea water (Fig. 1b).

As to the distribution of inorganic nitrogen forms, approaching the sea boundary of the calculation area, the content of ammonium increases and of nitrate and nitrite decreases; respectively in the zone of sea water influence the level of ammonium increases with depth and of the other forms decreases (Fig. 1c-1e).

In conclusion, it should be stressed that the model can be used for calculating other characteristics of water quality in the zone of river/sea water interaction and for obtaining the spatial-temporal variability of these characteristics, not only for the Ob' gulf, but also for the other arctic estuaries with a pronounced halocline.

References

1. Aizatullin T.A., Leonov A.V. Kinematics of transformation

- of nitrogen compounds in natural water. - Hydrochemical materials, 1975, vol.44, pp.177-183.
2. Aizatullin T.A., Leonov A.V. Kinematics of transformation of nutrient compounds and oxygen consumption in sea water (mathematical modeling). - Oceanology, 1975, vol. 15, No.4, pp.622-633.
 3. Doronin Yu.P., Ivanov V.V., Svyatsky A.Z. Mathematical modeling of the processes of river/sea water interaction in the mouths of rivers of the Arctic zone. - Proc. of the 5th All-Union Hydrological Congress, vol.9 "River mouths", L., Gidrometeoizdat, pp.163-170.
 4. Yeremenko Ye.V. Modeling of transformation of nitrogen compounds for water quality management in waterways. - Water resources, 1980, No.5, pp.110-117.
 5. Yeremina T.R. A mathematical model of spreading of a conservative mixture in a stratified estuary. Methods of hydrophysical studies: Abstracts of the 3d All-Union School-Workshop, Svetlogorsk, May16-26, Kalinigrad: AN SSSR, 1989, 87 p.
 6. Ivanov V.V., Svyatsky A.Z. Numerical modeling of sea water intrusion to the river mouths at a seasonal temporal scale. Water resources, 1987, No.5, pp.116-122.
 7. Ozmidov R.V. Diffusion of mixtures in the ocean. L.: Gidrometeoizdat, 1986, 278 p.

ESTIMATE OF THE CHANGE IN THE YENISEY RIVER INFLOW TO THE KARA SEA AS AFFECTED BY INDUSTRIAL ACTIVITIES IN ITS BASIN

A.I. Shiklomanov(AARI)

The Yenisey river runoff significantly influences the Kara Sea regime. Since 1958 the hydrological regime of the Yenisey has been subjected to an intensive anthropogenic impact as a result of constructing hydroelectric power stations in its basin. That is why also the characteristics of its inflow to the Kara Sea change.

In order to assess the effect of economic activities in the Yenisey Basin on the characteristics of its hydrological regime, a numerical model of the runoff transformation of the Yenisey by 10-day time intervals based on the genetic runoff formula, was developed. The use of this method is suitable, as at a relatively small amount of initial information and easy computer implementation it provides satisfactory results in considerable zones of the basins. This allows its use for calculating runoff in large water catchment areas. Model verification using independent data has shown that the mean relative error of model water discharges does not exceed 10-12% and one can conclude that the used transformation scheme sufficiently reliably describes the process of unstable water motion in the channel network of Yenisey and its tributaries and can be used for reconstructing runoff hydrographs.

By using numerical model natural 10-day runoff hydrographs were reconstructed by means of the main sections of the channel network of the Yenisey Basin and at the downstream measuring section Yenisey-Igarka. On the basis of comparing reconstructed (natural) runoff values with actual (observed) ones an assessment of the effect of economic activities on the Yenisey runoff since 1958 has been made. During the period under consideration the Yenisey runoff was approximately 500 cu.km smaller, mainly due to water accumulation in barrier basins. And a particularly considerable runoff decrease of 40.5 cu.km/year was observed in 1962-1969 when Bratskoye and Krasnoyarskoye barrier basins were filled. Sig

nificant changes have also taken place in the intraannual runoff distribution, especially in the upper and middle current of the Yenisey. At the downstream measuring section near the Igarka town due to channel regulating in the basin, the winter low water runoff increased by 30-50 % and the flood water volume increased by 10%.

Sea ice (including Remote-Sensing)

ON THE QUESTION OF ICEBERGS IN THE ARCTIC SEAS

V.A. Abramov, Ye.G. Shvedov (the AARI)

Changes in the number of icebergs according to data of airborne ice reconnaissance during the period 1936-1993 in the Arctic Seas are investigated. A method for calculating the number of icebergs is presented. Seasonal and interseasonal changes in the number of icebergs, as well as some features of their spatial distribution are analyzed.

Icebergs that calve from the glaciers on Spitsbergen, Franz-Josef Land, Novaya Zemlya and Severnaya Zemlya are one of the components of the ice regime of the Arctic Seas.

The number of icebergs, their spatial distribution undergo changes both within a year and from year-to-year. The southern boundary of the iceberg extent also considerably varies and it is possible to consider it a climatic indicator /6/. Also, a great deal of attention is paid to the problem of iceberg distribution in connection with the increased activities on the shelf of these seas, since icebergs present a potential threat to off-shore and coastal structures.

The article is a continuation of earlier studies /1, 2, 6/ and its main aim is to assess the number of icebergs in the Barents and Kara Seas.

In conducting visual airborne ice reconnaissance icebergs were recorded by observers. If a group of icebergs was encountered, the position of the center of the group was recorded and the total number of icebergs was indicated. During flights data were recorded on the ice charts with a root-mean-square error from 2.2 to 12.6 nautical miles depending on conditions and the region of observations /3/.

The ice charts compiled on the basis of visual airborne ice observations are stored at the archive of the AARI /4/. It should be noted that airborne ice reconnaissance flights were conducted all-year-round, but in winter their frequency was much less than in summer. By using these charts, the database of icebergs was prepared. Its outline is given in /2/.

In the course of the work 2329 reconnaissance flights from 1936 to 1993 where about 40 000 icebergs were recorded, were analyzed.

The reconnaissance flights during the years under consideration covered a certain area along the flight route. Hence, information on the number of icebergs is incomplete. It was necessary to proceed from the number of icebergs observed along the flight routes to the possible number of icebergs over the whole of the study area. For this estimate a hypothesis of the uniform distribution of icebergs in the study region was assumed.

To address this objective the area of the seas covered by ice reconnaissance flights in a given month was calculated. Calculations took into account mean velocity of aircraft, the flight altitude, the surveillance width at a given flight altitude, duration of airborne reconnaissance and the number of the reconnaissance flights during a month. On the basis of this information the area of the sea which was surveyed during airborne ice reconnaissance every month was calculated. Then assuming the uniform distribution of icebergs, it is possible to calculate the number of icebergs in the whole study region. Thus, the number of icebergs over the whole study area by years and the number of icebergs per a 100x100 km square were calculated for the entire time interval. These data serve as a basis for studies.

On average from 1943 to 1989 there are annually 774 icebergs in the study region or 4 icebergs per 10000 sq. km (a 100x100 km square).

If one takes into account mean statistical iceberg dimensions /6/, then the volume of icebergs for a year in the study region is 0.18 cu.km. This is inconsistent with the calculated estimates of glaciologists equal to 4.61 cu.km of icebergs a year due to their calving from glaciers /5/. This difference with glaciological data may arise due to

incorrect estimates of the volume of an average iceberg, number of icebergs in the region or errors in calculations of glaciologists. A probable reason for the discrepancy in the results can be the fact that glaciers along with icebergs of considerable size produce a large number of smaller icebergs which melt and are destroyed in the regions of their production and it is impossible to record them.

The distribution of icebergs in the North-European Basin undergoes both changes within a year and from year-to-year. The chart in Fig. 1 illustrates the maximum concentration of icebergs in March during the period 1936-1993. The presented data show the distribution of icebergs in the Barents and Kara Seas and in the Arctic Basin.

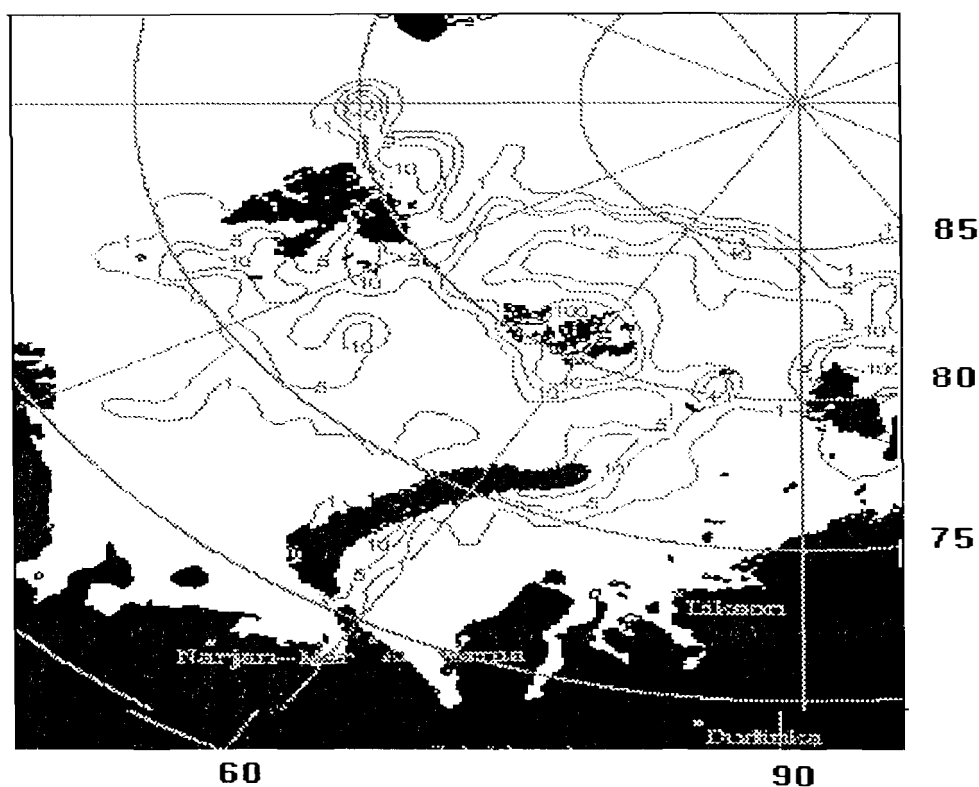


Fig.1 Spatial distribution of the maximum concentration of icebergs in March during the period 1936-1993.

One may note that in December-January icebergs are mainly centered near the centers of their production. In spring in connection with the break-up processes of fast ice, icebergs are exported and spread over the seas. In April-June icebergs are observed up to the coast of the Kola peninsula and in the south-western Kara Sea they are exported to Kara Gate strait. From August to October the decrease in the concentration of icebergs near the main centers of iceberg production and a simultaneous northward shift in the southern boundary of their export are observed.

Seasonal changes in the number of icebergs observed on the average in the area of 10 000 sq. km are shown in Fig. 2(a). Seasonal variations have two maxima: in April and in September and two minima: in January and in June-July.

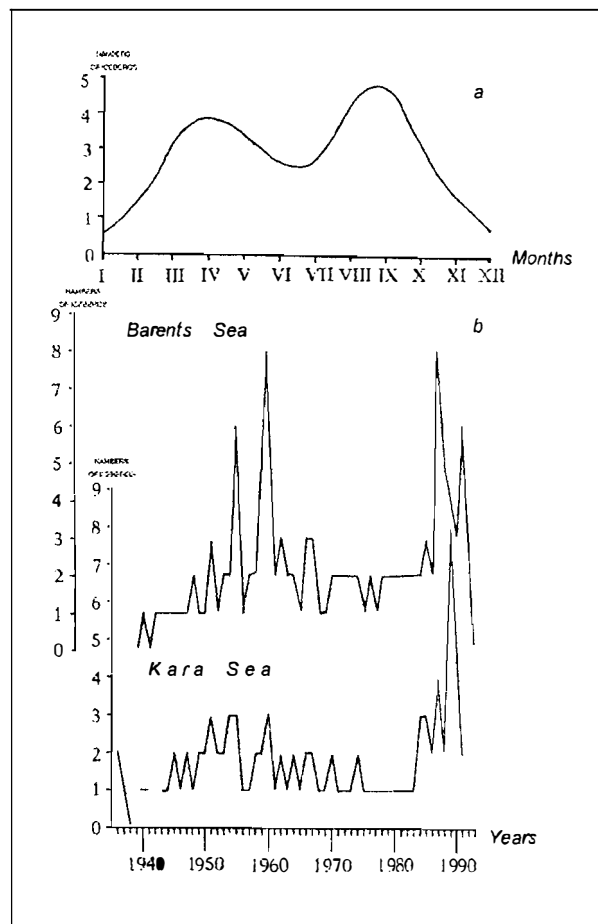


Fig.2 Seasonal (a) and Interannual (b) changes in the number of icebergs observed in the Barents and the Kara Seas on the average in the area of 10 000 sq.

Interannual changes in the number of icebergs in the Barents and the Kara Seas are shown in Fig. 2(b). As is seen, from the early 1950s to the early 1960s the number of icebergs in the Barents Sea increased. Then up to the mid 1980s the number of icebergs was reduced on the whole in the region. From 1985 there was an increase in the number of icebergs both in the Barents and the Kara Seas. In 1987 in the Barents Sea and in 1989 in the Kara Sea an extreme number of icebergs was recorded for the period under consideration. For the same time interval the northernmost southern latitude of the iceberg distribution in the eastern Barents Sea 71.8 N was recorded.

The maximum and minimum number of icebergs during a year is, probably, connected with seasonal variations in natural processes. Icebergs calved from glaciers in winter are accumulated off islands where fast ice and shallow water prevent their spreading. In March-April with the decay of fast ice, icebergs and melting ice cover, icebergs begin to spread over the area of the seas. This can account for the increase in icebergs in April. With the increase in air and water temperature icebergs begin to intensively melt and decay. In June their number decreases. With the increase in air temperature, production of icebergs by glaciers grows. In August-September the number of icebergs increases again. This, probably, accounts for the second maximum in seasonal variations of changes in the number of icebergs. At the beginning of winter the number of icebergs is reduced, since most of icebergs are destroyed by that time.

Thus, the analysis allowed us to reveal some features in the distribution of icebergs in the North-European Basin.

1. Abramov V.A. Icebergs in the North-European Basin. 2. Abramov V.A., Benzeman V. Yu., Klyachkin S.V., Shvedov Ye.G. Characteristics of the database of icebergs of the Arctic Seas and the Arctic Basin.
3. Bushuyev A.V., Loshilov V.S. Accuracy of airborne RI. - 1967. - vol. 257. - pp.84-92.
4. Charts of airborne ice reconnaissance in the Arctic Seas. - St. Petersburg: Archives of the AARI. - 1936-1989.
5. Koryakin V.S. Glaciers of the Arctic. - M.: - Nauka. - 1988. - 158 p.
6. Abramov V.A. Russian iceberg observations in the Barents Sea, 1933-1990. - Pol. Res. - 1992. - 11(2). - pp.93-97.

RUSSIAN ARCHIVED OBSERVATION DATA ON ICE THICKNESS IN THE KARA SEA

Ye. O. Aksenov, S.V. Brestkin, A. Ya. Busuyev, V.F. Dubovtsev, S. Yu. Nikolayev, V.S. Porubayev (the AARI)

Ice thickness is considered one of the most interesting ice cover characteristics both for basic studies in the Northern polar region and from the viewpoint of practice (navigation in high latitudes, oil-gas production on the shelf of the Arctic seas, ecology of polar regions, etc.). The AARI has accumulated a considerable amount of observation data on ice thickness using different observation methods. These observations include measurements of fast ice and drifting ice thickness, observations of the amount of ice hummocking and decay, age categories, measurements of the snow depth on the ice, observations of ice and snow melting from the upper surface, etc. (Fig.1).

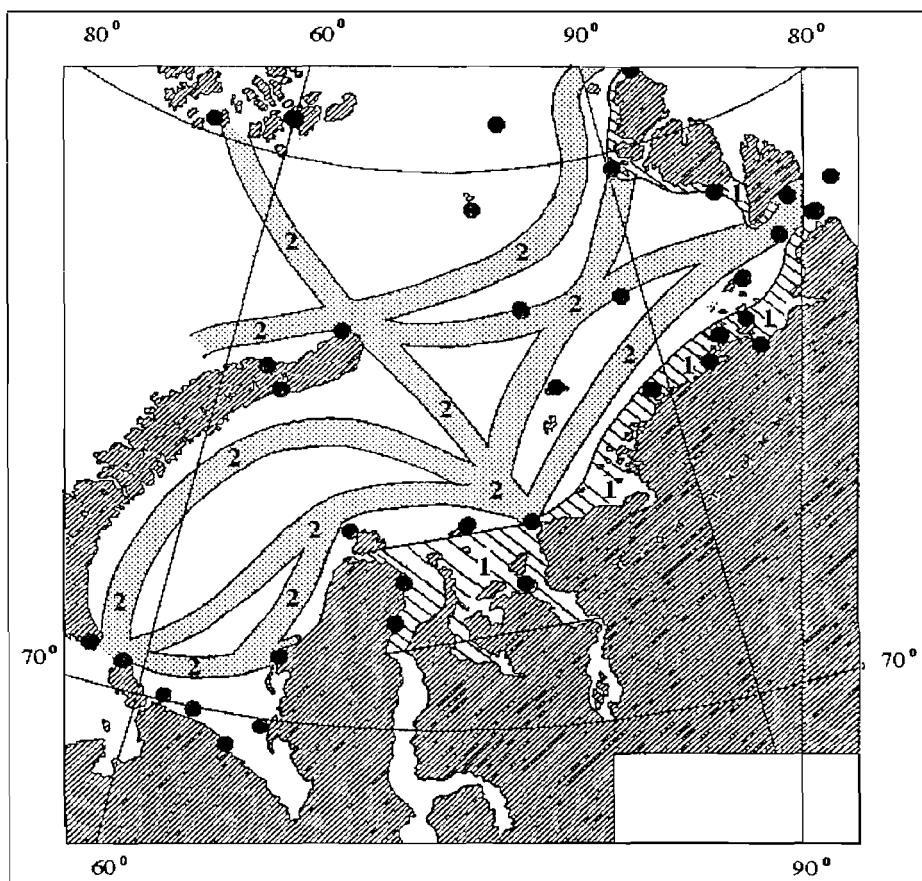


Fig. 1. Location of the polygons of area surveys of the ice thickness by hydrographic parties (1), measurements points at coastal stations (•), main routes of shipborne observations (2).

All observations of ice thickness can be divided into regular and episodic. Regular observations are observations which were carried out with an almost constant time interval (once in a 10-day period, once a month, once a year) in the given region. Such observations include measurements of fast ice thickness at polar stations at a fixed point and at linear short profiles; polygon surveys of fast ice in Vil'kitsky strait and its western approaches; polygon surveys of the Ob' Gulf and the Yenisey Bay; special shipborne observations of icebreakers when escorting ships along the Northern Sea Route and part of observation data of the airborne "Sever" expeditions.

Episodic observations include data of ice thickness measurements by hydrographic teams, geological expeditions, airborne "Sever" expeditions. Spatial scales of ice thickness measurements are from several hundred meters to several thousand kilometers. The spacing varies from several meters to several tens of kilometers.

When measurements were performed on fast ice during hydrographic expeditions, areal surveys with ice thickness and snow depth measurements (Fig. 1) were carried out. Also, the deformation extent of the ice cover was determined according to the scale of 5 arbitrary units of the amount of hummocking. Measurements were carried out in March-first 10-day period of May when ice thickness reaches the largest values or is close to them. Drilling of the ice cover of steady growth and measurements of its thickness by means of a stake were carried out. The accuracy of measurements was on the average (+-) 2 cm. Observations were made from 1958 to 1985. The total number of measurements was about 10 000. The distances between the points of measurements at the polygons were from 100 to 1000 m. The geolocation was by means of the triangulation grid near the coast and by notation (including satellite) at a distance from the coast.

The most complete and long historical observation series of the ice cover are data of measurements of fast ice that are carried out at the Russian polar stations. These direct instrumental observations are performed by means of common methods since 1913 up to present. Measurements begin in the fall from the moment the fast ice reaches the thickness of 10-20 cm and end during the spring-summer period at break-up of fast ice or when the degree of ice decay reaches 3-4 arbitrary units (Fig. 2). Measurements are performed on level ice, ice thickness and submergence depth are determined by means of a T-shaped stake //.

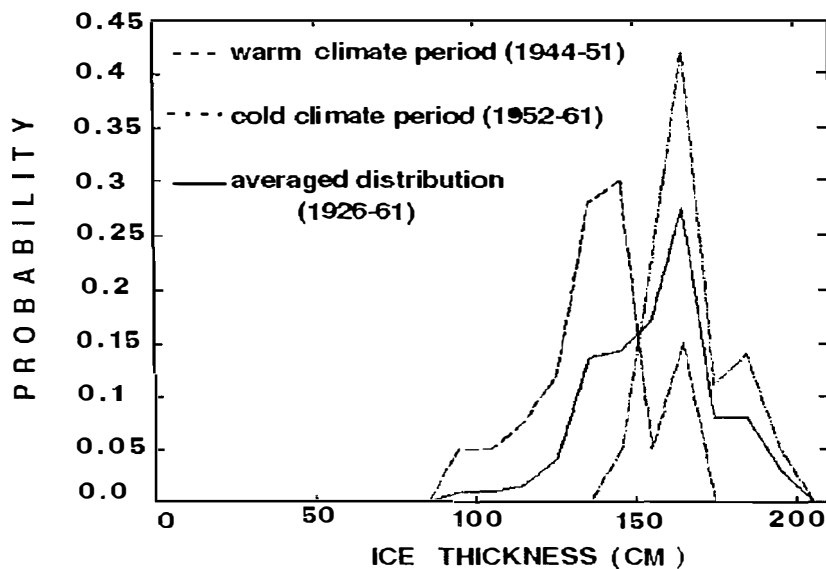


Fig. 2. Distribution of the maximum ice thickness at the Dikson polar station at the onset of melting in the observation data from 1926 to 1961.

From the onset of the period of melting observations are carried out daily. For other seasons measurements are carried out daily, every two days, every five days and every 10 days at ice thicknesses, respectively, up to 20 cm, from 20 to 50 cm, from 50 cm to 100 cm and above 100 cm.

The observation polygon which characterizes the entire observation region in the vicinity of the polar station is selected //.

For the period from 1913 (opening of the Yugorsky Shar station) up to present about sixty stations carried out observations in the Kara Sea. The station network covers the whole area of the Kara Sea including Vil'kitsky strait and the northern regions of the Kara Sea Franz-Josef Land and Severnaya Zemlya (Fig. 1). The volume of the data set is about 40 000 measurements.

Simultaneously with ice thickness measurements there were carried out measurements of the snow cover depth, observations of fast ice hummocking, degree of its decay and ice age categories were determined. Profile measurements of ice thickness were performed on fast ice near the polar stations from 1960 at two profiles 200-400 m long.

To select an optimal route for navigation of ships in the ice of the least thickness and the reduced amount of hummocking, areal surveys with measurements of ice thickness and hummocking were carried out from 1961 to 1971 in B. Vil'kitsky strait and at its western approaches in springtime (Fig. 3). Measurements were performed by means of a stake. The accuracy of observations was (+-) 1 cm. Polygon surveys of the Ob' Gulf and the Yenisey Bay were conducted using similar methods.

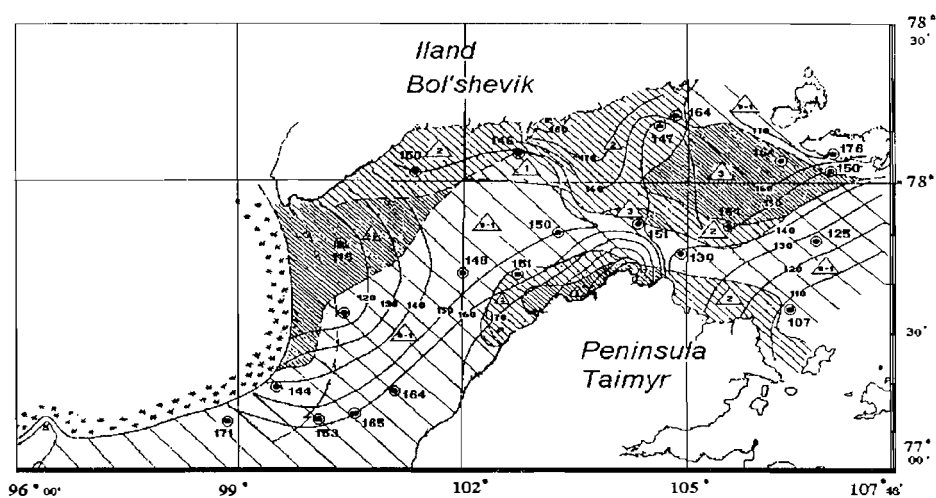


Fig. 3. An example of an ice-measuring survey of fast ice in the north-eastern Kara Sea, May 6-10, 1961.

A considerable amount of data on ice thickness and other ice parameters were obtained during special observations of icebreaking expeditions of the AARI from 1961 to 1987 when escorting transport ships along the traditional Northern Sea Route variant or along its high-latitude variants (Fig. 1). When shipborne ice observations along the route are carried out, relatively uniform zones with regard to the set of ice characteristics are delineated visually. The time and coordinates of the beginning and end of zones, as well as values of a number of ice characteristics determined onboard a ship are recorded. Most interesting of them are the ice thickness, amount of hummocking and decay of ice, the snow cover depth and partial concentration of ice of different thickness ranges or different age categories. The length of the uniform zones is from 2 to 30 nautical miles. Observation data are contained in the log of ship observations. A brief description of the cruises is presented in Table 1. The total volume of observations was about 7000 observations.

Ice thickness measurements were also performed by the high-latitude airborne "Sever" expeditions. Level ice was drilled and its thickness was measured by a stake, also the snow cover depth was measured. On the basis of airborne ice reconnaissance on the route the amount of hummocking and decay of the ice cover were determined. The expeditions cover the period from 1955 to 1993. From 1979 measurements were carried out basically at the same geographical points.

To successfully address a large number of research and practical objectives it is necessary to have a possibility for a composite ice thickness data processing. At present the AARI creates the database on ice thickness of the Arctic Basin: intermediate archives on magnetic media are created and ice thickness observation data are introduced into the database. The main difficulty for the combined analysis of the data of measurements obtained from different sources is the need for combining the observations performed using different methods, i.e. of observations performed with different accuracy and for different spatial-temporal scales.

Tabl.1 Special ship's observations from the ice thickness (1960-1987)

PERIOD OBSERVATION	ICEBREAKER	RESEARCH AREA
VI - IX 1960 VI - IX 1961 VI - X 1964	"MOSKVA"	BARENTS SEA, KARA SEA, LAPTEV SEA VLADIVOSTOK-MURMANSK
VI - IX 1960 VI - IX 1961 VI - X 1964	"LENINGRAD"	FRANZ JOSEF LAND, YENISEY BAY KARA SEA, LAPTEV SEA
VI - VIII 1967 VI - VIII 1976	"KIEV"	BARENTS SEA, KARA SEA
V - VII 1969 V - VII 1970	"MURMANSK"	FRANZ JOSEF LAND, YENISEY BAY KARA SEA, LAPTEV SEA
V-VI, XI-XII 1970 V-VI, XI-XII 1971 V-VI, XI-XII 1972 V-VI, XI-XII 1973	"LENIN"	MURMANSK-DUDINKA, MURMANSK-PEVEK (HLV)*
VII-IX 1974	"YERMAK"	KARA SEA, LAPTEV SEA
II-IX, XI-XII 1975 II-IX, XI-XII 1976 II-IX, XI-XII 1977 II-IX, XI-XII 1981 II-IX, XI-XII 1984	"ARKTIKA"	FRANZ JOSEF LAND, KARA SEA, LAPTEV SEA
XII-II 1977 XII-II 1978 V-VII 1980 V-VII 1982	"KAPITAN SOROKIN"	KARA SEA, YENISEY BAY KARA SEA, YENISEY BAY OB' GULF OB' GULF
V-VII 1978 II-III 1985 III-VI 1987	"SIBIR"	BARENTS SEA-CHUKCHI SEA (HLV)* (nuclear) KARA SEA, YENISEY BAY KARA SEA, LAPTEV SEA, NORTH POLE
IV-VI 1986	"ROSSIA"	FRANZ JOSEF LAND, MURMANSK- PEVEK (nuclear)

(HLV)* - High-latitude variants of the Northern Sea Route.

References

1. The Manual for hydrometeorological stations and posts, Part I, Hydrological observations at coastal stations and posts, Leningrad, Gidrometeoizdat, 1984, 310 p.

STUDIES OF SEA ICE DYNAMICS IN THE KARA AND LAPTEV SEAS FROM SATELLITE IMAGES

V. Yu. Aleksandrov, T. V. Rakhina

Introduction

The ice drift in the Arctic Basin governs ice exchange with the Arctic Seas and influences ice conditions. A large-scale circulation of sea ice in the Arctic Ocean has been quite well investigated from data of drifting stations and buoys. The polar High and the Icelandic and Aleutian Lows, continuously interacting, govern the rate and the direction of shifts of ice massifs in the Arctic Basin, contributing to the development or the attenuation of the Transarctic ice flow and the anticyclonic ice gyre. In the Laptev Sea the northward and north-westward drift prevail all season long. In winter in the Kara Sea the northward ice export prevails and in spring-summer - westward, south-westward and southward drift directions.

However, mesoscale sea ice dynamics in the Kara and Laptev Seas has been comparatively little investigated, since it requires deployment of a large number of drifting buoys. Hence, the only technique for mesoscale drift studies is a regular analysis of successive satellite images covering the same regions of the Arctic Ocean.

Main results

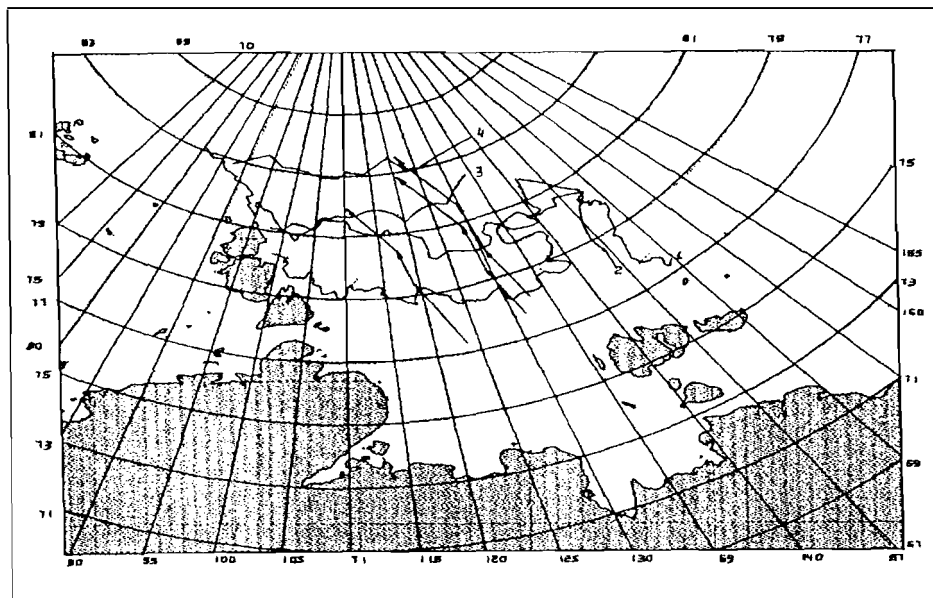
Algorithms and software evolved at the AARI allow the determination of the ice drift from successive images of one and the same region in the interactive mode /1/. The geographically located images using orbital data and correction by ground control points, are visualized on a computer screen; the geographical coordinates of any image pixel are determined. As a rule, ice floes and discontinuities in the ice cover that are distinguished on successive satellite images are chosen for determining the drift. For estimating sea ice dynamics there are used images in the visible and IR ranges, as well as satellite radar images which do not depend on weather conditions and natural illumination.

Studies of the possibility for regular drift determinations from visual satellite images received from NOAA and "Meteor" were made. For this purpose a series of AVHRR NOAA images for the period August-September 1993 covering the region of the Laptev Sea was processed /2/. A spatial drift structure for the western and eastern regions of the Laptev Sea was obtained for this period. The analysis and comparison with data of the drifting Argos buoys has shown good agreement of the obtained drift vectors both in value and direction. However, due to constant clouds, it was impossible to obtain drift data in the central sea region.

Satellite radar images are most suitable for studies of sea ice dynamics due to their independence on light and weather conditions. Radar images from the "Okean" satellite can be used for this purpose. In order to investigate a possibility for a regular drift determination from these images, a series of 80 images of the Laptev Sea was selected. It covered the period from the onset of autumn freezing of the sea in 1987 to the onset of melting in summer of 1988. The ice drift for this period was determined over the whole area of the sea. By analyzing the retrieved images, the trajectory of separate ice floes was traced and the drift for the entire study period was determined and the shift in the boundary of multiyear ice was obtained (Fig. 1a). The possibility for studying the drift of large ice massifs in the ice cover was shown. The obtained data confirm that the drift in the Laptev Sea is north-westward.

The possibility of determining the ice drift in the Kara Sea from satellite radar images is shown in Fig. 1b.

a



b

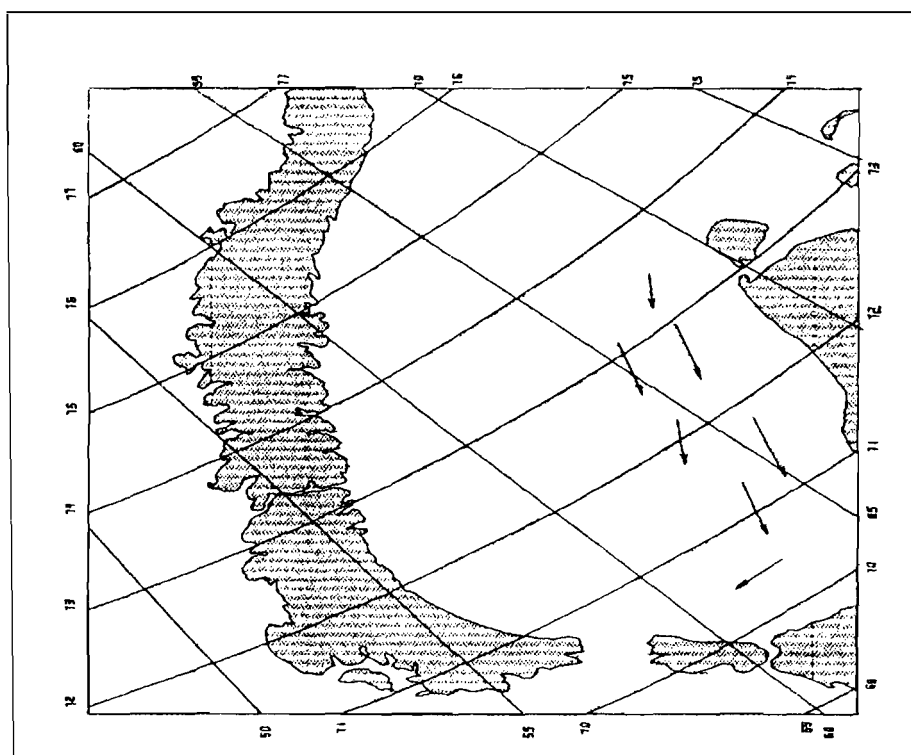


Fig. 1. Results of the drift determination from successive "Okean" images for different regions of the Arctic.

a) the Laptev Sea (05.11.1987-10.01.1988-29.03.1988-06.05.1988)

1 - November 2 - January 3 - March 4 - May b) the Kara Sea (30.12.1994-08.01.1995)

Conclusion

The analysis performed has shown the use of satellite images in studies of the ice cover dynamics to be very effective. Radar images allow regular drift monitoring independently of meteorological conditions.

At present an interactive image processing technique for the ice drift determination from successive satellite images is used. It allows a reliable ice drift determination, but it is time-consuming. Thus, to obtain data for large time intervals is difficult. Hence to achieve greater accuracy in determining the drift and reduce labour, software for automated determination of the drift vectors is being elaborated. Methods of cross-correlation, floe contour coincidence are used by tracking the drift from pairs of images.

References

1. A.V. Bushuyev, Yu.D. Bychenkov . - Study of sea ice distribution and dynamics from TV images of "Meteor". - Temporal instruction. - L., Gidrometepoizdat, 1978, 133 p.
2. V.Yu. Aleksandrov, H. Eiken, T. Martin. - Ice drift determination in the Laptev Sea from satellite images and buoy data. - In: Scientific results of the LAPEX-93 expedition, St. Petersburg, Gidrometeoizdat, 1994, pp.174-179.

VERY DANGEROUS ICE PHENOMENA IN BARENTS AND KARA SEA

V.A. Voevodin, V.V. Panov (AARI)

Force, duration, frequency and distribution area of wind-induced ice compaction are discussed on the basis of volumetric observational material on ice compaction from aircraft, helicopters, icebreakers and vessels. Main regularities of ice compaction both in summer and autumn-spring periods have been shown. Seasonal variability has been described. An account of spatial temporal structure of compaction has been given. Different types of spatial distribution of compaction: local, zonal and regional have been considered. The influence of hydrometeorological and other factors on compaction including speed, direction and duration of wind, types of location of baric systems etc have been presented. A diagram of zones with different degrees of compaction under cardinal winds, relationships between the degree of compaction and distance to the coast under coastward winds, types of center location for baric structures under heavy compaction and other data of prognostic importance as well as an example of the forecast of compaction developed together with co-authors have been given. Different aspects of the influence of compaction on navigation including lower ship speeds in ice due to different degrees of compaction, nip of icebreakers as well as the influence of compaction on the formation of "ice cushion" (a phenomenon of adhesion character) on boards of icebreakers. A negative influence of this phenomenon on navigation and others (ships icing, "ice river" - extremal ice drift) have been given.

**FIRST-YEAR BARENTS AND KARA SEA ICE: CALCULATED MEAN
MULTIYEAR MONTH VALUE OF MECHANICAL STRENGTH, ELASTIC
MODULI AND POTENTIAL RESISTANCE**

V.P. Gavrilov, S.M. Kovalev, G.A. Lebedev, O.A. Nedoshivin (AARI)

To calculate mechanical parameters of ice there are proposed to use the next hydrometeorological data as original ones: air temperature, ice thickness, snow cover thickness, temperature and salinity of water under ice layer. The scheme of ice strength calculation and equations for determination of elastic moduli and potential resistance are given.

Potential specific energy (J/cub m) of destruction of ice cover cubic element with side equal to its thickness, estimated as a ratio of square of ice compressive strength to Young modulus is a good illustration of estimating of potential resistance.

Spatial-temporal variability of this characteristics for thin, medium and thick first-year ice of the Barents and the Kara seas are discussing.

DISTRIBUTION OF ICEBERGS IN SEPARATE REGIONS OF THE BARENTS AND KARA SEAS

Yu. P. Gudoshnikov, G.K. Zubakin, A.K. Naumov (the AARI)

Studies of the probability characteristics of iceberg distribution in separate regions of the Barents and Kara Seas were performed using data of airborne reconnaissance and shipborne observations carried out by Russia and Norway during the period from 1888 to 1991 in the region restricted to coordinates: 67 - 86 N, 0 - 100 E /1-4/.

For correct statistical processing and analysis of the results of iceberg location, the repeated detections of icebergs during a month were excluded from the total observation set if several routes of airborne reconnaissance flights passed across the study region within this interval. The filtration of the detections was as follows. On the basis of the available observations of the drift of icebergs with "Argos" buoys /1/, the mean rate of the daily displacement of icebergs was determined for the northern Barents Sea. For this purpose the component excited by periodic forces was filtered. Then, if several reconnaissance flights during a month were available, each of the observations within a monthly interval was compared to observations falling on a later date. If the distance between the fixed points turned out to be less or equal to the expected one (taking into account mean rate) for the time interval under consideration, then it was assumed that two observations of one and the same iceberg were available. Of two observations the observation with the least number of icebergs was rejected.

The primary analysis of the set has shown the maximum number of icebergs (99) to be recorded on August 6, 1960 in the region north of Franz-Josef Land with coordinates 80.41 N and 54.55 E. It should be noted that probably, in this case bergy bits during the summer decay of icebergs were detected. This suggestion is confirmed by the fact that during this airborne reconnaissance 664 icebergs (or bergy bits) were recorded. The next accumulation of icebergs at one point second in number (90) was recorded on October 2, 1989 approximately in the same region north of the Georg Land (coordinates of 80.52 N, 50.00 E). The total number observed during this reconnaissance flight was 373 icebergs. There are 45 cases when more than 100 icebergs were observed during one reconnaissance flight.

For further estimate of the maximum possible number of icebergs once per N year by using the general iceberg drift pattern, iceberg records were selected from the database for 6 separate squares with a size 2 x 10 by latitude and longitude, respectively. For the same regions an analysis of the seasonal variability of the number of icebergs was performed. For this purpose mean monthly number of icebergs was calculated for each of the squares and then for comparison these values were normalized to the area of 10000 sq. km and to the mean monthly number of the reconnaissance flights. Coordinates of the regions and their areas are given in Table 1.

For this study we used the theory of statistics of extreme values whose practical application is presented in detail in the known monograph of E. Gumbel /5/.

The preliminary analysis of the distribution allowed us to conclude that its type was exponential (Fig. 1).

The verification of the hypothesis using the χ^2 criterion with a probability > 0.99 has confirmed the theoretical distribution to describe the process satisfactorily /6/. As a result of calculations, the theoretical distribution parameters were determined for all study squares and then the maximum possible number of icebergs in the study squares once in 5, 10, 25, 50 and 100 years were calculated (Table 2).

Table 1

Coordinates of the regions and their areas

N sq.	Coordinates		S area in sq.km
	Latitude	Longitude	
1	75-77	20-30	59709
2	78-80	55-65	47094
3	74-76	40-50	63880
4	76-78	65-75	55521
5	74-76	60-70	63880
6	78-80	40-50	47094

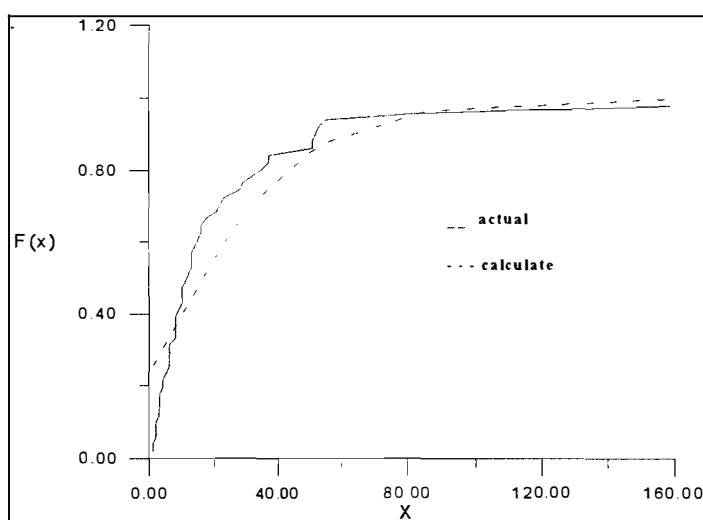


Fig. 1 The distribution function of the number of icebergs

For example, Fig. 2 presents a diagram of the distribution function for the square No.6 with the calculated 95% confidence intervals where ... is the presented variable /5/.

Table 2

The maximum possible number of icebergs once in N years

No. of the region	Period, years						
	2	5	10	20	25	50	100
1	12	27	36	45	48	57	66
2	23	47	63	78	83	98	113
3	5	14	20	25	27	32	37
4	9	21	29	37	40	47	55
5	18	29	40	50	53	64	74
6	17	43	60	77	82	98	114

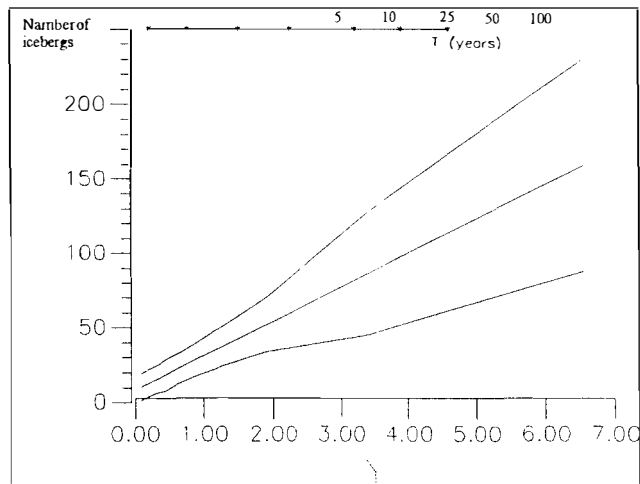


Fig. 2 The distribution function of the maximum number of icebergs for region 6.

As a result of the statistical processing of initial data, the diagrams of the distribution of mean monthly number of icebergs were obtained from multiyear values for the six delineated squares. For comparison of the results, the number of the observed icebergs was subjected to normalizing over the area (10000 sq. km), since the area of the selected squares was different. Further, we are dealing with a number of icebergs normalized to the area and to the mean monthly number of the reconnaissance flights.

The analysis of the diagrams shows that in square No. 6 (Fig. 3) the maximum of icebergs falls on April, then drifting and being partly destroyed, the icebergs leave this square and shift toward squares No. 1 and No. 3. In square No. 3 the maximum of icebergs falls on June. This is probably, explained by the import of icebergs which were formed in square No. 6 and in other regions. Then, the number of icebergs in this square in September decreases actually to zero due to their export and thermal decay.

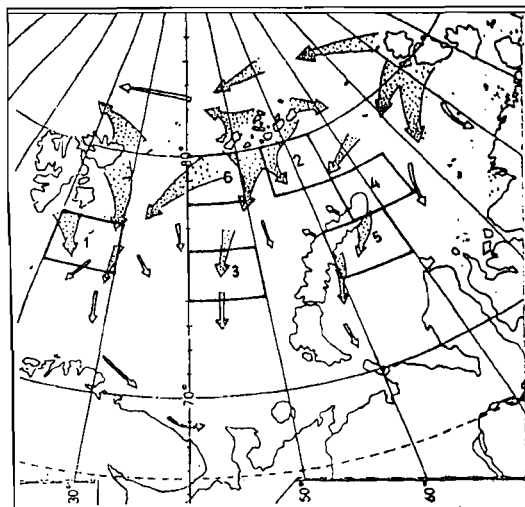


Fig. 3 The general drift pattern of icebergs

In square No. 1 the pattern is more smoothed, which is attributed to the import of a large number of icebergs from other regions where they were formed earlier than in square No. 6. In this square there is a similar reduction in September due to the same reasons.

The accumulation of icebergs in square No. 2 ends in March and their number in this square for four months steadily reduces due to their export and decay. Part of them shifts to square No. 4 where the maximum in April-June is clearly observed and some part, probably, moves to square No. 3 where together with icebergs from square No. 6 it governs a well-pronounced maximum. A small number of icebergs in square No. 2 in January can be attributed to the absence of the sufficient number of observations in connection with the reduced reconnaissance flights.

In square No. 5 the maximum number of icebergs is observed in September, then their number decreases, icebergs are quickly destroyed and leave the square partly moving to square No. 4 where the second local maximum is observed in November.

The obtained results are quite consistent with the general pattern of the drift and production of icebergs in the study region (Fig. 2).

The calculated distribution functions and control strips for the six squares allowed detection of the maximum possible number of icebergs once in N years for the six regions of the Barents and Kara Seas. Although these regions do not reflect a complete pattern of the spatial distribution of icebergs in the western Arctic, they, however, provide some understanding of the density of icebergs in the regions of their production and transit.

References

1. Doronin N., Vinje T. IDAP 92. Eastern Barents Sea Buoy Deployment. Vol. 1: Cruise Report, 1992.
2. Gudoshnikov Yu., Zubakin G., Naumov A. Iceberg distribution in the Region of Svalbard. AARI Project Report, 1994.
3. Abramov V., Zubakin G. Russian iceberg observations, 1970-1989. Project Report, 1992.
4. Vinje T., Zubakin G., Nikiforov A. Russian iceberg observations, 1936-1969. Project Report, 1992.
5. Gumbel E. Statistics of Extremes. Columbia University, Press N.Y., 1962.
6. Himmelblau David M. Process Analysis by Statistical Methods. John Willey and Sons, Inc., 1970.

ICEBERGS OF THE WESTERN ARCTIC (MORPHOMETRY, DISTRIBUTION AND DYNAMICS).

G.K. Zubakin , W. A. Abramov. Yu. P. Gudoshnikov, A. A. Dementiev, (AARI)

Present paper is based on results of five years long joint investigations of icebergs fulfilled by AARI and INTAARI on the one hand and by NPI and IDAP on the other hand. It includes also last studies carried out according to 'Rosshelf' company orders and is a peculiar review of this problem.

Data base was formed as a result of analysis of Russian and Norwegian archives (air reconnaissance and vessel observations), which is necessary for investigation and practical purposes.

Data ordered by months and years allowed us to calculate statistical characteristics, to reveal peculiarities of seasonal course and interannual variability and to compare these characteristics with other parameters of climatic system.

Places of iceberg calving and zones of their transit were revealed. Amounts of outflow and supply of glaciers production to the Western Arctic seas (the Barents and Kara seas) were determined. Maps of the mean monthly and maximum iceberg distribution were prepared.

Estimates of morphometric characteristics of the iceberg and of their volumes were fulfilled using not numerous measurements.

The distribution of extreme iceberg number in separate regions is described by the first limiting distribution.

The stochastic estimates of the iceberg number with return periods N years are of great importance for offshore constructions for oil and gas exploitation, because they are necessary for risk analysis. Such data were obtained for the Stockman condensate field region, for the Western Svalbard and for the south-western part of the Kara sea.

The estimates of iceberg drift velocities were calculated using materials of the IDAP expeditions in the years 1990 and 1992. The ARGOS automatic buoys deployed on the large icebergs allowed us to evaluate the mesoscale and synoptic variability of the drift velocities and to trace the general drift for 3-6 months (and up to 1 year). The data on the iceberg dynamics are of their own value and they also may be used as a test material for validation of stochastic and hydrodynamic models, which are developed in the 'Arctic-shelf' laboratory.

DYNAMIC-STOCHASTIC MODEL OF DRIFTING ICEBERG

B.V. Ivanov, Yu.P. Gudoshnikov, (AARI)

New dynamic-stochastic model for calculation of iceberg drift is represented. Surface pressure data for forecasting iceberg drift was used. A quantitative relationship between speed and direction iceberg drift and geostrophic wind, tides and mesoscale ocean calculation was revealed.

FEATURES OF ICE CONDITIONS IN THE BARENTS SEA DURING THE SPRING-SUMMER PERIOD 1993-1994 AND TENDENCIES TOWARD THEIR CHANGES IN THE LAST DECADE

Ye. U. Mironov, O.I. Babko (AARI)

Introduction The ice cover of the Barents Sea significantly influences physical processes in the boundary layers of the ocean and the atmosphere. Of particular importance appears to be the constant presence of the ice edge through the annual cycle which represents a well-pronounced frontal zone with large gradients of most hydrological and hydrochemical characteristics and enhanced biological activity. To identify features of the ice edge distribution and other parameters of ice conditions is significant for comprehensive studies of natural environment of the region.

Results A comparison of the main parameters of ice conditions (ice cover extent, ice edge position, multiyear ice area, ice thickness) during the spring-summer period 1993-1994 with mean multiyear data was performed. The ice cover extent of the sea or its separate regions is an integral indicator of ice conditions. Fig. 1 shows anomalies in the ice cover extent of the Barents Sea during the seasons under consideration. Ice conditions in the spring-summer season of 1993 were much easier than mean multiyear ones, except for August and September when there was ice advection from the Arctic Basin and the area of ice basically did not reduce during this period. Ice conditions in spring-summer of 1994 were much more favourable than mean multiyear ones. During May-September a large negative anomaly in the ice area and ice edge position was observed (see Fig. 1).

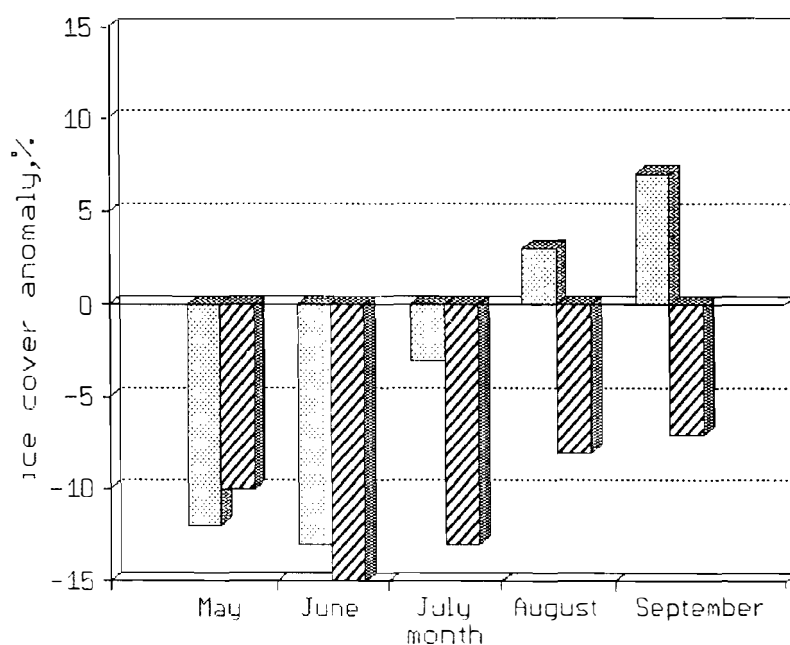


Fig.1 Anomalies of the ice cover extent in the Barents Sea during the spring-summer period 1993-1994.

1993
 1994

An analysis of the interannual variability of ice cover extent and ice edge position has shown that in recent years predominantly easy ice conditions were formed. During the last decade there were 8 years with a negative anomaly in the ice cover extent, including 4 years with a large negative anomaly (Table I).

Respectively, an easy type of the ice cover distribution was formed - the ice edge position and close ice boundaries are considerably more northward than mean values, a minimum amount of multiyear ice, etc. The period from 1985 to 1994 is characterized by the most favourable ice conditions in the spring-summer season over the whole series of observations from 1928 (Fig. 2) including the known period of warming in the Arctic (Zakharov, 1981; Zubakin, 1987).

Table I

Anomalies of the ice cover extent (in á units) in the Barents Sea in spring-summer during the last decade Year May June July August September

Year	May	June	July	August	September
1985	- 0.1	- 0.3	- 1.3	- 0.9	- 1.0
1986	+ 0.3	+ 0.2	- 0.5	- 0.4	- 1.0
1987	+ 0.7	+ 0.4	+ 0.5	- 0.1	- 0.2
1988	- 0.4	- 0.2	- 0.2	- 0.5	+ 0.3
1989	- 2.5	- 0.8	+ 0.1	+ 0.7	+ 2.3
1990	- 2.7	- 1.5	- 1.8	- 0.7	- 0.2
1991	- 0.8	- 0.8	- 1.1	- 0.2	- 1.0
1992	- 3.2	- 1.9	- 1.0	- 0.7	- 0.6
1993	- 1.2	- 1.2	- 0.3	+ 0.4	+ 1.3
1994	- 1.0	- 1.4	- 1.7	- 1.3	- 1.4

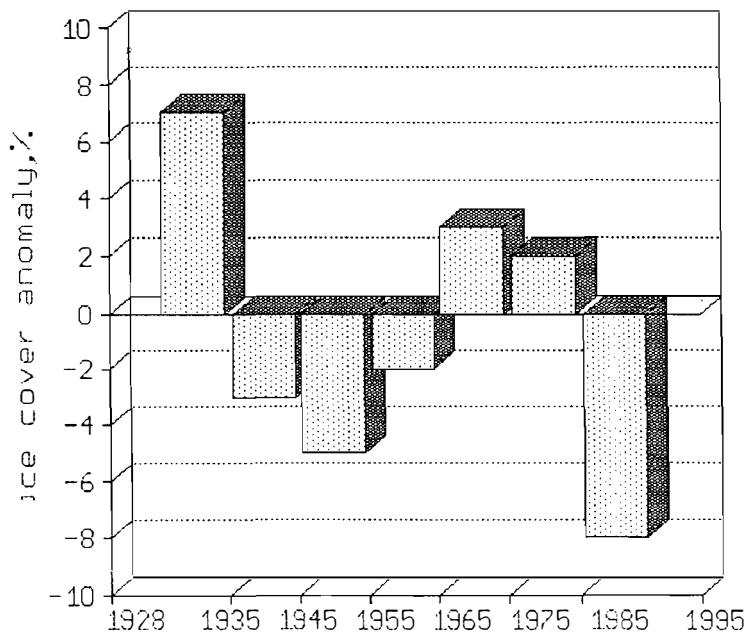


Fig.2 Anomalies of the ice cover extent in the Barents Sea in June by decades.

Conclusion As is evident from this analysis, for comprehensive environmental studies of the Barents Sea area and optimal planning of oceanographic expeditions it is important to take into account the features of sea ice distribution and a long-range forecast of their seasonal changes.

References

1. Zakharov V.F. Ice of the Arctic and current natural processes. - Leningrad, Gidrometeoizdat, 1981. - 136 p.
2. Zubakin G.K. Large-scale variability of the ice cover state in the seas of the North-European Basin. - Leningrad, Gidrometeoizdat, 1987. - 160 p.

Fig. 1. Anomalies in the ice cover extent of the Barents Sea during the spring-summer period 1993-1994.

Fig. 2. Anomalies in the ice cover extent in the Barents Sea in June by decades.

MODELLING THE VARIABILITY OF THE ICE COVER, TEMPERATURE AND SALINITY OF THE ARCTIC OCEAN

I. Polyakov, S. Kolesov and A. Naumov (the AARI)

The main aim of the work is to estimate the behaviour of the "ice-ocean" system on climatic scale. The employed model is a simplified version of a coupled sea ice-ocean model (Polyakov et al. 1994). It has a number of similar formulations with the model (Mellor & Kantha 1989). However, we have used a slightly different approach to parameterization of the ocean-to-ice heat flux. Also, the description of the ice cover dynamics and thermodynamics in a coupled model is based on ice thickness and concentration represented in the form of the distribution functions. This governs a more realistic simulation of the variability of the ice mass and thickness, since different rate of melting/growth of young and multiyear ice is taken into account.

Model description

Ice model

The main equations for the partial volume $h_i A_i$ and concentration A_i have the form

$$\partial(h_i A_i)/\partial t + \partial(u h_i A_i)/\partial x + \partial(v h_i A_i)/\partial y = R(h_i A_i), \quad (1)$$

$$\partial A_i/\partial t + \partial(u A_i)/\partial x + \partial(v A_i)/\partial y = R(A_i), \quad (2)$$

where h_i is the partial ice thickness, u , v are the ice drift rates, $R(h_i A_i)$ and $R(A_i)$ is the rate of the thermodynamic increase or decrease in the partial ice volume and concentration, respectively.

For determining the right-hand terms (1) and (2) the heat balance equation is used (Semtner 1976):

$$H_{\downarrow} + LE_{\downarrow} + \epsilon_s LW_{\downarrow} + (1 - \alpha_s)SW_{\downarrow} - \epsilon_s \sigma T_{srf}^4 + k_s/h_s(T_I - T_{srf}) = 0 \quad (3)$$

where H_{\downarrow} is the sensible heat, LE_{\downarrow} is the latent heat, LW_{\downarrow} is the incoming longwave radiation, α_s is the snow albedo, 0.99; σ is the Stefan-Boltzmann constant, k_s and h_s are heat conductivity and thickness of snow, T_I and T_{srf} is the surface temperature of ice and snow, respectively. A similar form of equation (3) with minor changes is used for the case of the ice without snow and open water.

Equation (3) allows obtaining new values of T_I and T_{srf} . If T_{srf} is higher than the temperature of melting 273.15 K, then T_{srf} is assumed to be equal to 273.15°K and the remaining energy is lost due to snow melting

$$-\Delta h_s = \Delta t/Q_s [H_{\downarrow} + LE_{\downarrow} + \epsilon_s LW_{\downarrow} + (1 - \alpha_s)SW_{\downarrow} - \epsilon_s \sigma T_{srf}^4 + k_s/h_s(T_I - T_{srf})], \quad (4)$$

where Q_s is the heat capacity of snow, 110 MJ/m³. If the calculated T_{srf} is higher than 273.15°K, then snow falls out on the surface. The rate of the snowfall is prescribed by the climatic mean (Parkinson 1978). On the bottom surface the ice thickness changes according to the formula

$$\Delta h_i = \Delta t/Q_I [k_I/h_i(T_b - T_I) - F_{\uparrow}], \quad (5)$$

where Q_I is the heat capacity of ice, 302 MJ/m³. k_I is the heat conductivity of ice, 2.04 W/(m°K); F_{\uparrow} - is the sea-to-ice heat flux. Parameterization of this flux in the model has the form

$$F_{\uparrow} = \rho_w c_p K_H \partial T/\partial z, \quad (6)$$

where ρ_w is water density, c_p is the specific heat capacity of ice, 4.194.19 KW/m³; K_H - is the mixing coefficient. The temperature gradient $\partial T/\partial z$ is assumed to be proportional to the difference between the freezing temperature and the temperature at the first 2.5 m level in the ocean model.

Ocean model

The heat and salt balance equations have the form

$$\partial T/\partial t + \partial(UT)/\partial x + \partial(VT)/\partial y + \partial(WT)/\partial z = A_H \Delta T + \partial/\partial z [K_H \partial T/\partial z] + \delta(T), \quad (7)$$

$$\partial S/\partial t + \partial(US)/\partial x + \partial(VS)/\partial y + \partial(WS)/\partial z = A_H \Delta S + \partial/\partial z [K_S \partial S/\partial z] + \delta(S). \quad (8)$$

Here, U , V , W are speed components of the current, A_H is the horizontal turbulent exchange coefficient, Δ is the Laplace operator, the symbol δ means the convective adaptation of temperature and salinity (Bryan 1969). In this work we have neglected advection and horizontal heat and salt diffusion. Hence, in equations (7) and (8) only the first term in the left-hand part and two last terms in the right-hand part are preserved. Parameterization of the vertical turbulent exchange coefficients K_H and K_S is given in (Polyakov, 1994). They depend on the vertical gradients of the horizontal speed (equal to zero in these experiments) and the vertical gradients of the corresponding characteristic.

For the case of ice melting an additional portion of desalinated water is added to the upper ocean layer (Makshtas 1991) and it differs for different ice age gradations. The temperature of melting is calculated taking into account water salinity. New water salinity and temperature in the surface ocean layer are calculated as mean weighted characteristics. For the case of ice freezing, part of the water proportional to the ice thickness change is removed from the upper ocean layer.

Results

Calculations were performed at the point located in the Beaufort Sea ($\varphi=79.8^\circ$). Data of the Atlas of the Arctic Ocean (1980) were used. The initial vertical temperature and salinity distribution is taken from (Polyakov&Timokhov 1994). The absence of the ice cover was used as initial conditions. The vertical resolution in the ocean was 2.5, 5, 10, 15, 20, 25, 30, 40, 50, 75, 100, 150, 200, 300, 500, 1000, 2000 and 3000 m. The duration of calculations was 50 years and the system has achieved the equilibrium state.

The calculated snow surface temperature for six ice age gradations (0.05, 0.20, 0.40, 0.95, 1.60 and 3.50 m) and for open water is shown in Fig. 1. Due to a considerable difference in the surface temperature the model simulated a significantly different change in the mass of young and multiyear ice. There is good agreement between the values of the heat balance equation components on the multiyear ice surface (3.50 m) and data of Parkinson (1978).

Fig. 2 presents seasonal variability of the ice and snow thickness. The values of the ice and snow thickness are close to mean climatic estimates of the characteristics for the given region obtained from observation data (Romanov, 1992).

Fig.3 and 4 show the calculated upper ocean temperature and salinity. Their variability looks like a real one and qualitatively corresponds to the earlier obtained results in (Melloe & Kantha 1989). During the warm season the model simulated ice melting and as a result, the decrease in salinity accompanied by the increase in the freezing temperature. With time the salinity minimum and the temperature maximum extend to the lower ocean layers. From July to November an intermediate temperature minimum at a depth of about 25 m is observed.

Fig. 5 presents ocean-to-ice heat flux values. Mean flux of 1.2 W/m^2 does not contradict the estimates of Maykut and Untersteiner (1971), $2-4 \text{ W/m}^2$. However, it distinctly differs from 0.33 W/m^2 in (Mellor & Kantha 1989). Relatively smooth variations of the flow are interrupted by a sharp increase in its values. We have investigated the reason for such a behaviour of the flow. Fig. 5 presents a number of levels in the ocean model that are entrained in convective mixing. Each of the successive

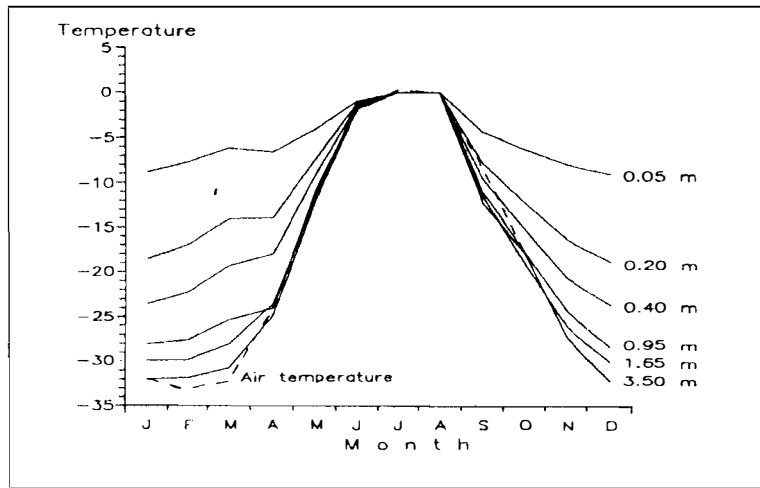


Fig.1 The calculated snow surface temperature for different ice thickness. The dashed line indicates surface air temperature. The point is located in the Beaufort Sea.

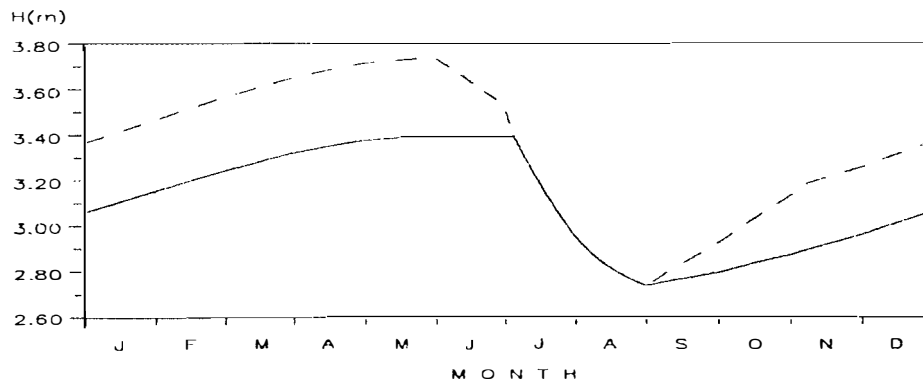


Fig.2 The calculated equilibrium thicknesses of ice (solid line) and snow (dashed line).

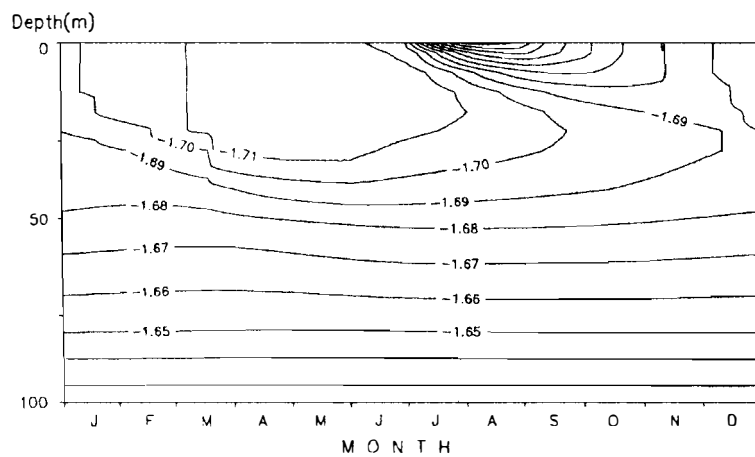


Fig.3 The calculated upper ocean temperature. The isolines are drawn across 0.01 degrees.

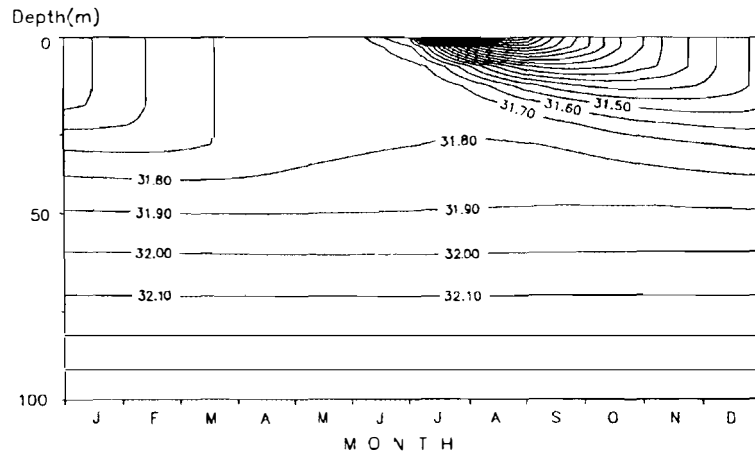


Fig.4 The calculated upper ocean salinity. The isolines are drawn across 0.1 ppt (part per thousand).

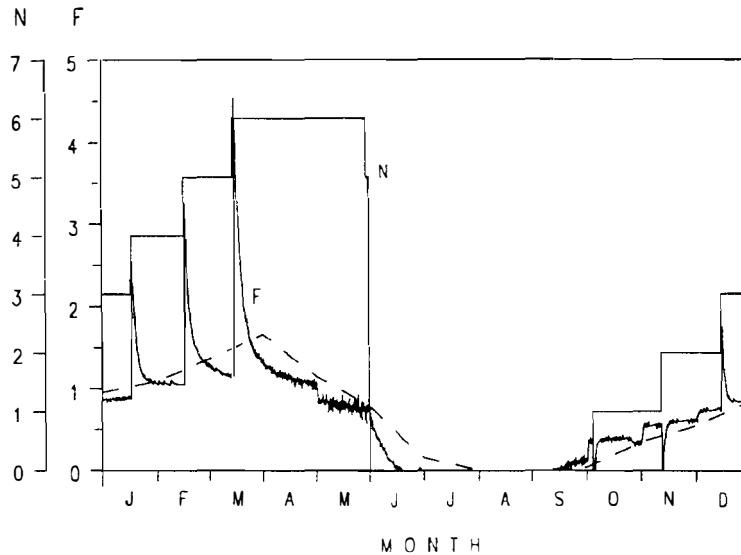


fig.5 The calculated ocean-to-ice heat flux F (W/m^2) and the number of levels in the ocean N entrained into convective mixing. The dashed line indicates mean monthly values of the flow F .

layers involved in convective mixing bring an additional portion of heat to the upper ocean layer. This causes a sharper temperature gradient in the subice layer, since the freezing temperature of water changes relatively little.

For estimating the dependence of the behaviour of the system on vertical resolution in the ocean we have repeated the experiment with constant spacing of 2.5 m by the vertical in the upper 100 m layer. Equilibrium values of ice and snow thicknesses are practically independent on the vertical grid interval. This means that the ice mass is sensitive to integral values of the flow F_{\uparrow} and does not respond to its short-term disturbances generated by convection. Variations of F_{\uparrow} obtained in the experiment are comparatively smoothed, the curve has a larger number of peaks of smaller amplitude. The temperature and salinity distribution in the upper ocean layer is similar to that obtained in the preceding part of the work.

References

1. Bryan, K. A numerical model for the study of circulation of the world oceans. 1969, *J. Comput. Phys.*, 4, 347-376.
2. Gorshkov, S.G. Atlas of Oceans. Arctic Ocean. Moscow. Military Defense Publishing House. 1980, 190 pp. - in Russian.
3. Makshtas, A.P. The heat budget of Arctic ice in the winter. Published by International Glaciological Society. 1991, Cambridge CB2 1ER. UK. 77 p.
4. Maykut, G.A. & Untersteiner, N. Some results from a time-dependent thermodynamic model of sea ice. 1971, *J. Geophys. Res.* 76. 1550-1575.
5. Mellor, G.L. & Kantha, L.H. An ice-ocean coupled model. 1989, *J. Geophys. Res.*, 94, 10937-10954.
6. Parkinson, C.L. A numerical simulation of the annual cycle of sea ice in the Arctic and Antarctic. 1978, NCAR Cooperative Thesis No. 46. The Ohio State University and National Center for Atmospheric Research, 191 p.
7. Polyakov, I.V. Maintenance of the Arctic Ocean large-scale baroclinic structure by the M2 tide. 1994, *Polar Research* 13(2), 219-232.
8. Polyakov, I.V., Kulakov, I.Yu., Kolesov, S.A., Naumov, A.K., Dmitriev, N.Eu. Coupled ice-ocean dynamics model of the Kara Sea. 1994, Tech. Rep. 4-YA-94. Arctic and Antarctic Research Institute. 194 p.
9. Polyakov, I.V. & Timokhov, L.A. Mean temperature and salinity fields of the Arctic Ocean. 1994, *Meteorologiya i gidrologiya (Meteorology and Hydrology)*. 7, p.68-75. - in Russian.
10. Romanov, I.P. The ice cover of the Arctic Basin. 1992, S.Petersburg. 211 p. Semtner, A.J. A model for the thermodynamic growth of sea ice in numerical investigation of climate. 1976, *J. Phys. Oceanogr.*, 6, 379-389.

THE KARA SEA SATELLITE SEA SURFACE TEMPERATURE MEASUREMENTS IN SEPTEMBER 1994

V.G.Smirnov, A.V. Grigoryev (AARI)

Methods for sea surface temperature measurements using IR-radiometry, are part of the non-contact methods for environmental studies and are widely employed in oceanographic studies. To improve such methods is of particular importance for remote regions of the Russian Arctic Seas which are characterized by a high percentage of cloudiness and the absence of reliable estimates of atmospheric absorption within the various ranges of the IR-radiation region.

The work analyzes the NOAA-11 AVHRR IR-images of the Kara Sea retrieved in St. Petersburg on 2 and 9 September 1994 during the Russian-Norwegian expedition aboard the R/V "Ivan Petrov". Only two comparatively small sea regions were delineated due to extremely heavy clouds during the expedition activities and a non-regular satellite data receiving in the HRPT mode: west of the Yamal peninsula (region 1) and east of Novaya Zemlya (region 2). Calculation of the technical albedo values and brightness temperatures T_b were performed using the algorithms recommended in /3/ with a corresponding non-linearity correction of the thermal channels.

Fig. 1 (a, b, c) presents the T_b temperature charts for the indicated regions. Fig. 1d presents a chart of sea surface temperature distribution based on data of contact measurements during the period August 22 to October 4, 1994. The albedo values of the underlying surface were used for delineating the cloud-free sea regions. Mean water surface temperatures from data of contact measurements for regions 1 and 2 were 4.0 and 2.0..C, respectively.

An assessment of sea surface temperatures (SST) based on satellite data was performed using eight different algorithms of a two-channel (channels 4 and 5) atmospheric correction in a splitted window. The results of calculations are given in the table. Evidence on the algorithms 1-4 (see the table 1) are presented in an overview /1/. The algorithm 5 was used in /5/. The algorithms 6 and 7 were specially developed for NOAA-11 /4/. The algorithm 8 was also specially developed for NOAA-11 based on observation data in the central Arctic in summer at the drifting polar station NP-26 /2/.

The algorithms in the table were created for different regions and seasons and the results of calculations illustrate what errors in SST can occur when the model of atmospheric correction is incorrectly chosen.

Let us note that the algorithms 5 and 8 are considered the most suitable (by regional indication) algorithms given in Table 1, for estimating SST for the Kara Sea. This is also confirmed by sufficiently close SST estimates obtained on the basis of these algorithms. However, there is a significant discrepancy (more than 3 C) between the SST values and data of contact measurements. This is in our opinion (assuming the algorithms 5 and 8 being more or less reliable) can be related to the time difference of the remote sensing and contact measurements and an imperfect approach used for comparison of the temperature fields obtained by principally different methods. Possible hypotheses that during the period of remote sensing measurements there were sharp subsurface vertical temperature gradients or an oil pollution film cannot be checked on the basis of available data.

It is obvious that the activities in this direction should be continued including purposeful composite oceanographic, meteorological and aerological subsatellite experiments in the Arctic Seas. Such experiments on the regional basis along with available archived data will allow considerable improvement in the existing algorithms of atmospheric correction and possibly, taking into account the specific conditions of the regions of the Arctic Seas, creation of original algorithms.

ATMOSPHERIC ATTENUATION CORRECTION

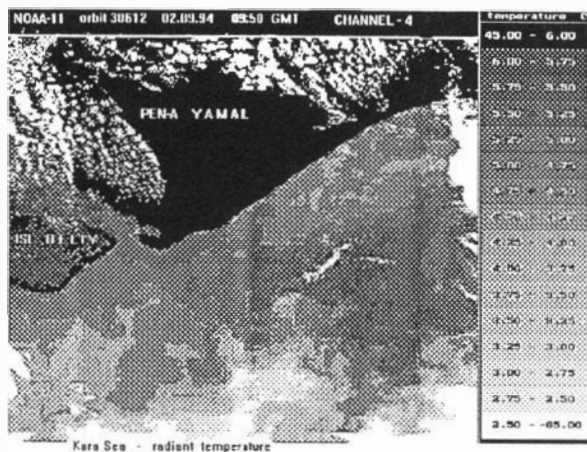
№	Investigators	Algorithms *	SST °C	
			Reg.1	Reg.2
1.	Deschamps and Phulpin (1980)	$SST=2.686(ch.4)-1.626(ch.5)-1.1$	6.61	4.14
2.	McClain et al. (1983)	$SST=1.035(ch.4)+3.046(ch.4-ch.5)-10.784$	9.56	7.16
3.	Price (1984)	$SST=(ch.4)+3.33(ch.4-ch.5)$	11.22	8.95
4.	Singh (1984)	$SST=1.699(ch.4)+0.699(ch.5)-0.240$	5.56	3.00
5.	Deschamps (1986)	$SST=(ch.4)+2.63(ch.4-ch.5)-2.18$	7.59	5.24
6.	NOAA/NESDIS MCSST DAY SPLIT (1990) NOAA-11	$SST=1.0155(ch.4)+2.50(ch.4-ch.5)+0.7*(ch.4-ch.5)*(SEC\ sza^{**}-1)-4.99$	8.85	6.46
7.	NOAA/NESDIS CPSST DAY SPLIT (1990) NOAA-11	$SST=(0.19069(ch.5)-49.16)/(0.20524(ch.5)-0.17334(ch.4)-6.78)*(ch.4-ch.5+0.789)+0.92912(ch.5)+0.81(ch.4-ch.5)*(SEC\ sza^{**}-1)+18.82$	7.42	4.51
8.	J.Key and M.Haefliger (1992)	$SST=-1.76899+3.6654(ch.4)-2.66249(ch.5)-0.39676*[(ch.4-ch.5)*SEC\ sza]$	7.92	5.68

* All temperatures in the above equations are in Kelvin

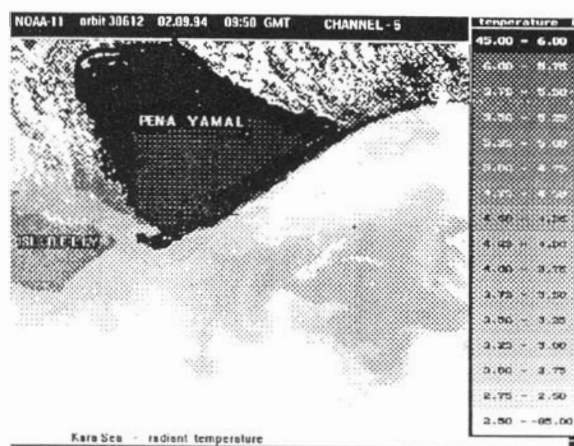
** satellite zenith angle

Reg.1: $T_b\ ch.3 = 1.72^{\circ}C$ $T_b\ ch.4 = 4.31^{\circ}C$ $T_b\ ch.5 = 2.30^{\circ}C$

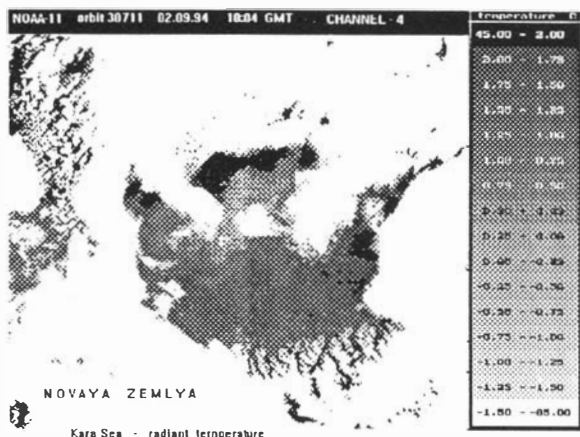
Reg.2: $T_b\ ch.3 = -1.24^{\circ}C$ $T_b\ ch.4 = 1.72^{\circ}C$ $T_b\ ch.5 = -0.45^{\circ}C$



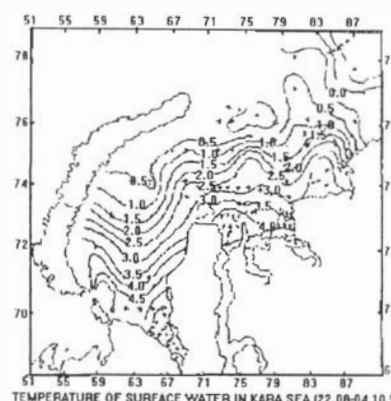
a)



b)



c)



d)

(brightness)

Fig. 1. Charts of the brightness temperature of region 1 (a,b) and region 2 (c), d - a chart of surface water temperature of the Kara Sea from data of contact measurements.

Reference

1. L.Di, D.C. Rundquist. One-step algorithm for correction and calibration of AVHRR level 1b data. Journal of the american society for photogrammetry and remote sensing, Vol. LX, No. 2, 1994, p. 165-171.
2. J.Key, M. Haefliger. Arctic ice surface temperature retrieval from AVHRR thermal channels. Journal of geophysical research, Vol. 97, No.D5, 1992, p.5885-5893.
3. L. Lauritson, e.a. Data extraction and calibration of TIROS-N/NOAA A-G radiometer, NOAA Tech. Memo., NESS 107, 81 pp., NOAA, Boulder, Colo., 1979.
4. NOAA, NOAA Polar Orbiter Data User's Guide, U.S. Dept of Commer., NOAA, NESDIS, Boulder, Colo., Feb. 1991.
5. P.Pagano, e.a. Use of AVHRR data in the air-sea interactions. Proceedings of the 5th AVHRR data user's meeting, Tromso (Norway), 1991, p. 243-252.

**USAGE OF THE DATA ON SEA ICE IN THE GRID FORMAT FOR THE
BARENTS AND KARA SEAS AREAS FOR THE AIMS OF ICE INFORMATICS**
V.M.Smolynitsky, V.E.Borodachev, I.E.Frolov, S.V.Klyachkin, Ey.G.Shvedov (AARI)

By January 1995 data bases involving stereographically gridded (in GRID format) comprehensive sea ice information are developed for 1953-1991 time period for North Polar region area including Barents Kara and other shelf seas. Both data contence including such sea ice characteristics as total, partial concentration, stages of ice development, stages of ice melting, hummocks and fractures spatial concentrations and data base technical parameters including qualitively new archiving format, mesh size equal to 25 by 25 km and temporal step equal to 7-10 days correspond to practically optimal from the point of accuracy conversion of actual historical series of sea ice charts, prepared at AARI.

Following guidelines for regional usage for shelf seas areas are proposed for the created data bases:

(1) Browse of ice condition historical series for shelf seas area in the form detailed maps in polar stereographic projection.

(2) Gaining mostly accurate for today statistical estimates of temporal and spatial variability features for mentioned above ice cover characteristics. At present a number of climate (multiannual) parameters is gained for each mesh point, including standard and robust estimates for distribution function parameters and temporal trends, study of their large- and mesoscale variability and relationship with processes in ice cover is started.

(3) Recovering of such phisical parameters of sea ice which direct measurements for large scale areas are or were in past difficult. Following parameters may be gained easier than others: mean thickness of the level sea ice on the basis of stages of development data (result is gained in the form of separate data base) and effective thickness of ice, that is using amendments on melting and hummocks. With a help of other hydrometeorological parameters (sea water temperature and salinity, air temperature) recover of, e.g., strength properties of sea, ice is possible (at present fields of flexure strength module are estimated).

(4) Gaining initial and test data patterns for numerical modelling of sea ice evolution. Here application of different methods of objective analysis in order to carry out smoothing, interpolation and extrapolation procedures seems reasonable. Developed technique and software are based either on point by point approximation of ice characteristics values by individual polynomial with definite radius of influence or on approximation of values for grid parts by a sum of orthogonal Chebyshev polynomials, thus involve field smoothing and recovering, including interpolation to more detailed grid. Test calculations carried out for Kara sea area reveal good concordance for approximated and actual fields.

FEATURES OF CHANGES IN SUMMER ICE CONDITIONS OF THE KARA SEA IN RECENT YEARS

V.A. Spichkin, A.Ė. Yegorov A.G. (AARI)

The ice cover of the Kara Sea significantly influences natural processes in marine environment. In winter the sea surface is covered by fast and drifting ice. In summer from July to September the area becomes ice-free. This fact governs different effects of interaction between the active sea layer and the atmosphere. The largest annual variations of such effects occur in summertime depending on the intensity of ice disappearance in the sea.

Since the Kara Sea is located in the area of active large-scale interaction between the cold polar region of the Central Arctic and the warm subpolar region of the North Atlantic, there is a considerable disturbance in zonality. Hence, 8 regions were delineated in the Kara Sea on the basis of uniformity of changes in summer ice conditions (Fig. 1).

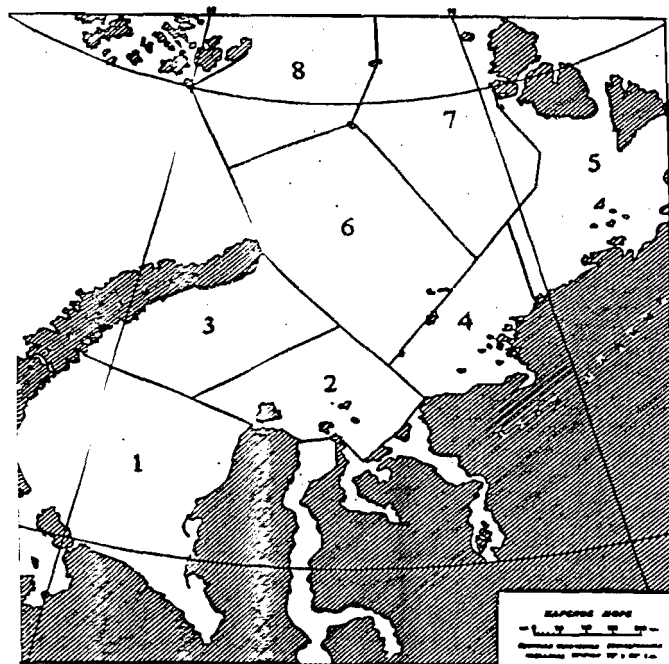


Fig. 1. Ice-geographical regioning of the Kara Sea 1 - Yamal-Yugorsky region 2 - Ob'Yenisey region 3 - Novozemel'sky region 4 - Severozemel'sky western region 5 - Severozemel'sky eastern region 6 - Kara western region 7 - Kara eastern region 8 - Kara north-western region

Each of the uniform ice regions is characterized by spatial-temporal features of ice disappearance in summer which are sufficiently well taken into account by the local-genetic typification of ice conditions. The combinations of typical anomalies in the amount and distribution of ice in the uniform ice regions form the features of summer ice changes over the whole area of the sea.

In 1983-1994 when comprehensive sea expeditions were carried out in the south-western Kara Sea, the anomaly of ice conditions was negative, and in the north-eastern sea region - positive (Fig. 2,3). This combination of anomalies has been steadily observed from 1988.

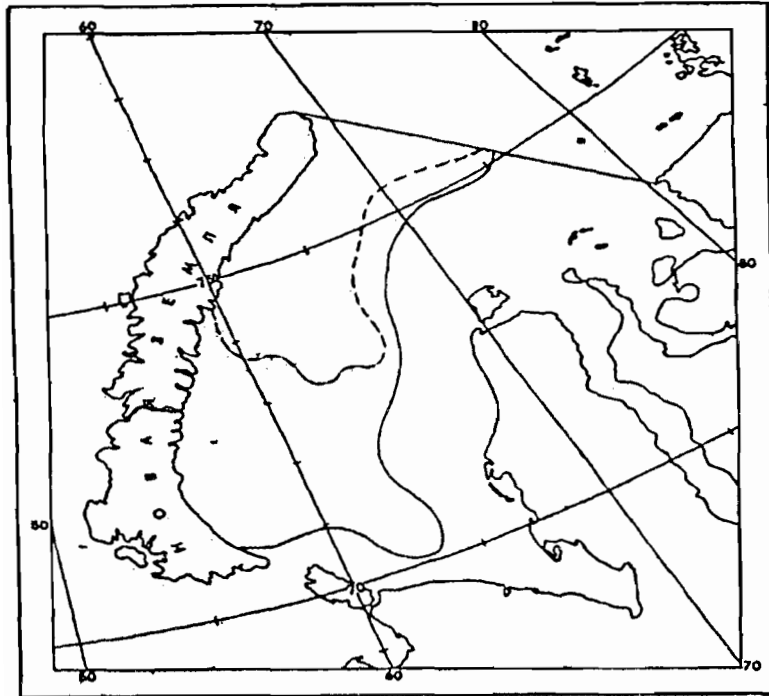


Fig. 2. Position of the boundary of close ice in early July. mean multiyear (-) and for the period 1988-1994 (-)

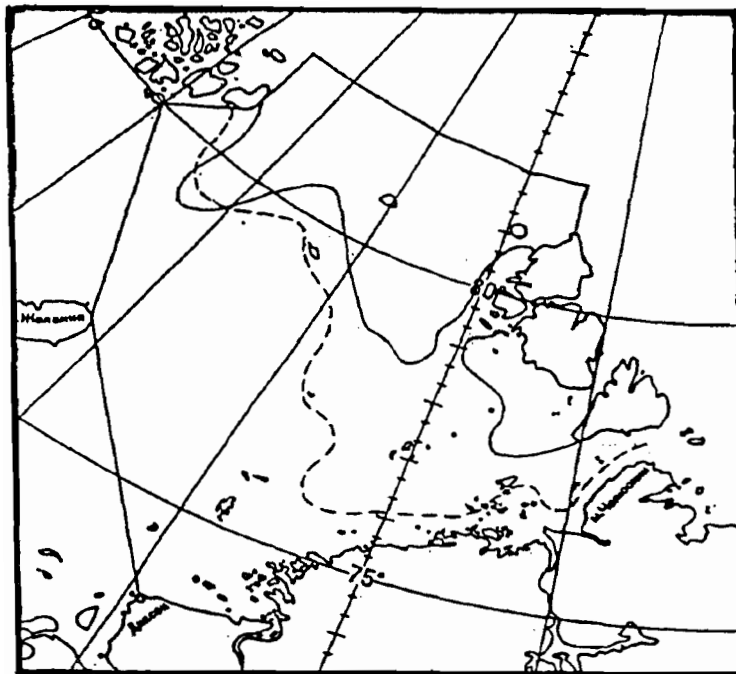


Fig. 3. Position of the boundary of close ice in late August. mean multiyear (-) and for the period 1988-1994 (-)

For the last 7 years anomalously easy conditions are formed in the south-western Kara Sea: the area of close ice and total ice cover extent in the second half of July-early August is usually 20-25% less than mean multiyear values (Fig. 2). For the period 1988-1994 from 2 to 9 cases of large negative anomalies in 10-day values of the close ice areas and ice cover extent were annually observed in uniform regions of the south-western Kara Sea. As a result of active disappearance of close ice, the area was ice-free almost one month earlier than on the average. The largest anomaly in ice conditions was observed in the Yamal-Yugorsky uniform region where the duration of the ice-free period on some segments - in the vicinity of Kara Gate strait, the Yugorsky peninsula and the Yamal coast was up to 3-4 months. The main cause for intensive ice melting in these years was an anomalously early onset of melting of the ice cover, as well as the presence of extensive zones of open water in the Ob'-Yenisey and Yamal polynyas.

In the north-eastern Kara Sea predominantly heavy ice conditions were observed for the last 7 years: the area of close ice and total ice cover extent in the region in August-September exceeded mean multiyear values by 10-15% (Fig. 3). For the period 1988-1994, 3-4 large positive anomalies in 10-day values of the area of close ice and ice cover extent were observed annually, on the average, in uniform regions of the north-eastern Kara Sea. As a result, much of the area was not cleared of ice at all and only on local segments in the western part of the region the duration of the ice-free period was about a month. The largest anomalies in ice conditions were mainly observed in the Severozemel'sky eastern and western uniform regions where the excess of the ice cover extent over the normal value was up to 30%, on the average. The major cause for a delayed melting of ice was the absence of the Central Kara Flaw Polynya in these years, as well as summer ice advection along the western coast of Severnaya Zemlya. The year 1993 was an exception when easier ice conditions were formed due to extremely insignificant development of fast ice along Taimyr.

The anomalous development of ice conditions, as well as a non-uniform ice disappearance in different parts of the Kara Sea, considerably affect the distribution features in oceanographical data collected in the expeditions of 1993-1994. It is probable that the recorded distributions of oceanographic and biological parameters can reflect not only the typical position or features of the anomalous distribution of sea ice in each specific year, but also an exceptional fact that similar features are steadily preserved for the last 7 years.

Currently, there are indications that a long period of a uniform anomaly in the development of ice processes in the Kara Sea is coming to an end. In the next few years one may expect a large diversity in anomalies of the ice cover extent in natural sea regions.

It seems that optimal planning and implementation of oceanographic studies should take into account seasonal variations in the state of the ice cover. Forecasting of the distribution of ice with different periods in advance and detailing of ice parameters over the Kara Sea area is performed in the Department of Ice Regime and Forecasting of the AARI.

STOCHASTIC COMPUTER SIMULATION OF THE MORPHOMETRY OF LEVEL DRIFTING ICE

I.V.Stepanov, V.A.Likhomanov (AARI)

For numerical modelling of sea ice drift, ice loads on ships and shelf structures, and for resolving some other problems, information about ice cover as a set of separate floes taking into account their size, shape, position, etc. is desirable as initial data.

In terms of the probability theory, the ice cover can be considered as a sample of some random vector function of spatial and time coordinates. In a special case of homogeneous level drifting ice, the computation procedure for constructing such a sample can be based on transforming the Gaussian random field using a jump function [1]. With regard to the problem under consideration, this method is as follows.

First, a sample of the Gaussian scalar random field is found

$$\eta_N(\bar{x}) = \frac{1}{\sqrt{N}} \sum_{j=1}^N \zeta_j(\bar{x}, \bar{\Omega}_j), \quad (1)$$

$$\zeta_j = \sqrt{2} q_j \sin[\bar{r}^T(\bar{x}_0 + \bar{x}) + \pi/4];$$

where \bar{x} - is the radius-vector of a random point of the field; $\bar{\Omega}_j = (q_j, \bar{r}_j)$, $j = 1, \dots, N$ are independent samples of a random parameter $\bar{\Omega}_j = (q, \bar{r})$; N - is the number of samples of the field ζ_j ; \bar{r}_j - is a sample of a two-dimensional random vector with the distribution density f_r ; q_j - is a sample of a Rayleigh distributed random value that is extended symmetrically to the negative semi-axis; \bar{x}_0 is the initial non-stochastic vector.

Assuming the ice cover to be a homogenous random field, the density of the probability f_r can be assumed to be dependent only on the argument vector modulus. The expression for the function f_r will only depend on the desirable form of the correlation function of the field $\rho_\zeta(\bar{x}) = \rho_0(|\bar{x}|)$.

In particular, for $\rho_0(|\bar{x}|) = [1 + \alpha^2|\bar{x}|^2]^{-3/2}$

density $f_r(u) = [\exp(1 - |u|/\alpha)] / (2\pi\alpha^2)$.

A sample of the random vector modulus $|\bar{r}|$ can be obtained by means of the formula $\alpha \ln(\gamma_1, \gamma_2)$, where γ_1 and γ_2 - are samples of a random value which is uniformly distributed on $[0, 1]$. The selection of the most suitable form of the correlation function of the fields ζ_j and, respectively η_N , can be made using the results of modelling since the available a priori data are not sufficient for such a selection. The components of the vector $\bar{r} = (r_1, r_2)$ are equal

$$r_1 = |\bar{r}| \cos\phi; \quad r_2 = |\bar{r}| \sin\phi,$$

where ϕ , like γ_1 and γ_2 - is a sample of a random uniformly distributed value $[0, 1]$. For generation of Rayleigh distributed random numbers symmetrically extended to a negative semiaxis, one can use a modelling formula

$$q_j = \chi \sqrt{-\ln \gamma},$$

where $\chi = -1$ or 1 with equal probability; γ - a sample of a random value, uniformly distributed on $[0, 1]$. All marginal distributions of the field η_N , determined by the formula (1) are asymptotically normal according to the central limiting theorem. At numerical simulation it is necessary to be restricted to a finite value N which can be determined by comparing the estimated statistically and the required theoretical distribution laws. It may be assumed that $N=10 \dots 20$ will provide for acceptable accuracy.

Obtaining a sample of the Gaussian field (1) allows proceeding to the generation of the simulated ice cover proper as a set of separate floes of a random form. As initial parameters

governing the ice cover, let us take its concentration p , expressed in tenths, as well as medium sizes of the floes along the axes of coordinates l_x and l_y , which characterize the forms of floating ice.

Let us perform a non-linear transformation of the initial Gaussian field $\theta(x, y)$

$$\theta(x, y) = \psi \left[\eta_x \theta(x, y) \psi \left(\frac{\theta(x, y)}{a} \right) \right] = \begin{cases} 0, & \theta(x, y) \leq a \\ 1, & \theta(x, y) > a \end{cases} \quad (2)$$

where $a = \Phi^{-1}(1 - p/10)$; Φ^{-1} is a function reverse to the distribution function of a standard random value. Then $\theta(x, y) = 1$ governs the connected areas each of them being considered as a separate floe. Part of the area where $\theta(x, y) = 0$, corresponds to open water.

The prescription of the threshold a by the indicated way in transformation (2) provides the required ice concentration value. In order to obtain mean sizes of the ice floes along the x-axis equal to the prescribed ones l_x by means of modelling, it is necessary to select a corresponding value of the correlating function parameter. For instance, for the correlating function

$\rho(r) = \exp(-\alpha^2 |r|^{3/2})$ the parameter α is equal to

$$\alpha = \frac{2\pi(1/10) \exp(a^2/2)}{\sqrt{3}l_x}$$

The floe size along the y-axis is achieved by changing the scale along y . For illustrating the application of the algorithm described,

Fig. 1 shows the results of computer modelling of uniform small floes of 2/10 in concentration observed in the Barents Sea in the course of the international expedition "Tundra-Ecology-94" aboard the research expedition vessel "Akademik Fedorov" in summer of 1994. Both the qualitative similarity of full-scale and simulated ice cover and coincidence in concentration are achieved.

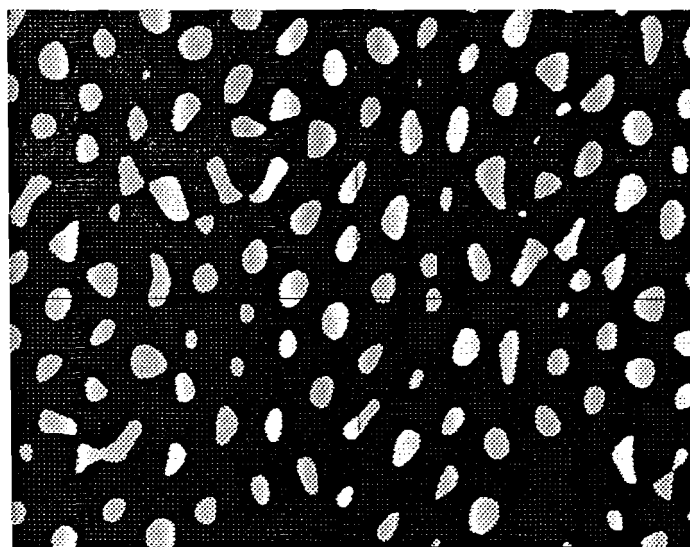


Fig.1 Results of stochastic simulation of uniform small ice floes with concentration 2/10.

Generalization of the method described also allows simulating the non-uniform ice cover. In particular, the ice cover formed of floes and medium floes with small floes and ice cake between them is often observed. In this case, generation of independent Gaussian fields is performed by means of formula (1) which are then transformed according to (2) and superimposed onto each other.

Each of the floes, in addition to its form in the plan is characterized by thickness. It is common to describe a spatial distribution of ice thicknesses by the Gramm-Sharlier law. However, in the first approximation one can assume the normal distribution, i.e. assume assymetry and kurtosis to be zero. Further, it could be possible to improve the method for generation of ice thicknesses taking into account, for instance, that small floes and ice cake which fill the space between the floes are, as a rule, younger and, hence, less thick.

References

1. Shalygin A.S., Palagin Ya.I. Applied methods for statistical modelling. - Leningrad: Mashinostroyeniye. Leningrad Branch, 1986. - 320 p.

METHODS AND TECHNIQUES FOR "IN-SITU" TESTS OF THE ICE COVER MECHANICAL CHARACTERISTICS

V.P. Tripol'nikov (AARI)

For exploration and production of mineral resources and fuel on the Arctic shelf some activities can be carried out on the ice cover surface. For in-situ determination of the bearing capacity of the ice cover, four stages of tests were performed at the AARI: 1) traditional measurements of the ice thickness and environmental conditions and the use of reference technical literature; 2) determination of the effective rigidity of the ice cover by investigating the wave processes of the flexural-gravitation resonance produced by aircraft; 3) determination of the ice elastic and creep characteristics in the bore-holes by the pressiometry method; 4) calculation of time intervals of ice resistance without destruction at heavy loads.

Expedition studies on the drifting ice traditionally included measurements of the ice thickness and its temperature. However, the strength of the ice specimens was tested under the laboratory conditions simulating the ambient conditions of the ice cover. These data are summarized /1/ and allow us to use different equilibrium models to work out the design estimates of the loads destructing the ice /2/. For calculations of the temporal bearing capacity of the ice cover it is also necessary to have data on the cylindrical rigidity of the ice plate and the ice creeping strength.

The wave process in the ice cover is excited by a moving load (Fig. 1) /3-10/.

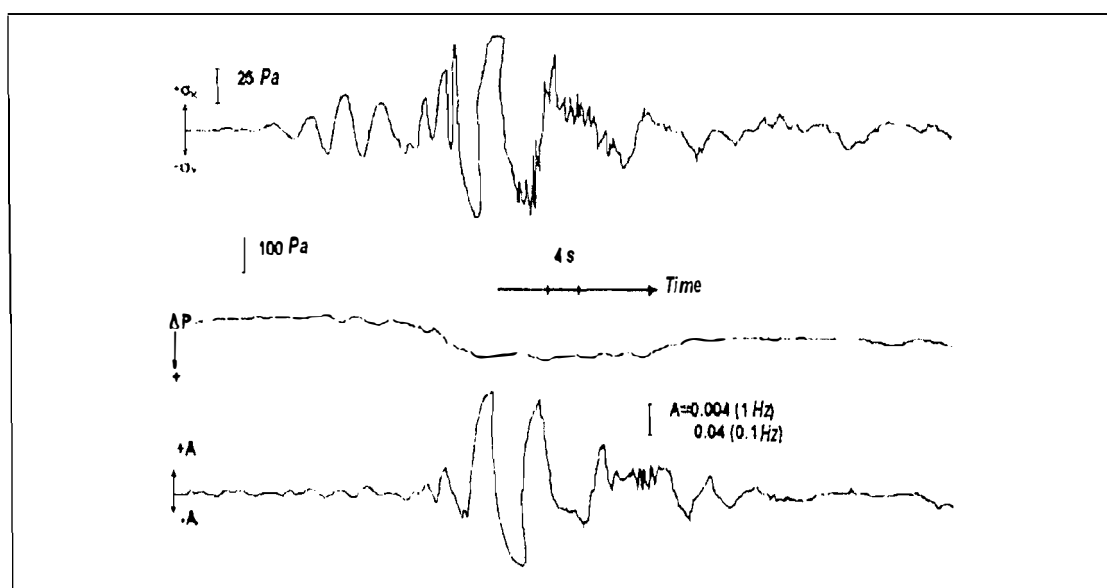


Fig. 1. An example of wave recording in the ice cover 1.9 m thick excited by aircraft; σ_x - stress in the ice, A - the flexure amplitude, ΔP - pressure at the bottom ice surface.

The general qualitative characteristics of the processes which are consistent with theoretical understanding /3-6/ are as follows: 1) the period of resonance fluctuations depends on the ice thickness and its elasticity modulus; 2) there is phase correlation of the ice flexure (A) and stresses (σ) when the load passes across the observation point; 3) stresses and strains of compression-stretching in the horizontal plane can be translated as forward and backward longitudinal waves from the flexural wave under the load; 4) the water pressure on the lower ice surface depends not on the ice flexure phase, but on the load phase.

According to the theory of an idealized model /3/, the spatial and temporal frequencies of the wave pattern in these processes are functions of the complex Eh^2 , with the scale of

correspondence between the frequencies and the complex Eh^2 being always local. In the vicinity of an off-shore structure on the shelf the goal is to detect the anomalous changes in the ice cover rigidity under the influence of weather and pollution. Also important is the question about the dates of normal rigidity restoration after correction of the conditions. The ice thickness (h) should be measured by drilling. Having one and the same mechanical system "ice-basin" and repeating the measurements during the aircraft flight at the same height and with the same speed along the line of sensors on the ice, we obtain a relative change in the Young's modulus (E) from frequency changes.

The absolute values of the characteristics of ice elasticity and creeping can be obtained by pressiometric ice tests in the bore-holes. Let there be a uniform isotropic ice plate which is infinite in the horizontal plane. There is a vertical cylindrical bore-hole with smooth walls where a pressiometer sonde is placed tightly contacting the bore-hole sides. Let also l_0 be the height of the sonde, r_0 - the bore-hole radius, μ - the Poisson's ice coefficient, P - the pressure of the sonde on the walls of the bore-hole, V_0 - the sonde volume. By solving the differential equilibrium equation with the boundary conditions /11/ and then the energy balance equation, we can obtain the equilibrium equation relating the pressiometer readings to the elastic medium characteristics at a purely elastic ice response:

$$\frac{P(1+\mu)}{E} \cdot \left(1 + \frac{3r_0}{l_0} \cdot th \frac{h-l_0}{4r_0}\right) = \frac{\Delta V}{2V_0} \quad (1)$$

If the pressure in the pressiometer sonde is set to exceed the prolonged ice creeping strength - $\sigma_{i\infty}$, then the equilibrium mechanism will be different. The energy dissipated in the process of creeping (in the form of heat and sound),

$$Q = \int_V \sigma_i \varepsilon_{ci} t_i dV, \quad (2)$$

where t_i - current time from the moment of loading, ε_{ci} - the rate of plastic creeping strain. In the bore-hole area the elastic strains and stresses decrease with the increase in r so that at some distance $r=r'$ creeping stops and is replaced at this boundary by ice elasticity:

$$\sigma_i(r') = \sigma_{i\infty} = \frac{Pr_0^2}{(r')^2} \cdot f(z) \quad (3)$$

For briefness let us take the case $(z)=1$. One can assume that the creeping rate

$$\varepsilon_{ci}(r) = \varepsilon_{ci} \cdot \frac{r_0^2}{r^2}, \quad (4)$$

where ε_{ci} - the rate at the bore-hole wall. After substituting (3) and (4) and integrating by r from r_0 to r' , we obtain

$$Q = -t_i P \varepsilon_{ci} \left(1 - \frac{\sigma_{i\infty}}{P}\right) \cdot V_0 \quad (5)$$

The energy dissipated in the ice in the process of creeping is being equalled to the change in the sonde operation by the value $(P - \Delta P)(V_0 + \Delta V_{oi}) - PV_0$, where ΔP - the pressure release in the process of prolonged creeping strain, ΔV_{oi} - the expansion of the sonde chamber (over the entire time t_i from the beginning of loading). We obtain the instant balance equation:

$$t_i \cdot \varepsilon_{ci} \left(1 - \frac{\sigma_{i\infty}}{P} \right) = \frac{\Delta V_{oi}}{V_o} - \frac{\Delta P}{P} - \frac{\Delta P}{P} \cdot \frac{\Delta V_{oi}}{V_o} \quad (6)$$

The pressimeter which is capable of operating in a complex with IBM PC, was developed by the AO "Morinzheologija" (Riga). The objectives of the static flexure of an infinite elastic plate which is assumed to be both uniform and isotropic on a hydraulic basement, are considered in [12,13]. This model is suitable for determining the ice cover bearing capacity in the water areas. Let us designate $P(x, y)$ - the load distribution function, β - the coefficient of the hydraulic base. For calculating the guaranteed bearing capacity of the ice cover it is necessary to determine the maximum flexural compression stresses which should not exceed the prolonged creeping strength. It can be shown that the maximums of elastic stresses (both shear and volumetric) should be estimated as follows:

$$\max \sigma = \pm \frac{3(1-\mu)P}{h^2 \beta^2} \quad (7)$$

If the maximum stresses exceed the prolonged creeping ice strength, then the development of accelerating ice creeping is possible. In this case the bearing capacity cannot be considered guaranteed.

Practice has shown that in this mode in some time after load application, three cracks occur in the ice cover originating from the maximum flexural point divided by azimuthal angles of 120° . The time for forming of the macrocracks (the latent destruction period) is equal to:

$$t^* = \frac{1}{2} \cdot \sum_{h_e}^{\frac{h_e}{h}} \frac{dz}{(\Delta h) / t_i^*}, \quad (8)$$

where $(\Delta h) / t_i^*$ - the rate of destruction (erosion of the plate material) as a result of creeping, h_e - the plate thickness with brittle cracking at a given static loading. The minimum thickness of the erosion layer is equal to a linear size of a stable microdefect in the form of a crack (according to Griffith), i.e.

$$\Delta h_{min} = \frac{1}{\pi} \frac{K_{1c}^2}{\sigma_i^2}, \quad (9)$$

where K_{1c} - the coefficient of the ice crack bearing for the cracks of separating [14]. The time of erosion (ice creeping) according to [15]:

(10) where A, n, λ - empirical constants. For example, according to data [14] $K_{1c} \approx 0,1MH \cdot i^{-3/2}$ for freshwater ice at temperatures from 0° C to -40° C. Also, for freshwater ice [14] we have $A = 132 (\text{MPa})^n \cdot \tilde{n}^\lambda$, $n = 1,35$, $\lambda = 0,68$, $\sigma_{i\infty} = 0,51$ MPa. At these empirical values of the ice characteristics we obtain the loading of a concentrated type from the formulas (8)-(10)

$$t_{max}^* = 2062h \left(1 - \sqrt{\frac{\sigma_i}{\sigma_{t0}}} \right) \cdot \frac{\sigma_i^2}{\sigma_i^2 - \sigma_{i\infty}^2}, \quad (11)$$

(11) where t^* - in seconds, σ_i - in MPa, σ_{t0} - temporal ice resistance at brittle destruction. Calculations of the time interval of the ice cover resistance without destruction at critical loads allows situations to be distinguished by the risk degree.

References

1. "A letter on the methods for calculating ice strength limits" , 2d edition, ed. by B.A. Fedorov, AARI, 1988.
2. Masterson D.M., Straudberg A.C. Creep and relaxation in floating platforms - an analysis of case histories. - Proc.Symp. "Physics and mechanics of ice", Copenhagen, 1979. (Translation: Creep and relaxation in floating platforms - an analysis of case histories. Vol. Mechanics. Physics and mechanics of ice. Mir., M., 1983; ed. by R.V. Goldstein).
3. D.Ye. Kheisin. Ice cover dynamics. L., Gidrometeoizdat, 1967, 215 p.
4. Bukatov A.Ye., Zharkov V.V. Modeling of three-dimensional flexural variations of the ice cover at motion in the area of pressures. Marine Hydrophysical Journal, 1990, No. 4, pp.10-15.
5. Bukatov A.Ye., Zharkov V.V., Zavyalov D.D. Three-dimensional flexural-gravitation waves at non-uniform compression. - PMTF (Novosibirsk), 1991, No. 6, pp.51-57. Copenhagen, 1979.
6. Bukatov A.Ye., Zharkov V.V. Three-dimensional disturbances in the exponential-stratified basin with the ice cover at motion in the constant pressure field. Izv. AN., ser. Physics of the atmosphere and the ocean., 1993, Vol.29., No.5, pp.681-687.
7. Squire V.A., Langhorne P.J., Robinson W.H. et al. Moving loads on sea ice. - Polar record, 1987, No.23 (146), pp. 569-575.
8. Takizava T. Deflection of a floating sea ice sheet induced by moving load. - Cold Reg. Sci. and Techn., 1985, No. 11, pp.171-180.
9. Gavrilov V.P., Tripol'nikov V.P. Results of investigating the flexural-gravitation resonance in sea ice. - Theory and strength of icebreaking ship: Gorkovskiy polytechnical institute, 1982, pp.28-34.
10. Sytinsky A.D., Tripol'nikov V.P., Kheisin D.Ye. A method for determining physical-mechanical ice constants under natural conditions". The author's certificate No. 181350. - Inventor's Bull., 1966, No.9.
11. Landau L.D., Lifshits Ye.M. The theory of elasticity. M., Nauka, 1965.
12. Korenev B.G. Some objectives of the theory of elasticity and heat conductivity resolved in Bessel's functions. M., Fizmatgiz, 1960, 458 p.
13. Ogibalov P.M. Shells and plates. MGU Izd., 1969, 695 p.
14. Liu H.W., Miller K.J. Fracture toughness of freshwater ice. - J.Glaciology, 1979, vol.22, pp.135-143.
15. Zaretsky Yu.K., Fish A.M. A typical feature of ice deformation at uniaxial compression. Proc./AARI, 1975554, Vol.324, pp.458.

DESTRUCTION OF ICE BY EXPLOSIONS

V.P. Tripol'nikov (AARI)

Motions of ice objects in the sea under the effect of currents and wind and icing of structures create obstacles for operations and present a possible threat to off-shore structures, especially during the construction stage.

In critical situations ice destruction is a radical means for reducing the ice loads on off-shore structures. By using a minimum number of explosions, a stamukha is raised from the bottom, ice is loosened for damping the ice ram and ice frozen to the structures, is separated from them. Obviously, the explosion should not damage the structure and have an adverse environmental influence. For this purpose experiments and calculations are required.

The curves of the pressure waves provide understanding of the character of the shock impact in the environment. The shock wave curve in water at a deep explosion of trotyl is given in Fig. 1. At explosions of trotyl charges near the bottom ice surface (Fig. 2) the pressure curve has a more steep backfront drop. Fig. 3 presents a pressure curve in water at explosion of a single trotyl charge placed into a bore-hole in the ice cover at a depth equal to half the ice thickness. Fig. 4 presents the curves resulting from explosion of several trotyl charges placed in different bore-holes in the ice cover, by one current impulse. The curves of the pressure waves at explosion of powder charges in water are given in Fig. 5.

According to the similarity principle in the explosion theory, the shock wave pressure peak (P^*) is function of the complex $\gamma = \sqrt[3]{m/r}$ where m - the charge mass in kg, r - the distance from the charge center in m. For calculating the underwater deep explosion the formula /1/, /2/ is used:

$$P^* = 53.3 \cdot A \gamma^{1.13}, \quad (1)$$

where A - a trotyl equivalent of the specific heat energy of the explosive, P^* - in MPa. Experimental data on the shock wave levels and pressure waves from explosions of different explosives are given in Fig. 6. At explosions of the ice cover by trotyl charges placed in water near the lower ice surface, the experimental data are grouped near the functional dependence (1). The shock waves recorded in water from the explosions of trotyl charges placed in the ice cover at a depth equal to half its thickness, have a trotyl equivalent $A=0.2$. The explosions of small spherical and large extended gas charges "methane plus oxygen" under the ice according to P^* yield a result at a plane (Fig. 6) where calculation of γ is based on the mass of fuel mixture component and r is counted from the edge of the gas cavity. These results are strongly influenced by the method of initiating the gas mixture explosion. The radius of the zone of ice crushing can be estimated as follows. A strong shock wave carries energy /3/

$$U = (P^* + P_0) \left(1 - \frac{\rho}{\rho^*}\right) / 2\rho, \quad (2)$$

(2) where P^* - the pressure peak, ρ^* - the density peak in a strong shock wave, P_0 - pressure in the medium ad infinitum, ρ - medium density before the explosion. With spreading of the strong shock wave the material destruction stops somewhere which means attenuation of the wave up to the level of the adiabatic pressure wave. Here the density relation can be expressed through relative deformation in the medium ε^* :

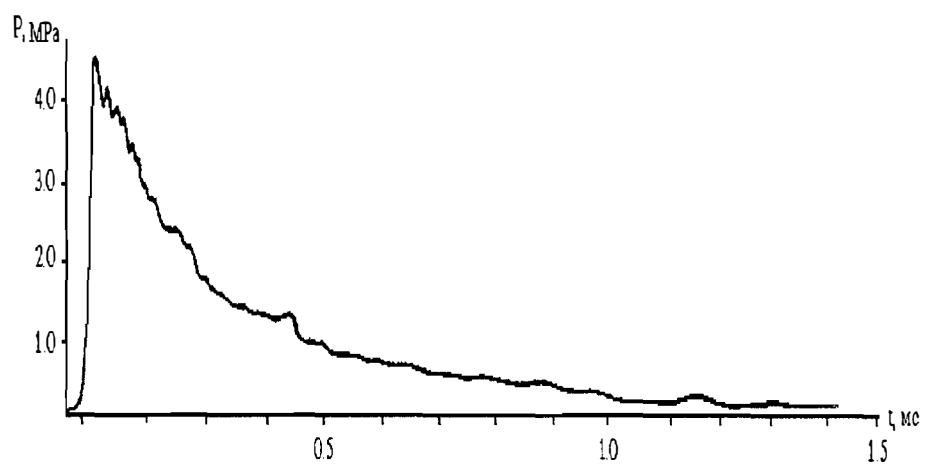


Fig. 1. The curve of the shock wave from trotyl explosion in water (a deep explosion).

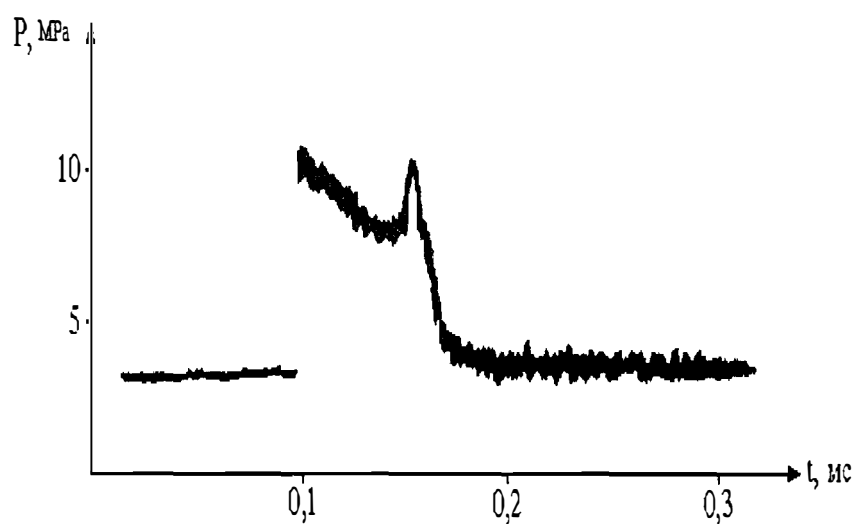


Fig. 2. The curve of the shock wave pressure in water near the bottom ice boundary at a deep explosion of the trotyl charge.

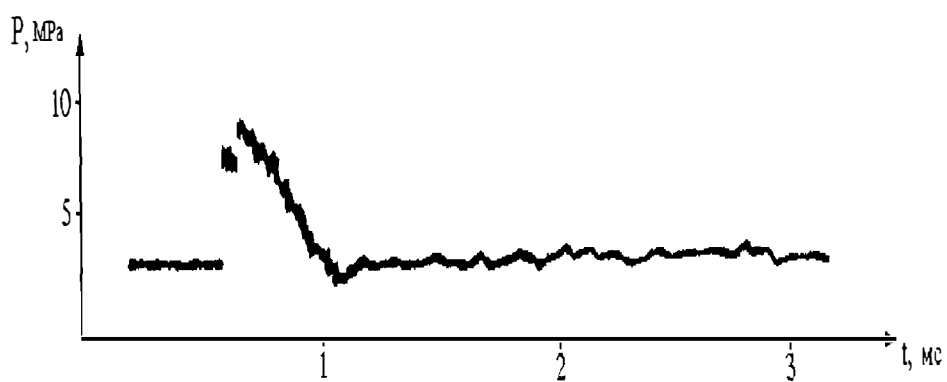


Fig. 3. The curve of the shock wave pressure in water near the bottom ice boundary at the explosion of a single trotyl charge at a depth equal to half the ice thickness.

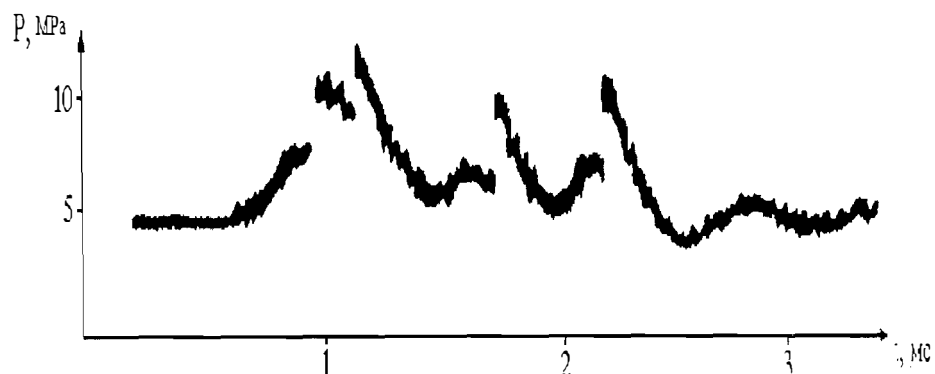


Fig. 4. The curve of the shock wave pressure in water near the bottom ice boundary of a group of single trotyl charges at a depth equal to half the ice thickness at a distance of 1 m from each other.

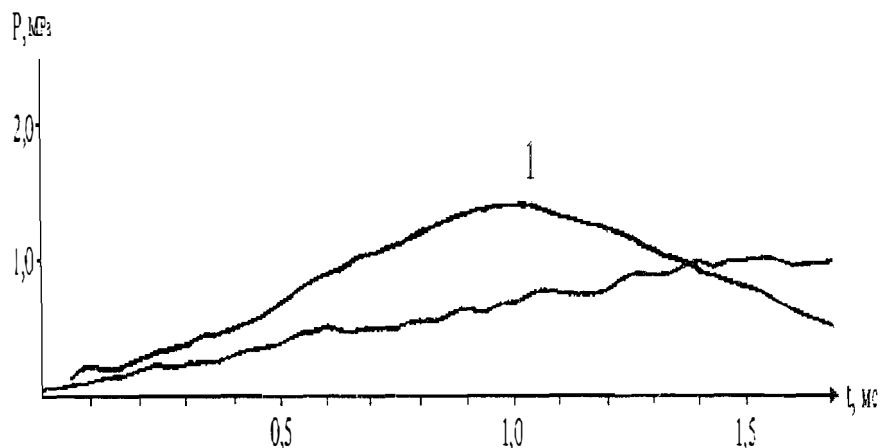


Fig. 5. The curve of the compression waves at the explosions of the powder charges: 1 - cannon, 2 - gunpowder.

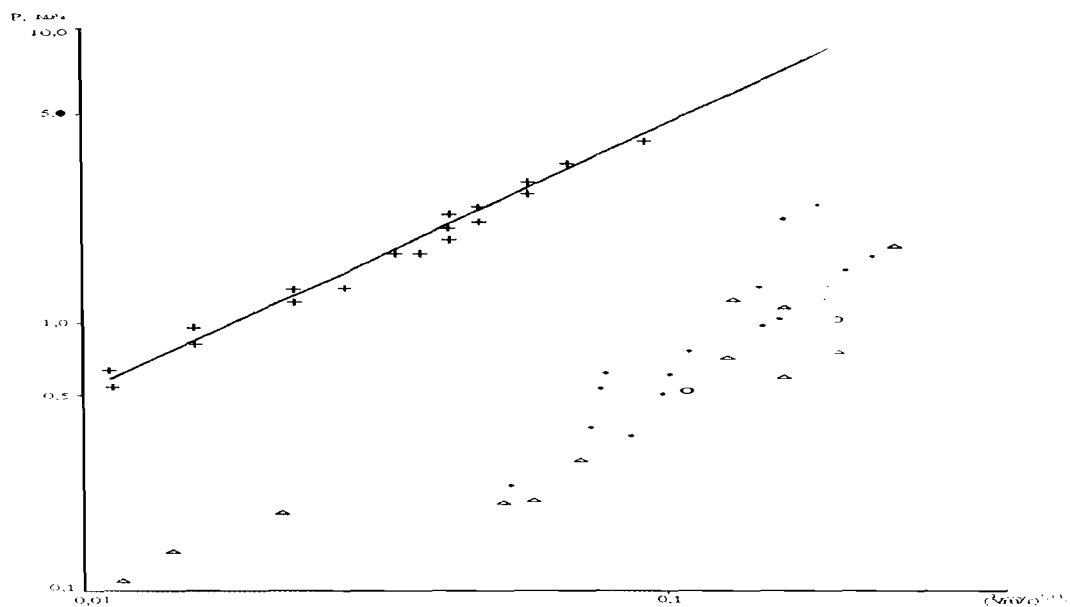


Fig. 6. Pressure at the front of the shock waves (or compression waves) in water at the explosion of different explosives under the ice cover. — approximation (1) for deep underwater trotyl explosions; + - trotyl explosions near the bottom ice boundary; ● - trotyl explosions in the middle of the ice cover mass; Δ - explosions of fuel-air mixtures under the ice initiated by trotyl; ○ powder explosions under the ice;

$$\frac{\rho}{\rho^*} \approx 1 - 3\varepsilon^* \quad (3)$$

The molecular relations in the ice are distributed in a mosaic way according to structure. Hence one can speak about the cohesion distribution of ice - σ_k (in pressure units) which withstands the destructive action of a strong shock wave. An energy condition for material destruction by the strong shock wave will be:

$$\frac{3}{2}(P^* + P_0) \cdot \varepsilon^* \geq \frac{\sigma_k^2}{2E}, \quad (4)$$

where E - the Young's modulus and hence, as extreme value of $\varepsilon^* = \sigma_k/E$

$$P^* + P_0 \geq \frac{1}{3} \sigma_k, \quad (5)$$

Therefore the radius of the explosion crushing zone is equal to

$$R^* \approx \frac{P_0 Q}{\sigma_k/3 + P_0} \cdot \sqrt[3]{m}, \quad (6)$$

where Q - the specific energy characteristic of the explosive. Beyond this zone the ice becomes partially less strong and can be destroyed by a mine effect.

For investigating the residual ice strength after the explosions the following methods were used. A cling instrument cooled in advance to deep temperatures (-50°C) is frozen to the ice mass under study. Then this instrument is sharply torn away from the mass with some amount of the test ice which remains at the entire contact surface of the instrument. The separating force is recorded by a dynamometer. The ratio of the force to the contact area of the instrument with the ice can be considered the estimate of time resistance to stretching. Fig. 7 shows the results of the tests before and after the explosion of trotyl charges under the ice cover. The left histogram in Fig. 7 shows the residual ice strength at the surface formed by the explosion, the right one (the dashed line) - the initial ice state with regard to the strength (before the explosion).

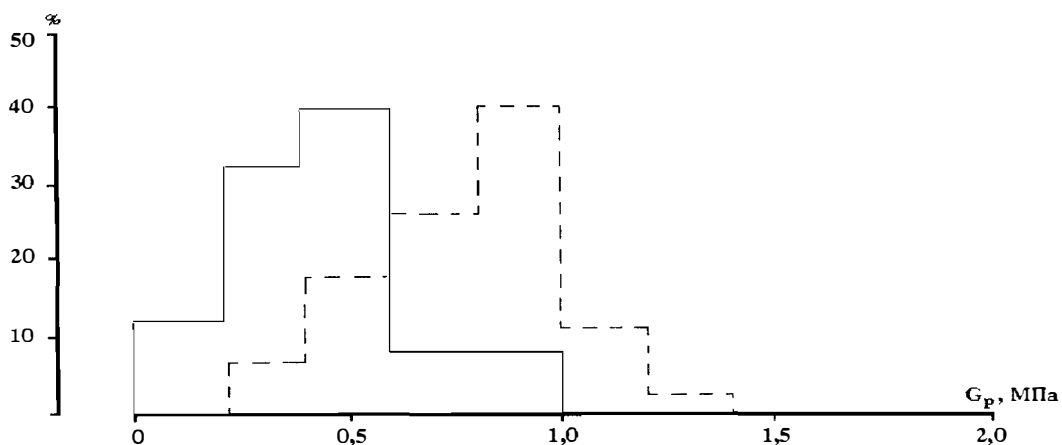


Fig. 7. Histograms of the results of measurements of the strength of first-year sea ice.

The application of trotyl can be limited due to technical and ecological considerations. The least impact takes place at explosions of gaseous mixtures, as well as at flameless explosions of thermal expansion whose force is regulated by the gas mixture composition and the method for initiating the explosion /4, 5/. According to the law, the application of explosive technologies should be approved by the State Mining-Technical Inspection which adopts the "Project of explosive works on the ice in the region of NN-off-shore structure". The project should be based on the results of studies which have direct relevance to the forthcoming explosion works.

References

1. Koup P. Underwater explosions. M., IL., 1950.
2. Yakovlev Yu.S. Explosion hydrodynamics. L.; Sudpromgiz, 1961, 312 p.
3. Zeldovich Ya.B., Kompaneyets A.S. A theory of detonation. M., Gostekhizdat, 1955.
4. Margolin A.D., Krupkin V.G. The development of a bubble in liquid in the presence of the gas-release source. "Physics of burning and explosion", 1985, No. 2, pp.76-81.
5. Tripol'nikov V.P. "Explosion evaporation of cryogenic liquid as a shock means". - Abstracts of the Third International Symposium "Mining in the Arctic", St. Petersburg, 1994, 90 p.

SPATIAL-TEMPORAL VARIABILITY OF ICE COVER STRUCTURE OF THE KARA SEA DURING ITS FORMATION AND GROWTH.

M.V.Strakhov, K.P.Tyshko, V.I.Fedotov, N.V.Cherepanov (AARI).

Multiyear full-scale studies of the ice cover in the Kara Sea allowed the main characteristics of the ice formation mechanisms and spatial-temporal variability of its structure to be revealed. The diverse characteristics are governed by a complexity of the hydrological regime of the water body and primarily by an intensive outflow of freshwater from the Ob'-Yenisey basin. In the zones of the fresh-/sea water contact, as well as in the zones of open water in winter (flaw polynyas, fractures and cracks in the drifting ice) the most favourable conditions for dynamic ice formation are created. The processes of dynamic ice formation are, as a rule, related either to water supercooling or to the heat outflux from the open water surface. The following structural-genetic ice types prevail in these regions: shuga, frazil ice and water-snow ice (formed when a considerable number of snow crystals fall to the water surface). In the ice cover these ice types are characterized by disoriented structures, the isometric form of crystals and the reduced salinity.

The results of laboratory and full-scale studies of different supercooling mechanisms of water and frazil ice formation have shown the heat outflux from the open water surface to be the most ice productive and widespread in the autumn-winter season. The ice crystals can form both at the surface and within the surface layer and the cooling value can reach 0.2-0.3 C /3/. The wind force and to a very small extent the current speed can have the largest influence on the value of ice production in polynyas and fractures (Fig. 1a).

The other mechanisms of water supercooling and formation of frazil ice have more local spreading and are mainly observed in the coastal regions of the intensive outflow of freshwater. These processes occur both at mixing of fresh- and sea water (Fig. 1b) and at their sharp layering (Fig. 1c).

On the whole, the dynamic conditions of ice formation are characteristic of much of the Kara Sea area during formation of the stable ice cover and of its most dynamic regions during the entire autumn-winter season. With ice thickness growth, the conditions for its formation become gradually stabilized and ice of dynamic type is gradually replaced by steady congelation ice formation. As a result, an oriented ice structure begins to develop with ice crystal growth in the direction of the basal plane (0001). This period is characterized by one more important feature of the spatial-temporal variability of ice cover structure, namely, its spatial orderliness. This phenomenon which forms well-pronounced unidirectional C-axes of crystals under the effect of currents with stable directions is typical both of fast ice and drifting ice of low mobility. Based on the results of multiyear studies of the ice cover of the Kara Sea, a map-diagram of the spatial orderliness of its structure was prepared (Fig. 2a).

The obtained set of all data on the spatial-temporal variability of the ice cover structure in the Kara Sea has allowed its schematic regioning according to prevailing structural-genetic ice types. The method of regioning was developed on the basis of the distribution of mean monthly multiyear air temperatures and ice thicknesses, as well as on data on its crystalline structure. For choosing the prevailing structural-genetic ice types and for facilitating schematic regioning of the Kara Sea ice cover, all structural-genetic classification of first-year ice /2/ was subdivided into two main groups: congelation ice with prevailing parallel-fiber structure and ice of dynamic or shuga type with an isometric form of crystals. This division of all ice types into two groups also took into account the fact that their physical properties have the largest differences.

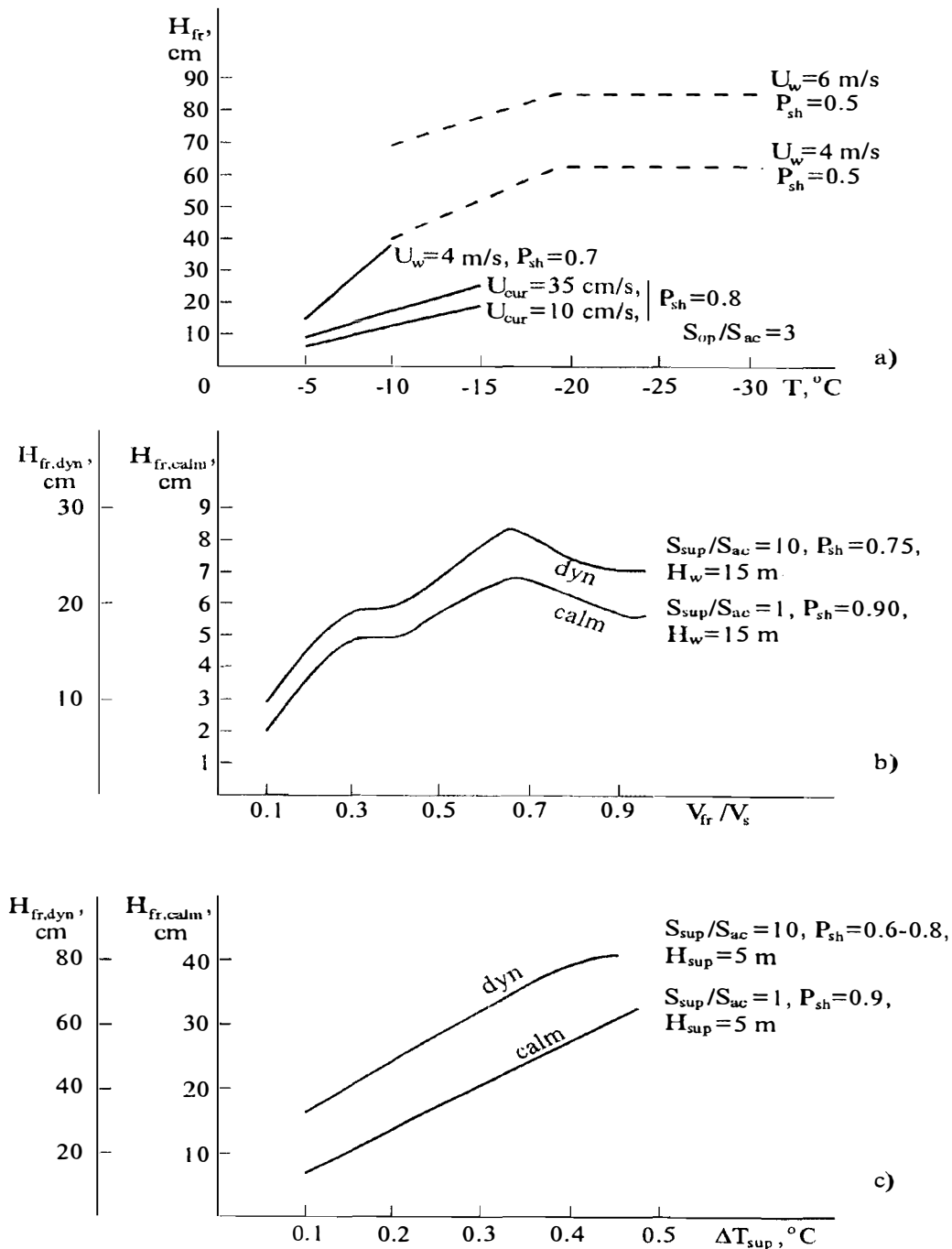


Fig. 1. Thickness of the formed frazil ice layer (H_{fr}): a) during a day in the open water zone under varying hydrometeorological conditions, as well as under calm ($H_{fr,calm}$) and dynamic ($H_{fr,dyn}$) conditions depending on b) mixed volumes of fresh (V_{fr}) and sea water (V_s) and c) the value of supercooling (ΔT_{sup}) of the contact layer between fresh and sea water.

----- - from data of Shuki U, Massaki W. f_3/S_{op} , S_{ac} - the area of open water surface and accumulation of crystals of intrawater ice, S_{sup} - the area of supercooled water surface, P_{sh} - porosity of shuga in its mixture with water, U_w , U_{cur} - wind and current speed, H_w - sea water layer depth, H_{sup} - thickness of the supercooled water layer.

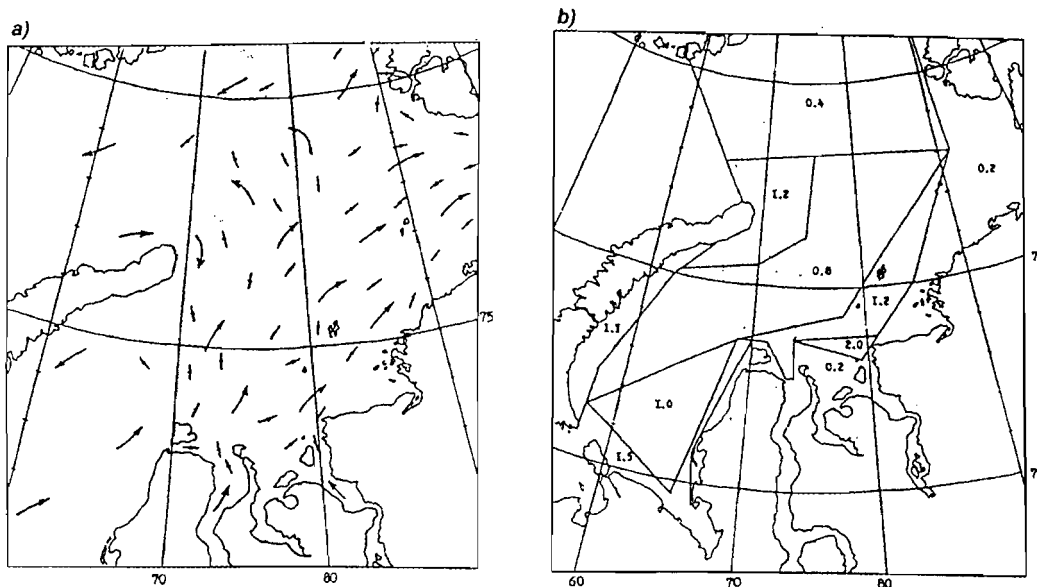


Fig. 2. A map-diagram a) spatial orderliness of the ice cover structure in the Kara Sea and b) distribution of the coefficient of dynamic ice formation in April.

—> - the direction of surface currents /4/,
 —•— - orientation of C-axes of ice crystals.

The degree of dynamic ice formation in each of the regions was determined by means of the respective coefficient K_d

$$K_d = (1 - H_{con} / H_{act}) \times H_{cal} / H_{act} + (H_{act} / H_{cal} - H_{con} / H_{act}) \quad (1),$$

where H_{con} - thickness of the congelation ice layer, H_{act} - actual ice thickness at mean monthly air temperatures, H_{cal} - ice thickness at mean monthly air temperatures calculated by Zubov's method [1].

The expression for calculating the coefficient of dynamic ice formation (1) was chosen assuming that the maximum dynamic ice formation is observed in the regions where ice export and renewal (the left term) occur regularly and also in the regions where the ice cover growth occurs due to the formed ice of dynamic or shuga type. The varying variability ranges of the K_d coefficient have approximately correspondent variability of the content of the ice of dynamic type in the entire ice cover layer, especially in the region with prevailing congelation formation (Table 1).

Table 1

The character of ice formation depending on the K_d

coefficient variability K_d	Content of ice of dynamic type, %	Character of ice formation
0 - 0,5	0 - 20	Congelation
0,5 - 1,0	20 - 40	Prevailing congelation
1,0 - 1,5	40 - 60	Congelation-dynamic
1,5 - 2,0	60 - 80	Prevailing dynamic
> 2,0	80 - 100	Dynamic

The obtained mean monthly maps-diagrams of the ice cover structure from October to April (Fig. 2b presents a map-diagram for April) served as a basis for a similar regioning of the ice cover by the main physical and physical-mechanical ice properties.

Reference

1. Zubov N.N. Sea water and ice. - M., 1938 - 451 p.
2. Cherepanov N.V. Classification of ice of natural water bodies/Proc. AARI, 1976, v.331, pp.77-99.
3. Shuki U., Massaki W. Rapid frazil ice production in coastal polynya: laboratory experiments/ Proc. NIPR-Symp.Polar Meteorol. and Glaciol., 1989 - No.2 - p.117-126.
4. Weeks W.F., Gow A.J. Preferred crystal orientations along the margins of the Arctic Ocean/J.Geophys. Res., 1978 - vol. 84 - N C10 - p. 5105-5121.

ICE COMPRESSION AND LOCAL DEFORMATIONS OF AN ICE FLOE IN THE ARCTIC OCEAN

V.N. Smirnov, I.B. Sheikin, A.I. Shushlebin (the AARI)

Introduction

The development of instrumental observation means allowed estimating the values of sea ice strains, their properties and some typical features. Studies (Legen'kov, 1992) were mainly performed at ice camps of small- (103 m), medium- (104 m) and large (105 m) scales. Strain observations at local (1 m) measurement bases can be of large applied and scientific significance. Composite local observations of the deformation processes of sea ice by means of the distributed systems of stress-, strain-, tilt- and seismometers were used for studying the dynamic processes in the ice cover of the Arctic Basin (Bogorodsky and Smirnov, 1980). Some typical features of the local strains were revealed during the experiment in Fram strait (Manley et al., 1982). Local observations were also used for solving some applied objectives, in particular, for estimating the ice loads on off-shore structures (Niemenlehto and Nordlund, 1986). On the whole, one may note that deformation of a separate ice floe reflects a wide range of oceanographic and atmospheric processes and can serve as an additional information source for their studies.

Observation results and their analysis

Observations were performed during the drift of the "NP-28" station on an almost round ice floe with a mean diameter of 1500 m and a thickness of 4 m which was in the massif of close ice and was separated from it by a belt of smoothed hummocks. Three quartz strainmeters were the main component of the measurement system (Smirnov, Shushlebin, 1988), deployed at a point according to the equiangular array whose maximum sensitivity was 10.. In addition, strain-, tilt- and seismometers were used. The general work program of the station included meteorological and hydrological measurements and the satellite coordinate measurement system.

For the work period of the station in 1987-1989 a piecewise continuous data series on local strains was obtained. For analysis a small portion of the record for April 1988 was chosen when the station was in the area of active dynamical processes. The obtained results allowed some preliminary conclusions which can be useful for planning further studies.

A two-dimensional tensor representation of the theory of elasticity of the mechanics of continuous media served as a basis for the mathematical model (Niemenlehto and Nordlund 1986). Main ratios and the deployment array of strainmeters are given in Fig. 2. The strain tensor components, divergence and deviator, as well as main strains and their directions were calculated from the calibrated and detrend data. The results of calculations, given in Fig. 1, show that at the background of a quasiharmonic deformation of a small amplitude (0..107h) the process of ice compression is well-pronounced (107..115h) and is accompanied by intensive hummocking according to visual observation data. By analysing the synoptic situation from surface atmospheric pressure and satellite TV images it is found that compression is governed by the intrusion of a continental cyclone to the region of Severnaya Zemlya Island. During the period April 18-21 the continental cyclone interacting with an extended high pressure area over Yakutiya, central Arctic and Greenland exited to the Laptev Sea and then turned to Severnaya Zemlya. The cyclone speed was about 500-700 km a day. Data of attendant meteorological parameters, as well as the calculated drift velocity and direction are given in Fig. 1.

It is known that any strain can be represented in the form of superposition of the comprehensive compression strain and shear strain and any deformed state of the

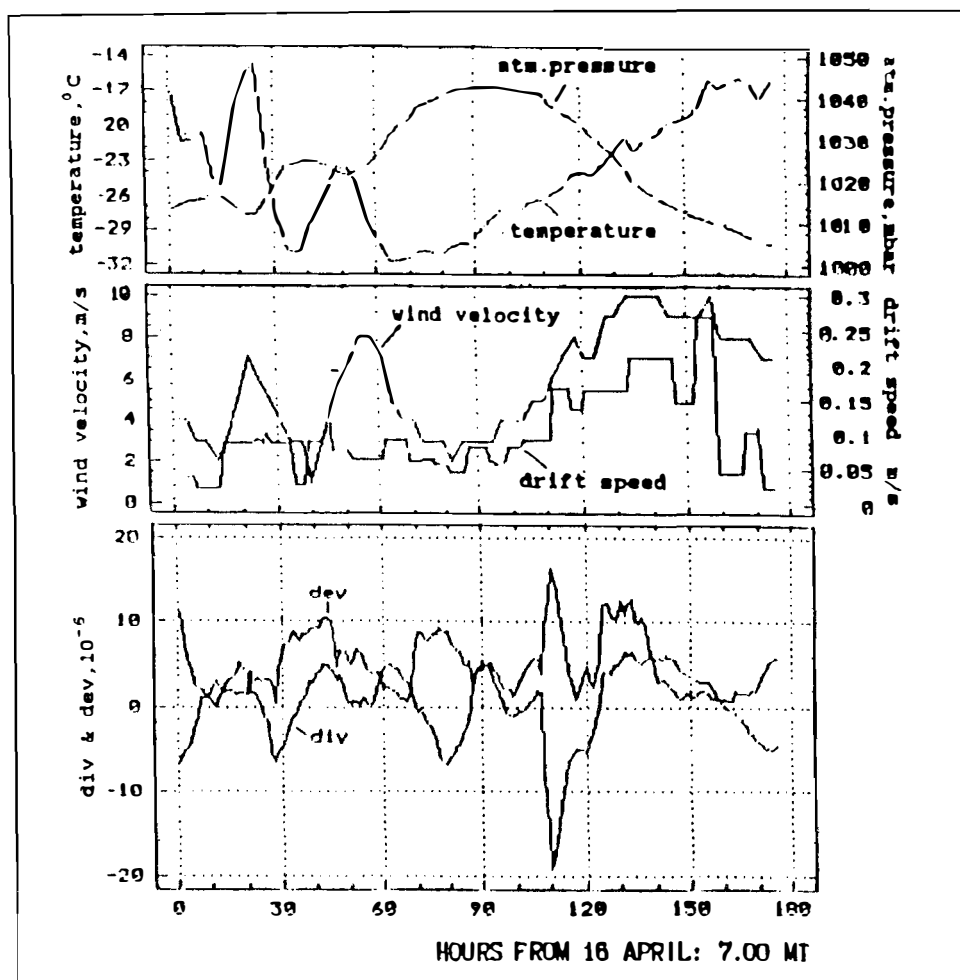


Fig. 1. Atmosphere temperature and pressure, wind speed, drift rate, divergence and deviator of the strain tensor.

object under study in the form of a point in the strain space whose coordinates are divergence and deviator of the strain tensor (Nye, 1976). The results of observations in this representation are shown in Fig. 2. The main patch of the points connected with the background quasiharmonic deformation includes more than 90% of all events. The points outside the patch belong to the process of compression and are grouped along the regression line with the regression coefficient being close to one, which coincides with the theoretical estimates of the ratios of normal and tangential stresses (Kolesov, 1979). The statistical analysis of the diagram allows determining a confidence level of the amplitude of background strains and formulate a criterion for determining the compression events. For investigating the nature of background deformation, the length of the series under consideration is not enough. However, one should note the periodicity of the processes of ice cover divergence-convergence, a relatively constant strain amplitude and direction which may be governed by the regional features of tidal processes.

A detailed analysis of the compression process allows determining its duration, increase and decrease rates, as well as the duration of ice hummocking. The latter characteristics can be connected with a smooth decrease in the intensity of strains at the peak of compression due to redistribution of strains at hummocking. The duration and intensity of compression suggest a possible development of plastic strains, however,

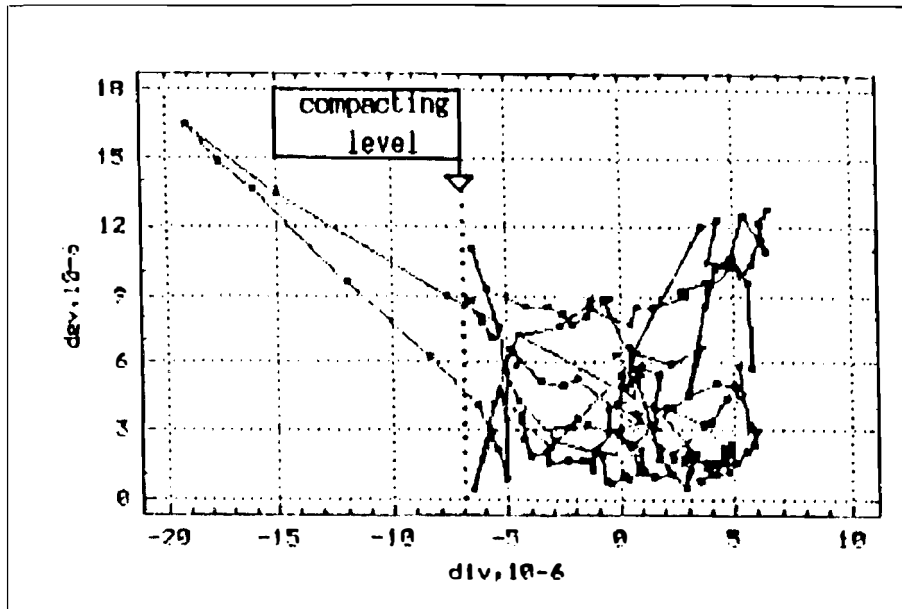


Fig. 2. Data in the strain space.

their estimates on the basis of measurements at one point are difficult due to background strains.

Comparison of the obtained results allows us to underline three facts.

1. The beginning of the compression process surpasses the cyclone front by about a day, if one assumes the front to be a moment of the maximum rate of the pressure drop which coincides with the time of the maximum wind and drift speed in our case. This confirms the conclusions of Smirnov (1988) and suggests that in close ice cover there is an additional mechanism for momentum transfer which is responsible for spreading of the compression process. The mechanism of elastic-kinematic interaction of separate ice floes can be such a mechanism. In this case the compression process can be presented in the form of the compression impulse or the frontal wave of compression emanating from a distant dynamical source.

2. A rapid shift of the station for 24 hours on April 21-22 after the cyclone front arrival is accompanied by an increase in the intensity of shear strains in the absence of compression strains. This deformed state is characteristic of the longitudinal uniform and cross-non-uniform velocity field. The orientation of the shear strains indicates the presence of the drift rate cross gradient and allows estimating its sign.

3. Wind speed and the drift rate correlate quite well, however, their directions differ in about 45-60 degrees and this difference is preserved for 2-3 days. A comparison of the directions of surface pressure isobars, wind and drift speed direction, as well as the orientation of the compression axis show the absence of direct relations between these two factors. However, the drift trajectory of the stations "NP-28" can be considered isobaric if the directions of isobars in the eastern sector of the central Arctic are averaged. Compression can also be considered isobaric if isobar directions are averaged for the Laptev Sea region. The mechanism for a spatial correlation of the phenomena under consideration can be synoptic circulation in the boundary layer of the ocean in the first case and propagation of the compression impulse through the ice cover in the second case.

Conclusions

1. Local deformation of the ice floes as a result of the effect of the synoptic-scale dynamic processes can be identified with a prescribed confidence level at the background of different strains related to thermodynamic processes in the ice cover. An analysis of local strains allows an objective assessment of the main characteristics of the compression processes of sea ice - intensity and direction of compression, duration of compression and hummocking, rates of their increase and decrease. As a result, an instrumental method for monitoring the ice cover stress-strain state can be developed by measuring local strains in sea ice.

2. An analysis of the obtained results allowed identifying two successive stages of the ice cover response to the synoptical process. The stage of intensive compression accompanied by sea ice hummocking surpasses the stage of the maximum drift rate by almost a day which is basically characterized by zero divergence and significant shear strains. The spatial delay of the area of the maximum ice drift localized along the cyclone front is 500-800 km relative to the area of the compression processes.

References

1. Legen'kov A.P. Strains of the drifting ice in the Arctic Ocean. 1992, St. Petersburg. Gidrometeoizdat.
2. Bogorodsky V.V., Smirnov V.N. Relaxation processes in the ice fields of the Arctic. 1980, DAN AN SSSR. vol. 250, No.3, pp.589-591.
3. Smirnov V.N., Shushlebin A.I. Results of observations of natural deformations of ice floes. 1988. Izvestiya AN SSSR. Physics of the Earth, No. 12, pp.75-78.
4. Manley, T.O., L.A. Codispodi, K.L. Hunkins, H.R. Jackson, E.P. Jones, V. Lee, S. Moore, J. Morison, T. Packard and P. Wadhams The "Fram 3" Expedition. 1982, EOS, 63(35), pp.617-636.
5. Niemenlehto J.J., Nordlund O.P. In-Ice Field Measurements for an Ice Load Estimation. VTT Symposium 71, Polartech '86, International Offshore and Navigation Conference and Exhibition, Helsinki, Finland, 27-30 October 1986, vol. 2, pp.762-778.

RESULTS OF STUDIES OF THE EFFECT OF WIND-INDUCED WAVES AND SWELL ON THE ICE COVER OF THE BARENTS SEA

V.N. Smirnov, V.A.Nikitin, A.I.Shushlebin, I.B.Sheikin (AARI)

The short-term ice dynamics in the vicinity of the ice edge is, to a great extent, governed by wind and waves.

The drift station was occupied on a first-year ice floe 55-56 cm thick at the base of the ice "tongue" of 4000 sq. miles in the area (Fig. 1). The amount of hummocking of the ambient ice was 2 arbitrary units (according to the national scale of 5 units) at ice concentration of 9-10/10. Four tiltmeters and three stress meters were set up. Wind observations were made at a height of 20 m.

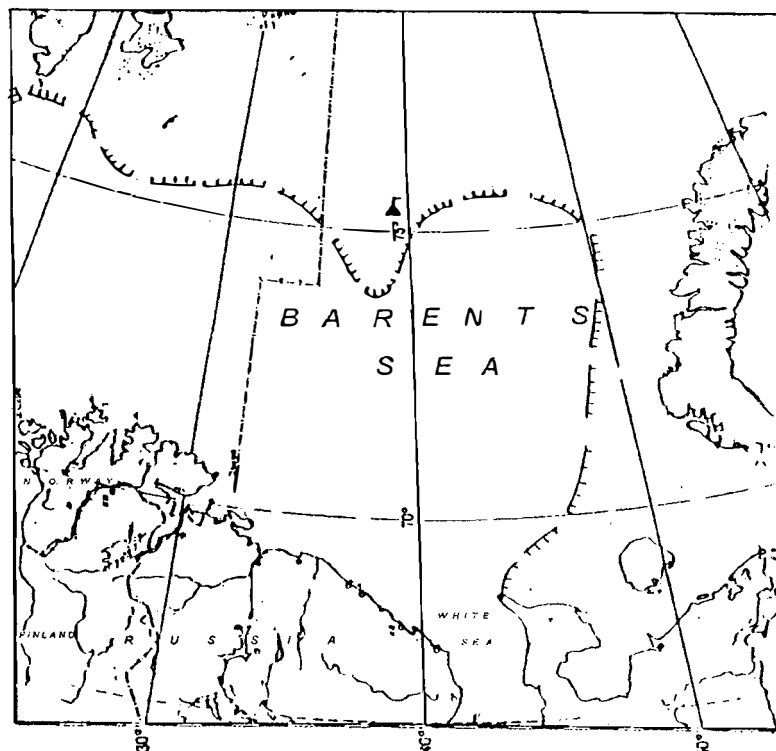


Fig. 1. Ice edge during the observation period (end of February - beginning of March 1986).

The analysis of the ice cover tilts has shown the sector of the arrival of waves to the observation point to be 200-225 ...

Fig. 2 presents meteorological parameters which are compared with a maximum hourly range of stretch-pressure stresses in the ice induced by propagation of gravitation waves under the ice cover.

Fig. 3 presents the amplitude spectra of stress oscillations in the surface ice layer to which the numbers from 1 to 18 were assigned .

Spectra 1,2,3,17,18 are governed by remote sources of swell. Spectra 6,7,10,11,12 are typical of the wind-induced waves. South wind (February 27) resulted in the significant development of waves near the ice edge which caused a change in the spectrum in approximately 12 hours. The change in the wind direction from western to southern (February 28, 2 hours) resulted in the changed spectrum in 5 hours (9, 10) and from southern to north-western (February 2, 8 hours) - in 9 hours.

Thus, the delay in the ice cover response to the change in the synoptic situation varies over a wide range (from 5 to 12 hours).

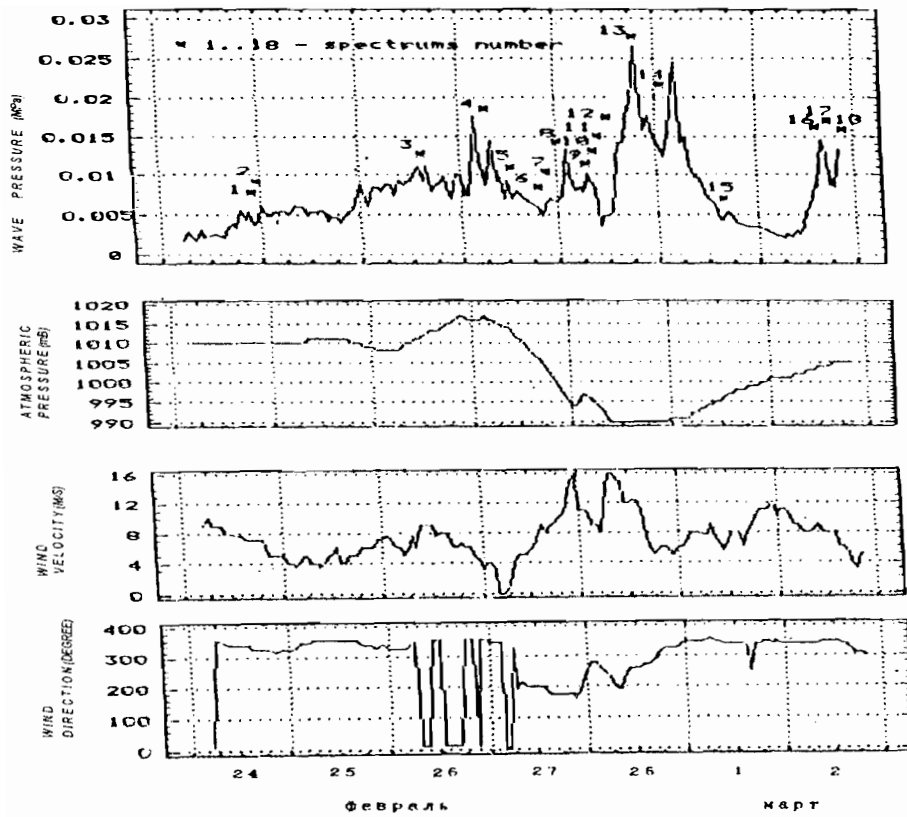


Fig. 2. Wave stresses and meteorological parameters during observations.

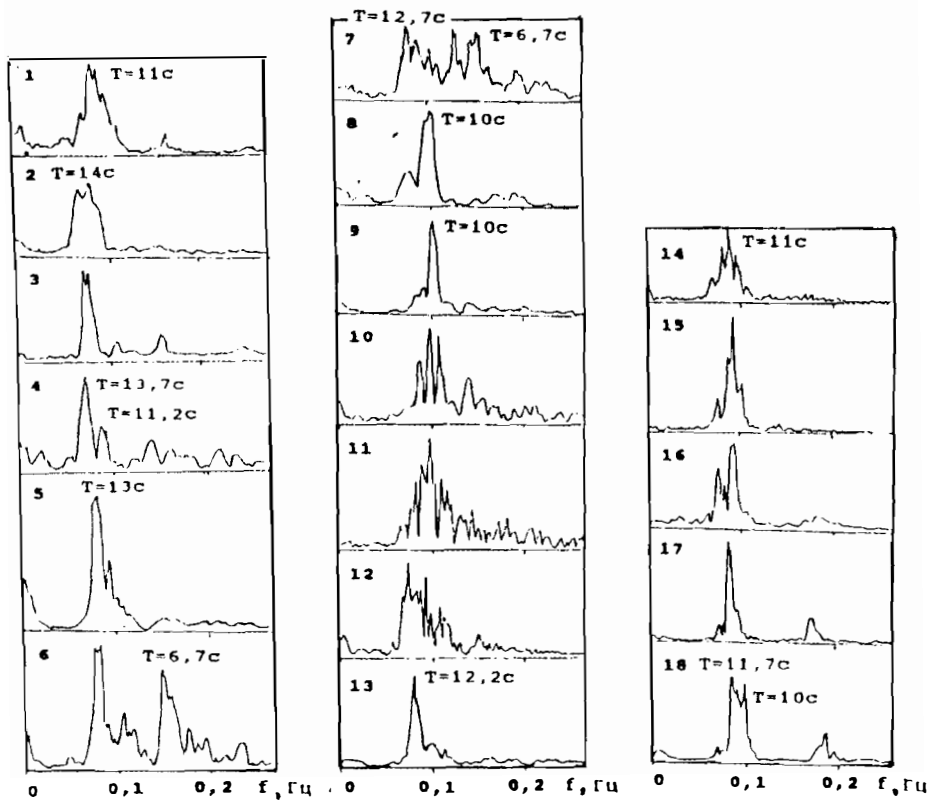


Fig. 3. Amplitudinal spectra of stress oscillations in the surface ice layer.

In the Barents Sea waves with a period of 7 s prevail, their occurrence frequency is 85% (the USSR Register, 1974). The constituent oscillations with periods more than 7 s prevail in the spectra which is attributed to the filtering properties of ice.

On February 2 at 15 hours the wind changed its direction from western to northern. At 16 hours on March 2, the spectrum 16 became similar to spectrum 1. Thus, full time of the ice cover "tongue" adapting to new meteorological conditions was about 49 hours.

The change in the wind direction to the northern one resulted not only in the changed spectral composition of the waves, but in pressure on the ice as well. One can estimate the tangential stress ... occurring at wind interaction with the ice cover surface which was about 0.22 H/m.. for our case. The total force F of pressure on the ice tongue ofin the area is estimated to be 2800 MH. Then, a normal stress at the base of the "tongue" at the extent of its base

$L = 75$ miles was 0.034 MPa. On February 28 at 3 hours the wind changed its direction and

was northern for 2 days. Wind pressure from water on the ice "tongue" disappeared. However, maximum stresses caused by the wind and the presence of swell were reached at 7 hours on February 28, i.e. in four hours after the onset of the wind change. The minimum of stresses was recorded at 20 hours on March 1 (more than 1.5 days have passed from the time of the wind change). The difference in stresses was about 0.025 MPa. Regretfully, the background level of stresses in the ice is unknown. It is difficult at present to draw any conclusions by comparing the stress values governed by wind and the calculated values.

A spectral express-analysis of the ice cover oscillations in combination with meteorological observations can serve as a basis for creating a method for ice state forecasting.

References

1. The USSR Register. "Wind and waves in the oceans and the seas". - "Transport" Publ. House, Leningrad, 1974, 359 p.

Part “Meteorology”

CURRENT CHANGES IN CLIMATE OF THE KARA SEA REGION

Ye.I.Aleksandrov, N.N. Bryazgin, A.A.Dementyev (The AARI)

An increase in air temperature in high latitudes of the Northern Hemisphere was observed from the mid- 1960s. In the second half of the 1980s the increase in temperature was slightly slower in the Northern Hemisphere, whereas at temperate latitudes this process was characterized by the highest temperatures for the period of instrumental observations /AARI, 1992; WMO, 1993/. In the Northern polar area the increase in temperature was most intensive at the end of the 1970s and the beginning of the 1980s. However, the temperature changes are not synchronous in different regions, which is governed by differences in spatial-temporal scales of the processes forming the temperature field in each of the regions.

For estimating current climatic tendencies in the Kara Sea region, the interannual changes in air temperature and monthly precipitation during cold and warm periods and on the whole for a year were considered. For this purpose, annual and seasonal charts of differences for each element between the period 1981-1990 and the preceding decades beginning from the period 1941-1950, were constructed.

An analysis of the charts of differences showed the highest annual temperatures with regard to the period 1981-1990 to be observed in the Kara Sea region in the 1940s and the 1950s. Annual air temperatures in the 1940s exceeded those of the 1980s by more than 2° C over much of the area. During the period 1951-1960 the source of higher temperatures was reduced in the area and was located in the region of the northern part of Novaya Zemlya and in the north-eastern Barents Sea. In the 1960s and 1970s annual air temperatures over the Kara Sea region were lower than in the 1990s, but not much. As is seen from Fig. 1, the main temperature increase was observed south of the Kara Sea coast.

The main contribution to the formation of the annual air temperature over the Kara Sea area is made by temperature changes in the colder period. As is seen from Fig. 1, the largest temperature differences regarding the last decade were observed during the periods 1941-1950 and 1951-1960. In the 1940s the air temperature in winter was 3° C higher than during the period 1981-1990 over much of the sea area. In the 1950s the difference was about 2° C. The largest air temperature contrast over the sea area and the adjacent territory of West Siberia was noted in the 1940s. The latter indicates that warming of the 1930s-1940s in this part of the Arctic was developing over the Kara Sea and during the past decades over the continental regions. The Kara Sea region in this case was at the periphery of the region of the current increase in air temperature.

In summertime the changes in temperature in the preceding decades were not so large as compared with the last decade. The temperature differences vary within +/-0.5°C.

An analysis of spatial distribution of differences in the annual and seasonal precipitation sums has shown that during the colder season there is observed large spatial uniformity in the distribution of the sign of precipitation differences. The differences of the same sign cover not only the Kara Sea area, but also a considerable part of the adjoining territory of West Siberia. In all decades under consideration the amount of precipitation in winter was greater than during the last decade. The largest amount of precipitation for the cold season was observed in the 1960s, during the period of the lowest air temperatures (for the whole study period). The main source of large values of differences was located in the northern part of the sea almost in all decades (Fig. 1).

In the warmer season the non-uniformity in the distribution of the sign of precipitation differences increases. Likewise in winter, there is a decrease in the precipitation amount in summer from the 1940s up to the 1970s. In the 1980s in the southern half of the sea the precipitation amount increased, whereas in the northern sea half it continued to decrease.

Fig. 2 presents interannual changes in temperature and precipitation sums for the Kara Sea region. As is seen, on the whole during the study period there is observed a well-pronounced linear trend toward cooling in temperature for the autumn and winter seasons and for a year over the Kara Sea region beginning from the 1940s. In the spring and summer seasons there is a weak trend toward the temperature increase. Within the study period there are noticeable short-period variations including the temperature increase from the mid 1960s. During the last decade the temperature changes have a trend for a decrease which is well-pronounced in the autumn and winter seasons. In summer and especially in spring there is a clear trend toward the increased air temperature.

Multiyear precipitation variations show a general trend for a decrease in the amount of precipitation. The annual amount of precipitation from the mid 1930s was non-uniformly decreasing and in the 1970s it decreased by 20-25% (or by 70 mm) relative to the 1930s-1940s. At the end of the 1970s a trend for the increase in precipitation has appeared. The precipitation maximum in the region during all years of observations was recorded in 1989 (more than 300 mm), but in 1990 precipitation was below the norm by 20-30 mm.

A comparison of interannual variations of temperature and precipitation shows good correlation of their changes in some periods. The increased air temperature at the end of 1970s and the beginning of the 1980s in autumn and winter corresponds to the decreased precipitation amount. However, the increase in the precipitation amount in the colder season which followed it from the mid -1980s, coincides with the temperature decrease.

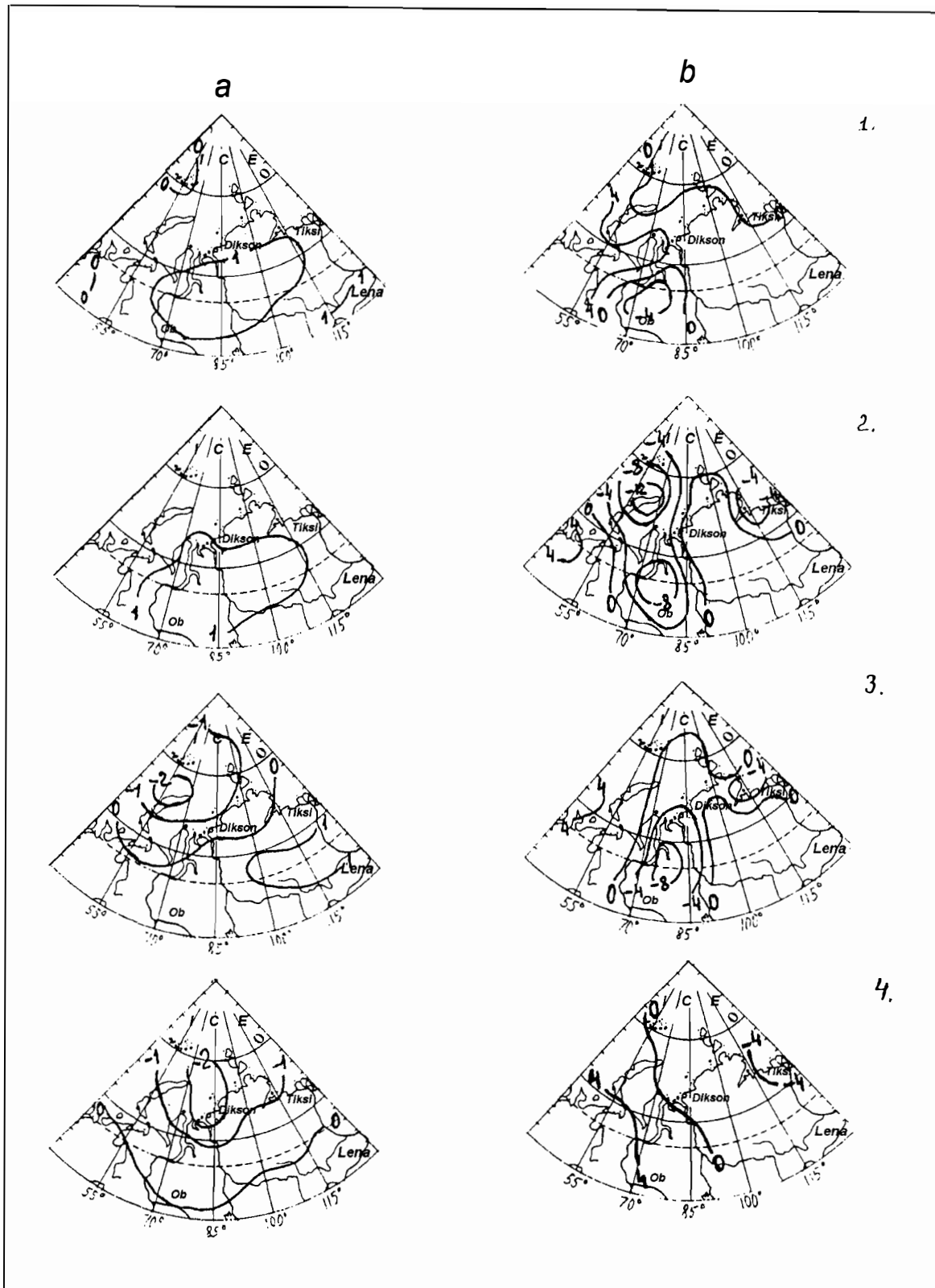


Fig. 1 Spatial distribution of the differences in annual temperature (A) and annual amount of precipitation (B) between separate periods. 1 - 1981-1990 and 1971-1980, 2 - 1981-1990 and 1961-1970, 3 - 1981-1990 and 1950-1960, 4 - 1981-1990 and 1941-1950.

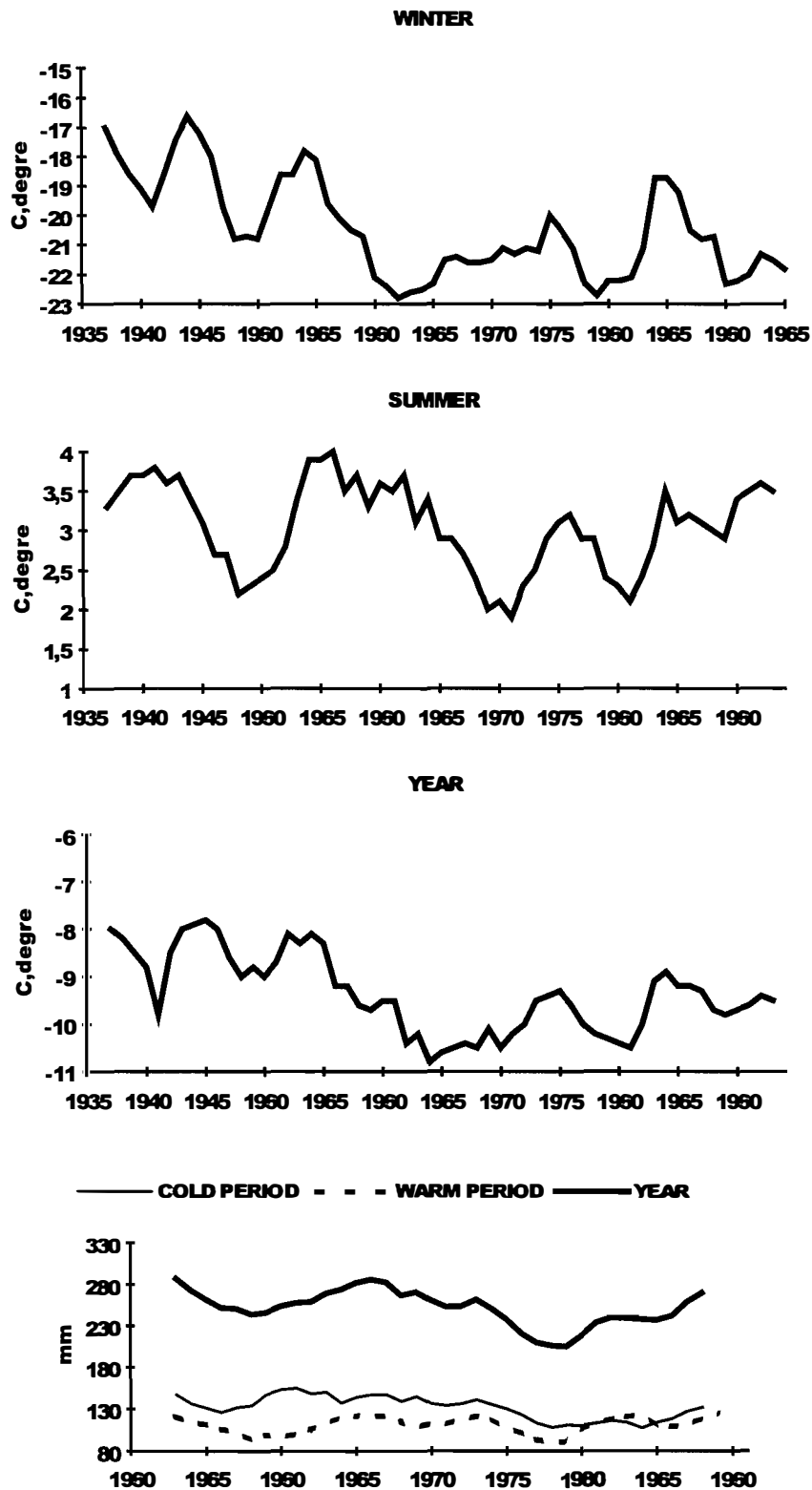


Fig. 2. Interannual changes in 5-year running air temperature and precipitation

The tendencies in the variations of temperature and precipitation sums are closely related to changes in atmospheric circulation. The distribution of the number of days with the forms of atmospheric circulation according to Vangengeim, shows that in the 1970s the number

of days with the eastern form of circulation (E) was observed to prevail and the number of days with a zonal form of circulation (W) was minimum. This situation resulted in the enhanced meridional exchange between high and temperate latitudes which led to a more intensive air temperature increase in the Kara Sea region in the 1970s-beginning of the 1980s. During the last decade the number of days with the E form has decreased and the number of days with a zonal circulation form has increased. This governed the trend for a decreased annual temperature and the increased sums of precipitation from the mid -1980s.

References

1. Data of climate monitoring in polar regions of the Globe. - St. Petersburg: the AARI, 1992. - 120 p. (In Russian).
2. WMO statement on the status of the global climate in 1993. - Geneva - Switzerland, 1994, WMO - No. 809. - 20 p.

DRIFTING SNOW TRANSPORT IN THE KARA SEA

N.N. Bryazgin, A.A. Dementyev (AARI)

During the cold season of the year (October-May) the drifting snow is very frequent in the Arctic. As a result of the drifting snow, there is redistribution in the depth and density of the snow cover. In the Arctic Seas the snow cover on the ice is non-uniform. Due to drifting, snow is accumulated in some places (snow-drifts, sastrugi), and is blown away from the ice surface in other places /3/.

In the Kara Sea mean multiyear dates of the formation of a stable snow cover refer to the third 10-day period of September in the north-eastern region and only to the third 10-day period of October in the south-western sea. The dates of the formation of a stable snow cover vary significantly. Thus at the Amderma station the snow cover can become stable from September 24 to November 21 and at Dikson Island - from September 11 to October 20 /1/.

The snow cover decay at these stations occurs in the period May 9 to June 13 (Amderma) and May 25 to July 11 (Dikson). Table 1 presents mean multiyear dates.

Table 1

Mean dates of appearance, formation, decay and disappearance of the snow cover

Station	First appearance	Formation of the stable cover	Decay of the stable cover	Disappearance
Amderma	28 IX	12 X	4 YI	15 YI
Beliy Island	22 IX	4 X	28 YI	29 YI
Viese Island	18 YIII	12 IX	23 YI	25 YI
Golomyaniy Island	28 YIII	12 IX	28 YI	29 YI
Uyedineniye Island	28 YIII	20 IX	20 YI	25 YI
Dikson Island	18 IX	1 X	14 YI	18 YI
Ruskiy Island	2 IX	20 IX	1 YII	3 YII

Mean snow depth in the Kara Sea varies from 25 to 50 cm at the end of winter. The largest snow depths are presented in Table 2. Their maximum values are observed in May.

Table 2

The largest mean depth (cm) of the snow cover at the Kara Sea Islands

Station	IX	X	XI	XII	I	II	III	IV	V	VI
Beliy Island	5	2 9	3 4	4 4	5 1	7 3	6 3	6 6	7 1	6 6
Viese Island	1 0	2 1	3 8	4 6	4 7	4 8	5 5	6 4	7 0	6 0
Golomyaniy Island	1 4	2 2	2 7	3 6	3 2	3 1	3 4	3 9	4 7	3 9
Dikson Island	8	2 2	1 7	2 2	2 6	2 7	2 7	2 8	3 8	1 6
Russkiy Island	2 4	2 7	3 3	3 3	4 5	5 3	4 8	5 0	6 3	5 9

Only a thin upper layer of the snow cover and solid precipitation participate in the snow transport. The duration of the drifting snow in the Kara Sea is significant. One event of the drifting snow can last for 5-6 days in succession. Mean duration is from 50 to 200 h for a month and more than 2000 h for a season. The snow transport at the hydrometeorological stations is not usually measured, only the duration of the drifting snow is recorded. However, a series of observations of the intensity of the snow transport at different heights from 0 to 5 m was conducted using experimental measurements of the "Tsiklon" instrument. It turned out that the intensity of the snow transport depends on the wind speed and the height above the snow cover level. The drifting snow begins at a wind speed of 6-8 m/s (the height of measurements is 10 m above the ground level).

A methodology for calculating the amount of the snow transport was developed [2]. The total intensity of the snow transport is calculated using the formula:

$$\int_Z^H q * dh$$

where Q is the total intensity of the snow transport in the whole drifting snow layer, g/cm²; q is the intensity at various levels; H is the drifting snow height; Z is the snow surface roughness.

The calculation formula of intensity: $Q = (0,24 * U^{3,44}) * t, \tilde{a} / \tilde{m}^2 * g,$

where t is the duration of the drifting snow. If the density of the drifting snow is equal to 0.17 g/cm^3 , then the formula for calculating the volumes of the snow transport:

$$V = (0,00014 * U^{3,44}) * t, \text{ m}^3/\text{m}.$$

In accordance with a large variability in the duration of the drifting snow and the wind speed, the Kara Sea is characterized by a large variability in the volumes of the snow transport (Fig. 1). On the whole for the sea from 500 to 700 m^3 of snow across the linear meter perpendicular to the wind direction is transported (in different directions) during the drifting snow season. The largest snow transport is recorded at the southern sea coast where strong local winds are observed. Thus in the Amderma region up to 1880 m^3 is transported, in the Yenisey Gulf up to 1750 , in Vilkitsky strait up to 1300 m^3 . The snow transport is mainly from the south - from the south-eastern to the south-western direction. 45% of the snow transport volumes falls on these directions. For the other directions the snow transport is distributed by 5-10% for each of the eight direction gradations (rhombs).

Conclusion. The amount of the snow transport is calculated on the basis of experimental measurements. In the Kara Sea the snow cover becomes stable on September 24, on average, and decays on June 21. The extreme dates can differ by 15-20 days. The snow cover depth varies from 25 to 50 cm at the end of winter. The snow transport volumes are 500 - 750 in the sea and up to $1880 \text{ m}^2/\text{m}$ at the southern coast for the winter season.

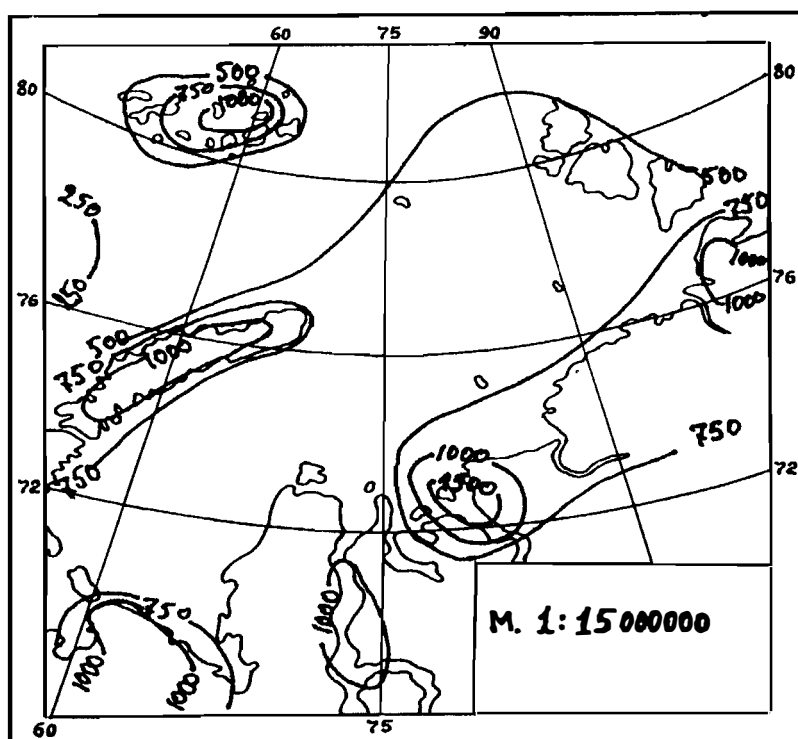


Fig. 1. The snow transport volume in the Kara Sea, m^3/m .

References

1. Atlas of the Arctic. M., GUGK, 1985.
2. Bryazgin N.N., Voskresensky A.I. Solid precipitation and snow transport under conditions// Materials of glaciological studies. M., 1982. No. 43, pp.79-85.
3. Buzuyev A.Ya., Romanov I.P., Fedyakov V.Ye. Variability of the snow distribution on ice of the Arctic Ocean// Meteorology and Hydrology, 1979, No.9, pp.76-84.

**CONCENTRATION OF LARGE CONDENSATION NUCLEI AT
AIRBORN
ATMOSPHERIC SOUNDING OVER THE BARENTS AND KARA
SEAS**

B.F. Sadovsky, A.G. Sharapov, B.I. Ogorodnikov(KPCI)

Introduction

Large condensation nuclei with the particle size of 0.1-0.3 μm are the most stable global fraction of aerosols in the atmosphere. These particles are transported over large distances and their transport is governed by the general laws of turbulent atmospheric mixing. They play a large role in forming the cloud layer. By origin, large condensation nuclei are subdivided into marine, continental and anthropogenic. To clear up the concentrations of such aerosols over the basins of the Barents and Kara Seas a number of studies were carried out for some years from the laboratory-aircraft AN-24. The experiments were performed in the troposphere at the heights up to 6 km taking into account the influence of cloudiness, air temperature, wind direction and force and other factors. Based on synoptic charts, the region from where the arctic air was transported, was determined taking into account two-three preceding days.

Methods

Two laser aerosol spectrometers designed at the Karpov Institute with multichannel amplitude analyzers of integral and differential types were installed onboard aircraft. The main measurements were conducted using the instrument of a differential type, while the instrument with an integral analyzer

was used for calibration. The design of the instrument allowed recording the particles with a diameter of $0.2 \mu\text{m}$ and more. At a short-term voltage amplification at the photoelectric multiplier one could record the particles with a diameter of $0.11 \mu\text{m}$. The air transport through the capillar for counting the particles was $20 \text{ cm}^3/\text{min}$ at the total flow of $500 \text{ cm}^3/\text{min}$. For operational tracing of the change in the concentration of particles the measurements were performed for 0.5 min. During this time the distance passed by aircraft was about 3.5 km.

Main results

The work under different weather conditions has shown that the concentration of large condensation nuclei is greatly influenced by the meteorological conditions, the temperature factor, cloud distribution by altitude, the prehistory of the particles and conditions for their formation. In the free atmosphere at heights from 0.5 to 6.5 km the concentration of particles was in the range from tenths of fractions to several thousands in a cm^3 , depending on the state of the atmosphere and the processes which preceded the sampling time, the spectrum of particles was strongly transformed.

It is found that near the clouds at their edges and above the upper cloud edge the concentration of large condensation nuclei is 10-15 times greater than in the cloud itself. Directly over the cloud the concentration is usually comparable with the background level observed at a distance from the cloud, but at atmospheric disturbance the concentration of particles is large. Thus at a height of 5.5-5.7 km the measured concentration was from several units to 26 cm^{-3} , whereas directly near the cloud it is from 900 cm^{-3} . The presence of a weak haze is always accompanied by the increase in condensation of large condensation nuclei up to tens and hundreds of particles in cm^{-3} . More than 80% of the spectrum of such particles was represented by particles of $0.2 \mu\text{m}$. At small concentrations of aerosols or "fresh" clouds, the particles of the size of $0.2 \mu\text{m}$ comprised 93-98% and sometimes 100%.

In old "air dispersion" systems at relatively low concentrations a significantly transformed aerosol spectrum

at the heights of 2-3 km was observed. The particles of the size of 0.2-0.3 μm comprised sometimes 30-50% and with a diameter more than 2 μm up to 27%. In these cases with the increased content of particles more than 1-2 μm in size, the maximum in the size distribution of particles shifted to the region of 0.3-0.5 or 0.5-0.7 μm . During temperature inversion an anomalous large number of the background particles above the clouds were observed (at the heights of 2-3 km up to 400 cm^{-3} at the background concentration at this time of about 20 cm^{-3}). In strongly transformed "old" systems the particles with a size of 0.2-0.3 μm comprised only 5-8% and of 1.5-2 μm more than 38-44%. By mass the micron particles constituted more than 90%. In the surface layer (at the heights less than 1 km) at a small absolute concentration only particles with a size of 0.2-0.3 μm were practically observed.

Conclusion

Unlike the continental air dispersion systems where size distribution can be approximated by the formula:

$$dN/d\ln r = Cr^{-\beta},$$

the value $\beta=3$ and the C-constant is in the size region from 0.2 to 0.8, for marine aerosols of the polar basin β was within 0.4-0.47, according to our data.

The value of the mass concentration of aerosols calculated from measurements of the number of particles assuming their density to be 1, was within 0.002-0.01 mg/cm^3 in all measurements.

RESULTS OF A FULL-SCALE EXPERIMENT ON STUDY OF SOLAR RADIATION ABSORPTION IN THE UPPER LAYER OF THE KARA SEA (AUGUST-SEPTEMBER 1994)

Myakoshin O.I., Makshtas A.P., Nagurny A.P.

Processes of sea/air energy exchange govern to a great extent the thermal, dynamical and ice regime of the Arctic Seas. The shortwave solar radiation flux is one of the main components of the heat budget of the upper active sea layer. Some new data on the hydrooptical characteristics of the Kara Sea area in summer were obtained during the Russian-Norwegian expedition "KAREX-94".

For measurements of incoming and scattered solar radiation and its calculations based on the heat influx at different depths an experimental underwater balansometer was used. It was designed at the St. Petersburg Electrotechnical University and allows measurements in the spectral range of 0.3 +3 mkm up to depths of about 15 m. Measurements were performed at oceanographic stations under favourable meteorological conditions: weak waves and the height of the Sun more than 10°.

Taking into account the specific features of oceanographic conditions, the obtained data can be divided into three groups (Fig.1):

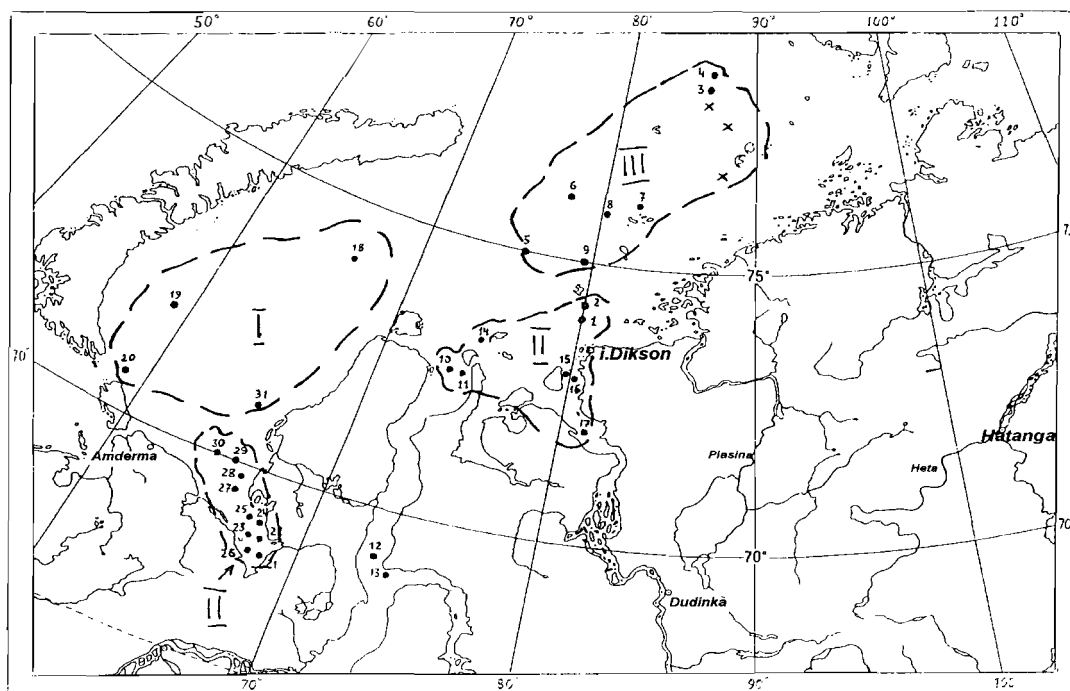


Fig. 1. The geographical position of oceanographic stations at which the hydro-optical measurements were made. — : boundaries of the uniform oceanographic regions.

1. The region of the Novozemel'sky gyre. 2. The coastal-mouth region. 3. The north-eastern Kara Sea. For illustration, Fig. 2 presents the distributions of incoming, scattered and absorbed radiation in the layer , as well as of the attenuation coefficient obtained at oceanographic stations of each of the groups.

The attenuation coefficient (c) was calculated on the basis of the Buger's law by the formula:

$$C = -\frac{1}{\Delta Z} \ln \frac{J_{i+1}}{J_i}$$

where J_{i+1} , J_i - is incoming radiation measured at the levels Z_{i+1} , Z_i , $\Delta Z = Z_{i+1} - Z_i$. For the cloud-free sky the depth Z was calculated taking into account the height of the Sun and the effect of light refraction in sea water.

Table I presents mean values of the attenuation coefficient for the three data groups identified.

As is seen, in all of the three groups the attenuation coefficients are maximum for the upper 0.5 m layer which is connected with intensive absorption of the near- infrared portion of the incoming radiation. The largest attenuation coefficient is typical of the coastal mouth region (group 2) which is governed by the enhanced level of suspended particles discharged by rivers and, respectively, by large scattering of shortwave radiation. Some increase in the attenuation coefficient in the 4-5 m layer of which is absent in other regions is also of interest. Probably, this is related to the near bottom turbid flows characteristic of the shallow mouth zones of the sea.

A comparison of data of hydrooptical and oceanographic observations has shown that a significant influx of shortwave radiation (4-8 W/m²) under the pycnocline also occurs in the coastal mouth region. In view of the important role of the heat flux to the bottom boundary of the ice cover formed in the Arctic Seas which is governed by the heat content of water below the pycnocline (Gudkovich et al., 1979), this effect is worth to be further investigated.

Table 1

Mean attenuation coefficients for groups 1, 2, 3

Layer (m)	Group 1	Group 2	Group 3
0-0.5	0.77	1.43	0.45
1-2	0.29	0.21	0.33
4-5	0.16	0.38	0.26

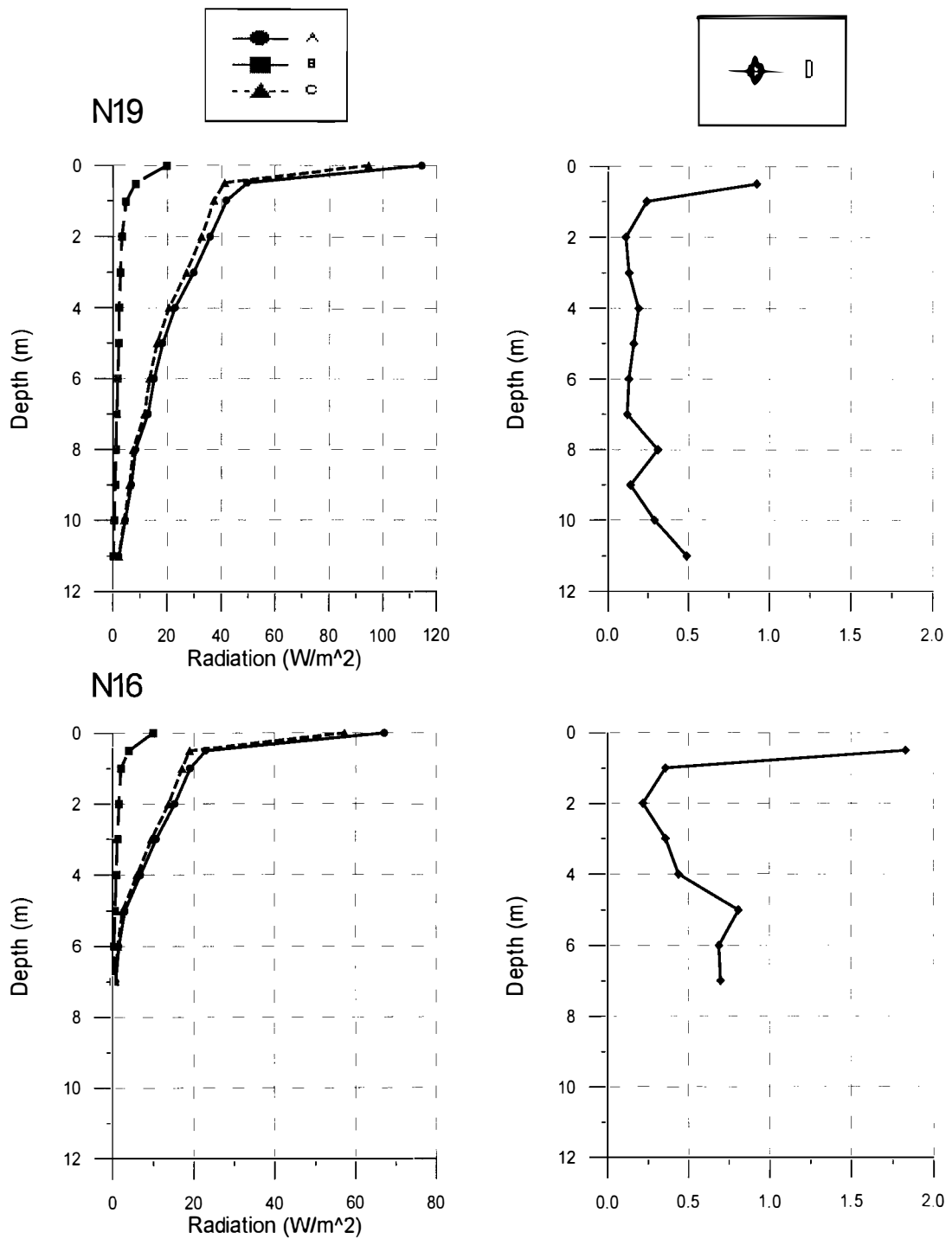


Fig. 2. Vertical distributions of incoming (A), scattered (B) and absorbed (C) solar radiation and of the attenuation coefficient (D) at stations 19 (cloud cover 1/0, height of the Sun 20.2 °); 16 (cloud cover 8/5, height of the Sun 20.2°);

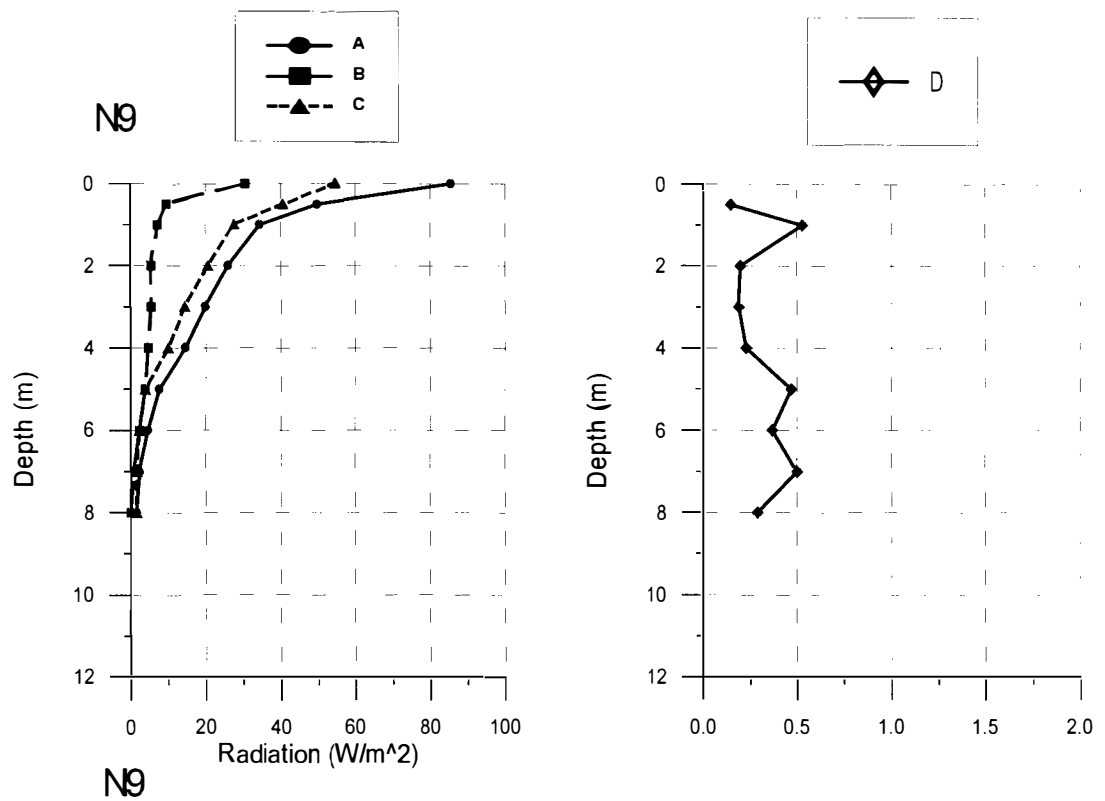


Fig. 2. Vertical distributions of incoming (A), scattered (B) and absorbed (C) solar radiation and of the attenuation coefficient (D) at station 9 (cloud cover 1/1, height of the Sun 22.6°).

References

1. Gudkovich Z.M., Gladkov M.G., Lukyanchikov S.N. 1979. Ice cover volume and ice thickness distribution in the south-eastern Laptev Sea at the end of winter of 1976. In: Poles-North-76, Part II, L., Gidrometeoizdat, pp.16-20.

Sea chemistry and contamination

RADIOACTIVE CLIMATE OF THE KARA SEA FROM THE RESULTS OF RUSSIAN-NORWEGIAN CRUISE IN 1992.

L.M.Ivanov, T.M.Margolina (MHINUAS), A.I.Danilov, M.Y.Kulakov, V.K.Pavlov (AARI).

The ^{137}Cs and ^{137}Sr concentrations in the dissolved and suspension forms measured in the Russian-Norwegian cruise of 1992 were utilized by the method of spectral reconstruction developed in Ivanov, Eremeev and Kirwan, 1992; Ivanov, Kirwan and Margolina, 1995. The radionuclide fluxes across the external boundary of the Kara Sea were calculated. The contributions of the various factors to the generation of the sea radioactive climate were being indicated.

It was demonstrated that the total amount of the ^{137}Cs in the dissolved and suspension forms were equal to 15.8 and 0.2~TBq, respectively. The similar value for the ^{137}Sr in the dissolved form was 8.62~TBq. The estimations of the annual mean transport for the radionuclide through the strait Kara gate given 53.6, 0.24 and 2.34~TBq for the ^{137}Cs in the dissolved and suspension forms and the ^{137}Sr in the dissolved form, respectively.

There are some peculiarities in the conclusions the relative to radioactive pollution of the Kara Sea following from the present calculations. In our opinion the present radioactive climate of the Kara Sea can be generated by the radioactive pumping through the strait Kara gate and the draining of radionuclides through the Vilkitsky strait and open boundary of the Kara Sea. Apparently, the contribution of radionuclide transport from rivers and atmosphere in the generation process is more weak.

**POTENTIAL RADIOECOLOGICAL SITUATION IN THE REGIONS OF THE
BARENTS AND KARA SEAS.**

V.N.Lystsov (RSC KI)

The current radioecological situation in the seas of the Russian Arctic does not present a radioecological problem. However, the great potential sources for radionuclide pollution of the Barents and Kara Seas do exist. There were identified five major areas of problems connected with possible radioactive pollution. They include nuclear submarines and nuclear icebreakers decommissioning, spent nuclear fuel and radioactive waste treatment, dumped nuclear waste and material, sunken nuclear submarines. Significant features for all the problem areas are formulated and suggestions for necessary practical steps are made.

INVESTIGATION OF SEDIMENT RADIOACTIVE CONTAMINATION AT THE KOLA BAY.

A.A. Namjatov (MTAHEM)

In 1994 Murmansk Department for Hydrometeorology and Monitoring of Environment there have been carried out works concerning studies of the bottom sediments radioactive contamination on the territory of the civil enterprise "Atomflot".

The main part of the samples collection was carried out on board the ship "Victor Buinitsky". Samples collection was carried out in the centres of squares 100 x 100 m dimension (84 samples). Besides, 7 samples were collected from the moorings of the Repairing-Transport Enterprise "Atomflot". All samples were gamma-spectrometrical analyzed and Pu-239,240 were determined in 8 samples.

Minimal value of Cs-137 was about 2 Bq/kg of dry weight, and maximal value was 43.0 Bq/kg of dry weight. Though in the Cs-137 distribution a certain regularity should be traced: maximal values were observed most often along the moorage line.

Co-60 was determined only in 8 samples out of 84 samples collected. In one of the samples Co-60 concentration was determined on the level of minimal-detecting value, in other samples Co-60 concentrations range was 3.0-27.0 Bq/kg d.w.

Eu-154 was detected in 15 samples out of 84 collected samples., in 7 samples - Eu-154 concentrations were either on the level or less than minimal allowable concentration. In other samples range of Eu-154 contents change varied between 3.0-123 Bq/kg d.w.

Out of 84 samples collected Eu-152 was detected in 15. Out of these in 6 samples its contents was on the level or lower than minimal detective value., maximal meaning was 55 Bq/kg d.w.

In the collected samples of bottom sediments determination of Pu-239,240 was carried out. These nucleids contents was 0.53-1.00 Bq/kg d.w.

**RESULTS OF THE EXPRESS-SURVEY OF THE NOVAYA ZEMLYA BAYS
RADIOACTIVE POLLUTION**

G.A. Nejdánov, L. Yu. Kazennov, RRC "Kurchatov Institute"

Water and bottom sediments of the seven bays of the Novaya Zemlya archipelago were surveyed with the aim of quick assessment of the environment state at the sites of previous radioactive waste dumping. The measurements were conducted from the deck of the expeditionary ship by a submerged gamma-spectrometer of high sensitivity.

Analysis of spectrometric information obtained shows an absence of any meaningful pollution signs except several points of registrations of negligible bottom sediments pollution indications.

**RUSSIAN-NORWEGIAN JOINT INVESTIGATIONS OF THE MARINE
ENVIRONMENT RADIOACTIVE CONTAMINATION IN THE AREAS OF
RADIOACTIVE WASTE DUMPING IN THE KARA SEA**

A.I.Nikitin, V.B.Chumichev ("Typhoon"), P.Strand (NRPA), L.Foyn (IMR)

Since 1992 in a frames of the joint Russian-Norwegian Commission for Cooperation in the Environmental Sector the joint work of the specialists of Russia and Norway on investigation of radioactive contamination in the Northern Sea Areas was started. The joint research in this direction was initiated because the both sides were worried about the consequences of the former USSR practice of radioactive waste dumping into the Kara and Barents Seas. The investigations were conducted on board research vessel "Victor Buinitsky" of Roshydromet Murmansk Area Department.

The joint expedition was carried out in 1992 with the purpose of the general radioactive contamination level estimation in the Kara and Barents Seas. One of the main conclusions based on the results from this expedition was that now there are no influence of the waste dumped on the general level of radioactive contamination in the regions of the open Kara and Barents seas.

However the local effects directly in the dumpsites for radioactive waste can not be excluded and so in 1993 were started a joint investigations directly in the most potential dangerous dumpsites for solid radioactive waste in the Kara Sea (the dumpsites where along with the other radioactive waste the objects with spent nuclear fuel were dumped). In 1993 investigations were carried out in the dumpsites in the Tsivolki and the Stepovogo Fiords in the east coast of Novaya Zemlia Ilands and in the dumpsite in Novaya Zemlia Trough. In 1994 the investigations were continued: the survey was carried out in the most important from radioecological point of view dumpsite in the Abrosimov Fiord and continued the investigations in the Stepovogo Fiord. The information on the content and volume of the observations fulfilled is given in the presentation.

During the joint investigations some of the dumped objects were located and observed, along which were two nuclear submarine reactor compartments containing reactors with unloaded spent fuel in Abrosimov Fiord and submerged in the Stepovogo Fiord nuclear submarine with reactors containing spent nuclear fuel. The detail information on the located and observed objects is given in the presentation.

According to the preliminary measurements results received on board research vessel "Victor Buinitsky" during the joint 1994 Russian-Norwegian expedition, there are observed in the Abrosimov and Stepovogo Fiords the places with high level of bottom sediment radioactive contamination, especially in the vicinity of the containers with radioactive waste dumping areas. High levels of bottom sediment radioactive contamination (for Cs-137 up to 2000 Bq/kg dry weight in the Abrosimov Fiord and up to 60000 Bq/kg in the Stepovogo Fiord) are existed only closely (practically near the walls) to the dumped containers. On the distances about dozens metres from the objects the same levels as typical for most part of the fiords aquatory are observed.

Elevated levels of bottom sediment radioactive contamination (less essentially than near containers) are determined also closely to some submerged objects with spent nuclear fuel. For example, closely to one of the reactor compartments submerged in the Abrosimov Fiord Cs-137 bottom sediment contamination levels up to 400 Bq/kg are detected. This fact is a sign that some leakage of radioactivity from the objects of this type exist and dumped objects with spent fuel are potential source of marine environment radioactive contamination.

So, due to the joint investigations we have a good progress in estimation of existing consequences of radioactive waste dumping into the arctic seas and scientific basis for potential concequenses estimation is created. The results received during the joint work allows us to give some first priority recommendations on monitoring of marine environment radioactive contamination in the west part of the Russian Federation Arctic Region:

1. Now the most actual task is an estimation of potential concequenses of the objects with spent nuclear fuel dumping. The same investigations as carried out in Abrosimov Fiord in 1994

ones is necessary to continue in another Kara Sea dumpsites with the purpose to receive the basic scientific information for the future work on marine environment radioactive contamination monitoring.

2. The presence in the Kara Sea of the dumpsites with potentially dangerous objects containing spent nuclear fuel, and also a severe situation in the region with radioactive waste management require to organize in the region a joint work of Russian and Norwegian specialists on marine environment radioactive contamination on a regular base.

FEATURES OF ORGANIC MATTER DESTRUCTION IN WATER OF THE BARENTS AND KARA SEAS

G.A. Korneyeva, V.P. Shevchenko (IORAS); G.I. Ivanov (ARROI)

For the first time a comprehensive study of the spatial distribution of particulate matter and hydrolytic enzymatic activities for estimating the quality and destruction rates of organic matter in water of the Arctic Seas was performed. Also, an analysis of the results taking into account the hydrological conditions (based on the results of the 9th cruise of the R/V "Professor Logachev" in August-September 1994) was performed. The parameters under consideration reflect a structural-functional approach to investigating the organic matter and its transformation. Study of particulate matter in water and the features of concentration of particulate organic carbon as an ecosystem component is required for understanding the processes of current sedimentation and for assessing the ecological state of the area. The hydrolytic enzymatic processes in the water column reflect the molecular mechanisms of interrelated transformations of organic matter. Due to the high rates, the enzymatic processes are decisive in transformation of organic matter and its redistribution for living organisms during the entire period of life at the Earth /more than 3.5 billions of years /Sidorenko, Tenyakov, 1991/. The enzymatic processes are capable to provide the rates of destruction of natural organic polymers 10^9 - 10^{13} times exceeding the rates of similar chemical reactions in the absence of enzymes /Keleti/.

The enzymes produced by living substance, are active not only in the organism cells, but also in the habitat medium. Thus high biochemical activity of microorganisms with regard to destruction of organic matter in sea water is related to the action of extracellular enzymes released in large quantities to the medium both as a result of natural functions and at decomposition of biota after its death. According to literature and data obtained, the extracellular enzymes are capable to accumulate in the natural-immobilized state on particulate matter and to preserve their activity. Since the enzymes are only catalysts of the destruction reactions of the organic matter and are not destroyed at that, their action can be traced for a long time, including the zones remote from their genesis. Unfortunately, no sufficient attention was paid to studies of the enzymatic processes at the ecosystem level.

The considered processes of enzymatic destruction of natural polymers which belong to organic substances of protein and polysaccharide nature /Biogeochemistry of the boundary zones of the Atlantic Ocean, 1994/, up to lower molecular compounds - peptides, aminoacids, sugars are the key stages in the detrital food chains providing rapid utilization of high molecular compounds from the medium by microorganisms.

The results of studies of particulate matter in water and hydrolytic enzymatic activities are given in Fig. 1. As is seen, the least quantity of particulate matter and only traces of hydrolytic activity or its absence at all were observed in the northern Barents Sea (stations 73-76). The concentration of particulate matter varied from 0.09 to 0.19 mg/l. Calculation of the kinetic parameters of enzymatic destruction of proteins has shown that in this region the effective constant of the reaction rate of the 1st order by substrate k_1 was less than 0.003 1/h and the destruction rate of v - less than 0.40 mg/l an hour which corresponds to the protein turnover of more than 300 h. A decisive influence on water structure and the hydrochemical regime in this region is produced by the water exchange with the Arctic Basin / Volume: Biogeochemistry of organic matter, 1962/. Hence it can be concluded that the surface layer of arctic water which is underlied by Barents water, is poor in marine particulate matter and the processes of the organic matter destruction are extremely slow. The easternmost station of this transect (st. 78) was the only exception.

At the transect from the Spitsbergen archipelago to the Kola peninsula (st, 81-88) the total particulate matter was 0.10-0.37, increasing from south to north. The distribution of enzymatic hydrolytic activities was non-uniform which, probably, reflects the features of the

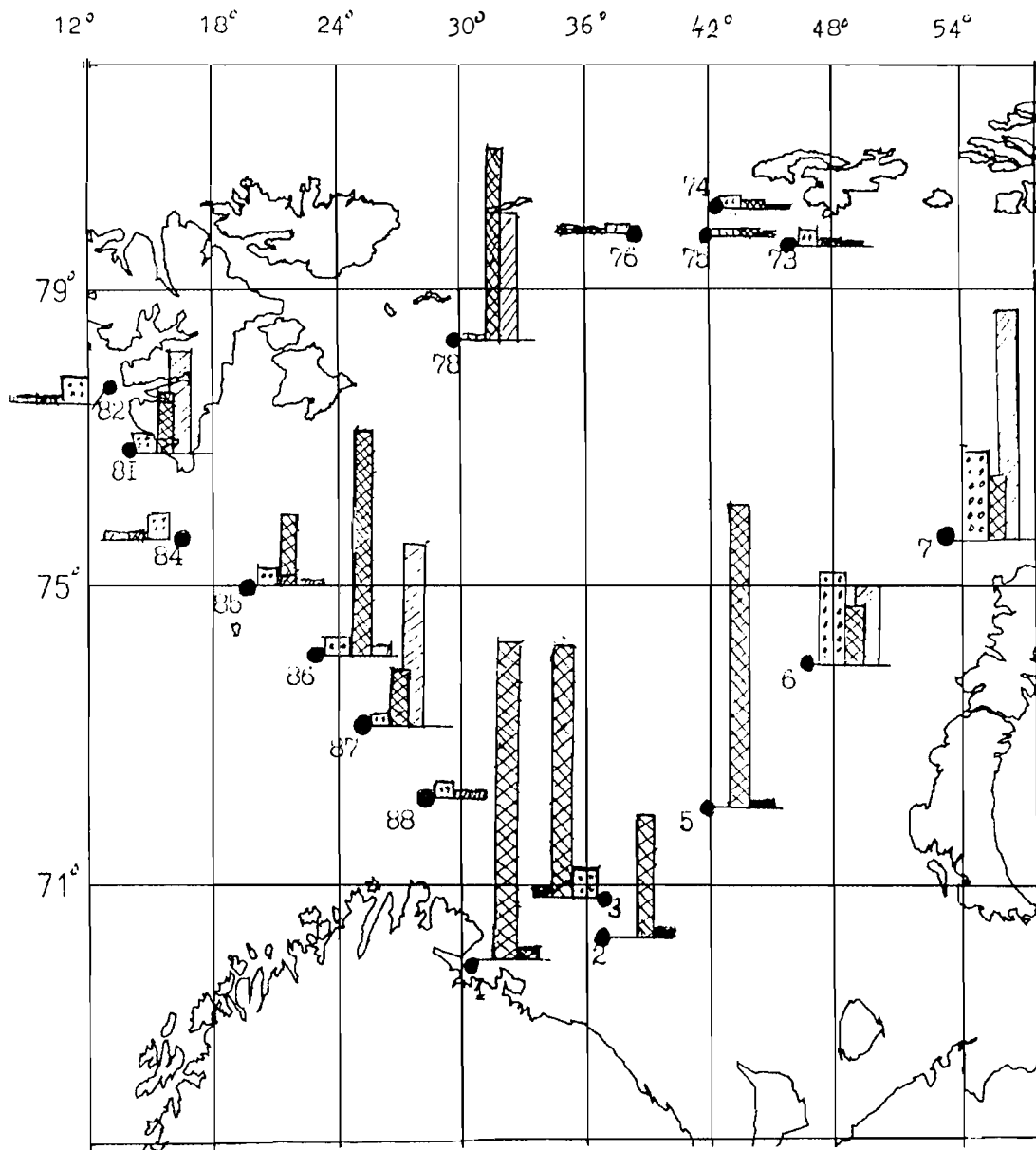


Fig. 1. Distribution of the quantity of particulate matter in water (\square , 1 cm = 1 mg/l), proteolytic (\boxtimes , 1 cm = 10 e.u./l) and amylolytic (\boxdot , 1 cm = 20 e.u./l) enzymatic activities in the Barents Sea area.

hydrochemical water regimes in the northern and southern parts of the transect including the Nordkapp and the central regions of the Barents Sea. The k_1 values for the hydrolysis of proteins varied from 0.003 to 0.018 1/l and v - from 0.40 to 2.12 mg/l an hour which corresponded to the time of the turnover of proteins from 298 to 57 h. The elevated values of hydrolytic enzymatic activities were observed in the middle part of the transect where the axis of the warm Nordkapp current passes (Tantsyura, 1973/).

Large concentrations of particulate matter in water of 1.58-1.52 mg/l were detected in the eastern sector of the central Barents Sea at stations 6 and 7 adjacent to Novaya Zemlya. However, the proteolytic enzymatic activities here were low. The kinetic indicators for them were: k_1 0.003-0.004 1/h and v 0.4-0.5 mg/l an hour. In the southern part of this transect at the

background of the largest values of the proteolytic activities (k_{10} from 0.019 to 0.023 1/h and v from 2.27 to 2.37 mg/l an hour, the time of the turnover of proteins was 51-57 h).

The trace values of the amylolytic enzymatic activities indicated the inhibition of the destruction processes of polysaccharide of alpha-glucane type. The obtained data confirm published data about the insignificant discharge of the sedimentary material and the slow rates of bottom sedimentation for the Barents Sea. Destruction of proteins and polysaccharides as the main classes of natural organic polymers in sea water is also slow, as compared to the Baltic and Black Seas.

During this cruise data on sea water in the north-eastern Kara Sea (st. 11-69) were also obtained. In the north-eastern region of the St. Anna trough the elevated values of the total particulate matter - 0.50-0.86 mg/l were recorded at the stations near the ice floe edge. This was in agreement with high amylolytic enzymatic activities corresponding to the rates of the turnover of alpha-glucanes up to 10 h. The largest values of enzymatic activities were determined in the water sample from a crack in the ice floe near Graham-Bell Island (Frantz-Josef Land archipelago) where an intensive diatom blooming was observed. The proteolytic enzymatic activity was 552 e.u./l which corresponded to the extremely high rates of the protein turnover - less than 3 h. This was consistent with the recorded large productivity in these regions at the end of summer governed by active phytoplankton development near the ice floe edge /Bobrov, 1985; Sakshang and Skjodal, 1989/. The quantity of particulate matter in the sample was maximum and was equal to 3.85 mg/l.

References

1. Biogeochemistry of organic matter of the Arctic Seas. Ed. by I.S. Gramberg, Ye.A. Romankevich. M.: Nauka, 1982, 240 p.
2. Biogeochemistry of the boundary zones of the Atlantic Ocean. Ed. by Ye.A. Romankevich. M.: Nauka, 1994, 400 p.
3. Bobrov Yu.A. Influence of temperature and light on primary production. In: Life and conditions for its existence in the pelagic zone of the Barents Sea. Ed. by G.G. Matishov. Apatity. 1985, pp.115-125.
4. Keleti T. Grounds of enzymatic kinetics. M.: Mir, 1990, 350 p.
5. Sidorenko Sv.A., Tenyakov V.A. On the nature of organic matter in rocks of the Early Precambrian. - The RAS papers, 1991, vol. 321, No. 5, pp. 1080-1083.
6. Tantsyura A.I. Seasonal changes of currents of the Barents Sea. Proc/PINRO, 1973, No.34, pp.108-112.
7. Salshang E., Skjodal H.R. Life at the ice edge. Ambio, 1989, Vol. 18, pp. 60-67.

**RESULTS OF HYDROCHEMICAL STUDIES IN THE KARA SEA DURING THE
EXPEDITION "YENISEY-93"**

V.S. Latyshev (AARI)

The results of the determinations of hydrochemical elements during the expedition from 7 August to 15 September are presented. They include determinations of salinity, oxygen, silicon, phosphates, concentration of hydrogen ions, alkalinity, nitrates, nitrites, salt composition elements (Cl, K, Na, Ca, Mg) heavy metals, chlororganic pesticides in the Yenisey Bay, Ob' Gulf and the central Kara Sea. By using hydrochemical parameters zones of estuaries and boundaries of river water spreading that were tracked in the vicinity of the northern tip of the Novaya Zemlya Island, were delineated. The characteristics of the vertical hydrochemical structure are presented. Zones of stagnant water in the near bottom layer with a large deficit of dissolved oxygen reaching up to 20% are revealed. Supplies of mineral nutrients are estimated and a high level of nitrate nitrogen in the Ob' Gulf water is observed (more than 1000 μ l).

COMPOSITION OF AEROSOLS OVER THE NORTH-WESTERN KARA AND BARENTS SEAS IN AUGUST-OCTOBER 1994

V.P. Shevchenko (IORAS), G.I. Ivanov (ARROI), A.A. Vinogradova, A.A. Burovkin (IORAS), L.Ya. Grudinova (MER)

Importance of aerosol studies in the Arctic is governed by possible ecological implications of anthropogenic impact of large industrial regions of the Northern Hemisphere on the Arctic atmosphere. Studies of aerosol composition in the Arctic are carried out in the Norwegian, Danish, USA and Canadian Arctic for more than 30 years /Barrie, 1986/. In the Russian Arctic only separate studies in this area were performed /Vinogradova et al., 1993/. From 1991 scientists of the Institute of Oceanology of the RAS under supervision of Academician A.P. Lisitsyn conduct studies of aerosols above the Arctic Seas.

Materials and methods

In August-October 1994 in the 9th cruise of the R/V "Professor Logachev" in the St. Anna trough (the north-western Kara Sea) and in the Barents Sea 19 samples of aerosols were collected by nylon meshes and 10 samples by filtration through the AFA-HA filters (Fig. 1). During sampling by means of the mesh method 5-10 nylon meshes with an area of 1 sq.km each and the cell size of 0.8 mm were suspended in the bow part of the ship for 8-24 hours. After exposition the meshes were washed in distilled water, then this water was filtered through Iavsan nuclear filters with a pore diameter of 0.45 μm . During sampling by the filtration method 65-525 cu. m of air was pumped through the AFA-HA-20 filters by means of a home-made sampler. Sampling by both methods was performed onboard the moving vessel at the adverse wind. In samples collected by the mesh method the substance composition of non-salt particles was investigated using a scanning electronic microscope JSM-U3 (Japan). The content of different chemical elements in the samples was determined by means of the instrumental neutron-activation analysis method at the Institute for Geochemistry and Analytical Chemistry of the RAS (Moscow).

Results and discussion

According to data of electronic-microscopic studies, coarse ($>1 \mu\text{m}$) non-salty aerosol particles sampled by the mesh method, mainly consist of mineral particles with a size of 5-20 μm and organic substance (vegetation fibers, pollen, diatom algae). Soils of the land regions surrounding the study site (Fig. 1), are the main source of mineral particles, although during certain time periods long-range transport also makes a significant contribution /Maenhaut et al., 1989/. Vegetation fibers up to several hundreds of μm long and pollen of terrestrial plants are transported by wind over hundreds of kilometers and the cells of diatom algae with a size of 5-50 μm are torn away by wind from the surface microlayer of sea water and are discharged to the near water air layer. As a result, the content of organic carbon in the mesh aerosol samples reaches 20-30% of the dry weight of the sample. Porous fly ash of 5-50 μm in size and smooth spheres of combustion of 0.5-10 μm in diameter were observed in a small amount in most mesh aerosol samples. The amount of these typically anthropogenic particles injected to the atmosphere with the emissions of metallurgic, mining plants, thermal power stations and boilers increases near Murmansk at the inflow of air masses from the Kola peninsula. For example, many combustion spheres were recorded in Sample 17. The maximum content of fly ash was recorded in the Kola Gulf at the roadstead of Murmansk.

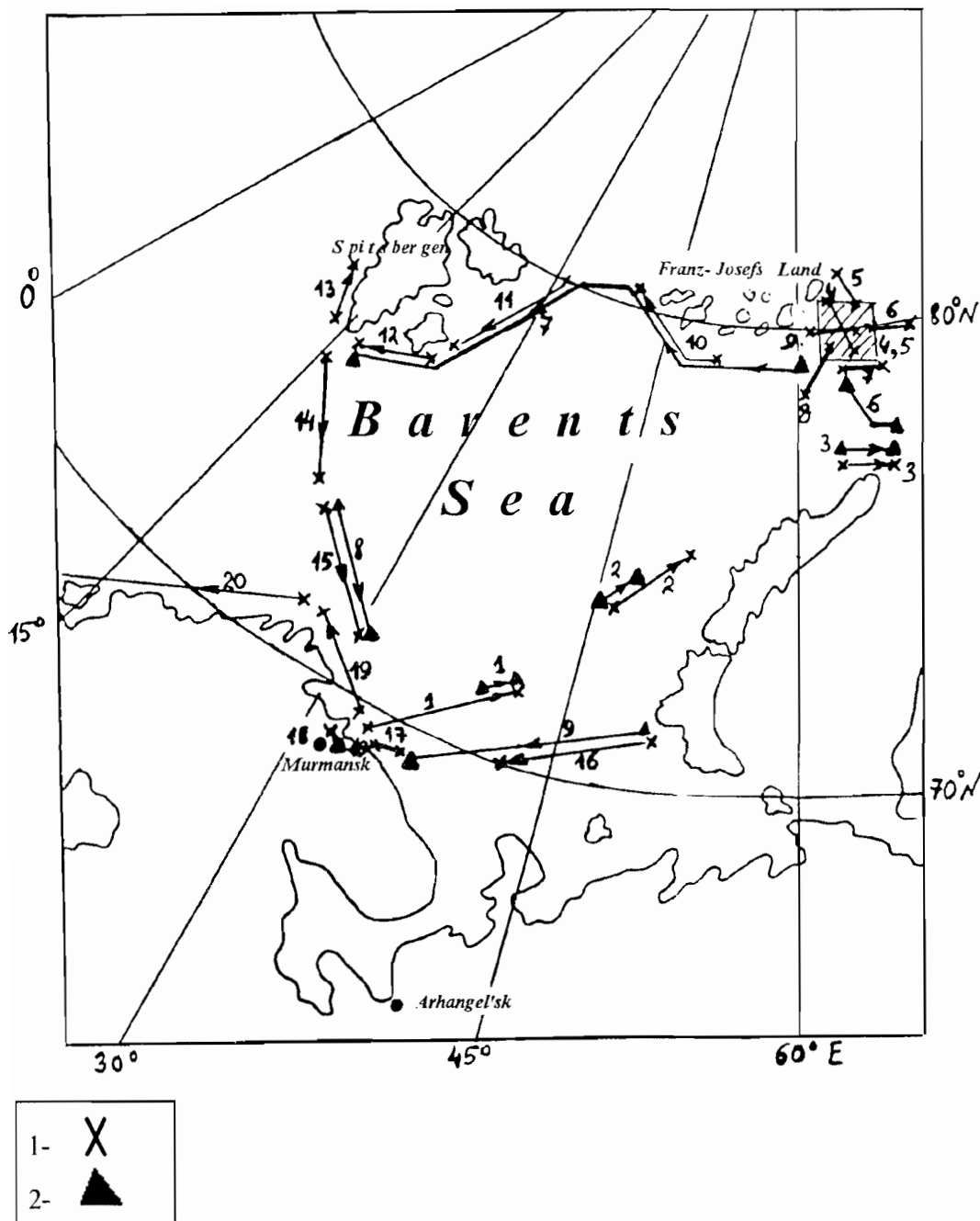


Fig. 1. A scheme of aerosol sampling in the 9th cruise of the RV "Professor Logachev": 1 - mesh sampling; 2 - filtration samples.

The enrichment coefficients (EC) of aerosols by chemical elements relative to mean composition of the Earth's crust were calculated by the formula:

$$EC = ((El. / Sc)_{\text{sample}}) / (El. / Sc)$$

where El. and Sc - are concentrations of the given chemical element and of Scandium in the sample and in the Earth's crust /Taylor, 1964), respectively.

On the whole, the enrichment coefficients (Fig. 2) are at the level typical of the summer Arctic atmosphere /Vinogradova et al., 1993; Maenhaut et al., 1989/. The highest enrichment coefficients of the mesh samples by such elements as Co, Ni, Cu, Zn were observed in sample

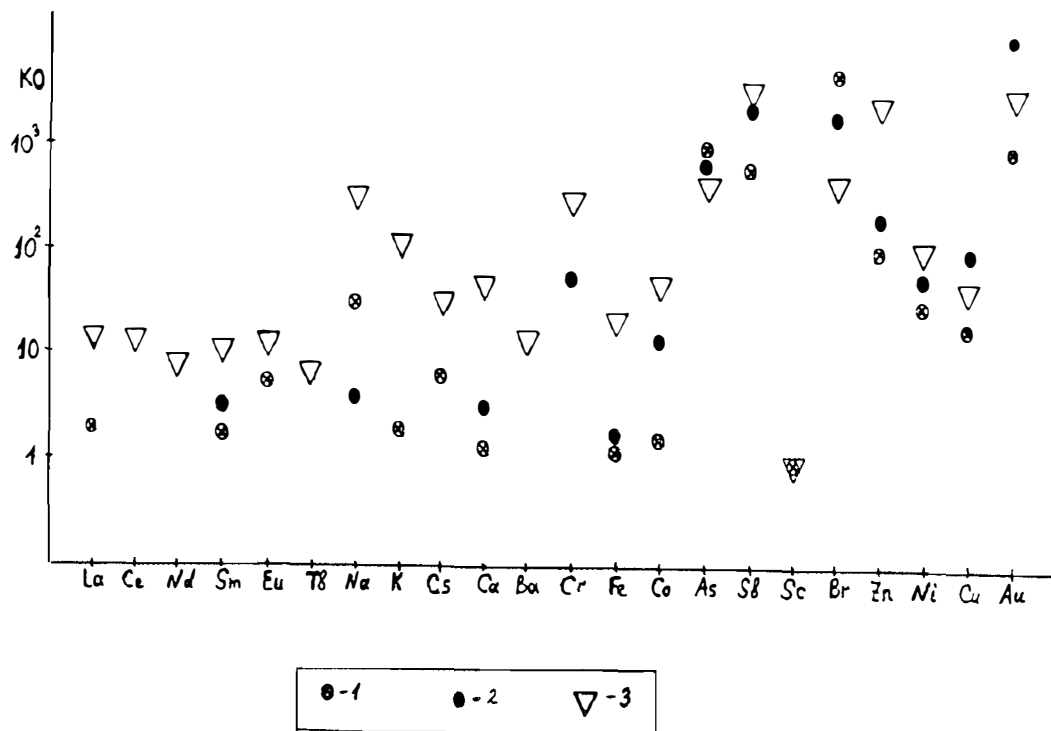


Fig. 2 Enrichment coefficients (EC) of filtration samples of aerosols collected in various regions of the Arctic: 1 - Spitsbergen, winter 1983-1984 /Maenhut et al./; 2 - Severnaya Zemlya archipelago, winter 1985, 1986, 1988 /Vinogradova et al., 1993/; 3 - St. Anna trough and the Barents Sea, August-October 1994 /this work/.

17 collected near Murmansk. As mentioned, a large number of anthropogenic combustion spheres are present in this sample.

Data on the enrichment coefficient and results of a pair correlation analysis allow us to divide chemical elements into 4 groups: 1) typical crustal (Sc, rare-earth elements, Th); 2) marine (Na, Br); 3) anthropogenic (As, Ni, Cu, Se) and 4) mixed crustal-anthropogenic (Fe, Co, Zn) origin. Comparatively large enrichment coefficients of rare-earth elements and Fe in filtration samples (10-15) are, probably, related to the fact that aerosols collected by filtration, mainly consist of sea salt which is characterized by enrichment with these elements /Savenko, 1994/.

On the whole, our data do not indicate a considerable anthropogenic aerosol pollution above the St. Anna trough and the Barents Sea. Enrichment of aerosols by many chemical elements has mainly natural reasons. The aerosols near the Kola peninsula at the transport of air masses from the industrially developed regions are the only exception.

The authors gratefully acknowledge the assistance and help of Academician A.P. Lisitsin. The work was fulfilled at a partial support of the Russian foundation of basic studies (Grant 93-05-12100).

References

1. Vinogradova A.A., Malkov I.P., Polissar A.V., Khramov N.N. Elementary composition of surface atmospheric aerosol in the Arctic regions of Russia. - *Izv. AN SSSR. Physics of the atmosphere and the ocean*, 1993, vol. 29, No. 2, pp.164-172.
2. Savenko V.S. Factors determining distribution of chemical elements in oceanic aerosol. - *Reports of the Academy of Sciences*, 1994, vol. 339, No. 5, pp.670-674.

3. Barrie L.A. Arctic air pollution: an overview of current knowledge. -Atmospheric Environment, 1986, v.20, N 4. P.643-663.
4. Maenhaut W., Cornille P., Pacyna J.M., Vitols V. Trace element composition and origin of the atmospheric aerosol in the Norwegian Arctic.-Atmospheric Environment, 1989, v.23, N 11. P.2551-2569.
5. Taylor S.R. The abundance of chemical elements in the continental crust-a new table. - Geochem. Cosmochim. Acta, 1964. V.28. P.1273-1285.

**THE DIAGNOSTIC TECHNOLOGIES DEVELOPMENT FOR
ATMOSPHERIC POLLUTION TRANSPORTS TO THE KARA
AND BARENTS SEAS ESTIMATIONS *)**
V.F.Romanov, V.E.Lagun (AARI)

1. The Norwegian, Barents and Kara Sea areas are known, as high atmospheric cyclone concentration regions. Most of drifting eddies initiate intensive atmospheric currents, blowing over industrial and agricultural American, European and Asian territories, where could involve and carry a lot of different pollutants. During climate periods synoptic circulation conditions form prevailed pollution transports, determined the climate transportation conditions.

Usually in the different kinds of human activity, including strategic planning and adequate emergency reactions development, the most desirable information on contamination should include the prevailed background atmospheric transports (mean currents and transient eddy fluxes) and the anomalous transports. First could show the typical transportation picture, sources influenced the given area, typical trajectories and prevailed eddy variability for current climate conditions. The second could illuminate a certain synoptic circulation anomalies, having intensive daily transports to the given region from injections, what could be comparable with a background values.

In the first kind of practical problems we have information on contaminants concentration atmospheric distribution. Using data on circulation, we should get the prevailed and dispersive pollution fluxes vector field, showing the spacial redistribution and typical sedimentation on surface. The second kind is more wide spread and complexive. We have information on the power injections distribution and circulation data. We have to generate the atmospheric transports (fluxes vector fields) and contaminants concentration and sedimentation power distributions.

The pollution background prevailed climate transference estimations are very important for general state and possible tendencies understanding. On the other hand, the typical synoptic eddy scales determine necessary resolution (daily and 200 km) for accurate statistical climate estimations, to get prevailed transport values in the synoptic fluctuations climate ensemble. Thus, it is necessary to have the daily circulation and pollutant data fields, as climate length totality. Then we have to estimate a prevailed

transport fields small differences on the background the intensive, big amplitudes daily fluctuations.

The most preferable way for analysis is the averaged climate circulation data diagnosis, used the dynamic-statistical synoptic eddies effects simulation. The diffusive transport conception could not always be applied for prevailed eddy transports simulation, because substances could transfer even to regions, having the higher concentration level, or opposite a gradient with prevailed winds and really have the eddy-advective transport nature, requiring the new theory.

We could propose the diagnostic technologies for mentioned problems. Technologies could be easily realised, but included a complex theory and data generalizations. The first is directed to the climate background and eddy prevailed transports estimations. It restores the atmospheric circulation statistics, using averaged climate data on the pressure distribution and cyclones frequencies (determining the potential energy field) only. Results characterize the global (or hemispherical) pollutants redistribution from sources to the given regions, as different mean and eddy components, corresponded to circulation processes.

Then classification determines the anomalous synoptic situations, characterized intensive transports phenomena from a powerful sources to given regions, as determined dates.

**) translated by the author*

The three dimensional pollution transports model is realized for detailed analysis during these selected periods and should give detailed information on the contaminants redistribution from a certain sources and sedimentation on the surface also.

2. The background climate transports diagnosis technology is based on the dynamic-statistical synoptic eddy circulation variability simulation. The daily circulation pictures climate ensemble is performed as two ensembles sum. The first includes complete synoptic eddy totality during a given climate period. The second is represented by the circulations consequence,

have not been disturbed by synoptic eddies. The data have showed a preferable way to determine the spacial synoptic eddy definition, as a certain atmospheric area, limited by external closed isobaric line. According to data analysis, drifting cyclones could be presented, as moving air masses, but only half. The mass

turbulent fluxes lower troposphere convergence forms the vertical mass coming up through the cyclones flash, where divergence produces a mass export from cyclone volume. Thus, the drifting eddies could be presented as moving and rotated air masses only half and as diabatic synoptic waves the second half at the same time. It means, the moving eddies(determined, as synoptic pressure systems) drift speed, related to the cyclones transference wave speed, produces the mass eddy-advective flux. It is proportional to approximately one half the cyclone mass motion, having the cyclone drift speed.According to the air mass rotation,proportional to synoptic speed vorticity, there is another eddy transport component,formed by eddy mass rotations around the eddy "vertical" axes and connected with prevailed synoptic vorticity.

Thus it was considered, that instanteneous speed V_L could be expended in the next form for not desturbed mean currents (MC):

$$V_L(x_L, t) = v_L + \psi_L$$

and for synoptic eddies (SE), partialy analogous to the Helmholtz expansion:

$$v_L(x_L, t) = \alpha^* (u_L + \phi_L) + \varepsilon^{Li3} \xi_L (\omega_3 + \phi_3), \quad \text{where: } L = 12$$

-is the horizontal coordinate index; u_L -synoptic pressure system drift speed; ω_3 -synoptic vorticity; symbol $\tilde{\omega}_3$ indicates the subsynoptical fluctuations; $\xi_L = x_L - X_L$ -is a radiusvector, x_L -current coordinate and X_L -the mass center coordinate for SE; ε^{Li3} -Levi-Chivita antisymmetric three rank tensor; $\alpha^* = 1 - (\pi / 4)(I_E w / H u_L) \approx 040 \div 060$ -the mass leaking coefficient.

Designating: ρ -is the volume mass or pollution concentration density and P -pressure, we have to expend: $\rho = \rho_m + \delta_s \rho$ and $P = P_m + \delta_s P$, where ρ_m and P_m - the not disturbed background variables

and $\delta_s \rho$, $\delta_s P$ are the synoptic anomalies. It is well understanding, that due to typical prevailing a certain synoptic anomalies at some places, the temporal averaging $\langle \dots \rangle$ should

give us: $\langle \rho \rangle = \rho_m + \delta\rho$ and $\langle \mathbf{P} \rangle = \mathbf{P}_m + \delta\mathbf{P}$, where $\delta\rho$ and $\delta\mathbf{P}$ are not equal to zero and express the prevailed climate spacial anomalies.

Then we do separate the spacial instanteneous fields as synoptic eddy volumes and not disturbed currents and carry out a spacial smoothing operation for both components, using a smoothing scale $l_m > l_E$, where l_E is typical eddy scale. As result, we have smoothed variables and subsynoptic scale fluctuations for eddy totality and for background currents. Then we do average fields by time t_m -climate period, included a long enough eddy totality (for instance, monthly values, averaged during 10 years). The eddy mean values we should define as averaged during a periods sum, which characterized by eddy presence and background values, as averaged during t_m .

Averaging spacially and temporally the mass volume density (pollution volume concentration)balance equation, we could get the averaged balance equations system for eddy climate pictures and for background circulations combination. Equations include the spacially smoothed and temporally averaged variables, determined according to the climate averaged circulation data and correlations, related to the subgrid fluctuations input in averaged transports and mass exchange between eddy and background circulation ensembles. The first kind of correlations is related to the subsynoptic and small-scale turbulent fluctuations influence and could be traditionally simulated as turbulent diffusion effectes. The second kind is related to the synopticscale anomalies correlations and expresses the prevailed and dispersive statistical effectes both. Using closure hypothesis, based on the data analysis, we have parameterized the every correlation in the eddy ensemble mass density balance equation and balance for the background atmospheric currents. The respected terms in equations are described the next transportation processes: - eddy mass transport due to eddy drift and spacial density inhomogeneouty;- eddy mass transport due to eddy drift and the drift speed spacial inhomogeneouty;- eddy mass rotational transport due to motions, formed by prevaled synoptic vorticity;- stochastic turbulent diffusive transports, connected with subsynoptic and synoptic scale fluctuations; -the vertical re-

distribution from the given layer to upper atmosphere, where vertical prevailed circulation is parameterized by prevailed synoptic vorticity; - subsynoptic turbulent exchange between eddy and not disturbed currents ensembles and finally -the mass exchange between ensembles due to cyclogenesis and cyclolysis processes.

The background mass density balance equation includes:-the advective inputs due to speed and mass distribution inhomogeneities; -subsynoptic turbulent exchange;-vertical redistribution; -the eddy mass input to the background fields due to eddy destabilization with density and drift speed spacial inhomogeneities, connected with eddy drift transports;-eddy-background fields turbulent exchange and the same eddy formation or disappearing processes effects.

The coefficients, appeared according to parameterizations are determined due to special data assimilation procedure. Using US National meteorological Center (NMC) data we have estimated every term in the balance equations and have got a local temporal density change distribution. Then we could estimate a hydrostatic surface pressure anomaly time tendency and compare with data. The coefficients have been changed to satisfy a good agreement between computed local temporal change of the surface pressure anomaly and data. Thus the every term in equations was determined by data. Equation was used for coefficients estimations.

Results have showed, that non diffusive eddy-advective transport components, connected with prevailed effects of eddy drift and prevailed vortex rotations, have an important role in the total transportation picture. Those components are formed by the regulated synoptic variability (prevailed) components. And only stochastic variability part is connected with diffusivity.

Thus, we have determined every variable, which is included in the density balance equations. Therefore, we can estimate the every transport component and additional influxes (sedimentation, chemical transformations and so on). It is easy to understand, that the similar procedures could be applied for any pollution component diagnosis. It is clear, that exposed technology could be applied for vertically averaged troposphere description, for different atmospheric layers diagnosis and for three dimension simulation. It is determined by specific diagnosis objectives and available information, including vertical pollution and circulation

structure approximation abilities. We have simulated many year climate winter tropospheric mass transports for the Island Low area climate conditions. The mass advective-eddy transport vectors, connected with prevailed eddy drift speed show the well expressed jet, directed to the North-East, along the climate prevailed cyclone trajectories. It is very powerful transportation, but it is well known, that most of transient eddies have lose their motion over Norwegian and Barents seas. Thus, corresponded transport component decreases. The most of stagnated cyclones could characterize by strong winds, and as result, mass could transfer with rotational transport component, connected with prevailed synoptic vorticity. This component forms a well expressed meridional jets at the Western (southward) and Eastern (northward) Northern Atlantic areas. These meridional currents present the statistical eddy motions prevalence and could support the pollution transference to the Arctic regions through the polar frontal zone. Synoptic stochastic variability transports component, could not play an important role in the total climate transportational picture. The subsynoptic diffusivity have the same structure, but is not so intensive. The most effective transports are formed by prevailed eddy drift speed and prevailed vorticity effects. Those transports form the regular transportation picture and well-expressed influx areas. The background circulation transports effectivity is much lower. The same results could characterize the global or hemispheric transportation picture.

3. Sometimes the current daily circulation could be characterized by a long distance very intensive jets formation, blowing from injections to the Arctic regions. Those short-period streams (a few days) could be very different, relative to a mean prevailed transports, but their high effectivity (due to very intensive currents and wind orientation, connected the injections and Arctic regions) could produce a short period significant Arctic contamination.

For those anomalous synoptic-scale transport situations determining the special classification is necessary. It must select in the daily current conditions a certain periods, characterized by : 1) very intensive air-mass transports to the arctic and 2) air mass transports from powerful injections.

Now we do develop a method for circulation analysis to get objective information on the daily transports intensity and trajectories selection, which come from injections.

The NMC-data (geopotential, temperature, humidity and wind speed) have been used for transport diagnosis during selected anomalous conditions. The spatial and temporal data resolution is 2.5 degree and 12 hours. Diagnosis includes the vertical motions and cloudiness distribution estimation. The regional three-dimensional atmospheric pollution transport model was applied for anomalous synoptic-scale transport diagnosis. The mass balance equation,

included advective transports, horizontal and vertical diffusion, dry and moist precipitation, cloudiness dissolving and chemical transformations was used for admixture concentration, transports and output pollutants from the atmosphere. Thus, model included every important synoptic-scale pollution transport properties to the Arctic for wide pollutants totality (sulphur dioxide, sulphates, ammonia and so on). The spatial resolution for horizontal was 20 km and 300 m along vertical. Results showed the well-expressed advective transference prevailing, relative to the turbulent diffusion and pollution absorption by clouds water drops and precipitation washing effects importance. According to diagnosis the cloudiness presence provides the surface pollution concentration decrease from 3 to 10 times.

Thus, the current climate global or hemispheric transport diagnosis and the regional synoptic-scale anomalous detailed transports, physical and chemical effects diagnosis technology combination provides a complete information on the total pollution redistribution and detailed regional anomalous situations.

Biology, Sedimentology

PARTICULATE LIPID DISTRIBUTION IN THE OB' RIVER ESTUARY AND THE SOUTHERN KARA SEA

Aleksandrova O.A., Shevchenko V.P. (IORAS)

Studies of particulate lipid composition and distribution in the area of river/sea water mixing under Arctic conditions can provide information on the features of the processes of accumulation and transformation of organic matter in this region. Data on lipid distribution in the Arctic Seas are few, especially for the Kara Sea /Romankevich et al., 1982/.

Sampling of particulate matter was carried out in the 49th cruise of the R/V "Dmitry Mendeleev" in September 1993. At six stations along the submeridional transect Ob' estuary - southern Kara Sea (up to 76 N) (Fig. 1) 19 samples were collected from the surface, the pycnocline and the near-bottom layer.

Separation and identification of 8 classes of lipids (hydrocarbons, wax and sterol esters, fatty acid methyl esters, sterols, mono- and diglycerides, polar lipids) were performed using TLC-FID (thin layer chromatography with flame-ionization detecting) method on IATROSCAN TH-10 Mark III equipment /Ackman, 1982/.

The particulate lipid concentration at the Ob' transect varies over a wide range - from 18.4 to 2666.0 $\mu\text{g/l}$ (Fig. 2). The lipid content in organic particulate matter is from 4.06 to 58.22%. Marine stations are characterized by higher values of lipids in organic matter (39%, on average), as compared to the estuary values (14%, on average), i.e. by about 3 times. Also, at the marine stations the content of lipids in organic matter increases with depth and at the estuary stations decreases. The absolute particulate lipid concentration ($\mu\text{g/l}$) decreases a little with depth, however, in the near-bottom layer their content increases reaching surface concentrations or exceeding them by 1.5-2 times. The main components in the composition of particulate lipids at the transect Ob'-Kara Sea are hydrocarbons (0.07-68.8, 32.14%, on average, of the total lipids), polar compounds (6.9-74.50, 29.85%, on average), wax and sterol esters (1.61-35.0, 13.04%, on average), mono- and diglycerides (4.35-60.91, 12.52%, on average) (Fig. 3). Secondary components are fatty acid methyl esters (5.14%, on average), free fatty acids (4.56%, on average), triglycerides (2.32%, on average) and free sterols (1.04%, on average).

The main distribution features of the particulate lipid fractions at the transect Ob'-Kara Sea are: the maximum of absolute concentrations of total lipids observed in the near-bottom layer governed by resuspension of the upper layer of bottom sediments /Medvedev, Potekhina, 1990/ and the maximum of concentrations of polar fraction, probably, related to the peak in the numbers of microorganism /Mitskevich, Namsarayev, 1994/. It is suggested that the enhanced concentrations of mono- and diglycerides in the surface layer of the water column and in the estuary part of the transect are governed by the influence of the temperature regime of the Arctic Basin on the degradation intensity of triglycerides which are important components of the Arctic marine and brackish organisms /Parrish, 1988/.

The lipid composition reflects the differences in the processes of organic substance transformation in the estuary and the sea zones of the transect. Distribution of hydrocarbons (the increase in relative concentrations with depth in the sea part of the transect and the decrease in the estuary part), as well as fatty acid esters (the maximums of absolute concentrations) mark most clearly the biogeochemical barriers separating these two systems.

A complicated hydrological situation of the Kara Sea including stratification of the water column and river/sea water interaction /Burenkov, Vasil'kov, 1994/, is reflected in the increase of the absolute lipid concentrations and in the presence of the maximum of polar fraction in the pycnocline.

Composition and content of particulate lipids depend, to a great extent, on the peculiar composition of the arctic community of the organisms in the Kara Sea /Vinogradov et al.,

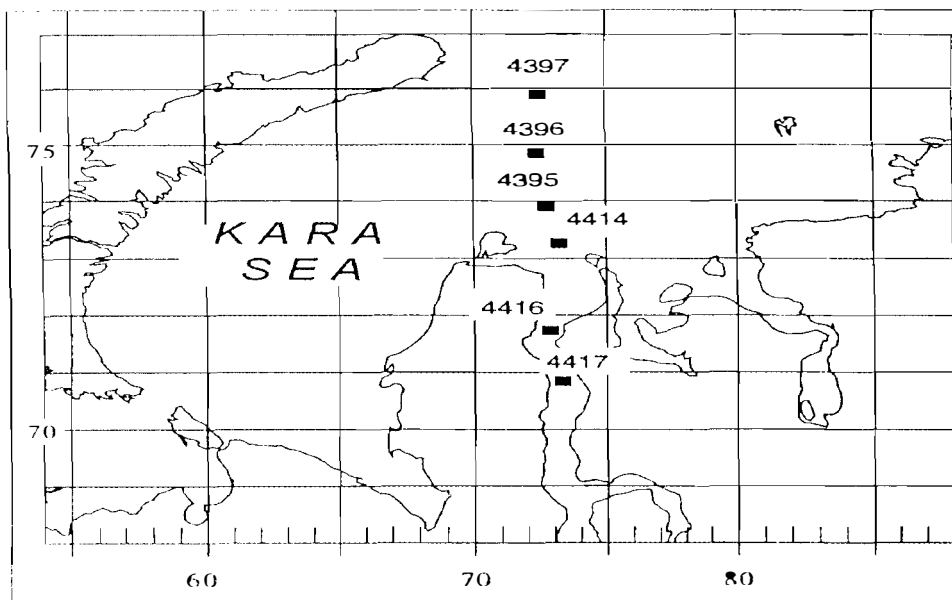


Fig. 1. A scheme of the sampling stations.

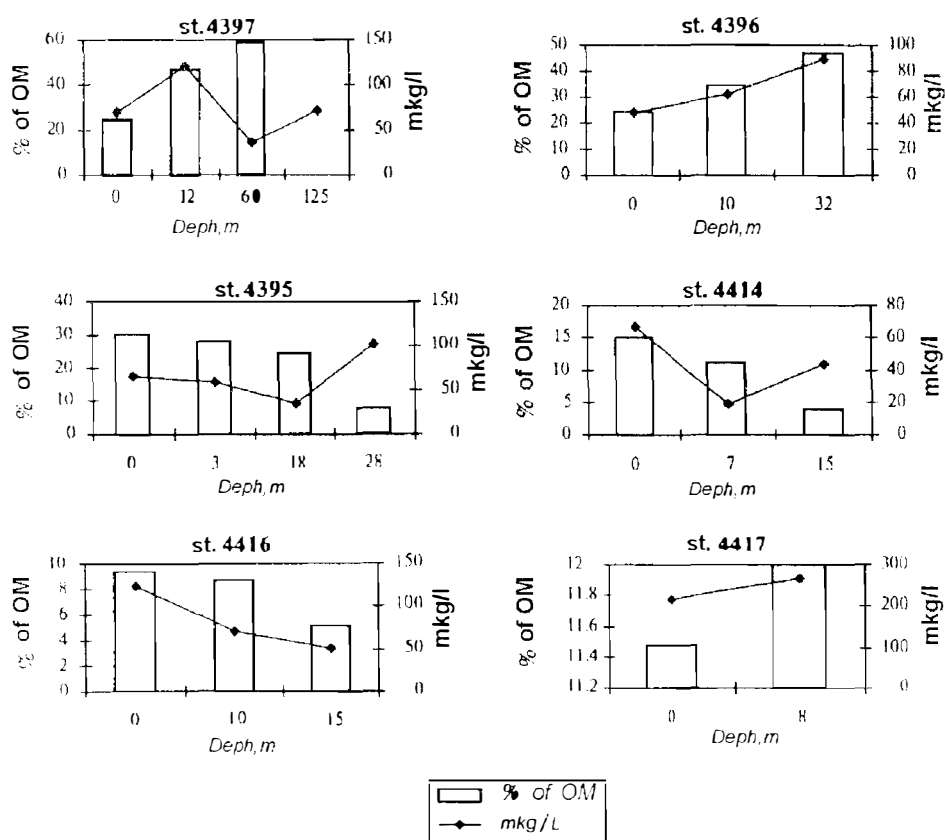


Fig. 2. Distribution of the total absolute ($\mu\text{g/l}$) and relative (% of organic matter (OM)) lipid content at the transect.

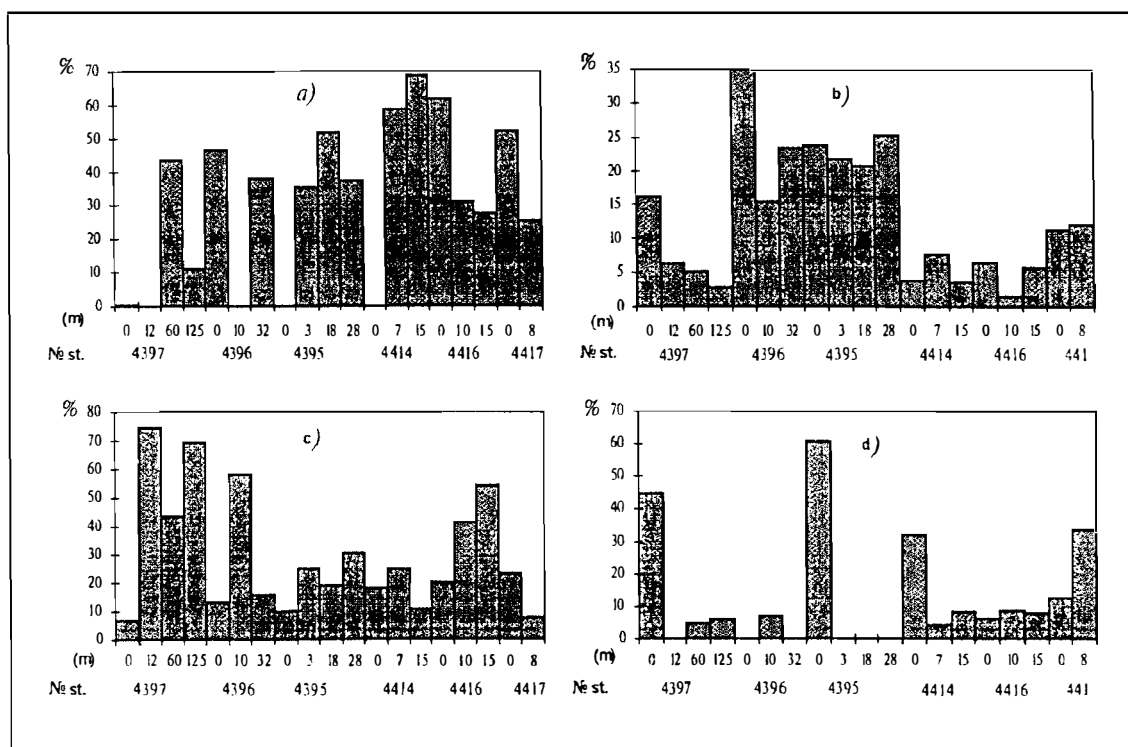


Fig. 3. Distribution of percentage of prevailing fractions in particulate lipid composition at the transect: a) hydrocarbons; b) polar lipids; c) wax and sterol esters; d) mono- and diglycerides.

1994/ governed by the need for accumulating reserve lipids. The identified maximums of the wax and sterol esters, as well as of triglycerids correspond to the areas of the largest biomass values of zooplankton species typical of the northern seas.

References

1. Burenkov V.I., Vasil'kov A.P. On the influence of the continental outflow on distribution of the hydrological characteristics of water in the Kara Sea. - *Oceanology*, 1994, vol. 34, No.5, pp.652-661.
2. Vinogradov M.Ye., Shushkina Ye.A., Lebedeva L.P., Gagarin V.I. Mesoplankton of the eastern Kara Sea and the estuaries of Ob' and Yenisey. - *Oceanology*, 1994, vol. 34, No.5, pp.716-723.
3. Medvedev V.S., Potekhina Ye.M. Quantitative distribution and dynamics of particulate matter in the south-western Kara Sea. - In: *Current sedimentation processes on the shelves of the World Ocean*. Ed. by N.A. Aibulatov. M.: Nauka, 1990, pp.110-120.
4. Mitskevich I.N., Namsarayev B.B. (1994). Numbers and distribution of bacterioplankton in the Kara Sea in September 1993. *Oceanology*, 1994, vol. 34, No.5, pp.704-708.
5. Romankevich Ye.A., Danyushevskaya A.I., Belyayeva A.N., Rusanov V.P. biogeochemistry of organic matter of the Arctic Seas. M. : Nauka, 240 p.

HYDROBIOLOGICAL RESEARCHES IN THE GULF OF PETCORA OF THE BARENTS SEA AND ITS PROSPECTS

A. E. Antsulevich, N. V. Maximovich, I. A. Stogov (BISPb SU)

The Gulf of Petchora is one of most important fishery basins of Russian NW. In last period it was involved into activity, connected with exploratory drilling for oil and fresh oil transportation. These circumstances does put in the forefront the nature conservation tasks, where the biological methods of environmental control and mitigation have a particular place. This kind of tasks can be resolved only on base of hydrobiota's background structural parameteres knowledge, but available data are extremely insufficient and fragmentary.

There are investigations of plankton and bottom communities were executed on all duration of the Gulf in collaboration with State Establishment "LARGE" in frames of AARI research program. They makes it possible to characterize the basin in the whole and to enrich substantially the data available. The greatest number of zooplankton species (14) was observed at the Petchora river outfall, where only freshwater animals are inhabits with dominants *Bosmina longirostris* and *Keratella cohlearis*. Some less of species were discovered in the distal part of the Gulf where marine crustacean *Microcalanus pygmaeus* and *Pseudocalanus elongatus* are the dominants. The specific content of the central part is more poor, there are only 5-7 species were found and one brackish form *Limnocalanus grimaldii* is prevail, which is not typical both for river mouth and marine part of the Gulf. The similar peculiarities were registered in bottom communities distribution, which are influented as well by bottom grounds quality. There is typical freshwater fauna at the river mouth, it is represented by oligochetes, larvae of insects, leeches and bivalves. Close to the distal part of the Gulf there is ally 47 and tunicates, having nothing similar to the river outfall faunistic complex. It is peculiar to the central part an impoverishment of benthic fauna, where just relict crustaceans as *Mesidot heantomon* and *Mysis oculata relicta* are predominaa species of bottom organisms were collected with more than one half of them were recorded firstly for the Gulf of Petchora. Generally the number of bottom organisms species is expect in 4-5 times more, what could be confirmed by data from the nearby and better studied areas of water.

If plankton communities gives the possibility to evaluate the rapid environmental changes, the bottom communities successions does characterize integral conditions and their displacements. These two approaches together makes it possible to trace in complex the impact of pollution as well as other impacts to the aboriginal ecosystems.

PHENETIC ANALYSIS OF GENETIC POLYMORPHISM OF SOME INVERTEBRATE AND PLANTS NATURAL POPULATIONS IN THE NORTH-WESTERN AREA OF THE WHITE SEA FOR THE ECOLOGICAL STUDIES OF STUDENTS BIOLOGISTS.

L.V.Barabanova, L.V. Bondarenko, K.V. Kvitko, V.D. Siminenko (SPbSU), S.A.Kozhin (LNPI)

It must be emphasized that the constantly increasing of the adversely anthropogenic affecting on the structure and the nature plants and animals population dynamics brings now the threat and can have the serious environmental impacts: the animals and plants associations. The threats of the different intensity now one can observe in the areas of water and the coastal regions of the Baltic, Barents and Kara seas.

The background of the skilled biologists, connected with the ecological problems, is the main factor for the timely establishing the reasons for the environment pollution and threats forecasting of the animals and plants biocoenosis.

Such work is carried out within 15 years by the Biological faculty of the State University of SPb during the summer practical students work. The program of this practical work consists of the sections " *invertebrate zoology*" and "*higher and lower plant botanics*". In these sections the students are become acquainted with species variety of the invertebrate and plants, inhabiting in the areas of water in the north-western part of the White Sea and its coasts. The program also includes the "*genetic excursions*", the main purpose of which is to train the students to use the common methods to reveal the intraspecific variability - genetic polymorphism of the marine and freshwater invertebrate and plants.

The White Sea now is rather clean. It allows to describe phenetically the reasonable intact natural animals populations and plants in this region, to reveal some objects, which are accessible to such investigations, and also the populations appropriated for monitoring. Such investigations can be useful for carrying out the same works in the sea areas with the purpose to reveal the factors, disrupting the natural populations structure and dynamics. The phenetic method of the natural populations analysis, which allows to fulfil the populations genetics studies of the objects (the genetics analysis of which is a difficult and impossible task), is used as a main methodological approach to carry out the genetic practical students work. The practical work consists of the excursions in the coastal region littoral near the Marine Biostation of the State University of SPb, during which the students are trained for true phenetic estimation of the population structure, animals and plants species, which are the result of the previous investigations. The students also collect the material, the analysis of which needs the laboratory investigations.

The objects, which meet the requirements to be accessible, numerical and have the lightly indentified features, are selected as a studying material. The summer period within the end to the middle of July is considered to be the optimum for the collecting and the analysis of the natural material in the north-western part of the White Sea.

During the practical work the students estimate two or three different populations of one species, inhabiting in the ecologically different regions. For the laboratory analysis it is enough to use microscopes, binocular magnifiers and the dyes assortment for the polymorphism revealing in the chromosome stage. The mathematical statistics method (Kenuy, 1979) is used to compare with the results.

Some objects, the populations of which were used by the students for the comparative analysis of the genetic polymorphism, can be considered to be the genetic practical work results within 15 years.

Using the natural material the students are to be acquainted with the examples of hereditary and nonhereditary variability including the main propositions of the populations genetics and the phenetic method of their investigation, and with the revealing and quantitative polymorphism studying methods.

The modificational variability is shown by the example of the features variability in the fucus balanus (*Balanus*) populations of the contrast ecological niches. Observation of many

objects makes it possible to analyse the interpopulational genetic polymorphism on the features: the form of the white spot on the leaves of clover (*Trifolium*) (Fig. 1) (Brewbaker, 1952; Carnahan et al., 1952), the corolla colour of the geranium (*Geranium*), the colour and design shells of two *Littorina* species, the colour and design shell of the *Isopods*, the chromosome polymorphism of the typified buffalo gnats (*Simuliidae*) and chironomids (*Chironomidae*) family (Fig. 2).

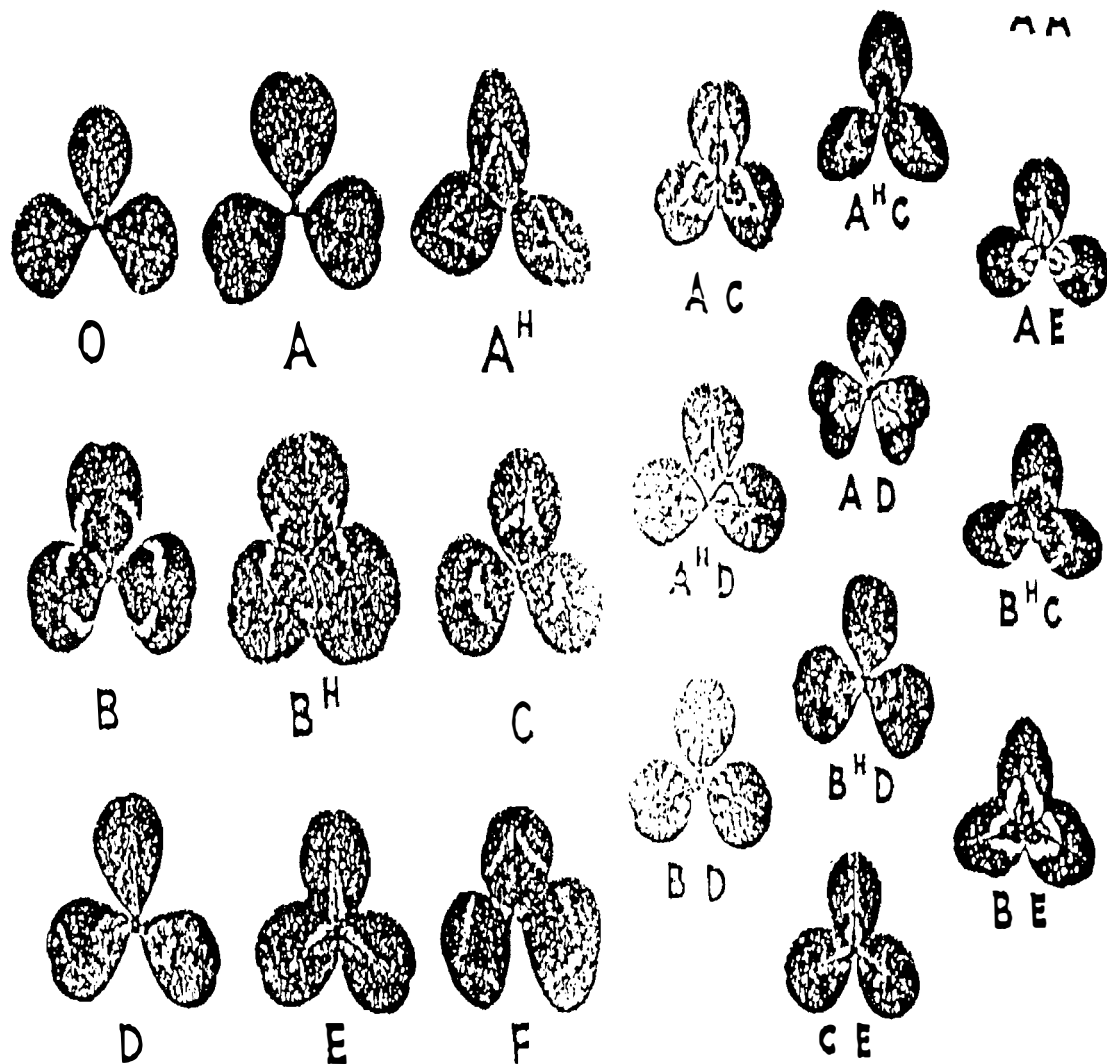


Fig. 1 Polymorphism to the leaves design of the Dutch clover (*Trifolium repens*)

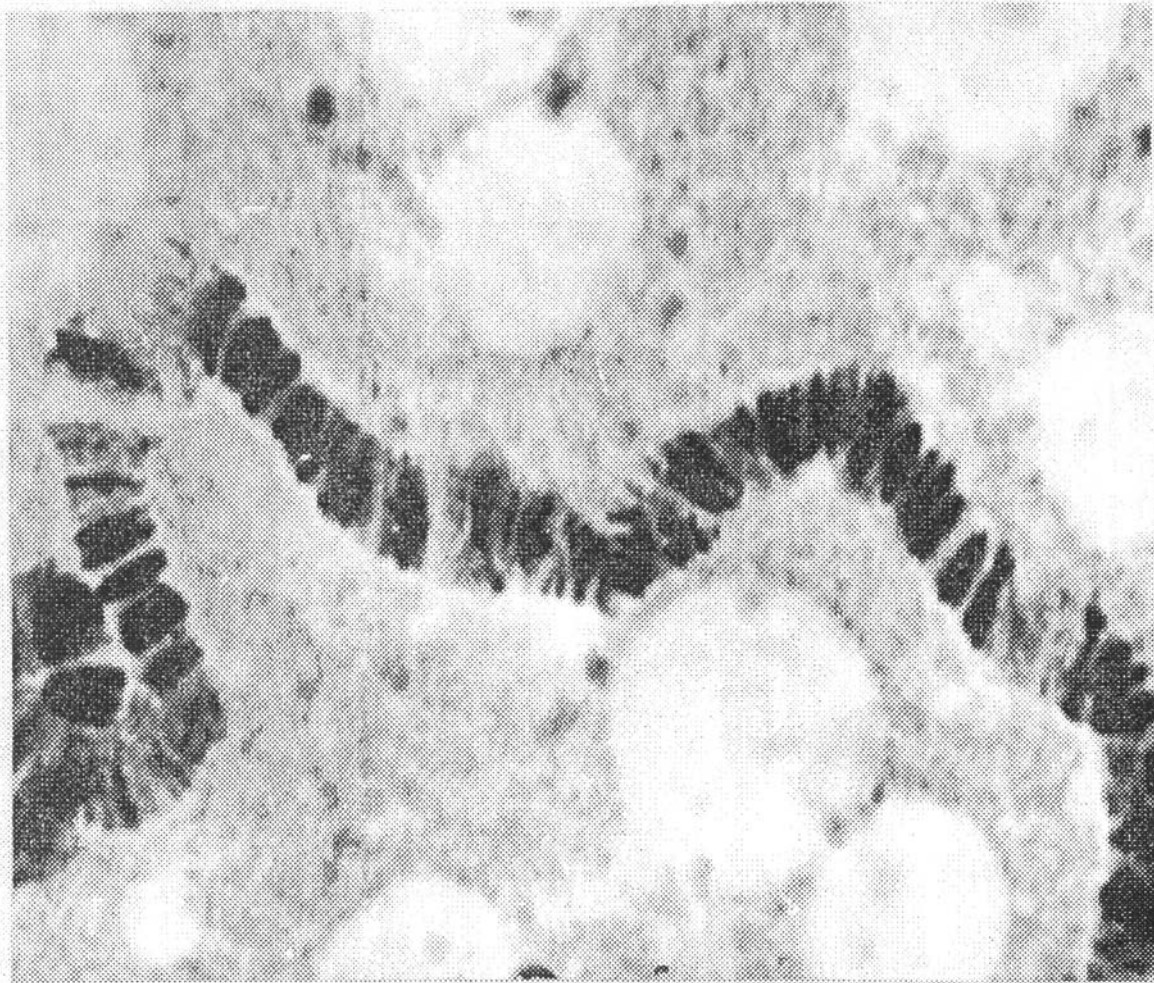


Fig. 2 Polytene chromosomes of two-winged insects.

The role of the structure and dynamics populations studying for the ecological monitoring and the threat environment forecasting is shown by the example of the investigating populations. Within many years the analysis of the genetic structure dynamics of the natural populations allows to discuss the fundamental propositions in biology connected with the microevolutional changes in the visible period (Levontin, 1978).

The students analyse the natural cereals and conifers populations in order to estimate the mutational and combinative variability. The role of the combinative variability in the genetic variety extending of the populations is being viewed (Fig. 3). Sexual reproduction is the main feature of the combinative variability. The sexual reproduction in the species evolution by the variability analysis of the higher and lower plants sex features - sexual dimorphism of the dioecious plants: fucus, polytrichum flax (*Linum*), sorrel (*Rumex*), common nettle (*Urtica dioica*), is being discussed during the genetic practical work.

The morphological and physiological plants provisions for the cross-pollination - primrose heterostyly (*Primula*), crane's-bill protandry (*Geranium*), cereals protogyny are being shown.

The genetic practical work experience will allow the students to use the genetic methods in the ecological estimation investigations of the threat influence to the living organisms.

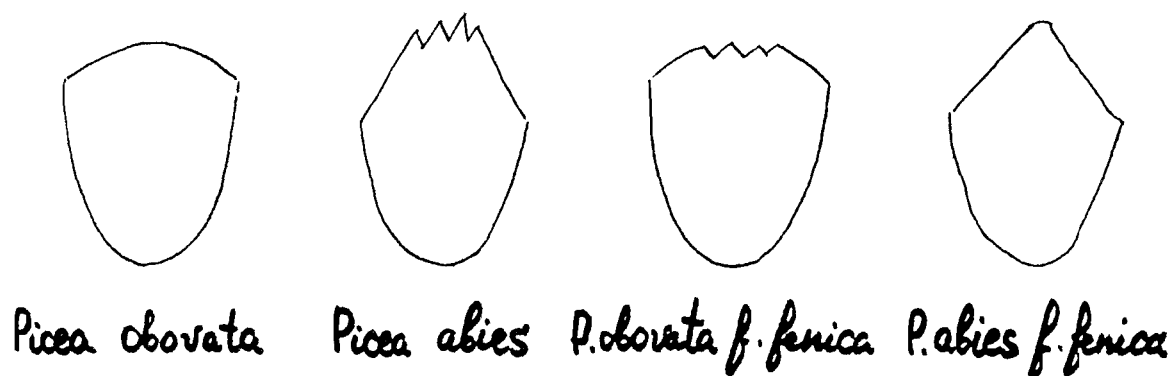


Fig. 3 The seed scale form of the clean and hybrid fir-tree types.

References

1. M.G.Kenuy Fast statistical calculations, M., Statistika, 1979, 69 p.
2. R. Levontin Genetic basis of evolution, M., Mir, 1978, 349 p.
3. J.L.Brewbaker V-leaf marking of white clover, Journal of heredity, 1952, pp 115-123
4. H.L.Carnahan, H.D.Hill, K.G.Brown Inheritance and frequencies of leaf markings in white clover, Journal of heredity, 1952, pp.109-114

The previous theses title:

Interspecies variability studying in the natural populations for the training of the specialists-ecologists.

ENVIRONMENTAL CONTROLLING FACTORS REFLECTED IN THE KARA SEA SEDIMENTARY LIPIDS*)

A.N.Belyaeva(IORAN)

Introduction

There are two most important controlling environmental factors of polar marine environment: the pronounced oscillation of primary productivity caused by the long period of polar night and extremal life conditions of marine organisms under seasonal ice cover and in low temperature sea water resulted in various biochemical adaptations.

Arctic seas, in addition to these factors, are distinguished from the Antarctic seas by high riverine input. The main questions appear to be key considerations in understanding the influence of polar environmental factors on carbon cycle and organic matter accumulation in sediments are as follows:

- (1) What is the relative importance of various source sedimentary organic matter?
- (2) How, and to what extent, is organic matter reworked by bacteria?
- (3) Are there any specific biomarkers of polar biosynthesis and terrestrial organic matter in sediments?
- (4) What is the mechanism of incorporation and preservation of different organic compounds in sediments?

In this regard, the Kara Sea being the most heavily loaded by riverine runoff (about 1350 km³ per year), is particularly suitable for the study of interrelation of organic matter and environmental factors. Sedimentary lipids including the large number of marker compound have been chosen for detailed study. Fifteen samples of surface and subsurface sediments (up to 380 cm) were retrieved on the transect from the Ob River mouth to the northern part of the Kara Sea up to 76° N during 49th cruise of r/v "Dm.Mendeleev" (Fig. 1)

Results and discussion

(1) Terrestrial derived lipids predominated over autochthonous ones in alkane, fatty acid and fatty alcohol patterns characterised by prevailed content of higher plants organic matter discharged by the Ob River (Fig.2). However, terrestrial imprint in surface sediments was not uniform along the transect. Spatial variability of main lipid fractions as well as their content in total lipids did not show correlation with primary productivity or distance from the Ob River mouth. Instead, factors controlling sedimentation most likely influenced on accumulation of various lipids in sediments

(2) Bacterial derived fatty acids, i.e., branched iso- and anteisoacids, in the examined sediments (9.5% of total acids in average) evidenced that bacterial transformation processes are not suppressed in the Kara Sea in relation to low temperature environment. Instead, average bacterial fatty acid content is comparable with correspondent values obtained in the Bohai Sea (Bigot et al., 1989).

The highest content of fatty acids of primary bacterial origin was found in the sediments nearest to the Ob River mouth (Fig.2). Bacterial fingerprint was supported also by alkane pattern. These data support the conclusion (Peulve et al., 1993) that arctic estuarine areas are distinguished by intensive bacterial organic matter transformation from marine shelf sediments.

*) *translated by the author*

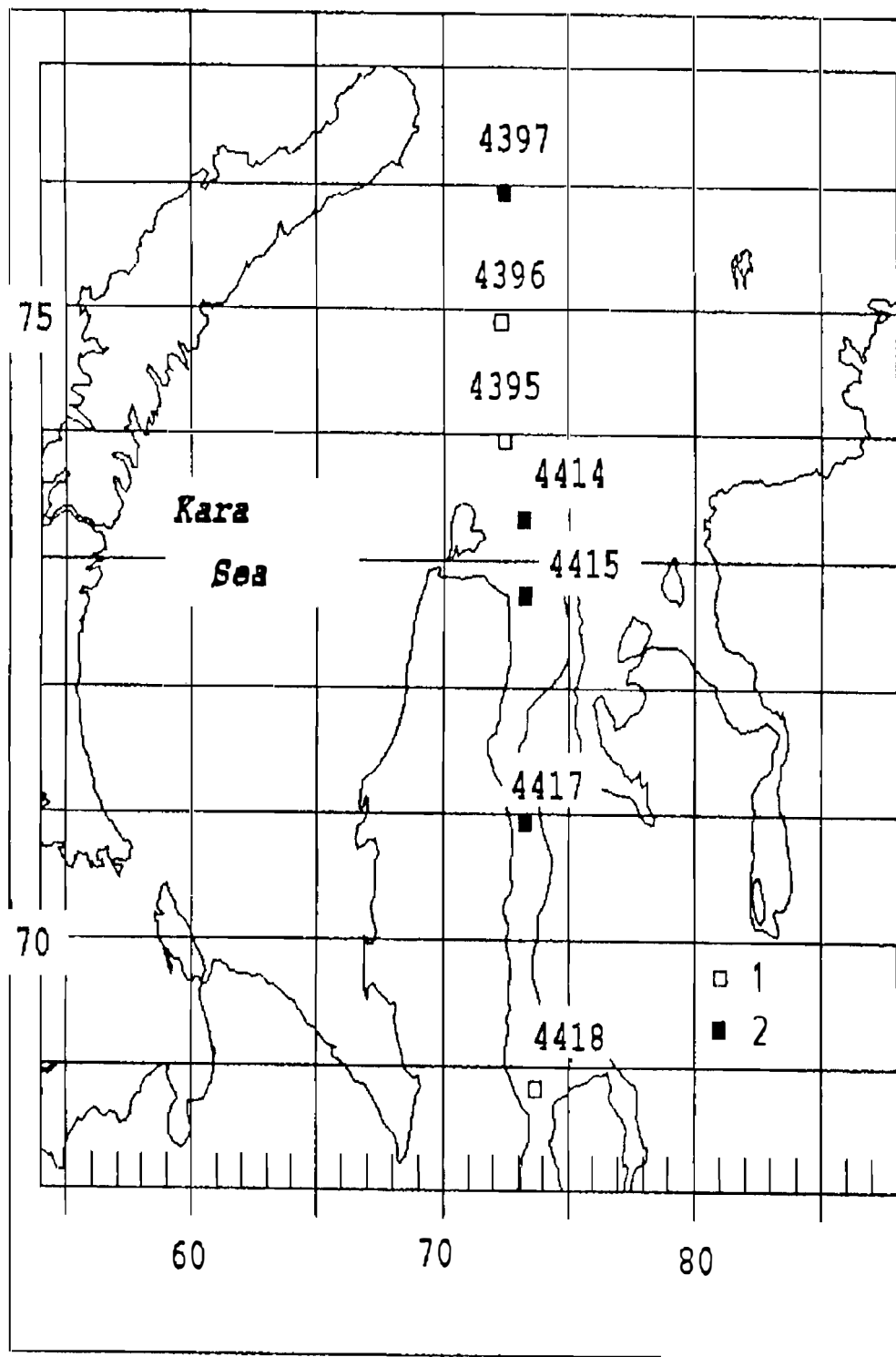


Fig. 1 Sample site location in the Kara Sea
 1 - surface sediment;
 2 - sediment cores.

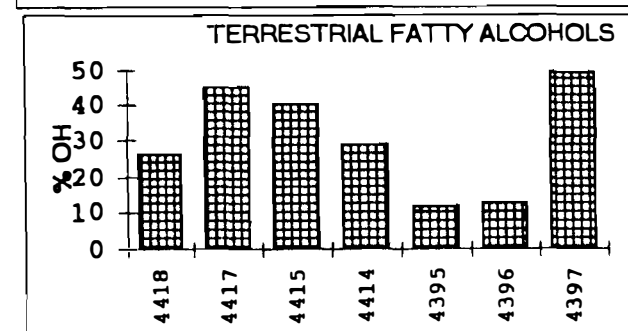
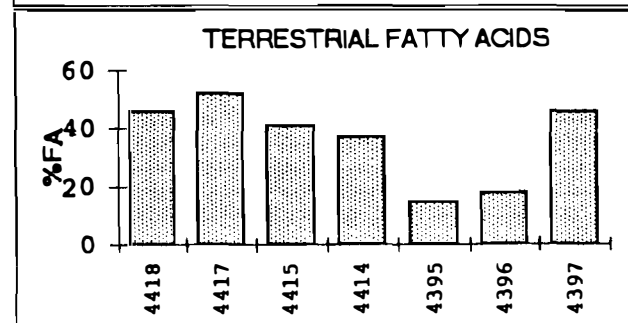
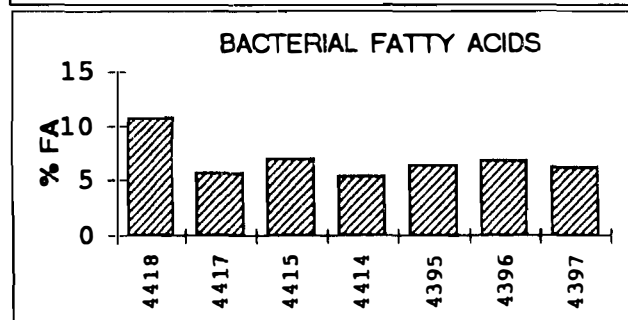
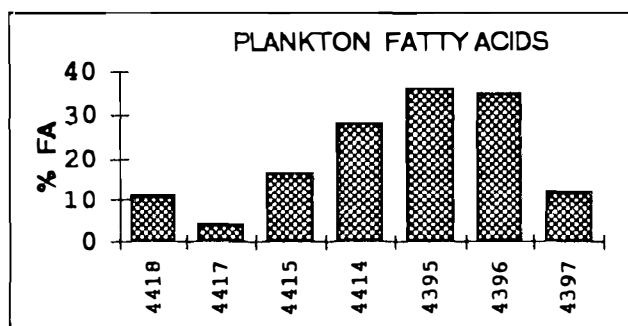
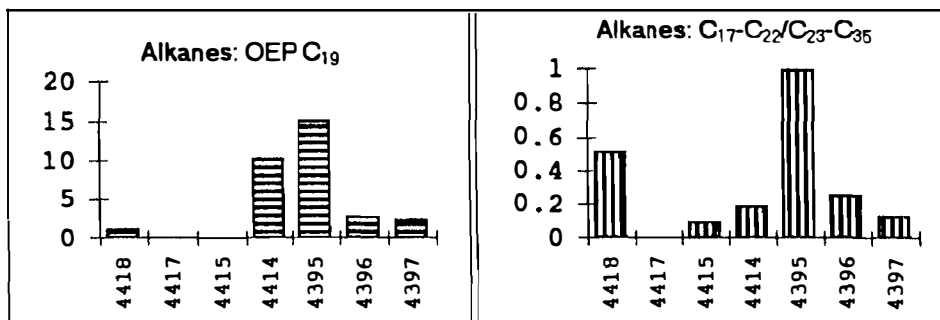


Fig.2 Source-specific lipid distribution in the surface sediments

(3) Specificity of arctic biosynthesis reflected in sedimentary lipids by occurrence of polyunsaturated fatty acids C_{16:4}, C_{18:4} and C_{16:2}. These compounds are thought to originate from membrane lipids with increased unsaturation providing suitable specific gravity.

The ratio of identified dehydroabietic acid derivatives to their predecessors - abietic acid derivatives strictly derived from terrestrial organic matter tends to increase from the Ob River mouth to the North of the transect. These compounds seem to be promising indicators of terrestrial organic matter transformation during its transport to the site of accumulation in sediment.

(4) Diagenetic resistance of terrestrial and unsaturated fatty acids seems to be closely related to their incorporation into complex lipids. Thus, main mechanism of selected preservation of different organic constituents in sediments most likely consists of formation of stable large complex compounds.

Diagenetic transformations reflected in lipids by increased proportion of high molecular, i.e., terrestrial compounds in alkanes, fatty acids and alcohols. In contrast, strictly derived from higher terrestrial plants abietic and dehydroabietic acid derivatives decreased in total lipids in cores indicating their diagenetic transformation into final pathway products.

In conclusion, lipid sedimentary molecular markers seem to provide the reliable basis for assessment of organic matter source and transformation processes as well as for the estimation of background state of natural organic matter cycling in the polar environment.

References

Bigot, M., Saliot, A., Cui, X. and Li J. (1989) Organic geochemistry of surface sediments from the Huanghe estuary and adjacent Bohai Sea (China). *Chem. Geol.* **75**, 339-350

Peulve, S., Broyelle, I., Sicre M.-A., Bouloubassi, I., Lorre, A., Saliot, A., de Leeuw, J.W. and Baas, M. (1993) Characterisation of the organic matter in an Arctic delta (Lena River) using biomarkers and macromolecular indicators. In: *Organic Geochemistry. Poster Session 16th Int. Meet. Org. Geochem.*, Stavanger, 393-397

A RELATIONSHIP BETWEEN THE PRODUCTION-DESTRUCTION PROCESSES IN SEA WATER OF THE KARA SEA

V.I. Vedernikov, G.A. Korneyeva, V.P. Shevchenko (IORAN)

Comprehensive studies of surface water were performed in the southern regions of the Kara Sea which is most subjected to freshening by rivers with large water content among the Siberian seas. Vast brackish water areas of the estuaries and the near-mouth zones create peculiar conditions for functioning of the plankton communities. Based on the results of the 49th cruise of the R/V "Dmitry Mendeleev" at the end of the summer season of the seasonal succession of plankton (1993), a comparative study of the structural components of the ecosystem (total particulate matter, particulate organic carbon - POC, concentration of chlorophyll "a" - CHL), as well as of functional characteristics (primary production - PP and hydrolytic enzymatic activities - EA) responsible for destruction of the main natural polymers - proteins, polysaccharides, their derivatives and complexes was carried out. The work describes distribution of these indicators and their relationship at the Yenisey and Ob' transects.

The Yenisey transect With distance to the open sea from south to north at the background of the small-scale variability there is a tendency for a decrease in the study parameters with the salinity increase from 0.046 to 29.68 ppt.

The total particulate matter varied from 0.23 to 1.25 mg/l in the seaward part of the transect and from 1.68 to 8.87 mg/l in the near-mouth area. The concentration of POC varied from 0.091-0.163 to 0.234-0.82 mg/l, respectively.

A jump-like change in the concentrations of CHL, PP and EA occurred in the regions of intensive mixing of fresh river water with brackish water of the estuaries (stations 4410-4413) and at transition to the open sea zone adjoining the Yenisey Bay (stations 4401-4402).

On the whole, the Yenisey transect was characterized by a high content of CHL in the upper mixed layer which was more than 1 mg/l for seaward regions, more than 2 mg/l at stations 4401 and 4402 and more than 5 mg/l in the near-mouth area. The values of PP did not exceed 22 mgC/m³ a day in the seaward regions, increasing up to 50 mgC/m³ a day in brackish water and were maximum - 104.6 mgC/m³ a day in the zone of mixing of brackish and fresh waters.

High rates of enzymatic destruction of polysaccharides of alpha-glucane type were observed in the transient zone from river to brackish water - 236 e.u./l, which corresponded to the following kinetic parameters /Keleti, 1990/: a constant of the effective rate of the 1-order reaction by substrate $k_1=0.18$ 1/h, effective polymer hydrolysis rate $v=2.25$ mg/l an hour and turnover of 5.5 h. At the other stations of the transect either trace values of amylolytic activities or no traces at all were observed. The proteolytic enzymatic activity in water samples was changing non-uniformly with the maximums in the transient zones of various types of water (see above), whose value increased from north to south from 36 to 74 e.u./l. The kinetic constants of the enzymatic hydrolysis of proteins calculated from these activities, were K_1 from 0.015 to 0.030 1/h, v from 1.82 to 3.73 mg/l an hour and the turnover of proteins varied from 32 to 66 h.

The Ob' transect At the northern stations of the Ob' transect (stations 4395-4397) at the surface water salinity more than 17 ppt and the temperature less than 2 C, the total particulate matter was small, being 0.31-0.84 mg/l and the concentration of POC varied from 0.10 to 0.16 mg/l which was close to similar parameters of the seaward zone of the Yenisey transect. In the direction from north to south there was an increase in the total particulate matter and the POC concentration with the maximum in the upper part of the Ob' estuary at stations 4417-4419 where the salinity was less than 1 ppt. The maximum values of particulate matter were 11.7-115.3 mg/l and the concentration of POC - 0.90-4.10 mg/l. The concentration of POC in dry substance of particulate matter was 3.05-4.18 ppt which indicates the dominance of terrigenous particles.

In the seaward zone of the transect the CHL concentrations did not exceed 1 mg/m³ and the PP - 14.0 mgC/m³. With the salinity decrease and temperature increase at more southern stations the CHL concentration increased. The highest rate of its change was observed in the middle part of the Ob' estuary at stations 4417 (CHL concentration 5.72 mg/m³) and 4418 (21.7

mg/m³); the PP increased up to 36.8 and 22.9 mgCm³. The values of these indicators correlated with large values of particulate matter (see above).

The distribution of hydrolytic enzymatic activities was non-uniform. The largest values of amylolytic activities were recorded in the zone of mixing of brackish and sea water (stations 4395 and 4414) - 78 and 198 e.u./l which corresponded to k₁ 0.053-0.144434 1/h, v 0.66-1.68 mg/l an hour and the polysaccharide turnover from 19 to 7.5 h. The proteolytic enzymatic activity varied from 8 to 86 e.u./l which corresponded to the kinetic indicators of protein destruction: k₁ 0.003-0.036 1/h v 0.40-4.42 mg/l an hour and the protein turnover from 28 to 297 h. For processing the expedition results the investigated stations were conventionally divided into three groups in accordance with water salinity: sea stations - S=23-32.4 ppt (9 stations), zones of mixing of sea and brackish water - S=10-23 ppt (8 stations) and zones of freshened water - S=0-9.9 ppt (10 st.).

As is seen from the Figure 1, the averaged values of surface water layer characteristics decrease in the direction - freshened water-mixed brackish and sea- sea water.

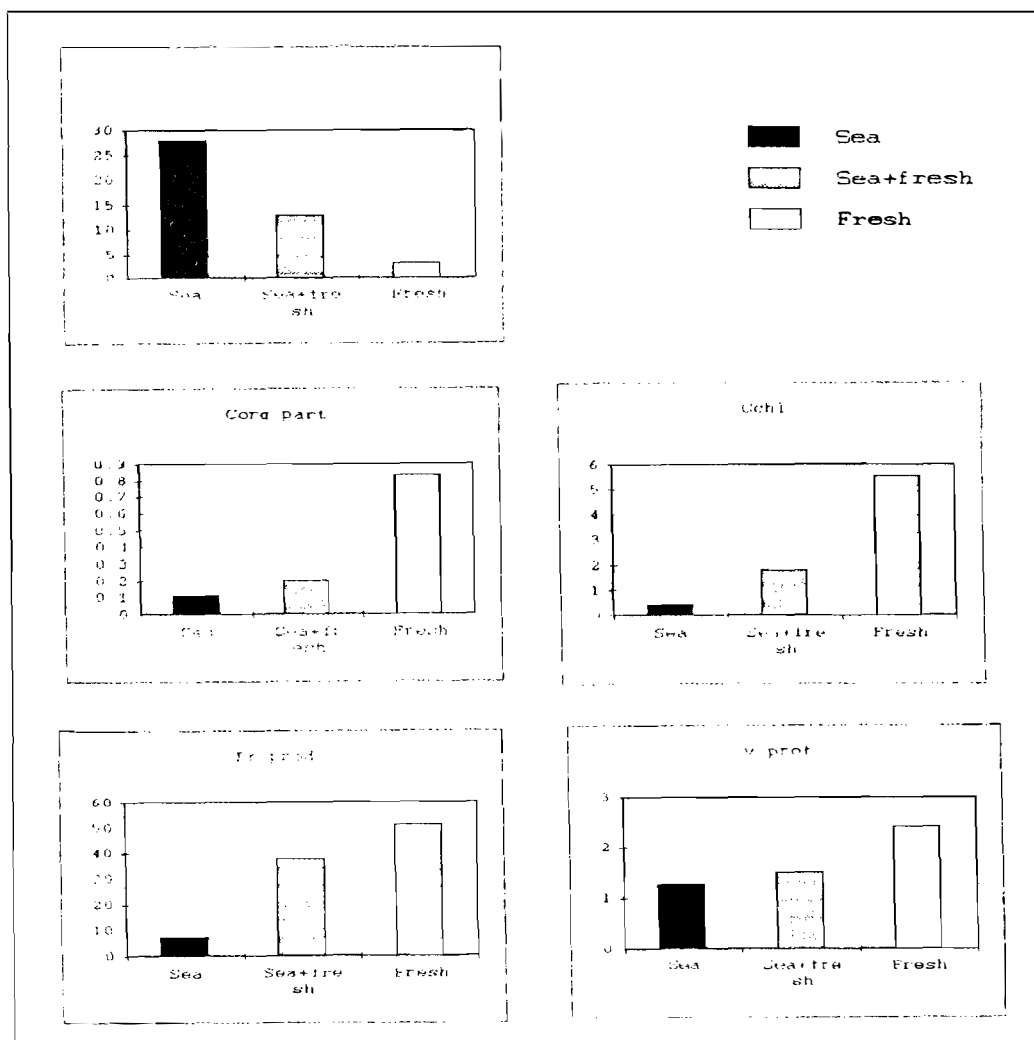


Fig.1 istribution of hydrochemical and hydrobiological indicators in surface water of the southern Kara Sea.

This allows a conclusion that in the southern Kara Sea both structural and functional indicators of the ecosystems have a reverse dependence on water salinity. The production-destruction processes in the area are directly dependent on each other since with the increase in POC and CHL concentration, the values of PP of phytoplankton and the rate of enzymatic destruction of proteins increase.

The obtained results show that probably, at the river-sea boundary due to active precipitation processes of the material transported by rivers, there is a decrease in the amount of POC and CHL concentration in surface water. Also, there is a drop in the functional characteristics of the ecosystem - primary production of phytoplankton and rates of destruction of organic matter.

On the whole, the low level of PP of phytoplankton and the rates of destruction of organic matter in the study sea regions is attributed to the influence of the factors, typical in the North, which are adverse for photosynthesis - low insolation level, low temperatures and water transparency.

Reference

1. Vedernikov V.I., Demidov A.B., Sud'bin A.I. Primary production and chlorophyll in the Kara Sea in September 1993. - *Oceanology*, 1994. Vol. 34, No. 5, 693 p.
2. Keleti T. Grounds of enzymatic kinetics. M.: Mir. 1990, 350 p.
3. Korneyeva G.A., Shoshina Ye.V., Makarov V.N. Features of enzymatic destruction of organic polymers in sea water in the light and in darkness. - *Izv. RAN, biology series*, 1995, No.3, 460 p.
4. Lisitsin A.P., Vinogradov M.Ye. An international high-latitude expedition to the Kara Sea (the 49th cruise of the R/V "Dmitry Mendeleev")/*Oceanology*, 1994. Vol.34, No. 5, 643 p.
5. Shevchenko V.P., Severina O.V., Maiorova N.G., Ivanov G.V. Quantitative distribution and composition of organic matter in the Ob' and Yenisey estuaries. - *MGU Vestnik, hydrology series*, 1994.

MARINE BIRDS IN THE KARA SEA ECOSYSTEM; COVERAGE AND PERSPECTIVE STUDIES.

M. V. Gavrilov (AARI)

In spite of their small numbers sea birds inhabiting the Kara Sea are considered to be an integral component of its ecosystem. Their investigation should become a composite part of the program for comprehensive studies of the environment of the region.

Up to recent time the study of sea birds in the region was not of a systematic character and much of evidence was obtained on an opportunity basis during general faunistic or geographical studies. The only exception is the international project the "Ivory Gull" initiated in 1993. Species composition of sea birds nesting in the Kara Sea is not rich, being typical of the inland seas of the Siberian shelf. The Ivory Gull - a species included in the Red Book, is, undoubtedly, a peculiar feature of the region. An overwhelming majority of the nesting population of this species in Russia and about half the world population inhabit the Kara Sea islands. Distribution of nesting grounds of sea birds is generally known. The main colonies of sea colonial birds are situated on the coasts of archipelagos and minor islands. At present the western coast of the Northern Land and a number of minor islands of the western Taimyr coast have been sufficiently well studied. Practically nothing has been known about the distribution of sea birds on the eastern coast of Novaya Zemlya. Quantitative accounts are carried out only in a number of colonies. The main feature of the quantitative structure of the population of sea birds of the Kara Sea is a significant prevalence of Gulls over Alcidae.

The data practically on all aspects of biology related to the use of marine biotopes are extremely fragmentary and sometimes of a purely speculative character. The observations of the distribution of birds over the area along the coast of Novaya Zemlya were performed in the 20s and in a small zone in 1992. The first quantitative pelagic accounts of sea birds over the Kara Sea area were made by the author jointly with V. Bakken (NPI) in summer of 1994 in the framework of the expedition "Ekotundra-94". An increased abundance of sea birds was found in the ice zone adjacent to the Vil'kitsky strait and along the ice edge.

For comprehensive studies of sea birds it is necessary to combine both terrestrial and pelagic observations. Quantitative accounts at sea in different biological seasons simultaneously with an oceanographic survey appear to be promising both for addressing purely biological problems and for planning nature protection activities, this being particularly important under conditions of a planned large-scale shelf exploration.

MULTIDISCIPLINARY INVESTIGATION OF THE SEA-BOTTOM ENVIRONMENT OF THE WESTERN RUSSIAN ARCTIC

I.S.Gramberg, G.I.Ivanov, V.L.Ivanov (ARROI), Yu.K.Bordukov (NMG), V.D.Kryukov (PMGSE)

Recent changes in Russian foreign policy and related warming of global geopolitical climate allowed to focus attention of the international community on high priority habitation problems, among which environmental vulnerability of the Arctic is of supreme concern to the whole mankind.

It has been recognized that during past 30 years the Arctic, particularly its western sector, was converted into a dump for a variety of harmful pollutants, inclusive of radioactive waste. The Eurasian Arctic shelf is believed to be most heavily contaminated and for that reason represents an immediate goal for complex geoecological investigations.

VNII Okeanogeologia and other branches of Association "SEVMORGEOLOGIA" has a large experience of geo-ecological and ecological-geochemical studies. Methodic of geoecological mapping of the shelf is created in 1983 - 93. Small scaled geo-ecological mapping is done in Barents, Kara Seas and Ladoga Lake.

Scientific-Industrial Association "SEVMORGEOLOGIA" has carried out on complex geo-ecological investigations of the Western part of the Arctic including Norwegian, Barents, Kara, White, Pechora Seas and eastern part of Greenland sea through 1991-94. The goals of these investigations was to assessment the antropogenous impact on main components of the Arctic environment - bottom sediments, near-bottom waters, and biota. Total number of complex stations was about 800.

Marine cruises were organized aboard research vessels "Geolog Fersman" (1992-93) and "Academic Alexander Karpinskiy" (1991), "Professor Logachev" (1994).

Specialists of VNII Okeanogeologia carried on scientific leadership as well as description, cultivation and conservation of cores. Specialists of Polar Marine Expedition (PMGRE) and Murmansk Arctic Geological Expedition (MAGE) carried on technical operations and interpretation of hydrophysical and geoacoustic data. Scientist of St.Petersburg University, Zoological Institute, GosIOPAS, Regional Centre "Monitoring of the Arctic", Institute of Hygiene and military troop N 70170 also had participated.

Complex investigations included geoacoustic, hydrophysical, lythological-mineralogical, ecological-geochemical and hydrobiological studies. The anthropogenic influence on basic components of the natural environment - surface bottom sediments, bottom waters and biota was investigated.

Data on biotesting and concentration of pollution in water, bottom sediments and benthos (chlororganic components, heavy metals Fe, Cu, Co, Mn, Ni, Pb, Sn, Zn, Cd), phenols, synthetic surface-active matters, radionuclides, oil hydrocarbons and polycyclic arenes) allow to give the complex geological estimation of condition of the natural environment of the Western Arctic sector on the transregional level, to estimate back ground concentrations, to determine zones of the maximum influence on the natural environment, to project the network of the Arctic ecological monitoring.

Preliminary results show: (i) significant concentrations of radionuclides are not found out in the bottom sediments of the Barents, Greenland and Norwegian Seas. Just minor exceedings over the background are observed; (ii) considerable part of radionuclide contaminants supplied by relatively warm water of Gulf Stream is confirmed; (iii) available data suggest transnational nature of contamination in the Barents sea-bottom environment and, possibly, in other parts of the Arctic system characterized by large-scale circulation processes. It is clear that environmental problems in the Arctic can be solved only through international intellectual, financial and logistic cooperation and implementation of complex multidisciplinary studies based on unified methodological approach.

CURRENT STATE OF BOTTOM FAUNA AND STRUCTURE OF BOTTOM COMMUNITIES IN THE PECHORA SEA

Denisenko S.G., Denisenko N.V., Frolova Ye.A., Anisimova N.A. (MMBI), Sandler (FIMI), S.Dale(AN)

Studies of bottom fauna of the south-eastern Barents Sea were initiated in the middle of the last century and first quantitative sampling of benthos was carried out in the 1920s. The results of these studies were included into classic works of Zenkevich and Brotskaya (1927; 1939). In 1958-1959 specialists from the Murmansk Marine Biological Institute have repeated the benthic survey of this part of the sea and published several articles on quantitative distribution of some large systematic groups and their most mass representatives (Streltsov, 1968; Khodkina, 1964). The next benthic survey was performed by the Polar Research Fishery and Oceanography Institute at the end of the 1970s. Based on these materials, some works concerning quantitative distribution of a number of systematic groups in the region, were also published (Antipova, 1978; Anisimova 1984; Denisenko, 1990). Discovery of oil resources in the Pechora Sea (the official name of the region east of Kolguyev Island from 1935) has become the cause for a renewed interest of scientists and in 1992-1993 specialists of the MMBI jointly with Finnish and Norwegian scientists have performed the fourth benthic survey. At 70 stations more than 220 quantitative samples (Fig. 1) were collected. Material was sampled in 2-4 replicas by "Okean" and Van Vien grabs with the working areas of 0.25 m² and 0.1 m², respectively. The number of replicas depended on the filling of the grab which was mainly governed by the granulometric composition of bottom sediments. Samples were washed through a synthetic siever with a cell size of 0.75 mm and fixed by 4% formalin neutralized by hexamin or sodium tetraborate. After primary examination the material was placed into 70 ° alcohol. Identification of taxa was made by the MMBI specialists with participation of the Zoological Institute (calibration determinations for some groups).

Determination of the dominating species in bottom communities was based on the values of their production characteristics calculated by the formula:

$$P_i = K_i * B_i^{0,75} * N_i^{0,25},$$

where B_i - the biomass of the i -taxon (species), N_i - the numbers of the i -taxon, K_i - the exchange coefficient typical of the specific taxon and determined for 3 °C (from literature).

The similarity of the stations was calculated by the Chekanovsky-Soerensen index for quantitative data (Pesenko, 1982) taking into account the production characteristics of each species:

$$C_z = 2 * \min(P_{ij}, P_{ik}) / (P_{ij} + P_{ik}),$$

where P_i - the production characteristic of the i -species at the j - station, P_{ik} - the production characteristic of the i -species at the k -station. Interpretation of the results was by computer.

Taxonomic processing of samples has shown 618 taxa of bottom invertebrates in them which is almost three times as large as observed in the 1920s (Zenkevich, 1927). Such a large difference in the species abundance of bottom fauna is, probably, governed by the progress in taxonomy and systematics of some groups for the past 70 years and by methodological features of collection of actual data.

The number of species in the samples varied from 20 to 93 and was minimum at the stations with well-sorted sand sediments. By the number of species, such systematic groups as mollusks, polichaetae, crustaceans (on the whole) and pearl weeds also dominated.

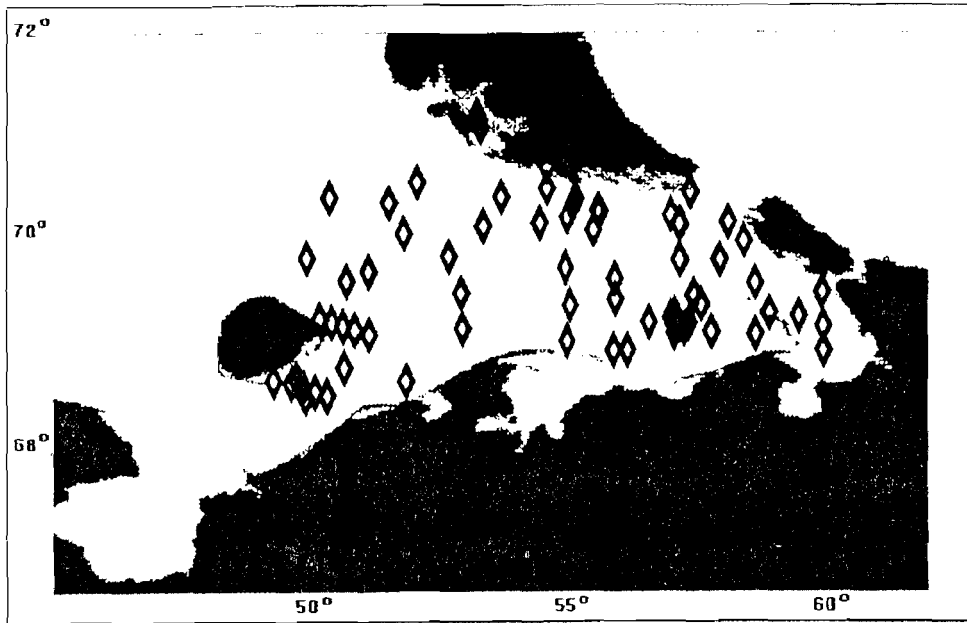


Fig. 1. A scheme of benthic stations in the Pechora Sea in 1992-1993.

Quantitative representativity of separate large taxa of zoobenthos in the study region was also governed by the character of bottom sediments.

Fig. 2 presents distribution of the total numbers of bottom animals.

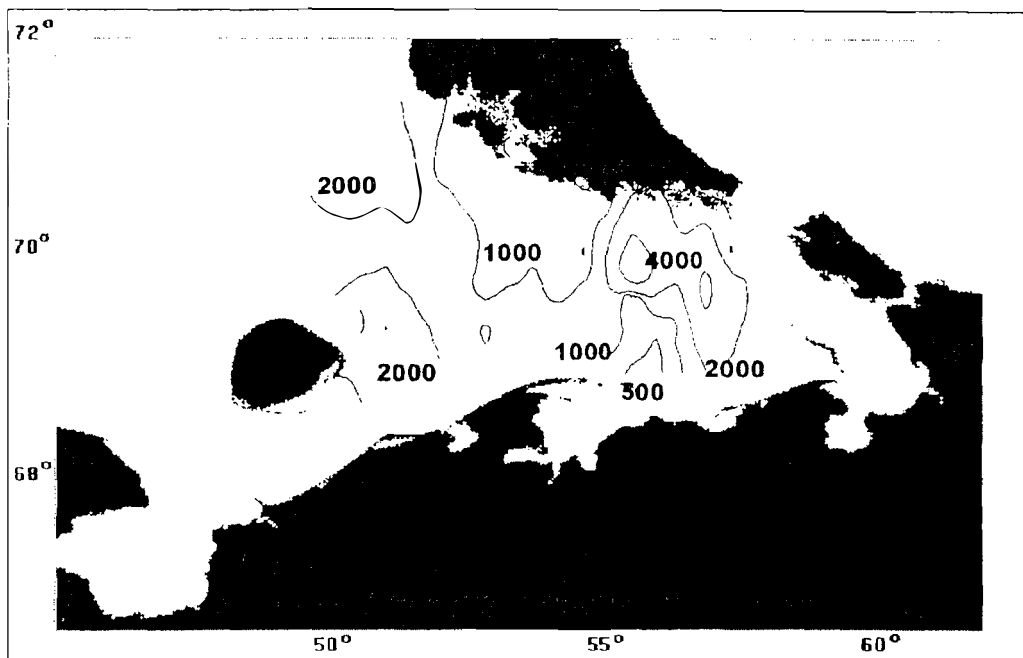


Fig. 2. Distribution of population density of benthic organisms (ind./m²) in the Pechora Sea in 1992-1993.

The number of individuals in various parts of the Pechora Sea varied from 384 to 6732 ind./ m². The largest density of the populations is observed in the central part south of Novaya Zemlya and in the strait between Kolguyev Island and the mainland, the lowest - in the freshened region at the exit from the Pechora Bay.

The amount of the total biomass varied from 1.5 to 536 g/ m² (Fig. 3) and was characterized by enhanced values (more than 400 g/ m²) in two zones. One is in the north-western and the other one in the eastern Pechora Sea. The main portion of the biomass at most stations was composed of bivalve mollusks.

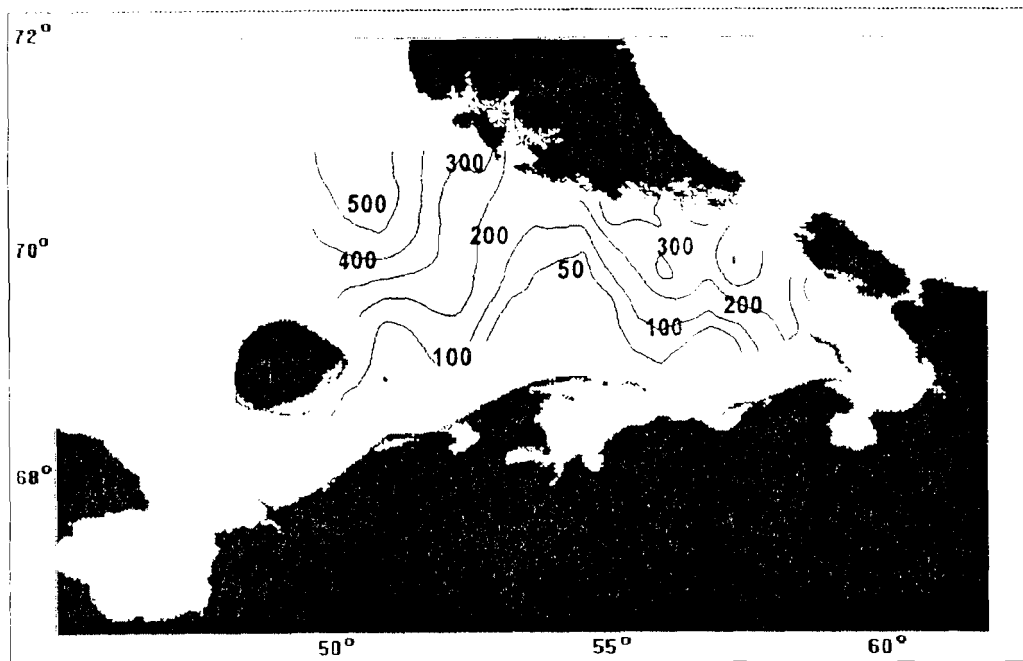


Fig. 3. Distribution of benthic biomass (g/m²) in the Pechora Sea in 1992-1993.

Cluster diagrams based on data 1992-1993 have allowed us to identify 7 bottom communities (Fig. 4). The most widespread community *Tridonta borealis* (the biomass -298±-52 g/ m²) is located at depths 25-100 m on soft and mixed bottom sediments. Another widespread community *Serripes groenlandicus* (the biomass 77±-19 g/ m²) was recorded in the shallow zone mainly on sand bottom sediments. The community *Ciliatocardium ciliatum* (the biomass 217±-35 g/ m²) was observed on mixed silty-sand sediments in the north-western and some shallow coastal zones. In the deep-sea zone of the Novaya Zemlya trough the community *Spiochaetopterus typicus* inhabits silts (the biomass of 231±-39 g/ m²). The community *Maldane sarsi* (the biomass 60±-18 g/ m²) was observed on silts with the underlying grey clay in the Novaya Zemlya trough and east of Kolguyev Island. Gravel bottom sediments in the Kara Gate strait are inhabited by the community *Chlamys islandica* (the biomass about 110 g/ m²). At the exit from the Pechora Bay there is observed the community *Ophelia limacina* with depleted species composition and a low biomass (1.5±-0.6 g/ m²).

The obtained results have shown a comparatively high extent of diversity of the bottom population and bottom communities in the Pechora Sea. The identified bottom communities in spite of methodological differences in clusters are, on the whole similar to those published (Brotskaya, Zenkevich, 1939).

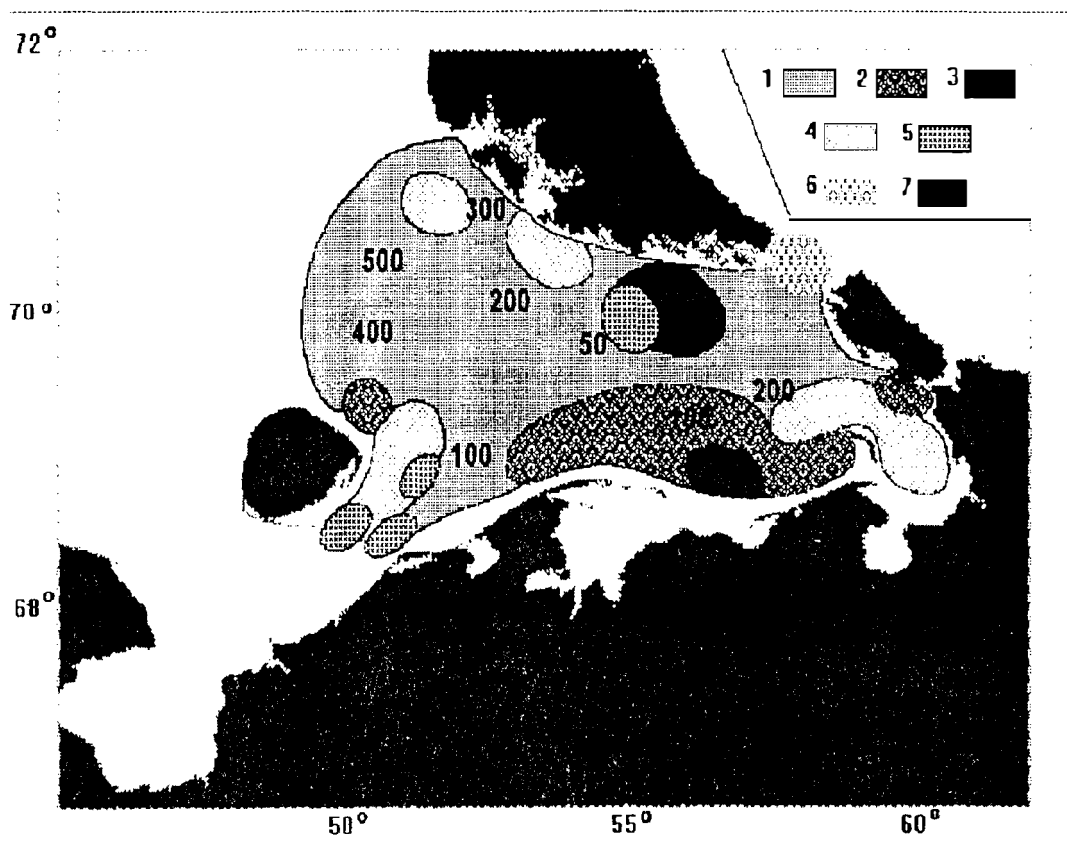


Fig. 4. A preliminary scheme of distribution of bottom communities in the Pechora Sea in 1992-1993:
 1 - *Tridonta borealis*; 2 - *Serripes groenlandicus*; 3 - *Spiochaetopterus typicus*; 4 - *Ciliacardium ciliatum*; 5 -
Maldane sarsi; 6 - *Chlamys islandica*; 7 - *Ophelia limacina*.

The quantitative development of fauna, like in the 1930s, is characterized by high biomass values. This fact allows us to consider the Pechora Sea a highly productive zone little subjected to anthropogenic impact.

Reference

1. Anisimova N.A. To the fauna and quantitative distribution of echinoderms of the Barents Sea. - Benthos of the Barents Sea. Apatity, Publ. by KF AN SSSR, 1984, pp. 32-44.
2. Antipova T.V. Preliminary data on species composition and quantitative distribution of bivalve mollusks of the Barents Sea. - Oceanology, 1975a, vol. 15, No. 2, pp.330-332.
3. Denisenko N.V. Distribution and ecology of pearl weeds of the Barents Sea. Apatity. Publ. by KNC RAN, 1990. 156 p.
4. Brotskaya V.A., Zenkevich L.A. Quantitative account of bottom fauna of the Barents Sea. Proc./VNIRO, 1939, vol. 4, pp. 3-150.
5. Zenkevich L.A. Quantitative account of bottom fauna of the Pechora region of the Barents and White Seas. Proc.of the Floating marine research institute, 1927, vol. 2, pp. 3-64.

6. Streltsov V.Ye. Quantitative distribution of Polychaeta in the southern Barents Sea. - Composition and distribution of plankton and benthos in the southern Barents Sea. M.-L., Nauka, Proc./MMMBI, 1996, No. 11 (15), pp. 71-91.

7. Khodkina I.V. Echinoderms in the southern Barents Sea. - New studies of plankton and benthos in the Barents Sea. M.-L., Nauka, 1964, pp. 41-75.

GREEN ALGA CHORICYSTIS (SKUJA) FOTT - A PARASITE OF THE WHITE SEA MUSSEL (MYTILUS EDULIS L.)

*K. Kvitko (SPbSU), V. Andreyeva, Ja. Kirsanova, N. Maximovich, L. Tichonova, A. Migunova,
Ju. Minichev (BIRAS)*

For the past 15 years Biological Institute of SPb. University has been engaged in the research of natural and artificial colonies of *Mytilus edulis* in the White Sea. In cooperation with Zoological Institute of the Russian Academy of Sciences they have prepared some recommendations for the mussel mariculture. The first harvest of mollusks was gathered from these semi-industrial plantations in 1988.

We found algae, parasite symbionts of mussels, in natural mussel colonies near the plantations of the mariculture. The algae recorded was assigned to *Choricystis* sp. (V. Andreeva and others, 1988). The goal of this work is to analyze the variety of natural algal isolates, mussel parasites.

1. Morphology and serological features of mussel parasites

Based on the morphological identification criteria (Komarek, Fott, 1983) we described alga, an isolate taken from mussels, as *Choricystis* sp. (V. Andreeva and others, 1988), a fresh-water genus distinguished from *Coccomyxa* by the absence of slime. There are dramatic changes in the growth and gametogenesis processes of infected mussels. The back of a shell becomes deformed (Fig. 1) because of the ceased secretion of shell matter on the affected areas of the mantle. The histological test suggested that algal colonies seemed to replace the gonad and inhibit the development of the gametogenesis stages on the areas free of algal colonies. Algae are inserted both in connective tissue and inside the alveoles. Usually they are surrounded by a "peralgal vacuole" (Fig. 2A,B). At a high level of infection the mussel growth stops, and their absolute parasitic castration takes place. These algae are similar in their influence on a mollusk to *Coccomyxa parasitica* found in hemocytes and *Placopecten magellanicus* tissue (K.S. Naidu (1971); R.W. Stevenson, R.G. South (1975)).

The immunofluorescent identification method for micro-organism cells has been used to describe the natural variety of symbionts. It was based on the phenomenon of the specific surface antigens in strain cells (Kinzie, Chee, 1983). Algal culture, a mussel parasite, which was used as a contributor of surface antigens, is an isolate F-1-1, i.e. the strain with a large proportion of bean-like cells (Fig. 2, D).

The specific polyclonal serum with antibodies against algal surface antigens was obtained through immunization of rabbits which were made 4 subcutaneous injections (per 122-156 million of living cells once a week). In order to keep the antibody titre at 210 a once-a-month injection was sufficient. The strain F-1-1 is protected by the author's certificate (K. Kvitko and others, 1989) as a source of antigens to identify parasitic algae, mussel inhabitants.

Serological and morphological strain characteristics are given in Table 1 below. Homology of isolates from mussels was unambiguous by all 5 features, nonspecific similarity of them with the strain F-1-1 was established for phycobionts from lichen. The algae of symbiotal origin have no similarity.

Table 1

Comparison of serological and morphological characteristics of algal cells of stains of symbiotic origin, CALU Collection (SPb University)

Strain code	Taxon	Ecological description (symbionts, free-living algae)	Serology**			Size (mkm)	
			AG	NIF	log2	HOM OL	length
F-1-1	Choricystis sp.,	mussel symbiont	++++	7	++	4,9	1,6
M-2-1	Choricystis sp.,	mussel symbiont	++++	9	+++	5,3	1,7
L-25	"-,	"-	++++	9	+++	3.7	1.8
M-53/1	"-,	"-	++++	9	+++	4.4	1.8
M-77/11	"-,	"-	++++	9	++	4.1	1.8
*216-2	Coccomyxa chodatii,	"-	++	2	+/-	6.3	1.5
*216-4	C.mucigera,	lichen phycobiont	0	0	0	7.6	1.8
*216-5	C.peltigerae,	"-	++++	5	0	7.6	1.8
*216-6	C.peltigerae,	"-	++++	9	+/-	8.0	2.0
*216-10	C.solorinae-bisporae,	"-	++++	3	0	7.6	1.6
*216-9A	C.simplex,	infusoria symbiont	0	1	0	9.4	2.2
*49.84	Coccomixa sp.,	lichen phycobiont	++++	1	+/-	5.9	1.2
826	Chlorella sorokiniana,	sponge symbiont	0	0	+/-	-	sphere
827	"-,	"-	++	0	+/-	-	"-
826	"-,	"-	0	2	+/-	-	"-
829	Ch.vulgaris,	Paramecium bursaria symbiont	0	4	0	-	"-

*) - taxa by (Schlosser, 1982);

**)- estimate of serological features in balls:

"NIF"-immunofluorescence,

"AG log2"- binary logarithm of the back titre of algal surface antigens, agglutination,

"HOMOL"- similarity with the strain F-1-1 by antigens (Wahterlony reaction).

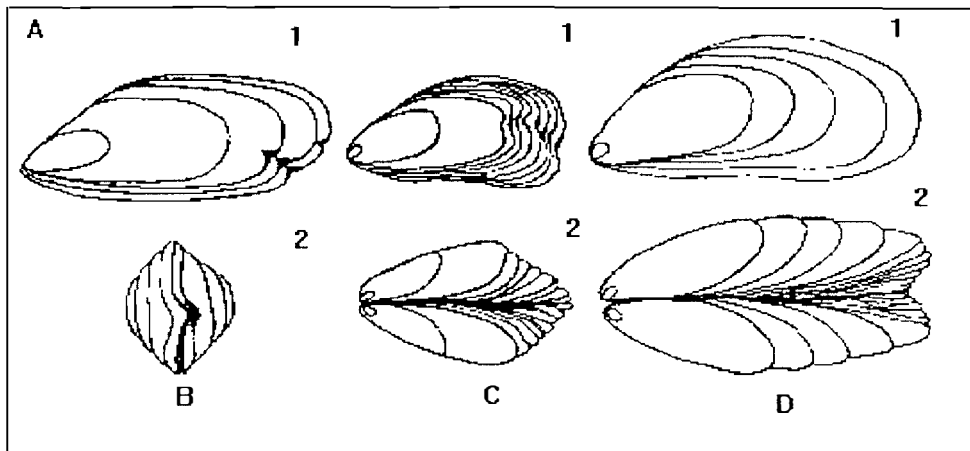


Fig.1 Different kinds of deformations in *Mytilus edulis* shells, infectious carriers (N.V.Maksimovich, A.V.Chemodanov, 1986)

- a- local slowing-down of the growth on the left valve;
- b- formation of a beak-like tumour on the "healthy" right valve towards the deformed area on the left valve (view of the back shall edge);
- c- slowing-down of the growth;
- d- termination of the growth (1- left valve, 2 - top view)

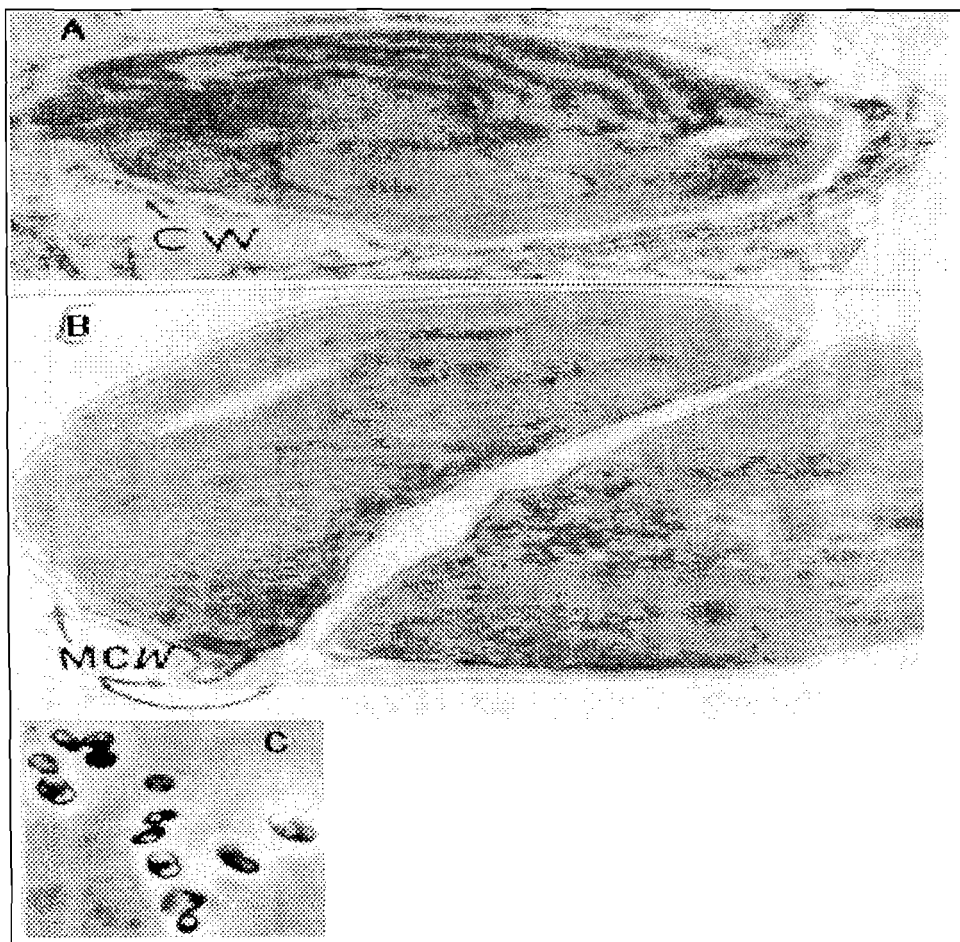


Fig.2 *Choricystis* sp. cells

- A - electron diffraction pattern of a mature algal cell in mussel tissues CW- cell wall;
- B - divided cell: 2 autospores partly surrounded by the mother cell wall (MCW);
- C - F-1-1 *Choricystis* sp. cells in the pure culture

2. Risk factors of mussel infection with algae *Choricystis.sp.*

There have been many attempts to estimate ecological factors contributing to algal parasitism in mollusks. V.L.Konstantinova and N.V.Maksimovich (1985) noted that the probability of being infected for mussels is mainly governed by their age, the portion of infected mollusks rises since they reach the age of 2-3 years. The second factor is the closeness to antropogenic sources. And the third one seems to be standing waters (Maksimovich and Chemodanov, 1986). But it is water freshening which is considered by K.V. Kvitko and others (1988) to be the principal risk factor because *Choricystis* genus is well known as fresh-water. At a salinity between 2ppm and 22ppm /Fig.3/ which took place in summertime along the coastline in the Podpakhta Arm, the occurrence frequency of infected mussels varied from 70-77 to 36 percent proportionally with the degree of freshening, and it sharply reduced to 0.4 percent at a salinity of 22ppm in the Chupinsky Roadstead.

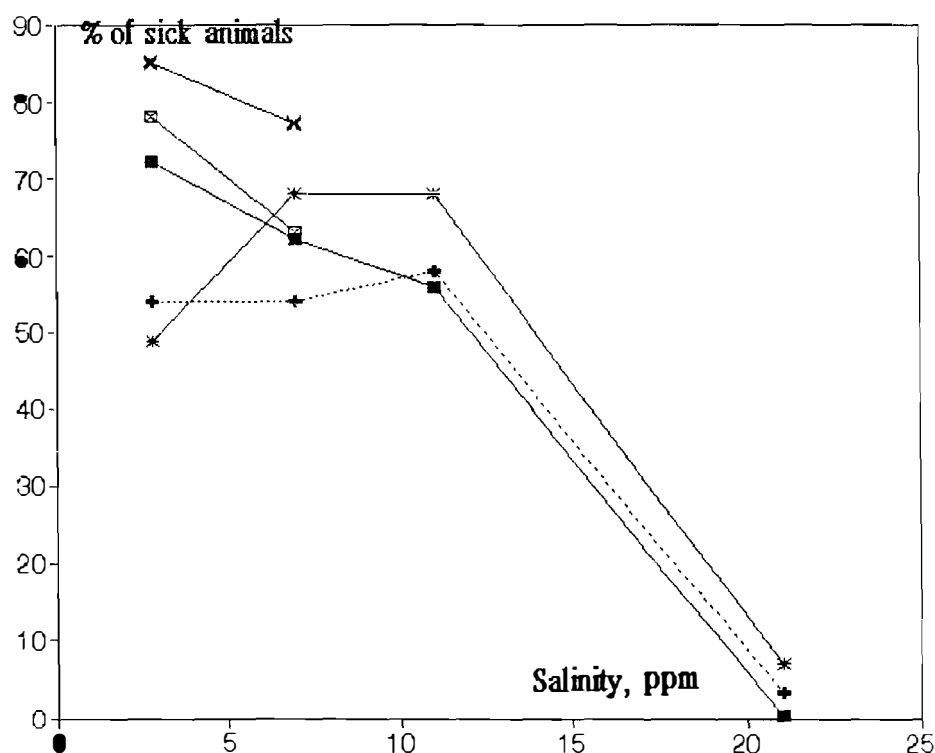


Fig.3 Water-salinity (ppm) dependence of the rate of mussel infection(%), eulittoral (intertidal) inhabitants
Samples were taken in the Podpakhta Arm along the coastline of Mys Gorely Island from the Keret river to the Chupinsky Roadstead

But there is a large proportion of infected mussels (60-70 percent) on the bank of Matrenin Island in the similar waters. Vernal freshening of the areas must be the main reason of it.

No infection with algae has been recorded neither in natural mussel colonies of the Chupinskaya Bay at a salinity of 25‰ or higher nor in mussels grown in the mariculture.

Thus, if the plantations are located in the water areas with a salinity less than 25‰ there is a potential hazard to the mariculture of the White Sea mussels located in estuaries to be infected

with Choricystis. It necessary to take it into consideration when one chooses an area for the mariculture.

References

1. V.M.Andreeva, K.V.Kvitko, Zh.G.Kirsanova. About the genus of alga, a symbiont of *Mytilus edulis* L. Abstracts for the Second All-Russian Conference "Ecology, biological productivity and some problems of the Barents Sea mariculture". Murmansk, 1988, pp. 251-252
2. K.V.Kvitko, Zh.G.Kirsanova, Yu.S.Minichev, N.B.Smirmova. Freshening is a comtributory factor for the mussel infection with Choricystis sp. The same, 1988, pp. 153-154
3. K.V.Kvitko, Zh.G.Kirsanova, L.N.Tikhonova, B.V.Gromov, Yu.S.Minichev. Choricystis sp. strain to obtain the antiserum intended for revealing of the algae. The author's certificate: SU 1678829 A1, priority from 24.04.1989. Inventor's bulletin N 35, 23.09.91
4. N.V.Maksimovich, V.L.Konstantinova. Composition and regularities of the symbiont distribution in the colonies of *Mytilus edulis* L. in the Kandalakshsky Bay. In the issue "Some problems of study, rational use and protection of the White Sea natural resources" (abstracts for the Regional Conference). Arkhangesk, 1985, pp.90-92
5. N.V.Maksimivich, A.V.Chemodanov. About the ecology of the natural colonies of *Mytilus edulis* in the Chupa Bay. Vestnik Leningradskogo Universiteta, 1986, series 3, issue 1, pp.84-92
6. Kinzie R.A., Chee G.S. Strain-specific differences in surface antigens of symbiotic algae. Microbiology, 1982, v.44,N 5, pp.1238- 1240
7. Komarek J.,Fott B. Chlorophyceae (Grünalgen). Ordnung: Chlorophyceae. In: Die Binnengewässer. Bd.16. Das Phytoplankton des Süßwassers. Systematic und Biologie. Teil 7. Hf.7 - stuttgart: E. Schweizerbartische Verlaagsbuch-handlung. 1983.1044 S
8. Naidu K.S. Infection of the giant scallop *Placopecten magellanicus* from Newfoundland with Endozoic algae. - J.Invertebr.pathology. 1971, N.17, pp.145-157
9. Schlosser U.G. Sammlung von Algenkulturen. - Ber. Deutsch. Bot. Ges. 1982.,Bd.95.S.181-276
10. Stevenson R.W., South R.G. Observations on Phagocytosis of *Coccomyxa parasitica* (Coccomyxaceae; Chlorococcales) in *Placopecten magellanicus*.- J. of invertebr. pathology. 1975, v.25, pp.307-311

ENVIRONMENTAL INFLUENCE TO THE GENETIC POLYMORPHISM OF SOME INVERTEBRATE AND BROWN ALGAE IN THE WHITE SEA BY THE PHENETICS POPULATION METHOD.

S.A.Kozhin (LNPI), L.V. Bondarenko, L.V.Barabanova, K.V.Kvitko, V.D.Simonenko (SPbSU)

Phenetics population method, the main idea of which is to find the natural populations of the individuals with different phenes (it is desirable - with contrast phenes), the quantitative and qualitative analysis of their variety, accumulation, dynamics, etc., allows to use the genetic methods and principles in order to analyse the natural organism populations, the genetic studying of which is difficult or impossible (Yablokov, Larina, 1985).

By this method the polymorphism monitoring of natural populations of some invertebrate and brown algae, which inhabit in the Kandalaksha Gulf littorals of the White Sea, was carried out within a decade.

The main purposes of these investigations are the following:

1. To reveal the objects with the distinct morphological polymorphism and contrast (or alternative) phenes. The objects were selected by the requirements that can be placed upon them. They are the following: the studying organisms population are to be the numerical and lightly available, the analysed features are to be identified.

2. To describe the phenotypic structure population of the selected objects by the quantitative accumulation estimating of phenes.

3. To compare the revealed polymorphism among the typified populations of different ecological niches, to estimate the most credible dominating ecological factor.

4. To study the dynamics of the phenetic polymorphism changes in the same populations within the multiyear observations, to find the stable and variable populations from the standpoint of their phenestruce.

Some objects, the phenetic population structure of which is being studied, (their accumulation density in littorals allows to analyse them without the population structure disrupting) were found within multiyear investigations.

Such objects are the following: *Littorina obtusata* - the littoral mollusk widely distributed in the investigated area of the White Sea and the northern seas. The main features of it in the genetic and population investigations are the high accumulation density and the rigorous rating to the littoral macrophytes, lacking of the plankton evolutionary stages, the small mobility of the adult individuals and the clearly marked polymorphism of colour and shell design. (Fig. 1.2). The phenotypical structure studying of two ecologically contrast *Littorina* populations within the period 1985-1995 showed the great difference in the concentration of the shell colour. The sand and silt *Littorina* population of littoral is characterized by the constant large proportion of the purple phenes and virtually lack of colour phenes. But the *Littorina* population, which inhabit in the stone littoral is characterized by large proportion of the orange, yellow and white shell colour of phenes by these purple. (Fig. 1) Analysis of the intra- and interpopulational variability with space and time is one of the main lines of the ecological and genetical natural populations studying. It allows to begin the revealing of variability features and factors, which have an influence on it (Battaglia, Bearmore, 1978).

Isopod *Jaera albifrons* is the good object for the investigations. It inhabits in littoral and sublittoral of cold and moderate waters of the Northern Atlantica and lives in stones and algae. *Jaera albifrons*, as all Isopods, are diclinous. She lays eggs to the bag, which is on the abdominal body side. This feature gives the great opportunity to carry out the genetic analysis of heritability of main colour (black, brown, orange, white) and the shell design of Isopods, because *Jaera* are extremely varied (Fig.3) to these features. Polymorphism analysis of colour and shell design showed that there are dark coloured

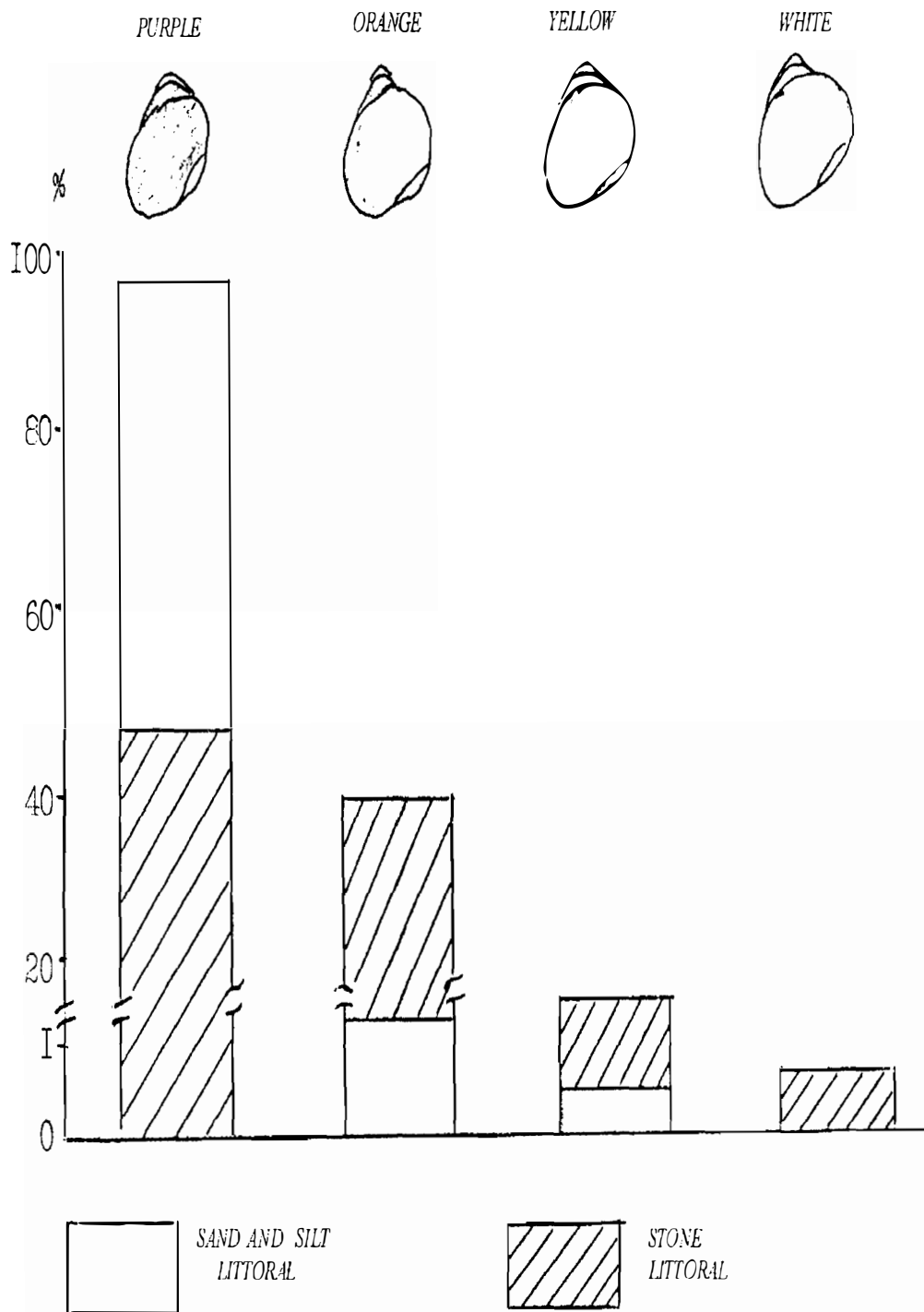


Fig.1 Frequency of the shell colour in the ecologically contrast *Littorina* populations within 1985-1995.

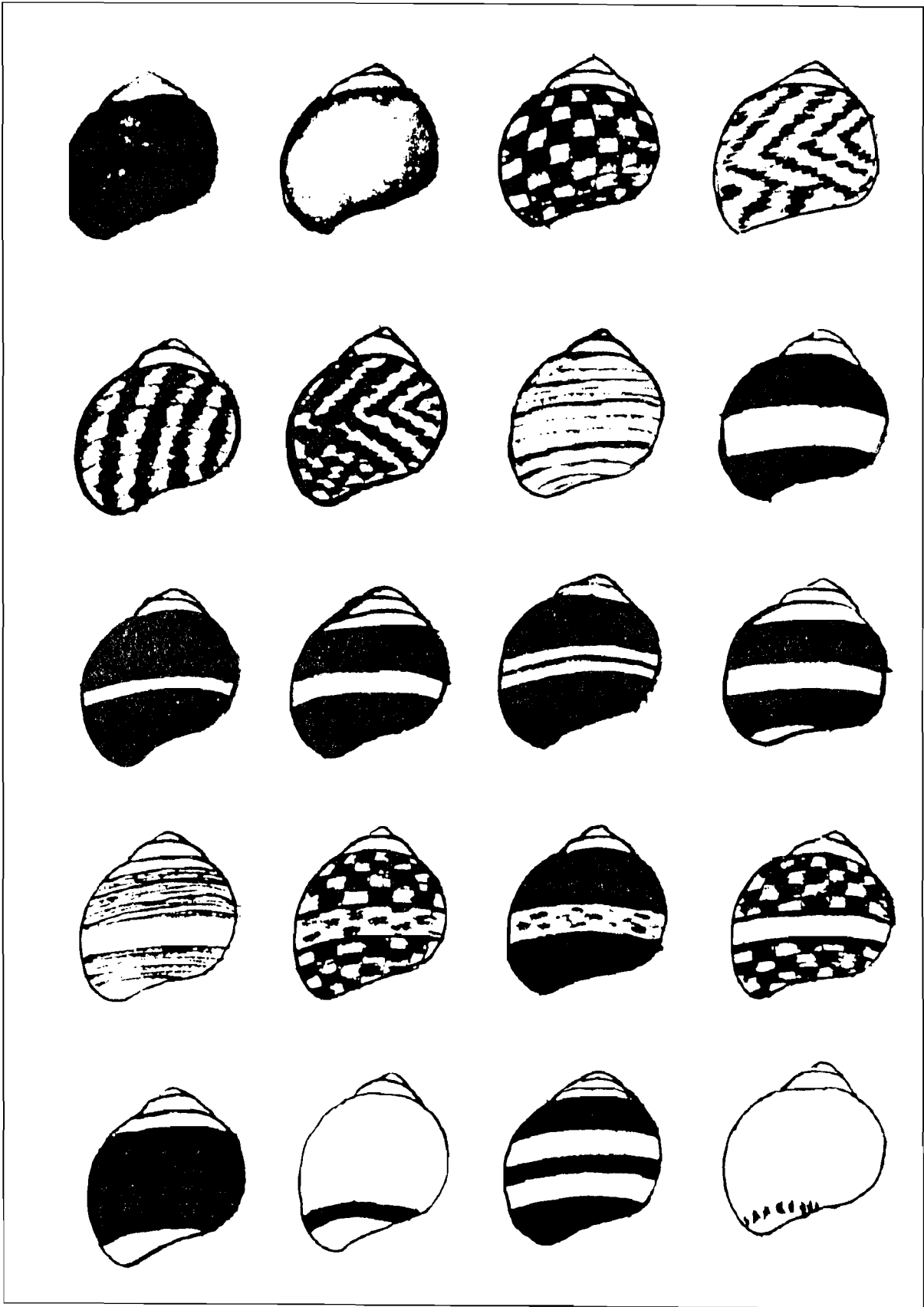


Fig. 2 Shell design phenes of *Littorina*

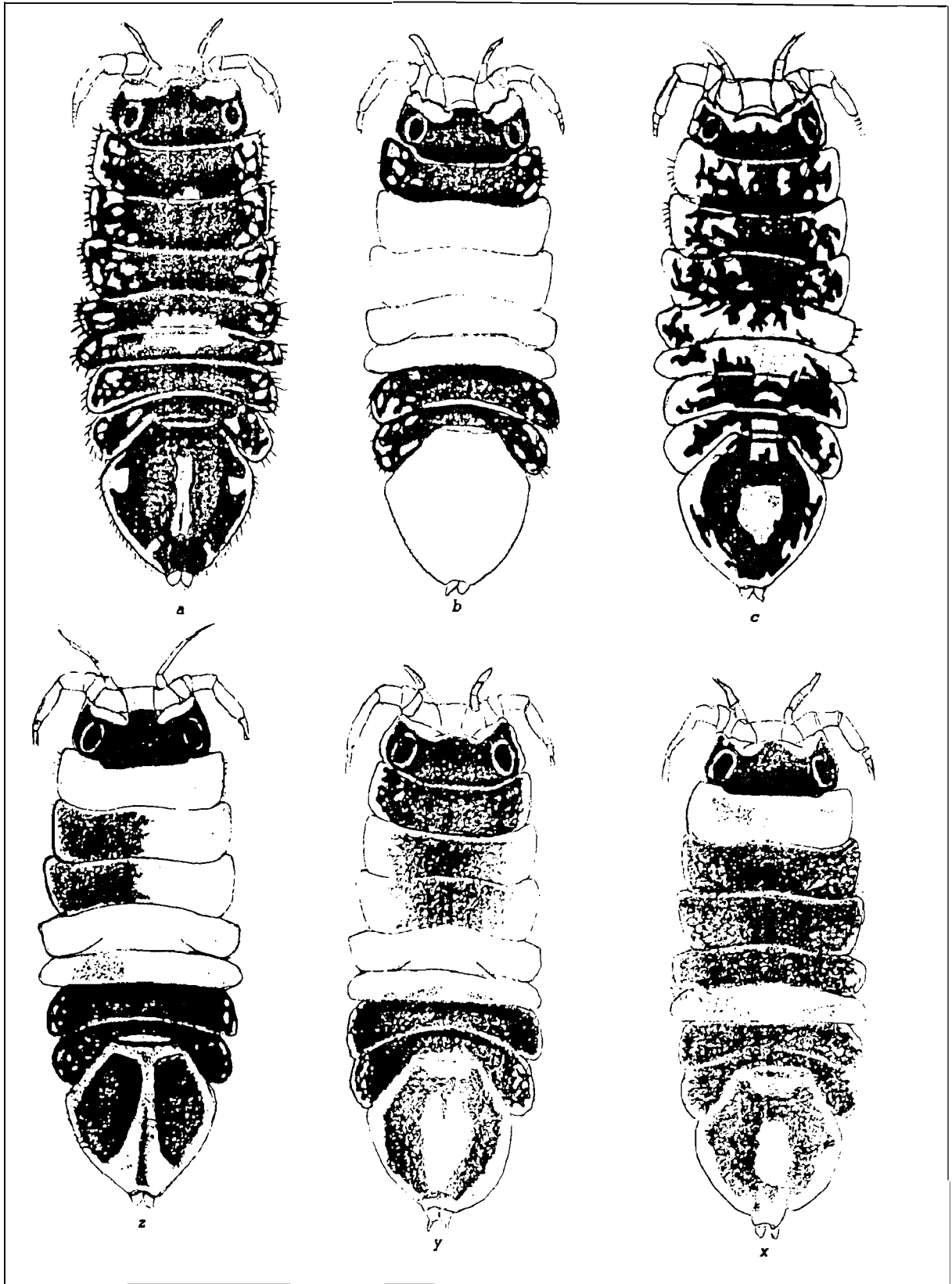


Fig. 3 Shell design phenes of *Jaera*

forms in all populations. But the ecologically contrast populations are characterized by the different phenes proportion of the other colour types. The shell design polymorphism analysis has considerable promise because the preliminary data show the concentration dynamics of some phenes in the investigated populations, and also in that rarity in nature (Fig. 3 x, y). Besides, the forms with different distribution of ontogeny pigment (it can be shown in the bilateral colour mosaicism) were found within investigations, carried out from 1993 to 1995 (Fig. 3 z).

The same ecological and genetical investigations are carried out by studying of the sea natural populations and freshwater invertebrate such as *Mytilus edulis*, *Macoma baltica*, *Littorina saxatilis* (representatives of the *Simuliidae* and *Chironomidae* families). All these objects are in the polar region and show different polymorphism types (leg colour of common mussel, colour and shell design of ark shells (*Bivalvia*) and *Littorina*, the different chromosome polymorphism types of dipterous).

In the northern seas areas of water there is the wide variety of algae. Bady wrack (*Fucus vesiculosus*) is the most plentiful (Vozzhinskaya, 1986). *Fucus* have the wide adaptational reaction. Besides they have some modificational changes. To estimate these reactions during the investigations within 1985-1995 two ecologically contrast populations of *Fucus* (they differ to reaction of desalination factor), which were compared to the features thallome accretion of the previous year, population puberty and the proportion of male and female plants, were investigated (Fig. 4).

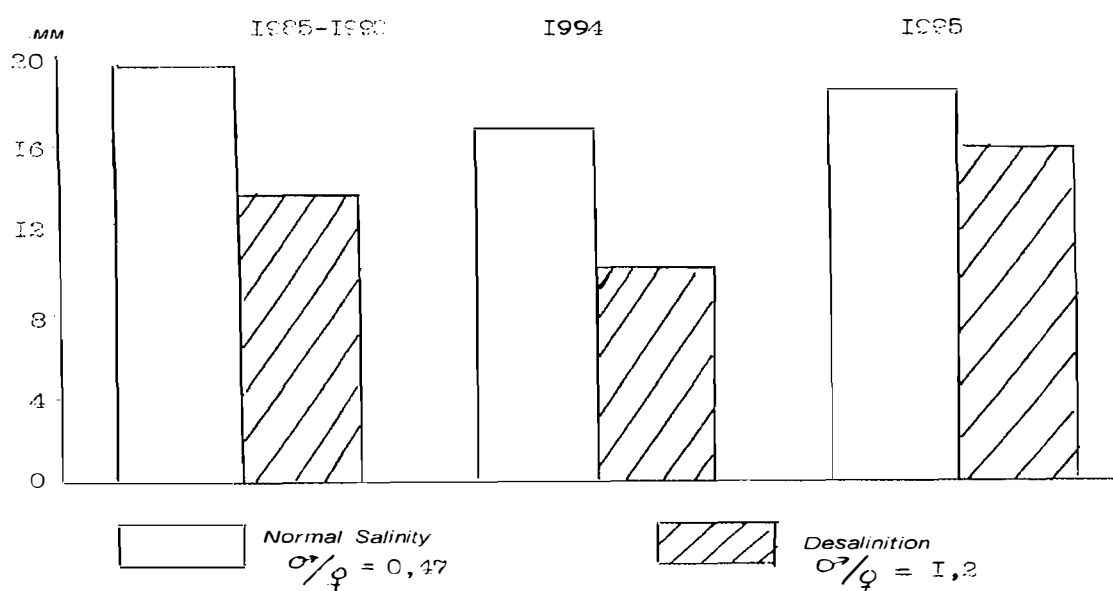


Fig. 4 Vegetative thallome accretion and the sex proportion in the fucus populations, which differ to desalination factor.

Desalination, as the main ecological factor, has an influence to vegetative thallome accretion and practically has no influence to puberty of the investigating fucus population. But, because of the influence of desalination factor, the proportion of male forms in population increases. It is necessary to emphasize the revealed disruption of the thallome dichotomy and its annual accretion within 1993-1994. These disruptions are the result of the environmental factor, which was not taken into consideration and affected adversely to the *Fucus* population within that period.

As the result of multitear investigations the phenestruure of the populations studying objects, which inhabit in Kandalaksha Gulf littoral of the White Sea, was described.

The contrast populations (which are in dependence of environmental factors), such as the populations with wide and narrow polymorphism, were found. The conducted Monitoring showed the departures of some phenes within some years in commonly stable populations. Studying of the natural littoral invertebrate populations and algae in the north-western part of the White Sea by phenetics population method showed its efficiency for investigation and quantitative description of the genetic polymorphism, for the analysis of the phenostructure population dynamics (monitoring) and for the ecological factors revealing. These factors rate this dynamics in the White Sea regions, which are not impacted yet. Proposed methods and the investigated marine organism species can be used to estimate the anthropogenic factors influence in the other (from the standpoint of anthropogenic pollution) Arctic seas.

Referances

1. V.B.Vozzhinskaya Bottom - dwelling macrophytes in the White Sea, M., Nauka, 1986, p.196
2. A.V.Yablokov, N.I.Larina Introduction to populations phenetics, M.,High school, 1985, p. 156
3. B.Battaglia, J.A.Bearmore Marine organisms in Genetics, Ecology and Evolution, N.Y.L., Plem.Press, 1978, p.758

Preliminary theses title:

Genetic polymorphism monitoring of the marine invertebrate and macrophytes in the White Sea as ecological investigational method.

GEOLOGICAL CORRELATION AND EVOLUTION OF THE EASTERN SVALBARD - FRANZ IOSEF LAND REGION: THE NORTHERN BARENTS SEA GEOTRAVERS

E.E.Musatov (ARROI) , A.Solheim (NP)

Joint investigations of Norwegian Polar institute and VNIIOceangeologia were carried out through 1991-1994. They included studies of cores from three deep wells drilled in 1970-th on Franz Iosef Land and broad exchange and examination of samples of igneous, metamorphic and sedimentary rocks collected on both archipelagos. During summer season in 1992 joint geological-geophysical investigations between Svalbard and Franz Iosef Land were carried out from the board of Russian research vessel "Geologist Fersman", including single channel seismic profiling, high resolution seismic acoustics, echosounding, magnetic records and coring of Quaternary sediments and sometimes Cretaceous rocks with gravity tube. Norwegian participants of the project were N.Heintz, H.Dypvik, A.Andresen, F.Gustavssen, ators of the project. and A.Nilsen. V.L.Ivanov, V.I.Bondarev, Yu.K.Bordukov, A.R.Sokolov, V.D.Dibner, E.G.Bro, A.N.Evdokimov, G.I.Ivanov, P.V.Rekant, T.M.Pchelina, V.I.Gurevich, M.V.Korchinskaya and O.R.Buzikova were involved from Russian side. Both authors of the report were coordinators of the project.

Lithology, mineralogy, textures and structures of rocks and unconsolidated sediments as well as forams, spores and pollen, ostracods were examined in labs of University of Oslo and VNIIOkeangeologia. Three main sequences were recognized in Mesozoic cover of the shelf: Triassic, Jurassic and Upper Jurassic-Lower Cretaceous. Sills and dikes of dolerites penetrate them in Franz-Victoria trough. Late Pleistocene glacial and Latest Pleistocene-Holocene glacial-marine and marine deposits are established in recent veneer on the shelf. Geological map of bedrock, map of Quaternary deposits, maps of thicknesses of Upper Cenozoic sediments, geomorphic and tectonic maps are compiled (scale 1:1 000 000).

FISH FAUNA OF THE KARA SEA: STATE OF KNOWLEDGE AND KEY RESEARCH GOALS

A. V. Neyelov, N. V. Chernova, (ZIRAS)

The fish fauna of the Kara Sea is now many times less understood than that of the adjacent Barents Sea. This is due to lesser fishery importance and rather severe ice conditions of this region. Only coastal areas and estuaries, rich in different fish species, primarily whitefishes, have been much studied.

According to the recent information 84 species and subspecies of fish-like vertebrates and fishes are counted in the Kara Sea fish fauna. Of these species registered, 23 (27,4 percent) turned out the pure fresh-water ones (Table 1). Usually they are observable in some areas of the Kara and Ob Bays, the Yenisey and Piasina River estuaries, where the salinity is not high (up to 5‰). The only exception is ninespined stickleback (1,2 percent) which lives even in sea water, but can spawn nowhere but in fresh water. Thus, this species can be placed in a separate group (Table 2).

Table 1

Fresh-water fishes rare in brackish water

1. Fam. Petromyzontidae
 1. *Lethenteron japonicum kessleri* (Anikin, 1905)
2. Fam. Acipenseridae
 2. *Acipenser ruthenus* L., 1758
3. Fam. Cyprinidae
 3. *Rutilus rutilus lacustris* (Pallas, 1811)
 4. *Leuciscus idus* (L., 1758)
 5. *L. leuciscus baicalensis* (Dybowski, 1874)
 6. *Carassius carassius* (L., 1758)
 7. *C. auratus gibelio* (Bloch, 1783)
 8. *Phoxinus phoxinus* (L., 1758)
 9. *Ph. czekanowskii* Dybowski, 1869
 10. *Ph. percunurus* (Pallas, 1814)
4. Fam. Cobitidae
 11. *Cobitis tainia* L., 1758
5. Fam. Esocidae
 12. *Esox lucius* L., 1758
6. Fam. Osmeridae
 13. *Hypomesus olidus* (Pallas, (1814)
7. Fam. Salmonidae
 14. *Hucho taimen* (Pallas, 1773)
8. Fam. Coregonidae
 15. *Coregonus tugun* (Pallas, 1814)

(Continuation)

9. Fam. Thymallidae
 16. *Thymallus arcticus* (Pallas, 1776)
 17. *Th. thymallus* (L., 1755)
10. Fam. Gadidae
 18. *Lota lota* (L., 1758)
11. Fam. Cottidae
 19. *Cottus poecilopus* Heckel, 1836
 20. *C. sibiricus* Kessler, 1899
 21. *C. kessleri putorania* Korjakov et Sidelev, 1976
12. Fam. Percidae
 22. *Perca fluviatilis* L., 1758
 23. *Gymnocephalus cernua* (L., 1758)

Table 2

Brackish-water fishes

1. Fam. Cottidae
 1. *Trigloopsis quadricornis* (L., 1758)

In any kind water (everywhere).

1. Fam. Gasterosteidae
 1. *Pungitius pungitius* L., 1758.

Of other 60 species, 13 (21,6 percent) were found to belong to anadromous and semianadromous (mostly whitefishes and salmonids) (Table 3), and 1 species, four-horn sculpin, was a typical brackish-water (1,2 percent) spawning at a salinity up to 24‰ (Table 2).

Table 3

Anadromous and semianadromous fishes

1. Fam. Petromyzontidae
 1. *Lethenteron japonicum* (Mertens, 1868)
2. Fam. Acipenseridae
 2. *Acipenser baeri baeri* Brandt, 1869
 3. *A. b. stenorhynchus* A. Nikolski, 1896
3. Fam. Salmonidae
 4. *Salmo salar* L., 1758
 5. *Salvelinus alpinus* (L., 1758)

(Continuation)

4. Fam. Coregonidae

6. *Coregonus autumnalis* (Pallas, 1776)
7. *C. lavaretus pidschian* (Gmelin, 1788)
8. *C. muksun* (Pallas, 1814)
9. *C. nasus* (Pallas, 1776)
10. *C. peled* (Gmelin, 1788)
11. *C. sardinella* Valenciennes, 1848
12. *Stenodus leucichthys nelma* (Pallas, 1773)

5. Fam. Osmeridae

13. *Osmerus mordax dentex* Steindachner, 1870

Many of typical marine species (46) are able to live at a salinity up to 25 ‰ (Table 4), but they spawn at a salinity higher than 24 ‰. Only 17 species are strictly stenohaline, and they cannot live at a salinity less than 34-35 ‰. Thus, no more than 29 marine species are considered, to a greater or lesser extent, as euryhaline, they can be seen in sea water with a wide range of salinity (up to fresh water), for example, navaga and arctic flounder.

Table 4

Marine fishes of the Kara Sea

1. Fam. Squalidae

1. *Somniosus microcephalus* (Bloch et Schneider, 1801)

2. Fam. Clupeidae

2. *Clupea pallasii suworovi* Rabinerson, 1927

3. Fam. Osmeridae

3. *Mallotus villosus* (Muller, 1776)

4. Fam. Gadidae

4. *Arctogadus borisovi* Drjagin, 1932
5. *Boreogadus saida* (Lepechin, 1774)
6. *Eleginus navaga* (Pallas, [1814])
7. *Gadus morhus morhua* L., 1758

5. Fam. Cottidae

8. *Arctiellus atlanticus atlanticus* Jordan et Evermann, 1898
9. *A. atlanticus europaeus* Knipowitsch, 1907
10. *A. scaber* Knipowitsch, 1907
11. *Gymnocanthus tricuspis* (Reinhardt, 1831)
12. *Icelus bicornis* (Reinhardt, 1840)
13. *I. spatula* Gilbert et Burke, 1912
14. *Myoxocephalus scorpius* (L., 1758)
15. *Triglops pingeli* Reinhardt, 1838
16. *T. nybelini* Jensen, 1904

(Continuation)

6. Fam. Cottunculidae
17. *Cottunculus sadko* Essipov, 1937
7. Fam. Agonidae
18. *Leptagonus decagonus* (Bloch et Schneider, 1801)
19. *Ulcina olriki* (Lutken, 1876)
8. Fam. Cyclopteridae
20. *Cyclopterus lumpus* L., 1758
21. *Cyclopteropsis jordani* Soldatov, 1929.
22. *Eumicrotremus derjugini* Popov, 1926
9. Fam. Liparidae
23. *Liparis fabricii* Kroyer, 1847
24. *L. gibbus* Bean, 1881
25. *L. tunicatus* Reinhardt, 1837
26. *Careproctus micropus* (Gunther, 1887)
27. *C. "reinhardti"* Kroyer, 1862 complex.
28. *C. ramula* (Goode et Bean, 1880)
10. Fam. Zoarcidae
29. *Gymnelus retrodorsalis* Le Danois, 1913
30. *G. viridis* (Fabricius, 1780)
31. *Lycodes eudipleurostictus* Jensen, 1902
32. *L. pallidus pallidus* Collett, 1879
33. *L. polaris* (Sabine, 1819)
34. *L. reticulatus* Reinhardt, 1838
35. *L. rossi* Malmgren, 1865
36. *L. sagittarius* McAllister, 1975
37. *L. seminudus* Reinhardt, 1838
38. *L. jugoricus* Knipowitsch, 1906
39. *Lycenchelys kolthoffi* Jensen, 1904
11. Fam. Lumpenidae
40. *Anisarchus medius* (Reinhardt, 1836)
41. *Lumpenus fabricii* Reinhardt, 1836
42. *L. lampretaeformis* (Walbaum, 1792)
43. *Leptoclinus maculatus maculatus* (Fries, 1837)
12. Fam. Ammodytidae
44. *Ammodytes marinus* Raitt, 1934
13. Fam. Pleuronectidae
45. *Hippoglossoides platessoides limandoides* (Bloch, 1787).
46. *Liopsetta glacialis* (Pallas, 1776)

One can expect few marine species known for the Kara Sea to be increased since there are several species fished towards the West or East, primarily in the high-latitudinal Arctic and deep zones of the Polar basin. Now we know not more than 6 deep-water species (13 percent) in the northern Kara Sea. It is less than that in the Laptev Sea (A.V.Neyelov, N.V.Chernova, 1994).

Arctic fish species, both the fresh-water and anadromous as well as the marine ones, play the main role in the fish fauna. Cryopelagic species observable here is also the characteristic feature of the fish fauna. The presence of these species is permanently or temporary connected with the first-year or multi-year ice, for example, polar cod, blackbelly snailfish and, to a lesser degree, eastern-siberian cod and navaga. Only capelin and pacific herring can be considered as pelagic ones. The other marine fishes are benthic. The most important fish families among them are as follows: Zoarcidae (11 species or 23.9 percent), Cottidae (10 or 21,7 percent) and Liparidae (no less than 6 species or 13 percent).

All the anadromous and semianadromous fishes (whitefishes, salmonids and smelt) are of commercial fishery importance. Besides, some fresh-water species are very important for the local human use. As for marine fishes, only navaga, polar cod and, to a lesser degree, arctic flounder are also of fishery importance but their value is rather small as compared with whitefishes.

Four-horn sculpin, numerous here, plays a large role in trophic webs of shallow regions, bays and gubas included. It is not only a competitor in feeding of a number of valuable fish species, but its pelagic juveniles are also an important feed component for the other species, in particular for omul which is one of the most valuable fish here.

As to the state of knowledge on the fish fauna and the main research goals, a poor knowledge on the northern Kara Sea deep zones should be stressed. It is bathyal depths of the Kara Sea where fishes well known for farther western and eastern regions adjacent to the Arctic can be anticipated. Thus, one of the goals is to perform appropriate research in this region. It is necessary to determine the northern distribution boundary for semianadromous species, the peculiarities of distribution of brackishwater species over the shelf, the boundaries of the Arctic boreal and arcto-boreal shelf species penetration to the East, and the coastal fish fauna components of the Novaya Zemlia and Severnaya Zemlia Islands.

POLYCYCLIC AROMATIC HYDROCARBONS IN BOTTOM SEDIMENTS OF THE BARENTS-KARA SHELF *)

Petrova V.I. (ARROI)

Polycyclic arens (PAH) are among the basic pollutants along with heavy metals, radionuclides, oil-products, chlororganic compounds etc. Sources, ways of the supply and distribution of PAH in sediments for different areas of the World Ocean are subject of a considerable number of investigations. This is conditioned by the clearly defined mutagenic and carcinogenic activity of a row of PAH what in combination with a considerable molecular steadiness determines their high importance as markers for the estimation of the ecological condition of water areas (1,2,3,4,5).

It should be noted, however, that a level of the technogenic pollution in the majority of works are estimated on the absolute content of the PAH sum or one of basic contaminating matters of the PAH group - benz-a-pyren - without considering a natural geochemical background (6,7,8,9).

Available information uniquely suggests that the stable geochemical background of PAH of the natural genesis including tens of individual compounds with predominating 3-10 basic compounds exists in bottom sediments. Consequently, a strategy making possible to differentiate the technogenic constituent and geochemical background must be the basis for the ecological monitoring(10,11,12).

The strategy for the study of PAH developed by us is based on the organic-geochemical investigations which include a genetic diagnostics and typification of the organic matter in bottom sediments. It was shown on the basis of the correlative analysis that phenatrene [PHN], chrysene [CHR] and perylene [PER] can be related to the syngenetic dominants that is dominants which are genetically connected with the organic matter (OM) of bottom sediments. Perycondensed arens such as pyren [PYR] and benz-a-pyren [BAR] have, evidently, pyrogenous genesis, however, not uniquely antropogenic one. The natural processes such as volcanism, tectonic and hydrothermal relaxation also can be accompanied by forming pyrogenous PAH. This strategy has been tested on collections of bottom sediments selected during expeditional works of VNIIOkeangeologia in Northen and Southern polar zones of the World Ocean as well as in the equatorial zone (11,13,14,15).

Distribution of PAH is a very specific for an each water area. Consequently, the reliable estimation of the ecological condition implies both understanding ways for forming of the PAH geochemical background in a given region and the presence of a concrete qualitative and quantitative its characteristic.

The purpose of this investigation was to reveal a specificity of the geochemical background of PAH and factors influencing on its forming in sediments of the Western Arctic shelf. Sediments collected during expeditional works of VNIIOkeangeologia in 1991-1993 in Barents and Kara Seas have served as the object.

Sediments of the Barents Sea are clearly divided into three groups in accordance with organic-geochemical parameters and PAH content and distribution .

In sediments of the South-Western part of the Barents Sea shelf, contents of PAH are the least in the region, and the character of the distribution for individual compaunds indicates that the technogenic influence is insignificant. The ratio of the pyrogenous and background constituents are lower than in sediments of the Barents Sea.

Sediments in the deep, Nort-Eastern part of the Barents Sea are characterized by higher PAH contents and the original distribution of individual components.

*) *translated by the author*

The erosion by water and redeposition of black shale Jurassic formations in Franz Josef Land are, evidently, of considerable importance in forming OM of these sediments. This supposition is supported by the complex of litho-facial features of studied sediments as well as is in agreement with the data of the PAH distribution in the composition of so-called "black shales" (17).

The third group is presented by sediments from the Spitsbergen Island area: PAH contents in them are considerably higher than average values for Arctic shelf sediments. So high contents of PAH have been marked earlier in submerged sediments of trenches where the transformation level of OM has reached a protokatagenesis and in Cretaceous deposits opened by drilling at the Barents Sea shelf. Complex of organic-geochemical and lithofacial characteristics makes possible to connect the PAH distribution in this region with coaly stratas in Spitsbergen. Thereby, intensive decreasing of PAH contents along the Ulf-fjord profile betokens the erosion of coastal stratas more than loss of coal during a transportation (12,18).

Contents of PAH in estuarine and shelf sediments of the Kara Sea were not high and close to background ones. Thereby, the evident tendency of decreasing of components of terrigenous genesis and increasing of the relative content of phenanthrene and chrysene connected with hydrobiontic OM is traced in the direction of pelagial (6,7,16,19).

Pyrene has been identified in some samples and benz-a-pyrene has been not identified at all. Observed nature of the PAH distribution is very similar with that received by us ten years ago for sediments in this region. This fact allows to consider the given PAH distribution as background and the ecological condition is safe.

Conclusions:

1. The nature of the PAH distribution in the Western Arctic shelf sediments indicates a considerable variety of the geochemical background and a leading role of genetic and facial factors in its forming.
2. Majority of investigated sediments is characterized by the background distribution of PAH. Received information can serve as the basis for the ecological monitoring.
3. Estimation of the technogenic contamination level must be based on the local specificity of the background distribution of PAH.

Reference

1. Blumer M., Youngblood W. PAH in soils and recent sediments. (1985), *Science*, v.188, No.4, p.53-55.
2. Hites R., Laflamme R., Farrington J. Sedimentary PAH: The historical record. (1978), *Science*, v.198, No 25, p.829-831.
3. Laflamme R.E. and Hites R.A. The global distribution of PAH in recent sediments. (1978), *Geochim. Cosmochim. Acta*, v.42, p.289-303
4. Lipiatou E. and Saliot A. Fluxes and transport of anthropogenic and natural PAH in the western Mediterranean Sea. (1991), *Mar.Chem.* v.32, p.51-71
5. Rovinsky F.Ya., Teplitskaya T.A., Alexeeva T.A. Background monitoring of polycyclic aromatic hydrocarbons. (1988), *L.: Gidrometeoizdat*, 222 p., (in Russian).
6. Gearing J., Buckley D., Smith J. Hydrocarbon and metal contents in a sediment core from Halifax Harbour : a chronology of contamination. (1991), *Can.J.Fish.Aquat.Sci.* v.48, No 12, p.2344-2354.

7. Hites R., Laflamme R., Windsor J. et al., PAH in anoxic sediment core from the Pettaquamscutt River. (1980) , *Geochim.Cosmochim.Acta*, v.44, p.873-878.
8. Izrael Yu.A., Tsyban A.V.) Anthropogenic ecology of the Ocean, (1989, Leningrad, *Gidrometeoizdat*, 527p., (in Russian).
9. Wakeham S., Schaffner C., Giger W.) PAH in recent lake sediments. (1980),*Geohim.Cosmochim.Acta.*, v.44, p.403-429.
10. Brassell S., Eglinton G., Howell V. Paleoenvironment assessment of marine organic-rich sediments using molecular organic geochemistry . (1987) ,From : Brooks J., Fleet A., *Marine Petroleum Source Rocks*, Geological Society Special Publication No.26, p.79-98.
11. Killops S.D. and Massoud M.S. PAH of pirolytic origin in ancient sediments : evidence for Jurassic vegetation fires. (1992) , - *Org.Geochem.*, v.18, No.1, p.1-7.
12. Leith T., Weiss H., Mork A., e. a. Mesozoic hydrocarbon source-rocks of the Arctic Region.-in " *Proceeding of Arctic Geology and Petroleumm geology*".(1990) , Conference, Tromso.. p. 1-25.
13. Petrova V.I. Geochemistry of PAH of sediments for polar zones of the World Ocean. In: *Organic matter of bottom sediments of polar zones of the World ocean*. (1990), (A.Danyushevskaya ed), p.70-129, L., Nedra.(in Russian).
14. Smirnov B.A. A general scheme of hydrocarbons formation during organic matter sedimentation in the World Ocean. (1980) ,- *Oceanology*, v.20, No 5, p.856-865.(in Russian)
15. Tan Y. and Heit M. Biogenic and abiogenic PAH in sediments from two remote Adirondack lakes. (1981) , *Geochim. Cosmochim.Acta*, v.45, p.2267-2279.
16. Venkatesan M., Kaplan I. Distribution and transport of hydrocarbons in surface sediments of the Alaskan Outer Continental Shelf. (1982) , *Geochim.Cosmochim.Acta*, v.46, p.2135-2149.
17. Danyushevskaya A.I., Petrova V.I. Geochemical features of organic matter of black clays in the Eurasian continental margin. (1991) ,- *Geochemistry*, No.5, p.709-714,(in Russian).
18. Livshits Yu.Ya. Paleogenic deposits and platform structure of Spitsbergen. (1973) ,L., Nedra, 160 p., (in Russian).
19. Brawn G., Maher W. The occurrence, distribution and sources of PAH in the sediments of the Georges River estuary, Australia. (1992) , *Org.Geochem.*, v.18, No 5, p.657-668.

CURRENT ECOLOGICAL STATE OF BOTTOM COMMUNITIES IN THE BARENTS AND KARA SEAS: RESULTS OF STUDIES IN 1991-1994

V.B. Pogrebov, O.A. Kiyko, S.I. Fokin, V.V. Galtsova (RINCAN, ARROI, SPbSU, ZIRAS)

A review of literature and experience of our own studies shows that for monitoring purposes in the Arctic Seas, a special attention should be paid to ecological monitoring which corresponds to the population-species and biocenotic levels of organization. Among possible biological monitoring media, preference should be given to benthos. It is stable, characterizes the local situation and is capable to present changes in the ecosystem in retrospective. The "absolute" characteristics of biota which reflect the composition, abundance and structure of benthos are of priority for monitoring.

These considerations were taken into account during biological studies in the ecological cruises organized by the NPO Sevmorgeologiya in the western sector of the Russian Arctic. The main aim was to assess the ecological state of the studied regions at the transregional, regional and local levels. These regions included: the Barents and Kara Seas (with the adjacent territories of the White, Norwegian and Greenland Seas), the regions of Prirazlomnoye and Shtokman gas condensate fields, the St. Anna trough, nuclear testing grounds and dumping sites of radioactive wastes on the shelf of Novaya Zemlya (Fig. 1). At the present time the collected data and obtained statistical data are processed. The materials, ready for acquainting the scientific community, are presented below.

In total, during the field seasons 1994-1994 more than 1000 qualitative and quantitative samples of macro-, meio- and micro-benthos were collected. More than 3200 underwater photographs were analysed. To investigate the size-weight structure of zoobenthos populations, measurements and weighting of more than 2500 individuals representing 18 taxa, were performed. More than 200 samples for a chemical analysis of the content of persistent organochlorines (OCCs), heavy metals (HM) and radionuclides (RN) in benthos were collected.

For assessing long-term changes in bottom communities, a statistical comparison of our data with the results of studies in 1920-1930 and 1927-1945 was performed (Brotskaya, Zenkevich, 1939; Filatova, Zenkevich, 1957). Changes were estimated by abundance (in the course of a three-factor dispersion analysis) and benthic structure (based of the similarity coefficients of Soerensen and Brey-Curtis). Likewise, the role of the factors of the station location in the area and taxonomic belonging of hydrobionts in the bioaccumulation of pollutants was assessed.

In the course of systematic processing of materials, more than 500 species and groups of macrobenthos, 18 taxa of euand pseudomeiobenthos, 13 species of microbenthic infusoria and 23 species of flagellates were determined. The distribution of benthos on the shelf under study has its natural typical features. For the Kara Sea in all regions covered by data for a comparative analysis, the composition, abundance and structure of the bottom population are practically the same as described before. For the Barents Sea there are some differences between the results of our survey and previous studies. Statistically reliable local changes are observed in the biomass and a relative abundance of Sipunculoidea, Priapulioidea and Echinodermata, as well as in the fraction of the surface and subsurface deposit feeders. However, the difference in the total biomass of benthos is not statistically significant, as compared to the biomass recorded in the 1920s-1930s. There is a considerable coincidence not only in the trophical zones, but also in the biocenoses forming them. The structure of bottom communities described for the Pechora Sea in the 1920s-1920s and of biocenoses identified during these studies is 72-84% similar. For the most representative groups of invertebrates the difference in the biomass does not exceed 3%. The biocenoses are practically within the same boundaries. The size-weight structure of mass invertebrates reflects, as a rule, the ecological-physiological suitability of habitats for hydrobionts and does not indicate their stress state in

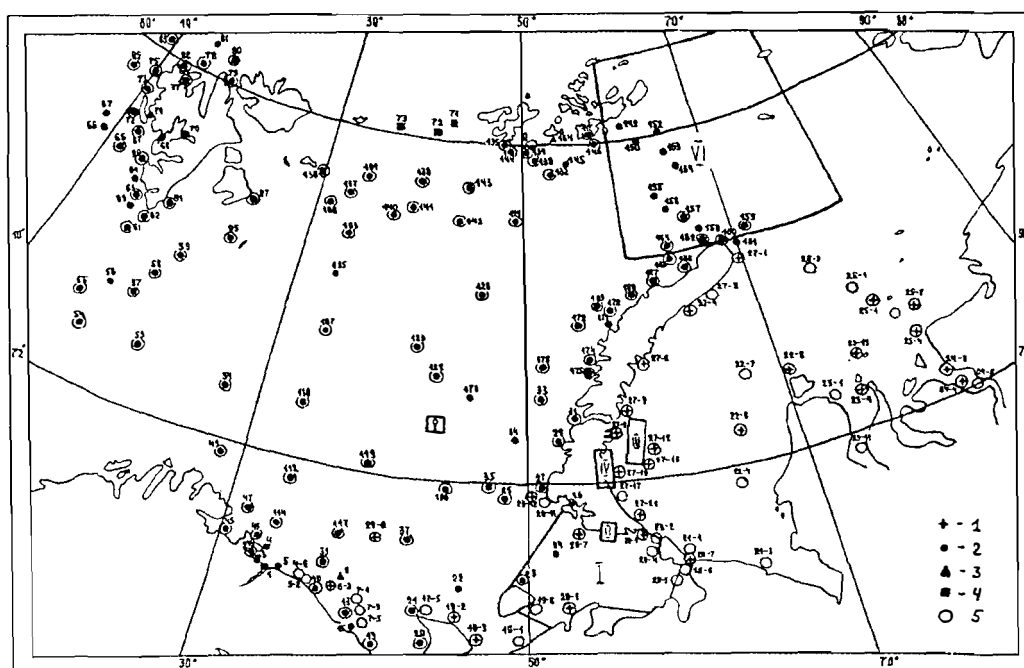


Fig. 1. Benthic stations examined on the west-arctic shelf of Russia at the transregional level in the course of geoecological expeditions 1991-1994, 1-4 stations of quantitative sampling, 1991-1994, respectively, 5 - stations of qualitative sampling. Roman figures designate the sites of regional and local studies discussed in the text.

any area. All this proves that most of the observed changes are governed by natural fluctuations and not by anthropogenic successions.

Single significant technogenic disturbances of bottom communities were observed near the Murman and Novaya Zemlya coasts. Thus near the Belushka settlement at a depth of 12 m which is favourable for habitation of algae and invertebrates, the species composition of benthos is limited to one species (polychaetae *Terebellides stroemi*) and the biomass does not exceed 0.1 g/sq.m. In the mouth of the Kolyma gulf the biomass of benthos is 2-10 times smaller than at the stations with similar environmental conditions; its structure is also disturbed.

Studies of meio- and microbenthos of the region under consideration were to a great extent descriptive. In this connection no assessment of the ecological state of the benthos by the indicated groups of hydrobionts was performed. These observations are suggested to consider preliminary and as a basis for forthcoming monitoring.

The content of OCCs and HM in the benthic groups indicates the absence of the spatial non-uniformity in their distribution and is similar to analogous indicators for the background regions. The presence of anomalous high concentrations of technogenic RN in biota was not recorded. An assessment of the RN concentration in the species collected in the coastal zone of Novaya Zemlya has shown the absence of their significant accumulation.

No changes in structure of bottom communities were found in the areas of radioactive waste dumping in the Novozemelsky trough and along the eastern coast of Novaya Zemlya from the Stepovoy Gulf to Abrosimov Gulf. In the Chernaya Bay where underwater nuclear explosions were made in 1955-1961, the disturbances in the group of microbenthic infusoria were recorded. They are manifested at the organism (Fig. 2), population-species and biocenotic levels of organization. Their probable cause is high concentration of plutonium in the bottom sediments of the bay (three orders of magnitude greater; Smith et al., 1993). It is interesting that the disturbances are not detected in the fauna of flagellates in the Chernaya Bay. This allows us

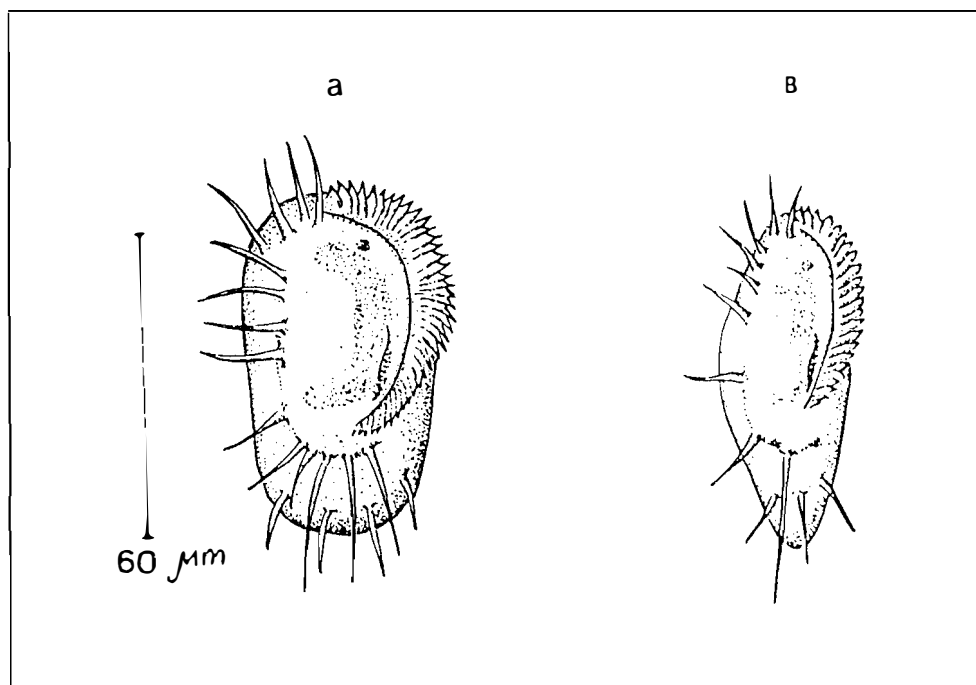


Fig. 2. Infusoria Euplotes sp. (Hypotrichida, Ciliopora) from the region at the entrance to the Chemaya Bay at Novaya Zemlya (a) and from its distant part (B).

to consider infusoria a "weak link" of marine bottom communities and hence a perspective object for ecological diagnostics of their state.

Generalizing the results of the studies performed, the current ecological state of the benthic in the Barents and Kara Seas can be considered close to a mean multiyear norm. The benthic indicators used for the assessment, indicate the presence of the anthropogenic press only at a local scale, predominantly in the narrow coastal zone at pollution or in the regions subjected in the past to a strong specific impact (Chernaya Bay).

References

1. Brotskaya V.A., Zenkevich L.A. A quantitative count of bottom fauna of the Barents Sea. - Proc./VNIRO, 1939, Vol. 4, pp.5-126.
2. Filatova Z.A., Zenkevich L.A. A quantitative distribution of bottom fauna of the Kara Sea. - Proc. Of the All-Union Hydrobiological Society. 1957, Vol. 8, pp.3-67.
3. Smith J.N., Ellis K.M., Matishov D. et al. Levels of radioactivity in Barents Sea sediments off Novaya Zemlya. Int. Conf. on Radioactivity in the Arct. and Antarc.: Abstr.Kirkenes, 1993 (No pages).

PERSPECTIVES OF STUDIES OF ECOLOGICAL TESTING GROUNDS IN THE ARCTIC

M.A. Sadikov (ARROI)

Works at the testing grounds aim to show the global and regional impact from the disturbance sources, both within and beyond them and are a composite part of the comprehensive regional study of the shelf. This should also be the goal of the ecological landing team "Arktika" (Dodin, Sadikov, Bordukov, 1994). Thus joint studies of the water areas and the coasts should allow us to investigate the tendencies for changes in the ecosystems, organize their tracing and determine a complex of nature protection measures.

The activities of the ecological team "Arktika" differ in principal from other activities here in additional studies of shallow and land zones, including pollution sources and medical-biological studies.

Knowledge of the regions of the most intensive anthropogenic impact is necessary and hence studies of the Yenisey, White Sea and Pechora testing grounds are of first priority.

The Yenisey testing grounds (the interfluvium of Yenisey-Pyasina) are considered from two viewpoints: as a source of discharge of technogenic products from a vast watershed area, where the nuclear complex facilities, pulp and paper, aluminum and chemical industries are present, and as a result of aerosol transport of the products of the Norilsk mining-metallurgic complex, as well as its discharges to the Pyasino lake and further to the Pyasina river. It is planned to find out the intensity of this discharge and the gradient of its fall for assessment of the global and regional anthropogenic impact on the Arctic shelf.

The NPA "Sevmorgeologiya" in 1973 carried out geoecological studies onboard the R/V "Geolog Fersman" in the south-eastern Barents Sea (Pechora Sea) with sampling of bottom sediments, suspended matter, water, bottom biota for oil organic matter, pesticides, radionuclides, heavy metals both in the entire substance and in its separate components characterized by increased accumulating properties.

For investigating the regional effect of the Usinsk pipeline accident (Komi Republic, autumn 1994) on the ecosystems of the Pechora coastal-marine zone (CMZ) including the shelf, shallow zone and the coast, it is advisable using the available materials as a reference, to supplement the complex of studies by mapping the tundra ecosystems, coastal swamps and peat-bogs, Iceland moss and mushroom layers. Also, impact sources (aerosol survey of the snow cover and sampling along the contours of the Usinsk accident area) and pathways of pollution transfer (lake-river systems and shallow zones) should be investigated.

The problem of studies of the Pechora CMZ is not of a regional character since coastal marine zones are global accumulators of pollution, including oil pollution which due to permanent currents and temporal shifts in the hydrosphere participates in the oceanic substance turnover falling out in the same CMZs or other. Hence information on the Pechora CMZ is not only a problem of Russia. The Pechora CMZ can serve as testing grounds for predicting the results of similar accidents in the other Earth's regions. Models based on the results of the Usinsk accident can be used as prototypes for exploration of mineral resources on the shelf of the North and Norwegian Seas. The oil impact on the spawning grounds of salmon and other migrating fishes within the Pechora CMZ can result in reduction of international fish resources. Available comparative data of the studies of the Pechora CMZ before the accident allow modelling of the situation at obtaining new data. For example, this was not possible during the Alaskan oil pipeline accident. The absence of modeling often results in inconsistent estimates of the impact of Novaya Zemlya nuclear testing grounds. Modeling will help mankind to be ready for possible environmental disturbances. At present a complex of problems can be resolved at the Pechora testing grounds on an operational basis which are impossible to simulate experimentally. Same applies to the White Sea testing grounds, which are a composite part of the White Sea-Baltic Sea system, where additional testing is also required.

The surveys of the NPO "Sevmorgeologiya" in the White Sea were conducted in 1991 onboard the R/V "Akademik Karpinsky". At the chart of the ecogeochemical regioning (see Fig.

in...) the region of the White Sea is in the south-western corner. Hence it is possible that there are marginal effects for charts with mono indications and differences of the statistical characteristics and relation systems from general class characteristics for the charts of integral indicators. Both of these shortcomings can be modelled, if necessary, by constructing similar charts only for the White Sea based on the same materials. But in view of their insufficient character for more detailed works, additional testing is necessary. If the White Sea and Severnaya Dvina are considered an integral component of the White Sea-Baltic Sea system, then the available data should be supplemented by data on the Ladoga and Onega lakes and the waterways connecting them, not mentioning the Neva river, the Gulf of Finland and directly the Baltic Sea so that the ecological problems of the north-western region of Russia and the adjacent states could be uniformly covered. This is a time-consuming work for a multiyear period which requires financing, although its importance is obvious. The need for such a work becomes clear from the overview of the available results for the White Sea where the situation is quite diverse and where of the eight landscapes identified at the western-arctic shelf of landscapes, the fragments of three landscapes are present. It should be mentioned that the landscape occupying the largest area in the Barents Sea, is absent in the White Sea.

The landscape of the western White Sea is characterized by enrichment of bottom sediments by nitrites, lead and manganese, to the lesser extent by organochlorines and phenols. It is also characterized by enhanced alpha- and beta-activities which are reflected to some extent by small increases in K-40.

In the middle part of the White Sea the bottom sediments also contain increased amounts of lead and phenols and for the near-bottom waters phenol pollution is replaced by oil hydrocarbon pollution (cold extraction by carbon tetrachloride). At the exit to the Barents Sea the bottom sediments are characterized by the minimum amounts of pollutants whereas in water the amount of oil hydrocarbons although decreasing still remains sufficiently large. It should be noted that zoobenthos is sharply enriched by lead, to a smaller extent by copper and cadmium, although in the bottom sediments the content of lead toward the Barents Sea decreases. It can also be mentioned that whereas in the first two landscapes mollusks prevailed, in the last one - echinoderms. It can also be indicated that the general characteristics of landscapes are given, rather than their parts located in the White Sea whose characteristics can be slightly different, although hardly different from the given one. This is also indicated by the classes of the geochemical fields. There are two such classes in the White Sea. The first one (western), beside the White Sea, is observed only in the Kara Sea going eastward from the northern island of Novaya Zemlya and it is enriched by all already enumerated components of bottom sediments (nitrites, lead, manganese, pesticides, phenols), water (phenols and oil hydrocarbons, zoobenthos (lead and cadmium)). The increased alpha- and beta-activities of bottom sediments associated with the maximum amount of K-40 in zoobenthos and its enhanced beta-activity are even more evident.

The class observed at the exit to the Barents Sea is typical only of this sea and is not observed at all in the Kara Sea. It is also characterized, like the landscapes, by the reduced differences of all the components described. At the charts of the White Sea with mono indications the White Sea is reflected by the same components with some additional detailing.

It should be mentioned that the largest variety of the geochemical and landscape fields is observed in the coastal zones and the central parts of the Barents and Kara Seas are occupied by the fields which are more common for them, but different for each of the seas. From these positions the fields of the White Sea are governed by a strong coastal influence, primarily from the side of the Kola peninsula, as well as by the outflow of the Onega and Severnaya Dvina rivers. Also, there were dumpings of non-identified chemical pollutants which resulted in a mass death of starfishes, i.e. even in the regional plan the situation in the White Sea is not the most safe on the western arctic shelf. The priority action could be a costwise closing of the White Sea by a perimeter with studies of the coastal land and the mouth parts of rivers. And although we speak all the time about the relative amounts, whose absolute values are sufficiently low, it is required to investigate their joint effect on biota with transfer to trophic food chains.

As mentioned, to clear up the ecological situation and to arrange nature protection actions at all polygons it is necessary to conduct a comprehensive ecological study with successive implementation of its integral parts. To fulfill this, financial support is required.

References

1. Dodin D.A., Sadikov M.A., Bordukov Yu.K. Some aspects of the radiation situation in the Arctic and directions of the ecological studies. 1994, St.-Petersburg, 138 p.

A CHART OF ECOGEOCHEMICAL REGIONING OF THE WESTERN ARCTIC SHELF OF RUSSIA

M.A. Sadikov (ARROI)

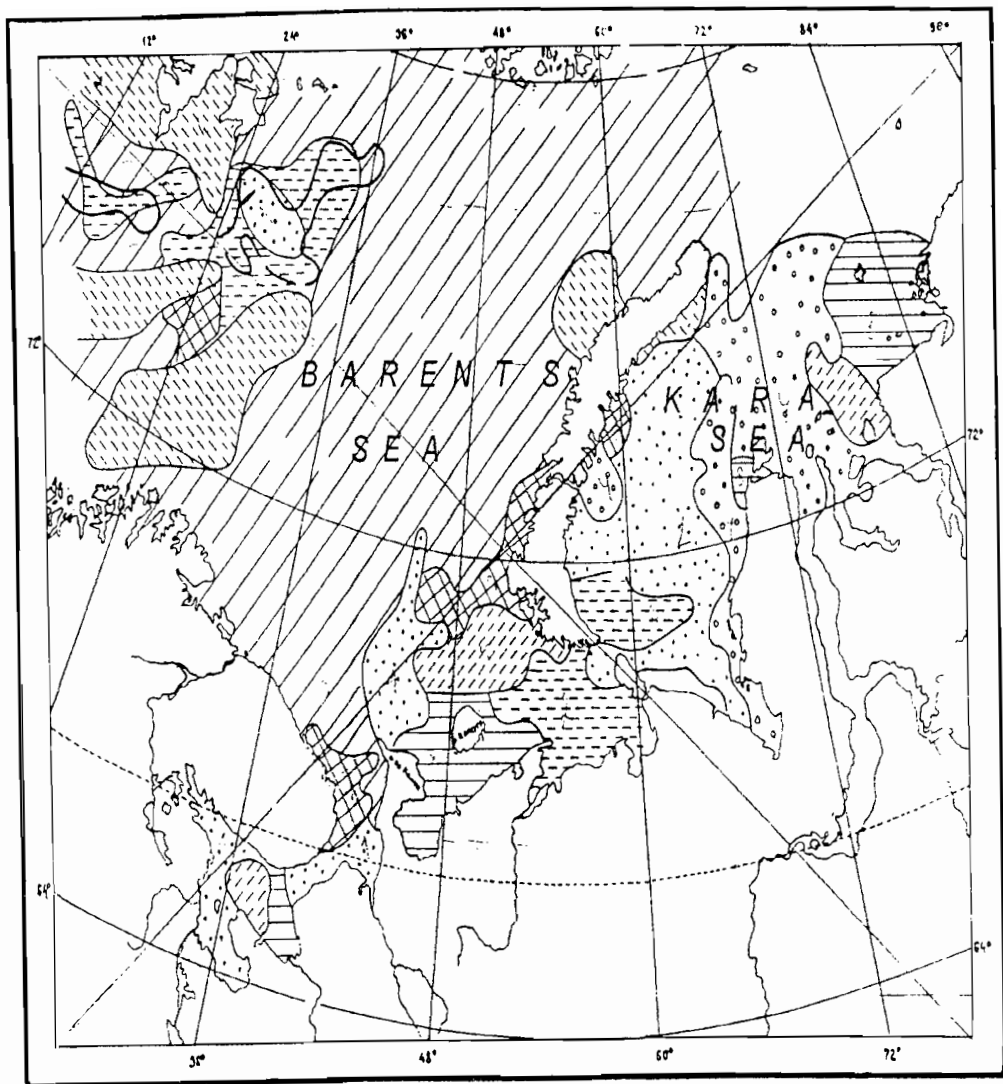
Classification of the territories is based on the technology created for information processing (Sadikov, 1988) which is being improved. It consists of multiple smoothing of local fluctuations which results in revealing the regional typical features. This is achieved by applying the systems approach (Sadikov, 1989) with regularization of space, use of integral indicators from the most informative indications of the studied media and their components, classification by potential functions taking into account the geographical coordinates and subsequent characteristics of the identified fields by the entire set of properties in the form of quantity formulas and structures of relations.

This processing can be applied, both to the ecological studies already performed and those under way, thus significantly increasing their effectiveness due to attaining a new property - revealing of the regional component. The following basic notions were used: of three ideologies of applied geochemistry, synergetic effects and new properties, matrix and raster methods of presenting the initial data, of one common (independent), intersecting and overlapping) space and their regularization, method of identifying extreme situations (exclusivity, charism) (Sadikov, 1972; Dodin, Sadikov, Shatkov, 1982).

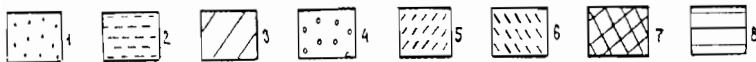
As a result of the proposed processing, the mono-indication and integral charts of regional changes are constructed. They differ in principle, from the charts of anomalies where the local fluctuations are assigned the status of general typical features (Sadikov, 1991; Dodin, Sadikov, Bordukov, 1994). At present such charts are constructed by geochemical indications which are characterised by the morphometric properties of media (bottom sediments, water, biota) for the Ladoga lake and the western shelf of Russia. The delineated landscapes are based on the indications which are usually used by investigators (Fig. 1, Table 1,2): three-dimensional space coordinates, granulometric composition and thickness of the surface sediment layer, physical-chemical properties of near-bottom water, the number of zoobenthos species and the ratio of their biomass, except for the coordinates subjected to a factor analysis. The number of the lanscapes and classes of geochemical fields delineated (usually five-eight) can be described in more detail by subclasses.

The proposed scheme of ecogeochemical regioning of the Arctic shelf (Fig. 2) reflects the results of studies in 1991-1992 by NPA "Sevmorgeologiya" onboard the R/V "Akademik Karpinsky" and "Geolog Fersman". Due to technical difficulties the chart presented in this publication is rather simplified, as compared to the constructed chart of the scale 1:5 000 000 which is much more diverse. The original chart is coloured and contains a large amount of information, including the concentrers of minimum and maximum values of indications for all media, granulometric composition, etc. The legend to the chart along with formulas of the classes (Table 3) which present contrasts (excess of the signal over the noise level) of indications from 1.5 up and from 1 down, shows their structure. Part of graphical annexes accompanying the chart as an album, is given in this publication (Dodin, Sadikov, Bordukov, 1994). It is seen (Fig. 2) that the third class which is absent in the Kara Sea, occupies much of the Barents Sea shelf (Table 2,3). In the Kara Sea where the fifth class is widespread the second to fourth classes are absent. The eighth class occupying the coastal shelf and the mouth river zones. is only observed in the Kara Sea. The greatest diversity of the fields is observed in the coastal zone and the central Barents and Kara Seas are occupied by the classes most widesperead over their areas. More detailed characteristics of the obtained results are beyond the scope of this article.

It is proposed to create an updated version of the chart using improved methods and new data in the near future.



km 0 100 200 300 400



Positive extreme fields 3-order

Fig. 1 Landscapes of the Arctic shelf

Table 1.

Characteristic landshafths of arctic shelf

N land	n object	%	deep m	bottom sediments					bottom waters			suspension
				gr	ps	al	pl	contrast	pH	O ₂	contrast	
1	152	8.3	124	7	25	25	42	NO ₂ 9.7 Pb 8.3 Mn 7.1 dde 2.2 fen 2.1 ddd 1.8 pcb 1.7 ddt 1.5	7.5	64	fen 6.4 SiO ₃ ,Cu 1.7	Cu 4.2 Zn 2.5 Cr 1.5
2	106	5.8	113	5	23	29	43	Pb 4.3 NO ₂ 3.9 Mn 2.2	7.8	62	fen 7.1 Zn 2.7 ohc,Cu 2 Ni 1.5	Pb 3.6 Fe,MnZ n 1.7 Cu 1.6
3	587	32.1	240	4	14	27	54	ohc,Mn 2.2 NO ₂ .pcb 2 Pb 1.8 ddd 1.6 fen 1.5	8.3	14	fen 9.3 Zn 3.2 Cu 3.1 NO ₂ 1.9 ohc 0.5	Pb 2.8
4	291	16	39	1	30	39	30	Pb 3.1 fen 2.3 Mn 2 Si 1.9 ddd 1.8 NO ₂ 1.7 ohc 0.4	7.7	91	SiO ₃ 8.7 Fe 5.6 ohc 4.4 Mn 2.9 Cu,Ni 2 Co,Sn, Zn,ssas 1.6	Fe 1.7 Cu,Mn 1.6
5	150	8.2	44	5	28	34	31	Pb 2.9 fen 2.8 ddd 2.7 ddt 2.5 dde 2.3 NO ₂ 2.2 Mn 1.9 Si 1.8 P 1.6	6.8	90	ohc 4.1 SiO ₃ 3.8 ssas 2.3 ddt 1.8 NO ₂ 1.6 Fe,ggcc 1.5	Zn 3 Cu 2.7 Cr 2
6	70	5.9	186	33	26	11	30	NO ₂ 3.7 pcb 1.9 ohc,Mn 1.7 ddt 1.5 fen 0.3	8.4	11	fen 15 Zn 5.8 Cu 3.9 ggcc 2.5 Ni 2.3 ddd 2 ddt 1.6 ohc 0.2 Sn 0.3	Pb,Cd 1.9 Zn 1.8 Ti 1.6
7	309	3.8	76	32	34	13	19	NO ₂ 4.3 pcb 3.5 ddd 2.2 dde 2 Pb,ohc 1.9	8	37	fen 15 ddt 2.3 Zn 1.9 ggcc 1.7 Pb,Cd 1.6	Cu 4.2 Zn 2.8 Cr 1.7 Cd 1.5
8	124	16.9	25	4	63	22	9	ddd 1.8 Pb 1.5 ohc 0.3 Zn,Ni 0.4	7	95	SiO ₃ 3.1 ohc 2.4 Fe,ssas 2.2 Mn 1.6	Fe 2 Cu 1.8 Zn 1.6

Foot-note: Gr - gravel, Ps- psammit (sand), Al- alevrit, Pl- pelite fractions. Tipe zoobentos: An - Annelidae, mol- Mollusca, ech -Echinodemata, ssas - synthetic surface-active substances, cyclic chlorinated hydrocarbons: agcc - alpha gexachlorcyclogexan, ggcc - gamma gexachlorcyclogexan; aromatic chlorinated hydrocarbons: DDT - dichlordifenilthreochloretan, dde, ddd - its derivatives, pcb - polychlorbifenils, gcb - gexachlorbenzol; pah - polycyclic aromatic glydrocarbons, ohc - oil carbon-hydrogens, fen - phenol , mas - biomassa, contrast - medians contrast.

Table 1.

(Continuation)

N lan d	zoobentos							formula
	%							
	A n	M o l	E c h	M a s	A n	M o l	Ech	
1	6	5 3	2 2	4. 5	1	9.1	0.7	Cu 5.9 Pb 3.3 pcb 1.9
2	7	6 ●	8	11	1. 4	21	0.3	Cu 16 Pb 6.8 pcb 1.9
3	2 2	1 7	3 3	1. 2	1. 6	1. 4	1.1	pcb 2.2 ddt 1.7 Pb,ddd 1.5
4	6	2 2	6 1	0. 9	1. 2	1. 6	1.7	Pb 5.9 Cu 4.2 Cd 3 pcb 1.7 gccc 0.2 ddd,dde ddt 0.3 agcc ●.4
5	3	5 3	2 6	2. 5	● 7	9. 2	1.6	Cu,Zn 1.6
6	1 6	1 4	4 ●	2. 2	2	2. 8	3.5	agcc,Fe 1.6
7	9	4 4	2 2	3. 4	1. 5	10	1.4	pcb 2
8	8	2 3	5 1	1. 9	1. 2	6. 6	1.6	Pb 7 Cu 2.5 Cd 2.4 ddd 0.4

Table 2

Extreme fields positive (exclusive) species
of the 2d and 3d orders
A. Landshafts

N order	n object	%	deep m	bottom sediments				bottom waters		suspension		
				gr	ps	al	pl	contrast	pH		O ₂ contrast	
3	30	1.6	172	7	9	23	61	ohc 2.8 NO ₂ 2.5 pcb 2 Mn 2.3 P 0.3 fen 0.4	8.4	9	fen 18 Zn 5.4 Cu 3.8 ddd 1.9 dde 1.7 Sn 0.1 ohc 0.3	Pb 9.4 Zn 3 Cu 2.1 Ti 1.8 Mn 1.7
2	129	6.9	197	30	21	14	36	NO ₂ 3.7 pcb, ohc 2 fen 0.4	8.4	9	fen 16 Zn 5.4 Cu 3.2 ggcc 2.3 Ni 1.9 ddd 1.6 ddt 1.5 Sn, ohc 0.3	Pb 2.0 Zn 1.8 Cd 1.7

B. Geochemistry fields

3	20	1.1	247	21	16	21	43	pcb 7.9 NO ₂ 3.9 Mn 2.1 ohc 1.8 ddt, ddd 1.6 Cs 1.5	9.3	17	fen 19 Zn 4.7 ggcc 3 Cu, Ni 2.7 Cd 1.9 ddt 1.8 ohc 0.2	Zn 1.8 Pb 1.6 Cd 1.5
2	58	3.2	260	2	8	21	69	ohc 2.9 ddd 2.2 Cs 2 Mn 3.8 Pb 2 ddt 1.8 pcb 1.6	8.3	11	fen 9.8 Cu 4.5 Zn 3 Pb 2.1 NO ₂ 2 ddt 1.6 ohc 0.1 Sn 0.3	Pb 4.9

Table 2

(Continuation)

A. Landshafts

N order	zoobentos							formula
	%							
	An	Mol	Ech	Mas	An	Mol	Ech	
3	7	61	6	4	1.2	.5	0.4	ddt 1.8 ddd 1.7 fen 1.6 dde 1.5
2	15	20	26	2.5	1.7	3.2	1.5	pcb 1.7 agcc 1.6 Fe 1.5

B. Geochemistry fields

3	8	20	28	3.9	1.7	2.7	1.3	pcb 1.7 agcc 1.5
2	26	18	32	0.5	1.4	0.5	0.5	Pb 1.8 ddd, ddt 1.6 Cu 1.5

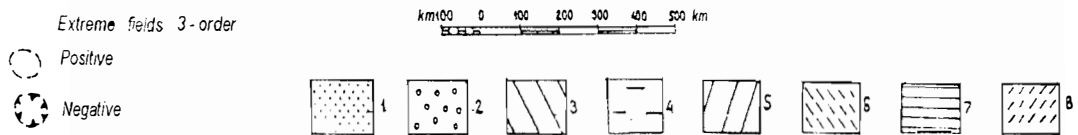
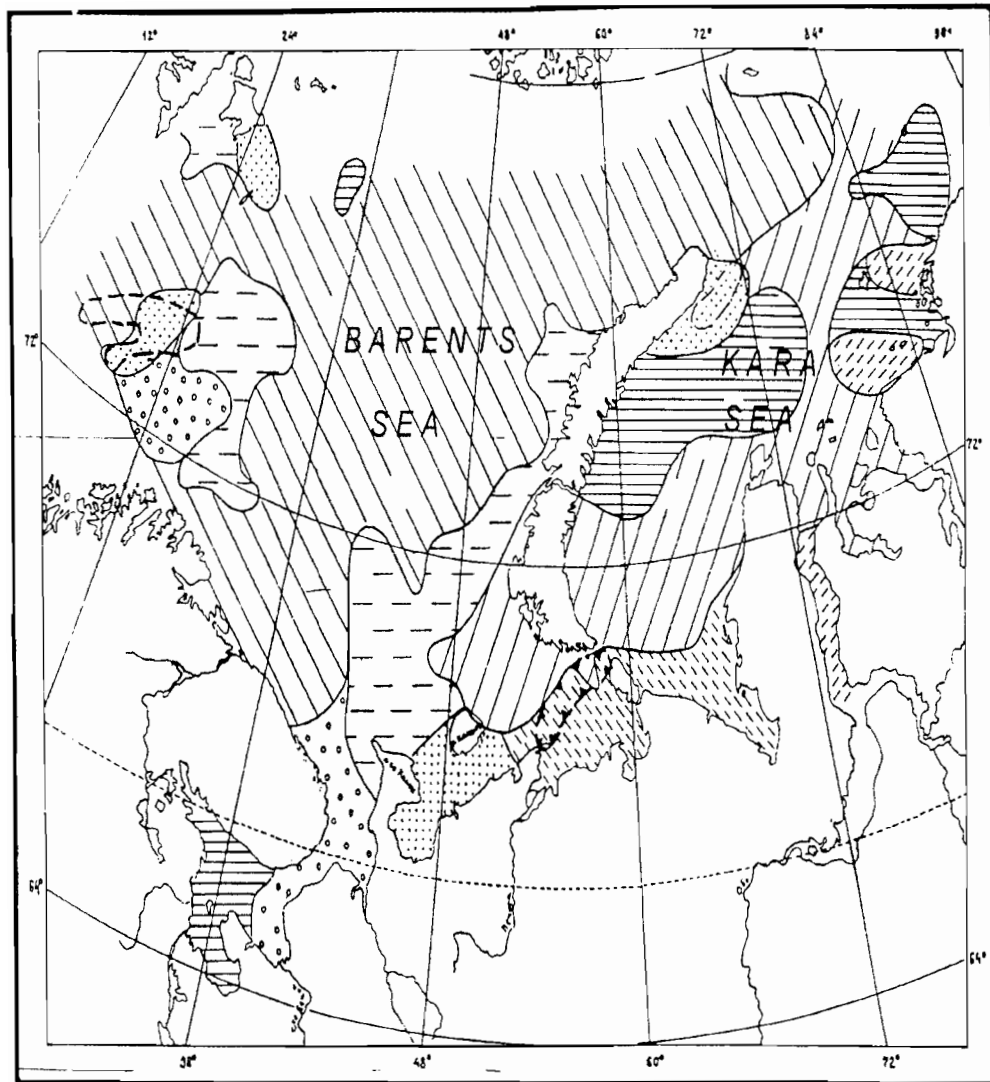


Fig. 2 Ecogeochemical regioning of the Arctic shelf

Table 3.

Characteristic classes geochemistry fields of arctic shelf

N classe	N object	%	deep	bottom sediments					bottom waters			suspension
				%					contrast			
			m	gr	ps	al	pl	formula	pH	O ₂	formula	formula
1	122	6.7	82	13	39	21	21	NO ₂ 2.4 pcb 2.2	7.4	71	ssas 2.1	Zn 2.4 Fe 1.6
2	208	11.4	51	15	34	24	25	NO ₂ 2.9 Pb, fen 2.7 pcb, ddd, ddt 2.4 dde 2.3 Mn 1.8	7.2	75	fen 4.5 ohc 3.3 SiO ₃ 3 ddt 2.1 ssas 1.9 ggcc 1.7 Pb 1.6	Zn 3.4 Cu 3.3 Cr 2.1 Mn, Pb 0.4
3	529	28.9	244	6	13	26	55	ohc 2.3 NO ₂ Mn 2.1 pcb 1.8 Pb 1.6 ddd 1.5	8.4	9	fen 1.1 Zn 3.8 Cu 3.5 pcb 2 ddt 1.8 NO ₂ , ggcc 1.7 ddd, Ni 1.6 Sn 0.2 ohc 0.3	Pb 3.4
4	176	9.6	170	16	30	22	33	NO ₂ 3.4 ohc 1.9 Pb 1.8 Mn 1.6 ddd 1.5	8.1	25	fen 1.3 Zn 3.5 Cu 2.4 ggcc 1.8 ddd 1.7 Cd 1.6 ohc 0.5	Cu 2 Zn 1.7 Cd 1.6
5	215	11.8	87	2	35	27	35	Pb 6.6 Mn 4.8 NO ₂ 4.4 ddd 1.9 fen 1.5	7.5	75	SiO ₃ 4.6 Fe 2.5 ohc, fen 2.7 Mn 1.7 ssas 1.6	Cu 1.8 Pb 1.7
6	239	13.1	21	2	50	37	12	NO ₂ 1.8 ohc, dde 0.1 ddt 0.3 Zn 0.4 Co 0.5	7.3	97	ohc 4.8 ssas 2.2 Fe 1.6 Cd 0.4 fen 0.5	Fe 2.4 Mn, Cu 1.9
7	116	6.4	119	4	25	24	45	NO ₂ 7.2 Pb 7 Mn 5.1 dde 3.1 fen 2.9 Si 2.4 ddd 1.9	7.2	74	SiO ₃ 4.6 Fe, fen 2.4 Cu 1.8 ohc 1.5	Cu 5.9 Zn 2.6 Pb 2.2
8	124	6.8	21		26	38	35	ddd 4.4 fen 3.6 Mn 2.5 Pb 2.8 Si 2.4 dde 1.8	7.9	98	SiO ₃ 17 Fe 10 Mn 4.4 Cu 3.1 P 2.4 Ni 2.3 ohc 2.1 Sn 2 Co 1.9 Zn 1.8 NO ₂ 1.6 ssas 1.5 fen 0.4 ggcc 0.5	Fe, Mn 1.6

Table 3

(Continuation)

N classe	zoobentos							formula
	%				Contrast			
	An	Mol	Ech	Mas	An	Mol	Ech	
1	6	23	29	1.6	1.1	3	1.4	pcb 1.6
2	4	42	33	3	0.7	10	2.8	pcb 2.1 Zn,dde 1.6 ggcc 1.5
3	20	20	32	1.4	1.5	1.4	1.1	pcb 2 ddt 1.8 ddd 1.6
4	20	29	27	1.7	1.9	5.4	1.3	ddt 1.7
5	9	39	32	3	1.2	2.5	0.6	Cu 10 Pb 6.8 pcb 1.8 dde 0.2 ggcc,ddd, agcc 0.3 ddt 0.5
6	5	28	55	6.2	1.4	17	1.7	Pb 9.8 Cu 7.7 Cd 1.9 pcb 1.6 ggcc 0.1 dde,ddd 0.2 ddt,agcc 0.3 Zn 0.4
7	8	35	42	1.1	1	3	1	Pb 3.1 Cd 2.2 pcb 1.8
8	6	27	57	1	1.3	1.7	1.5	Pb 6.5 Cd 4.5 Cu 4 ggcc,ddd dde,agcc ddt 0.1 Fe 0.5

The main aim of creating such sets of charts is to have a basis for delineating the testing grounds for more large-scale studies and predicting the ecological situation within the regions already identified, both on the whole and by subregions using separate indications and media. Obviously, all this cartographic material requires publication on an operational basis.

References

1. Dodin D.A., Sadikov M.A., Shatkov V.A. - L., Nedra, 1982. - 168 p.
2. Dodin D.A., Sadikov M.A., Bordukov Yu.K. Some aspects of the radiation situation in the Arctic and directions of ecological studies. - St. Petersburg. 1994, 138 p.
3. Sadikov M.A. Application of the factor analysis for assessing the "exclusivity"/ athemtical methods in geology. - L., 1972, pp. 22-23.

4. Sadikov M.A. Technology for geochemical predicting of copper-nickel fields/ Nickel bearing of basite-hyperbasite complexes of the Norilsk region. Apatity, 1988, pp.87-92.
5. Sadikov M.A. A systems approach in the methodology of predicting the deposits/ A Systems approach in geology. - M., 1989.
6. Sadikov M.A., Makedon I.D. Metrological provision of geochemical studies (methodological recommendations). - L., VNIIOkeangeologiya, 1990, 34 p.
7. Sadikov M.A. Multipurpose geoecological mapping/ Problems of geoecology of the water areas and the coasts. - St. Petersburg, 1991, pp.38-49.

STATE OF KNOWLEDGE OF ICHTHYOFAUNA OF THE BARENTS SEA

N.V. Chernova (ZIRAS)

State of knowledge of ichthyofauna of the Barents Sea is performed on base of analysis of the bibliography on biology and in less extent on fishery of marine fishes. Overwhelming majority of publications are devoted to commercial fish species, cod, haddock, polar cod, capelin, black halibut, plaice. Articles about noncommercial fishes, such as species of families Zoarcidae, Cottidae, represented rich here, are a few.

Number of publications in Russian on mentioned above commercial fishes are comparable with a number of articles in English which has been registrated. The second is concerned not only for the Barents Sea, but for the whole North Atlantic area (excluding the Baltic). Number of titles are: capelin 95 and 75, haddock 70 and 80, cod 181 and 170, polar cod 75 and 45, black halibut 30 and 45, plaice 23 and 70 accordingly. Number of English publications should be some less than existed as they are available for the author in less extent than Russian publications.

Materials on ecology of marine fishes of the Barents Sea published in Russian are poorly available for English-readers as a number of translated publications comprise from 0 to 35 % from a number of English titles on different species.

It is concerned equally with other commercial fishes, such as rockfishes, wolffishes, salmon.

QUANTITATIVE DISTRIBUTION OF SUSPENSION AND SUSPENDED ORGANIC CARBON IN THE KARA AND BARENTS SEAS

*V.P.Shevchenko, A.P.Lisitsin (IORAS), G.I.Ivanov (ARROI), O.V.Severina,
A.A.Burovkin, N.G.Maiorova, S.S.Shanin, Ye.A.Romankevich (IORAS),
L. Ya. Grudinova (MEP)*

The study of water suspension is necessary for an understanding of modern sediment accumulation processes and for an ecological assessment of the condition of the water area. In this regard the Arctic seas are scantily known. In the Kara and Barents Seas suspension was investigated by V.S.Medvedev and Ye.M.Potekhina /1986, 1990/, and suspended organic carbon - by A.N.Beliaeva and Ye.A.Pomankevich /Biogeochemistry..., 1982/. In addition to this research, some works on studying suspension concentrations in the lower reaches of the Ob and Yenisey rivers were also done /Telang et al., 1991/.

Initial information and methods

The studies of suspension in the estuaries of the Ob and Yenisey, the greatest Siberian rivers, were conducted during the 49th cruise onboard the R/V "Dmitry Mendeleev", September 1993. In the estuaries and the Kara Sea 343 samples of suspension and 171 samples of suspended organic carbon were taken. Besides, we also analyzed 210 samples of suspension and 85 samples of suspended organic carbon withdrawn in the Barents Sea and St. Anna Trough during the 9th cruise onboard the R/V "Professor Logachev", August-September 1994. The filtration of the water sampled with barometers was carried out through nuclear filters 47 mm in diameter (the pore diameter is 0.45 mkm) and light-fibrous filters GF/F, Whatman firm. More detailed working procedure is given in the paper by V.P.Shevchenko and co-authors /1995, in the press/.

Results and discussions

In September 1993 the highest suspension concentrations varying from 11.7 to 115.3 mg/l were observed in the upper Ob estuary at the stations 4417-4419 (Fig.1,2a), where a salinity was less than 1‰ /V.I.Burenkov, A.P.Vasilkov, 1994/. Notice that at the station 4418, the farthest one from the sea, the concentrations of suspension were in the range between 69.3 and 115.3 mg/l. At the salinity barrier (S=5-10 ‰) as a salinity increases, the suspension concentration reduces from 11.85 mg/l at the station 4420 (S=4.86 ‰) to 4.83 mg/l at the 4421 (S=16.88 ‰) at the expense of its coagulation and sedimentation /A.P. Lisitsin, 1982/. In the open sea on the Ob section (Fig.1, 2a) at the stations 4395-4397 the suspension concentrations in the surface layer were 0.31-0.84 mg/l. Deeper than 10-15m, under the pycnocline /V.I.Burenkov, A.P.Vasilkov, 1994/ the concentrations went to 0.10-0.24 mg/l, and then at a level of 10m above the bottom these was a rise to 1.03-9.71 mg/l. The content of suspended organic carbon (C_{org}) in the upper Ob estuary equaled 900-4100 mkg/l. As this takes place, the C_{org} concentration in the dry suspension was 3.05-4.18 percent, suggesting that the terrigenous particles were dominant. We registered a sharp decrease in the C_{org} concentrations which took place in the firth. For instance, at the station 4420 the concentration equaled 490 mkg/l, at the 4415 it was not higher than 330 mkg/l, and it was as low as 100-160 mkg/l in the open sea.

The suspension concentration in the upper Yenisey estuary (stations 4405-4413) was within 1.68-29.1 mg/l. At the River-Sea barrier the surface layer has a reduce in suspension concentrations from 8.8 mg/l at the station 4413 (S=6.82‰) to 1.79 mg/l at the 4404 (S=10.1‰). Moving offshore along the Yenisey section (Fig.1, 2b), from the station 4404 to the 4401, the

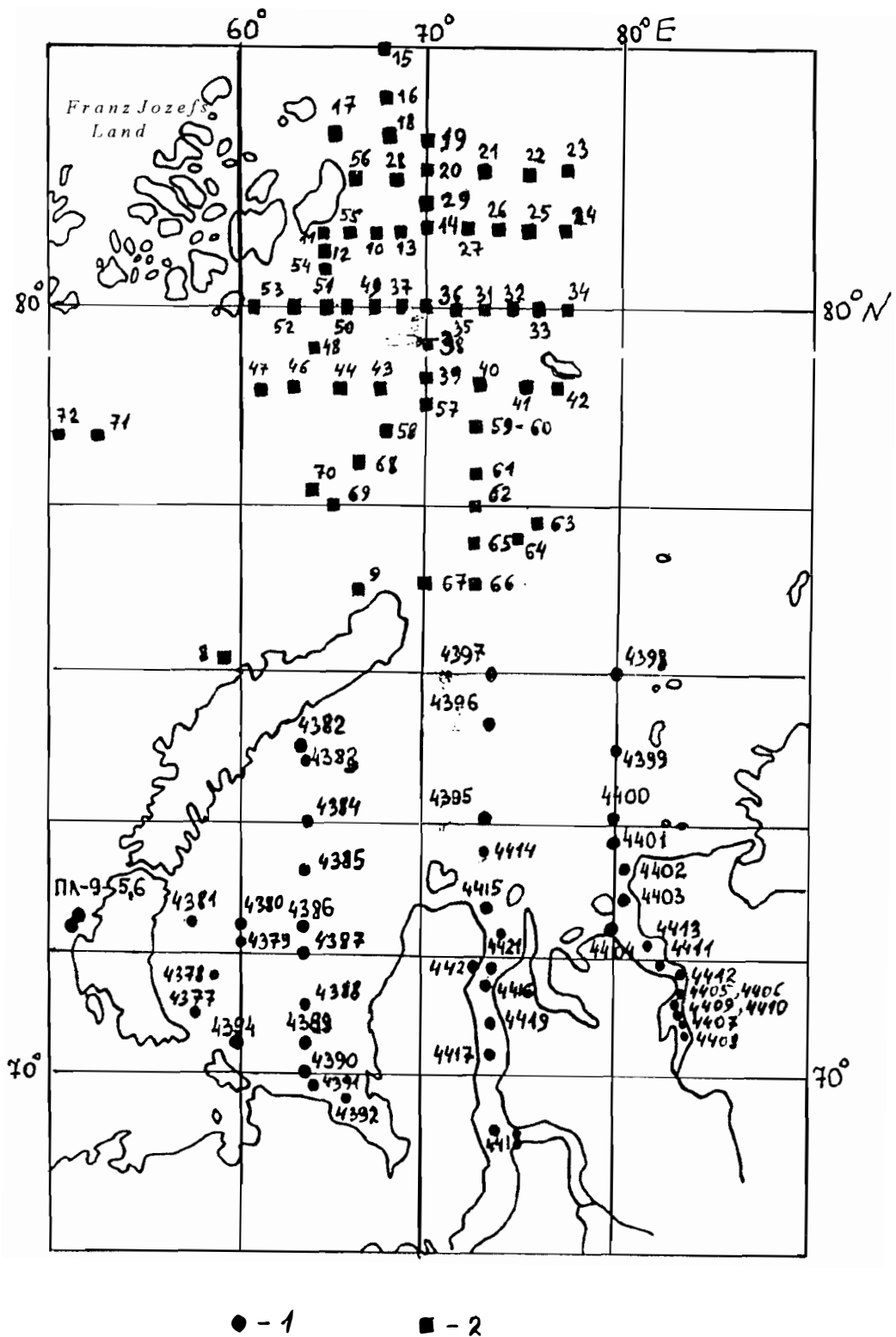


Fig.1 Stations for suspension sampling :
 1- 49th cruise onboard the R/V "Dmitry Mendeleev";
 2- 9th cruise onboard the R/V " Professor Logachev"

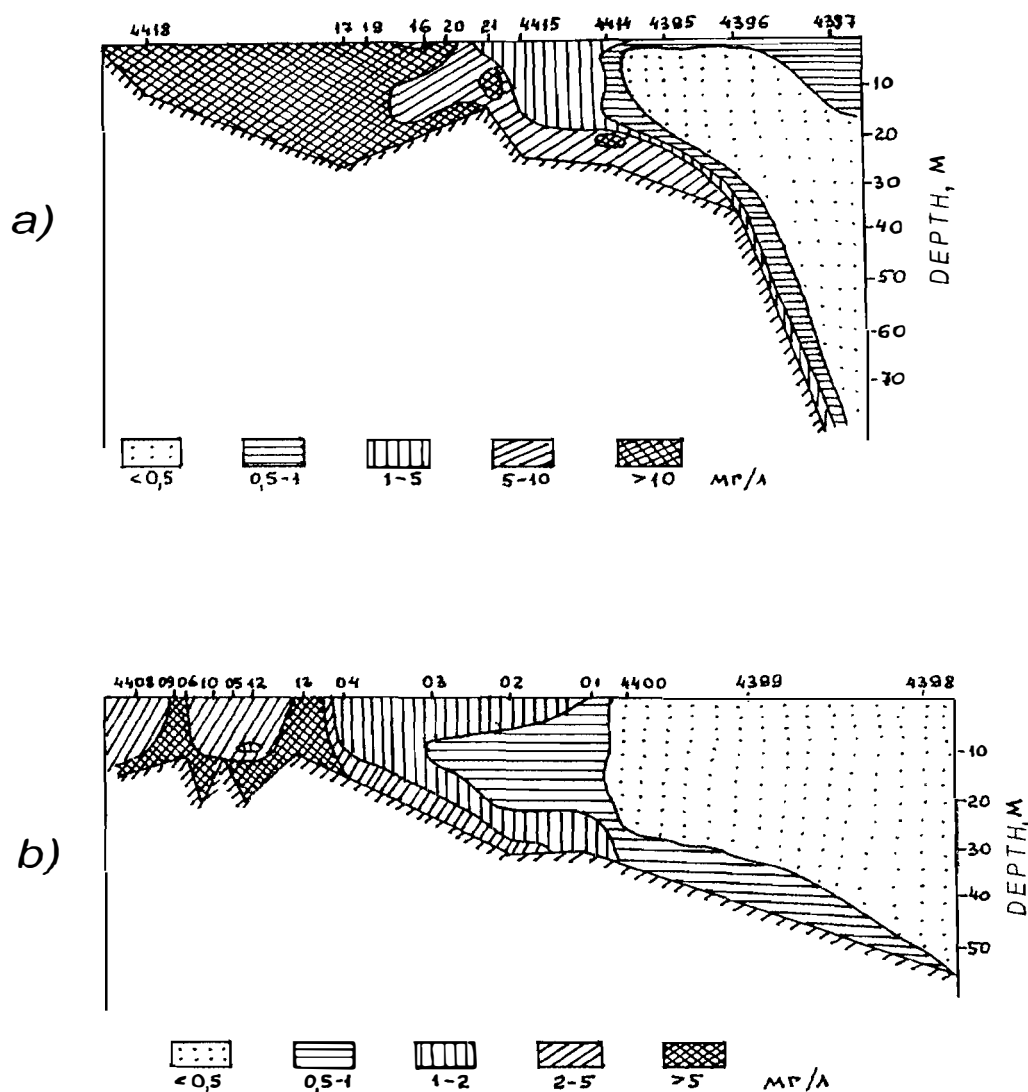


Fig.2 Quantitative suspension distribution in the Kara Sea, September 1993
 1- Ob section;
 2- Yenisey section

suspension concentrations fell to 1.05 mg/l, and in the open sea - to 0.23 mg/l. In the Yenisey estuary in the surface layer the concentrations of suspended C_{org} were in the range between 290-819 mkg/l, and they were as small as 91-105 mkg/l in the open sea.

The suspension concentration in the Ob estuary was several times as great as that in the Yenisey one. It is attributable to the character of rocks in the watershed basins (the Ob river flows on the Western-Siberian Lowland, where incoherent sediments are frequently observable, but the Yenisey crosses the region with prevailing crystalline rocks) /N.V.Koronovsky, 1984/.

The lowest suspension concentrations (< 0.5 mg/l) were recorded in the Western Kara Sea. The high values were not observed anywhere over this area except the stations 4382, 4384, 4386, 4387 in the 10 meter surface layer, where they were equal to 0.62-1.69 mg/l. It was caused by the bloom of Diatoms /V.V.Vavilova, private report/.

At these stations the suspension concentrations reduced quickly with increasing depth, and deeper than 10m they were less than 0.25 mg/l. This is because of the fact that both photosynthesis occurs mainly in the thin surface layer and there is a pycnocline at a depth about of 10m /V.I.Burenkov and A.P.Vasilkov, 1994/.

The suspension concentrations in the surface layers of the Barents Sea were as follows:

- 0.11 - 1.74 mg/l (on the average, 0.36 mg/l) in the St. Anna Trough;
- 0.07 - 0.37 mg/l (on the average, 0.18 mg/l) in the Franz-Victory Trough;
- 1.27 - 3.32 mg/l (on the average, 2.34 mg/l) in the Bezymainnay Bay.

In the St. Anna Trough the concentrations of suspended organic carbon at the surface level (0-1m) vary over a wide range (from 27 to 481 mkg/l). As this takes place, the greatest values (180-481 mkg/l) were observed in the SE St. Anna Trough, where an elevated phytoplanktonic productivity took place (the phenomenon has been described earlier in some papers, for example, Sakshaug, Skjoldal, 1989). In the Barents Sea the lowest concentration of suspended organic carbon was noted in its NE part; in the Western Barents Sea the concentrations varied between 43 and 160 mkg/l, and in the SE Barents Sea they equaled from 57 to 134 mkg/l.

Summary

The results obtained allow us to make the following conclusions:

1. The suspension concentration reduces as a salinity increases at the River-Sea barrier at the expense of the sedimentation of the river-transported material.
2. As a salinity increases, the proportion of C_{org} in suspended material increases, but the proportion of mineral matter reduces. It is because of changing the type of suspension from riverine to marine.
3. On vertical sections the highest suspension concentrations were recorded in the 10-15 meter surface (above the pycnocline) and near-bottom layers.

References

1. I.S.Gramberg, Ye.A.Romankevich. Biochemistry of the Arctic Seas organic material. M.: Nauka. 1982, p.240
2. V.I.Burenkov, A.P.Vasilkov. About the influence of the continental discharge on the spatial distribution of hydrological characteristics of the Kara Sea water. *Okeanologia*, 1994, v.34, #5, pp.652-661
3. N.V.Koronovsky. Brief course on regional geology of the USSR. M.: MGU press. 1984, p.334
4. A.P.Lisitsin. Cumulative sedimentation. In: Cumulative sedimentation in the ocean. Rostov-on-Don. 1982, pp.3-59
5. V.S.Medvedev, Ye.M.Potekhina. Quantitative distribution and some features of the suspension dynamics in the SE Barents Sea. *Okeanologia*, 1986, v.36, issue 36, pp.639-645
6. V.S.Medvedev, Ye.M.Potekhina. Quantitative distribution and some features of the suspension dynamics in the SW Kara Sea. In: Modern sediment accumulation processes on the World Ocean shelves. M.: Nauka, 1990, pp.110-120
7. V.P.Shevchenko, O.V.Severina, N.G.Maiorova, G.V.Ivanov. Quantitative distribution and composition of the suspension in the Ob and Yenisey river estuaries. *Vestnik Moskovskogo Universiteta. Geologia*. 1995 (in the press), v.41, pp. 77-86
8. E. Sakshaug, H.R.Skjoldal. Life at the ice edge. *Ambio*, 1989, v.18, pp.60-67

9. S.A.Telang, R.Pocklington, A.S.Naidu, E.A.Romankevich, I.I.Gitelson, M.I.Gladyshev. Carbon and mineral transport in major North American, Russian Arctic, and Siberian rivers: the St.Lawrence, the Mackenzie, the Yukon, the Arctic basin rivers in the Soviet Union, and the Yenisei. In: *Biochemistry of Major World Rivers*. SCOPE. 1991, pp.75-104

OCEAN SEDIMENT FLUXES IN THE KARA AND BARENTS SEAS

V.P. Shevchenko, A.P. Lisitsin (IORAS), G.I. Ivanov (ARROI), M. Ye. Vinogradov, A.A. Burovkin, V.V. Zernova, S.S. Shanin, Ye.A. Romankevich, (IORAS) A.V. Nescheretov (ARROI)

An ocean sediment flux moving from the surface water towards the bottom is an important link for many geochemical cycles. Values of sediment fluxes and their components as well as the composition of sediment particles allow us to use numerical methods when solving the issues of biogeochemistry, lithology, ecology and environmental protection. Of a particular interest is the study of sediment fluxes in the Arctic. A knowledge on the balance of organic carbon in the Arctic is essential to the development of the models of global climatic changes /Walsh, 1989/.

Background information and methods

The sediment fluxes in the Kara Sea and Ob and Yenisey estuaries were studied for the first time during the 49th cruise onboard the R/V "Dmitry Mendeleev", September 1993, within the International Program JGOFS (Joint Global Ocean Flux Study) /A.P. Lisitsin and others, 1994/. Small cylindrical sediment traps 185mm in diameter, the working part 490mm in height, were mounted at 23 buoy stations, the samples could be obtained from 13 of them. During the 9th cruise onboard the R/V "Professor Logachev", August-September 1994, 6 stations were equipped with the similar traps, 3 of the stations were successful (Fig.1). A polyethylene bottle with a volume of 100ml to accumulate sediments was screwed to the lower part of each cylinder. In order to prevent the accumulated material from being destructed by bacteria and eaten away by zooplankton 5 ml of 40% formalin were placed into most bottles before the installation was done. For comparison purpose several cylinders were left not to be poisoned. More detailed method for measuring sediment fluxes and studying sediment composition is given in the paper by A.P. Lisitsin and co-authors /1994/.

Results and discussions

At the station 4382 located near the Novozemelsky Trough (Fig.1) the sediment flux was equal to 25 mg/ m² /day at a level of 60m and 52.8 mg/ m² /day at a level of 100m, and the fluxes of C_{org} were 5.54 and 9.04 mg C/m²/day respectively. The major portion of sediments was pellets of Calanus species and Euphausiids. Separate Diatoms and Tintinnids were also found here. At the station 4386 the sediment flux reached 18.7 mg/ m² /day at a level of 33m, and the flux of C_{org} - 4.28 mg C/ m² /day. Many Diatoms of Thalassiosira nordenskioldii, the bloom of which was observed in the euphotic zone, were noted in these traps. The samples contained only separate pellets of Copepods.

The moderate sediment and C_{org} fluxes were seen at the stations 4389 and 4394 located in the SW Kara Sea. Here, as at the station 4382, the sediments were mainly presented by pellets. The smallest sediment and C_{org} fluxes were registered at the northern stations of the Ob and Yenisey sections (stations 4395, 4396, 4400). The trapped sediments at these three stations were composed primarily of pellets of Crustaceous and little balls of matter out of Diatoms.

Vastly greater sediment fluxes were observed in the Ob and Yenisey river estuaries, i.e. in the zone of the marginal filters development /A.P. Lisitsin, 1994/. At the station 4415 located at the outer boundary of the zone, where the Ob river and sea water mixed together, the sediment flux reached 1321 mg/ m² /day at a level of 22m (10m above the bottom) and the C_{org} flux - 26.7 mg/ m² /day. Fine-grained detritus and argillaceous particles were mainly found in the sediments, the content of C_{org} was not high, as low as 2.02 percent.

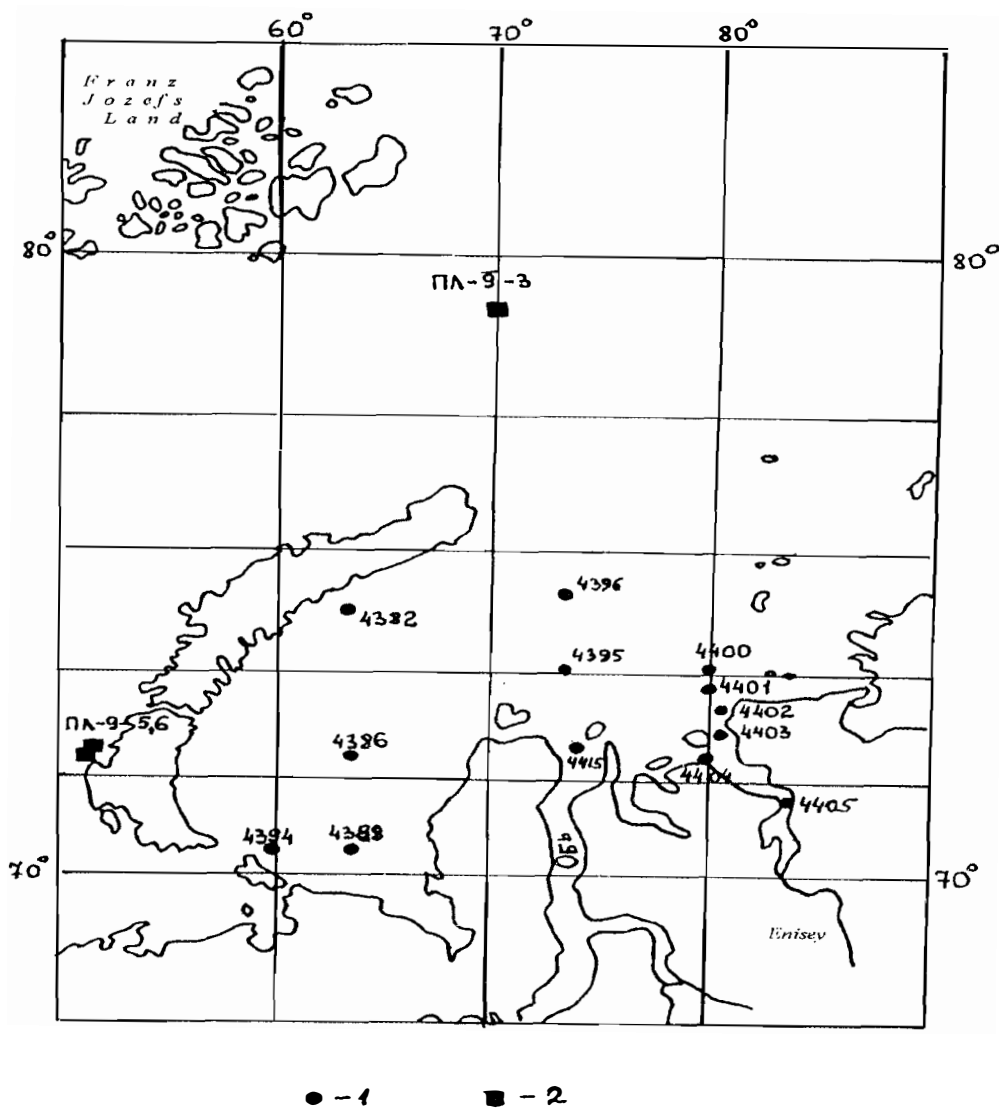


Fig.1 Sedimentation stations:

1- 49th cruise onboard the RV "Dmitry Mendeleev"; 2- 9th cruise onboard the RV "Professor Logachev"

When the content of the bottle-sampler of the formalin poisoned cylinder was compared with that of the poison free one possessed by the same trap, it was found that at some stations the poisoned bottles had a lot of zooplankton, but it was not practically found in the adjacent clear bottles /A.P.Lisitsin and others, 1994/. Thus, travelling into these traps zooplankton ("smimmers") successfully left the bottles without poison. While being inside these bottles it likely ate some sediment accumulated, but it could not get out the bottles poisoned. The obtained data on the influence of formalin as a preservative agree closely with the literature sources /Gardner et al., 1983/: formalin protects accumulated samples not only from being destructed by bacteria but from being eaten away as well.

In August 1994, in the central St. Anna Trough, the sediment fluxes reduced from 23.0 mg/ m²/day to 19.05 mg/ m²/day at a level of 55m at the expense of organic matter destruction, and then they increased to 27.9 mg/ m²/day at a level of 465m (50m above the bottom). The suspended C_{org} fluxes decreased from 10.74 to 1.68, and then rose to 3.44 mg/ m²/day at the same levels (Fig.2). The above changes in the fluxes are likely to point to the organic matter destruction during the particle settlement in the water column and to the bottom sediment resuspension in the near-bottom layer. The sharpest reduce in fluxes takes place in the upper layer of the Atlantic water mass (Fig.2). The sediments at this station were primarily presented by

amorphous aggregations of the "sea snow", the basis for them was provided with colonies and separate cells of Diatoms of *Thalassiosira*, *Chaetoceros*, *Navicula*, *Licmophora* and *Amphora* species. There were some representatives of migratory zooplankton died of formalin in the traps here, where Copepods of *Metridia longa* were prevailing.

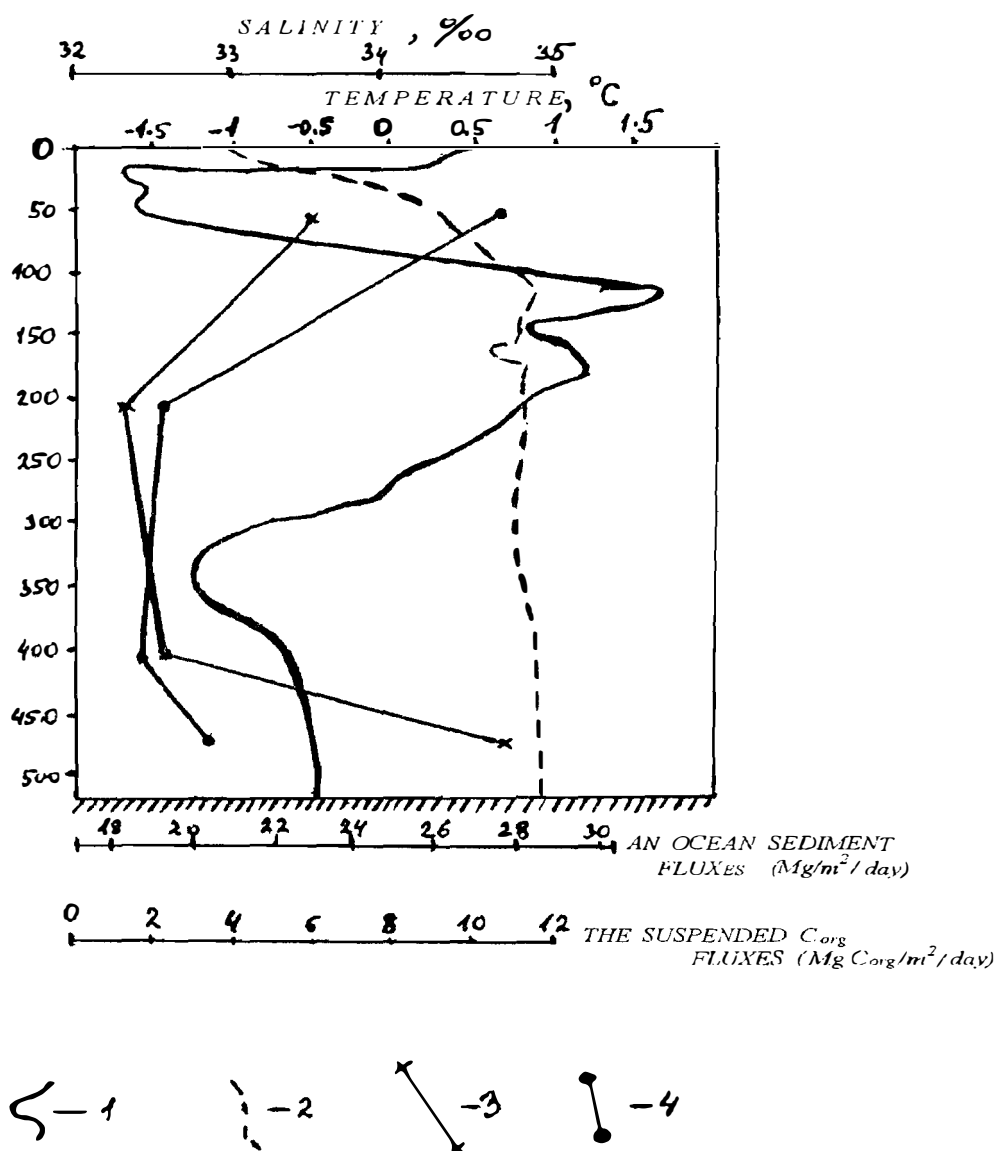


Fig.2 Temperature (1), salinity (2), sediment fluxes (3) and suspended C_{org} fluxes (4) at the station PL-9-3 (St. Anna Trough, August 10-20, 1994)

In late September, 1994 in the eastern Barents Sea, near the Yuzhny Island, Novaya Zemlia Archipelago, the sediment fluxes at the station 5 (a depth of the sea is 135m) were equal, on the average, to 62.9 and 42.5 mg/ m²/day at the levels of 35 and 95m correspondingly. The sediment composition is dominated by pellets of Crustaceous. Many Tintinnids were also recorded. The number of Diatoms was small. At the station 6 (a depth of the sea is 40m) the sediment fluxes reached 314 and 656 mg/ m²/day at the levels of 15 and 20m respectively, the sediment mainly consists of mineral particles, this is indicative of the bottom sediment resuspension.

Summary

The studies of sediment fluxes carried out in the Kara Sea and the Ob and Yenisey river estuaries, September 1993, and in the St. Anna Trough and eastern Barents Sea, August-September 1994, showed the following:

- low values of the sediment and C_{org} fluxes were measured in the open Kara Sea. The values are in agreement with the ideas of ultraoligotrophy of this water area. The sediment composition in the open Kara Sea is dominated by pellets of Copepods and Euphausiids, and flaky aggregations ("sea snow") as well;

- the sediment fluxes in the Ob and Yenisey estuaries are two-three orders greater than that in the open sea. This is due to the sediment settlement at the first global level of the cumulative sedimentation. The sediments here mainly consist of fine-grained terrigenous material of pelitic and aleuritic fractions.

References

1. A.P.Lisitsin. Marginal filter of oceans. *Okeanologia*, 1994, v.34. #5, pp.735-747
2. A.P.Lisitsin, V.P.Vinogradova, M.Ye.Vinogradova, O.V.Severina, V.V.Vavilova, I.P.Mitskevich. Sediment fluxes in the Kara Sea and Ob and Yenisey estuaries. *Okeanologia*, 1994, v.34. #5, pp.748-758
3. W.D.Gardner, K.R.Hinga, J.Marra. Observations on the degradation of biogenic material in the deep ocean with implications on accuracy of sediment trap fluxes. *Journal of Marine Research*, 1993, v.41. pp.195-214
4. J.J.Walsh. Arctic carbon sinks: Present and future. *Global Biogeochemical Cycles*, 1989, v.3.pp393-411

